INFLUENCE OF FORMATION ANISOTROPY AND AXIAL COMPLIANCES ON DRILLING PERFORMANCE

by

© Abdelsalam N. A. Abugharara

A Dissertation submitted to the

School of Graduate Studies

in partial fulfillment of the requirements for the degree of

Doctor of Philosophy

Faculty of Engineering and Applied Science

Memorial University of Newfoundland

August 2019

St. John's Newfoundland and Labrador

I. ABSTRACT

Drilling provides the path to reach and exploit underground oil and gas reserves. Drilling oil and gas wells can be vertical, inclined, or horizontal. However, as non-vertical drilling has become dominant, success in increasing oil and gas production has been led by horizontal drilling.

Trajectories of horizontal wells have three main curvature segments: vertical, inclined (diagonal or oblique), and horizontal, where the properties of the encountered formation during drilling may vary with inclination.

Rocks, classified as anisotropic (i.e. shale), whose properties are directional dependent or classified as isotropic (i.e. fine-grained and sandstone), whose properties are not directional dependent, have high influence on drilling performance, especially in nonvertical drilling.

The significant shift towards horizontal drilling has increased the interest in laboratory studies and research on directional drilling, particularly in shale, to evaluate the influence of anisotropy orientation on drilling performance (i.e. ROP), and therefore, choose optimal trajectory, enhance performance, and reduce costs.

This dissertation focuses on: (i) developing an experimental procedure for classifying rock anisotropy through oriented physical, mechanical, and drilling measurements, (ii) evaluating the influence of shale (as VTI rocks) anisotropy orientation on drilling parameters, and (iii) investigating the enhancement of the drilling rate of penetration (ROP) by implementing the novel drilling technique of passive Vibration Assisted Rotary Drilling (pVARD).

First, a laboratory baseline procedure was developed for a rock anisotropy characterization involving oriented physical, mechanical, and drilling tests on rock like materials (RLM). This research objective was to develop the procedure on synthetic rocks (RLM) as well as natural rocks, including shale, granite, and sandstone.

Second, detailed oriented physical, mechanical, and drilling measurements were taken for the determined isotropic and non-isotropic rocks in stage I, then aimed to interlink all results of all measurements, through which isotropic rock classifications can be enriched, and confirmed.

Third, compliant (i.e. pVARD) versus non-compliant (without pVARD) drilling was performed in various rocks for the purpose of evaluating the influence of axial oscillations on drilling performance. Also, the parameters behind enhancing ROP with compliant versus non-compliant were investigated in this research.

Last, a relationship between oriented strength and oriented drilling parameters for isotropic and anisotropic rocks was developed. This research aims to establish relationships between strength variation, drilling performance, and the main drilling parameters that influence ROP in different rock types for the purpose of rock isotropy / anisotropy evaluation.

II. ACKNOWLEDGEMENTS

I would like to express my sincere thanks and gratitude to my supervisor Dr. Stephen D. Butt, my co-supervisor Dr. John Molgaard, my supervisory committee members: Dr. Charles Hurich and Dr. James Yang. Their advice, support, guidance, and patience throughout the work of this research has been invaluable. I gratefully acknowledge and appreciate their technical expertise, critical thinking, and valuable comments on research, publications, and dissertation.

I would also like to thank the Atlantic Canada Opportunity Agency (AIF contract number: 781-2636-1920044), involving Husky Energy, Suncor Energy and the Research and Development Corporation (RDC) of Newfoundland and Labrador, for funding this research. I would like to acknowledge the academic offer and study opportunity, encouragement, guidance, and the financial support provided by the Libyan ministry of higher education through the Canadian Bureau for International Education (CBIE-Libya).

I would like to give my appreciation to all group members who provided me with assistance in the Drilling Technology Laboratory. Specifically, thanks are directed to Bashir Mohamed, Abourawi Alwaar, and Abdulsalam Ihmodai, for their help in experiments, as well as Shawn Organ, Steve, Steele, Wanda Aylward, and David Snook for help in technical support.

I am highly grateful to my parents and my wife who have been of a continues support and have given me patience and encouragement whenever challenges are encountered.

Last but not least, I thank my Lord, who provided for me a full and limitless support and assistance.

Table of Contents

III. LIST OF FIGURES

IV. LIST OF TABLES

V. LIST OF SYMBOLS, NOMENCLATURE OR ABBREVIATIONS

A	drilling rig stand
a	two channel digital storage Oscilloscope
AE	Acoustic Emission
AET	Axial Excitation Tool
AET	Axial Excitation Tool
AGT	Oscillation Generator Tool
AOT	Axial Oscillation Tool
AOT)	Axial Oscillation Tool
B	the rig base, on which K and G are fixed
b	square wave Pulser/Receiver
BHA	Bottom Hole Assembly
BHP	Bottom Hole Pressure
BTS	Brazilian Tensile Strength
C	dual rpm electric drill motor
c	rock sample
C11, C12, C22, C33, C44, C55, and C66	Elastic Constants
CBIE	Canadian Bureau for International Education
CBS	Conception Bay South
CCS	Confined Compressive Strength, (MPa)
D	suspended weight

d	shear wave sensor
DAQ-SYS	data acquisition system
DDWOB	Downhole dynamic weight on bit (kg)
DEM	Discrete Element Method
DOC	depth of cut, (mm/rev)
DOT	Drill-off-test
DTL	Drilling Technology Laboratory
e	shear wave sensor
E	Modulus of Elasticity
E-dy	Dynamic Modulus of Elasticity
Esw	swivel
Exp.	experimental
F	stand pipe
FEA	Finite Element Analysis
FR	flow rate, (l/min)
FRT	Friction Reduction Tool
FRT	Friction Reduction Tool
G	container for cuttings collection
H	three oriented shale samples cast in cement
HSW	High suspended weight, (kg)
HTI	Horizontally Transverse Isotropy
HTI	horizontally transverse isotropy
I	drill string

Ia(50)	Point load strength anisotropy index
IDP	input drilling parameters
Is	Point load strength index
IT	indirect tensile strength, (MPa)
IVP	Compressional Wave Velocity Index
Iσ (90)	UCS in vertical direction, perpendicular to rock bedding, (MPa)
Iσ (min)	minimum strength, MPa
Iσ C	uniaxial compressive strength anisotropy index
J	grooved flat steel plate for rpm measurement
K	load cell
L	data acquisition system, DAQ-SYS
LP	compressional wave travel length, (m)
LPT	linear position transducer
LS	shear wave travel length, (m)
LSW	low suspended weight (kg)
LTS	laser triangulation sensor
LTS	laser triangulation sensor
LVT	Lateral Vibration Tool
M	cutting collection system and drainage
MDP	multiple drilling parameter
MSE	mechanical specific energy
MSW	medium suspended weight (kg)

N	linear position transducer, LPT
NPT	non-productive time
O	laser triangulation sensor, LTS
ODP	output drilling parameters
OITS	oriented indirect tensile strength
OPLS	oriented point load strength
OUCS	oriented unconfined "uniaxial" compressive strength
OUSWV	oriented ultrasonic wave velocity
P	a 1000-liter water tank and pump unit
PDC	polycrystalline diamond compact bit
PFC-2D	Particle Flow Code-2 Dimension
PLI	Point Load Index
PLIT	point load index test
pVARD	passive Vibration Assisted Rotary Drilling
Q	sample holder fixed above the load cell
R	receiver connection
RDC	research and development corporation
RLM	rock like material
rms	root mean square
ROP	rate of penetration, (m/hr)
rpm, RPM	revolution per minute
σ	strength, (MPa)
Sim	simulation

ST	splitting strength
Sta-WOB	static WOB, (kg)
T	transmitter connection
TP	compressional wave propagation time, (sec)
TRQ	torque, (N-m)
TS	shear wave propagation time, (sec)
UCS	unconfined compressive strength, (MPa)
V mean	velocity mean value, (km/sec)
V min	velocity minimum value, (km/sec)
VA	velocity anisotropy
Vmax	velocity maximum value, (km/sec)
Vmean	mean velocity
VP	primary or compressional wave velocity, (km/sec)
VS	secondary or shear wave velocity, (km/sec)
VTI	Vertically Transverse Isotropy
VTI	vertically transverse isotropy
WOB	weight on bit (kg)
ρ	density, (g/cc), (kg/cc)
υ	Poisson’s ratio

CHAPTER 1: INTRODUCTION AND OVERVIEW

1.1 Introduction

Drilling is essential to oil and gas exploration and field development, either vertically, directionally, or horizontally. Drilling performance, focusing on Rate of Penetration (ROP) has been the key concern and demanding interest for oil and gas companies to reach hydrocarbon targets effectively and economically. ROP has been reported to be affected mainly by two factors: (i) drillstring and bottomhole assembly (BHA) factor and (ii) rock (drilled formation) factor. For several decades, research has been advanced, technologies have been invented, and methodologies have been developed to overcome challenges of drillstring and drilled formation and to enhance drilling performance and increase ROP. For the drillstring factor, this thesis utilized a Passive Vibration Assisted Rotary Drilling (pVARD) tool (compliant drilling) as a newly designed tool that enhances ROP against the conventional (rigid or non-compliant) drilling as a part of the investigation. For the formation factor, Rock Like Material (RLM), shale, fine-grained granite, and fine-grained sandstone rocks were the rock types used for the research of this thesis.

Rocks can be characterized as isotropic, where material properties are independent of orientation, or anisotropic, where material properties are not independent of orientation. Special cases of rock anisotropy include Vertical Transverse Isotropic (VTI) or Horizontal Transverse Isotropic (HTI), where the properties are uniform in either the vertical or horizontal plane and are different in the perpendicular direction. Anisotropy is an important characteristic of rocks in oil and gas drilling operations, and it is known that anisotropy of the formation drilled in deviated, extended reach, and horizontal wells can impact ROP, contribute to the borehole

deviation and wander from the intended well trajectory, cause wellbore instability, and ultimately increase the overall drilling cost.

The main aim of this thesis is to develop an empirical procedure that utilizes several testing components: ultrasonic wave measurement, strength measurement, and drilling measurement as a methodology for (i) rock anisotropy evaluation and (ii) drilling performance investigation utilizing pVARD technology.

1.2 Statement of the Problem

As drilling is the main application through which hydrocarbon reserves can be reached and exploited, efficient and successful drilling can be improved by considering rock anisotropy. One important parameter that has not been covered much in the literature review as a positive drive towards enhancing drilling performance is “rock anisotropy”. Although, anisotropy of rocks has been studied for the purpose of (i) describing its failure behavior and modes, (ii) investigating its negative impact on wellbore deviation and wellbore instability, or (iii) classifying rocks based on their isotropy / anisotropy for investigating the two above purposes. These studies were performed by following individual procedures or pairs at most. However, this thesis (i) develops a comprehensive procedure for rock anisotropy that involves several tests conducted on same rock types for the purpose of anisotropy classifications, (ii) investigates the influence of rock anisotropy (positive effect) on the main drilling parameters influencing ROP (efficient rock breakage with less energy consumed, less bit wear, etc.), and (iii) utilizes bit-rock interaction of anisotropic rocks in understanding pVARD behavior and its influence to enhance ROP.

1.3 Research Objectives and Thesis Organization

The objectives of this thesis are to develop an experimental procedure through which several techniques are applied to collectively draw a baseline for rock anisotropy classification. The procedure involves study of oriented ultrasonic wave velocities: compressional and shear wave velocities (VP and VS respectively), study of the oriented strength, as well as study of the oriented main drilling parameters. Tests were performed in three main orientations: vertical, diagonal or oblique, and horizontal. This research was conducted under stated three main research blocks: (i) rock anisotropy characterization, (ii) influence of rock anisotropy on drilling performance, and (iii) influence of pVARD on enhancing drilling performance. These main research blocks were conducted over the course of seven projects as described in the following main seven chapters including chapter 3 to chapter 9.

Chapter 2: Research methodology

This chapter is focused on describing the research methodology of the main seven chapters.

Chapter 3: Fundamental baseline development for rock anisotropy characterization

The focus of this chapter was to develop a fundamental rock anisotropy measurement and characterization procedure utilizing published anisotropy indices and to interlink some tests (physical, mechanical, and drilling) for the purpose of evaluating rock anisotropy.

Chapter 4: Study of rock anisotropy with emphasis on circular wave velocities and elastic moduli

The objective of this chapter was to confirm the isotropy of the RLM by building on experimental characterization conducted in chapter 3 by expanding the characterization to include other anisotropic and isotropic materials.

Chapter 5: Study of rock anisotropy with emphasis on conventional drilling performance and cutting analysis

The purpose of this project was to expand rock characterization implemented in chapters 3 and 4 to include conventional rotary drilling and cutting analysis.

Chapter 6: Study of the influence of anisotropy orientation on main drilling parameters

The work of this chapter received a conference award for best paper and was extended and published in a journal. The purpose of this project was mainly to develop a procedure for VP and VS circular measurements of shale, as well as to investigate the influence of shale anisotropic orientation on main drilling parameters studies in the two previous projects on isotropic rocks.

Chapter 7: Study of enhancing ROP using pVARD

This chapter was mainly focused on investigating the improvement of ROP using pVARD, as a compliant drilling system versus rigid, as a non-compliant drilling system.

Chapter 8: Investigation of the pVARD influencing parameters on enhancing ROP

The purpose of this chapter was (i) to investigate the parameters behind improving ROP using pVARD.

Chapter 9: Developing a comprehensive procedure for rock anisotropy characterization with the inclusion pf pVARD for rock anisotropy evaluation

This Chapter was focused on developing a comprehensive rock characterization procedure by including all testes and measurements that were conducted in the previous chapters and by involving pVARD and DDWOB.

1.4 Literature Review

This section contains the literature review of (i) rock anisotropy classification (ii) drilling methods with the emphasis on rotary drilling, (iii) influence of rock anisotropy on drilling performance, (iv) techniques for enhancing drilling performance and maximizing ROP, and (v) classifications of downhole vibrations and the advantages of controllable, non-destructive, and desirable vibrations on improving drilling performance. There will be reflective information at the end of each section addressing the contribution of this research with relation to each section.

1.4.1 Rock classification

This section includes detailed information on (i) general rock classifications with the emphasis on isotropy / anisotropy (Iso. / Aniso.), (ii) published methods and procedures for rock Iso. / Aniso. classification.

1.4.1.1 General rock classification

Generally, rocks are categorized based on how they were originally formed into three main groups including igneous, metamorphic, and sedimentary rocks. Table 1.1 summarizes general rock classifications based on their origin, sub-class and groups, texture ranges and examples, and values of material constant of intact rocks used for rock strength estimations in underground mining excavation [1]. The igneous rocks are formed as intrusive igneous rocks through a slow cooling process of the molten rocks “the Magma” within the subsurface of the earth, or as extrusive igneous rocks through quick cooling process of the molten rocks “the Lava” on the surface of the earth. The metamorphic rocks are formed by exposing previously existed rocks to heat and pressure that result in profound change in rock properties forming metamorphic rocks. The sedimentary rocks are formed by depositing sediments carried through various means including air, wind, ice, gravity, or flowing water near or at a distance from the source area of the sediments. Sedimentary rocks are the typical hydrocarbon source rocks (i.e. shale), typical rocks forming hydrocarbon migration paths (permeable or fractured rocks), and typical hydrocarbon reservoir rocks (sedimentary rocks with various permeability ranges).

Table 1.1. Main rock types based on their origin, sub-class and groups, texture ranges and examples, and values of material constant of intact rocks used for rock strength estimations in underground mining excavation [1]

Rock Type	Class	Group	Texture			
			Coarse	Medium	Fine	Very fine
SEDIMENTARY	Clastic		Conglomerates* Breccias*	Sandstones 17± 4	Siltstones 7 ± 2 Greywackes (18 ± 3)	Claystones 4 ± 2 Shales (6± 2) Maris (7 ± 2)
	Non-Clastic	Carbonates	Crystalline Limestone (12 ± 3)	Sparitic Limestones (10 ± 2)	Micritic Limestones (9 ± 2)	Dolomites (9 ± 3)
		Evaporites		Gypsum 8 ± 2	Anhydrite 12 ± 2	
		Organic				Chalk 7 ± 2
METAMORPHIC	Non Foliated		Marble 9 ± 3	Hornfels (19 ± 4) Metasandstone (19 ± 3)	Quartzites 20 ± 3	
	Slightly foliated		Migmatite (29 ± 3)	Amphibolites 26 ± 6	Gneiss 28 ± 5	
	Foliated **			Schists 12 ± 3	Phyllites (7 ± 3)	Slates 7 ± 4
IGNEOUS	Plutonic	Light	Granite 32 ± 3	Diorite 25 ± 5		
			Granodiorite (29 ± 3)			
		Dark	Gabbro 27 ± 3	Dolerite (16 ± 5)		
			Norite 20 ± 5			
	Hypabyssal		Porphyries (20 ± 5)		Diabase (15 ± 5)	Periodotite (25 ± 5)
	Volcanic	Lava		Rhyolite (25 ± 5) Andesite 25 ± 5)	Dacite (25 ± 3) Basalt (25 ± 5)	
		Pyroclastic	Agglomerate (19 ± 3)	Breccia (19 ± 5)	Tuff (13 ± 5)	

Hydrocarbon forms in, migrates through, accumulates at, and finally being extracted only from sedimentary rocks [2, 3, 4, 5, 6]. Figure 1-1 shows a typical hydrocarbon (i.e. petroleum or oil

and gas) system that consists of four main sections that include a mature source rock (an organic matter rich rock such as shale), the migration path of the hydrocarbon, the impermeable rock (seal or cap rocks), and the reservoir rocks (hydrocarbon accumulation area in the permeable rocks forming the hydrocarbon reservoir).

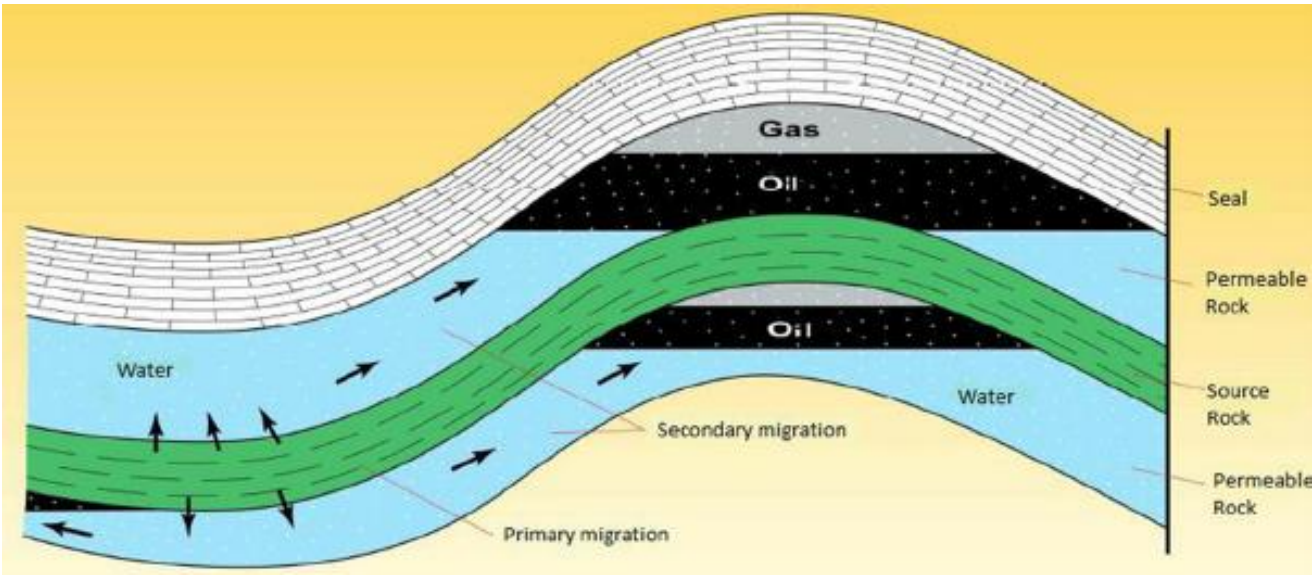

Figure 1-1.Typical petroleum system [7]

In this research most of the tested rocks were sedimentary rocks (i.e. shale and sandstones) with the addition to a synthetic rock-like-material (RLM) and a natural fine-grained granite for the purpose of developing laboratory procedure of rock anisotropy characterization of using rocks of various types and origins.

1.4.1.2 Isotropy / Anisotropy classification

Many researchers reported rock isotropy / anisotropy classifications [8, 9, 10]. These studies classified rocks into 5 main groups: isotropic, fairly anisotropic, moderately anisotropic, highly anisotropic, and very highly anisotropic based on indices that were proposed after intensive laboratory work. The laboratory work included two most common tests: (i) ultrasonic wave velocity tests and (ii) strength tests. The ultrasonic waves include compressional (primary) waves (VP) and shear (secondary) waves (VS) that propagate through the rock between the wave sender or transducer and the wave detector or receiver. The strength tests include UCS and PLI.

Each of these tests was conducted at least in three main directions. The directions were: vertical oblique and parallel to rock bedding, when the tested rocks have a visible bedding or foliation structure. Otherwise, these three orientations (vertical, oblique, and horizontal) are selected with the accordance to 1st quarter of the Cartesian coordinate system.

Table 1.2 shows the authors and their indices proposed for rock anisotropy classifications with respect to testing types.

Table 1.2. Authors and their proposed anisotropy indices with respect to test types

Author	Test type	Anisotropy Index	Equation
Tsidizi (1997)[9]	Wave velocity	Velocity Anisotropy (VA) Index	VA= [(Vmax-Vmin)/Vmean] (%)
Saroglou (2007)[8]			IVP =VP (0°)/VP (90°)
ISRM (1981) [11]	PLI	Point load strength anisotropy index	Ia(50) = Is (50) (90°) / Is (50) (0°)
ISRM (1985)[12]			
Tsidzi (1990) [13]			
Ramamurthy (1993) [10]	UCS	Uniaxial compressive strength anisotropy index	Iσc = σc (90°) / σc (min)

Table 1.3 , Table 1.4, and Table 1.5 show the anisotropy classification of rocks according to the Unconfined Compressive Strength (UCS) proposed by Ramamurthy 1993 [10], the anisotropy classification according to PLI proposed by ISRM 1985 [12], and anisotropic classifications according to wave velocity proposed by Tsidzi [9], respectively.

Table 1.3. Anisotropy classification according to UCS proposed by (Ramamurthy, 1993) [10]

Degree of compressive strength anisotropy, $I\sigma_c$	Descriptive term
1.0 - 1.1	Isotropic
1.1 – 2.0	Fairly anisotropic
2.0 – 4.0	Moderately anisotropic
4.0 – 6.0	Highly anisotropic
> 6.0	Very highly anisotropic

Table 1.4. Anisotropy classification according to PLI proposed by (ISRM, 1985) [12]

Degree of Point load strength anisotropy $I\alpha_{(50)}$	Descriptive term
1	Isotropic
1 – 2	Fairly – moderately anisotropic
2 – 4	Highly anisotropic
> 4	Very highly anisotropic

Table 1.5. Velocity anisotropy classification of some rocks (Tsidzi 1997) [9]

Degree of velocity anisotropy *VA* (%)	Descriptive term
< 2	Isotropic
2 – 6	Fairly anisotropic
6 – 20	Moderately anisotropic
20 – 40	Highly anisotropic
> 40	Very highly anisotropic

1.4.1.3 Influence of Anisotropy

Anisotropy has been determined through intensive studies that it has influences on rock properties and rock behavior when: (i) measuring oriented properties, (ii) applying loads for fracturing during oriented strength determination, and (iii) shear or tensile fracturing beneath

drill bits during rotary drilling. Anisotropy was reported to have an effect on rock physical and mechanical properties. Some of the influences of anisotropy are directly related to oil and gas operations include tendency of hole deviation in drilling [14, 15, 16, 17, 18] as well as well bore instability [19, 20, 21, 22, 23, 24]

1.4.1.4 Influence on Physical Properties

Physical properties are important characteristics of rocks that are always required to be determined for many engineering applications including oil and gas drilling as well as mining. The importance of determining the physical properties including the elastic moduli and seismic (i.e. low frequency waves for field applications) and ultrasonic wave velocities (i.e. high frequency waves typically used for laboratory applications) along with other physical properties comes in that the physical property measurement can (i) assist in determining the rock type, (ii) estimate other properties (e.g. mechanical properties) through correlations, and (iii) be less costly as well as are non-destructive tests. The inclusion of bedding, layering, cleavage, or foliations in the structure of the anisotropic rocks make influence the velocities of the seismic or ultrasonic waves when propagating in different directions. The assumption of rock isotropy has been the common practice in many engineering practices, however not considering rock anisotropy can produce inaccurate results in various magnitudes [25, 26]. As the rock physical anisotropy has been studied intensively, this dissertation uses the influence of the anisotropy on oriented ultrasonic wave velocities, elastic moduli, and stiffness constant as a sign to (i) characterize rocks based on isotropy and anisotropy, (ii) categorize them accordingly using the published wave anisotropic indices, and (iii) establish a connection towards studies of other properties including mechanical and drilling. Generally, studies

showed that seismic and ultrasonic waves are generally governed by density and elasticity of the material, through which the waves are propagating [9]. Other factors including grain size, mineralogy, and porosity were also studies for investigating their influence on wave velocities. In this regard, the objective of using the oriented ultrasonic wave velocity measurement was with the consideration of that isotropic rocks should have features distributed equally in all directions, therefore their effect on wave velocity would be similar. Unlike wise, laminated rocks, such as shale would have the density of bedding (discontinuities) varied with direction, therefore the highest density of bedding would be encountered when waves propagate perpendicular to bedding and the least when waves propagate parallel. Obtaining samples from rocks that they represent; three stages of sample production were introduced including (i) three cores need to be produced from the representative rock. Each core is obtained from a different direction of vertical, oblique, and horizontal) (Figure 1-2-a), (ii) Cube shaped sample [27, 28] (Figure 1-2-b), and (iii) one core sample obtained parallel to rock bedding [29] (Figure 1-2-c)

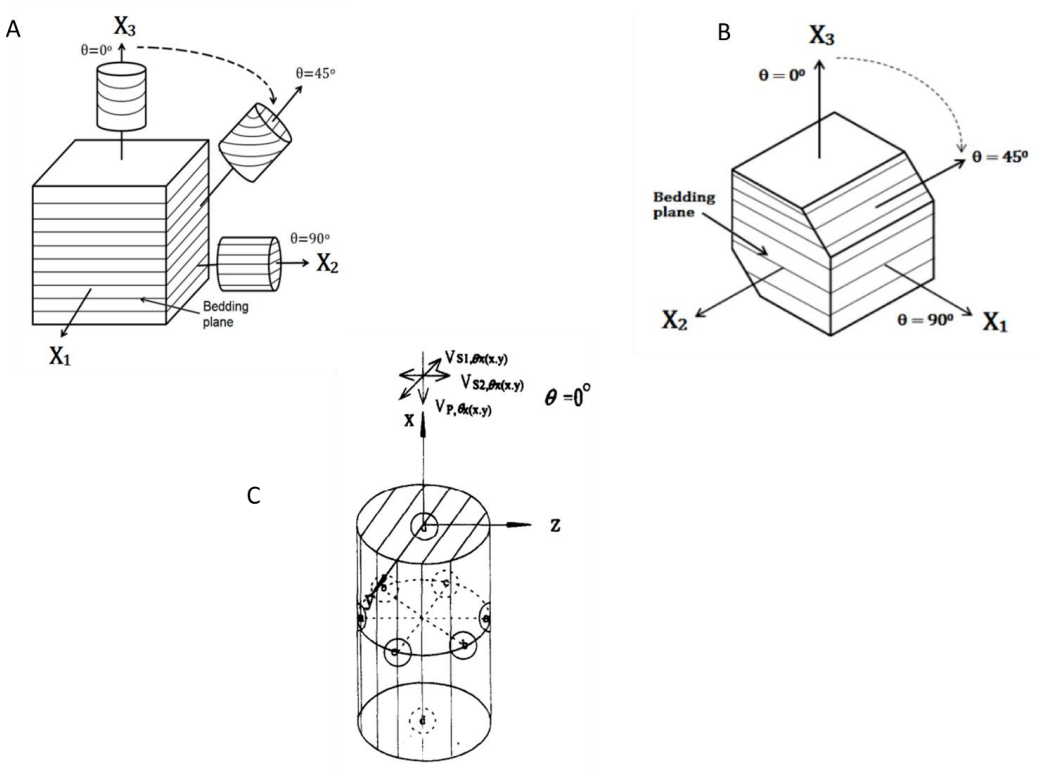

Figure 1-2. Number of samples required to obtain complete physical parameters for VTI rocks [27, 28, 29]

1.4.1.5 Influence on Mechanical Properties

Intensive studies were conducted to understand the relationships between the mechanical properties and behavior of anisotropic rocks and important problems encountered (wellbore caving in, deviations of wells, pre-mature wear and failure of downhole assembly, etc.) during: (i) hydraulic fracturing design, (ii) wellbore stability, and (iii) drilling operations through laboratory and field tests. These tests were performed various numerous conditions of loading, orientations, and confining pressures [30]. Other studies focused on the effect of the inner structure of rocks, which include permeability, porosity, inclusion of bedding, foliations, and cleavages, as well as mineral compositions on rock strength and their relationship with rock

anisotropy [31, 32, 33, 34]. McLamore and Gray [15] and Chenevert, M. E., and Gatlin [35] conducted some of the very comprehensive studies that were investigating the mechanical behavior of some sedimentary rocks containing visible features of foliations, bedding, or cleavage (e.g. slate, limestone, sandstone, shale). Some of their tests were conducted to determine the compressive strength under various levels of confining pressure with constant pore pressure. The testes were performed in several inclinations (degrees between the anisotropy plane and the loading direction) between perpendicular and parallel to bedding with increments of 15 degrees. The type of tests was involved in the study of the mechanical and properties and behavior of anisotropic rocks include (i) UCS test, (ii) confined (triaxial) compressive strength (CCS) test, (iii) PLI test, (iv) Brazilian tensile strength (BTS) test, and indirect tensile strength (ITS) test. The main objective of these tests was at least on the following: (i) understanding the mechanical behavior of the anisotropic rocks under various conditions and in different orientations, (ii) analyzing the failure patterns from laboratory controlled environment to field operations, as well as through modelling, and (iii) investigating the failure mechanics using anisotropic rocks, in general, and natural vertically transverse isotropic shale, or simulated transversely isotropic rocks, in specific [15, 30 -48]. The main conclusion drawn from the above studies regarding understanding the influence of anisotropy on the mechanical behavior can be summarized as follow:

- The orientation of bedding, foliation, or cleavage plane to the applied stress has an important relationship with strength of anisotropic rocks.
- The strength of the anisotropic rocks increases with the increase of confining pressures, but the anisotropic strength behavior tends to decrease as pressure increases.

- For the compressive strength, the maximum strength of anisotropic rocks occurs when the loading direction is perpendicular and parallel to the anisotropic plane (i.e. bedding), and the minimum strength occurs at 30 degrees. However, some researchers reported that the minimum anisotropic strength occurs between 30 and 60 degrees.
- Anisotropic rocks rupture or deform during compressive test in one of three failure modes (Figure 1-3), depending upon two main factors: 1) orientation, 2) initial stress state, as follow:
    1. Shear faulting across or along the plane of anisotropy.
    2. Slip along the plane of anisotropy.
    3. Internal buckling (kinking).
- For the indirect tensile strength, the maximum strength of anisotropic rocks occurs when the loading direction is perpendicular to bedding, and the minimum strength occurs when the loading direction is parallel to bedding.
- Anisotropic rocks rupture during indirect tensile test in one of the five failure modes as follow (Figure 1-4):
    1. Pure tensile across the bedding.
    2. Pure tensile along the bedding.
    3. Shear failure across the bedding.
    4. Shear failure along the bedding.
    5. Mixed failure between shear and tensile.

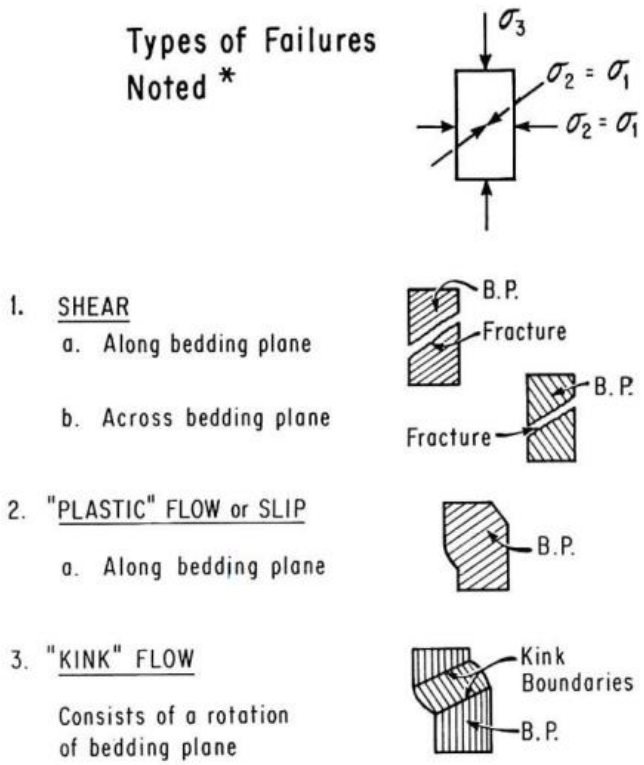

Figure 1-3. Three main fracture modes that occur in anisotropic rocks during compressive strength test [15]

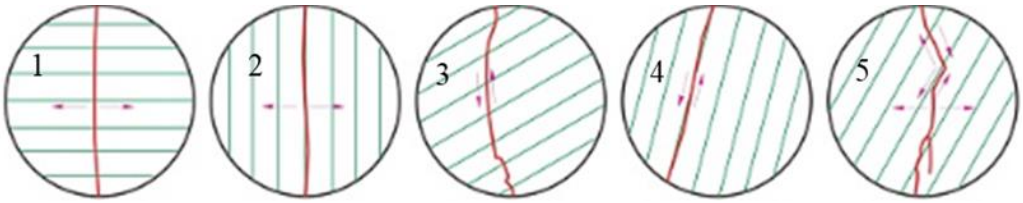

Figure 1-4. Five main failure modes of anisotropic rocks through indirect tensile test [39]

In relation with the research of this dissertation: (i) a connection between all three strength tests (UCS, PLI, IT) was made in the developed procedure for rock isotropy / anisotropy evaluation, where it was not performed before, and (ii) a three-point strength curve, which represent the strength in the three studied orientations, was developed for both isotropic and VTI rocks.

1.4.1.6 Characterization of Isotropic / Anisotropic Rocks

Rocks can be characterized to isotropic and anisotropic. Isotropy, which is the directional independency of rock property, is the simplest form, where anisotropy, which is the directional dependency of rock property, is considered the most complex form. VTI and HTI, whose property is symmetric in the direction perpendicular to the plane of isotropy. Wave velocity, compressive strength, and tensile strength are some of the properties that were studied in this thesis in both isotropic and VTI rocks. Figure 1-5 demonstrates the basic isotropy / anisotropy classifications.

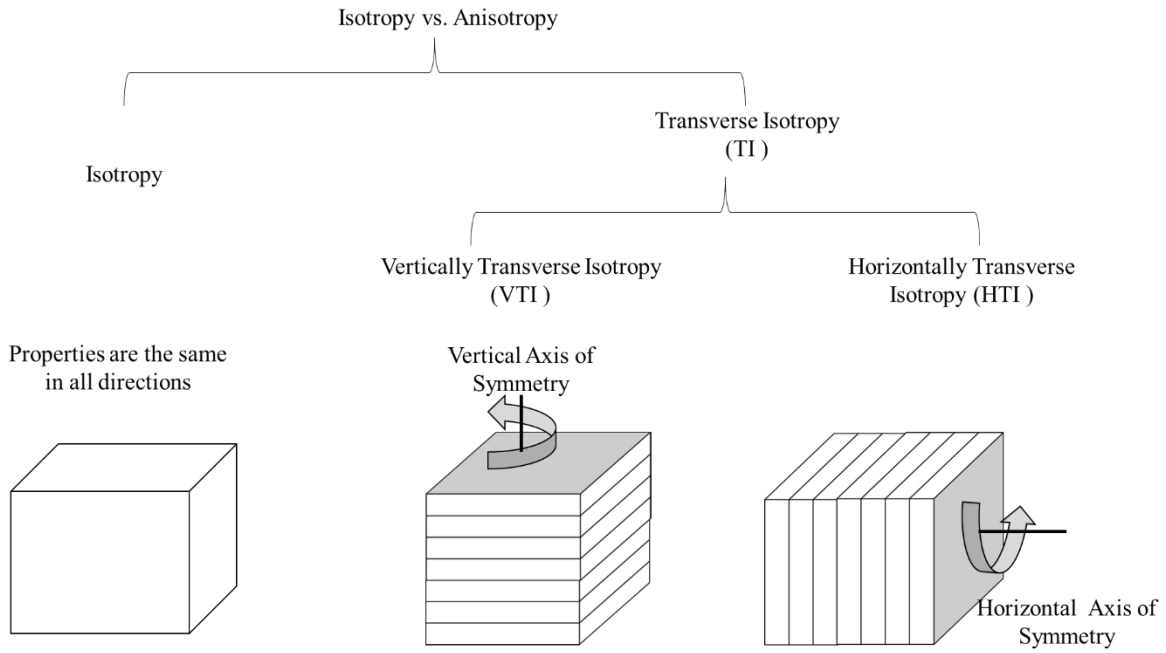

Figure 1-5.Classification of isotropy and transverse isotropy

For elastic characterization of rocks, Hock's law is expressed as in Equation 1:

$$\sigma ij = Cijkl * \varepsilon ijk \quad \text{.....1}$$

Where: σij is stress tensor, Cijkl is elastic constants, and $\varepsilon ijkl$ is strain tensor. With the introduction of the Voigt's notation [A, B, C] the (9 x 9) forth order stiffness matrix is simplified to the (6 x 6) stiffness matrix (Equation 2).

$$[c] = \begin{bmatrix} C_{11} & C_{12} & C_{13} & C_{14} & C_{15} & C_{16} \\ C_{12} & C_{22} & C_{23} & C_{24} & C_{25} & C_{26} \\ C_{13} & C_{23} & C_{33} & C_{34} & C_{35} & C_{36} \\ C_{14} & C_{24} & C_{34} & C_{44} & C_{45} & C_{46} \\ C_{15} & C_{25} & C_{35} & C_{45} & C_{55} & C_{56} \\ C_{16} & C_{26} & C_{36} & C_{46} & C_{56} & C_{66} \end{bmatrix} \quad \text{.....2}$$

Equation 2 is the stiffness matrix. It has 36 elastic constants. Due to the symmetry of the matrix, the 36 elastic constants are reduced to 21 independent elastic constants, which define the anisotropic materials.

For Orthotropic materials, which have three mutually perpendicular planes of material symmetry, their stiffness matrix has 9 independent elastic constants (Equation 3).

$$[c] = \begin{bmatrix} C_{11} & C_{12} & C_{13} & 0 & 0 & 0 \\ C_{12} & C_{22} & C_{23} & 0 & 0 & 0 \\ C_{13} & C_{23} & C_{33} & 0 & 0 & 0 \\ 0 & 0 & 0 & C_{44} & 0 & 0 \\ 0 & 0 & 0 & 0 & C_{55} & 0 \\ 0 & 0 & 0 & 0 & 0 & C_{66} \end{bmatrix} \quad \text{.....3}$$

For transverse isotropic material, the stiffness matrix has 5 independent elastic constants (Equation4).

$$[c] = \begin{bmatrix} C_{11} & C_{12} & C_{13} & 0 & 0 & 0 \\ C_{12} & C_{11} & C_{13} & 0 & 0 & 0 \\ C_{13} & C_{13} & C_{33} & 0 & 0 & 0 \\ 0 & 0 & 0 & C_{44} & 0 & 0 \\ 0 & 0 & 0 & 0 & C_{44} & 0 \\ 0 & 0 & 0 & 0 & 0 & \frac{C_{11}-C_{12}}{2} \end{bmatrix} \quad \text{.....4}$$

Where, C55 = C44 and C66 = (C11 – C12) / 2.

For the isotropic materials, there are only 2 independent elastic constants required to define the isotropic material.

In link to the research of this thesis, elastic constant was defined for the determined isotropic rocks (RLM and granite), as well as their stiffness matrices were defined in three orientations (vertical, oblique, and horizontal) as part of the procedure of the isotropic / anisotropic evaluation.

1.4.2 Rotary Drilling Method

As the most commonly used application, rotary drilling has been the dominantly adopted practice by oil and gas industry to reach hydrocarbons. With comparison to other drilling methods including percussion and rotary-percussion drilling methods, the rotary drilling is considered the most widely used techniques for most oil and gas well applications including: (i) vertical drilling, (ii) inclined drilling, and (iii) horizontal drilling. The fundamental rotary drilling process is demonstrated in Figure 1-6. However, there are six main systems, which each rotatory drilling rig consists of for efficient, safe, and economical drilling process including (i) rotary system, which is responsible for transmitting the torque to rotate the drill bit for fracturing the formation, (ii) mud circulation system, which is responsible for circulating

the drill mud for cutting removal and enabling the drill bit fracture new formation, (iii) hoisting system, which is responsible for raising and lowering drillstring components, (iv) power system, which responsible for power supplying to all systems to ensure smooth function of the drilling process, (v) well control and blowout prevention system, which is responsible for keeping the drilling conditions downhole stable and preventing a blowout through the drilling mud and Blow-Out Preventer (BOP), and (vi) well monitoring system, which is responsible for monitoring volume data of the drilling mud inlet and outlet for well control purposes.

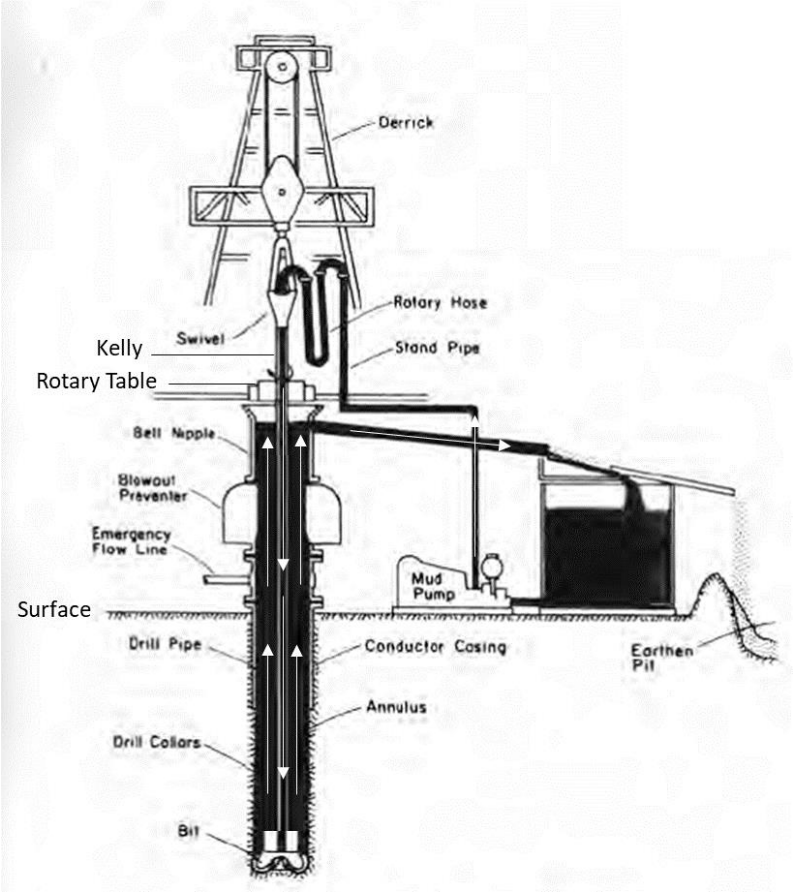

Figure 1-6. Sketch of fundamental rotary drilling process. After Bourgoyne et al. [49]

Three parameters are key for the efficient drilling process, which are: (i) weight on bit (WOB) sufficient for formation fracturing, (ii) rotary speed or revolution per minute (rpm) for chipping off and shearing formation, and (iii) fluid circulation for removing the formation fragmentations (cuttings) [49, 50, 51].

1.4.2.1 Influence of Rock Anisotropy on Rotary Drilling Performance

With the addition of the controlled input parameters (i.e. WOB, rpm, and flow rate), which make drilling process efficient when optimized, there are uncontrolled parameters that could affect the drilling process and reduce the drilling efficiency. Rock anisotropy have been reported to have influence on (i) borehole stability [19, 52], (ii) borehole deviation while drilling using different bit types including the polycrystalline diamond compacts (PDC) bit and the Roller Cone (RC) bit [14, 16, 18], and (iii) drilling ROP [17, 53]. Most of the previous studies that reported drilling in anisotropic rocks were performed for the purpose of eliminating or reducing the negative effect of rock anisotropy from deviating wellbores from the planned trajectories. However, the related research of this thesis to drilling in anisotropic rocks investigated the answer to the following question: Are there positive influences of rock anisotropy on drilling performance? what are they, if the answer is “YES”? For answering these questions, this research implemented what was recommended by the previous authors that studied the influence of rock anisotropy on wellbore deviation. Some of these recommendations are (i) optimal design of the drill bit and efficient distribution of the bit cutters, and (ii) utilizing the well-control devises and tools.

1.4.2.2 Techniques for Enhancing Rotary Drilling Performance and Maximizing ROP

Drilling efficiently can be achieved by operating at a maximum feasible rate of penetration (ROP) i.e. the depth of cut per unit time and at a minimum Mechanical Specific Energy (MSE), the energy required to remove a unit volume of rock [54-57]. Drill Off Test (DOT) is the typical practice to determine optimal drilling parameters for efficient drilling performance [57-59]. Understanding the relationships between drilling parameters and the drilling rate of penetration is a key for achieving optimal drilling performance [60]. With the addition to the conventional way of applying the drilling parameters at the surface, implementation of non-destructive and controllable axial oscillations to enhance drilling performance is addressed in Sec. 1.4.3.2.

1.4.3 Classifications of Downhole Vibrations and the Advantages of Controllable, Non-Destructive, and Desirable Vibrations on Improving Drilling Performance

Downhole vibrations always existed in drilling oil and gas wells. However, the severity, the type, and the reasons generating vibrations may vary. The downhole vibrations are interlinked to one another and some vibrations lead to generate others. For example, axial vibrations are experienced when drilling with Roller Cone Bit, or as a sign bit balling when drilling with PDC bit, or as a sign of excessive WOB when drilling hard formation in vertical wells. Some vibrations are caused by mass imbalance of drill string components, other are caused by encountering different lithologies, etc. [61, 62].

1.4.3.1 Types of downhole vibrations

Most encountered downhole vibration types are shown in Figure 1-7. Most of these vibrations are harmful and destructive. They cause either reducing drilling performance, damaging drilling tools, increasing drilling cost, or rising non-productive time. Therefore, detecting and monitoring destructive vibrations for the purpose of eliminating their effects have become important activity during drilling. However, detecting vibrations is not always applicable at the surface. For instance, forward whirl and backward whirl vibrations, which causes by drill string buckling severe WOB is difficult to detect at the surface, where the bit bounce vibration, which occurs as subsequence of the axial vibrations is generally caused by the use of RC bit can be detected at the surface [62].

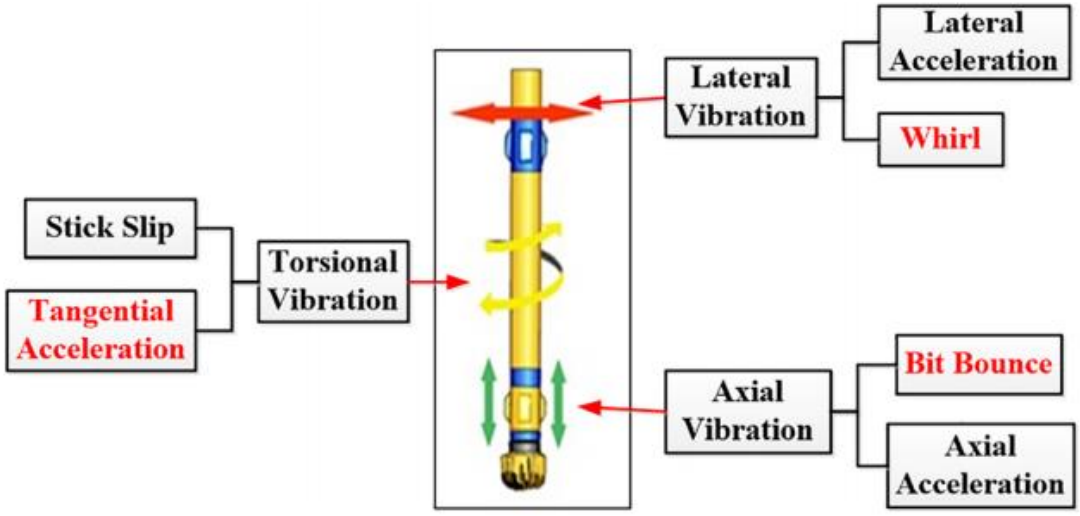

Figure 1-7. Classifications of downhole vibrations [61, 62]

1.4.3.2 Applications of Vibrations in Enhancing Drilling Performance and Increasing ROP

Conventionally, improving ROP requires increasing of the controllable input parameters WOB, rpm, torque, etc. to the optimized levels. However, such increase occurs only at the surface and then transmitted downward through the drillstring to the drill bit. Losses of the energy transmitted from the input parameters do occur before reaching the drill bit due to several reasons, among which are the drill string mechanical behavior, inclination of the well trajectory, etcetera. These encountered challenges in optimal transfer of the surface energy to the drill bit have driven oil and gas industry to consider near-the-bit technology for optimal energy transfer and drilling performance enhancement. These new techniques can be used to improve ROP involves installing special tools as part of the Bottom Hole Assembly (BHA) that utilize the parameters that are most influencing the ROP (i.e. WOB and rpm) to be increased, stabilized, or efficiently transmitted to the drill bit. Some of these applications are the utilization of the non-dangerous vibrations, which have been reported in several studies to be useful in improving downhole drilling conditions and therefore enhancing the drilling performance. de Bruijin et al. [59] reported up to 100% ROP improvement achieved through minimizing fluctuation in rpm by using a Turbodrill. Gaynor [63] reported the improvement of ROP in directional drilling using steerable straight-hole turbodrills, which provided eccentric bit rotation and controlled well deviations. Jansen et al. [64] reported a significant increase in ROP and reduction of downhole equipment failure by using an active damping system that acted as a tuned vibration damper that eliminated stick/slip and torsional drillstring vibration, the main two types of destructive vibrations. Motahhari et al. [65] reported maximizing ROP by using a Positive Displacement Motor (PDM) at the bit, whose performance data is coupled with an ROP model

to optimize drilling parameters including WOB and improving ROP. Alali et al. [66] reported ROP improvement by using Axial Oscillation Generator Tool (AGT), whose axial oscillation reduced friction, enhanced weight transfer, and improved ROP. Clausen et al. [67] reported maximizing ROP, limiting bit damage, and extending bit life by using an Axial Excitation Tool (AET) at the bit in vertical and non-vertical wells that generated downhole beneficial axial vibrations that led to ROP improvement. Gee et al. [68] reported field and mathematical simulation data that showed significant increase in ROP due to generating downhole benign vibration that enhanced weight transfer and reduced friction by using Axial Oscillation Tool (AOT) verses a Lateral Vibration Tool (LVT). Jones et al. [69] reported increasing drilling performance using a Friction Reduction Tool (FRT) that was effective in transmitting axial oscillation, reducing friction, and eliminating BHA damage, and significantly decreased the non-productive time. Wu et al. [70] reported a higher ROP and lower overall drilling cost by identifying the root cause of damaging stick / slip and axial vibrations and minimizing them to extend the life of the bit and BHA and to enhance drilling performance by applying Finite Element Analysis (FEA). Wang et al. [71] reported theoretical, laboratory and field results showing reduction of friction and improvement in ROP using a novel self-resonating oscillator. Wilson and Noynaert [72] reported ROP improvement not only due to reducing friction and enhancing weight transfer, but more importantly due to generating dynamic axial force by using an axial excitation tool (AET) in drilling non-vertical wells. Li et al. [73] and Akbari et al. [74] reported improvement in ROP by using downhole Vibration Assisted Rotary Drilling (VARD) through experimental and PFD-2D simulation, respectively. They found the excitation of controlled vibration at the bit could influence to increase ROP at a low WOB. Babatunde et al. [77] reported the influence of vibration frequencies at the bit on enhancing ROP using a

diamond drag bit. Xiao et al. [75] reported ROP improvement using an active vibration assisted drilling tool installed at the bit during laboratory coring with a diamond impregnated bit. Their experimental results showed that at any given WOB, the ROP was increased with higher amplitude of bit-rock vibration and with cutting size increased. Moreover, their spectral analysis of the Acoustic Emission (AE) indicated higher ROP with larger cutting size, higher AE energy, and lower AE frequency.

As a continuation of a series of investigations of the influence of downhole controlled and desirable axial vibrations (with various frequencies, amplitudes, compliances, etc.) performed by the Drilling Technology Laboratory at Memorial University of Newfoundland (DTL-MUN) [66, 67, 69, 75, 76, 77, 78,], DTL-MUN has been using PFC-2D to simulate drilling performance and investigate improving ROP, involving various conditions of pressure, rock properties, flow rates, vibration and non-vibration systems [67, 77, 78]. In link to the above reporting of the advantages of the non-dangerous and non-destructive vibrations in improving drilling performance, this research: (i) tested the newly developed pVARD with various configurations that generate different levels of axial oscillations using different rock types in laboratory, field, and PFC-2D simulation, (ii) investigated the reasons behind improving drilling performance using pVARD, and (iii) utilizing pVARD as compliant drilling versus non-compliant drilling in rock isotropy / anisotropy evaluation.

1.4.3.3 pVARD Tool

Implementing the pVARD tool in drilling has shown an enhancement in drilling performance. It induces useful axial oscillation that generates Downhole Dynamic Weight on Bit (DDWOB) and minimizes destructive vibrations to within the controlled and safe vibration window. A

laboratory and field prototypes were fabricated and tested to demonstrate the improvement of drilling performance by using pVARD (Figure 1-8)

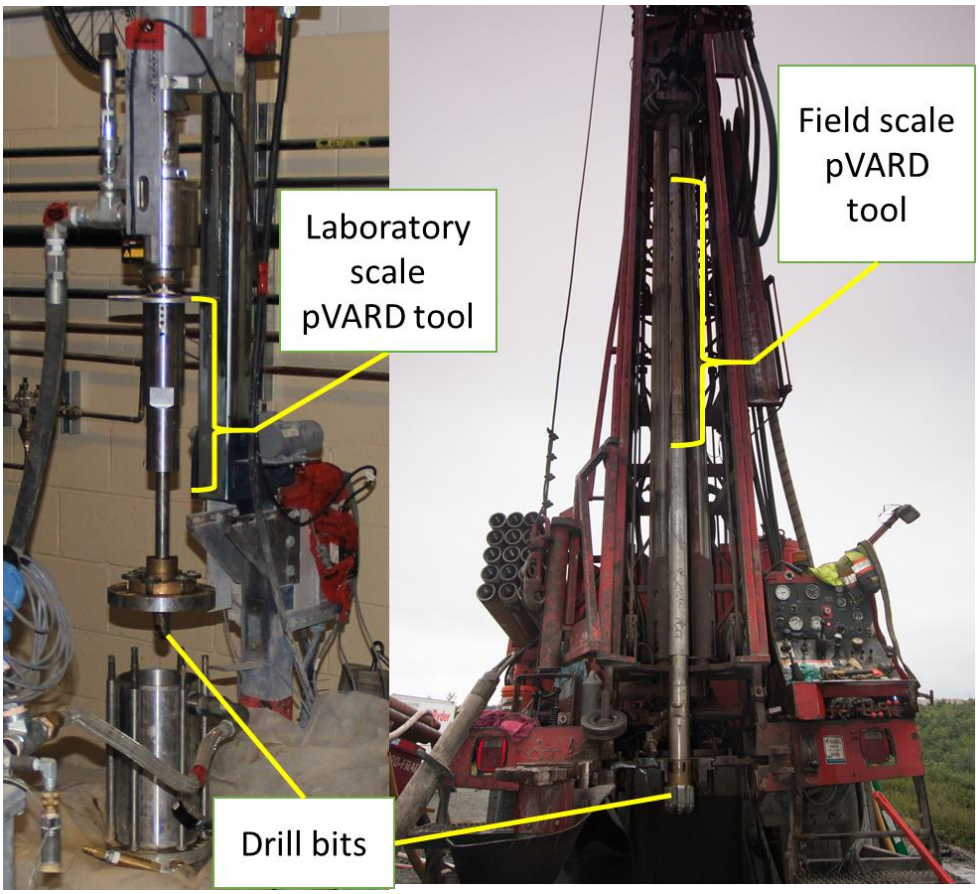

Figure 1-8. Laboratory and field scale pVARD tool. Modified after Rana et al. [77]

1.5 References

1. Brady, B. H. G., & Brown, E. T. (2007). Rock strength and deformability. In Rock Mechanics for underground mining (pp. 85-141). Springer, Dordrecht.

2. Creaney, S., & Allan, J. (1990). Hydrocarbon generation and migration in the Western Canada sedimentary basin. Geological Society, London, Special Publications, 50(1), 189-202.

3. Watts, N. L. (1987). Theoretical aspects of cap-rock and fault seals for single-and two-phase hydrocarbon columns. Marine and Petroleum Geology, 4(4), 274-307,

4. Hitchon, B., Gunter, W. D., Gentzis, T., & Bailey, R. T. (1999). Sedimentary basins and greenhouse gases: a serendipitous association. Energy Conversion and Management, 40(8), 825-843

5. Hu, L., Guo, Z., Feng, J., Yang, Z., & Fang, M. (2009). Distributions and sources of bulk organic matter and aliphatic hydrocarbons in surface sediments of the Bohai Sea, China. Marine Chemistry, 113(3-4), 197-211.

6. Littke, R., Baker, D. R., & Leythaeuser, D. (1988). Microscopic and sedimentologic evidence for the generation and migration of hydrocarbons in Toarcian source rocks of different maturities. In Organic Geochemistry In Petroleum Exploration (pp. 549-559). Pergamon.

7. Abel, M., Perrin, M., & Carbonera, J. L. (2015). Ontological analysis for information integration in geomodeling. Earth Science Informatics, 8(1), 21-36.

8. Saroglou, H., & Tsiambaos, G. (2007). Classification of anisotropic rocks. In 11th Congress of the International Society for Rock Mechanics. In: Ribeiro e Sousa, Otalla, Grossmann, editors. Taylor & Francis Group, London (p. 191).

9. Tsidzi, K. E. N. (1997). Propagation characteristics of ultrasonic waves in foliated rocks. Bulletin of the International Association of Engineering Geology, (56), 103-114.

10. Ramamurthy, T. (1993). Strength and modulus responses of anisotropic rocks. Comprehensive rock engineering, 1(13), 313-329.

11. ISRM 1981. Rock characterization, testing and monitoring, ISRM suggested methods. Pergamon Press, Oxford, U.K.

12. ISRM 1985. commission on Testing Methods. Suggested method for determining point load strength (revised version). Int. Journal Rock Mech. Min. Sci. & Geomech. Abstr, Vol. 22, pp. 51-60

13. Tsidzi, K. 1990. The influence of foliation on point load strength anisotropy of foliated rocks, Bull. Int. Association of Eng. Geology, 29: 49-58.

14. Brown, E. T., Green, S. J., & Sinha, K. P. (1981, October). The influence of rock anisotropy on hole deviation in rotary drilling—a review. In International Journal of Rock Mechanics and Mining Sciences & Geomechanics Abstracts (Vol. 18, No. 5, pp. 387-401). Pergamon.

15. McLamore, R., & Gray, K. E. (1967). The mechanical behavior of anisotropic sedimentary rocks. Journal of Engineering for Industry, 89(1), 62-73.

16. McLamore, R. T. (1971). The role of rock strength anisotropy in natural hole deviation. Journal of Petroleum Technology, 23(11), 1-313.

17. Karfakis, M. G., & Evers, J. F. (1987). Effects of Rock Lamination Anisotropy on Drilling Penetration and Deviation. International Journal of Rock Mechanics And Mining & Geomechanics Abstracts, 24(6).

18. Boualleg, R., Sellami, H., Menand, S., & Simon, C. (2006). Effect of formations anisotropy on directional tendencies of drilling systems. In IADC/SPE Drilling Conference. Society of Petroleum Engineers.

19. Ong, S. H., & Roegiers, J. C. (1993). Influence of anisotropies in borehole stability. In International Journal of Rock Mechanics and Mining Sciences & Geomechanics Abstracts (Vol. 30, No. 7, pp. 1069-1075). Pergamon.

20. Lee, H., Ong, S. H., Azeemuddin, M., & Goodman, H. (2012). A wellbore stability model for formations with anisotropic rock strengths. Journal of Petroleum Science and Engineering, 96, 109-119.

21. Dokhani, V., Yu, M., & Bloys, B. (2016). A wellbore stability model for shale formations: Accounting for strength anisotropy and fluid induced instability. Journal of Natural Gas Science and Engineering, 32, 174-184.

22. Bautmans, P., Fjær, E., & Horsrud, P. (2018). The effect of weakness patches on wellbore stability in anisotropic media. International Journal of Rock Mechanics and Mining Sciences, 104, 165-173.

23. Ong, S. H., & Roegiers, J. C. (1996). Fracture initiation from inclined wellbores in anisotropic formations. Journal of petroleum technology, 48(07), 612-619.

24. Kang, Y., Yu, M., Miska, S. Z., & Takach, N. (2009). Wellbore stability: a critical review and introduction to DEM. In SPE Annual Technical Conference and Exhibition. Society of Petroleum Engineers.

25. Kim, H., Cho, J. W., Song, I., & Min, K. B. (2012). Anisotropy of elastic moduli, P-wave velocities, and thermal conductivities of Asan Gneiss, Boryeong Shale, and Yeoncheon Schist in Korea. Engineering Geology, 147, 68-77.

26. Gu, M. (2018). Impact of Anisotropy Induced by Shale Lamination and Natural Fractures on Reservoir Development and Operational Designs. SPE Reservoir Evaluation & Engineering, 21(04), 850-862.

27. Meléndez-Martínez, J., & Schmitt, D. R. (2016). A comparative study of the anisotropic dynamic and static elastic moduli of unconventional reservoir shales: Implication for geomechanical investigations. Geophysics, 81(3), D245-D261.

28. Meléndez-Martínez, J., (2014). Elastic properties of sedimentary rocks, Edmonton, AB: University of Alberta.

29. Liao, J. J., Hu, T. B., & Chang, C. W. (1997). Determination of dynamic elastic constants of transversely isotropic rocks using a single cylindrical specimen. International Journal of Rock Mechanics and Mining Sciences, 34(7), 1045-1054.

30. Jaeger, J. C., Cook, N. G. W., & Zimmerman, R. W. (2007). Fundamentals of Rock Mechanics. 4th ed. UK: Blackwell

31. Fjaer, E., Holt, R. M., Raaen, A. M., Risnes, R., and P. Horsrud, 2008, "Petroleum Related Rock Mechanics", (53), Elsevier.

32. Chang, C., Zoback, M.D., and Khaksar, A., 2006, "Empirical Relations between Rock Strength and Physical Properties in Sedimentary Rocks", Journal of Petroleum Science and Engineering, 51(3), pp.223-237.

33. Pan, R., Zhang, G., Li, S., An, F., Xing, Y., Xu, D., and Xie, R., 2016, "Influence of Mineral Compositions of Rocks on Mechanical Properties", the 50th us rock Mechanics / Geomechanics symposium, American rock mechanics association, Houston, TX, USA, 26-29 June 2016.

34. Friedman, M., 1976, “Porosity, Permeability, and Rock Mechanics - A Review”, the 7th US Symposium on Rock Mechanics. American Rock Mechanics Association.

35. Chenevert, M. E., & Gatlin, C. (1965). Mechanical anisotropies of laminated sedimentary rocks. Society of petroleum engineers journal, 5(01), 67-77.

36. Li, H., Lai, B., Liu, H. H., Zhang, J., & Georgi, D. (2017). Experimental investigation on Brazilian tensile strength of organic-rich gas shale. SPE Journal, 22(01), 148-161.

37. Cho, J. W., Kim, H., Jeon, S., & Min, K. B. (2012). Deformation and strength anisotropy of Asan gneiss, Boryeong shale, and Yeoncheon schist. International Journal of Rock Mechanics and Mining Sciences, (50), 158-169.

38. Tien, Y. M., Kuo, M. C., & Juang, C. H. (2006). An experimental investigation of the failure mechanism of simulated transversely isotropic rocks. International journal of rock mechanics and mining sciences, 43(8), 1163-1181.

39. Ma, T., Peng, N., Zhu, Z., Zhang, Q., Yang, C., & Zhao, J. (2018). Brazilian tensile strength of anisotropic rocks: Review and new insights. Energies, 11(2), 304.

40. Steiger, R. P., & Leung, P. K. (1992). Quantitative determination of the mechanical properties of shales. SPE drilling engineering, 7(03), 181-185.

41. Park, B., & Min, K. B. (2013). Discrete element modeling of transversely isotropic rock. In 47th US Rock Mechanics/Geomechanics Symposium. American Rock Mechanics Association, held in San Francisco, CA, USA, 23-26 June.

42. Fjaer, E., Stenebraten, J. F., Holt, R. M., Bauer, A., Horsrud, P., and Nes, O. (2014) Modelling Strength Anisotropy. Rock Mechanics for Natural Resources and Infrastructure, ISRM-Specialized Conference 9-13 September, Goiania, Brazil.

43. Donath, F. A. (1961). Experimental study of shear failure in anisotropic rocks. Geological Society of America Bulletin, 72(6), 985-989.

44. Crawford, B. R., DeDontney, N. L., Alramahi, B., & Ottesen, S. (2012). Shear strength anisotropy in fine-grained rocks. In 46th US Rock Mechanics/Geomechanics Symposium. American Rock Mechanics Association, held in Chicago, IL, USA, 24-27 June.

45. Fjçr, E., & Nes, O. M. (2013). Strength anisotropy of Mancos shale. In 47th US rock mechanics/geomechanics symposium. American Rock Mechanics Association, held in San Francisco, CA, USA, 23-26 June.

46. Matzar, L. A., & Gamwell, C. G. (2013, January). Understanding Shale Failure from Laboratory Analysis to Field Operations. In 47th US Rock Mechanics/Geomechanics Symposium. American Rock Mechanics Association, held in San Francisco, CA, USA, 23-26 June.

47. Simpson, N. D. J., Stroisz, A. N. N. A., Bauer, A., Vervoort, A., & Holt, R. M. (2014, August). Failure mechanics of anisotropic shale during Brazilian tests. In 48th US Rock Mechanics/Geomechanics Symposium. American Rock Mechanics Association, held in Minneapolis, MN, USA, 1-4 June.

48. Ambrose, J., Zimmerman, R. W., & Suarez-Rivera, R. (2014, August). Failure of shales under triaxial compressive stress. In 48th US Rock Mechanics/Geomechanics Symposium. American Rock Mechanics Association, held in Minneapolis, MN, USA, 1-4 June.

49. Bourgoyne Jr, A. T., Millheim, K. K., Chenevert, M. E., & Young Jr, F. S. (1991). Applied drilling engineering, TX, Society of Petroleum Engineers.

50. Maurer, W. C. (1962). The" perfect-cleaning" theory of rotary drilling. Journal of Petroleum Technology, 14(11), 1-270.

51. Lummus, J. L. (1970). Drilling optimization. Journal of Petroleum Technology, 22(11), 1-379.

52. Zhang, J. (2013). Borehole stability analysis accounting for anisotropies in drilling to weak bedding planes. International journal of rock mechanics and mining sciences, 60, 160-170.

53. Thuro, K., & Spaun, G. (1996, January). Introducing the'destruction work'as a new rock property of toughness referring to drillability in conventional drill-and blast tunnelling. In ISRM International Symposium-EUROCK 96. International Society for Rock Mechanics and Rock Engineering

54. Teale, R. (1965, March). The concept of specific energy in rock drilling. In International journal of rock mechanics and mining sciences & geomechanics abstracts (Vol. 2, No. 1, pp. 57-73). Pergamon.

55. Hegde, C., Daigle, H., Millwater, H., & Gray, K. (2017). Analysis of rate of penetration (ROP) prediction in drilling using physics-based and data-driven models. Journal of Petroleum Science and Engineering, 159, pp. 295-306.

56. Pessier, R. C., Wallace, S. N., & Oueslati, H. (2012). Drilling performance is a function of power at the bit and drilling efficiency. In IADC/SPE Drilling Conference and Exhibition. Society of Petroleum Engineers. San Diego, California, USA. Paper No. SPE-151389-MS

57. Dupriest, F. E., & Koederitz, W. L. (2005). Maximizing drill rates with real-time surveillance of mechanical specific energy. In SPE/IADC Drilling Conference. Society of Petroleum Engineers. Amsterdam, Netherlands. Paper No. SPE/ IADC 92194.

58. Bourdon, J. C., Cooper, G. A., Curry, D. A., McCann, D., & Peltler, B. (1989). Comparison of field and laboratory-simulated drill-off tests. SPE drilling engineering, 4(04), pp. 329-334.

59. de Bruijn, H. J., Kemp, A. J., & Van Dongen, J. C. M. (1986). Use of MWD for Turbodrill Performance Optimization as a Means To Improve ROP. SPE Drilling Engineering, 1(04), PP. 309-314.

60. Mensa-Wilmot, G., Langdon, S. P., & Harjadi, Y. (2010, January). Drilling Efficiency and Rate of Penetration: Definitions, Influencing Factors, Relationships, and Value. In IADC/SPE Drilling Conference and Exhibition. Society of Petroleum Engineers.

61. Ren, Y., Wang, N., Jiang, J., Zhu, J., Song, G., & Chen, X. (2019). The Application of Downhole Vibration Factor in Drilling Tool Reliability Big Data Analytics—A Review. ASCE-ASME Journal of Risk and Uncertainty in Engineering Systems, Part B: Mechanical Engineering, 5(1), 010801.

62. Zhan, S., Ahmad, I., Heuermann-Kuehn, L. E., & Baumann, J. (2010). Integrated PoF and CBM strategies for improving electronics reliability performance of downhole MWD and LWD tools. In SPE Annual Technical Conference and Exhibition. Society of Petroleum Engineers.

63. Gaynor, T. M. (1988). Downhole control of deviation with steerable straight-hole turbodrills. SPE drilling engineering, 3(01), pp. 50-56.

64. Jansen, J. D., van den Steen, L., & Zachariasen, E. (1995). Active damping of torsional drillstring vibrations with a hydraulic top drive. SPE Drilling & Completion, 10(04), pp. 250-254.

65. Motahhari, H. R., Hareland, G., Nygaard, R., & Bond, B. (2009). Method of Optimizing Motor and Bit Performance for Maximum ROP. Journal of Canadian Petroleum Technology, 48(6), pp. 44-49

66. Alali, A., & Barton, S. P. (2011, January). Unique axial oscillation tool enhances performance of directional tools in extended reach applications. In Brasil Offshore. Society of Petroleum Engineers. Macaé, Brazil. Paper No, SPE-143216-MS.

67. Clausen, J. R., Schen, A. E., Forster, I., Prill, J., & Gee, R. (2014, March). Drilling with induced vibrations improves ROP and mitigates stick/slip in vertical and directional wells. In IADC/SPE Drilling Conference and Exhibition. Society of Petroleum Engineers. Paper No. IADC/SPE 168034.

68. Gee, R., Hanley, C., Hussain, R., Canuel, L., & Martinez, J. (2015, March). Axial Oscillation Tools vs. Lateral Vibration Tools for Friction Reduction–What's the Best Way to Shake the Pipe?. In SPE/IADC Drilling Conference and Exhibition. Society of Petroleum Engineers. London, England, UK. Paper No. SPE-173024-MS.

69. Jones, S., Feddema, C., Sugiura, J., & Lightey, J. (2016, March). A New Friction Reduction Tool with Axial Oscillation Increases Drilling Performance: Field-Testing with Multiple Vibration Sensors in One Drill String. In IADC/SPE Drilling Conference and Exhibition. Society of Petroleum Engineers. Fort Worth, Texas, USA. Paper No. SPE-178792-MS.

70. Wu, X., Karuppiah, V., Nagaraj, M., Partin, U. T., Machado, M., Franco, M., & Duvvuru, H. K. (2012, January). Identifying the root cause of drilling vibration and stick-slip enables fit-for-purpose solutions. In IADC/SPE Drilling Conference and Exhibition. Society of Petroleum Engineers. San Diego, California, USA. Paper No. SPE-151347-MS

71. Wang, P., Ni, H., & Wang, R. (2018). A novel vibration drilling tool used for reducing friction and improve the penetration rate of petroleum drilling. Journal of Petroleum Science and Engineering, 165, pp. 436-443.

72. Wilson, J. K., & Noynaert, S. F. (2017, March). Inducing Axial Vibrations in Unconventional Wells: New Insights through Comprehensive Modeling. In SPE/IADC Drilling Conference and Exhibition. Society of Petroleum Engineers.

73. Li, H., Butt, S., Munaswamy, K., & Arvani, F. (2010, January). Experimental investigation of bit vibration on rotary drilling penetration rate. In 44th US Rock Mechanics Symposium and 5th US-Canada Rock Mechanics Symposium. American Rock Mechanics Association. Paper No. ARMA 10-426

74. Akbari, B., Butt, S. D., Munaswamy, K., & Arvani, F. (2011, January). Dynamic single PDC cutter rock drilling modeling and simulations focusing on rate of penetration using distinct element method. In 45th US Rock Mechanics/Geomechanics Symposium. American Rock Mechanics Association. San Francisco, California. Paper No. ARMA-11-379.

75. Xiao, Y., Hurich, C., Molgaard, J., & Butt, S. D. (2018). Investigation of active vibration drilling using acoustic emission and cutting size analysis. Journal of Rock Mechanics and Geotechnical Engineering, 10(2), pp. 390-401.

76. Rana, P. S., Abugharara, A. N., Butt, S. D., and Molgaard, J., 2015, "Experimental and Field Application of Passive-Vibration Assisted Rotary Drilling (pVARD) Tool to Enhance Drilling Performance, " Proc. 49th US Rock Mechanics/Geomechanics Symposium, San Francisco, CA.

77. Babatunde, Y., Butt, S., Molgaard, J., & Arvani, F. (2011, January). Investigation of the effects of vibration frequency on rotary drilling penetration rate using diamond drag bit. In 45th

US rock mechanics/geomechanics symposium. American Rock Mechanics Association. San Francisco, California. Paper No. ARMA-11-527.

78. Zhang, J., Yang, J., & Butt, S. (2016, April). DEM simulation of enhancing drilling penetration using vibration and experimental validation. In Proceedings of the 49th Annual Simulation Symposium (p. 12). Society for Computer Simulation International.

CHAPTER 2: RESEARCH METHODOLOGY

2.1 Introduction

This chapter contains methodology, test setup and apparatus, materials and sample preparation techniques, and test procedure for research experiments and tests. The research procedure via oriented physical, mechanical and drilling measurements on two main stages is summarized in a detailed flow chart (Figure 2-1).

Flow Chart:

A laboratory Procedure of an Oriented Physical, Mechanical, and Drilling Study Evaluating the Oriented Drilling Performance in Isotropic and Anisotropic (VTI shale) rocks

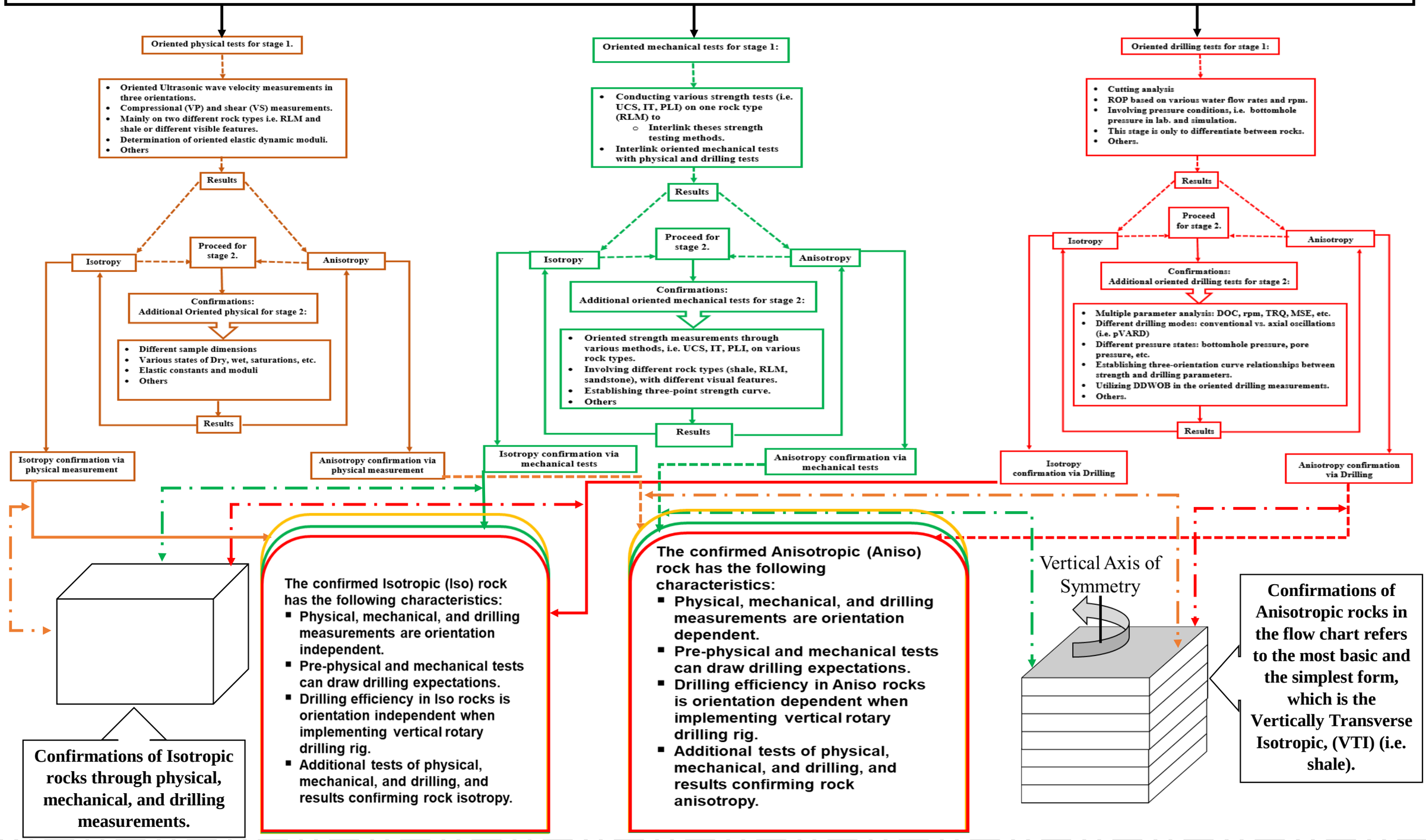

Figure 2-1. Summarized of two-stage research procedure via oriented physical, mechanical and drilling measurements evaluating isotropy / anisotropy of rocks

2.2 Fundamental Baseline Development for Rock Anisotropy Characterization

2.2.1 Methodology

This research involved several laboratory experiments to investigate the anisotropy of rock like materials (RLM) through measuring ultrasonic wave velocities, strength, and drilling performance as a function of WOB and flow rate. These were conducted in three main orientations: vertical, diagonal "oblique", and horizontal and consisted of several stages: (i) sample preparation, (ii) initial anisotropy determination though oriented ultrasonic wave velocity measurement on standard NQ cores samples, (iii) determination of oriented strength anisotropy, and (iv) evaluating oriented drilling performance as a function of WOB and three sets of flow rate.

2.2.2 Rock like material "synthetic rocks"

RLM is made of fine aggregate, Portland cement, and water. This synthetic rock product was the source for all RLM samples tested in all projects. According to research conducted by a Zhen Zhang a graduate student at Drilling Technology Laboratory (DTL), various rations of these three components lead to various strengths. This research was the first to investigate the anisotropy of medium strength RLM.

2.2.3 Ultrasonic method

Compressional "primary" and shear "secondary" wave velocities were measured in three main directions on NQ core samples and cubical samples using a high frequency ultrasonic method.

Some of the elastic moduli measured in the three directions include compressional wave modulus, shear wave modulus, elastic modulus, Lame' constant, bulk modulus, and Poisson's ratio. This test was conducted in accordance with ASTM standards.

2.2.4 Strength tests

In this research, tests were conducted to determine the strength of RLM in three orientations. Tests include (i) standard unconfined compressive strength (UCS) test using a commercial loading frame (i.e. Instron load frame), whose axial loading capability is more than 250 KN, (ii) axial and block point load index (PLI) tests using point load apparatus with the conical-end pistons, and (iii) indirect tensile (Brazilian tensile) strength test using a modified loading frame number ALPHA 3-3000 SD for splitting tensile strength test.

2.2.5 Drilling performance

Drilling was performed using fully instrumented non-compliant small drilling simulator with a dual cutter PDC bit for this project as well as for all projects of the research of this thesis. For this project, mainly RLM samples were drilled in three orientations, the same orientations indicated in all other tests: vertical or perpendicular, oblique or diagonal, and horizontal or parallel in case of rocks with bedding. Then the drilling rate of penetrations (ROP) as a function of five sets of static WOB and three sets of clean water flow rates was calculated from the recorded and stored data by the DAQ system that utilized LabVIEW software. Also, initial oriented drilling performance was investigated through oriented drilling in shale and RLM with similar drilling conditions of static WOB and mono-flow for preparatory step to the next research project.

2.2.6 Test procedure

For ultrasonic method: the ultrasonic technique was the method used for measuring VP and VS and was practiced for all projects of this thesis. For this project, compressional and shear wave velocity were measured from standard NQ core samples and block samples by using a TDS 1002B Two Channel Digital Storage Oscilloscope, Square Wave Pulser/Receiver Model 5077PR, and two panametrics shear-wave sensors. Shear wave couplant MOLYKOTE® was to ensure complete contact between sensors and rock samples. Recorded data is stored and later processed for VP and VS determination. Mean values of VP and VS and density together were used for calculating the oriented elastic moduli including compressional wave modulus (M), shear wave modulus (G), elastic modulus (E), Lame's constant (λ) bulk modulus (K), and Poisson's ratio (υ).

For strength tests: in accordance with ASTM Standards D7012-2014 for the unconfined compressive strength (UCS), D5731-2008 for the axial and block point load index (PLI), and D6931-2012 for the indirect tensile (IT), the oriented strength for RLM samples was determined.

For drilling performance: The small drilling simulator was the main laboratory drilling rig used for all drilling experiments conducted for all projects in this thesis. For this project, for each orientation, several RLM samples were drilled using the dual-cutter PDC bit for five depth intervals applying five different static WOBs, from low to high for each depth interval. This practice was repeated using three sets of clean water flow rates at 300 rpm.

2.3 Study of Rock Anisotropy with Emphasis on Circular Wave Velocities and Elastic Moduli

2.3.1 Methodology

This research investigates the isotropy of RLM. These rocks were tested in Sec. 2.1 in only three orientations, but here are tested by (i) applying more circular wave measurement, instead of only three directions, (ii) including another natural rock of fine-grained granite to examine the baseline procedure developed in Sec. 2.1, (iii) involving various drilling parameters as another step for rock isotropy / anisotropy evaluation through oriented coring tests.

2.3.2 Strength tests

Strength was measured for RLM samples (the same RLM source used for all projects of this thesis) using a modified point load apparatus by replacing the cone-end pistons by flat-end pistons for compressive strength determination. Samples of these tests were produced through a newly developed technique that categorized samples with respect to orientations (Figure 2-2).

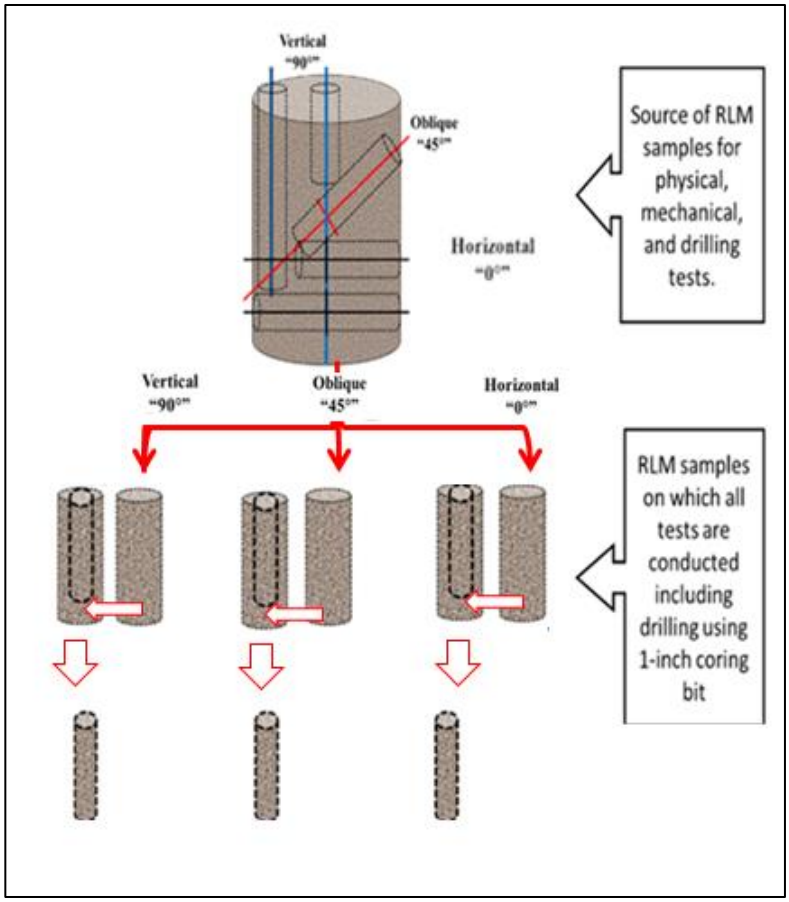

Figure 2-2. Developed procedure for producing RLM samples in three directions

2.3.3 Drilling performance

The small drilling simulator was used for this experiment using impregnated diamond coring bit. Coring in three orientations was practiced in RLM and green shale samples. The green shale samples were collected from the same query of the red shale (this query was the source of all green, grey and red shales that were encountered in drilling during the field trails prior to the start of this research). At the beginning, each shale type was investigated separately. However, after conducting X-ray diffraction analysis, it was found that red shale and green shale are of the same origin and have the same mechanical and physical properties, where the

grey shale (mainly tested in the field trails) was of a completely different shale than red and green shales. Therefore, subsequent research considered only “shale” without referring to its color.

2.4 Study of Rock Anisotropy with Emphasis on Conventional Drilling Performance and Cutting Analysis

2.4.1 Methodology

This project investigates mainly the isotropy / anisotropy of shale (referred to as red shale, as this project was conducted before performing X-ray diffraction analysis) through ultrasonic method, oriented drilling, and cutting size analysis. The purpose of the investigation was to (i) confirm shale vertically transverse isotropy (VTI) and (ii) evaluate shale oriented drilling performance with comparison to isotropic rocks’ drilling performance (Sec. 2.2. and Sec. 2.3.) and the associated shale cutting size analysis as a function of WOB and orientation. As shale oriented drilling of this project was the first of its kind of all projects of this thesis, the main purpose of the oriented drilling was only to investigate the contribution of VTI experiments (drilling performance and particle size analysis) to the study of isotropy / anisotropy evaluation (Sec. 2.2.). Therefore, there was no attention paid to installing drill string wonder prevention tools. The conclusion drawn from these drilling experiments and cutting size analysis was that VTI rocks provide different results as a function of orientation from that of RLM. However, it was the launching point for the subsequent projects.

2.4.2 Strength tests

The indirect tensile (IT) strength test applied on disks was another strength test added to this project. The IT test was performed using the modified point load apparatus with flat-end pistons. Disk samples were cut from cores produced from three orientations and there was no particular sub-orientation determined before loading to split. The only three indicated orientations were the orientations of cores, from which the disks were cut: vertical, oblique, and horizontal. The purpose of this oriented strength test was to support the strength tests involved in the baseline procedure indicated in Sec. 2.2.

2.4.3 Test procedure

For ultrasonic measurement: ASTM D2845-08 was followed for measuring VP, VS, and Elastic moduli for all RLM samples (these samples were the source for IT strength tests as well as drilling experiments).

For shale samples, first, VTI evaluation was determined through multiple position VP and VS measurement (Figure 2-3) performed on three shale block samples cut from the main shale rocks prepared for strength tests and drilling experiments of this project. Then, as a newly developed practice for oriented VP and VS measurement obtained from the same sample, the hexagon shale samples were produced (Figure 12).

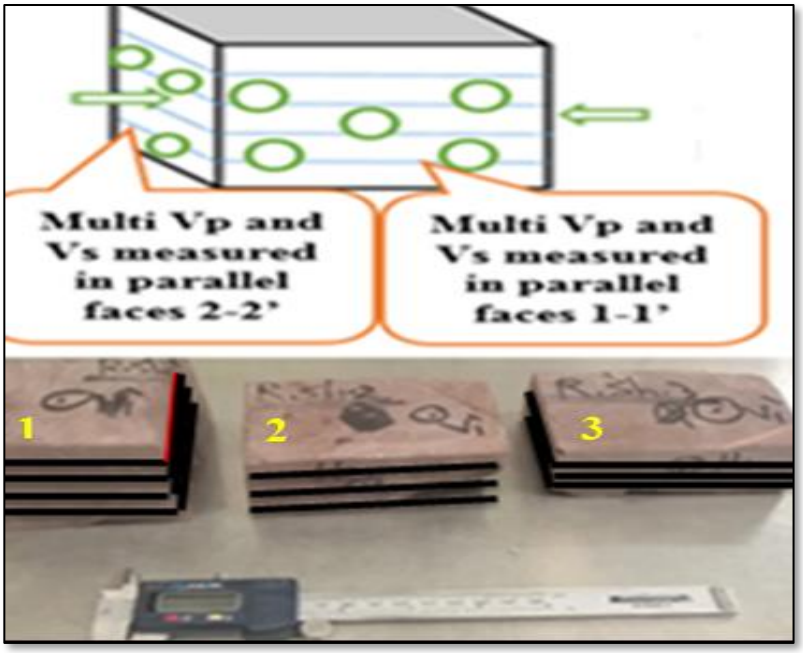

Figure 2-3. Repeated measurements of VP and VS parallel to shale bedding for shale VTI confirmation

Figure 2-4. Cube shape technique for VP and VS measurement
from the same hexagon shale samples

The mean values of oriented wave velocities, densities, and elastic moduli for both RLM and shale are summarized in Table 2.1and Table 2.2, respectively.

Table 2.1. Mean values of oriented wave velocities, densities, and elastic moduli for RLM

Table 2.2. Mean values of oriented wave velocities and density of shale

Orientation	Measurement								
	VP km/sec	VS km/sec	D g/cc	M GPa	G GPa	ν	K GPa	E MPa	λ GPa
0°	4.6	2.8	2.6	53.5	19.8	0.2	27.1	51.6	13.9
45°	4.8	2.9	2.3	52.6	20.1	0.2	25.8	53.9	12.4
90°	4.6	2.8	2.4	49.9	18.7	0.2	25.0	50.9	12.6

Rock Type	Orientation	Measurement		
Sample-1	0° (parallel)	4.9	3.2	2.7
	45° (oblique)	3.5	2.5	
	90° (Perpendicular)	1.9	1.1	
Sample-2	0° (parallel)	5.0	3.2	2.8
	45° (oblique)	3.5	2.5	
	90° (Perpendicular)	1.5	0.9	

For strength measurement: ASTM D3967-08 was followed in performing the IT test and determining RLM oriented strength through the following steps:

- Placing every disk between flat-end pistons
- Start loading the frame while recording the increase of pressure in the pressure gauge until failure
- Using equation 1 in calculating RLM oriented IT strength

$$\sigma t = 2P/\pi LD \quad (1)$$

- For shale strength, ASTM 5731-08 was followed to estimate shale strength only perpendicular to shale bedding through irregular lump test

For drilling experiment: The small drilling simulator was used for drilling RLM and shale samples in three orientations using a PDC bit and a constant water flow rate. Drilling experiments were performed under atmospheric pressure using conventional drill string (without involving external oscillation generating tools). Drained water with drilling cutting were directed to pass through the cutting collecting system. Five different static WOB were applied between the lowest: WOB = 75 kg and the highest: WOB = 209 kg. Table 7 summarizes input parameters for RLM and shale oriented drilling.

Table 2.3. Input parameters for RLM and shale oriented drilling

Parameter	Value				
Static WOB (kg)	75	108.6	142.2	175.9	209.5
rpm	300				
Flow rate (l/min.)	18				

For particle size analysis: ASTM C136/C136M-2014 was followed for sieving analysis procedure. The process of the cutting size analysis was performed through the following steps:

- A cutting collection system was fabricated and connected to the drilling rig.
- At the end of each drilling using one static WOB, cutting was collected separately and labeled with WOB, drilling run number, and rock type.
- After completing the drilling experiments, cuttings were oven dried.
- A commercial sieving shaker (i.e. octagon digital 2000 sieve shaker) was used for particle size analysis.
- Different size sieves were used: 0.85, 0.63, 0.59, 0.42, 0.25, 0.212, 0.177, 0.166, 0.15, 0.19, and 0.075 mm.

2.5 Study of the Influence of Anisotropy Orientation on Main Drilling Parameters

2.5.1 Methodology

This project (i) establishes shale three-point oriented strength anisotropy to be used as a one factor relationship with drilling parameters and (ii) investigates the influence of shale anisotropy on main drilling parameters including rate of penetration (ROP), rpm, depth of cut (DOC), and torque (TRQ) as a function of WOB using the conventional small drilling simulator. The novelty of this work is that it establishes the three-point strength anisotropy curve and then constructs relationships between this curve and the main drilling parameters.

2.5.2 Ultrasonic wave measurement

A new method of measuring VP and VS from one sample to ensure the real representation of shale was to conduct a circular measurement with small increments. Then, show the procedure of obtaining the sample preparation as well as the circular VP and VS as described in the following steps:

- Due to the sensitivity of obtaining shale cores in various orientations, coring parallel to shale bedding was a success.
    - Shale blocks were confined with cement.
    - When cement hardened, coring samples were obtained parallel to shale bedding
- Samples cored parallel to shale bedding enabled performing the circular measurement on one sample for more rock property representation (Figure 2-5).

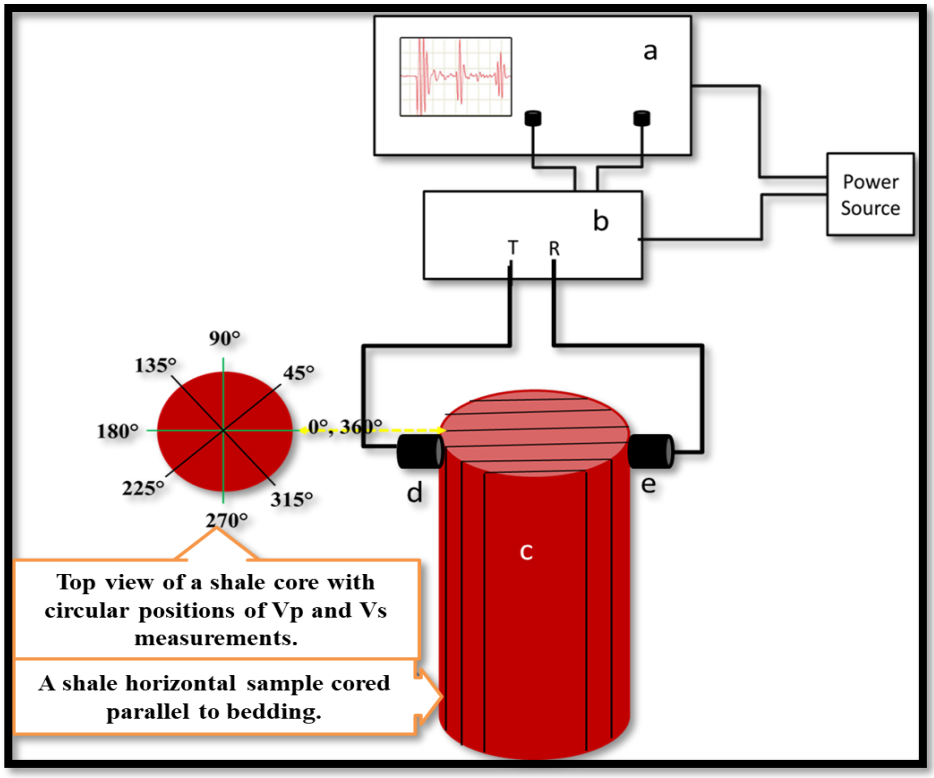

Figure 2-5. One shale sample cored parallel to bedding for more circular wave velocity measurement

2.5.3 Strength tests

Intensive strength measurement for RLM was performed using three testing methods of UCS, PLI and IT: (i) to determine RLM oriented strength, (ii) to establish a relationship between three-point strength isotropy / anisotropy for RLM with the main drilling parameters, (iii) to compare these using shale, and (iv) to establish a single factor strength drilling parameter relationship. For shale, the strength anisotropy curve depends on data collected from literature, however, shale-strength-anisotropy curve was plotted with drilling parameters of this research.

2.5.4 Drilling performance

The small drilling simulator was used for the drilling experiments using a PDC bit, a constant flow rate and a 300 rpm for drilling RLM and shale samples in three orientations were utilized. The drilling parameters involved in the analysis were ROP, DOC, rpm, and TRQ. All parameters (i) were analyzed as function to static WOB and (ii) were compared to three-point strength anisotropy curve (Figure 2-6).

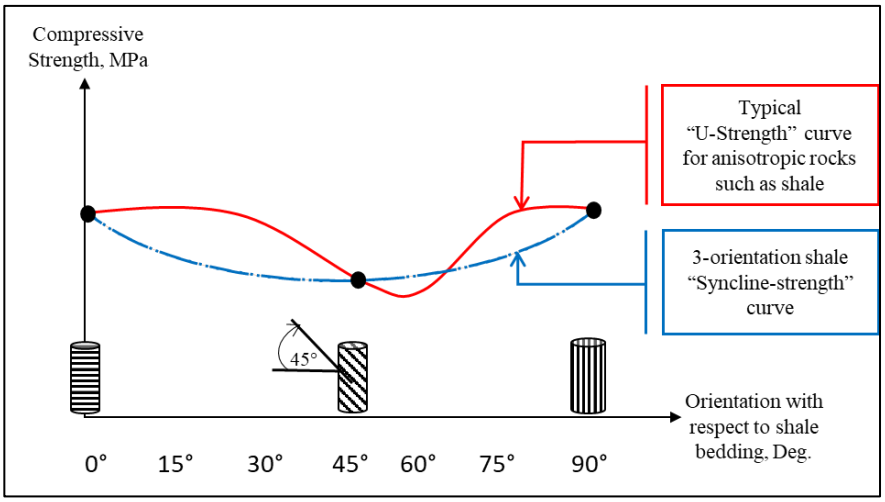

Figure 2-6. Three-point "orientations" strength anisotropy curve

2.6 Study of the Enhancement of ROP Using pVARD

2.6.1 Methodology

This project explored improving the drilling performance through increasing the drilling rate of penetration (ROP) by using the passive vibration assisted rotary pVARD tool in the laboratory and in the field. pVARD was designed to induce controllable axial oscillations that could increase ROP. pVARD was designed to have three different compliant configurations

that generate various magnitudes of the axial oscillations. The experiments of this project were conducted on mono-orientation RLM samples using PDC bit and involving various levels of water flow rates. The experiments also involved the drilling pressure environment and drilling system configuration that were summarized in Table 2.4.

Table 2.4. Drilling pressure environments and drilling system configurations

Rock type	Pressure	Temperature	drilling system
RLM	atmospheric	Room temperature	Rigid*
	pressurized		pVARD-low compliance (stiff)
			pVARD-medium compliance (medium stiff)
			pVARD-high compliance (soft)

* Without induced axial oscillations

2.6.2 Test procedure

The small drilling simulator was used for the drilling experiments using pVARD vs. rigid. A medium strength RLM was selected to be drilled in the laboratory using the laboratory scale pVARD vs. rigid in both atmospheric and pressurized conditions through the following steps:

- RLM cylinders (4 inch diameter * 6 inch long) were placed into the drilling pressure cell.

- Applying a pre-determined water flow rate (selected from several flow rates can be provided by the water pump) to provide optimal cleaning and cutting removal for best drilling performance as a function of flow rate (Figure 2-7).
- When the drilling was conducted under pressurized conditions, a back pressure was applied (the back pressure was applied by chocking the valve installed on the outlet flow line to apply back-pressure inside the drilling cell, where the rock sample was placed, that represented the bottomhole pressure and its value was determined by a pressure gauge installed between the drilling cell and the chocking valve).
- When the drilling was conducted under atmospheric pressure, then no back pressure was applied, and the chock valve was fully open.
- The required static WOB to establish a drilling performance curve was applied (Figure 2-7).
- Drilling process through drill-off-test (DOT) can be conditioned either by time or by depth intervals; a 1.5 cm of depth interval was the drilling depth for each drilling interval for this project.
- The variable parameters were WOBs, water flow rates, bottomhole pressure, and the drilling system of pVARD and rigid.
- Similar drilling experiments were conducted in a field trial using field scale pVARD (Appendix 2).
- The Particle Code Flow 2-Dimensssion (PFC-2D) simulation tool was utilized to simulate the laboratory experiments.

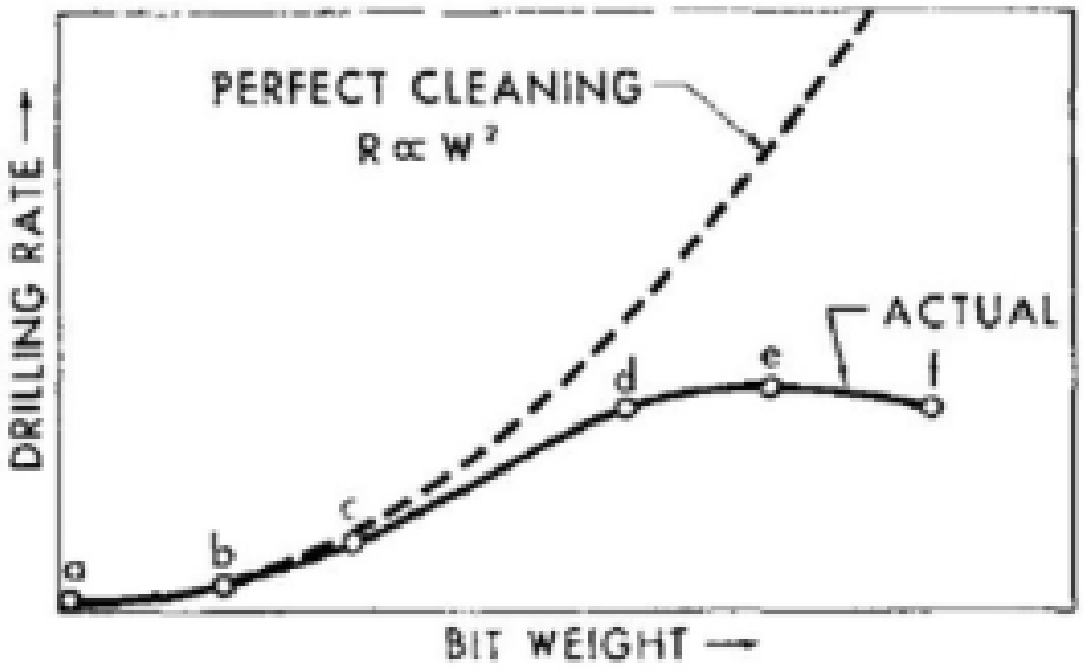

Figure 2-7. Perfect cleaning theory of rotary drilling [Maurer 1962]

2.6.3 Drilling performance

Drilling performance was analyzed based on Maurer curve (Figure *2-7*). The criterion was to select the highest ROP as a function of several associate parameters of (i) flow rate, (ii) drilling system of pVARD and rigid, and (iii) bottomhole pressure. The results show the positive influence of pVARD on drilling performance against rigid drilling.

2.7 Study of the potential pVARD parameters that Enhance ROP

2.7.1 Methodology

This project investigated the parameters of pVARD, as a complaint drilling, that result in enhancing the drilling performance against rigid, as non-compliant drilling. The experiments of this project involved drilling with the consideration of a downhole dynamic weight on bit (DDWOB) as a new parameter for shale drilling and coring.

2.7.2 Test procedure

The small drilling simulator was used for the drilling experiments as in the previous project, but with the inclusion of a load cell. The load cell, which was fixed beneath the sample holder, was used to record the DDWOB while drilling. The DDWOB recorded by the load cell was analyzed as a function of the applied static WOB, the drilled rock type, drilling system type, and pVARD configurations. Several WOBs were applied at each drilling system and pVARD configuration. The drilling experiments were conducted on shale samples that were determined to be VTI rocks in the previous projects. The drilling system type, pVARD configurations, flow rates, shale sample orientations, bit types are described as follows:

- Drilling experiments were conducted using rigid drilling and rigid coring against medium compliant pVARD configuration (this pVARD configuration was selected based on the results of the previous projects conducted on shale that showed that all pVARD configurations perform better than the rigid drilling and in several cases the medium pVARD configuration performed the best of all).

- The water flow rate was 7 liter per minute. This flow rate was kept constant for all drilling and coring experiments and was checked periodically after several runs to ensure it was constant.
- Shale samples were prepared either as cores, cored parallel to shale bedding, or as block confined with cement, to be drilled parallel to shale bedding for all experiments.
- Each drilling and coring tests were repeated several times under the same conditions for the purpose of providing sufficient data for this type of experiment of using the DDWOB as the first time of all thesis' projects.
- A PDC bit and impregnated diamond coring bits were used for shale drilling and coring, respectively.

2.8 Study of a Comprehensive Laboratory Procedure Evaluating Rock Anisotropy Using Fine-grained Sandstone Formation

2.8.1 Methodology

This project investigated rock anisotropy by following the baseline procedure developed (Sec. 2.2). This project was intended to be a comprehensive procedure based on the following points:

- This project used a single block of the same material: natural fine-grained sandstone as a source for samples for all tests.
- Samples were cored in three main orientations including vertical, oblique, and horizontal.
- This project involved all types of strength tests including UCS, PLI, and IT.
- More sub-orientations were included in IT tests with the addition to the main orientations.
- The IT fracture patterns, as a resultant of the sub-orientations, were monitored and analyzed.
- The oriented correlations between IT and PLI with UCS were involved in the analysis to support the procedure for rock isotropy / anisotropy evaluation.
- Drilling experiments of this project involved the two types of drilling systems, which included rigid and pVARD in drilling the same samples (each sample was drilled by rigid and pVARD).
- Drilling parameters were analyzed as a function of DDWOB and were used for rock isotropy / anisotropy evaluation.

2.8.2 Ultrasonic method

Mainly, circular VP and VS were measured from the oriented samples using the ultrasonic method. Preparation of sensors' locations for appropriate positioning around the samples were set by the technical service division at Memorial university of Newfoundland using advanced equipment to ensure a complete contact between sensors and rock surface and precise increments.

2.8.3 Strength tests

The point load apparatus was used for determining the oriented strength for all samples and through all tests: UCS, PLI, and IT. The apparatus was modified for the UCS and IT by replacing the cone-end pistons with flat-end pistons. The oriented strength values are correlated between UCS and PLI, as well as between UCS and IT as the first time for the purpose of rock isotropy / anisotropy evaluation.

2.8.4 Drilling performance

Drilling performance was analyzed as a function of DDWOB and orientation. Three static WOBs: low, medium, and high static WOBs were applied for all drilling experiments using rigid and pVARD systems. Drilling at each set of static WOB was repeated several times and then averaged for the final comparison between the two drilling systems in the three orientations, but as a function of the recorded DDWOB.

CHAPTER 3: BASELINE DEVELOPMENT OF ROCK ANISOTROPY INVESTIGATION UTILIZING EMPIRICAL RELATIONSHIPS BETWEEN ORIENTED PHYSICAL AND MECHANICAL MEASUREMENTS AND DRILLING PERFORMANCE

Abdelsalam N. Abugharara [a], PhD candidate

Abourawi M. Alwaar [a], Graduate Student

Charles A. Hurich [b], Associate Professor

Stephen D. Butt [a], Professor

[a] Drilling Technology Laboratory, Memorial University of Newfoundland, St. John's, NL, Canada A1B 3X5

[b] Department of Earth Sciences, Memorial University of Newfoundland, St. John's, NL, Canada A1B 3X5

This chapter is based on the objectives defined in section 1.3.1 and was presented at the ASME 2017 the 35th International conference on Ocean, Offshore and Arctic Engineering (OMAE-2016) held in Busan, South Korea, 19-24 June 2016.

3.1 Co-authorship Statement

The contributions of this collaborative work are described in the following six parts. 1) Identification of research topic is collaborative between all co-authors. 2) Design of

experiments are contributed by Abdelsalam Abugharara and the main supervisor Dr. S.D.Butt. 3) Preparation of cores and construction of ultrasonic and mechanical measurements are solely contributed by Abdelsalam Abugharara. 4) Performance of drilling experiments are cooperated by Abdelsalam Abugharara and Abourawi Alwaar, 5) Data analysis and discussion of results is a collaborative work contributed by all co-authors, 6) Manuscript preparation is mainly contributed by Abdelsalam Abugharara, with revision assistance provided by all other coauthors.

3.2 Abstract

This paper describes a baseline investigation to confirm the isotropy of rocks material through physical and mechanical measurements followed by oriented drilling. This baseline is intended to evaluate drilling experiments in anisotropic rock materials to determine the significance of the anisotropy on drilling performance. The conducted tests include oriented measurements of compressional and shear wave velocities (Vp and Vs, respectively), density, Elastic Moduli, Point Load Strength Index (PLI), Indirect Tensile (IT) strength, and Unconfined Compressive Strength (UCS). The oriented laboratory drilling experiments were conducted under various pump flow rates and several weights on bit (WOB). In this work, an isotropic rock like material (RLM) was developed using Portland cement and fine-grained aggregate. The tested RLM specimens were of medium strength of ~50 MPa. The RLM samples were cored in different orientations and then, tested and drilled according to these orientations. (e.g. 0°, 45° and 90°, representing horizontal, diagonal and vertical directions, respectively). Two main sets of lab tests were performed including pre-drilling and drilling tests. For the pre-drilling lab experiments, two main sets of tests were conducted to determine the physical and mechanical properties of samples (as outlined above) including PLI, IT, UCS, Vp, Vs, density and

corresponding isotropic Dynamic Elastic Moduli. For the drilling tests, a vertical lab scale drilling rig was used with a 35 mm dual-cutter Polycrystalline Diamond Compact “PDC” bit. The drilling parameters involved were flow rates, nominal rotary speed of 300 rpm, and various WOB under atmospheric pressure. The relationships between the drilling data were analyzed including drilling rate of penetration (ROP), depth of cut (DOC), and corresponding effective WOB. The results of all mechanical, physical and drilling measurements and tests show consistent values indicating the isotropy of the tested rock material. This consistency verifies that the drilling tests are free of bias associated with drilling orientation.

3.3 Introduction

Rocks can be characterized as isotropic, where material properties are independent of orientation, or anisotropic, where they are not. Special cases of rock anisotropy include Vertical Transverse Isotropic (VTI) or Horizontal Transverse Isotropic (HTI), where the properties are uniform in either the vertical or horizontal plane, respectively, and different in the perpendicular direction. Anisotropy is an important character of rocks in oil and gas drilling operations, and it is known that anisotropy of the formation drilled in deviated, extended reach and horizontal wells can impact the rate of penetration (ROP), contribute to borehole deviation and wander from the intended well trajectory, cause well bore instability. This is being investigated further in a parallel study to the one outlined in this paper and will be reported in future publications. However, to determine the influence of material anisotropy on drilling penetration, a baseline investigation of drilling penetration in an isotropic material was needed first. The proposed isotropic material is RLM composed of Portland cement and millimeter sized aggregate (essentially a fine-grained concrete) and which an Unconfined Compressive Strength (UCS) of ~ 50 MPa. This paper describes the characterization of the RLM to confirm its isotropic material

properties and oriented drilling experiments. The conducted experiments include physical measurements, mechanical measurements, and drilling tests. For the physical measurements, Vp and Vs are measured to determine the velocity anisotropy index (VA) as proposed by Tsidzi [1] for ultrasonic waves and by Brich [2] for description of seismic waves. For the mechanical tests, the Unconfined Compressive Strength anisotropy index (Iσ**C**) given by Ramamurthy [3] and Point Load Strength Anisotropy Ia(50) proposed by (ISRM, 1981) and (ISRM, 1985) [4, 5] were determined. In addition to those measurements, a drilling evaluation based on drilling performance in isotropic and anisotropic rocks is included. The drilling performance was evaluated by calculating the ROP. All tests were conducted in three different orientations (e.g. 0°, 45° and 90°, representing horizontal, diagonal and vertical directions, respectively). Recorded data, evaluated results, and work summary are reported.

3.4 Test Procedure and Apparatus

In this section, the procedure of sample preparation, conducted physical and mechanical measurements as well as the drilling tests and apparatus used are described.

3.4.1 Sample Preparation

In this work, the tested RLM samples were cast using Portland cement and fine-grained rock aggregates (grain size < 2mm). All samples were fan air dried for 48-hours, after which all measurements were taken. Samples were prepared according to ASTM D4543-08 [6]. Before conducting the mechanical tests (e.g. UCS, PLI, and IT), Vp and Vs were measured for all samples. The samples and type of conducted tests are summarized in Table 3.1.

Table 3.1. Summary of number of samples, type of tested conducted, and the orientation of tests

Test Type	Orientation	Direction representation	Sub-test Type	num. of samp.
PLI	90-Degree	Vertical	Axial	19
			Block	24
	45-Degree	Diagonal	Axial	13
			Block	15
	0-Degree	Horizontal	Axial	17
			Block	22
IT	90-Degree	Vertical		24
UCS	90-Degree	Vertical		2
	45-Degree	Diagonal		1
	0-Degree	Horizontal		4
Drilling	90-Degree	Vertical		7
	45-Degree	Diagonal		7
	0-Degree	Horizontal		7
				Total =162

3.4.2 Conducted Tests

Three sets of different tests were conducted on the RLM samples. The purpose of these tests is to determine the anisotropy percentage of the rock by measuring the Vp and Vs, and then utilizing the measured velocities and density in determining the dynamic elastic moduli.

3.4.2.1 Physical Properties' Measurements

3.4.2.2 Ultrasonic Method

This method is used to measure Vp, Vs, and to determine, with measured densities the corresponding dynamic elastic moduli (DEM) according to ASTM D-2845-08 [7]. Comparing to the available methods of sound velocities (e.g. low frequency sonic wave method and the frequency resonant method), the high frequency ultrasonic method is the more reliable and practical. The main influence for adopting the ultrasonic method in determining the wave velocities is the associated non-destructive test procedure, low cost, and more importantly high precision [8].

This method is applied for measuring Vp, Vs and the elastic constants are calculated then using the measured velocities and the bulk density. Vp and Vs can be affected by the inner structure of the tested material. Such factors include minerology, grain's size and distribution, density, porosity's percentage and type, weathering, water content, stress level, and temperature [8].

As the ultrasonic wave velocities increase with the increase of rock strength [8, 9], the work of this paper, exhibit that the measured Vp and Vs were found to be in same range in all orientations confirming using same rock of same strength of RLM. The measurements show small differences; though, due to the nature of experiments. Figure 3-1 shows the ultrasonic method equipment utilized in measuring Vp and Vs. The equipment includes TDS 1002B Two Channel Digital Storage Oscilloscope, Square Wave Pulser/Receiver Model 5077PR, and two Panametrics shear-wave sensors. Shear wave coupling was used to ensure complete contact between sensors and rock samples.

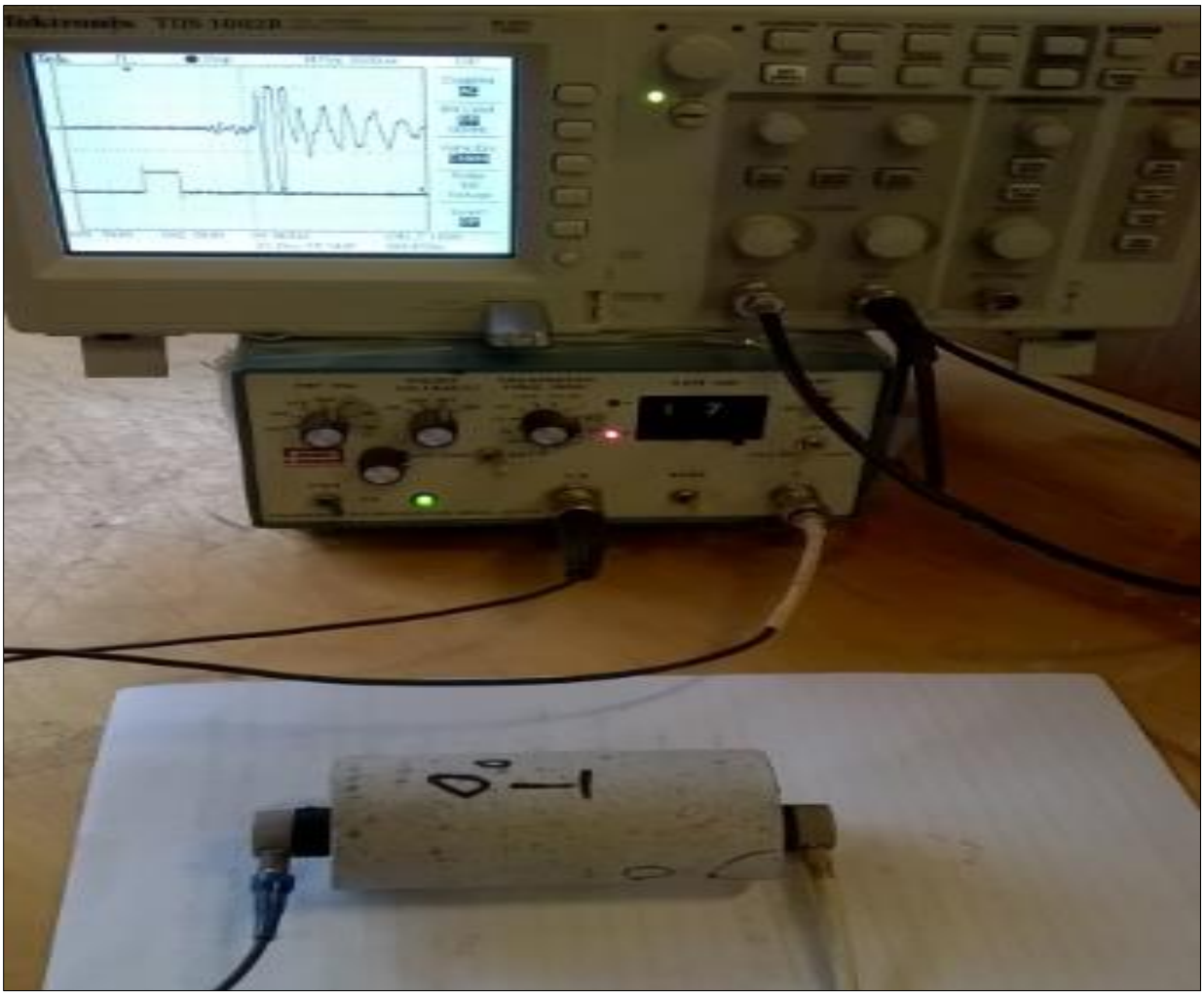

Figure 3-1. Apparatus used for VP and VS measurement

A sample of the recorded ultrasonic waves is shown in Figure 3-2 with the main associated parameters including Trigger, and arrival times.

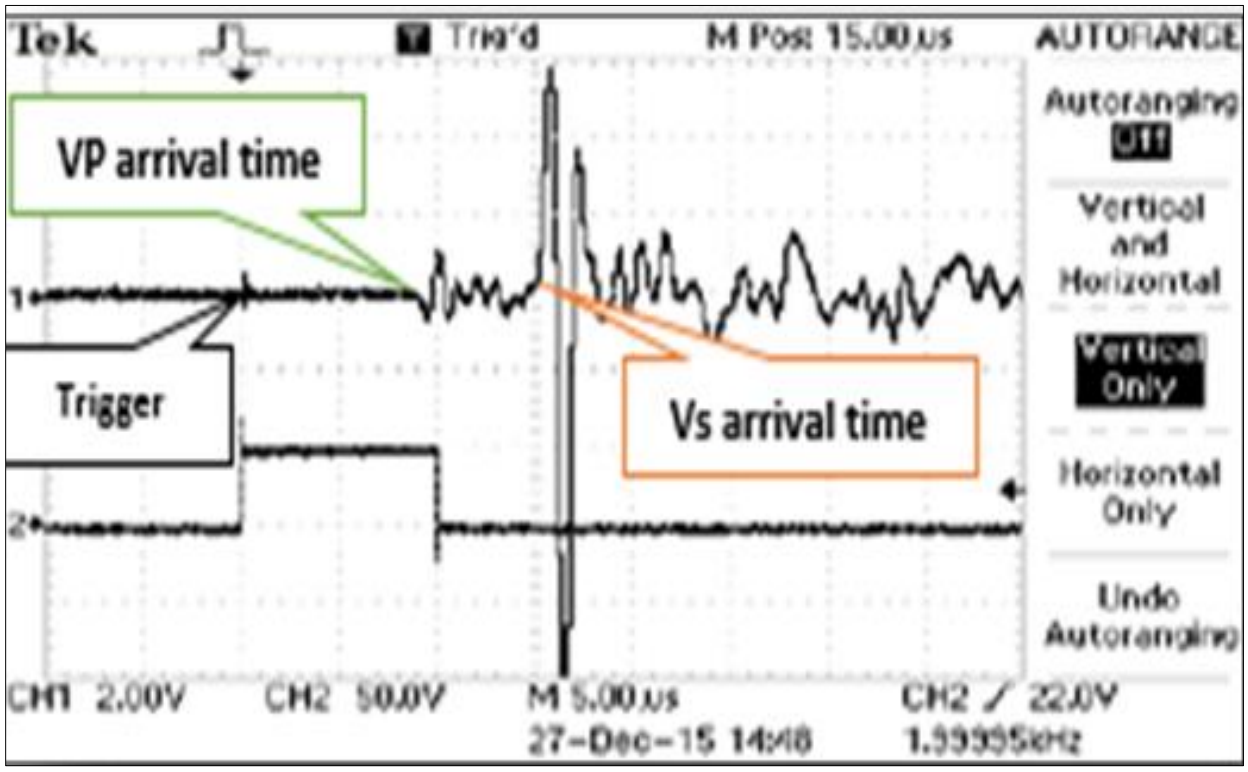

Figure 3-2. Sample of the recorded waves

The measured Vp and Vs and their relationship with density of all prepared samples for Axial and Block-PLI test in different directions are shown in Figure 3-3.

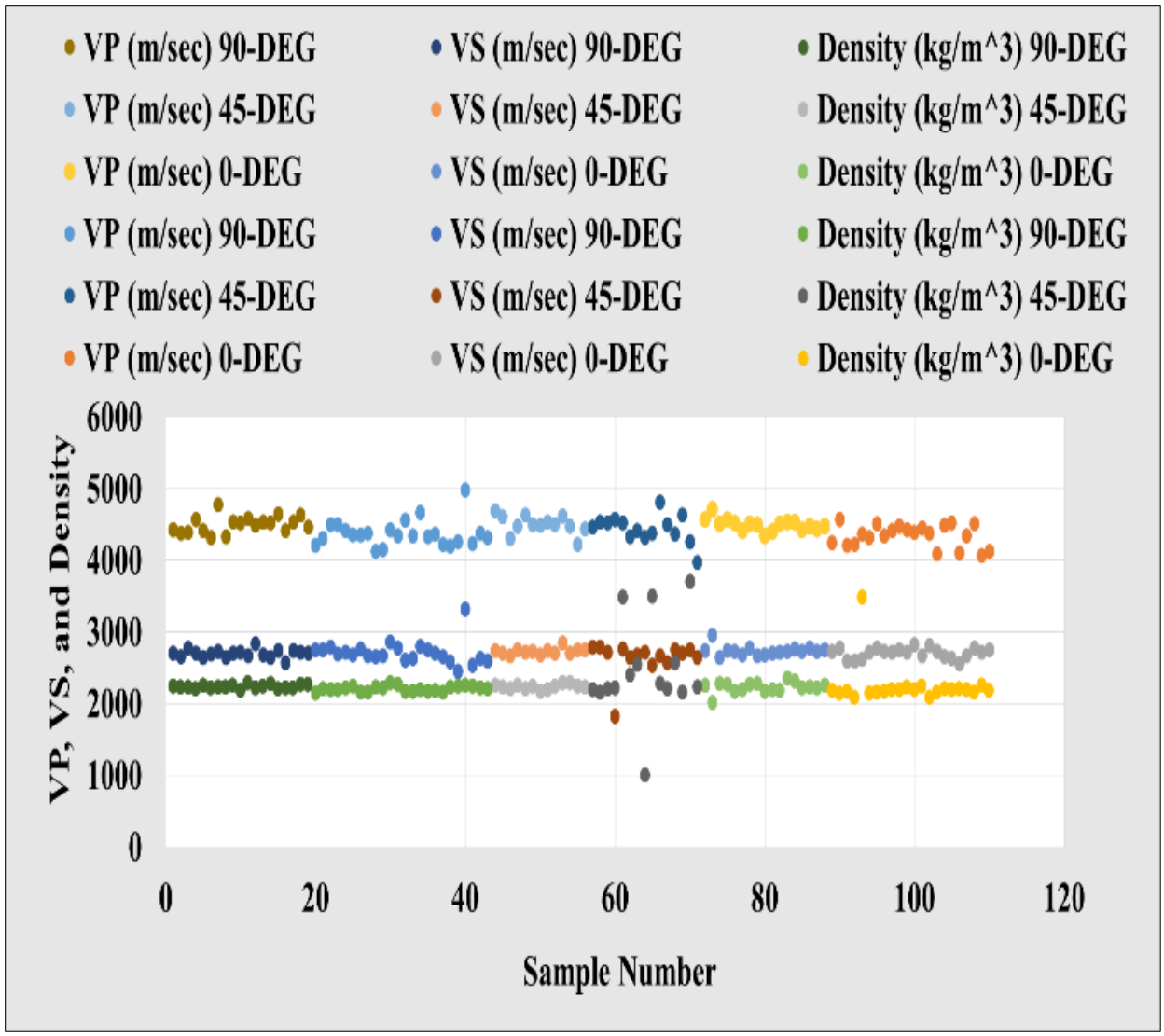

Figure 3-3. Vp, Vs, and Density of all samples of Axial and Block PLI tests in different orientations

The mean values of the measured Vp and Vs from the prepared samples for standard UCS test in different directions are shown in Figure 3-4.

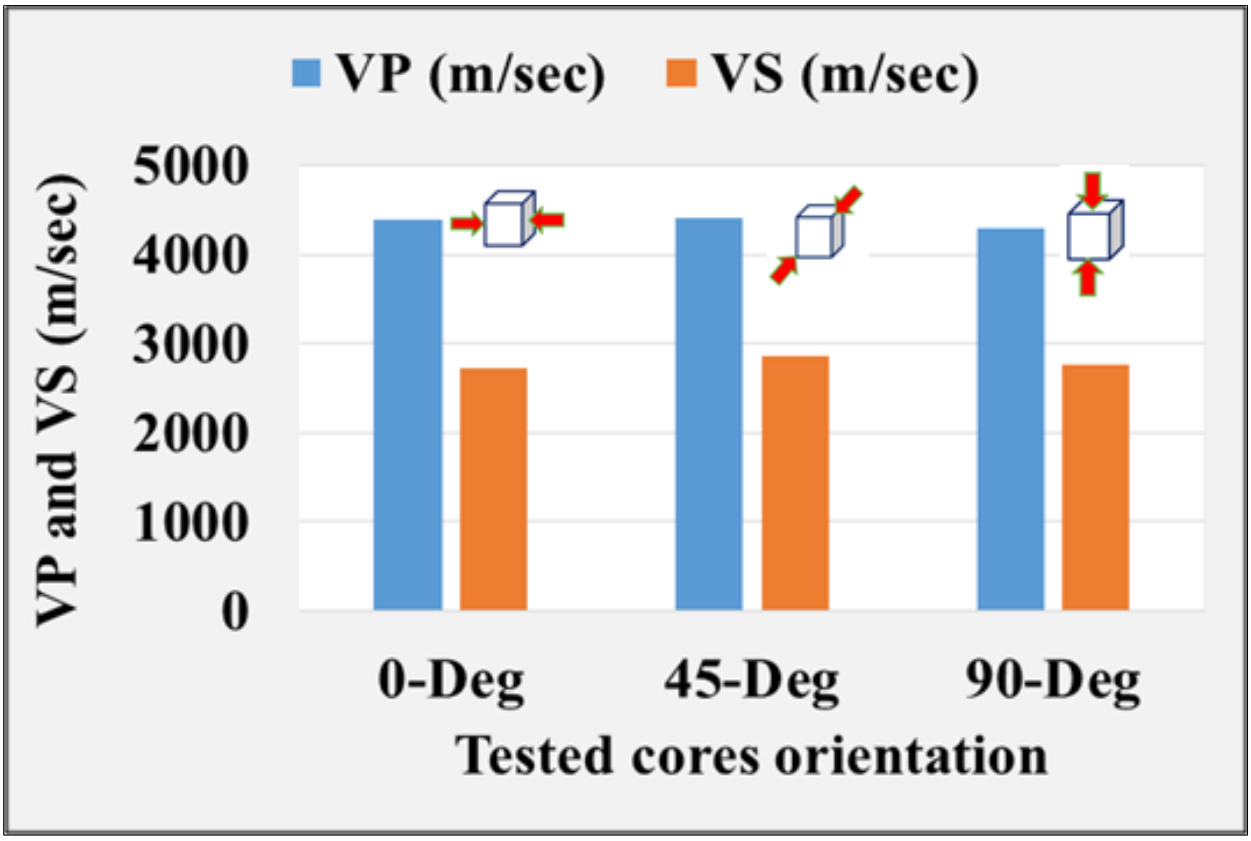

Figure 3-4. Mean values of measured Vp and Vs from standard samples for UCS test in different orientations

The mean values of the measured Vp and Vs from the prepared samples for Axial and Block-PLI test in different directions are shown in Figure 3-5.

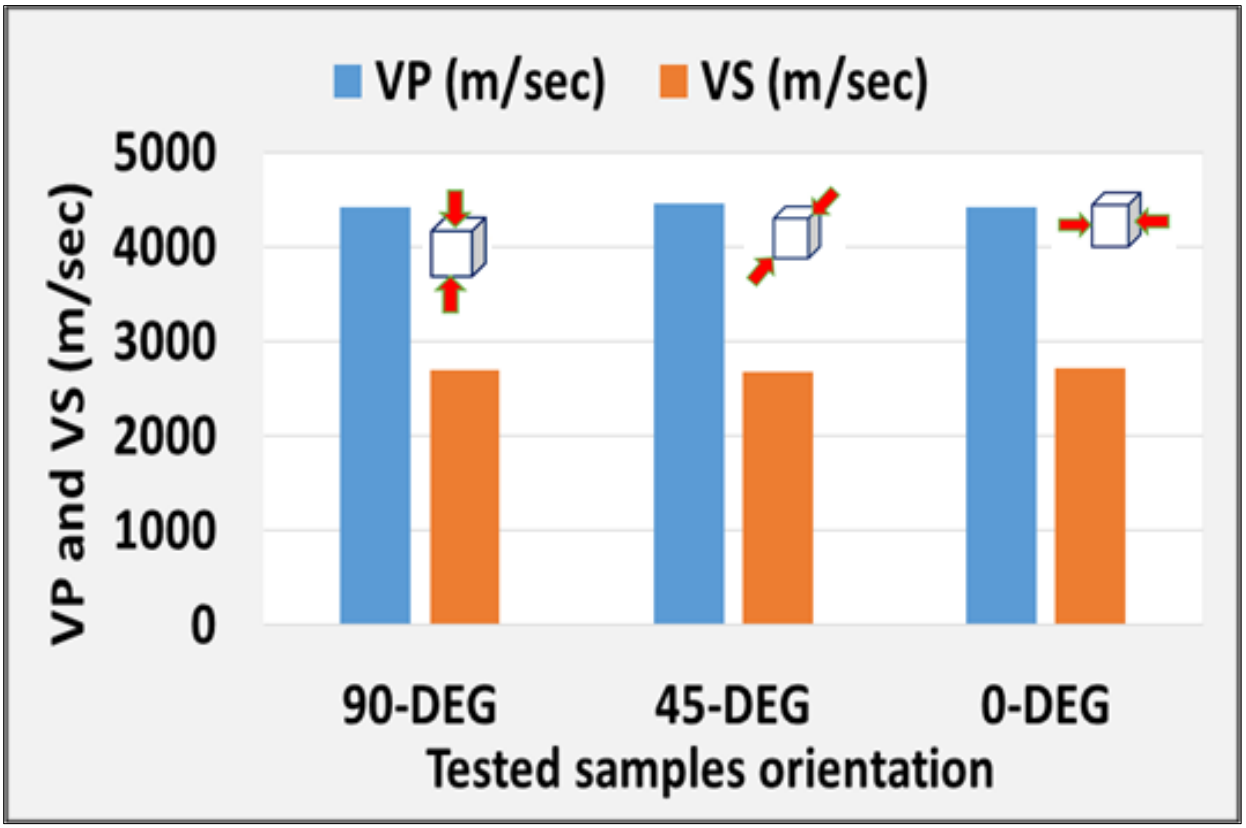

Figure 3-5. Mean values of the measured Vp and Vs of samples of Axial and Block-PLI test in different directions.

DEM were calculated based on measured velocities and densities. Figure 3-6, Figure 3-7, and Figure 3-8 show the mean values of the calculated Compressional wave Modulus, Shear wave Modulus, Elastic Modulus, Lame' constant, Bulk Modulus, and Poisson's ratio respectively. Based on velocity anisotropy index, VA proposed by Tsidzi [1], the VA of the RLM of his investigation is 0.0278 (%) < 2 confirming the isotropy of the tested material.

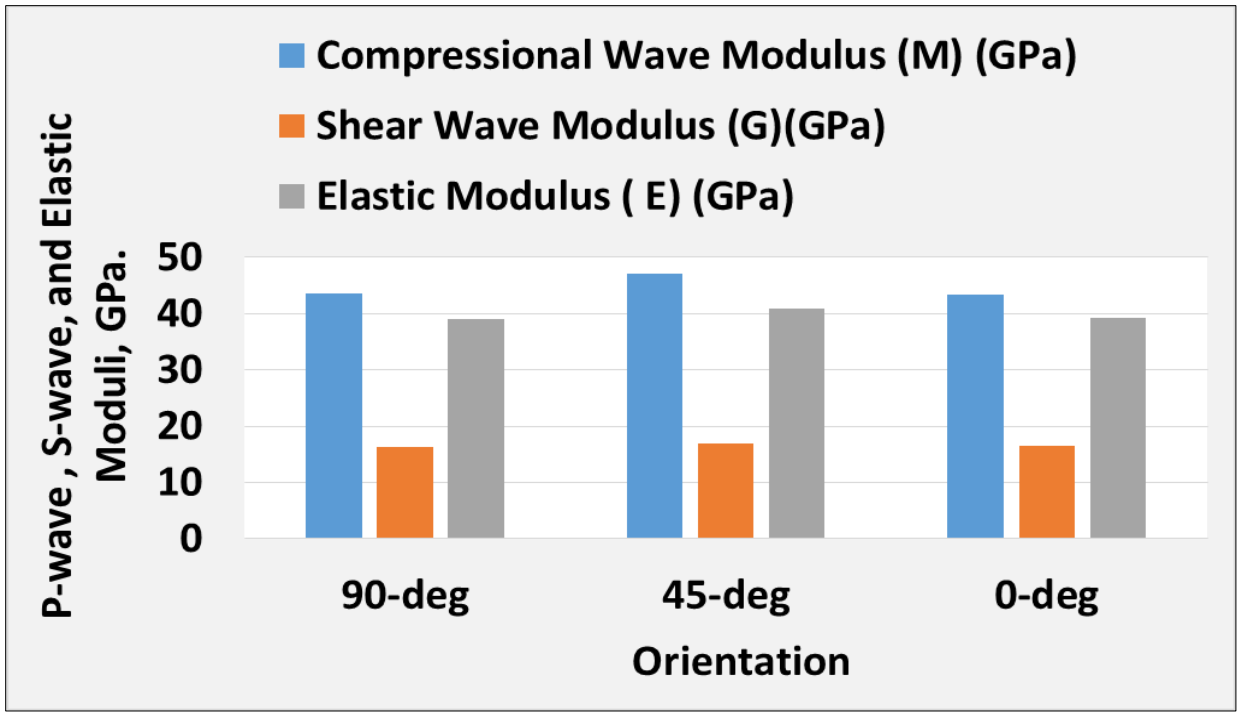

Figure 3-6. Mean values of P-wave, S-wave, and Elastic Moduli in three orientations

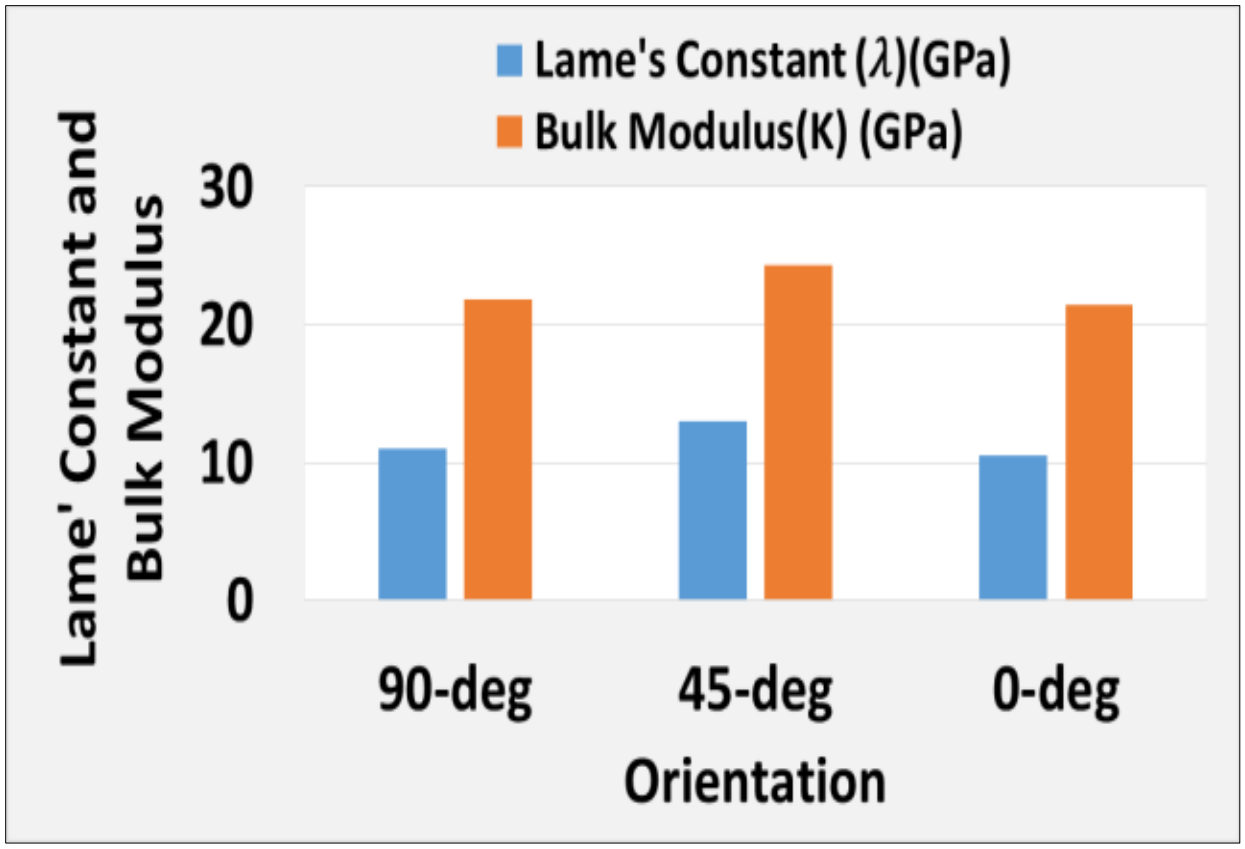

Figure 3-7. Mean of Lame' Constant and Bulk Modulus in three orientations

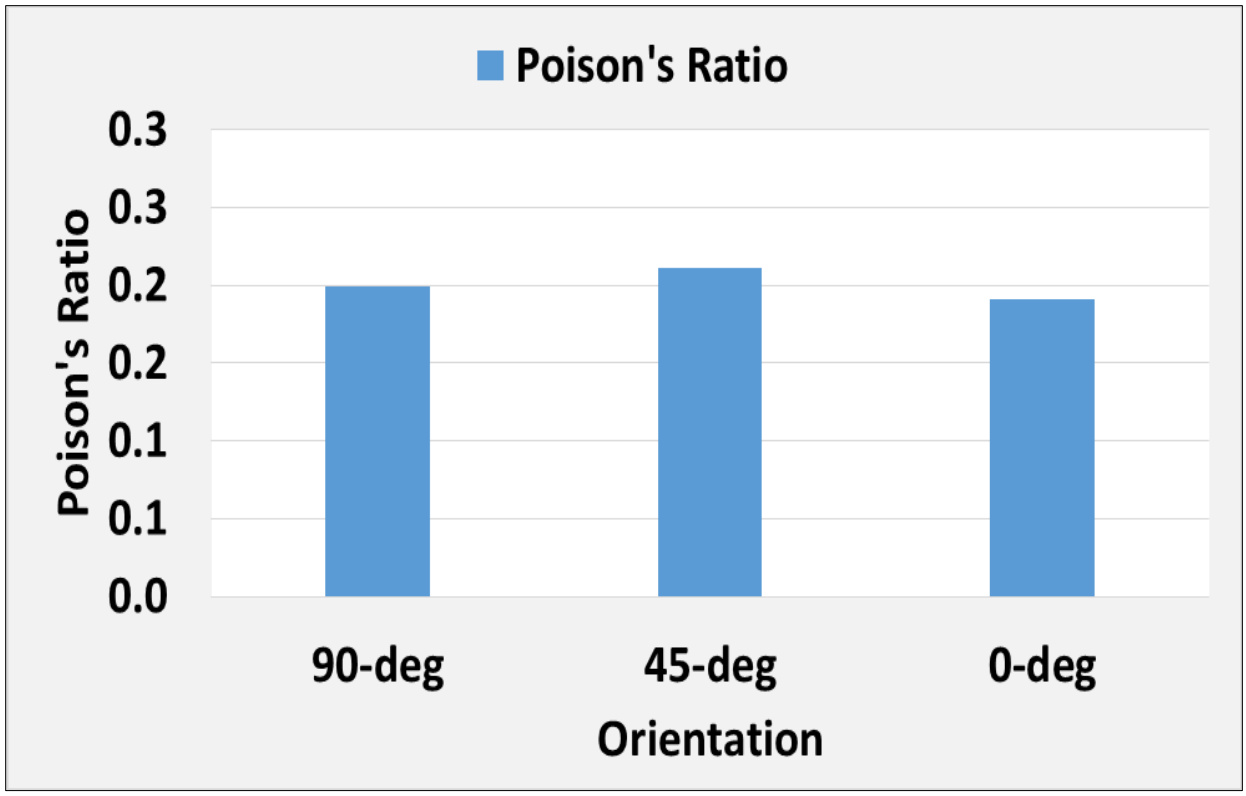

Figure 3-8. Mean value of Poisson's ratio in three orientations

3.4.2.3 Mechanical Tests

3.4.2.4 UCS Test

For this test, many standard NQ cores were obtained by using cylindrical coring bit with outer diameter of 47.6 mm. Grinder was used to ensure parallel ends. ASTM D4543-08- [6] was followed for ensuring appropriate sample preparation. Before conducting the mechanical tests, all measurements of Vp, Vs, and Density were taken for the samples. Figure 3-9 shows the samples cored in three different orientations to be tested for UCS.

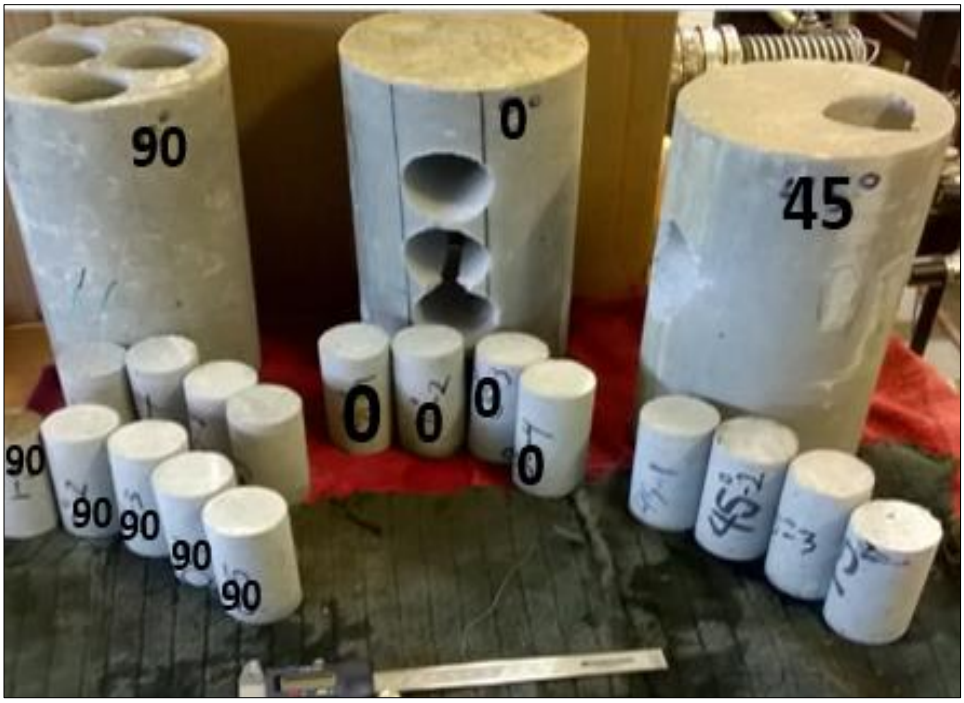

Figure 3-9. Samples of UCS test cored in different orientations

UCS was conducted for cores according to ASTM D7012-14 [10]. The UCS anisotropy of RLM of this paper was determined to be (1.059). This value falls between 1 and 1.1 using the method suggested by Ramamurthy [3] determining the isotropy of RLM. The mean values of the results of UCS tests are shown in Figure 3-10.

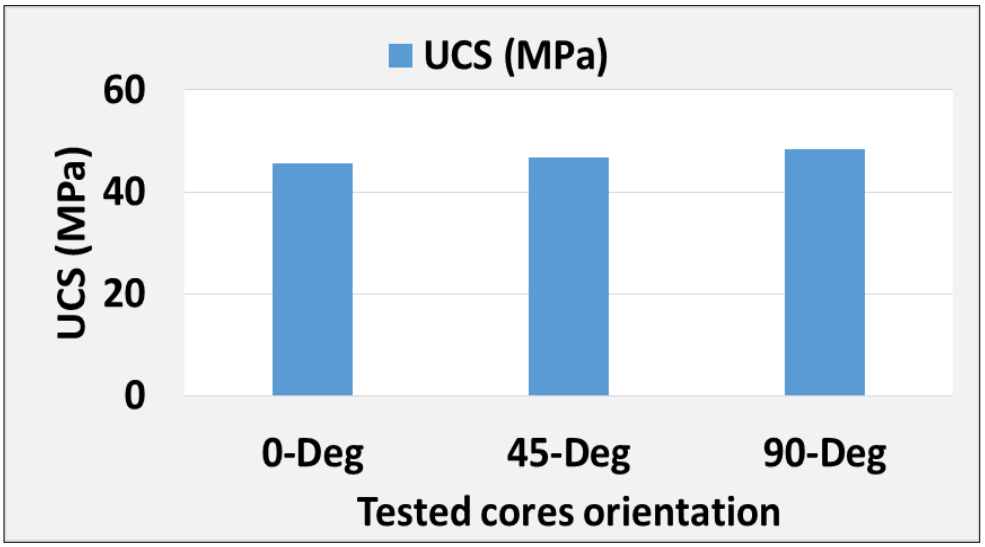

Figure 3-10. Mean values of UCS

Table 3.2 summarizes the recorded data for the standard cores for UCS test including Vp, Vs, and UCS.

Table 3.2. Mean values of Vp, Vs and UCS for the standard samples of UCS test

Orientations	AVG. density (kg/m^3)	VP (m/sec)	VS (m/sec)	UCS (MPa)
0-Deg	2338.5	4384.1	2718.5	45.6
45-Deg	2252.9	4404.1	2853.9	46.7
90-Deg	2408.6	4283.2	2766.7	48.3

3.4.2.5 PLI Test

In this test, two main types of samples were prepared for Axial and Block tests. ASTM D5731-08 [11] was followed for test procedure. Type of samples including Axial and Block tests' samples, orientation representation, and PLI tester are shown in Figure 3-11.

Figure 3-11. Samples of Axial and Block tests with PLI tester

The obtained result by this test followed the same trend of the previous tests in confirming the rock isotropy. However, some variations due to the nature of the test were observed. Such concern was highlighted by (Bowman et al. 2007) [12] and (Bowden et al. 1998) [13]. Bowman proposed that due to unrealistically high UCS estimating specific conversion factor "C" value in determining UCS, especially for weak rocks in the laboratory. Therefore, "C" was

determined for rocks tested in this paper to be “10.3” which gave reasonable UCS values comparing to using the standard “C” value of 24. Figure 3-12 shows the relationship between UCS values obtained by IT and Is(50). Such relationship provides a correlation that results a “C” factor that equals 10.3. Applying this factor using the equation (UCS = 10.3 Is), provides UCS values that are in the strength range of the tested samples by other methods. Figure 3-13 shows the UCS of PLI using different “C” factors.

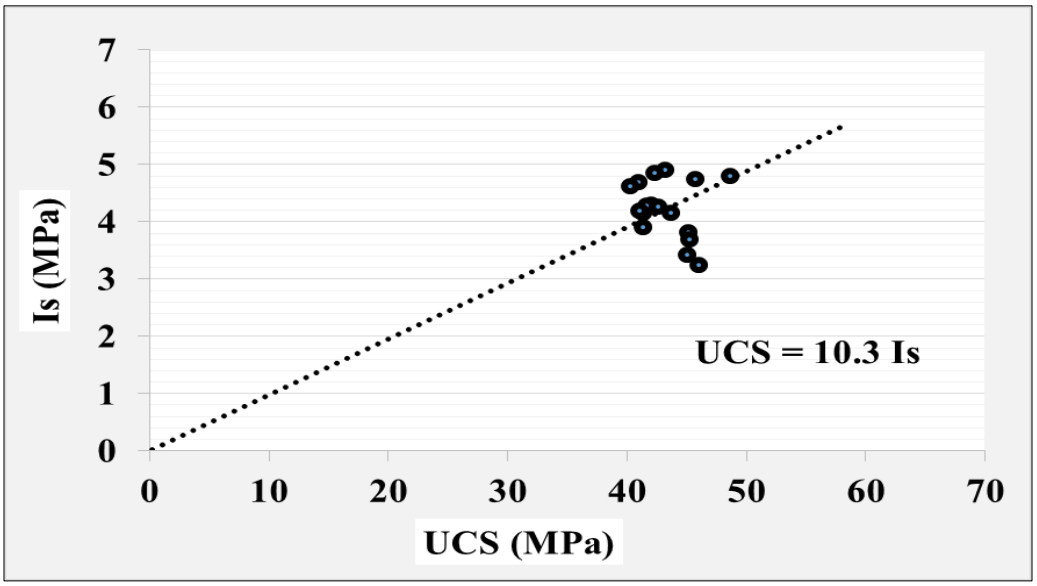

Figure 3-12. UCS Vs. Is

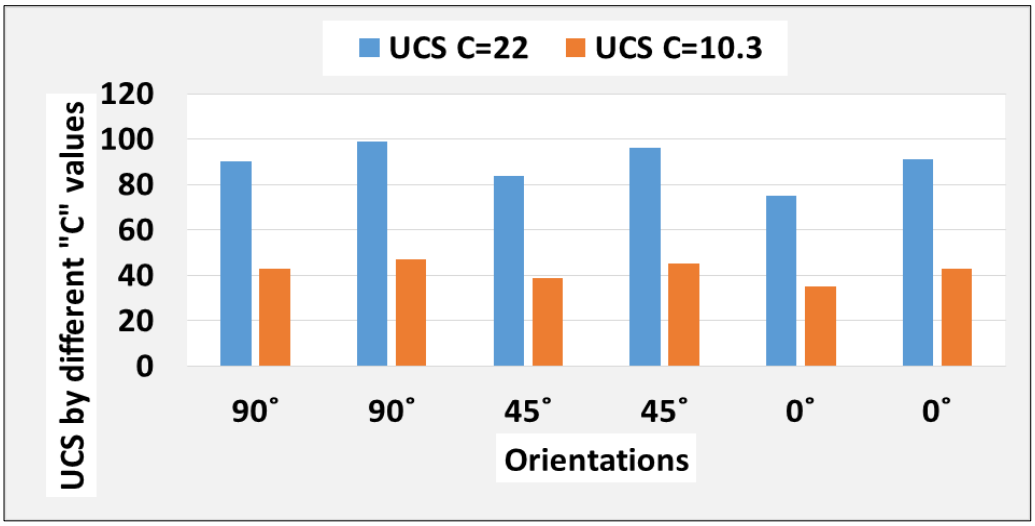

Figure 3-13. UCS values by PLI using different “c” factors

Comparison between the mean values of the obtained UCS by different methods is shown in Figure 3-14. This representation of the data shows close correlation between the UCS values determined by different testing methods (UCS and IT) and the PLI using C factor of 10.3.

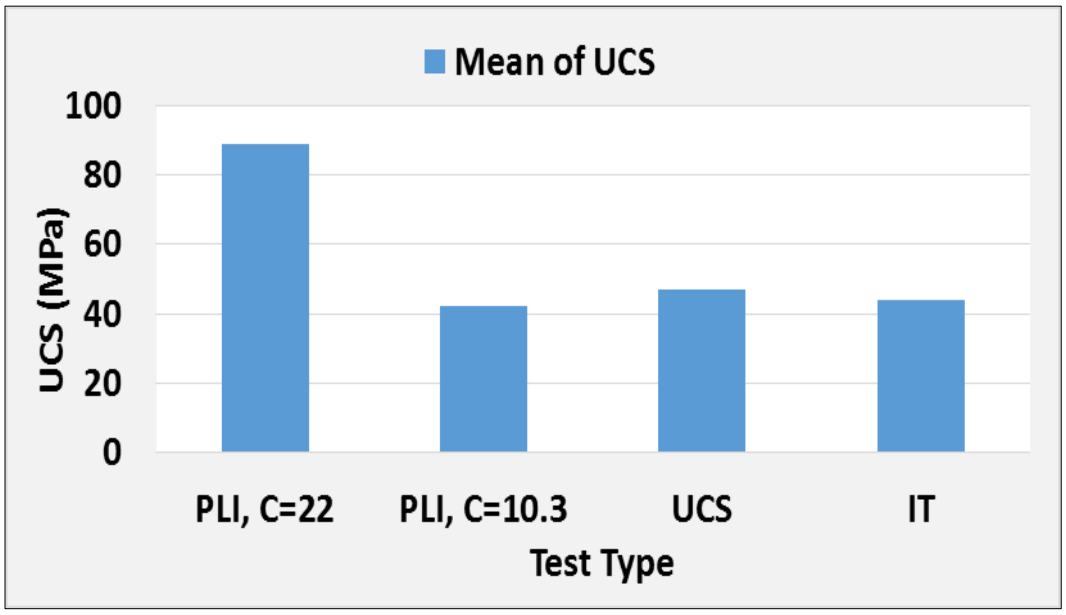

Figure 3-14. Mean Values of UCS values by different tests

3.4.2.6 IT test

In this section, another practical, fast and cheap, but reliable test was conducted. This test is the indirect tensile test (IT). It was performed in accordance to ASTM D6931-12 [14]. This test provided results of strength of the tested rock that is in the same range and compatible with strength results obtained from other tests reported in other sections of this paper. IT strength of the tested samples and their densities are shown in Figure 3-15. Figure 3-16 shows the relationship between the estimated strength by IT and PLI tests. The tested samples by IT are shown in Figure 3-17.

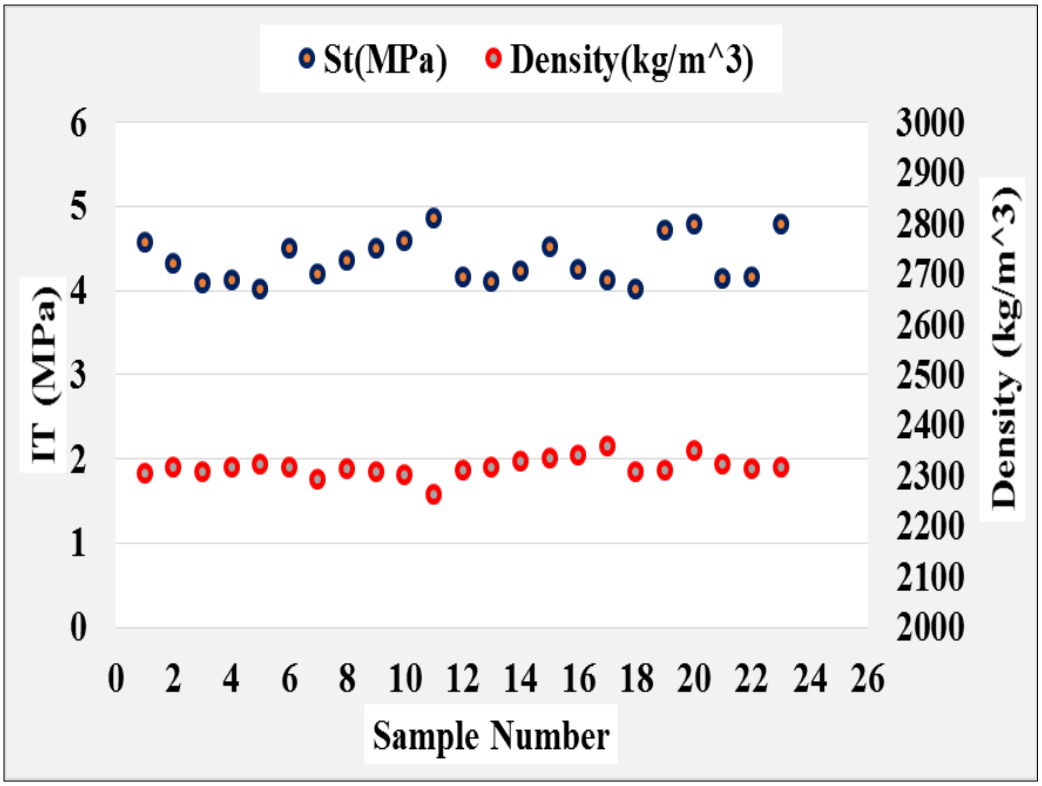

Figure 3-15. IT strength of the tested samples and their densities

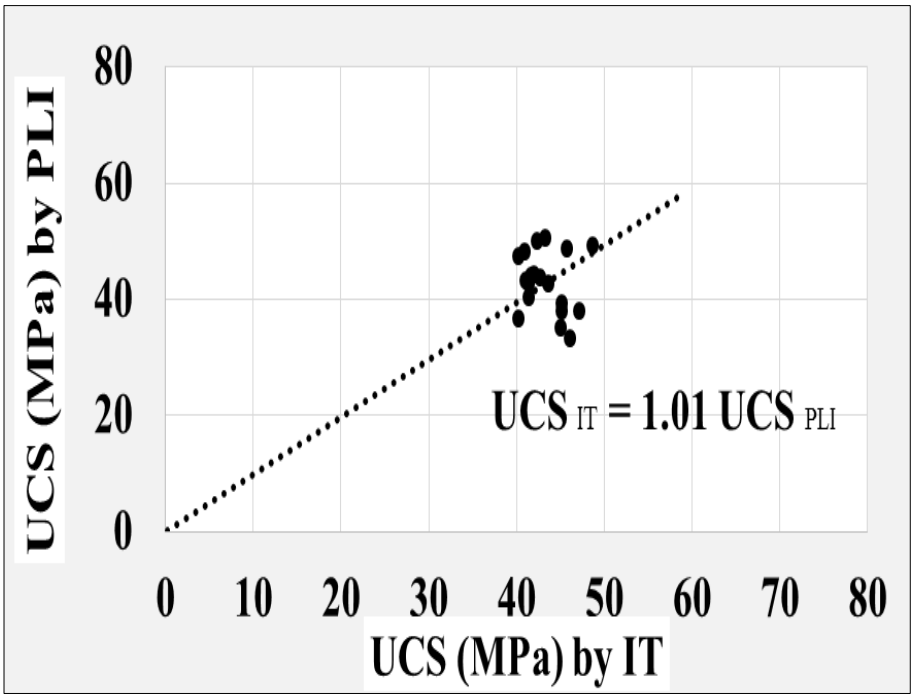

Figure 3-16. Estimated strength by IT and PLI tests

Figure 3-17. Tested Samples by IT test

3.4.2.7 Drilling Tests

In this section, drilling performance is evaluated based on oriented drilling in isotropic (RLM) and anisotropic rocks (Red Shale). For drilling experiments, a vertical laboratory drilling rig was used. The applied drilling parameters included inputs of five different WOB, three flow rates, and three orientations. The laboratory drilling rig used for these tests was described by Rana et al [15]. The hydraulic configuration of the drill bit used in these tests was previously fully examined by Khorshidian et al. [16]. In order to evaluate the drilling efficiency of the conducted drilling tests for the work of this paper, the depth of cut (DOC), (mm/rev.) of the cutters was calculated. A laser triangulation sensor (LTS) was used to calculate the actual DOC.

In all runs, DOC, which is equal to (ROP/rpm), was found to be greater than the chamfer of the drill bit cutter that is 0.15 mm. Figure 3-18 shows LTS and the grooves made on a rotating plate and a sample of the LTS recorded data, top and bottom respectively. ROP is calculated using the numerical recorded data shown in Figure 3-19. Then relationships between the calculated ROP and WOB as function of flow rates and drilling orientations were constructed. Figure 3-20 shows the relationships between ROP and WOB using three different flow rates and in three different orientations. The results showed consistent trend in the three drilled directions. The results confirm that drilling was conducted through isotropy rocks. Drilled RLM samples grouped with respect to their drilling orientation are shown in Figure 3-21.

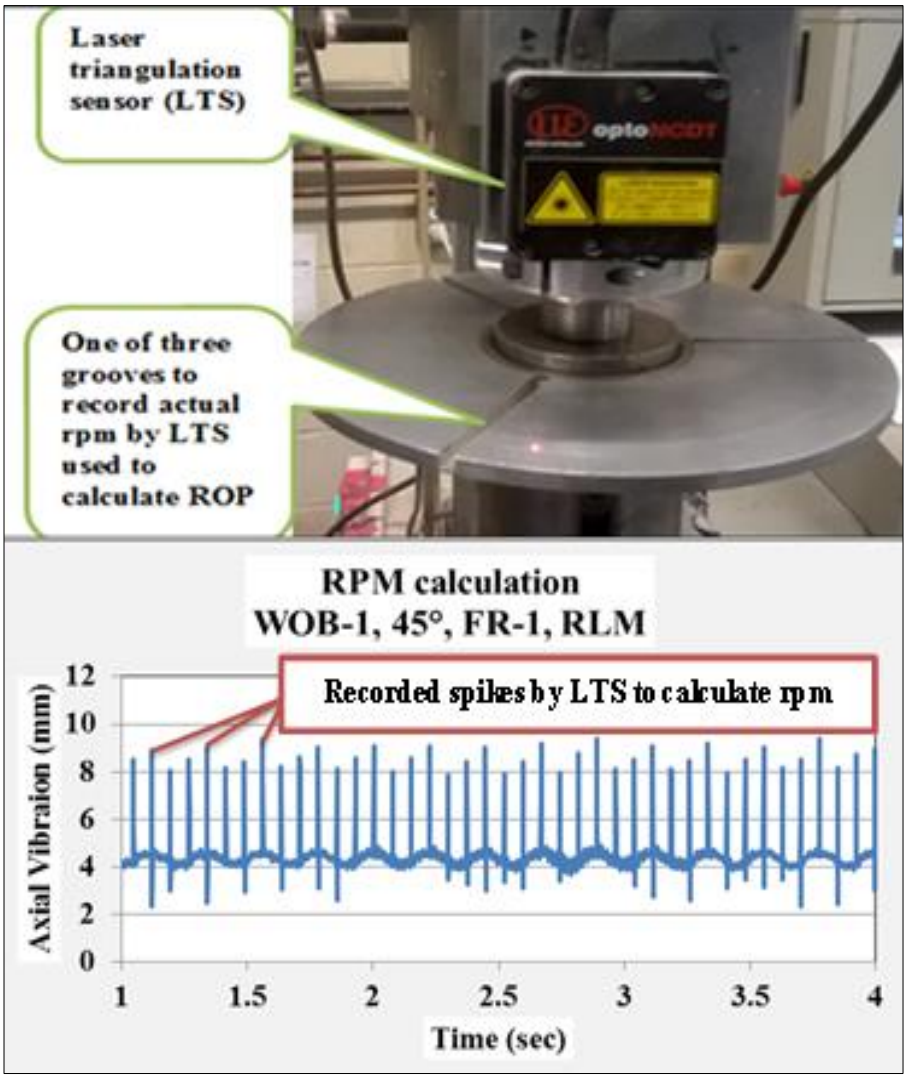

Figure 3-18. Top: LTS and grooved rotating plate for rpm calculation and bottom: recorded spikes by LTS to calculate rpm. For this run, RPM= 280

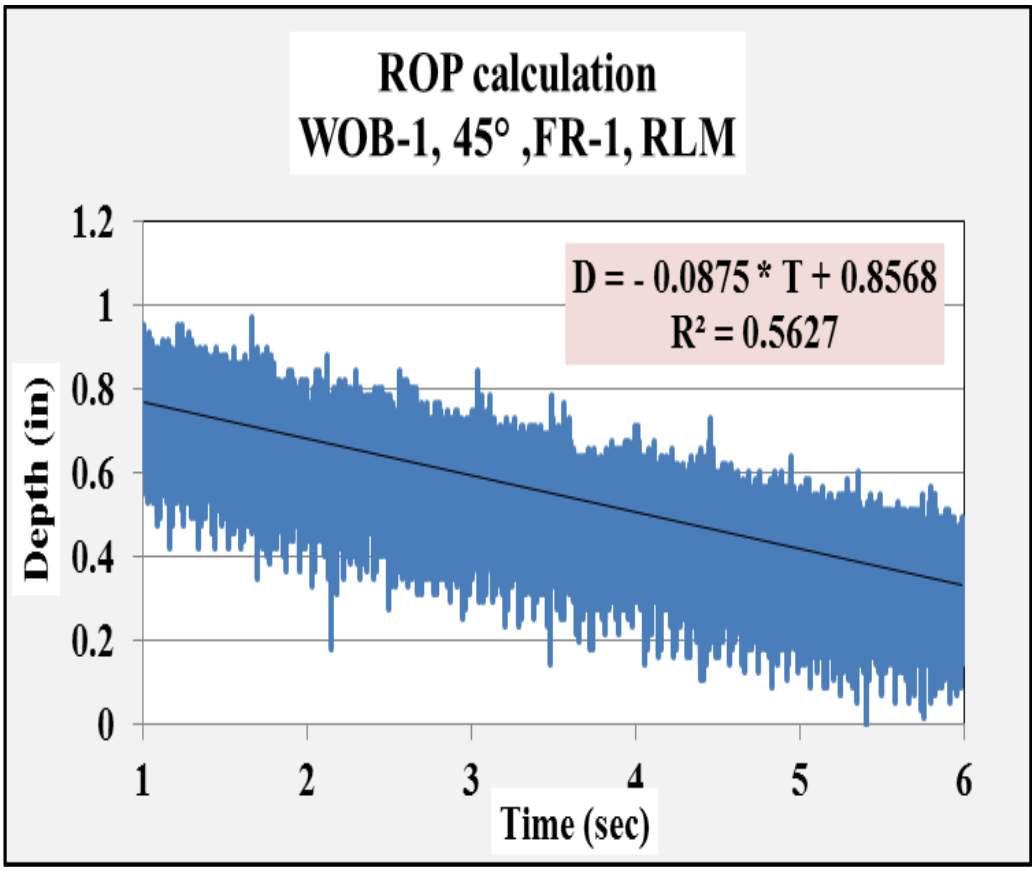

Figure 3-19. Sample of the recorded data used to calculate ROP. For this run, the slope = ROP of 8.00 (m/hr)

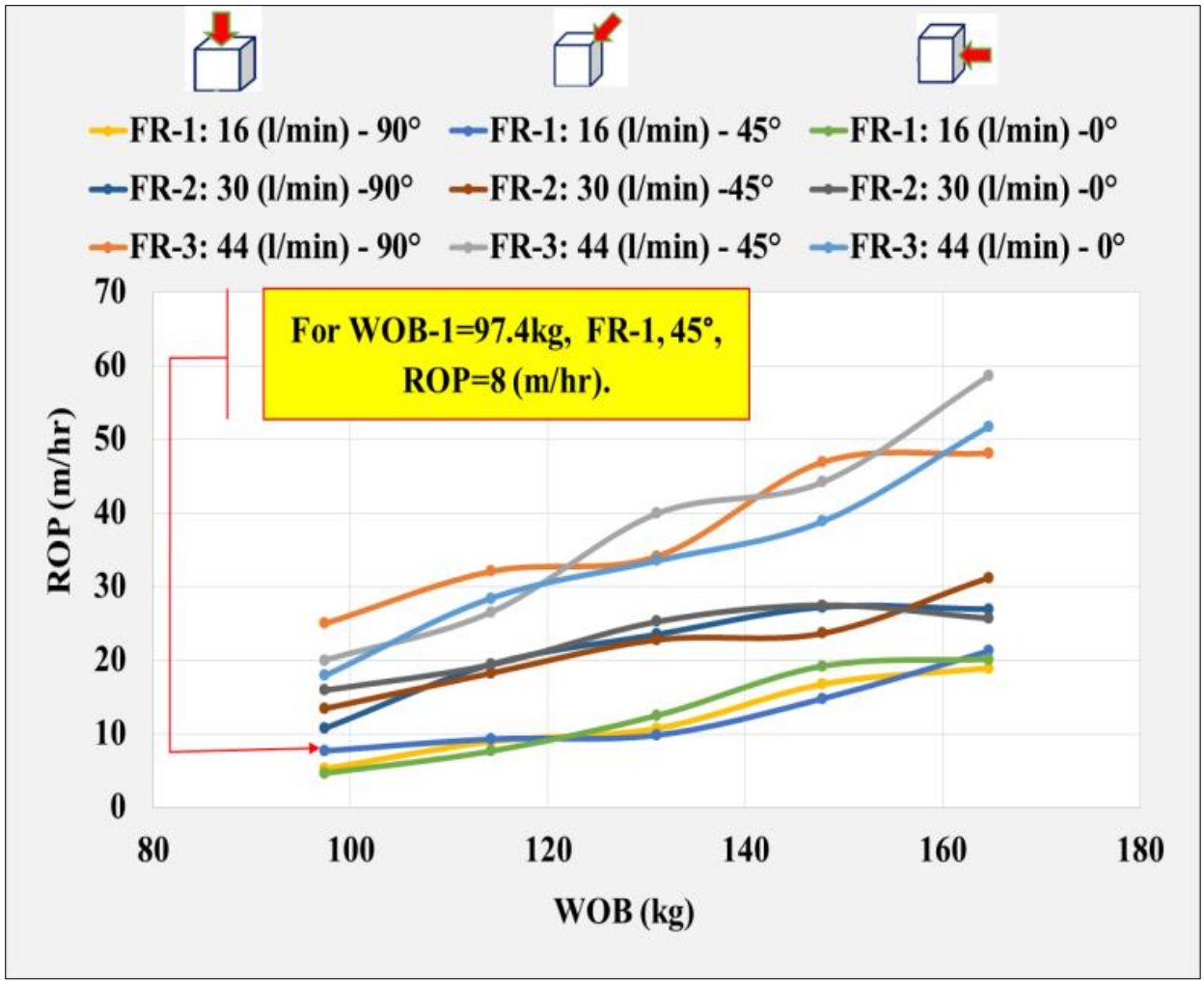

Figure 3-20. WOB Vs. ROP for three different flow rates and three different orientations

All data of lab drilling tests under different conditions of flow rates, orientations, and WOB are shown in Table 3.3.

Table 3.3.Test matrix of laboratory oriented drilling experiments including WOB, ROP, and DOC

Data of lab drilling tests (45 test runs in total)						
		1	2	3	4	5
Flow rate and orientation	WOB (KG)	97.43	114.25	131.06	147.87	164.69
FR-1: 16 (l/min) - 90°	ROP (m/hr)	5.25	8.94	10.73	16.75	18.93
	DOC (mm/rev)	0.40	0.68	0.74	1.16	1.26
FR-1: 16 (l/min) - 45°	ROP (m/hr)	8.00	9.28	9.81	14.78	21.23
	DOC (mm/rev)	0.46	0.68	0.68	1.03	1.42
FR-1: 16 (l/min) -0°	ROP (m/hr)	4.67	7.65	12.48	19.21	20.14
	DOC (mm/rev)	0.34	0.56	0.87	1.33	1.34
FR-2: 30 (l/min) -90°	ROP (m/hr)	10.76	19.44	23.50	27.21	26.91
	DOC (mm/rev)	0.81	1.43	1.63	1.89	1.79
FR-2: 30 (l/min) -45°	ROP (m/hr)	13.44	18.24	22.77	23.64	31.20
	DOC (mm/rev)	1.02	1.34	1.58	1.64	2.08
FR-2: 30 (l/min) -0°	ROP (m/hr)	15.91	19.37	25.23	27.47	25.68
	DOC (mm/rev)	1.21	1.42	1.75	1.91	1.71
FR-3: 44 (l/min) - 90°	ROP (m/hr)	24.98	32.06	34.10	46.90	48.11
	DOC (mm/rev)	1.89	2.43	2.37	3.26	3.21
FR-3: 44 (l/min) - 45°	ROP (m/hr)	20.02	26.52	39.92	44.19	58.64
	DOC (mm/rev)	1.52	1.95	2.77	3.07	3.91
FR-3: 44 (l/min) - 0°	ROP (m/hr)	17.92	28.42	33.50	38.86	51.77
	DOC (mm/rev)	1.32	2.09	2.33	2.70	3.45

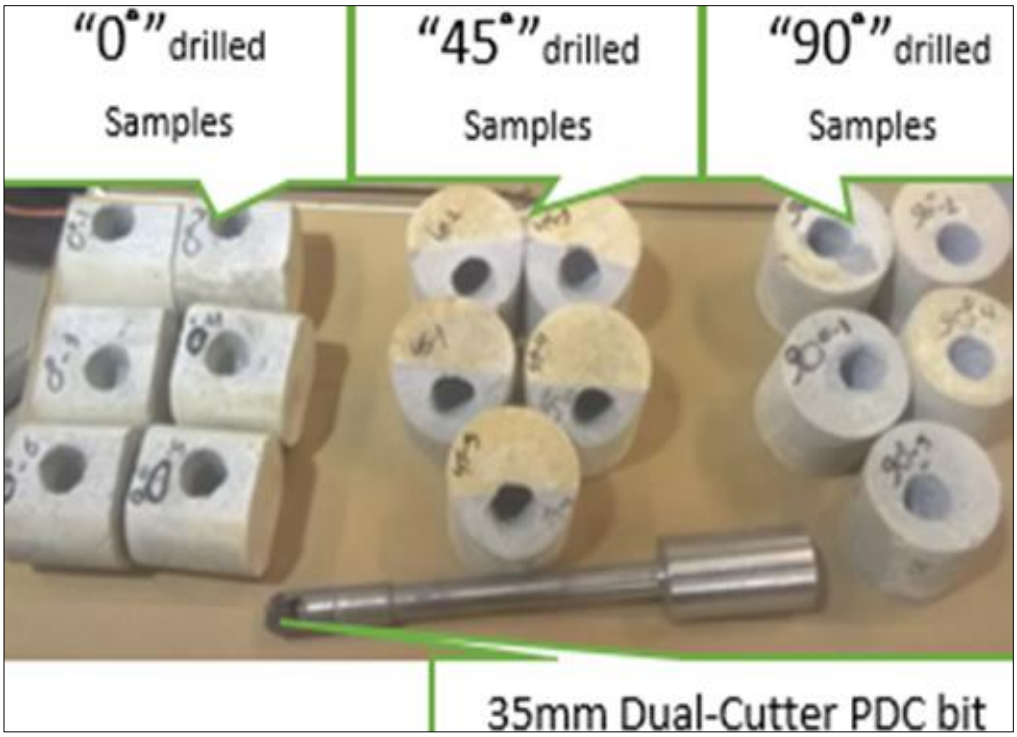

Figure 3-21. Some samples of drilling tests with PDC drill bit

RLM samples drilled in the three orientations are shown in Figure 3-21. For comparison study between oriented drilling performance in RLM as isotropic rocks and Red Shale as anisotropic rocks, Figure 3-22 shows results from drilling in both materials. Such results are a part of study done by Abugharara et al. [17] conducted on RLM and Red Shale and Table 3.4 includes the numerical data corresponding to the plots in Figure 3-22.

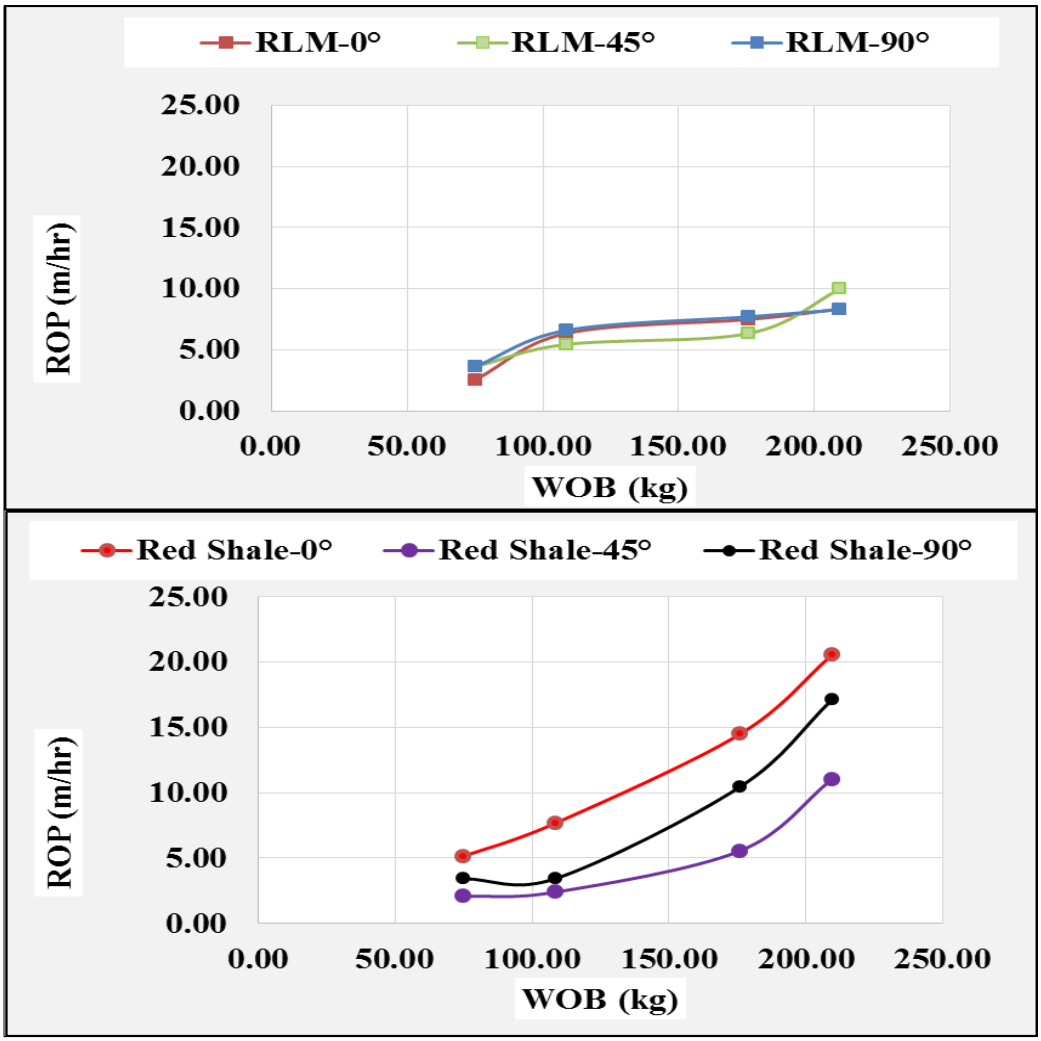

Figure 3-22. Drilling performance through RLM (top) and Red Shale (bottom)

Table 3.4. Calculated ROP for RLM and Red Shale

Oriented Drilling in RLM (Isotropic) and Red Shale (Anisotropic) rocks						
Conditions: atmospheric pressure and flow rate of ~ 18 (L/min)						
Rock Type	Rotation	WOB(kg)	75.00	108.61	175.85	209.46
RLM	0°	ROP (m/hr)	2.55	6.35	7.49	8.35
	45°		3.63	5.44	6.35	9.98
	90°		3.63	6.60	7.71	8.29
Red Shale	0°	ROP (m/hr)	5.13	7.68	14.48	20.54
	45°		2.06	2.40	5.55	11.03
	90°		3.43	3.43	10.44	17.12

3.5 Summary

The work of this paper covers a set of selective physical, mechanical and drilling measurements and tests, which can be summarized as follows:

- The physical measurements included calculating Vp, Vs, and DEM.
- The mechanical measurements included estimating the unconfined compressive strength of the rock by different methods.
- The drilling tests involved evaluating the penetration rate as a drilling performance indicator by applying various conditions of WOB, flowrates and orientations.
- The work was conducted on a medium strength concrete in three different orientations representing horizontal “0°”, diagonal “45°”, and vertical “90°” directions.
- The analysed result showed consistency confirming the isotropy structure of the tested rock in almost all the applied tests.

- A small degree of variation in the recorded measurements, in particular in PLI test was observed. The reason of the variation can be related to the change of the diameters of the tested samples with respect to the aggregates' size (e.g. <2 mm).
- The effect of the diameter in PLI test (ASTM D5731-08) is a dimension effect. However, the effect of the ratio between sample diameter and aggregates size has been observed. A related research focusing on such effect has been started and will be further investigated for future publications.
- Drilling performance evaluation can be emphasized as a new testing method for material anisotropic investigation along with the other testing methods included in this paper to determine the tested material anisotropy type and percentage.
- The methodology of the selective tests performed in this paper can be taken for examining rocks' anisotropy parallel to other available methods.
- The more tests applied, and measurements taken in more degrees between 0 and 90, the more accuracy of the decision can be regarding the rock anisotropy (%).

3.6 Future Work

The work of this paper will be taken as baseline for physical and mechanical measurements and drilling tests under various levels of pressures of well bottom-hole pressure while drilling and confining pressures while conducting the confined compressive strength (CCS) tests. The future work will, also be extended to cover some anisotropic rocks such as shale and new baseline for anisotropic materials will be proposed.

3.7 Acknowledgment

This work was done at the Drilling Laboratory Technology (DTL) at Memorial University of Newfoundland in St. John's, Canada. The project is funded by Atlantic Canada Opportunity Agency (AIF contract number: 781-2636-1920044), involving Husky Energy, Suncor Energy and Research and Development Corporation (RDC) of Newfoundland and Labrador. Financial support is also provided by the Ministry of Higher Education and Scientific Research, Libya. Special thanks to DTL members for their help in laboratory work, in particular M. Jalal Ahammad. Thanks to Mahmud Al Tarhouni for his feedback related to rock mechanics and geotechnical engineering. Thanks to Mark Pope in Mechatronics laboratory, Robert Murphy and David Snock in Technical Services, and Shawn Organ in the concrete lab for assistance in using their lab equipment.

3.8 References

1. Tsidzi, K. (1997). "Propagation Characteristics of Ultrasonic Waves in Foliated Rocks", International Association of Engineering Geology, (56), pp. 103-113.

2. Birch, F. (1961). "The Velocity of Compressional Waves in Rocks to 10Kilobars, Part 2," Journal of Geophysical Research, (66), pp. 2199-2224.

3. Ramamurthy, T. (1993). "Strength and Modulus Responses of Anisotropic Rocks", Compressive Rock Engineering, (1), pp. 313-329, Pergamon press, Oxford.

4. ISRM (1981). "Rock Characterization, Testing and Monitoring," ISRM Suggested methods, Pergamon press, Oxford, UK.

5. ISRM (1985). “Commission on Testing Methods, Suggested Method for Determining the Point Load Strength (Revised Version),” Int. Journal Rock Mech. Min. Sci. and Geomech. Abstr., (22), pp. 51-60.

6. ASTM Standard D4543. (2008). “Standard Test Method for Preparing Rock Core as Cylindrical Test Specimens and Verifying Conformance to Dimensional and Shape Tolerances,” ASTM International, West Conshohocken, PA, 2008, www.astm.org.

7. ASTM Standard D2845. (2008). “Standard Test Method for Laboratory Determination of Pulse Velocities and Ultrasonic Elastic Constants of Rock,” ASTM International, West Conshohocken, PA, 2008, www.astm.org .

8. Soroush, H., & Fahimifar, A. (2003). “Evaluation of Some Physical and Mechanical Properties of Rocks Using Ultrasonic Pulse Technique and Presenting Equations between Dynamic and Static Elastic Constants,” International Society for Rock Mechanics, Technology roadmap for rock mechanics, South African Institute of Mining and Metallurgy.

9. Onyia, E. C. (1988). “Relationships between Formation Strength, Drilling Strength, and Electric Log Properties,” the 63rd Annual Conference and Exhibition of the Society of Petroleum Engineers, Houston, 2-5 October.

10. ASTM Standard D7012. (2014). “Standard Test Methods for Compressive Strength and Elastic Moduli of Intact Rock Core Specimens under Varying States of Stress and Temperatures,” ASTM International, West Conshohocken, PA, 2014, www.astm.org.

11. ASTM Standard D5731. (2008). “Standard Test Method for Determination of the Point Load Strength Index of Rock and Application to Rock Strength Classifications,” ASTM International, West Conshohocken, PA, 2008, www.astm.org.

12. Bowman S.D., and Watters R.J. (2007). “Technical Note: A New, Highly Portable Point Load Test Device for Extreme Field Areas,” Environmental and Engineering Geoscience, XIII, (1), pp.69-73.

13. Bowden, A. J., Lamont-Black, J., and Ullyott, S. (1998). “Point Load Testing of Weak Rocks with Particular Reference to Chalk”, Quarterly Journal Engineering Geology. 31, (2), pp. 95-103.

14. ASTM Standard D6931. (2012). “Standard Test Method for Indirect Tensile (IDT) Strength of Bituminous Mixtures,” ASTM International, West Conshohocken, PA, 2012, www.astm.org.

15. Rana, P. S., Abugharara, A. N., Molgaard, J., & Butt, S. D. (2015). “Experimental Evaluation of Passive-Vibration Assisted Rotary Drilling (P-VARD) Tool to Enhance Drilling Performance,” the 49th US Rock Mechanics / Geomechanics Symposium, San Francisco, 28 June-1 July.

16. Khorshidian, H., Butt, S. D., and Arvani, F. (2014). “Influence of High Velocity Jet on Drilling Performance of PDC Bit under Pressurized Condition,” the 48th US Rock Mechanics / Geomechanics Symposium, Minneapolis, 1-4 June.

17. Abugharara, A. N., Alwaar, M. A., Hurich, A. C., and Butt, S.D. (2016). “Laboratory Investigation on Directional Drilling Performance in Isotropic and Anisotropic Rocks.” Accepted for presentation at the 50th US Rock mechanics / Geomechanics Symposium, American Rock Mechanics Association, Houston, TX, USA, 26-29 June 2016.

CHAPTER 4: IMPLEMENTATION OF CIRCULAR WAVE MEASUREMENTS AND MULTIPLE DRILLING PARAMETER ANALYSIS IN ROCK ANISOTROPY EVALUATION

Abdelsalam N. Abugharara [a], PhD candidate

Charles A. Hurich [b], Associate Professor

John Molgaard [c], Professor

Stephen D. Butt [a], Professor

[a] Drilling Technology Laboratory, Memorial University of Newfoundland, St. John's, NL, Canada A1B 3X5

[b] Department of Earth Sciences, Memorial University of Newfoundland, St. John's, NL, Canada A1B 3X5

[C] Department of Mechanical Engineering, Memorial University of Newfoundland, St. John's, NL, Canada A1B 3X5

This chapter is based on the objectives defined in section 1.3.2 and published in the proceedings of the 36th International Conference on Ocean, Offshore and Arctic Engineering held in Trondheim, Norway, 25-30 June 2017.

4.1 Co-authorship Statement

The contributions of this collaborative work are described in the following six parts. 1) Identification of research topic is collaborative between all co-authors. 2) Design of experiments are contributed by Abdelsalam Abugharara and the main supervisor Dr. S.D.Butt. 3) Preparation of cores and construction of ultrasonic and mechanical measurements are solely contributed by Abdelsalam Abugharara. 4) Performance of drilling experiments is contriputed by Abdelsalam Abugharara, 5) Data analysis and discussion of results is a collaborative work contributed by all co-authors, 6) Manuscript preparation is mainly contributed by Abdelsalam Abugharara, with revision assistance provided by all other coauthors.

4.2 Abstract

A laboratory procedure has been developed to evaluate the anisotropy of Rock Like Material (RLM), granite, red shale, and green shale. This procedure involves detailed anisotropy evaluation steps through implementing circular ultrasonic wave velocity measurements, representing physical measurement and multiple drilling parameters (MDP), representing drilling performance. The physical tests involved circular pattern measurements of compressional and shear wave velocities, VP and VS, respectively. The drilling tests involved drilling samples of each rock in different a 25.4 mm Diamond Coring bit. The MDP included the study of the variations of Rate of Penetration (ROP), bit cutter Depth of Cut (DOC), Revolution Per Minute (RPM), and Torque (TRQ). The MPD were studied as function of orientations under atmospheric pressure. In addition to the physical and drilling evaluation, mechanical tests, such as Oriented Unconfined Compressive Strength (OUCS) were also used in rock anisotropy evaluation. Concrete with fine aggregate and Portland cement is used as RLM for much of the laboratory work. This material was cast into cylinders measuring 101.6

mm by 152.4 mm and 203.2 mm by 203.2 mm, from which NQ; 47.6mm core samples were taken. Coring was performed in three main orientations including 0˚, 45˚, and 90˚. Characterization tests were performed on the RLM cores as they were conducted on the natural rock that included granite and red shale as isotropic and vertical transverse isotropic rocks, respectively. A fully instrumented lab-scale rotary drilling rig was used in conducting the drilling experiments. Details on the strategy for the tests on the anisotropy evaluation with results from laboratory work on natural rocks and RLM are reported. Result of the effect of shale anisotropy orientation on the drilling parameters that influence ROP as means of anisotropy evaluation are also, reported.

4.3 Introduction

Rock anisotropy has been a research topic of interest to many. Such study included evaluation and investigation of different properties of different types of rocks in different directions and interlinked the results of these studies to one another. Although, the methodologies of the studies were different, the goal behind them all was rock anisotropy evaluation. Some researchers focused their studies on the effects of the inner rock structure, including permeability, porosity and mineral compositions on the rock mechanical properties and their relations to the rock anisotropy [1-4]. Other researchers investigated rock physical properties by measuring the wave velocities, which could be influenced by the density of the media that waves propagated through and rock mechanical properties, such as strength under different conditions of confining pressures, loading rates, fluid saturations, and temperature. Some other researchers performed studies, which linked the physical properties and mechanical properties to drilling performance as a function of rock anisotropy [5, 6].

The work of this paper focuses on the anisotropy evaluation of RLM, granite, and red shale. The evaluation includes primarily a procedure of circular measurements of VP and VS and an oriented drilling performance with MDP evaluation. The evaluation also includes secondarily an OUCS of RLM.

4.4 Sample Preparation

Samples were prepared following a procedure described below to meet the type of test to be conducted. For RLM and granite rocks, samples of 47.6 mm were cored from larger samples in three main orientations. (i.e. 0°, 45°, and 90°; represents vertical, oblique, and horizontal directions, respectively). Then, samples of each orientation were separated into three groups, including the group of physical, mechanical, and drilling tests. All samples were prepared in terms of casting, dimension ratio, drying and surface grinding in accordance with ASTM standard procedures and the ISRM Suggested Methods for Rock Characterization, Testing, and Monitoring. For the physical measurement group, flat locations were prepared at intervals of 45° between 0° and 360° for placing the ultrasonic transducer and receiver sensors to measure the VP and VS. Figure 4-1 shows RLM and granite samples prepared for physical measurements.

Figure 4-1. Three RLM samples were cored in three different orientations (top), four granite rock core samples cored in vertical and horizontal directions from granite rocks (bottom). All seven samples were cored using 50.8 mm diamond coring bit and have prepared positions (flat surface by a grinder) for full circular Vp and Vs measurements

For the mechanical tests, samples of smaller diameter were cored from 47.6 mm RLM cores using a diamond coring bit. Calibrated Point Load Index (PLI) equipment with flat end steel plates was used in conducting OUCS. Figure 4-2 shows the calibrated and modified PLI apparatus and the OUCS RLM samples.

Figure 4-2. Calibrated point load index apparatus with flattened-steel-platens for OUCS test (top). OUCS RLM samples and the larger samples, from which the smaller samples were cored (bottom)

For drilling tests, samples of RLM and granite were prepared and drilled under the same conditions of water flow rate (FR), Weight On Bit (WOB), atmospheric pressure, and a rotary speed of (300 and 600 rpm). Figure 4-3 shows a RLM sample during drilling using a diamond coring bit.

Figure 4-3. RLM sample during drilling using a diamond coring drill bit

4.5 Conducted Tests

4.5.1 Ultrasonic Measurements

A full testing apparatus of the ultrasonic method used in this paper was reported by Abugharara, et al., 2016 [5]. RLM and granite as isotropic rocks were selected to be the main source of samples for the physical measurements. Figure 4-4 shows schematic drawing of the ultrasonic apparatus. The apparatus consists of **A**: TDS 1002B Two Channel Digital Storage Oscilloscope, **B**: Square Wave Pulser/Receiver Model 5077PR, **C**: Rock specimen, and **D** and **E**: Panametrics shear-wave sensors (Transducer and Receiver).

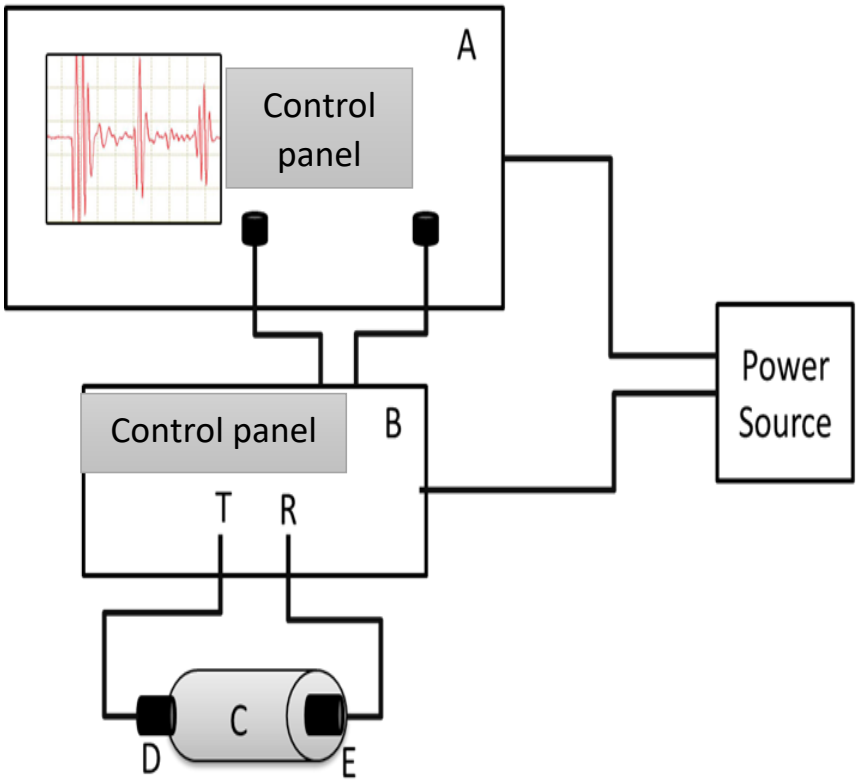

Figure 4-4. Schematic drawing of the ultrasonic apparatus

The results of VP, VS, and density of RLM and granite were measured in a circular pattern and are reported in Figure 4-5, Figure 4-7, and Figure 4-8. Figure 4-5 shows circular VP and VS measurements in RLM. The results plotted in this figure shows similarities in properties of the tested RLM samples cored in different orientations reflecting isotropy of the RLM.

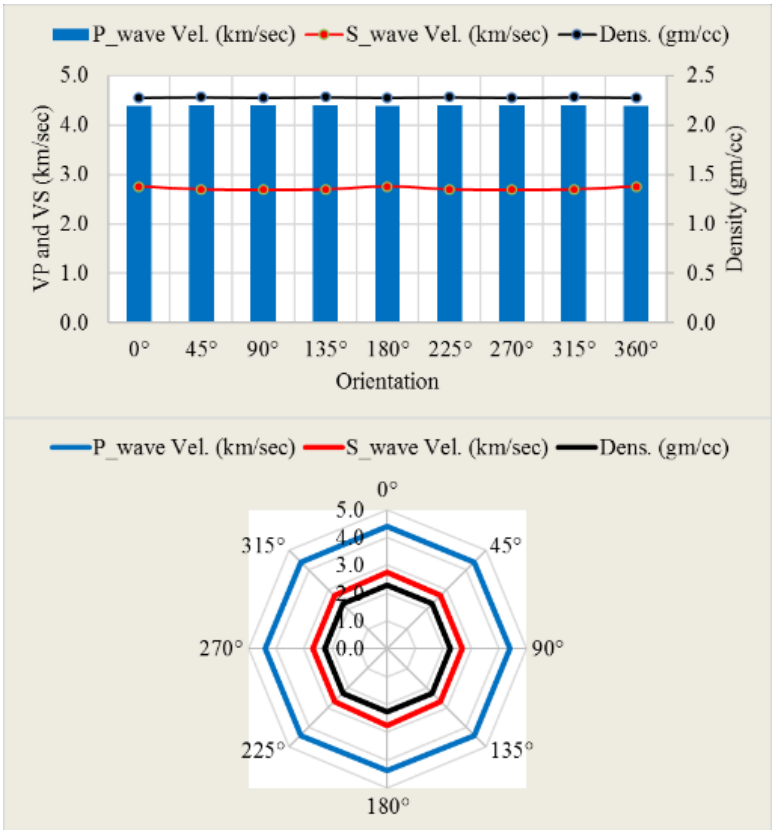

Figure 4-5. Full circular Vp and Vs measurement conducted on one sample of RLM

Full circular VP and VS measurements were also conducted on granite samples cored in vertical and horizontal orientations as shown in Figure 4-6. The results of the measurements are shown in Figure 4-7 and Figure 4-8, respectively. Like the RLM, the circular VP and VS measurements in granite showed the isotropy of the granite.

Figure 4-6. Granite rocks of different types with the obtained samples cored vertically and horizontally

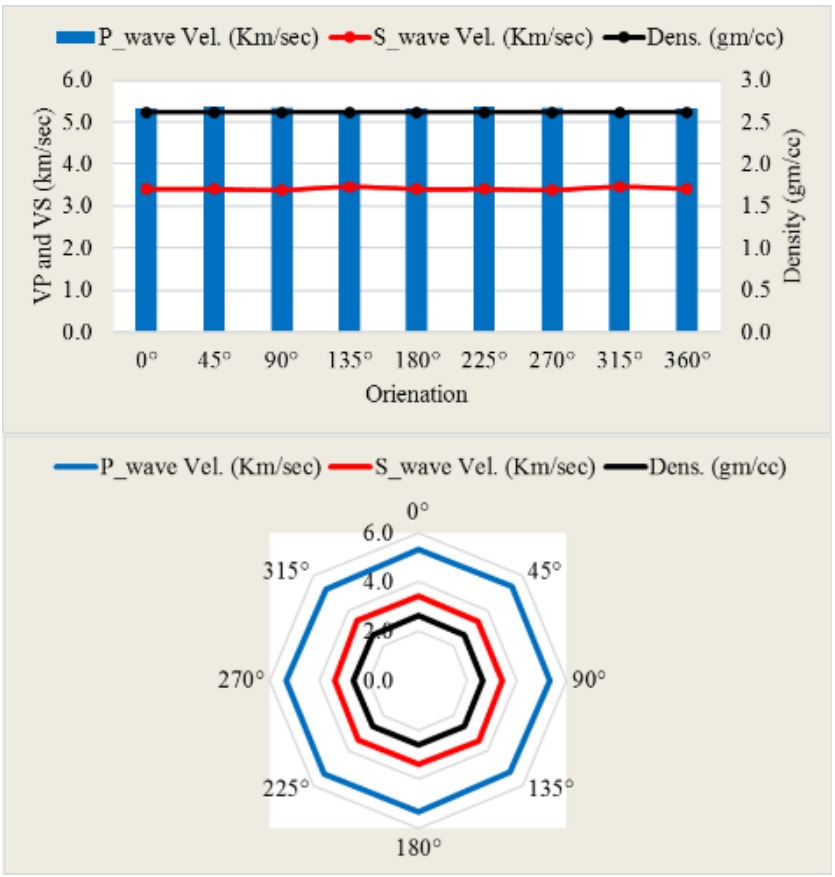

Figure 4-7. Full circular Vp and Vs measurement conducted on vertically cored granite sample shown in Figure 4-6

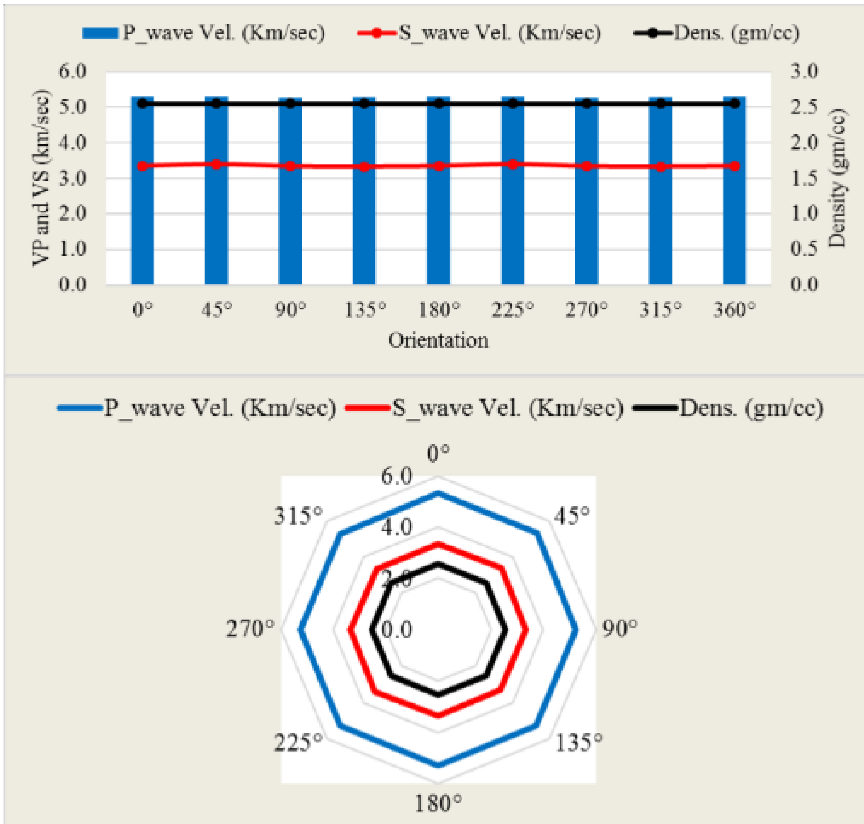

Figure 4-8. Full circular Vp and Vs measurement conducted on horizontally cored granite sample shown in Figure 4-6

According to Tsidzi [7], the measured VP and VS were used in determining the Velocity Anisotropy (VA) of RLM and granite. The VA (%) was determined using Eq. (1).

$$VA\ (\%) = \frac{Vmax - Vmin}{Vmean} \quad \ldots\ldots (1)$$

According to Tsidzi, [7], the tested rock is considered isotropic when VA is less than 2. In this study, the VA was 0.48% for RLM, and 0.86% for granite showing the Rock isotropy for RLM and granite.

For further confirmation of the isotropy of RLM and granite, the elastic constants were calculated to construct the oriented stiffness matrices in the three main orientations of 0˚, 45˚, and 90˚. Table 4.1 summarizes the equations used for calculating the elastic constants for RLM and granite as isotropic rocks.

Table 4.1. Equations used for calculating isotropic materials elastic constants, modulus of elasticity, and Poisson's ratio

Equations (ASTM: D2845-08)	
C11=C22=C33=ρ*VP^2	E=ρ*VS^2((3VP^2-4VS^2)/(VP^2-VS^2))
C44=C55=C66=ρ*VS^2	E=C44((3C11-4C44)/(C11-C44))
C12=C11-2C44	ν= 0.5((VP^2-2VS^2)/(VP^2-VS^2))
	ν= 0.5((C11-2C44)/(C11-C44))

Table 4.2 and Table 4.3 show the calculated stiffness matrices for RLM and granite, respectively in three orientations. The calculations were in accordance with ASTM Standards, D-2845-08 [11].

Table 4.2. RLM stiffness matrices in three orientations. The calculated constants show RLM isotropy

RLM_0Deg =

43.6400	9.1000	9.1000	0	0	0
9.1000	43.6400	9.1000	0	0	0
9.1000	9.1000	43.6400	0	0	0
0	0	0	17.2700	0	0
0	0	0	0	17.2700	0
0	0	0	0	0	17.2700

RLM_45Deg =

44.3200	11.1100	11.1100	0	0	0
11.1100	44.3200	11.1100	0	0	0
11.1100	11.1100	44.3200	0	0	0
0	0	0	16.6100	0	0
0	0	0	0	16.6100	0
0	0	0	0	0	16.6100

RLM_90Deg =

44.1500	11.3200	11.3200	0	0	0
11.3200	44.1500	11.3200	0	0	0
11.3200	11.3200	44.1500	0	0	0
0	0	0	16.4100	0	0
0	0	0	0	16.4100	0
0	0	0	0	0	16.4100

Table 4.3. Granite stiffness matrices in three orientations. The calculated constants show granite isotropy

Granite_0Deg =

73.0300	12.9200	12.9200	0	0	0
12.9200	73.0300	12.9200	0	0	0
12.9200	12.9200	72.0300	0	0	0
0	0	0	30.0600	0	0
0	0	0	0	30.0600	0
0	0	0	0	0	30.0600

Granite_45Deg =

75.8200	15.0700	15.0700	0	0	0
15.0700	75.8200	15.0700	0	0	0
15.0700	15.0700	75.8200	0	0	0
0	0	0	30.0600	0	0
0	0	0	0	30.0600	0
0	0	0	0	0	30.0600

Granite_90Deg =

73.0300	12.9200	12.9200	0	0	0
12.9200	73.0300	12.9200	0	0	0
12.9200	12.9200	72.0300	0	0	0
0	0	0	30.0600	0	0
0	0	0	0	30.0600	0
0	0	0	0	0	30.0600

The oriented Dynamic Elastic moduli (E-dy) and Poisson's ratio (ν) were also determined for RLM and granite in the three orientations. Table 4.4 summarizes the E-dy and ν for RLM and granite in three orientations in dynamic conditions utilizing the measurement of Vp and Vs. The measurements were in accordance with ASTM D-2845-08 [11].

Table 4.4. Values of the calculated E-dy and ν for RLM and granite. The result shows isotropy of RLM and granite

Rock Type	RLM		Granite	
Orientation	E	ν	E	ν
0-Deg	40.5	0.17	69.15	0.15
45-Deg	39.87	0.2	70.43	0.17
90-Deg	39.53	0.2	69.15	0.15

4.5.2 Mechanical tests

OUCS was the mechanical test performed in this paper on a carefully prepared RLM samples shown in Figure 4-2. The testing was in accordance with related ASTM standards and ISRM suggestions of RLM. The OUCS test was performed on the RLM samples obtained in different orientations following the procedure explained in Figure 4-9. Figure 4-9 shows the procedure of obtaining the RLM samples for OUCS tests. Figure 4-10 shows the result of the OUCS test conducted on RLM samples. Figure 4-10, also contains all the obtained result of this test, including the mean values of all three sets representing the three selected orientations.

The anisotropy classification, according to Ramamurthy [8] was adopted to evaluate the tested RLM samples using the modified point load apparatus shown in Figure 4-2.

$$I\sigma C = \frac{\sigma C\ (90°)}{\sigma C\ (\mathrm{min})} \quad \ldots\ldots\ldots\ldots\ldots \quad (2)$$

Using Eq. (2), rocks are classified as isotropy when $I\sigma C$ is between 1.0 and 1.2 according to Ramamurthy [8] and when $I\sigma C$ is equal or less than 1.1 according to Saroglou [9]. Figure 4-11 shows values of the MEAN-OUCS representing the values of table 5. By using Eq. (2) in

calculating the strength anisotropy using the values shown in Table 4.5, the result was (1.02) for RLM, showing the isotropy of RLM samples.

Table 4.5. Summary of mean values of OUCS for RLM samples shown in Figure 4-2

Sample #	[MEAN-UCS (MPa), (0°, 45°, 90°)]
0°-AVG	52.81
45°-AVG	52.52
90°-AVG	53.59

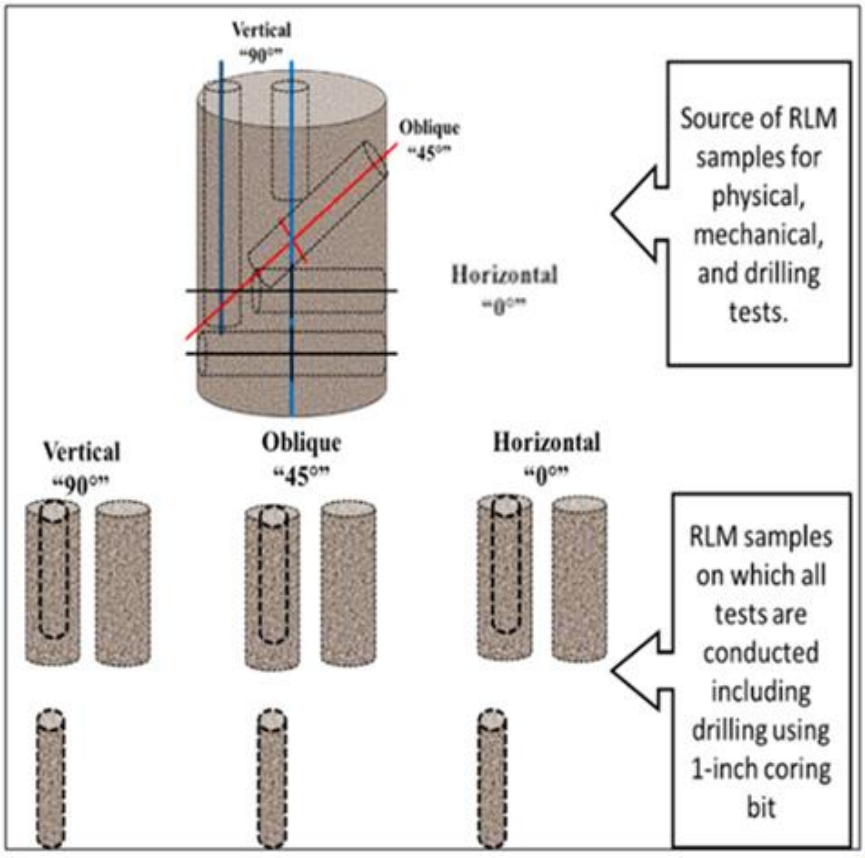

Figure 4-9. Procedure of obtaining RLM samples for drilling and OUCS tests

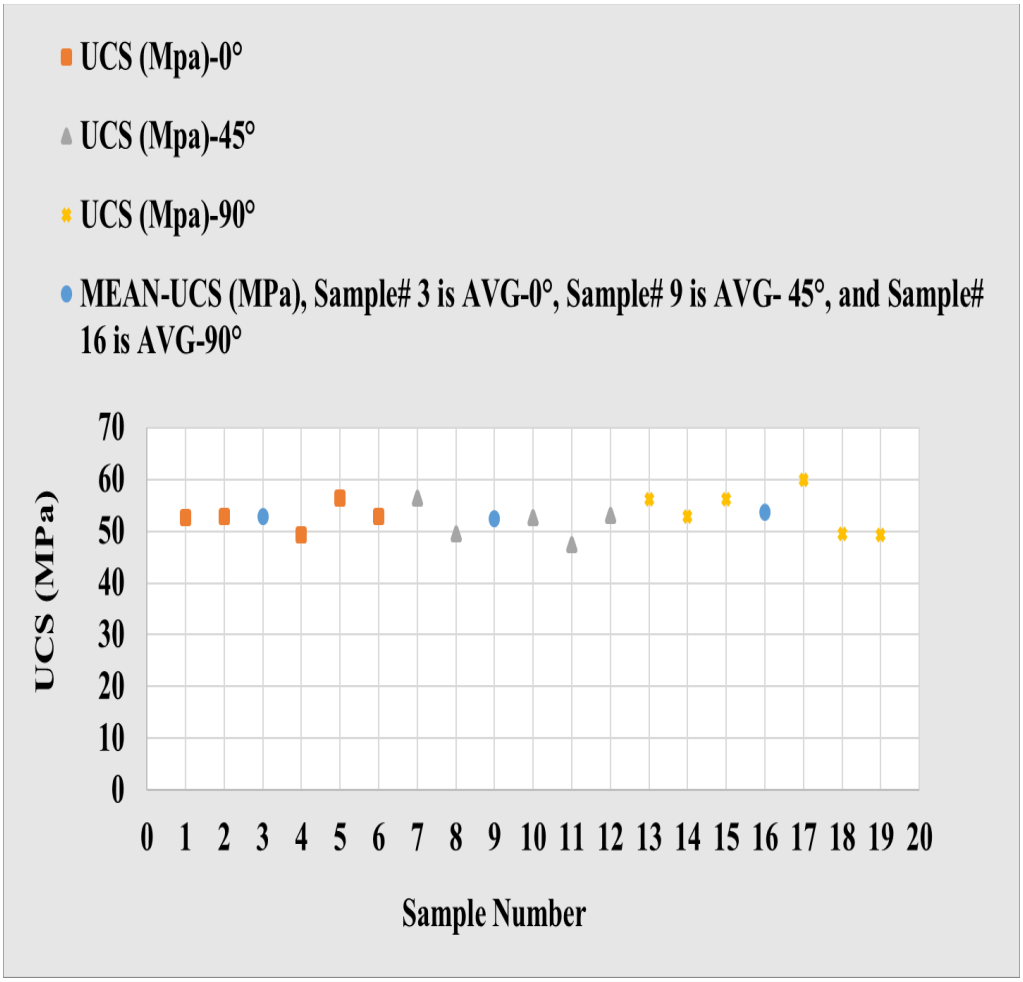

Figure 4-10. Summary of result of OUCS conducted on RLM samples shown in Figure 4-2

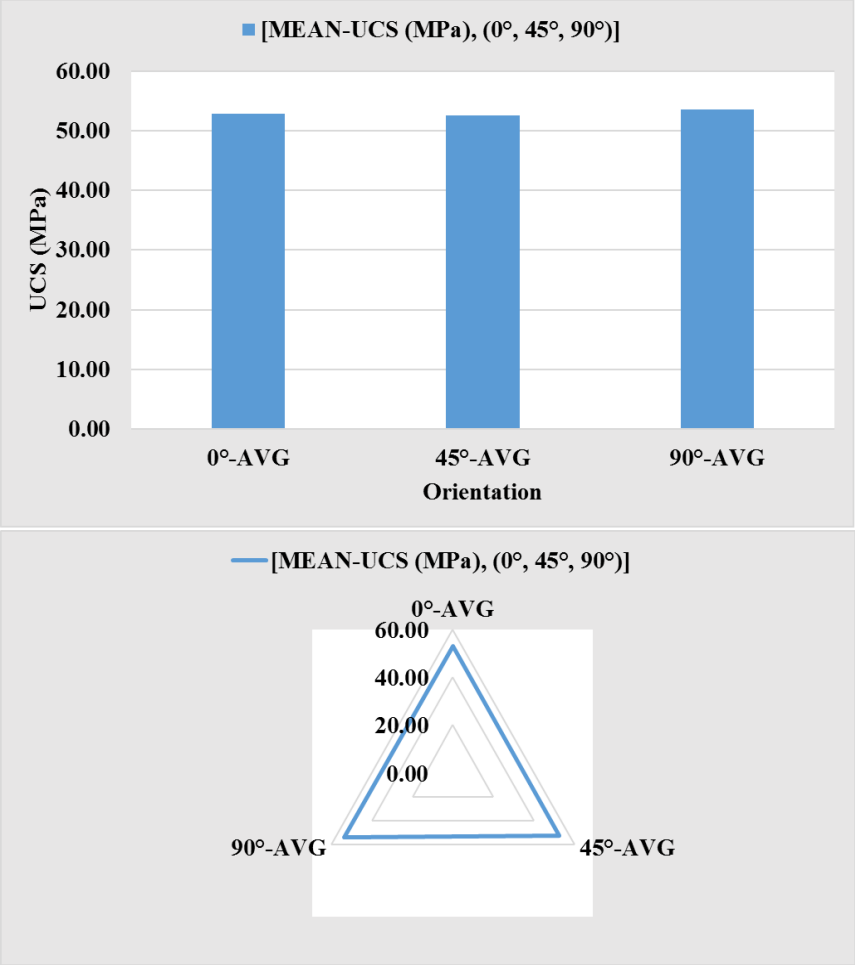

Figure 4-11. Summary of RLM mean-OUCS

4.5.3 Drilling tests

The drilling tests were conducted on samples of RLM and granite alike. However, the reported drilling data in this paper are only of drilling RLM samples, which were cored in different orientation to represent vertical, oblique and horizontal drilling on RLM samples. The drilling tests were conducted using a fully instrumented lab-scale rotary rig. The applied drilling parameters were always kept the same for each rock when drilling in all orientations to ensure consistency. The controlled drilling parameters included water flow rate of 5.6 l/min, rotary speed of 300 and WOB. The drilling was conducted under atmospheric pressure and the drill

bit used was 25.4 mm diamond coring bit. The recorded data included the current of the drill motor, axial displacement, rotary speed and WOB.

The purpose of the oriented drilling tests included in this paper is to evaluate, using multiple drilling parameter analysis, the anisotropy of the tested rocks. The evaluation is performed through constructing relationships between several drilling parameters with respect to the drilling orientation. The drilling parameters included in this evaluation are ROP, DOC, RPM, and Torque. The results of this evaluation provided confirmation of the isotropy of the tested RLM and granite as shown in Figure 4-12 to Figure 4-16. The isotropy of RLM and granite is further analyzed compared to results of drilling in anisotropic rock of green shale shown in Figure 4-17.

Figure 4-12 shows the relationship between WOB and ROP. This figure also shows that the ROP increases with the increase of WOB of drilling RLM samples in different orientations. The plotted data represents the WOB-ROP curve that is before the founder point and it confirms RLM isotropy. Figure 4-13 shows the obtained ROP when drilling RLM in the three orientations. The ROP-AVG shows the isotropy of the RLM. Figure 4-14 shows the DOC data determined when drilling RLM in the three orientations. The DOC-AVG data is at about same value at the same WOB in different orientations confirming the isotropy of RLM. Figure 4-15 shows the RPM results from drilling RLM samples in different orientations as a function of WOB. The plotted data of RPM-AVG shows about constant values in all drilling orientations at each WOB confirming the RLM isotropy. Figure 4-16 shows the torque results from drilling RLM in different orientations. The torque-AVG shows consistent TRQ values in all orientations confirming the isotropy of RLM. The above analyzed multiple drilling parameters, as mean values of each oriented parameter, provided the same result in each WOB confirming

the isotropy of the RLM isotropy through the drilling experiments, as was confirmed in the first and second sections of the conducted tests. This analysis procedure performed in this paper provides an experimental methodology that may be followed for rock anisotropy evaluations. Unlike the results of the above figures, which represent drilling in isotropic rocks, Figure 4-17 shows plotted data of DOC in different orientations obtained from drilling in shale samples showing an anisotropy of shale as reported by Abugharara, et al., 2017 [10].

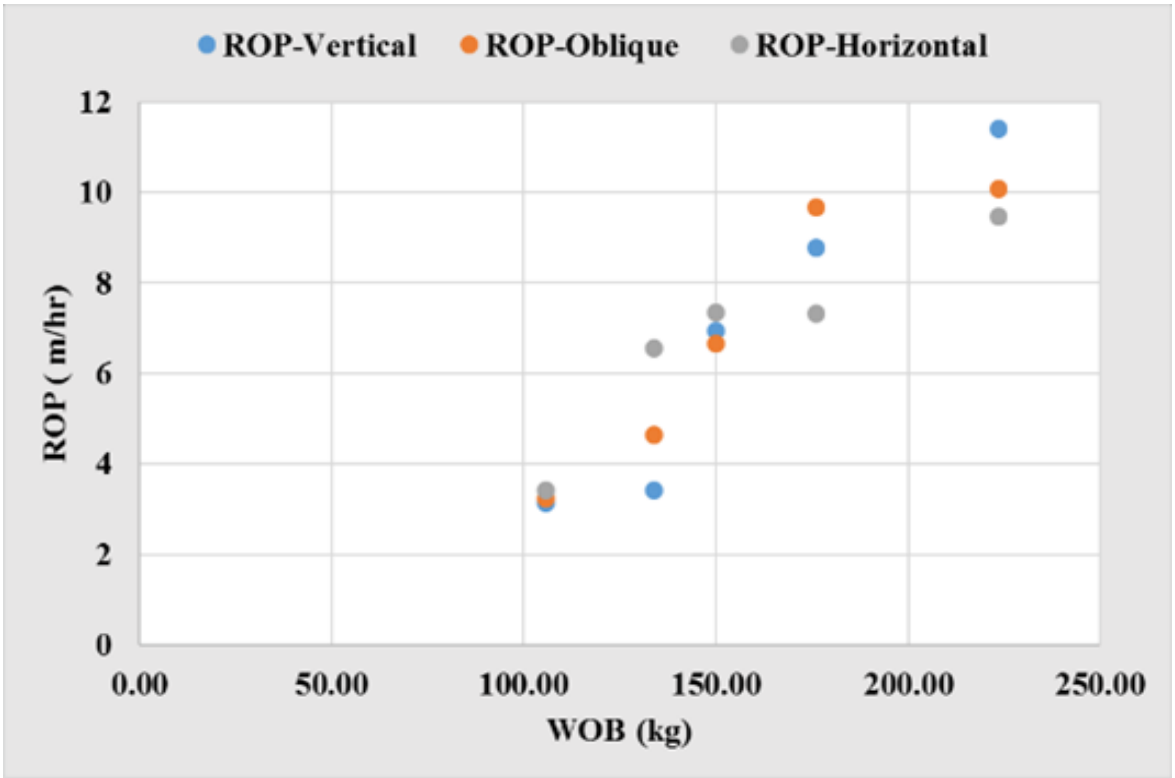

Figure 4-12. ROP of drilling RLM in different orientations

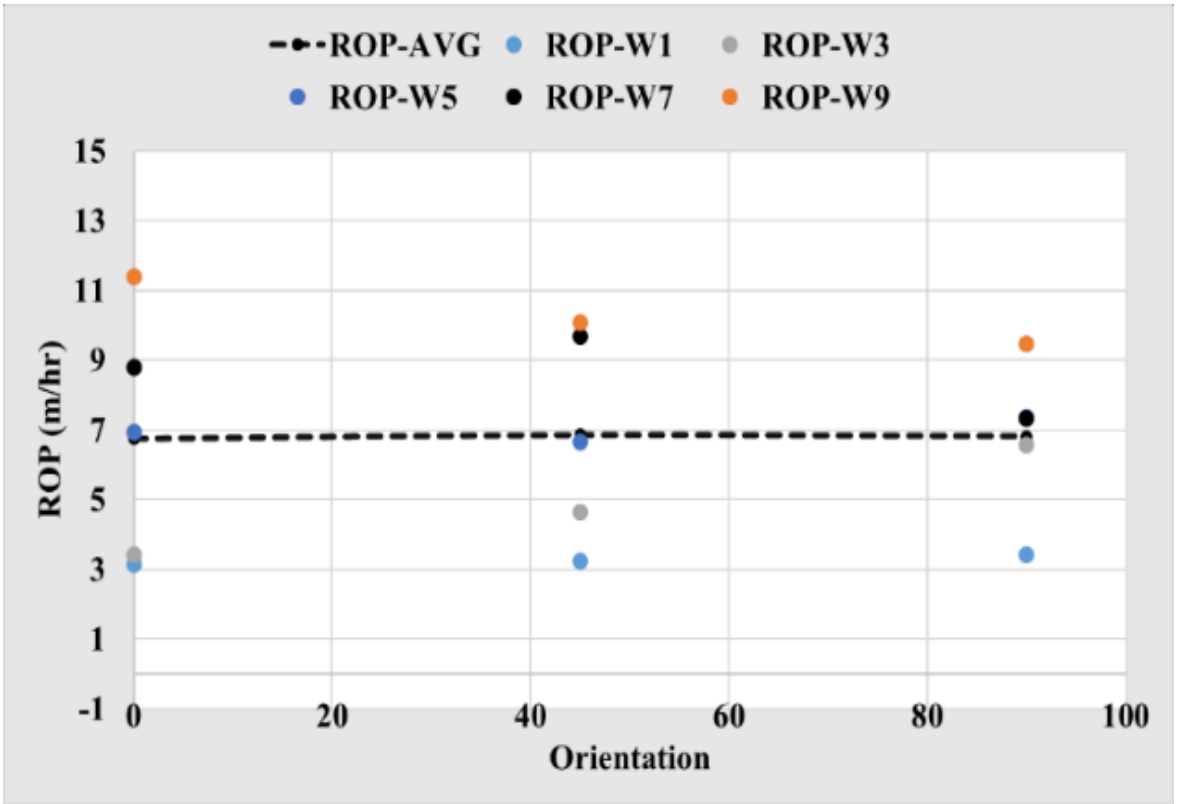

Figure 4-13. Result of ROP in drilling RLM samples in three orientations with increasing WOB. The ROP-average shows RLM isotropy

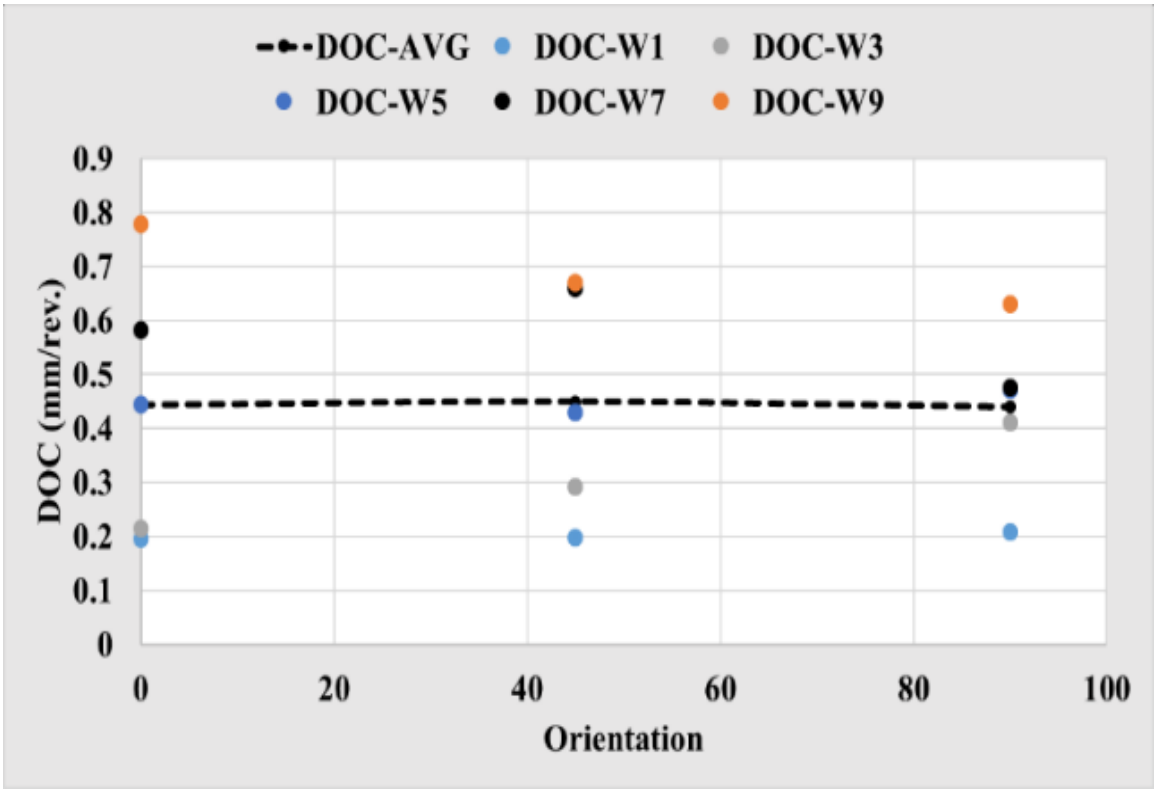

Figure 4-14. Result of DOC in drilling RLM samples in three orientations with increasing WOB. The DOC-average shows RLM isotropy

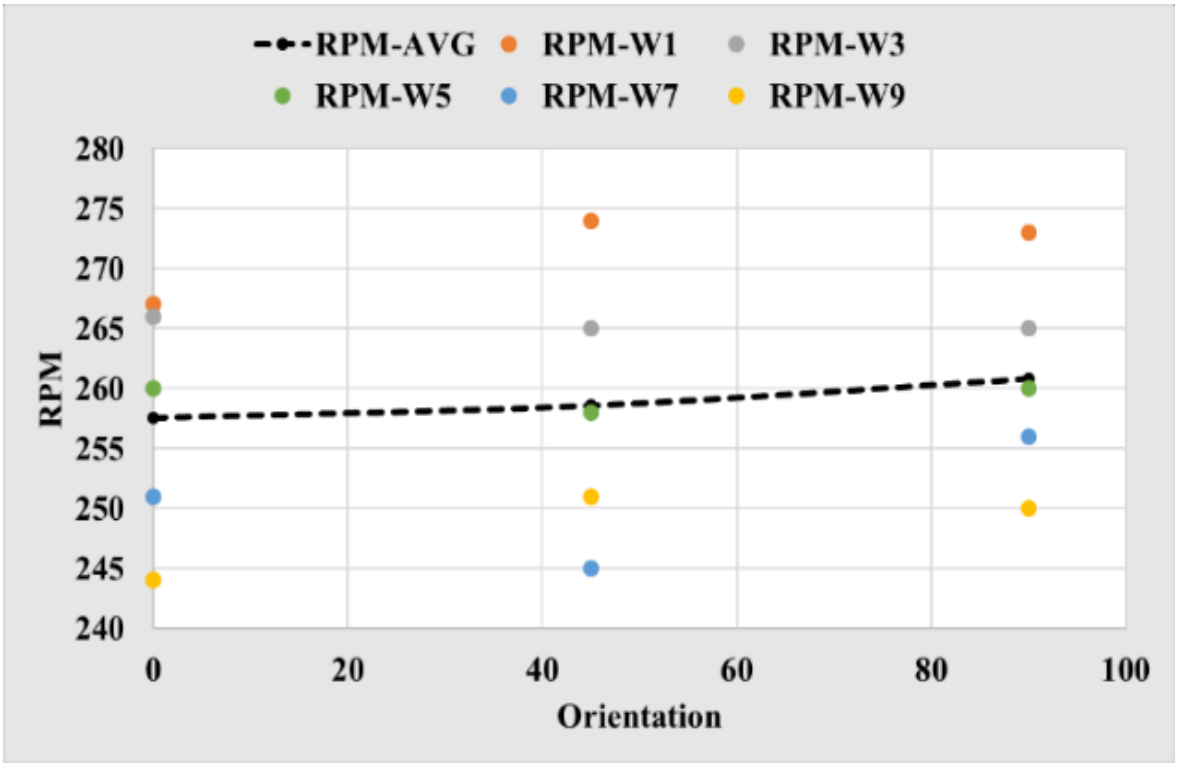

Figure 4-15. Result of rpm in drilling RLM samples in three orientations with increasing WOB. The rpm-average shows RLM isotropy

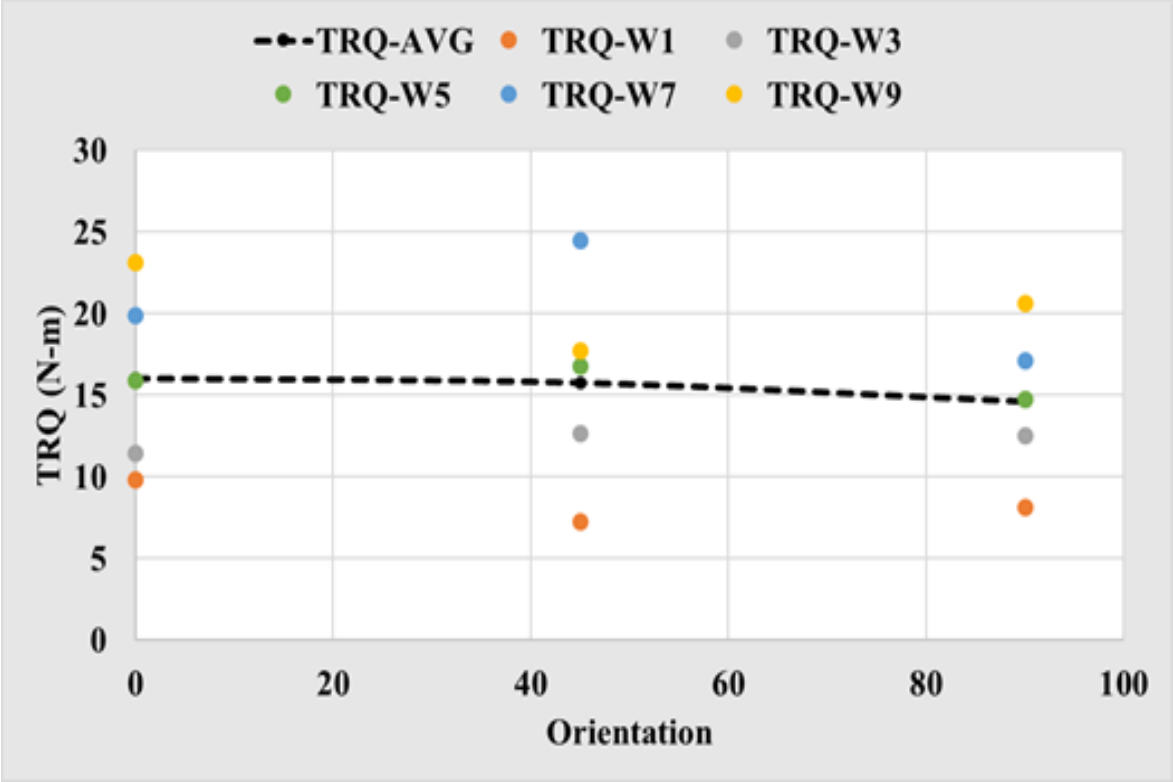

Figure 4-16. Result of ROP in drilling RLM samples in three orientations with increasing WOB. The ROP-average shows RLM isotropy

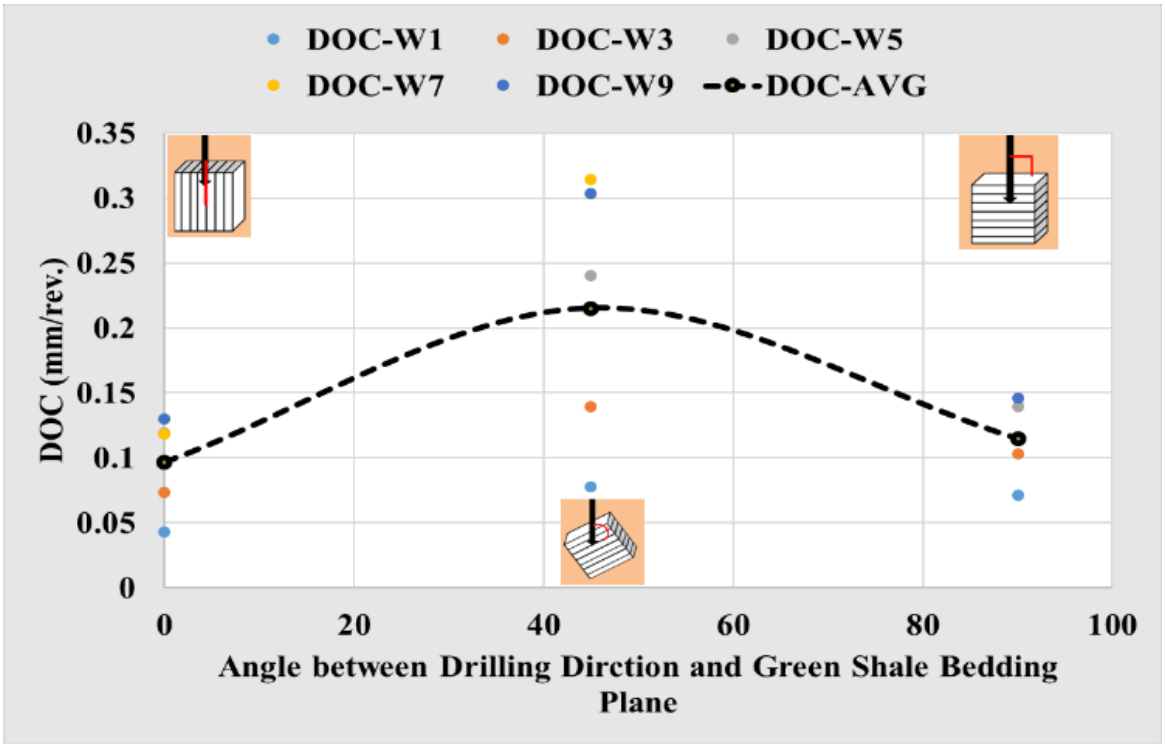

Figure 4-17. Result of DOC in drilling shale samples in three orientations with increasing WOB. The DOC-average shows shale anisotropy

4.6 Summary

This paper provides more detailed tests, particularly of physical and drilling tests performed on RLM and granite. Developed laboratory techniques in studying these rocks with respect to their anisotropy percentage is developed and added to the current procedures followed in evaluating rock anisotropy.

- The physical tests included in this paper involved a procedure of circular measurements of VP and VS. This procedure was applied on rock samples cored in different orientations (i.e. 0°, 45°, and 90°, representing vertical, oblique, and horizontal directions, respectively). Then circular measurements were taken on a circumference of each sample for detailed physical analysis.

- The circular VP and VS measurements confirmed the isotropy of RLM and granite and VTI of Red Shale.
- The mechanical tests involved only OUCS. The result of this test provided confirmation of RLM isotropy.
- The drilling experiments were also conducted using a newly developed procedure, which involved drilling in different orientations. Drilling parameters were studied and analyzed to further examine the rock anisotropy, including ROP, DOC, RPM, and Torque.
- In general, this paper describes the development of laboratory procedures for the physical, mechanical and drilling tests conducted on the same rock type and for same purpose of rock anisotropy evaluation provide a strong and collective set of data on which clearer decision of rock anisotropy can be made.

4.7 Future Work

- Conducting the developed testing techniques and procedures on more rock types for anisotropy evaluation under various conditions of pressure and loading rates.
- Including more drilling parameters such as drilling under flow pressure and involving confining pressure.

4.8 Acknowledgements

This work was done at the Drilling Laboratory Technology (DTL) at Memorial University of Newfoundland in St. John's, Canada. The project is funded by Atlantic Canada Opportunity Agency (AIF contract number: 781-2636-1920044), involving Husky Energy, Suncor Energy and Research and Development Corporation (RDC) of Newfoundland and Labrador. Financial

support is also provided by the Ministry of Higher Education and Scientific Research, Libya. Special thanks to DTL members for their help in laboratory work, in particular Abdlsalam Ihmoudah, Bashir Alrujbani and Peter Samaan.

4.9 References

1. Fjaer, E., Holt, R. M., Raaen, A. M., Risnes, R., and P. Horsrud, (2008). "*Petroleum Related Rock Mechanics*", (53), Elsevier.

2. Chang, C., Zoback, M.D., and Khaksar, A. (2006). "Empirical Relations between Rock Strength and Physical Properties in Sedimentary Rocks", Journal of Petroleum Science and Engineering, 51(3), pp.223-237.

3. Pan, R., Zhang, G., Li, S., An, F., Xing, Y., Xu, D., and Xie, R. (2016). "Influence of Mineral Compositions of Rocks on Mechanical Properties", the 50th us rock Mechanics / Geomechanics symposium, American rock mechanics association, Houston, TX, USA, 26-29 June 2016.

4. Friedman, M. (1976). "Porosity, Permeability, and Rock Mechanics - A Review", the 7th US Symposium on Rock Mechanics. American Rock Mechanics Association.

5. Abugharara, A.N., Alwaar, A.M., Butt, S.D., and Hurich, C.A. (2016). "Baseline Development on Rock Anisotropy Investigation Utilizing Empirical Relationships Between Oriented Physical and Mechanical Measurement and Drilling Performance", the 35th International Conference on Ocean, Offshore and Arctic Engineering, drilling Symposium, June 19-24, Busan, South Korea.

6. Abugharara, A.N., Alwaar, M.A., Hurich, A.C., and Butt, S.D. (2016) “Laboratory Investigation on Directional Drilling Performance in Isotropic and Anisotropic Rocks”, the 50th US Rock mechanics / Geomechanics Symposium, American Rock Mechanics Association, Houston, TX, USA, 26-29 June.

7. Tsidzi, K. (1997). “Propagation Characteristics of Ultrasonic Waves in Foliated Rocks”, International Association of Engineering Geology, (56), pp. 103-113.

8. Ramamurthy, T. (1993). “Strength and Modulus Responses f Anisotropic Rocks”, Compressive Rock Engineering, (1), pp.313-329, Pergamon press, Oxford.

9. Saroglou, H. and Tsiambaos, G. (2007). “Classification of Isotropic Rocks”, the 1th Congress of the international Society of Rock Mechanics, Taylor and Francis Group, London, ISPN 978-0-417-45084-3.

10. Abugharara, A. N., Hurich, C. A., Molgaard, J., and Butt, S. D. (2017). “Study of The Influence of Shale Anisotropy Orientation on Directional Drilling Performance in Shale”, Proceeding of the 36th International Conference on Ocean, Offshore and Arctic Engineering, drilling symposium, June 25-30, 2017, Trondheim, Norway.

11. ASTM Standard D2845. (2008). “Standard Test Method for Laboratory Determination of Pulse Velocities and Ultrasonic Elastic Constants of Rock,” ASTM International, West Conshohocken, PA, www.astm.org.

CHAPTER 5: LABORATORY INVESTIGATION ON DIRECTIONAL DRILLING PERFORMANCE IN ISOTROPIC AND ANISOTROPIC ROCKS

Abdelsalam N. Abugharara [a], PhD candidate

Abourawi M. Alwaar [a], Graduate Student

Charles A. Hurich [b], Associate Professor

Stephen D. Butt [a], Professor

[a] Drilling Technology Laboratory, Memorial University of Newfoundland, St. John's, NL, Canada A1B 3X5

[b] Department of Earth Sciences, Memorial University of Newfoundland, St. John's, NL, Canada A1B 3X5

This chapter is based on the objectives defined in section 1.3.3 and was presented at the 50th US Rock Mechanics / Geomechanics Symposium (ARMA) held in Houston, TX, USA, 26-29 June 2016.

5.1 Co-authorship statement

The contributions of this collaborative work are described in the following six parts. 1) Identification of research topic is collaborative between all co-authors. 2) Design of experiments are contributed by Abdelsalam Abugharara and the main supervisor Dr. S.D.Butt. 3) Preparation of cores and construction of ultrasonic and mechanical measurements are solely

contributed by Abdelsalam Abugharara. 4) Performance of drilling experiments is contributed by Abdelsalam Abugharara, 5) Data analysis and discussion of results is a collaborative work contributed by all co-authors, 6) Manuscript preparation is mainly contributed by Abdelsalam Abugharara, with revision assistance provided by all other coauthors.

5.2 Abstract

Successful drilling through shale with the optimal performance requires intensive research on controlled laboratory oriented drilling. The work of this paper is to evaluate oriented drilling, representing directional drilling in shale using a lab-scale drilling rig. Comparison study between drilling in shale and synthetic rock-like materials (RLM) of similar strength is included. The samples of shale and RLM were prepared to be characterized and drilled in different orientations (i.e. 0°, 45° and 90°) with respect to bedding for shale-samples and to the corresponding selected axis for RLM-samples. Physical measurements and mechanical tests were conducted to characterize the rocks and determine their anisotropy. Laboratory drilling experiments were performed using a 35mm dual-cutter PDC bit. Various weights on bit (WOB) were applied with constant water flow rate under atmospheric pressure. Drilling cuttings were collected and analyzed. Relationships between WOB, drilling rate of penetration (ROP), depth of cut (DOC), and drilling cutting size were determined. Results show increase of ROP and DOC with increasing WOB. Results also show that cutting sizes increase with the increase of WOB and they can exhibit the material anisotropy. Such result can assist in a better planning of drilling in shale to enhance drilling performance, especially in deviated wells.

5.3 Introduction

With the increasing interest by oil and gas companies in comprehensively understanding shale, in particular oil shale and shale gas as it plays an important role in unconventional reservoir exploration and production, intensive laboratory studies on shale come to play major role. Numerous laboratory studies have been focused on shale characterization and determining anisotropy % and type. However not much emphasis was put on relationships between drilling performance and rock anisotropy as function of bedding orientation. The work of this paper focuses on investigating shale anisotropy through oriented drilling and drill cuttings analysis with comparison to artificial rocks (RLM). Also, to evaluate drilling performance in both rock types.

An intensive work on RLM isotropy determination through multi-testing-methodologies was carried by Abugharara et al., 2016 reported that the tested RLM is isotropic rocks and was selected for further studies including the work of this paper.

Many field, laboratory, and numerical studies were conducted to study the physical and mechanical properties of the anisotropic rocks and the fracture modes and propagation. Alharthi, 1998 reported that most of sedimentary and metamorphic rocks show some degree of anisotropy. In general, shale is characterized to be anisotropic (Sodergeld and Rai, 2011).

Lashkaripour, 2000 and Crawford et al., 2012 indicated that shale strength is also anisotropic. In particular, the strength as mechanical property of shale and wave velocities of shale were investigated by Fjaer and Nes, 2013, Ambrose et al., 2014, Simpson el al, 2014, and Mighani et el., 2016. Those studies observed that shale strength estimated by UCS, CCS, and BTS is the highest perpendicular and parallel to bedding, but it decreases towards 45° and 30°. Wave

velocities, on the other hand are highest when propagating parallel to bedding, lowest when propagating perpendicular to bedding and medium when propagating in 45°.

Anisotropy and drilling ROP relationship was also investigated. Brown et al., 1981, Boualleg et al., 2007, Karfakis and Evers, 2007, Park and Min, 2013, and Thuro and Schormair, 2008 reported the influence of rock anisotropy on hole deviation tendency and drilling ROP. Thuro and Schormair, 2008 concluded using PFC2D that drilling progress and ROP are highest when drilling perpendicular to bedding and decreases with the decrease of the angle between bedding plane and drilling direction until reaching the lowest when drilling parallel to bedding. Altindag, 2003 reported that drilling ROP can be estimated by means of coarseness index and mean particle size, where Pfleider and Blake, 1953 indicated that a relationship between cutting size and shape with ROP was observed. However, as a main part of this paper, a new approach of a relationship between the ROP and cutting sizes as a function of rock anisotropy and rock orientation was investigated.

One of the latest studies that included intensive field and laboratory studies conducted by Drilling Technology Laboratory (DTL) at Memorial University of Newfoundland, Canada, started in 2014, also involved shale study.

In September 2014, DTL conducted drilling field trails during which three wells of about 120 m of each were drilled penetrating different shale formations. The formation dipping angle was about 12 deg. It was estimated before drilling through a comprehensive surface survey reported by Reyes et al., 2015. The drilling operation was rotary drilling and the drilling mode varied between conventional and vibrational drilling. Several types of drill bits including PDC, TSP and roller cone bits were used. The drilling performance was investigated as a function of

drill bit type, depth, penetrated formation type, drilling mode, etc. Collected drilling cuttings were analyzed. A geological cross-section of the drilling site was constructed.

For the laboratory studies, samples were cut from numerous shale rocks that were collected from an adjacent exposed formation in the drilling site that was estimated to be drilled in all wells after determining the dipping and the strikes of the formations and was confirmed by cutting analysis. Due to the challenge faced in obtaining shale core samples, a suggested method by Mele'ndez-Marti'nez, 2014 was followed to determine wave velocities for oriented samples and for physical characterization.

In general, samples of RLM and R-Shale were prepared, physically and mechanically characterized, and drilled in three main orientations (0°, 45° and 90°).

The data obtained by this analysis provides a direct link between standard approaches for assessing material anisotropy and the effects of anisotropy on drilling performance.

5.4 Experimental Equipment and Procedure

5.4.1 Physical Measurements

The main technique for measuring the physical properties practiced in this paper is the ultrasonic method. The objective of this is to evaluate the anisotropy structure of the tested material. Such physical anisotropy determination by the ultrasonic method can be analyzed with other anisotropy data obtained by mechanical tests (Sec. 2.3) and drilling experiments (Sec. 2.4). Compressional wave (Vp), and shear wave (Vs) velocities and densities were recorded for samples of different rock types before conducting the mechanical or drilling

experiments. The recorded waves were measured with respect to different orientations. Moreover, the dynamic elastic moduli of RLM were calculated according to ASTM D2845-08, 2008. Figure 5-1 shows the average recorded Vp, Vs, and measured density of RLM samples in three different directions. Figure 5-2 shows the dynamic elastic moduli of all tested samples of RLM. For RLM samples, the obtained Vp and Vs were about the same in all directions. This similarity in wave measurements can be taken as an indication of the isotropy of the tested RLM samples. Other mechanical measurements and drilling tests and cutting analysis support this observation.

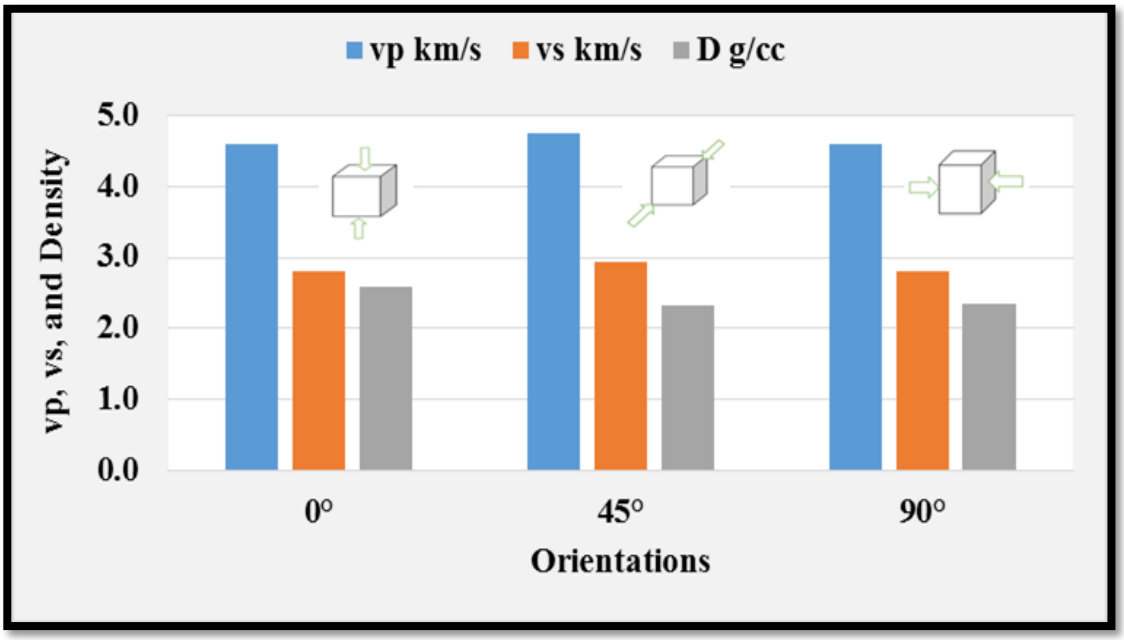

Figure 5-1. Oriented density and wave velocity measurements of RLM

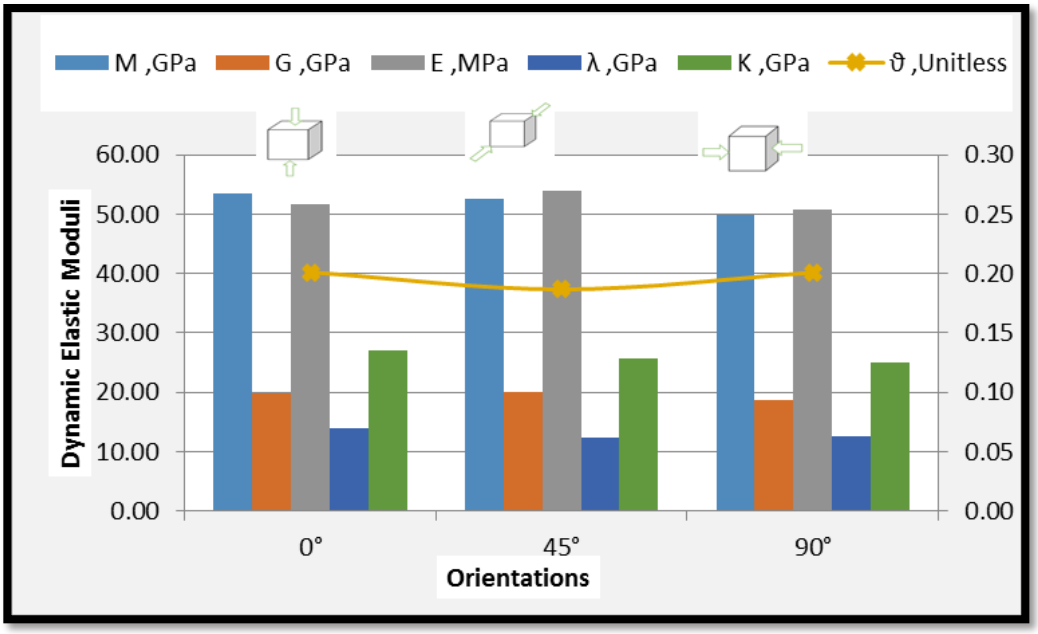

Figure 5-2. The oriented dynamic elastic moduli of RLM

Table 5.1 provides a summary of averaged measured values of Vp, Vs and Density of RLM. It also provides the mean values of RLM dynamic elastic moduli including M: Compressional wave Modulus, G: modulus of rigidity, ϑ: Poisson's ratio, K: bulk modulus, E: Young's modulus of elasticity, and λ: Lame's constant.

Table 5.1. Mean values of oriented Vp, Vs, density, and dynamic elastic moduli of RLM

Orientation	vp	vs	D	M	G
	km/s	km/s	g/cc	GPa	GPa
0°	4.60	2.80	2.58	53.54	19.83
45°	4.76	2.94	2.32	52.55	20.09
90°	4.60	2.81	2.35	49.85	18.65
Orientation	ϑ	K	E	λ	
	Unitless	GPa	MPa	GPa	
0°	0.20	27.10	51.62	13.88	
45°	0.19	25.76	53.94	12.37	
90°	0.20	24.99	50.88	12.56	

Wave velocities were also determined for R-Shale samples in the three orientations. However, due to limited samples of shale, the dynamic elastic constants will be conducted on more samples for future work for accuracy and confirmation. In the meantime, the wave velocities exhibit the anisotropy of R-Shale samples. Figure 5-3and Figure 5-4 show the recorded Vp and Vs and the measured density of two sets of R-Shale samples.

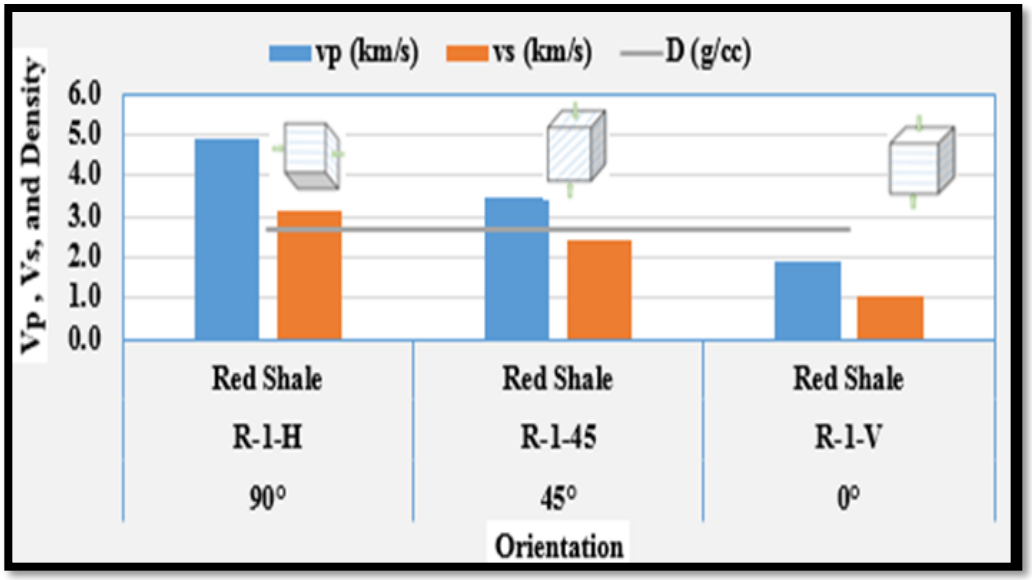

Figure 5-3. Oriented density and wave velocity measurements of R-Shale-1

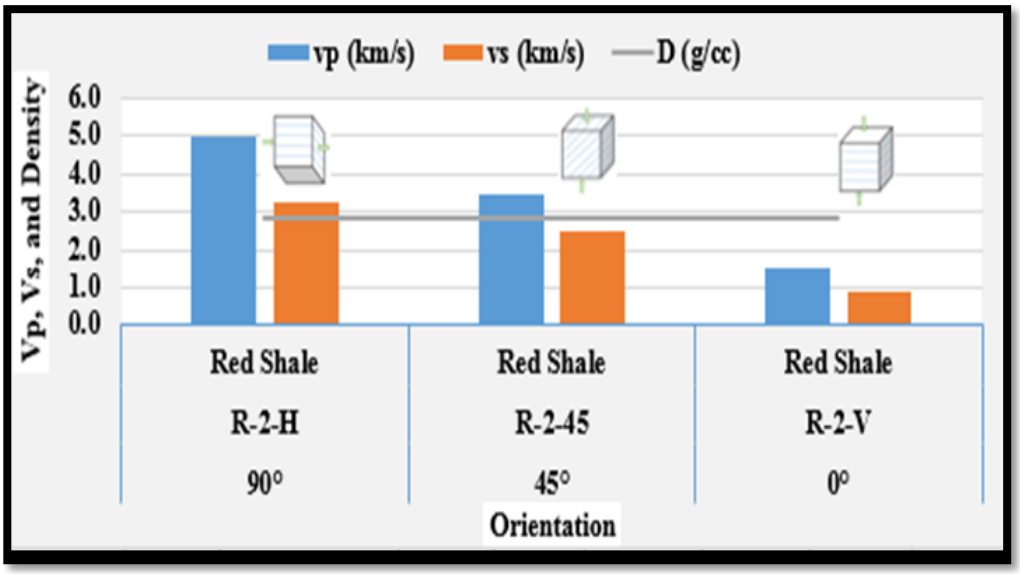

Figure 5-4. Oriented density and wave velocity measurements of R-Shale-2

Table 5.2 summarizes the mean values of Vp, Vs, and density of R-Shale samples.

Table 5.2. Mean values of oriented Vp, Vs, and density of two R-Shale samples 1, and 2, respectively

Orientation	Spec.#	vp (km/s)	vs (km/s)	D (g/cc)
90°	R-1-H	4.92	3.16	2.71
45°	R-1-45	3.49	2.45	2.71
0°	R-1-V	1.89	1.05	2.71
90°	R-2-H	5.01	3.22	2.81
45°	R-2-45	3.49	2.45	2.81
0°	R-2-V	1.48	0.87	2.81

For evaluating the Transversely Isotropy (TI) of R-Shale, multi measurements were taken on several R-Shale samples that were cut from same larger rock. Most of the measurements were taken parallel to bedding to confirm the shale Vertically Transversely Isotropy (VTI). The measured Vp and Vs in directions parallel to bedding of R-Shale in various locations are summarized in Table 5.3. Figure 5-5 shows all values of Vp and Vs measured parallel to R-Shale bedding in various positions on parallel faces and the mean values of Vp and Vs, top and bottom; respectively. Figure 5-6 shows the tested R-Shale samples and the positions of the measurements.

Table 5.3. All and mean values of the measured Vp and Vs of several R-Shale samples in directions parallel to bedding in various locations

Spec.#	Spec. rock type	Faces set #	All values		Mean values	
			Vp	Vs	Vp	Vs
			(km/sec)		(km/sec)	
R-Shale-1	H1-1'	1-1'	4.93	3.19	4.86	3.16
	H2-2'	1-1'	4.93	3.25		
	H3-3'	1-1'	4.79	3.08		
	H4-4'	1-1'	4.79	3.13		
R-Shale-2	H1-1'	1-1'	5.14	3.18	4.86	3.11
	H2-2'	1-1'	4.61	3.04		
	H3-3'	1-1'	4.61	3.04		
	H4-4'	2-2'	4.94	3.14		
	H5-5'	2-2'	4.94	3.14		
	H6-6'	2-2'	4.94	3.14		
R-Shale-3	H1-1'	1-1'	4.84	3.19	4.87	3.19
	H2-2'	1-1'	4.84	3.26		
	H3-3'	1-1'	4.84	3.26		
	H4-4'	2-2'	4.97	3.07		
	H5-5'	2-2'	4.86	3.16		
	H6-6'	2-2'	4.86	3.21		

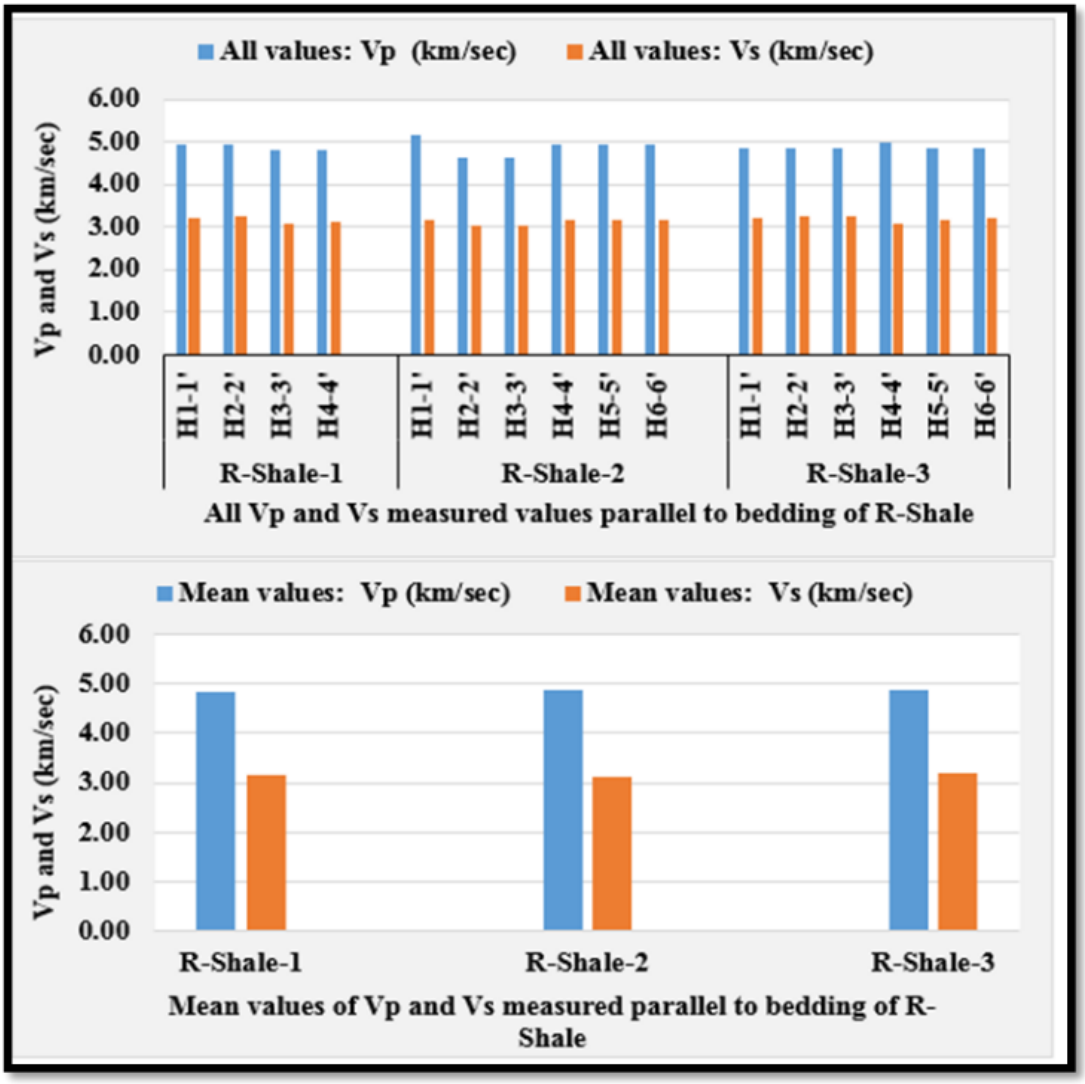

Figure 5-5. All and mean values of Vp and Vs measured in parallel direction to R-Shale bedding

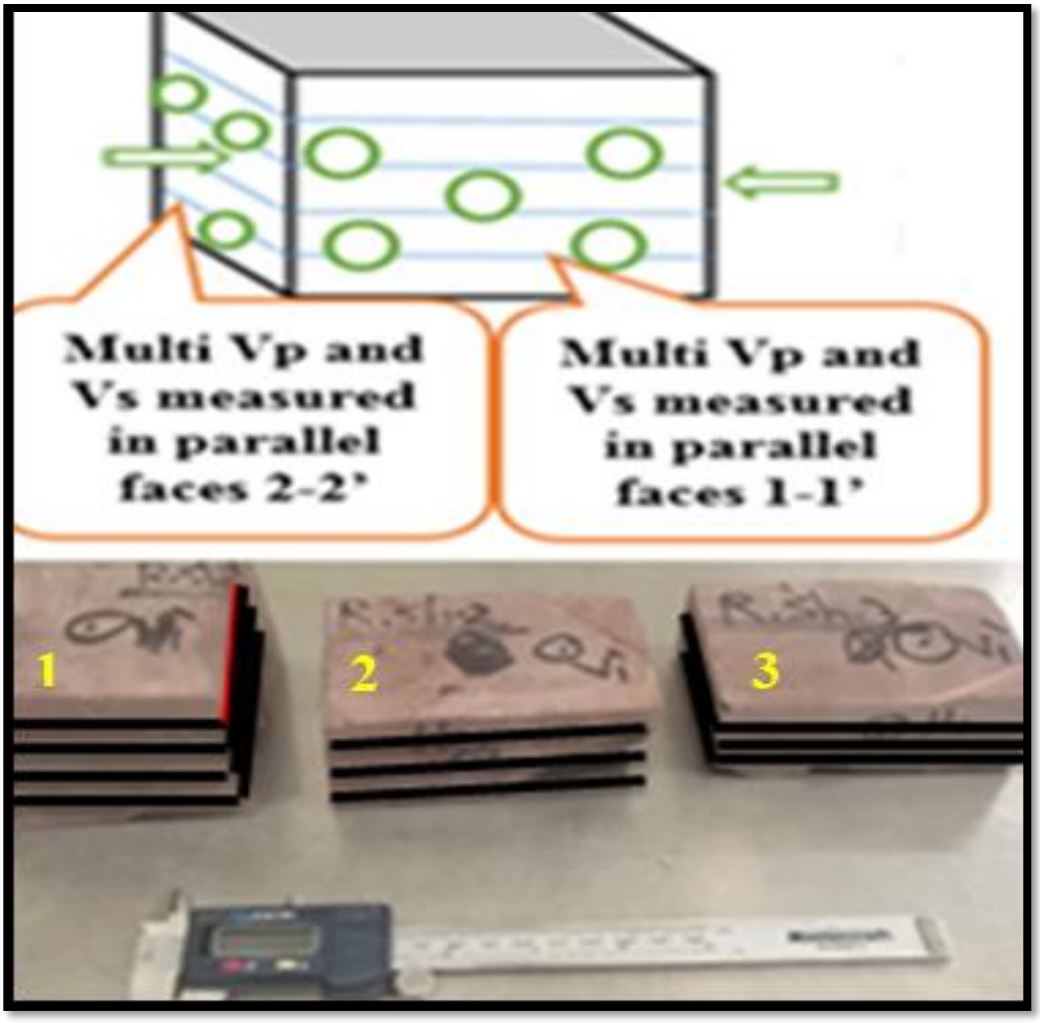

Figure 5-6. Multi measurements of Vp and Vs in two sets of parallel faces in parallel direction to R-Shale bedding to ensure horizontal layers of shale.

5.4.2 Mechanical Measurements

For RLM samples, the indirect (disk splitting) tensile test according to ASTM D3967-08, 2008 was performed to estimate the tensile strength (σt). The test was conducted on disks cut from ~ 2 inch cylindrical specimens cored in different orientations. Figure 5-7 shows the average values of the tensile strength (σt) of RLM in the three denoted orientations.

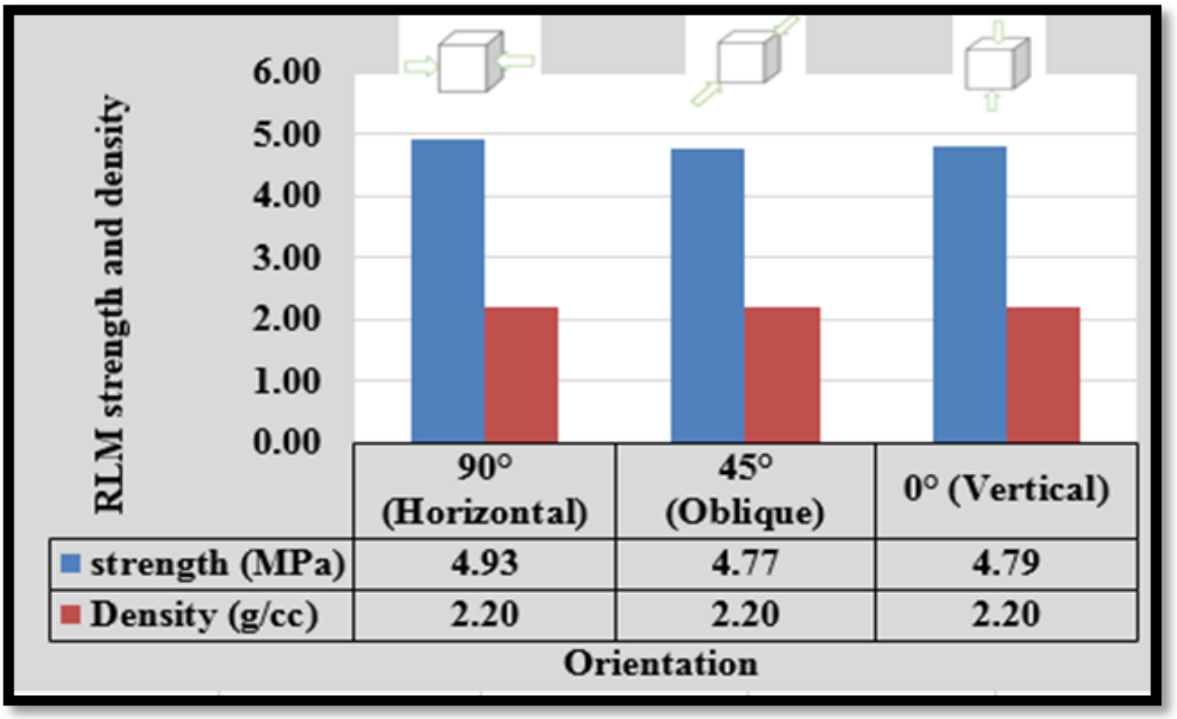

Figure 5-7. Mean values of oriented (σt) of RLM by splitting test

Figure 5-8 shows the RLM disks in different orientations before and after splitting cut from ~ 2 inch samples cored from 4 inch RLM cylinders as source of the disks, and the splitting apparatus (Modified point load apparatus). The average σt values of ~ 4.8 MPa was obtained in all orientations.

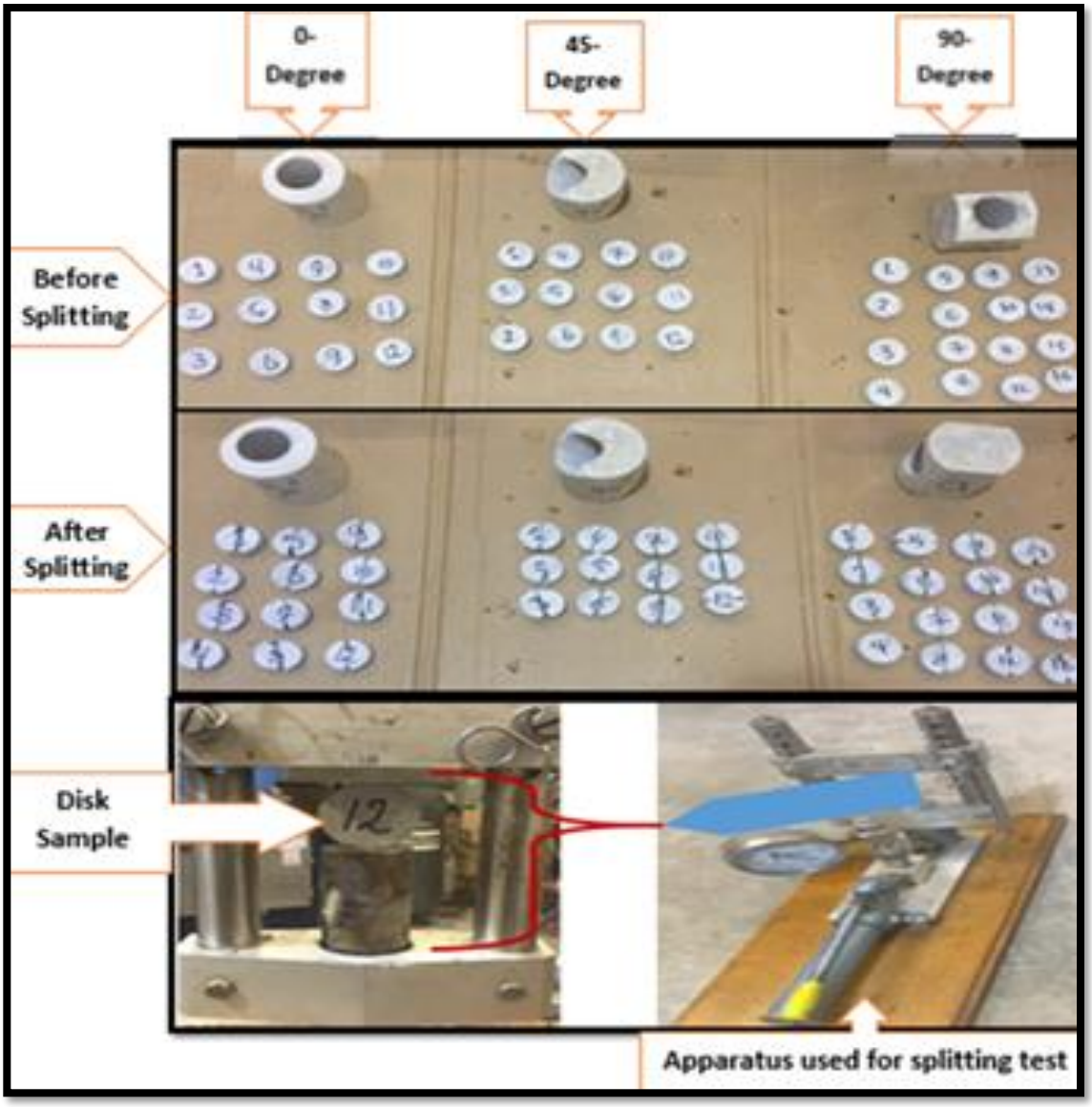

Figure 5-8. RLM samples before and after testing with splitting test apparatus

For R-Shale, the point load index (PLI) test was performed on irregular lump samples following ASTM D5731-08, 2008. The samples were tested only vertically as a result of difficulties associated with obtaining samples in other orientations to perform this test. Figure 5-9 shows R-Shale samples for the physical characterization and for point load index test in tow states; before and after failure, respectively.

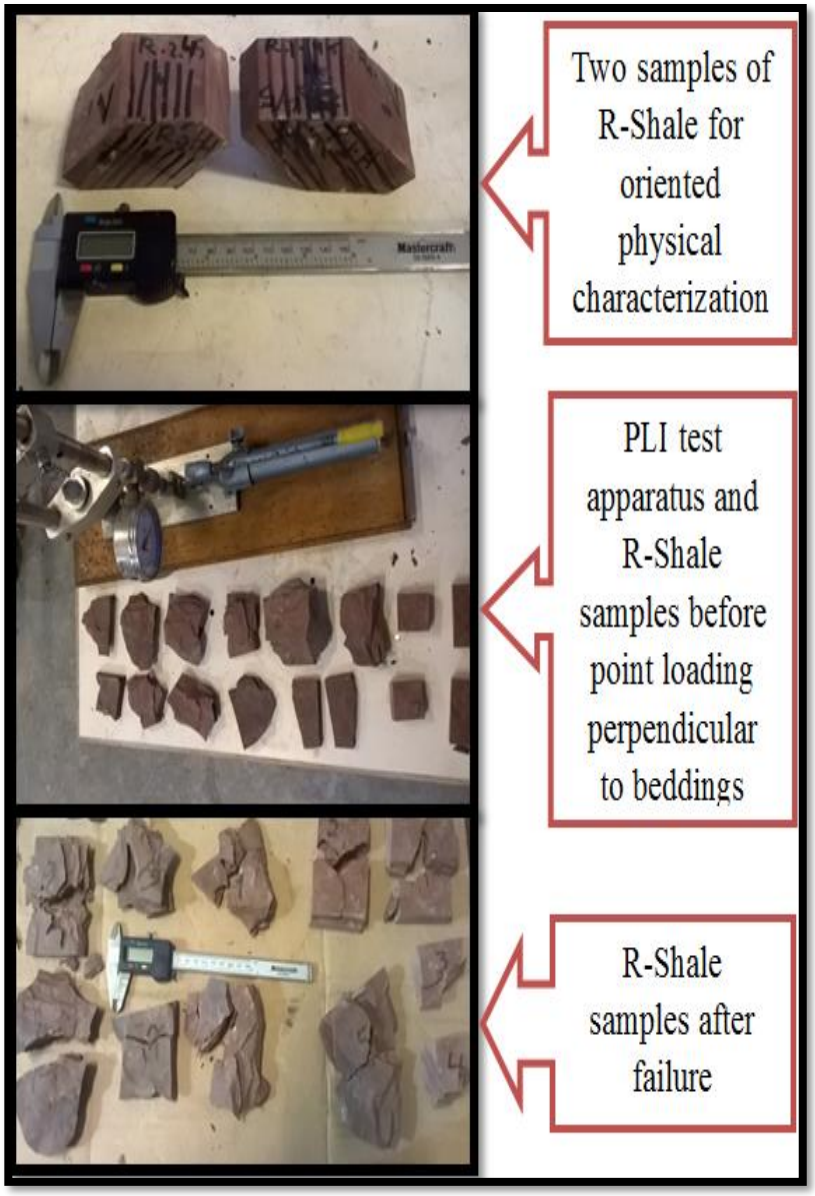

Figure 5-9. R-Shale samples for oriented physical characterization and point load test

Table 5.4 contains the estimated UCS values of R-Shale samples obtained by point load perpendicularly to bedding. The mean value of the PLI = 2.7 MPa.

Table 5.4. Summary of PLI test values of R-Shale samples

Result of PLI test conducted on R-Shale samples perpendicular to beddings						
Ref.	**Orientation**	**Test type**	**Is**	**UCS**	**Is avg**	**UCS avg**
1	Vertical "0º "	Lump	4.03	88.72	2.68	58.87
2			3.13	68.84		
3			2.47	54.36		
4			3.38	74.29		
5			1.53	33.72		
6			1.60	35.16		
7			2.18	48.02		
8			3.16	69.46		
9			2.60	57.22		

5.4.3 Laboratory Drilling Experiments

5.4.3.1 Laboratory Drilling Apparatus

Laboratory drilling experiments were performed using a lab- scale drill rig shown in figure (10). The drill bit used was a 35 mm dual cutter PDC bit. The drilling tests were conducted under atmospheric pressure. The water flow rate of 18 L/min was utilized to clean-off the drilled hole and to remove the cuttings towards the cutting collection system.

Figure 5-10. Laboratory drilling simulator conventional drill rig

5.4.3.2 RLM and R-Shale Samples Preparation for Drilling Experiments

RLM samples were cast in one direction (vertical direction). They were cut in three directions and drilled accordingly afterwards. On the other hand, as the R-Shale samples are laminated

structure they are weak and easy to split when being drilled, in particular when cut into small samples. To avoid splitting R-Shale, the cut samples were stabilized by casting them in cement. Hence, the samples were drilled afterwards according to the desired orientation. Figure 5-11 and Figure 5-12 show the R-Shale and RLM samples after drilling in different orientations, respectively.

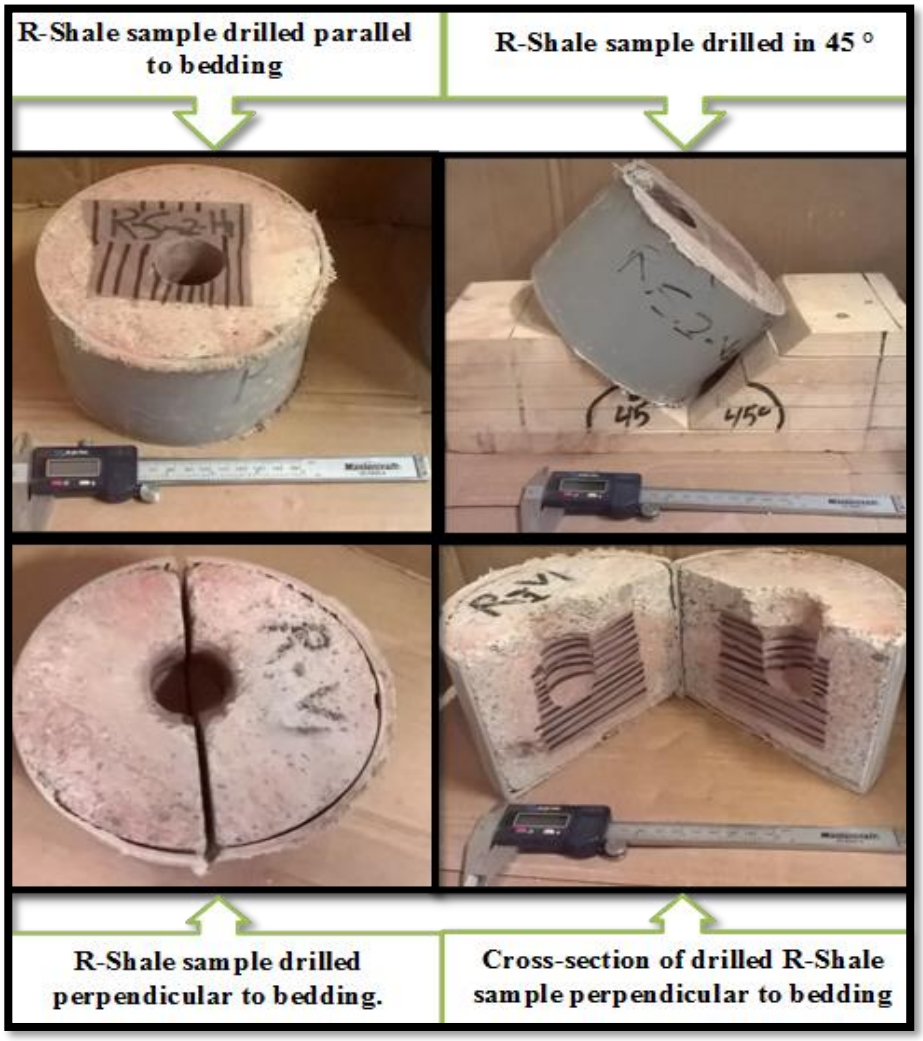

Figure 5-11. RLM and R-Shale samples after drilling in different orientations

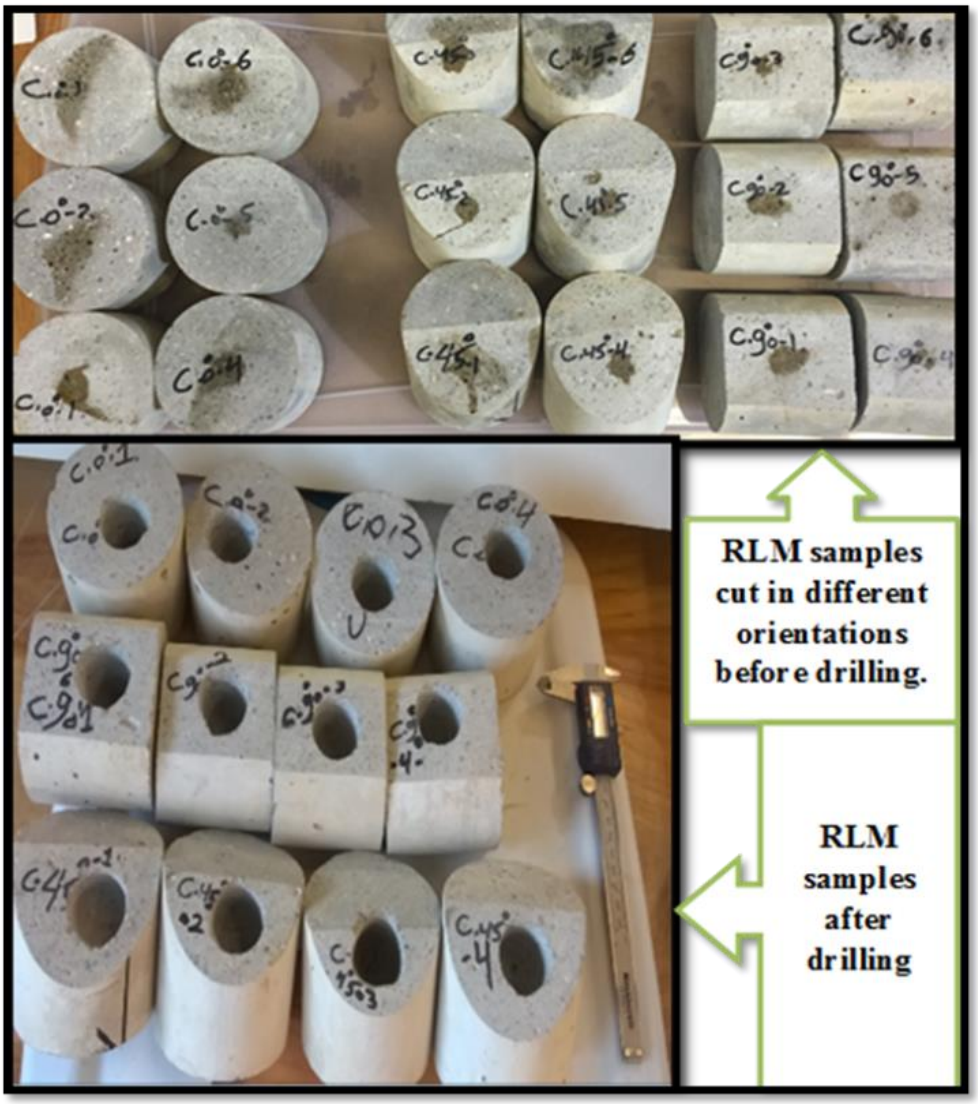

Figure 5-12. RLM samples before and after drilling

5.4.3.3 Drilling Cuttings' Collection

While drilling, a 75µ-m (0.0030 inch) sieve was used. Cutting samples of all drilled RLM and R-shale samples in the designated orientations were collected. A standard pre-sieving procedure for drying was followed. Two main points to consider here were emphasized in the

literature review related to cutting analysis. First, the cutting size increases with the increase of the ROP. Second, the relationship between ROP and cutting size should be the same in all directions when drilling an isotropic material (i.e. RLM) and varies when drilling an anisotropic material (i.e. R-shale). The obtained result of drilling cuttings analysis (Sec. 3.1.2) supported this. Drilling an isotropic material is orientation independent. However, drilling in R-Shale is orientation dependent. Therefore, achieving high ROP in drilling in shale may require selection of the best orientation as well trajectory. Figure 5-13 shows the cutting samples and cutting sieving apparatus.

Figure 5-13. Cutting samples and cutting sieving apparatus

5.5 Laboratory Experiments Results

5.5.1 Drilling Performance

During drilling, different sensors were used to measure various drilling parameters including a laser sensor to measure axial vibration to evaluate the bit-rock interaction and LVDT to measure drill bit displacement. A DAQ system utilizing LabVIEW was used to record data while drilling. ROP and DOC were calculated and plotted as a function of static WOB.

5.5.1.1 WOB vs. ROP and DOC

To provide WOB, several steel plates are used to feed the suspended weight. Relationships between WOB vs. ROP and DOC were constructed as a function of well trajectory represented by drilled samples bedding orientations. Summary of WOB, calculated ROP, and DOC is displayed in Table 5.5.

Table 5.5. Drilling parameters of WOB, ROP and DOC for RLM and R-Shale

Rock Type	Rotation	Drilling Flow Rate ~ 18 (L/min)					
RLM	0°	WOB(kg)	75.00	108.61	142.23	175.85	209.46
		ROP (m/hr)	2.55	6.35	9.53	7.49	8.35
		DOC (mm/rev)	0.19	0.50	0.80	0.50	0.67
RLM	45°	ROP (m/hr)	3.63	5.44	14.42	6.35	9.98
		DOC (mm/rev)	0.28	0.43	1.01	0.46	0.68
RLM	90°	ROP (m/hr)	3.63	6.60	7.56	7.71	8.29
		DOC (mm/rev)	0.23	0.50	0.53	0.54	0.58
R-Shale	0°	ROP (m/hr)	5.13	7.68	11.49	14.48	20.54
		DOC (mm/rev)	0.35	0.52	0.77	0.97	1.38
R-Shale	45°	ROP (m/hr)	2.06	2.40	3.39	5.55	11.03
		DOC (mm/rev)	0.16	0.18	0.24	0.39	0.76
R-Shale	90°	ROP (m/hr)	3.43	3.43	7.01	10.44	17.12
		DOC (mm/rev)	0.23	0.23	0.47	0.70	1.15

The revolutions per minute (RPM) were determined by using the laser sensor. The recorded data at the final stage as plotted in Figure 5-14 shows the relationships between WOB and ROP as s function of orientation of RLM (top) and R-Shale (bottom).

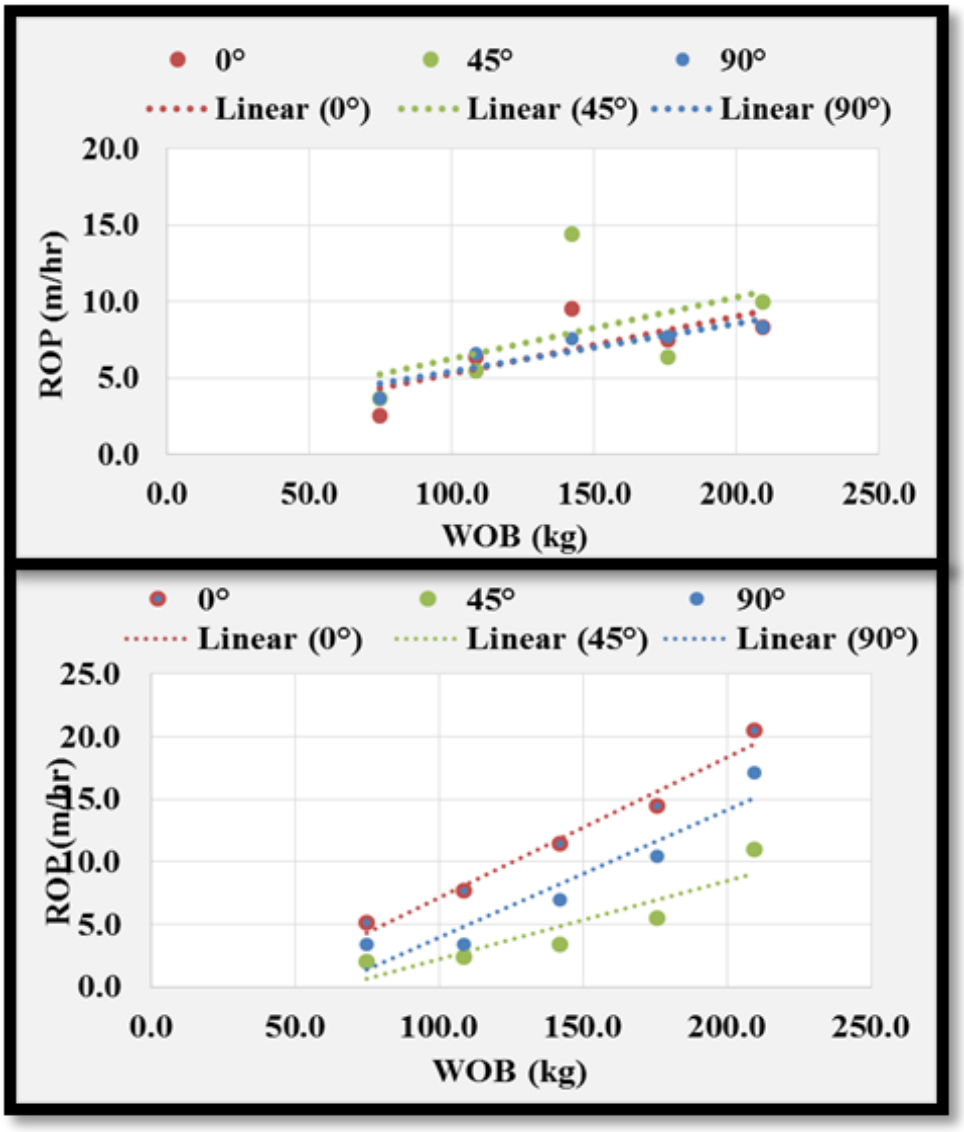

Figure 5-14. Oriented relationship between WOB and ROP of RLM (top) and R-Shale (bottom)

5.5.1.2 Cutting Size Analysis

The collected cuttings were in small volumes; however, most of the sieving analysis procedure was according to ASTM C136/C136M-14, 2014. The set of sieves used in cutting analysis included the following mesh sizes in mm:

0.85, 0.63, 0.59, 0.42, 0.25, 0.212, 0.177, 0.166, 0.15, 0.09, and 0.075

The results of the cutting analysis can be summarized as follows:

- For RLM, the cutting size distribution in % follows same trend when drilling in different orientations. Such matching in size distribution confirms the anisotropy of the drilled rocks.
- Similar matching trends were noticed in low WOB: (W1=75kg) as well as in high WOB: W9=209 kg.
- Drilling in RLM as an isotropic rock is orientation independent. Figure 5-15 (top and bottom) shows the distribution of cuttings collected from drilling RLM.
- For R-Shale, the cutting size distribution in % follows same trend when drilling in different orientations. Such matching in size distribution confirms the anisotropy of the drilled rocks.
- Such mismatching trends were noticed in low WOB: (W1=75kg) and in high WOB: W9=209 kg.
- Drilling in R-Shale as an anisotropic rock is orientation dependent. Figure 5-16 (top and bottom) shows the distribution of cuttings collected from drilling R-Shale.

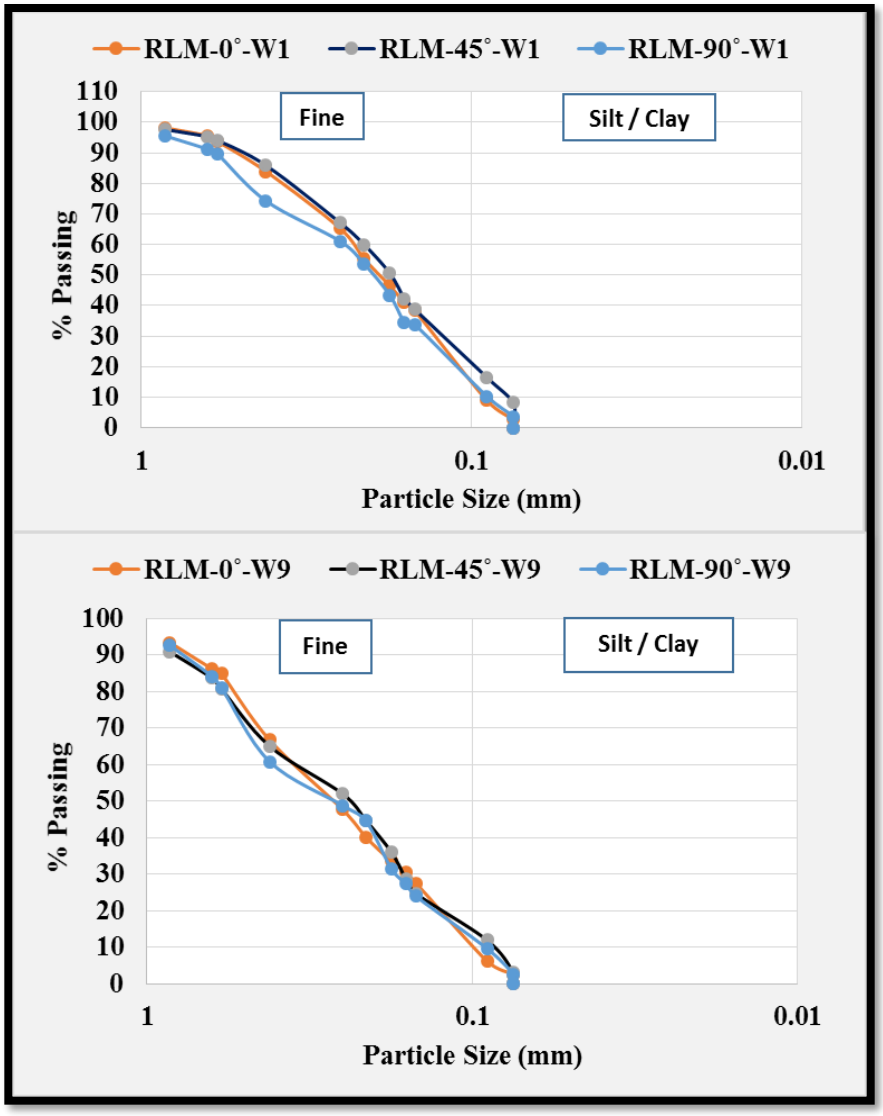

Figure 5-15. Cutting size analysis with the increase of WOB in drilling RLM in the three orientations 0º, 45º, and 90º. Figures show matching distribution confirming isotropy of RLM

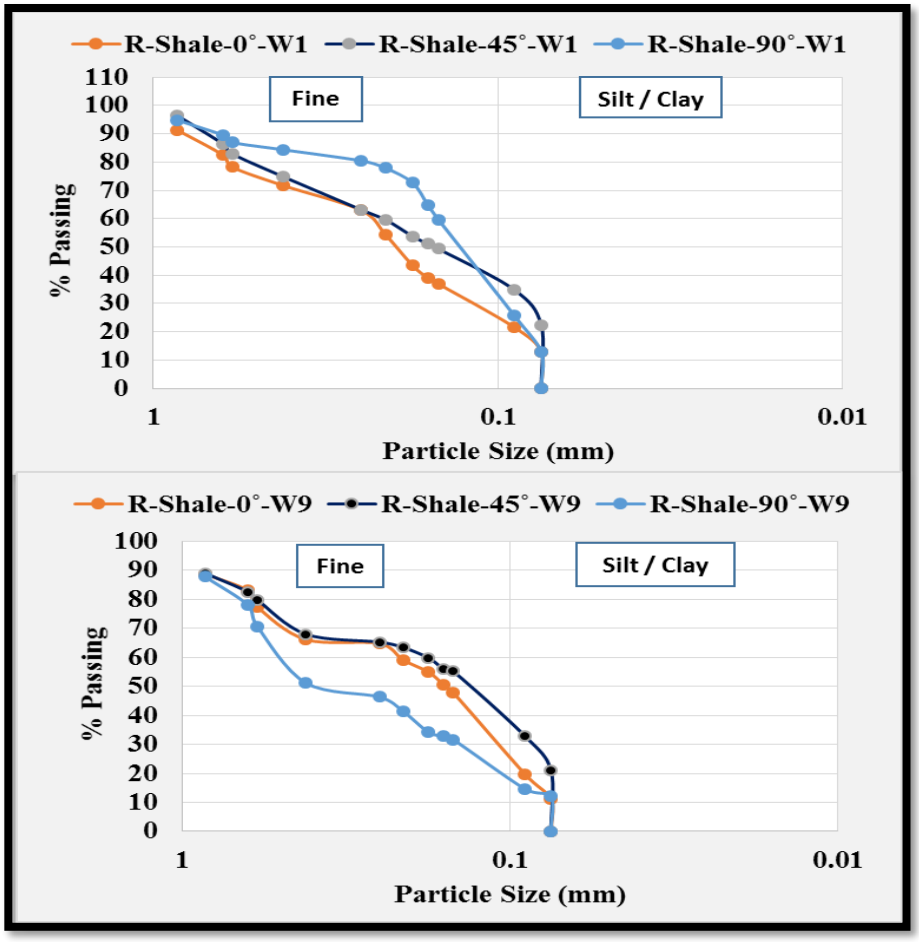

Figure 5-16. Cutting size analysis with the increase of WOB in shale drilling in the three orientations 0º, 45º, and 90º. Figures show mismatching distribution confirming shale anisotropy

5.6 Conclusion

Several physical and mechanical measurements and drilling tests were conducted as work of this paper. Conclusions of those measurements and tests are summarized as follows:

- Physical measurements using ultrasonic method conducted on RLM showed material isotropy, where same applied measurements conducted on R-shale showed material anisotropy.

- In particular, beside R-shale anisotropy exhibition, oriented Vp and Vs through R-shale in three different angles in couple samples exhibited special anisotropy of Vertically Transversely Isotropy (VTI). Investigation of such VTI has started using more angles representing more orientations of cores and cupped shaped samples will be reported in future publications.
- However, multi Vp and Vs measurements have been taken in parallel direction to R-Shale's bedding and showed same values of VTI.
- Mechanical measurements through indirect tensile tests conducted on disks cut from cylindrical samples cored in different orientations of RLM showed the RLM isotropy. Where PLI test was only conducted in perpendicular direction to R-shale bedding represents R-shale strength in this direction. R-shale strength determination in other directions to be conducted for R-shale anisotropy or VTI confirmation are under investigation and will be reported in future publications.
- Laboratory drilling experiments were conducted under constant water flow rate and rotary speed under atmospheric pressure. Recorded data of drill bit travel; bit-rock interaction through axial motion and vibration, as well as the actual rpm while drilling were all recorded by utilizing precise sensors. Such obtained data assists in calculating ROP and DOC. ROP and DOC are plotted against WOB.
- ROP, DOC, as well as the cutting size % obtained from RLM exhibit same trend with respect to orientations confirming the isotropy of RLM.
- ROP, DOC, and the cutting size % obtained from R-Shale exhibit various trends with respect to different orientations proposing R-Shale anisotropy.

5.7 Future Work

- More samples cut in various orientations, longer drilling intervals under various conditions of pressure and flow rates, and larger quantity of cuttings will be considered for larger window of data recording and analysis.
- An expanded study on more new shale types of grey and green shale will be included.
- More tests will be conducted under pressurized conditions through which the rock behavior as a function of anisotropy and orientation will be investigated and reported. Also, wave velocities propagating through isotropic and anisotropic samples while loading and applying confining pressure will be monitored, investigated and reported.

5.8 Acknowledgement

This work was done at DTL at Memorial University of Newfoundland in St. John's, Canada. The project is funded by Atlantic Canada Opportunity Agency (AIF contract number: 781-2636-1920044), involving Husky Energy, Suncor Energy and Research and Development Corporation (RDC) of Newfoundland and Labrador. Financial support is also provided by the Ministry of Higher Education and Scientific Research-Libya.

5.9 References

1. Abugharara, A. N., Alwaar, A. M., Butt, S. D., and Hurich, C. A. (2016). Baseline development on rock anisotropy investigation utilizing empirical relationships between oriented physical and mechanical measurement and drilling performance. Proceeding of the

ASME 2016, 35th International Conference on Ocean, Offshore and Arctic Engineering, drilling symposium, OMAE2016, June 19-24, 2016, Busan, South Korea.

2. Al-Harthi, A. A. (1998). Effect of planar structures on the anisotropy of Ranyah sandstone, Saudi Arabia: Engineering Geology, 50, no. 1-2, 49-57, HTTP://DX.DOI.ORG/10.1016/S0013-7952(97)00081-1.

3. Sondergeld, C.H., and Rai, C.S. (2011). Elastic anisotropy of shale: The leading Edge, 30, 324-331, http://dx.doi.org/10.1190/1.3567264.

4. Ajalloeian, R., and Lashkaripour, G.R. (2000). Strength anisotropies in mudrocks: Bulletin of Engineering Geology and the Environment, 59, no. 3,195-199, http://dx.doi.org/10.1007/s100640000055.

5. Crawford, B. R., and DeDontney, N.L. (2012). Shear strength anisotropy in fine-grained rocks. American Rock Mechanics Association, the 46th U.S. Rock Mechanics/Geomechanics Symposium, ARMA, 12-290.

6. Fjçr, E., and Nes, O.-M. (2013). Strength anisotropy of Mancos shale. American Rock Mechanics Association, the 47th US Rock Mechanics/Geomechanics Symposium in San Francisco, CA, USA, 23-26 June 2013.

7. Ambrose, J., Zimmerman, R. W., and Suarez-Rivera, R. (2014). Failure of shales under triaxial compressive stress. American Rock Mechanics Association, the 48th US Rock Mechanics/Geomechanics Symposium in Minneapolis, MN, USA, 1-4 June 2014.

8. Simpson, N. D. J., Stroisz, A., Bauer, A., Vervoort, A., and Holt, R. M. (2014). Failure mechanics of anisotropic shale during Brazilian tests. American Rock Mechanics Association,

the 48th US Rock Mechanics/Geomechanics Symposium in Minneapolis, MN, USA, 1-4 June 2014.

9. Mighani, S., Sondergeld, C. H., and Rai, C. S. (2016). Observations of tensile fracturing of anisotropic rocks. Society of Petroleum Engineers. SPE Journal, doi:10.2118/2014-1934272-PA

10. Brown, E.T., Green,S.J., and Sinha, K.P. (1981). The influence of rock anisotropy on hole deviation in rotary drilling- A review. Int. J. Rock Mech. Min. Sci. and Geomech. Abstr. Vol. 18, pp.387 to 401, 1981, United Kingdom.

11. Boualleg, R., Sellami, H., Rouabhi, A., Menand, S., and Simon, C. (2007). Effect of rocks anisotropy on deviation tendencies of drilling systems. 11th Congress of the International Society for Rock Mechanics, pp. 1221-1224. Tylor and Francis Group, London, ISBN: 978-0-415-45084-3.

12. Karfakis, M.G., and Evers, J.F. (1987). Technical Note: Effects of rocks lamination anisotropy on drilling penetration and deviation. Int. J. Rock Mech. Min. Sci. and Geomech. Abstr. Vol. 24, pp.371-374, 1987, United Kingdom.

13. Park, B., & Min, K.-B. (2013). Discrete element modeling of transversely isotropic rock. American Rock Mechanics Association, the 47th US Rock Mechanics/Geomechanics Symposium in San Francisco, CA, USA, 23-26 June 2013.

14. Thuro, K and Schormair, N. (2008). Fracture propagation in anisotropic rocks during drilling and cutting, Geomechanics and Tunnelling, Volume 1, Issue 1, PP. 8–17, 2008.

15. Altindag, R. (2003). Estimation of penetration rate in percussion drilling by means of coarseness index and mean particle size. Rock Mechanics and Rock Engineering. 36(4):323-332.

16. Pfleider, E. and Blake, R.L. (1953). Research on the cutting Cutting Action of the Diamond Drill Bit. Mining Eng. 5: 187-195.

17. Reyes, R., Kyzym, I., Rana, P. S., Molgaard, J., and Butt, S.D. (2015). Cuttings analysis for rotary drilling penetration mechanisms and performance evaluation. American Rock Mechanics Association, the 49th US Rock Mechanics/Geomechanics Symposium in San Francisco, CA, USA, 28 June -1 July 2015.

18. Mele'ndez-Marti'nez, J. (2014). Elastic properties of Sedimentary rocks, Edmonton, AB: University of Alberta.

19. ASTM D2845. (2008). Standard test method for laboratory determination of pulse velocities and ultrasonic elastic constants of rock, ASTM International, West Conshohocken, PA, 2008, www.astm.org.

20. ASTM D3967. (2008). Standard test method for splitting tensile strength of intact rock core specimens, ASTM International, West Conshohocken, PA, 2008, www.astm.org.

21. ASTM D5731. (2008). Standard test method for determination of the point load strength index of rock and application to rock strength classifications, ASTM international, West Conshohocken, PA, 2014, www.astm.org.

22. ASTM C136/C136M. (2014). Standard test method for sieve analysis of fine and coarse aggregates, ASTM international, West Conshohocken, PA, 2014, www.astm.org.

CHAPTER 6: EXPERIMENTAL INVESTIGATION OF THE EFFECT OF SHALE ANISOTROPY ORIENTATION ON THE MAIN DRILLING PARAMETERS INFLUENCING ORIENTED DRILLING PERFORMANCE IN SHALE

Abdelsalam Abugharara [a], PhD candidate

Bashir Mohamed [a], Graduate student

Charles Hurich [b], Associate professor

Jone Molgaard [c], Professor

Stephen D. Butt [a], Professor

[a] Drilling Technology Laboratory, Memorial University of Newfoundland, St. John's, NL, Canada A1B 3X5

[b] Department of Earth Sciences, Memorial University of Newfoundland, St. John's, NL, Canada A1B 3X5

[c] Department of Mechanical Engineering, Memorial University of Newfoundland, St. John's, NL, Canada A1B 3X5

This chapter is based on the objectives defined in section 1.3.4 and was accepted by Journal of Energy Resources and Technology for publication in October 2019 issue, Vol. 141.

6.1 Co-authorship Statement

The contributions of this collaborative work are described in the following six parts. 1) Identification of research topic is collaborative between all co-authors. 2) Design of experiments are contributed by Abdelsalam Abugharara and the main supervisor Dr. S.D.Butt. 3) Preparation of cores and construction of ultrasonic and mechanical measurements are solely contributed by Abdelsalam Abugharara. 4) Performance of drilling experiments are cooperated by Abdelsalam Abugharara and Bashir Mohamed, 5) Data analysis and discussion of results is a collaborative work contributed by all co-authors, 6) Manuscript preparation is mainly contributed by Abdelsalam Abugharara, with revision assistance provided by all other coauthors.

6.2 Abstract

The influence of shale anisotropy and orientation on shale drilling performance was studied with an instrumented laboratory drilling rig with a 38.1 mm dual-cutter PDC bit, operating at a nominally fixed rotational speed with a constant rate of flow of drilling fluid - water. However, the rate of rotation (rpm) was affected by the weight on bit (WOB), as was the torque (TRQ) produced. The WOB also affected the depth of cut (DOC). All these variables, WOB, RPM, TRQ, and DOC, were monitored dynamically; for example, RPM with a resolution of one-third of a revolution (samples at time intervals of 0.07 s.) The shale studied was from Newfoundland, and was compared with similar tests on granite, also from a local site. Similar tests were also conducted on concrete made with fine aggregate, used as “Rock-Like-Material” (RLM.) Shale samples were embedded (laterally confined) in concrete while drilled in directions

perpendicular, parallel, and at 45° orientations to bedding planes. Cores were produced from all three materials in several directions for the determination of oriented physical properties derived from ultrasonic testing and unconfined strength (OUCS) correlations. In the case of shale, directions set relative to the bedding. In this study both primary (or compression) velocity, Vp, and shear ultrasonic velocity, Vs, were found to vary with orientation on the local shale samples cored parallel to bedding planes, while Vp and Vs varied, but only slightly, with orientation in tests on granite and RLM. OUCS data for shale, published elsewhere, supports the OUCS theory of this work. The OUCS is high perpendicular and parallel to shale bedding and is low oblique to shale bedding. Correlations were found between the test parameters determined from the drilling tests on local shale. As expected, ROP, DOC and TRQ increase with increasing WOB, while there are inverse relationships between ROP, DOC, TRQ with rpm on the other hand. All these parameters vary with orientation to the bedding plane.

6.3 Introduction

The demand for laboratory studies on shale anisotropy has recently increased significantly due to many reasons, including the advancement of well control technology maintaining well trajectory and eliminating well deviation tendencies induced by shale anisotropy [1-5]. Also, the increase of shale oil and gas production, which has resulted from horizontal drilling and hydraulic fracturing [6-10]. Consequently, there is more focus on considering shale anisotropy in drilling, well completion, hydraulic fracturing, and reservoir development [11]. The oriented measurements of the physical and mechanical properties of shale are some of the main laboratory research areas of interest in many research institutes. In addition to the oriented measurements of shale physical and mechanical properties, the Drilling Technology Laboratory

at Memorial University of Newfoundland and Labrador (DTL-MUN) - Canada has studied oriented drilling performance in isotropic and anisotropic rocks, determining oriented physical and mechanical properties [12-18]. These studies show many influences on the strength of rocks in general, and on shale more specifically. Some of these influences include the content of mineral types and inner structures. In particular, the properties of shale are influenced mainly by the bedding structure, clay content, and compaction magnitude of the shale layers. For shale, the physical properties, relative to bedding orientation, can be determined by measuring the velocity of Vp, and Vs. Likewise, for the oriented mechanical properties. The mechanical characteristics of shale have two main strength patterns. The first pattern is the shear fracture pattern, which can be observed in unconfined and confined compressive strength tests (referred to as UCS and CCS; respectively). The second pattern is the tensile strength pattern, which can be observed in tensile tests [16, 19-26]. Moreover, the study of drilling in shale is a research topic of interest. Physical and mechanical properties determined in the laboratory have been used to enhance drilling performance and optimize shale HF applications [6, 27, 28]. DTL-MUN has been conducting research that evaluates shale drilling techniques as a function of shale bedding orientations, using different drill bit types under different flow rates [16, 17]. This research investigates the shale drilling performance in relation to other important drilling parameters including rotary speed (rpm), Depth of Cut (DOC), and Torque. Some of parameters are kept nominally constant as inputs, but they may nevertheless vary due to some encountered drilling conditions. These variations are also of interest in this paper.

6.4 Experimental Procedure

6.4.1 Wave Velocity Measurement

The compressional and shear wave velocities were determined using the Ultrasonic technique. The measurements were in three orientations: vertical, oblique, and horizontal. Moreover, the

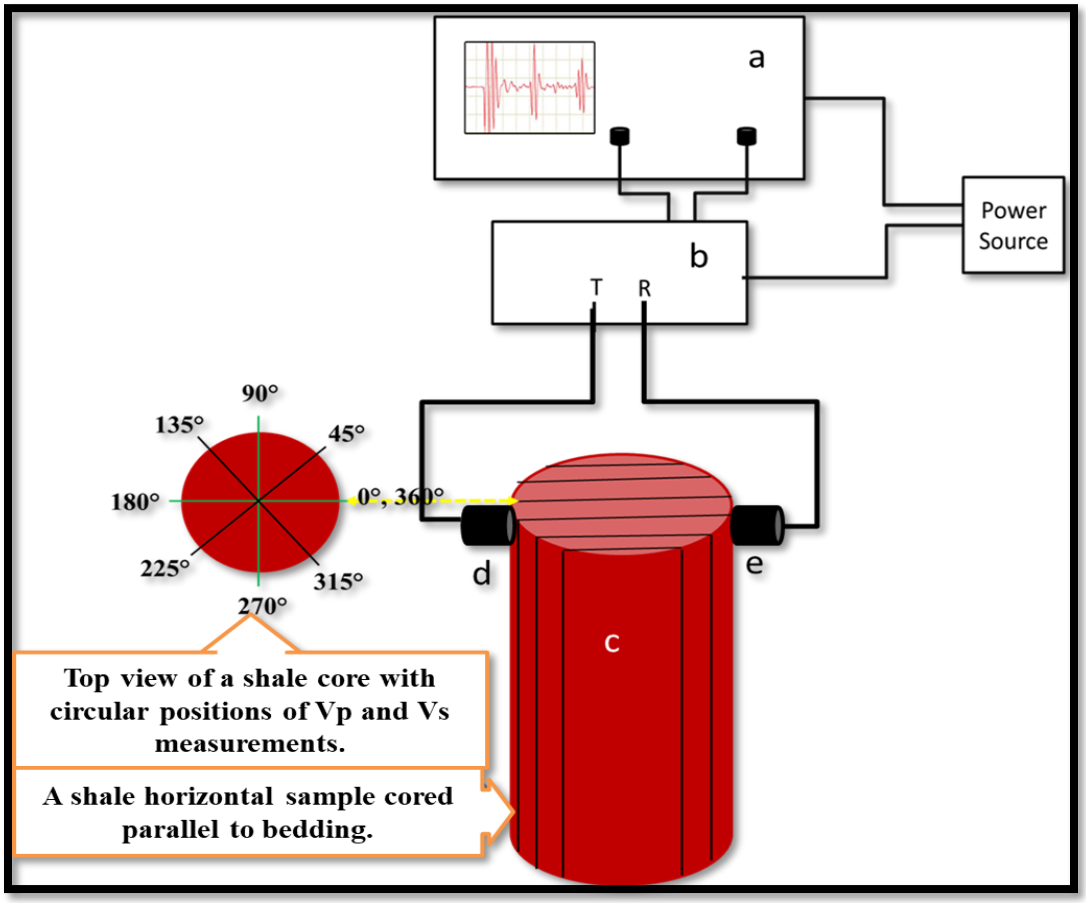

Figure 6-1. Procedure of shale physical property measurement with ultrasonic diagram and Vp and Vs measurement with respect to shale bedding

velocities were measured at 45° increments, from 0° to 360°, as shown in Figure 6-1. For example, Vp and Vs at 0° are measured when the transmitter is at point "d" and the receiver is at point "e", and Vp and Vs at 180° are measured when the transmitter is at point "e" and the receiver is at point "d".

6.4.2 Strength Measurement

Oriented strength determination was conducted in three main orientations. The limitation for shale oriented measurements are due to the challenge of obtaining samples in the other orientations and the availability of oriented strength data in the literature. The oriented RLM strength was determined using a flat-end-piston loading tester (a modified version of the point load testing apparatus) on standard cores. The vertical shale strength was estimated using the Point Load Strength Test (PLST). Figure 6-2 shows a procedure of estimating oriented strength of RLM and vertical strength of shale. The RLM OUCS and shale vertical strength values are summarized in Table 6.1 and Table 6.2, respectively.

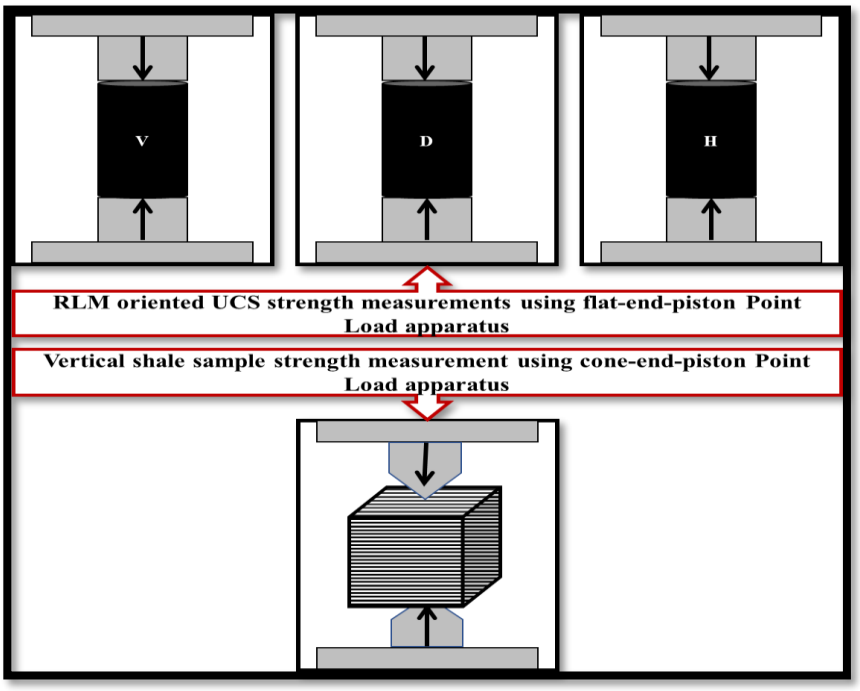

Figure 6-2. Procedure of RLM OUCS and shale point load tests parallel to bedding

Table 6.1. Mean (AVG) oriented values for RLM samples

Results of RLM oriented unconfined compressive strength (OUCS) in MPa			
Orientation	**0°**	**45°**	**90°**
OUCS values	**53**	**56**	**53**
	53	**49**	**56**
	49	**53**	**60**
	56	**47**	**50**
	53	**53**	**49**
OUCS-AVG	**53**	**52**	**54**

Table 6.2. UCS result for shale samples using point load index apparatus conducted perpendicular to shale bedding

Test Number	UCS (MPa)
1	**54**
2	**74**
3	**48**
4	**69**
5	**57**
7	**34**
8	**69**
9	**35**
10	**89**
6 (AVG)	**59**

6.4.3 Drilling Experiments

A fully instrumented small-scale drilling rig as described in Figure 6-3 middle was used to drill samples in three orientations. The three orientations were selected according to the three main trajectories encountered in oil and gas horizontal drilling, which include vertical, oblique, and horizontal as shown in Figure 6-3 left. Figure 6-3 right shown shale samples after drilling in different orientations.

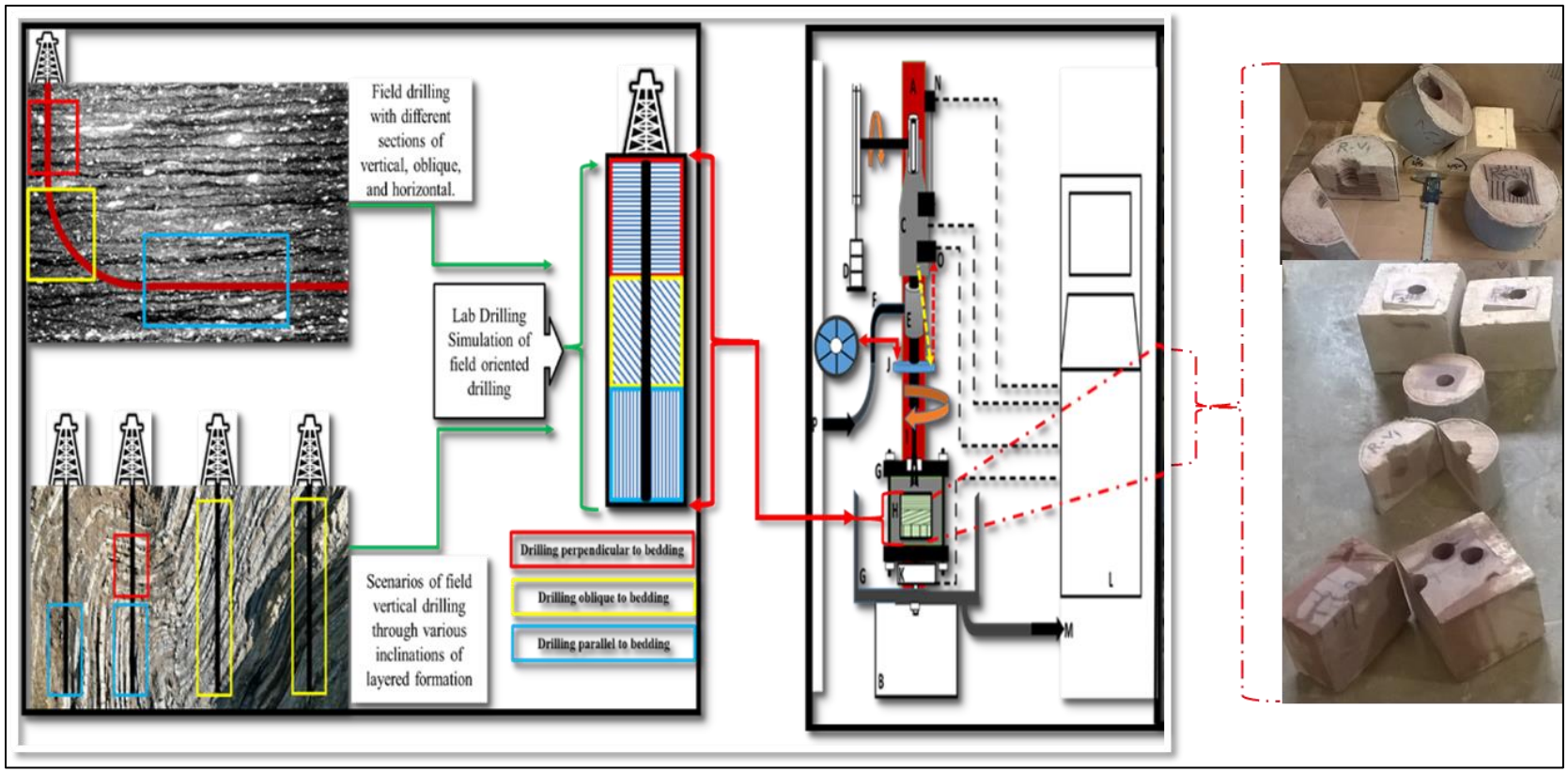

Figure 6-3. Subsurface scenarios of anisotropic rock, left, laboratory drilling rig diagram, middle, and cast shale samples drilled in three orientations, right

In shale, the vertical drilling is perpendicular to shale bedding, horizontal drilling is parallel to shale bedding, and oblique drilling is at 45° with the shale bedding. In RLM, the vertical drilling is parallel to y-axis of the cylinders, horizontal drilling is parallel to x-axis, and oblique drilling is parallel to 45° between vertical and horizontal directions in the Cartesian coordinate system of the original RLM cylinder as shown in Figure 6-4. In the drilling experiments WOB is the primary input variable, the rate of flow of the drilling fluid- water is constant. The drill string rotational speed is provided by an AC electric motor, but the rpm varies a small amount with the torque, and so the actual rpm is measured and used also as a variable. Other variables determined were ROP, DOC, and Torque.

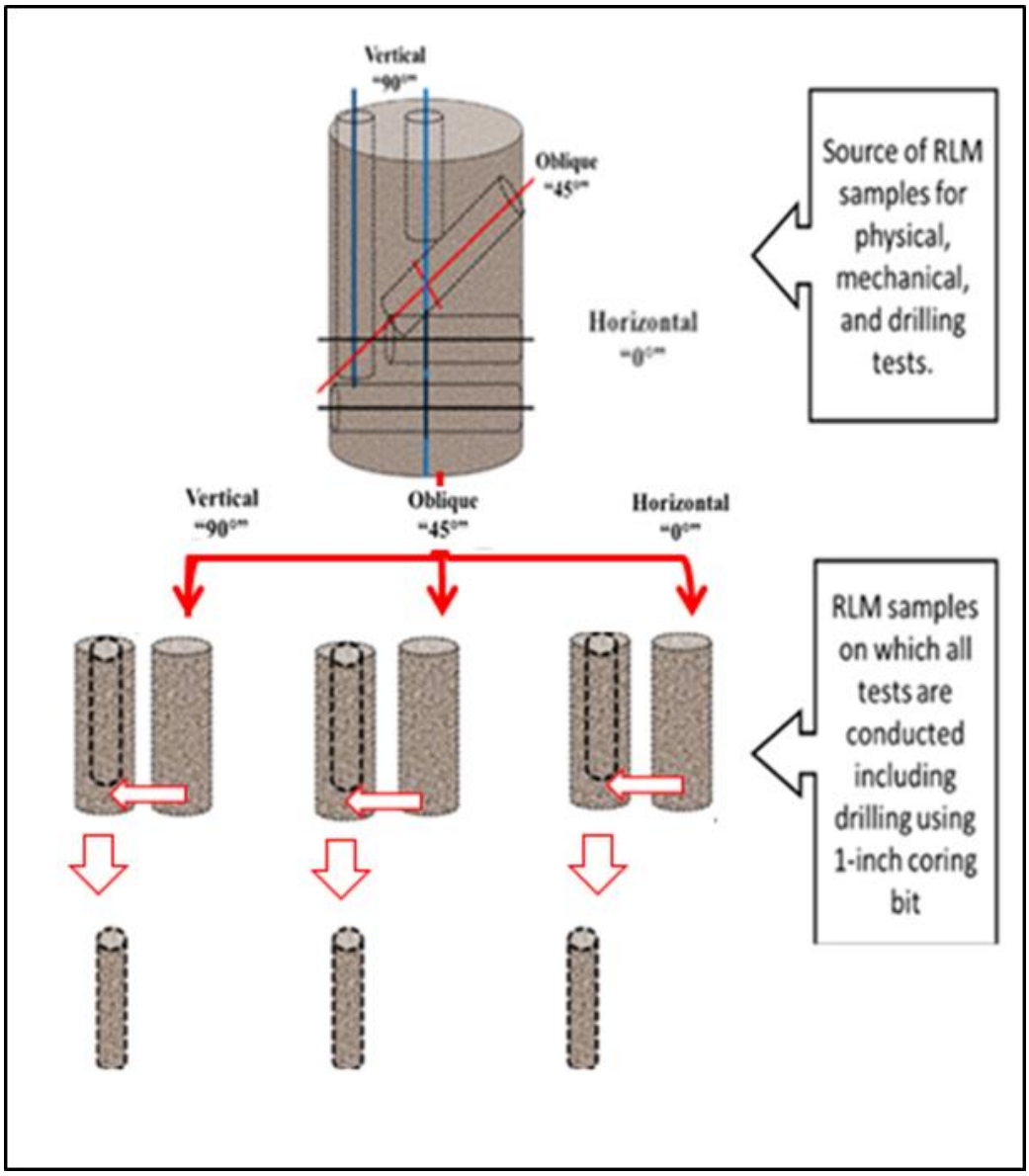

Figure 6-4. Preparation of RLM cores for determination of oriented samples for physical, Vp, Vs and mechanical measurements

6.5 Sample Preparation

Samples were prepared as cores in accordance to ASTM standards and ISRM suggested methods for wave velocity and strength tests. The RLM samples were cored in three orientations, including vertical, oblique, and horizontal. The granite samples were cored in vertical and horizontal orientations. Unlike the RLM and granite coring, samples of shale were cored in only one orientation, which is parallel to shale bedding as shown in Figure 6-5.

Figure 6-5. Core samples of, top left: RLM, top right: granite, and bottom right and left: shale

As challenges were encountered when coring shale due to bedding breakage and splitting, a special technique was developed specifically to overcome such challenges. Shale rocks were first cut into cubes by a diamond saw. Then, they were cast in cement after determining shale bedding orientations. Lastly, 50.8 cm and 101 cm diamond coring bits were used for coring. It was observed that coring parallel to shale bedding was the most successful for retrieving intact cores. This was because of the larger contact area between the layers compared to oblique and perpendicular coring.

Figure 6-4 shows the procedure of RLM sample preparation includes: (i) casting of 15.24 cm diameter, 30.48 cm long, from which 4.76 cm diameter cores are drilled using NQ core barrel in three orientations as indicated (each set in a particular orientation in separate cylinders), some used for physical tests. (ii) Smaller diameter cores were produced from these for OUCS tests.

6.6 Conducted Tests

6.6.1 Oriented Wave Velocity

The differences in the inner structure of rocks, such as shale bedding can affect the wave velocities. This effect can be determined by several techniques, including ultrasonic method. The purpose of conducting these measurements was to categorize the tested rocks as isotropic or anisotropic. Figure 6-1 shows the ultrasonic apparatus, which includes (a) TDS 1002B two channel digital storage oscilloscope, (b) square wave Pulser/Receiver Model 5077PR, and (c and d) two Panametrics sensors. Shear wave coupling was used to ensure complete contact between sensors

and the surface of the tested rock samples. Measurement of Vp and Vs for all tested rocks in this paper was conducted using Equation 5-1 and Equation 5-2, respectively.

$$Vp = 0.001 * \mathrm{LP/TP} \quad \text{(Equation 5-1)}$$

$$\mathrm{Vs} = 0.001 * \mathrm{LS/TS} \quad \text{(Equation 5-2)}$$

Where Vp and Vs are compressional and shear wave velocities in (km/sec), Lp and Ls are compressional and shear wave travel lengths in (m), and Tp and Ts are compressional and shear wave propagation time in (sec); respectively. The attenuation and high quality of couplant are two main concerns that were addressed to ensure high quality data and accurate measurements.

6.6.2 Oriented Strength

The purpose of these tests was to establish a relationship between the results of the oriented strength obtained from the oriented mechanical tests and the results of oriented drilling. The mechanical data for shale in this paper mainly depended on data collected from the literature. This data is plotted based on the 3-orientation "syncline-strength" theory of this paper, which is mainly formed by two high strength values at 0° and 90° and one low strength value at 45°, as shown in Figure 6-6. Figure 6-7 shows the oriented shale strength collected from the literature. A number of laboratory studies of shale strength and modelling have been conducted in many research centers. Many papers have reported confined and unconfined compressive strengths (CCS and

UCS, respectively), some reported shale tensile strength through Indirect Tensile (IT) tests and Point Load Index (PLIT) tests [16, 19-26]. Several empirical correlations support the shale strength pattern theory of the U-Strength curve [29-32]. Modelling of the shale strength using various types, including Plane of Weakness model, Patchy Weakness model, Bonded Particle model, and Smooth Joint model are also in agreement with the other shale strength methods [25, 26, 33, and 34]. They all agreed with the pattern of shale strength.

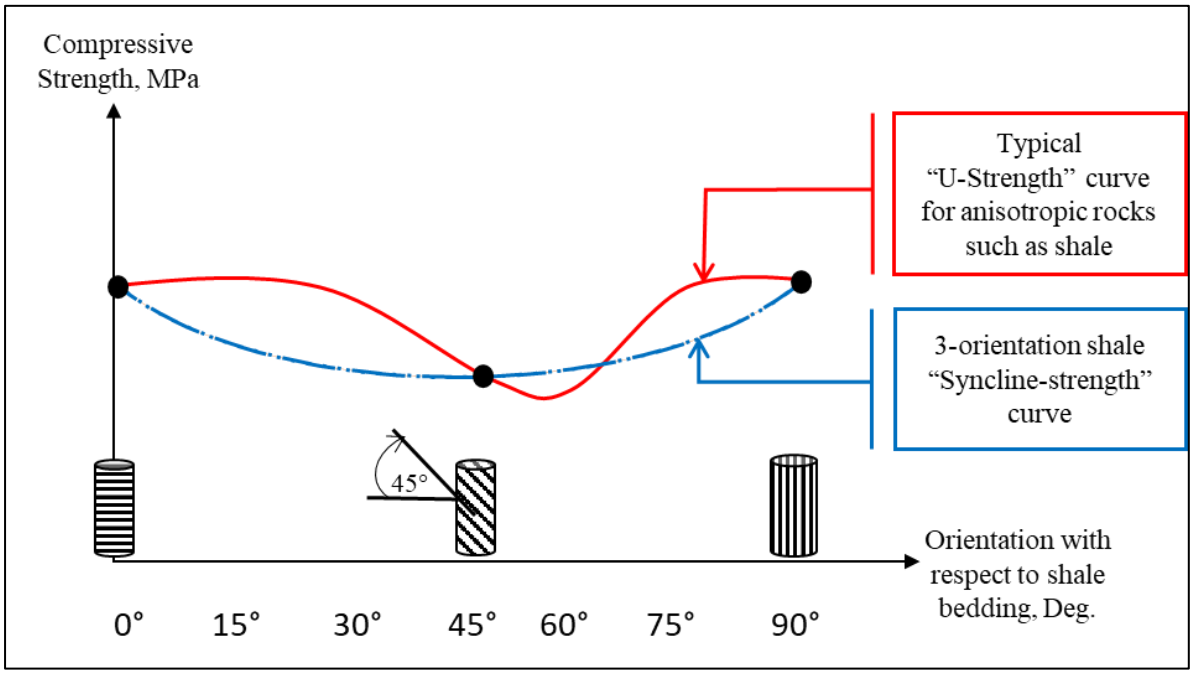

Figure 6-6. Diagram of anisotropic typical "U-Strength" curve and 3-orientation "syncline-strength" curve

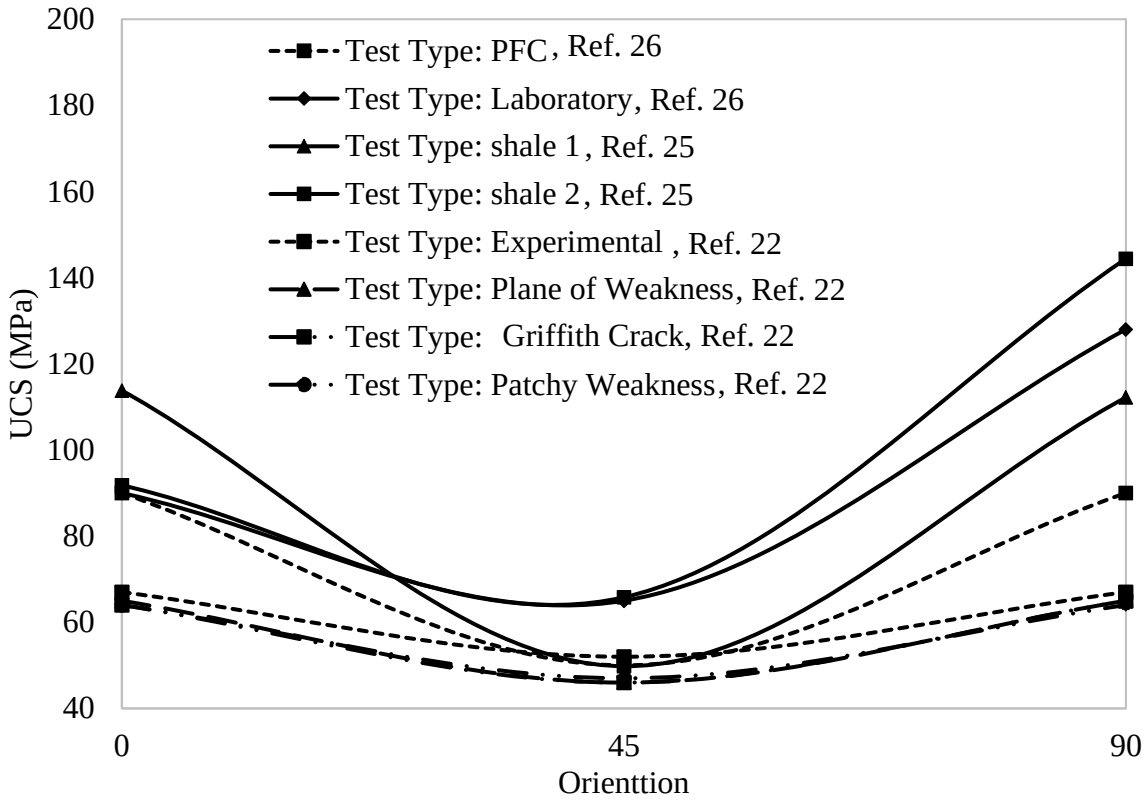

Figure 6-7. Literature data of shale OUCS following the 3-Orientation "syncline-strength" curve

6.6.3 Oriented Drilling

The objective of these experiments was to categorize the tested rocks through oriented drilling in conjunction with strength tests. Also, to evaluate the influence of isotropy and anisotropy of rocks through the evaluation of the drilling results. The drilling experiments were conducted mainly on shale as a VTI rock and on RLM as isotropic rocks. The purpose of conducting the drilling tests on RLM was for comparison and validation of the oriented shale "strength - ROP" theory presented in this paper. A coring bit was used for coring shale and RLM, while the drilling tests were performed on shale and RLM using a 38.1 mm dual cutter polycrystalline diamond compact (PDC)

bit. A fully instrumented laboratory scale rotary drilling rig shown in Figure 6-3 middle was used for drilling. A nominal 300 rpm was the input rotary speed, but the actual rpm was calculated as described in Figure 6-8. A constant flow rate of clean water was used to remove cuttings, clean the hole, ensuring continuous contact between rock and the drill bit and preventing non-productive time spent on fracturing cuttings into smaller pieces. The drilling parameters measured by sensors connected to a DAQ System with professional LabVIEW software, included drill bit travel for measuring drilling depth, actual rpm, consumed current, and WOB. Drilling performance was then evaluated by constructing relationships between WOB vs. ROP, DOC, rpm, and Torque performed on data recorded from drilling in different orientations focusing primarily on drilling in shale. Although shale cutting process under single cutter PDC bit has been extensively studied, but mainly perpendicular to shale bedding (35- 37). The work reported here, however, uses a dual cutter PDC in drilling shale in three orientations. The drilling parameters are also analyzed based on drilling shale in these three orientations with a comparison to drilling RLM.

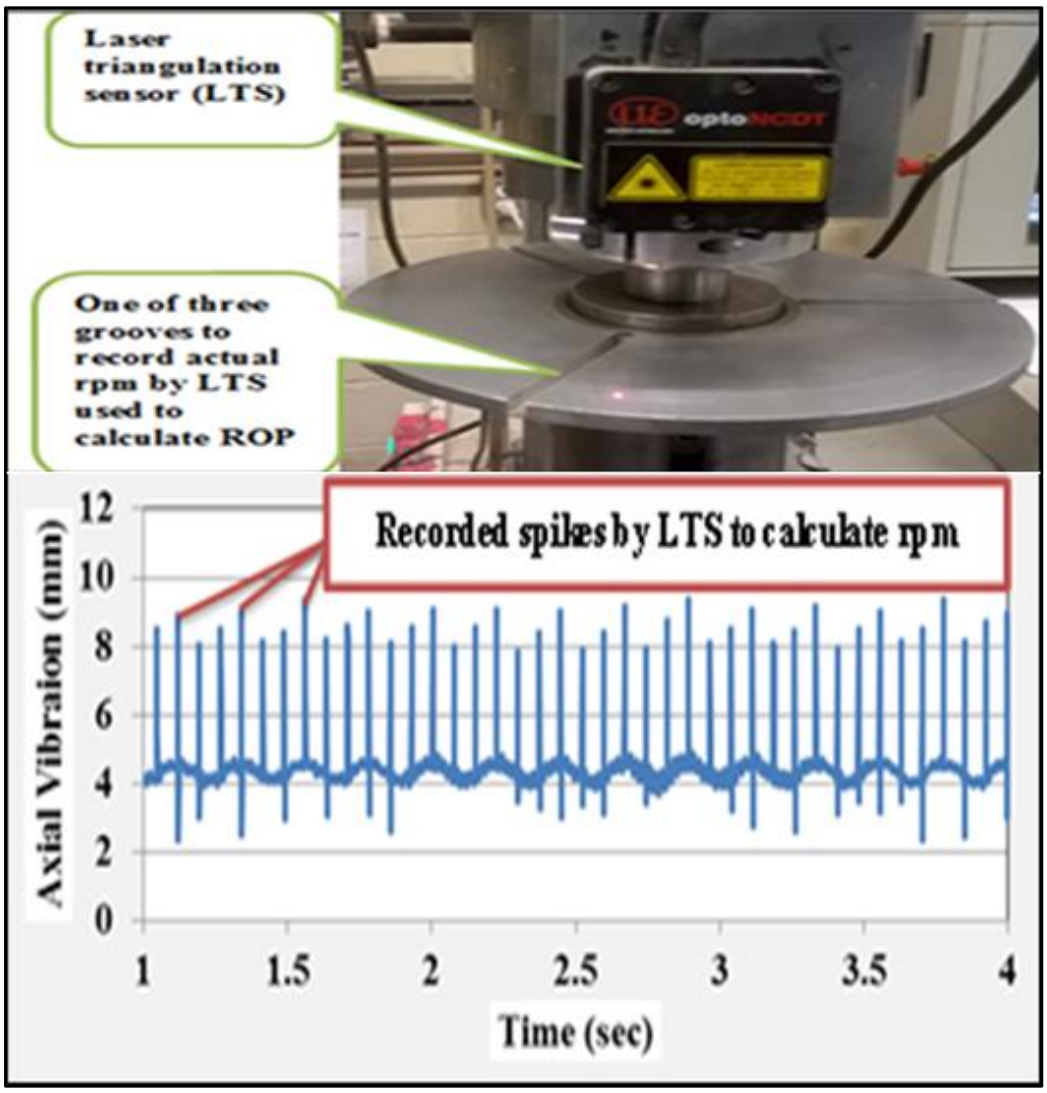

Figure 6-8. Operational rpm determination utilizing the LTS. Abugharara et al., 2016 [17]

6.6.4 Data Recording System

The drilling parameters were recorded by many sensors connected to a data acquisition system (DAQ) system with a minimum sampling rate of 1000 Hz. The sensors include a draw wire linear position transducer (LPT) that measures axial displacement between the motor head and the drill pipe used to calculate the ROP, a laser triangulation sensor (LTS) (Figure 6-8) that measures (i) the relative displacement between the motor head and drill pipe (ii) the actual rpm, and also a Hall Effect sensor that is in line with the electric motor and measures the motor current used in determining the torque.

6.7 Results and Discussion

6.7.1 Oriented Wave Velocity

Rock physical properties (Vp and Vs) can be affected by rock inner structure such as rock lamination. The magnitude of the influence of rock lamination on Vp and Vs variation is orientation dependence. Laboratory study of this affect and understanding its relationship with the lamination orientation could assist in determining the subsurface rock type and its inclination when being encountered in wells, only based on the physical data gathered at the surface. As anisotropic rocks, shale bedding inclinations, which affect shale physical properties were measured. Results of the oriented Vp and Vs were also obtained from RLM and granite core samples for comparison. Results of oriented Vp and Vs for RLM, granite, and shale are displayed in Figure 6-9 to Figure 6-14; respectively. RLM and granite exhibit isotropy, and shale exhibits Vertical Transverse Isotropy (VTI).

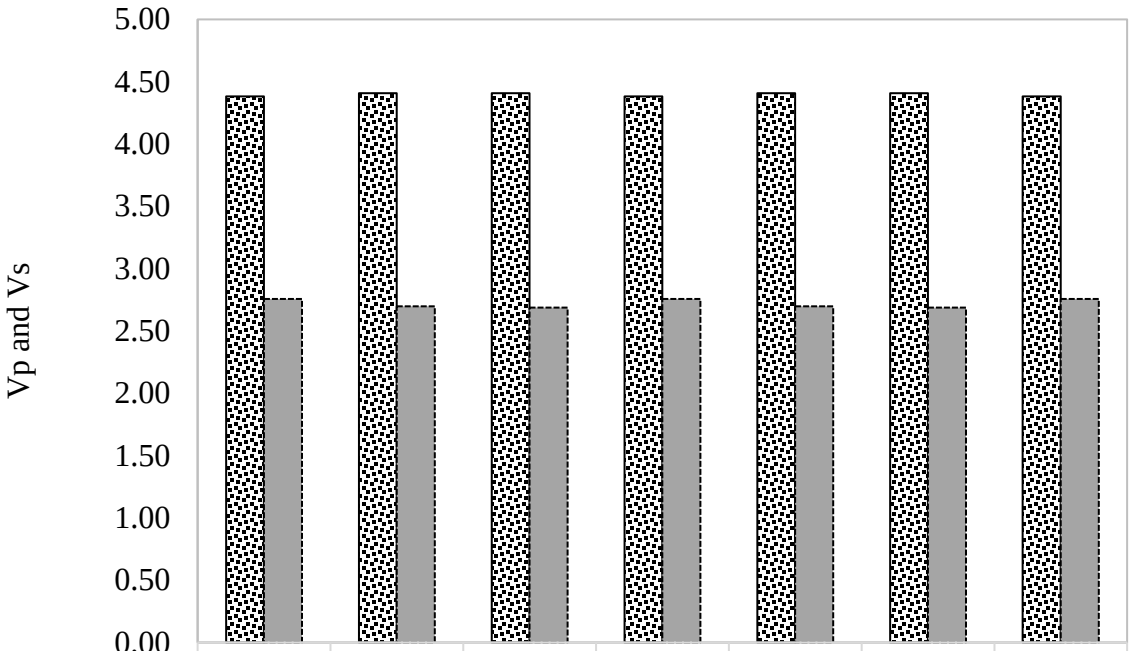

	0°	45°	90°	180°	225°	270°	360°
Vp (km/s)	4.38	4.41	4.41	4.38	4.41	4.41	4.38
Vs (km/s)	2.76	2.70	2.69	2.76	2.70	2.69	2.76

Figure 6-9. Circular wave measurements conducted on an RLM core using bar chart

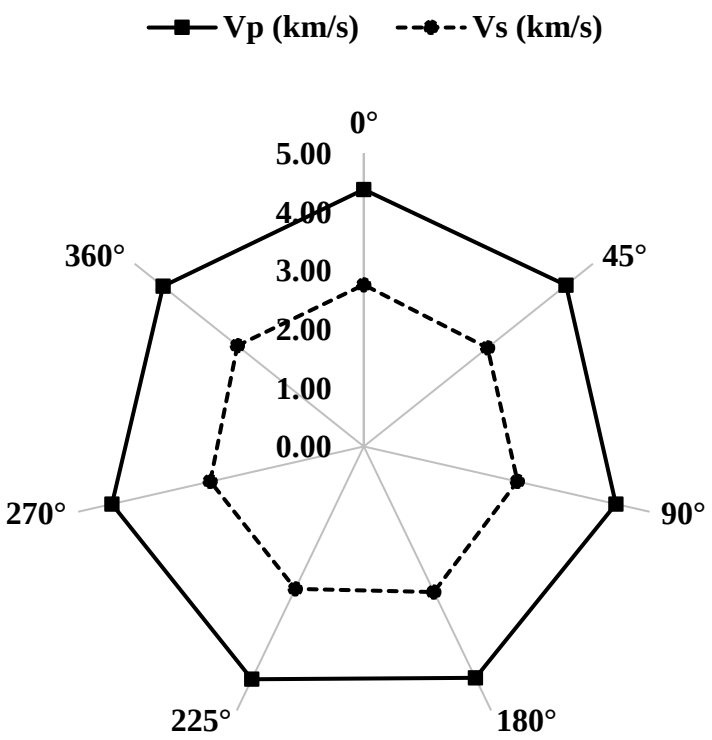

Figure 6-10. Circular wave measurements conducted on an RLM core using radar chart

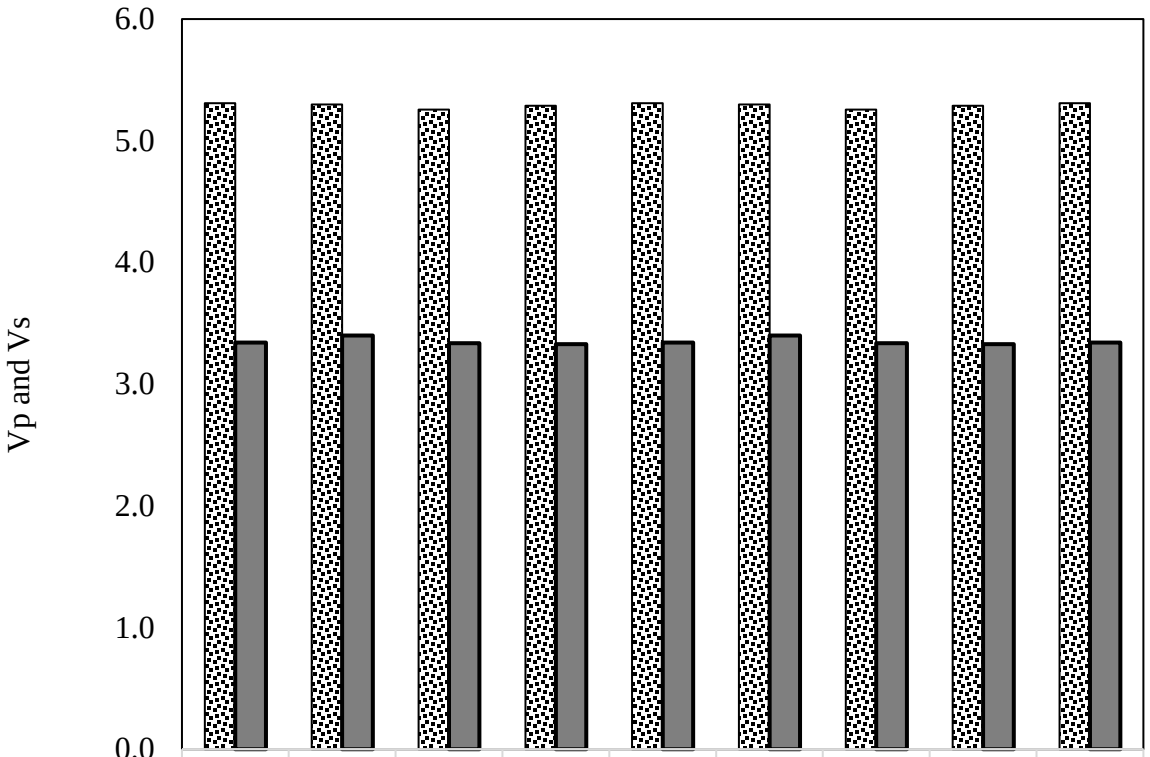

	0°	45°	90°	135°	180°	225°	270°	315°	360°
Vp (km/s)	5.3	5.3	5.3	5.3	5.3	5.3	5.3	5.3	5.3
Vs (km/s)	3.3	3.4	3.3	3.3	3.3	3.4	3.3	3.3	3.3

Figure 6-11. Circular wave measurements conducted on a horizontal granite core using bar chart

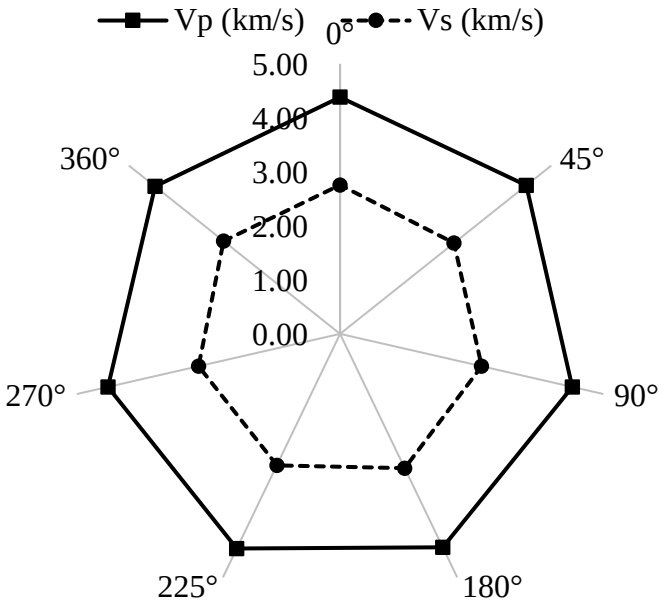

Figure 6-12. Circular wave measurements conducted on a horizontal granite core using radar chart

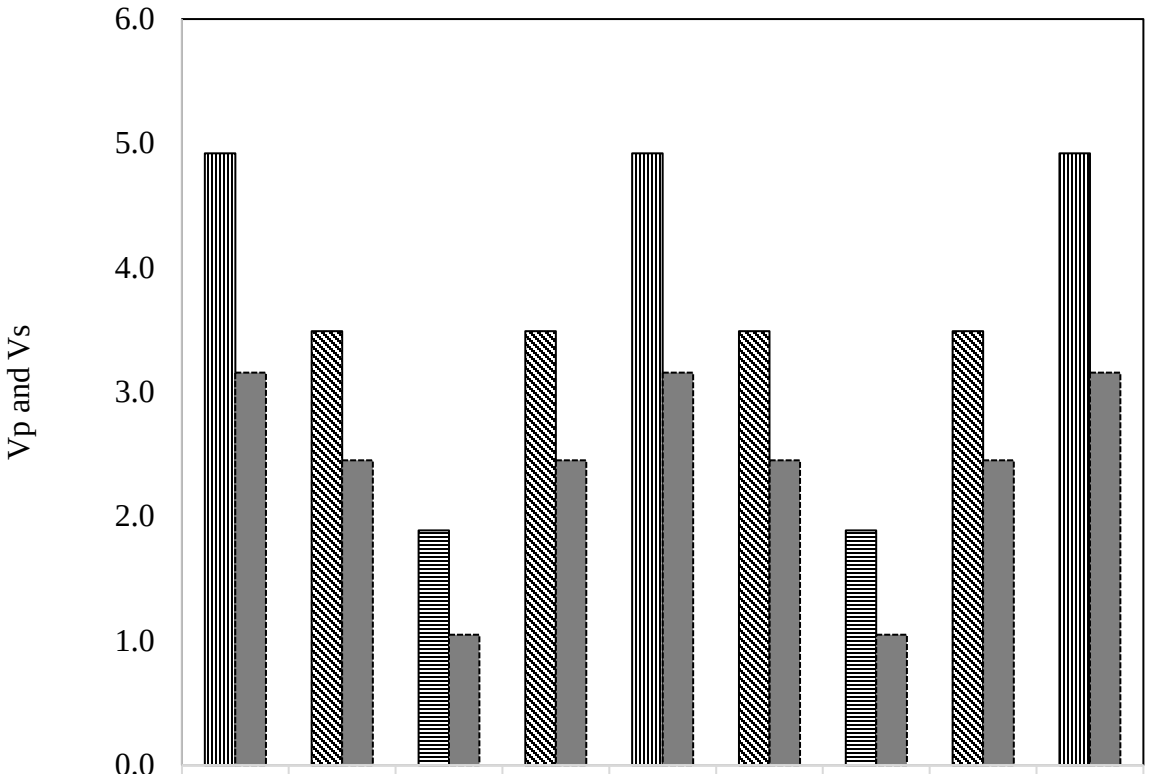

	0°	45°	90°	135°	180°	225°	270°	315°	360°
Vp (km/s)	4.9	3.5	1.9	3.5	4.9	3.5	1.9	3.5	4.9
Vs (km/s)	3.2	2.5	1.0	2.5	3.2	2.5	1.0	2.5	3.2

Figure 6-13. Circular wave measurements conducted on a shale sample cored parallel to the bedding using bar chart

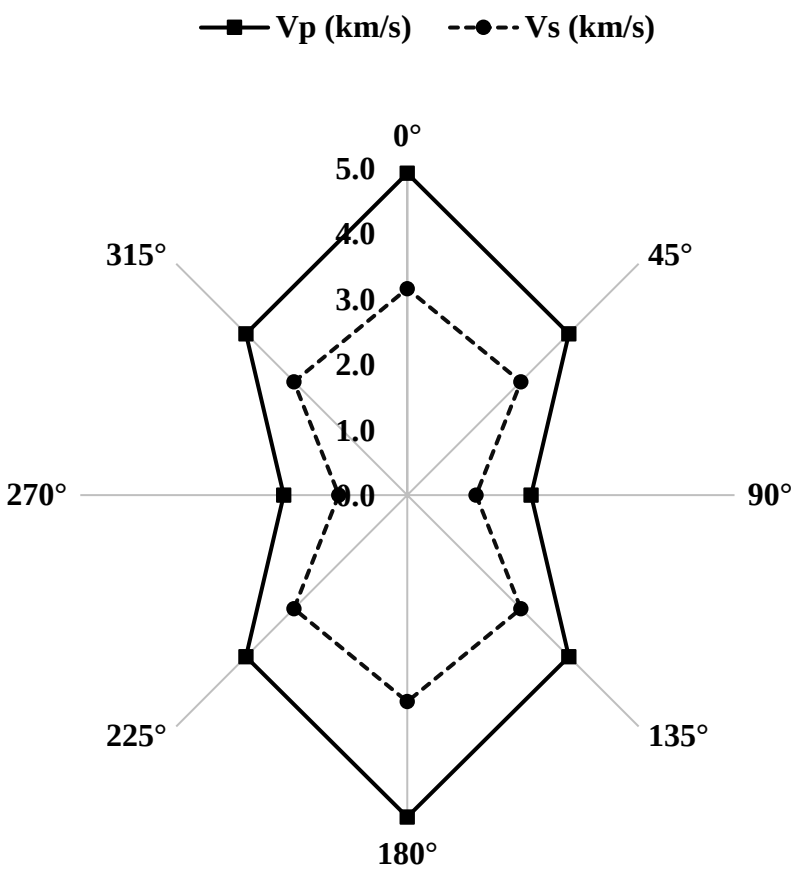

Figure 6-14. Circular wave measurements conducted on a shale sample cored parallel to the bedding using radar chart

6.7.2 Oriented Strength

Shale bedding inclinations can affect the mechanical properties through strength variation, which can be evaluated by strength tests conducted in different orientations. The main strength tests, include unconfined compressive strength (UCS), confined compressive strength (CCS), point load index strength (PLI), and indirect tensile (IT) strength. The oriented strength for RLM samples was also determined and summarized in Table 6.1. The result exhibits RLM isotropy and supports the result of the oriented wave velocity that are shown in Figure 6-9 and Figure 6-10. Strength tests using the point load apparatus were performed on irregular-shape shale samples. The results were expected to vary due numerous reasons, including the variation of sample shape and size. However, the purpose of this test was to obtain an average shale strength perpendicular to shale bedding. The results of this test are summarized with their averaged value of 59 MPa. Literature data was the main source for the oriented shale strength. This data showed variations in the oriented shale strength that corresponds to the orientation of shale anisotropy, showing shale strength is orientation dependent. Shale strength in the UCS and the CCS tests which perform shear fractures is the highest at the orientations of 0° and 90° (perpendicular and parallel to shale bedding, respectively). On the other hand, shale has low strength value between 45° and 60°. This is demonstrated in the typical "U-Strength" curve shown in Figure 6-6 and Figure 6-7. However, the pattern of shale strength in the IT test leading to tensile fracture mode has two reported modes. First, the lowest strength is at 0° (parallel to bedding) and highest tensile strength is at 75° to 90°, increasing in the degrees in between [22, 25]. Second, the lowest tensile strength occurs at about 15° and a higher shale tensile strength occurs at about 0° and the highest strength occurs at about 90° (parallel and perpendicular to shale bedding respectively) [23]. By selecting three shale

strength orientations, a “syncline-strength” curve is constructed as the study base for this work as shown in Figure 6-6. Based on this, the ROP and the drilling parameters that positively influence ROP (i.e. DOC and TRQ) are inversely proportional to shale strength and the actual rpm is directly proportional to shale strength. Table 6.3 contains published data from several references showing the oriented strength of some shale types as a result of experimental and numerical UCS tests. Figure 6-15 shows the relationship between the oriented strength of shale and ROP, as a single

parameter effect as proposed in this work. This relationship is further analyzed by involving more drilling parameters.

6.7.3 Oriented Drilling

In petroleum engineering, drilling performance can be significantly influenced by shale anisotropy and inclination. This can be evaluated by drilling the shale in different directions. Then, the influence of direction vs. rock anisotropy on drilling performance can be evaluated using one of several parameters. However, the more drilling parameters included in the evaluation, the more

Table 6.3. Various oriented shale strengths of several published data

Orientation	Reference # 22				Reference # 26		Reference # 25	
	Test Type				Test Type		Shale Type	
	Experimental	Plane of Weakness	Griffith Crack	Patchy Weakness	PFC	Laboratory	shale 1	shale 2
0	67	65	64	64	90	90	113.8	91.8
45	52	46	46	47	50	65	49.8	65.8
90	67	65	65	64	90	128	112.2	144.4

accurate and reliable data and results achieved. In this work, laboratory drilling experiments were performed on different rock types, including shale and RLM. The parameters analyzed and the results are reported in the following sections.

Table 6.4. Various sets and values of WOB used in drilling experiments

Set	Value
W1	**97**
W3	**114**
W5	**131**
W7	**148**
W9	**165**

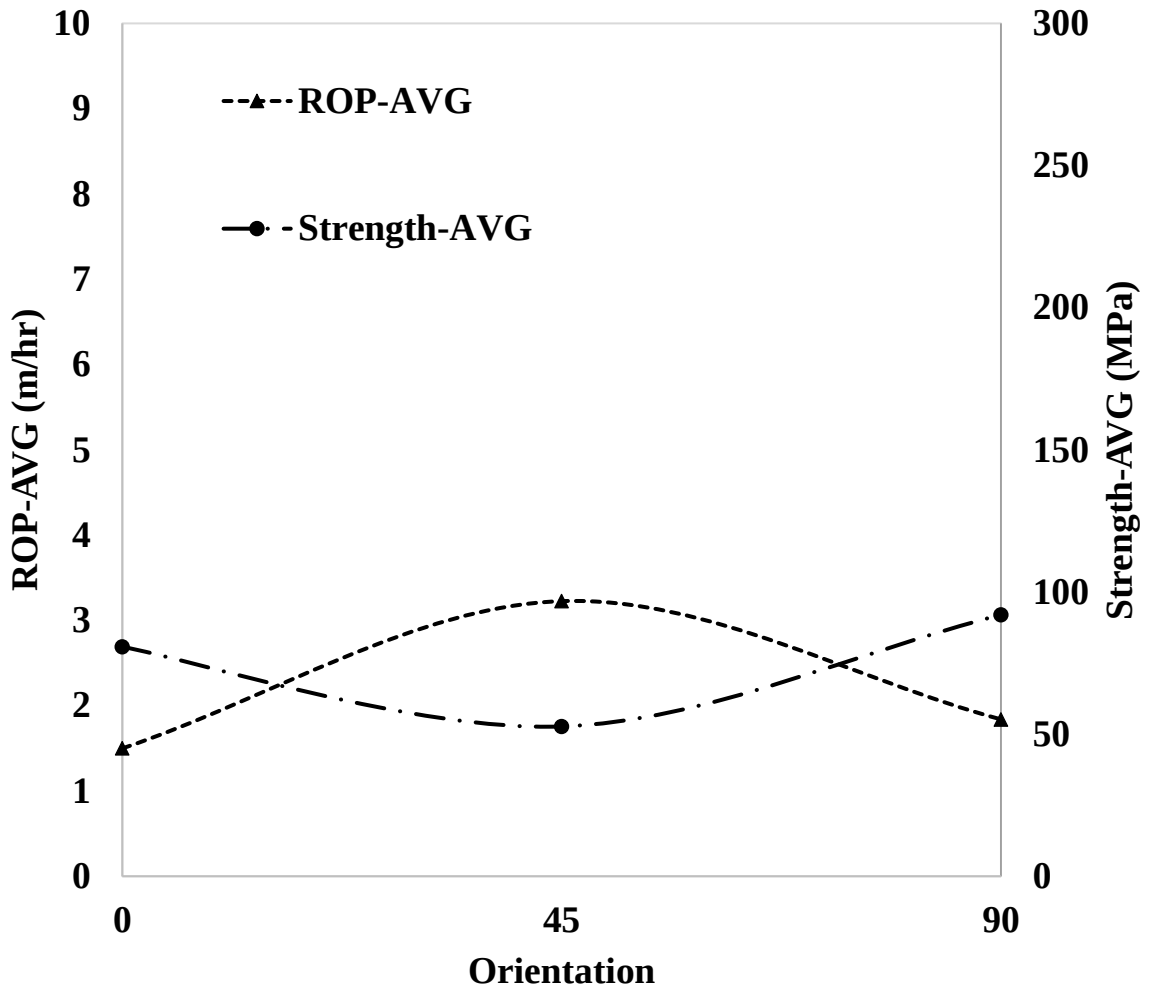

Figure 6-15. Relationship between shale strength-AVG in Figure 6-7 and shale ROP-AVG of this work

6.7.3.1 Single-Parameter Analysis

The results of the oriented drilling tests conducted on shale are shown in Figure 6-16 through Figure 6-20. Figure 6-16 shows ROP increase with the increase of WOB. Various WOB sets and values are shown in Table 6.4. The data shows the ROP in the oblique direction is the highest compared to the ROP perpendicular and parallel to shale bedding. Figure 6-15 demonstrates that ROP is significantly affected by shale strength due to shale bedding orientation, which is demonstrated in Figure 6-6 and Figure 6-7. This relationship is translated to higher ROP at 45° due to low shale shear strength by using the PDC bit (PDC follows shear fracture when drilling). Moreover, the relationship shows the ROP is low at 0° and 90°, where shale shear strength is highest that is further demonstrated in Figure 6-16 and Figure 6-17. Figure 6-18 shows the trend of the DOC resulted from drilling shale in three different orientations at different levels of WOB. These results show higher DOC at 45° due to the lowest encountered strength, which results bit cutter to be inserted deeper into the formation. Figure 6-19 shows the trend of rpm, at different levels of WOB as a result of drilling in shale in different orientations. In Figure 6-19, the rpm has an inverse relationship to the ROP and DOC. An increasing of DOC leads to an increasing of the ROP, but, in reverse, it leads to the reduction of rpm, which indicates the involvement of higher resistance when the bit cutters get deeper in the formation as a result of increasing WOB. Figure 6-20 shows the trend of the torque (TRQ) as a result of drilling shale in different orientations. The variations of torque at each level of WOB leads to the increasing of ROP and DOC but causes reduction in rpm.

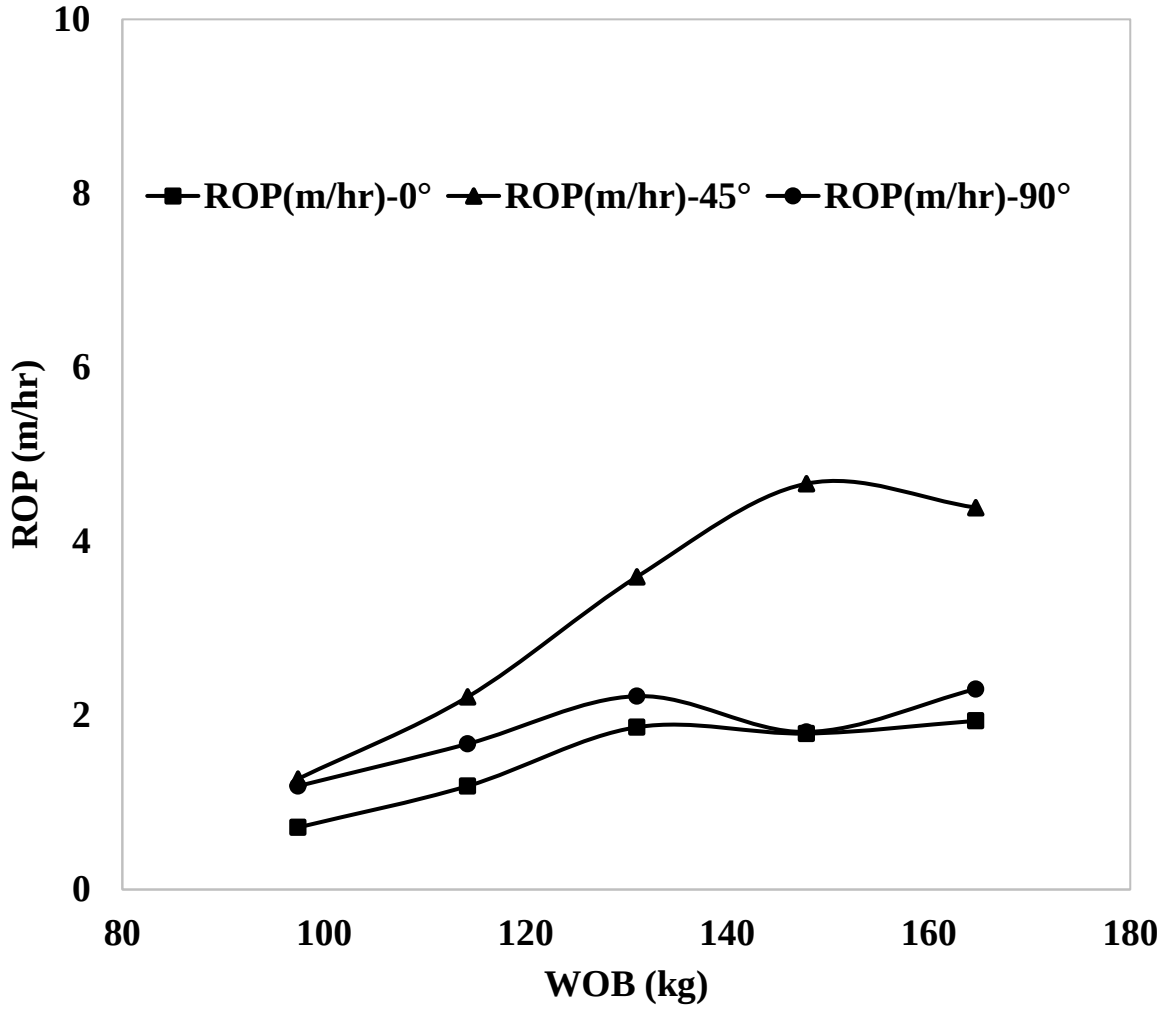

Figure 6-16. Oriented shale ROP at various sets of WOB

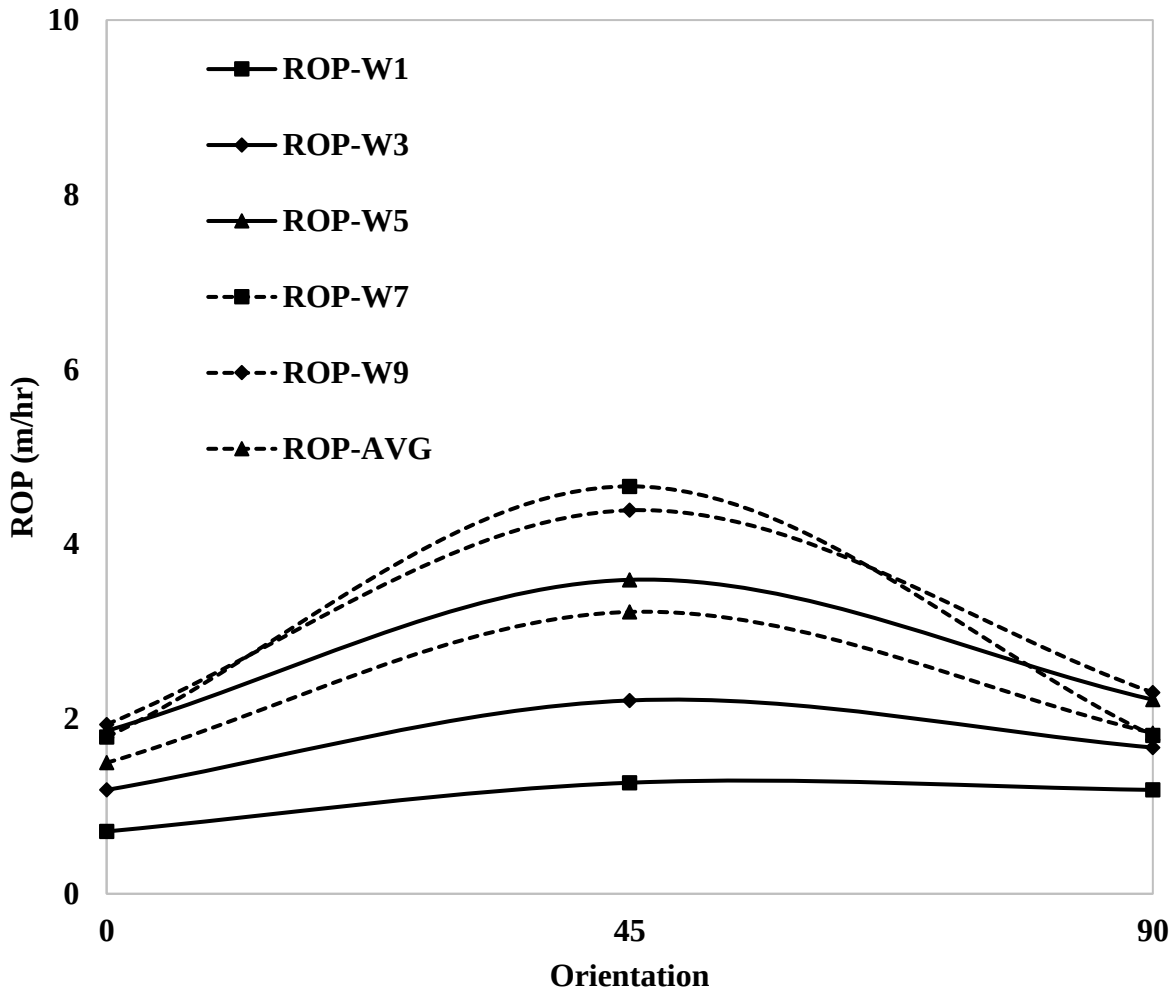

Figure 6-17. Oriented shale ROP at various sets of WOB

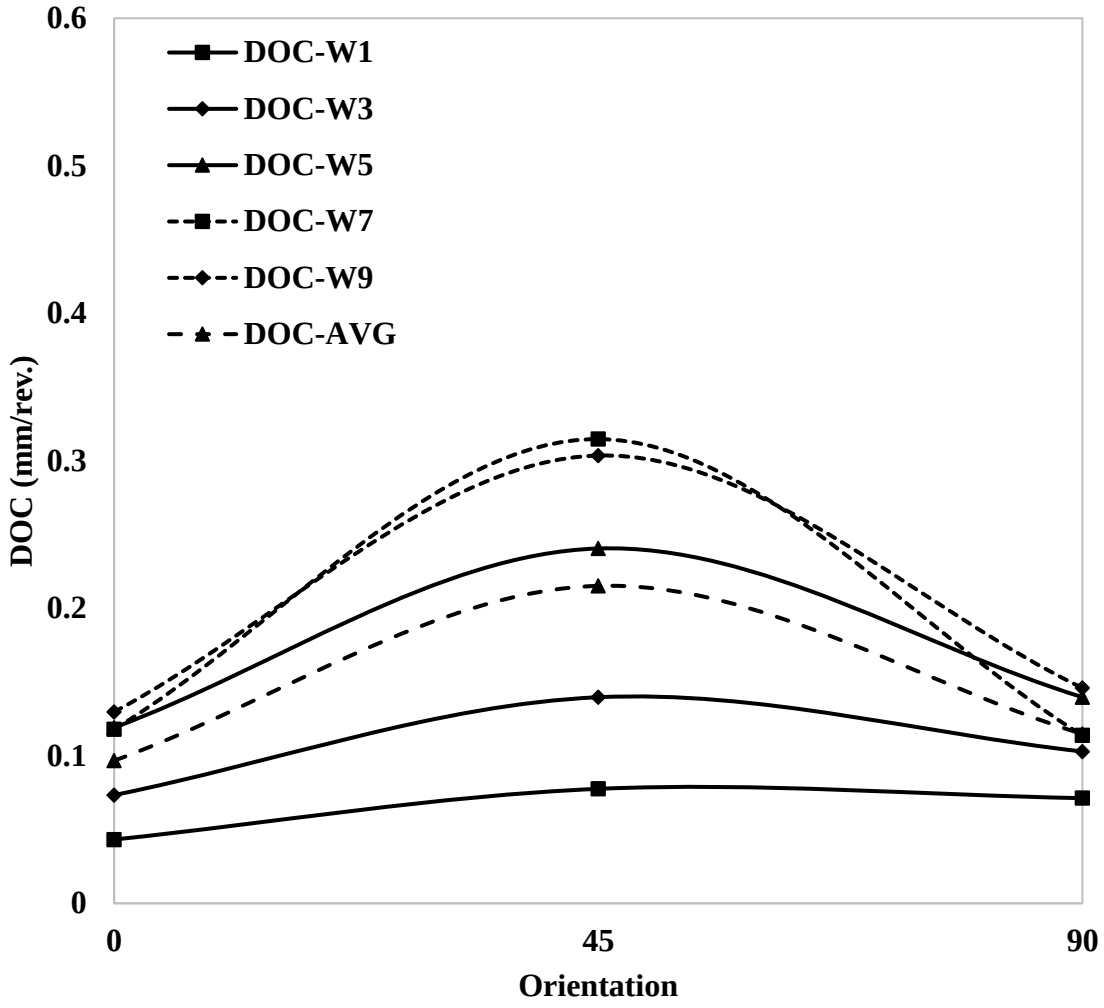

Figure 6-18. Oriented DOC at various sets of WOB from shale drilling

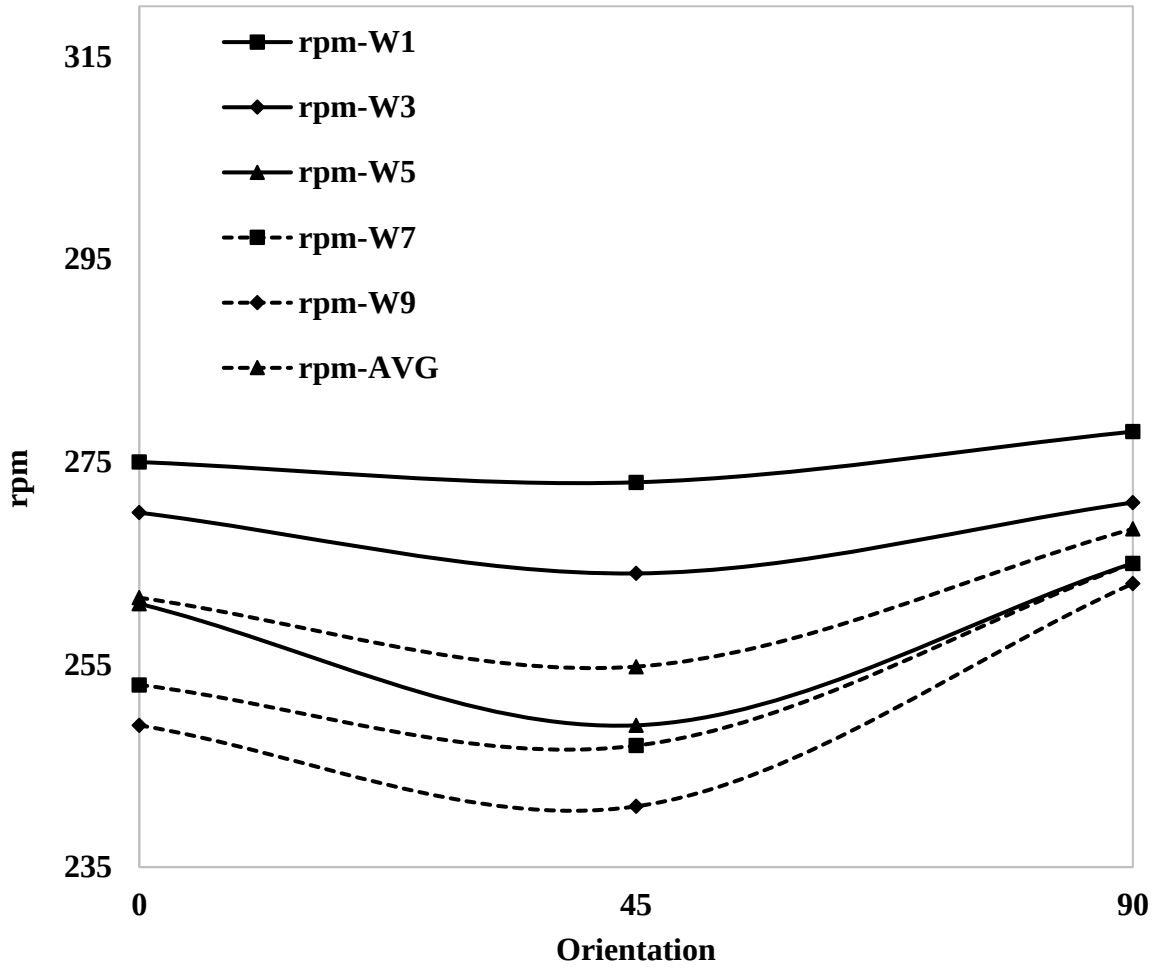

Figure 6-19. Oriented actual rpm at various sets of WOB from shale drilling

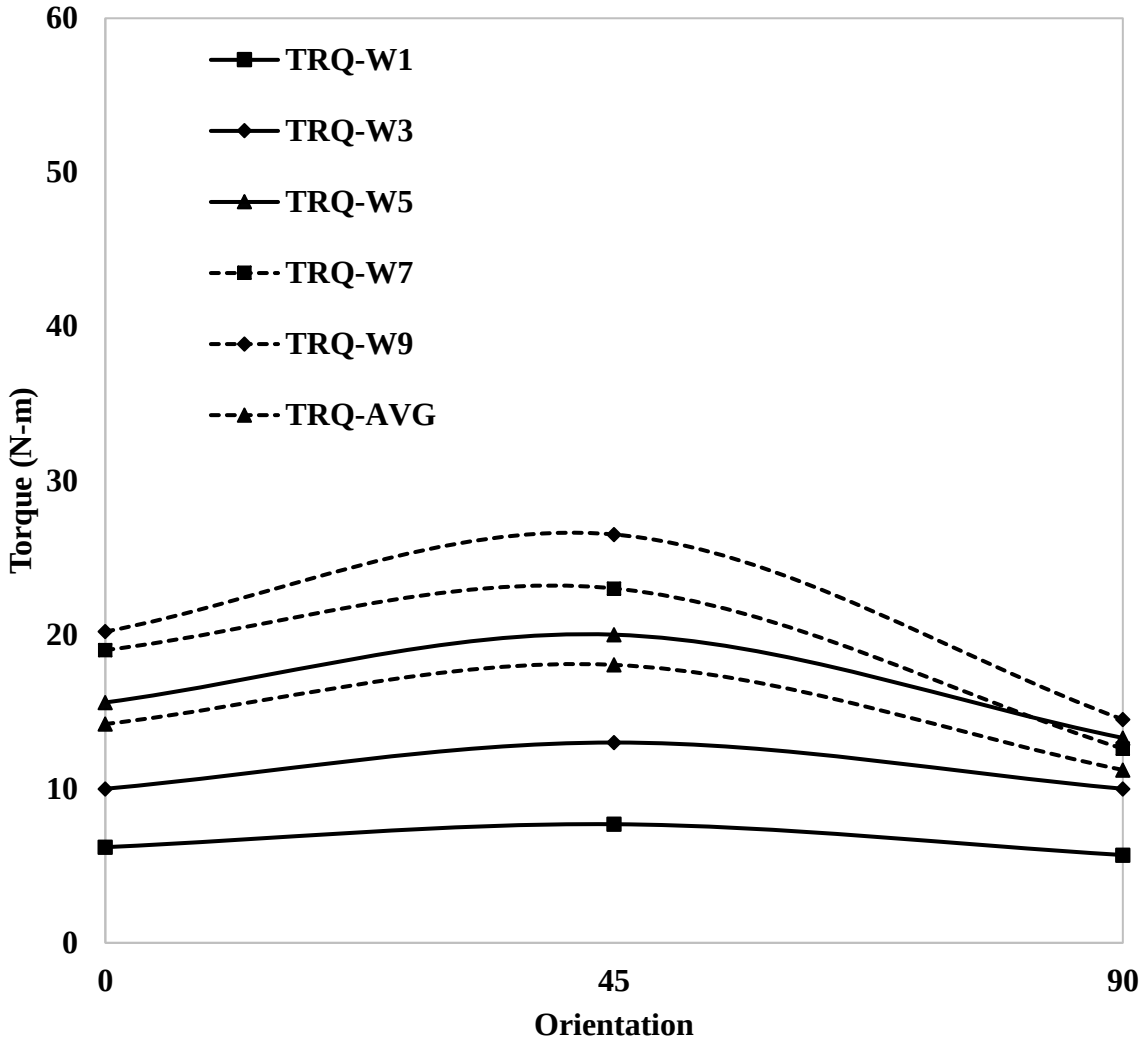

Figure 6-20. Oriented torque at various sets of WOB in shale drilling

6.7.3.2 Dual-Parameter Analysis

In this section, three parameters are analyzed, including DOC, TRQ and rpm versus ROP. Figure 6-21 through Figure 6-23 show relationships between average values of DOC, torque and rpm to

each other and to the ROP. Figure 6-21 displays a direct proportion relation between DOC and ROP. Figure 6-22 shows a direct proportion relation between ROP and TRQ. The increase of TRQ shown here is because of the increase of DOC. Conventionally, the increase of rpm results in increasing ROP; this is true when the other parameters are constant. However, when the increase of ROP is accompanied by an increase of TRQ, the rpm might decrease to a level that does not negatively affect ROP. The decrease of rpm shown in Figure 6-23 is related to the increase of the DOC that leads to the increase of TRQ and results high ROP.

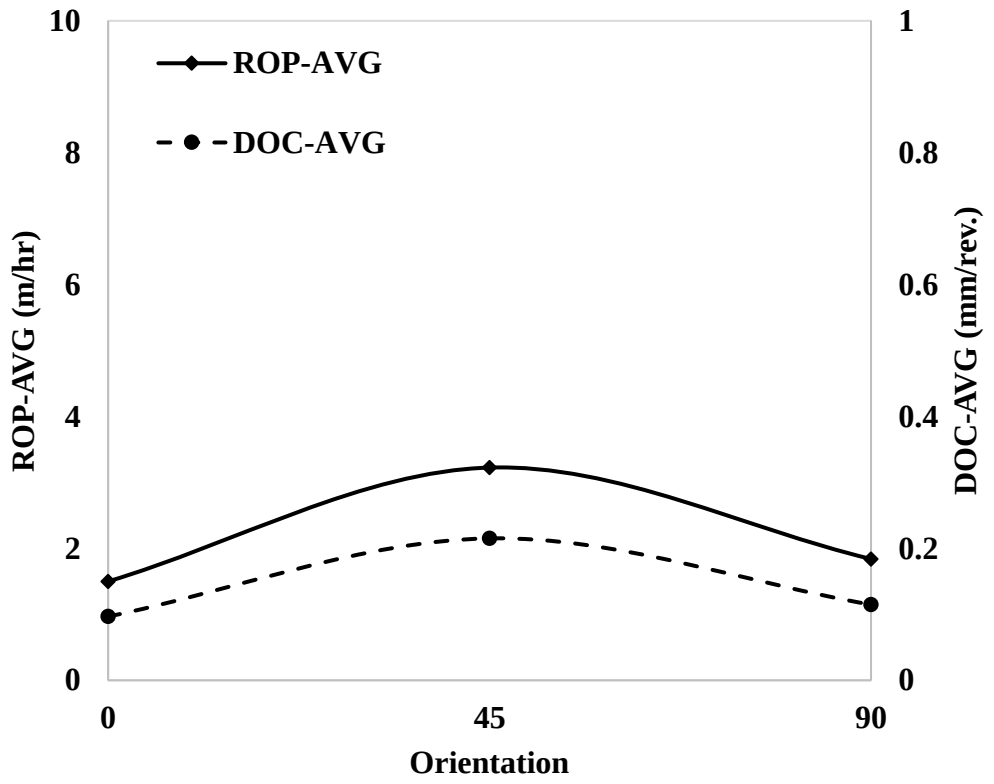

Figure 6-21. Relationship between average values of oriented ROP and oriented DOC from shale drilling

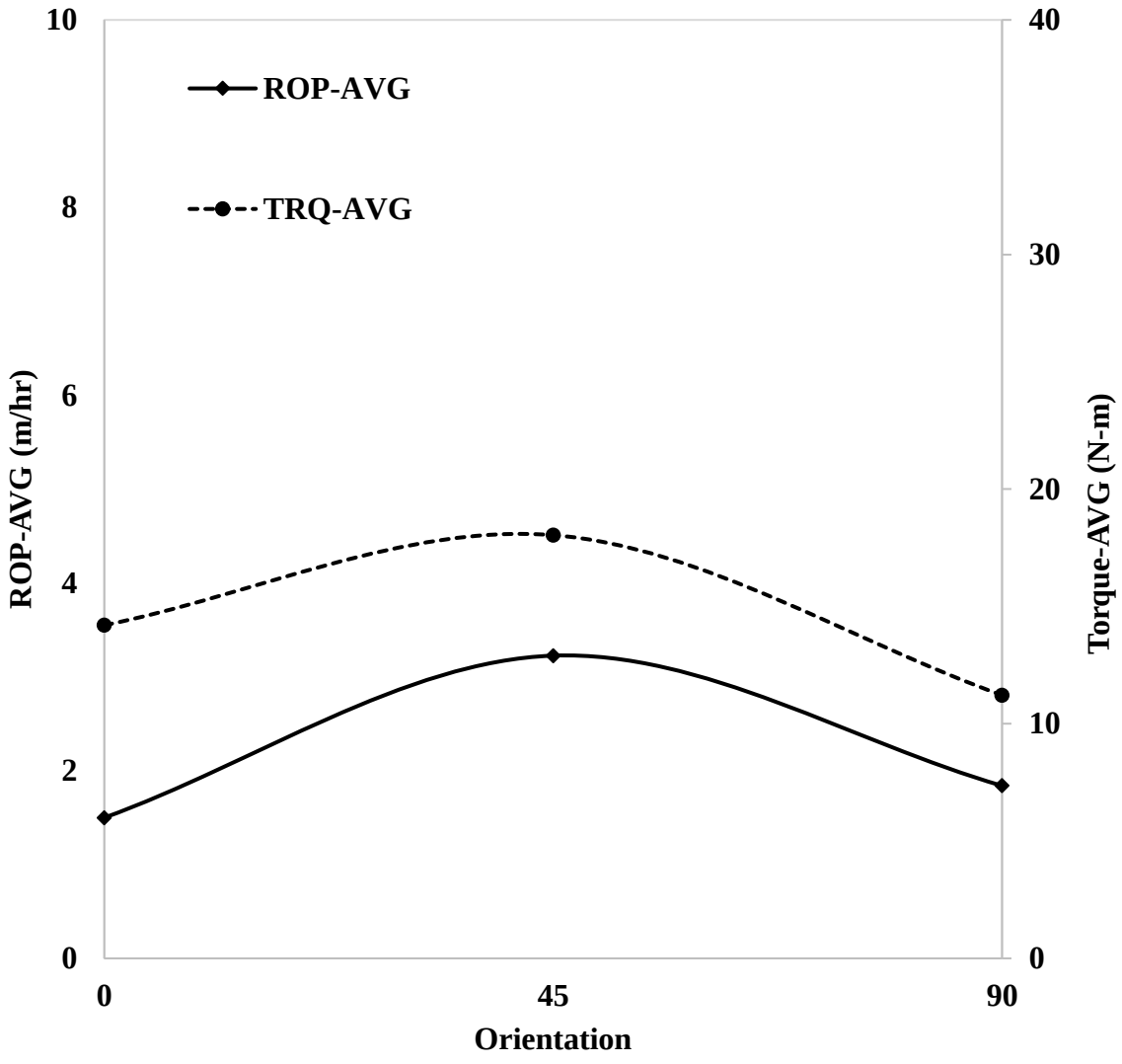

Figure 6-22. Relationship between average values of oriented ROP and oriented TRQ from shale drilling

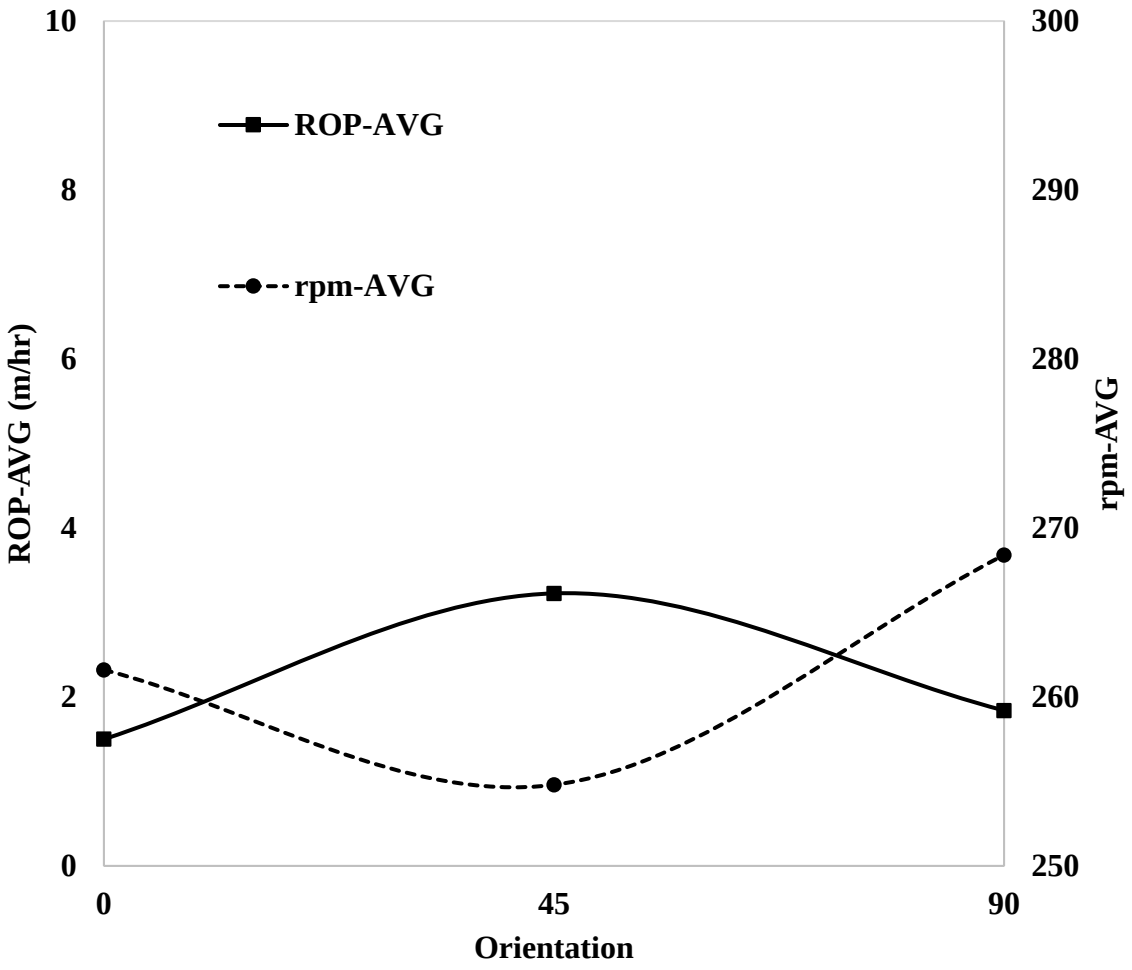

Figure 6-23. Relationship between average values of oriented ROP and oriented rpm from shale drilling

6.7.3.3 Isotropy vs. Anisotropy Study Analysis

In this section, RLM oriented drilling parameters are provided as a comparative analysis of the oriented drilling of the Isotropic (Iso) versus Anisotropic (Aniso) rocks. The purpose of this analysis is to evaluate, based on the averaged data, the response of each drilling parameter, DOC, rpm, and TRQ with ROP in both rock types and to develop a general procedure, through which rock isotropy or anisotropy can be determined by interpreting the results of the oriented drilling performance. As drilling parameters of isotropic rocks, such as RLM are orientation independent, Figure 6-24 through Figure 6-26 show the relationships between DOC, TRQ, and rpm with ROP in three orientations with very low variations indicating RLM isotropy.

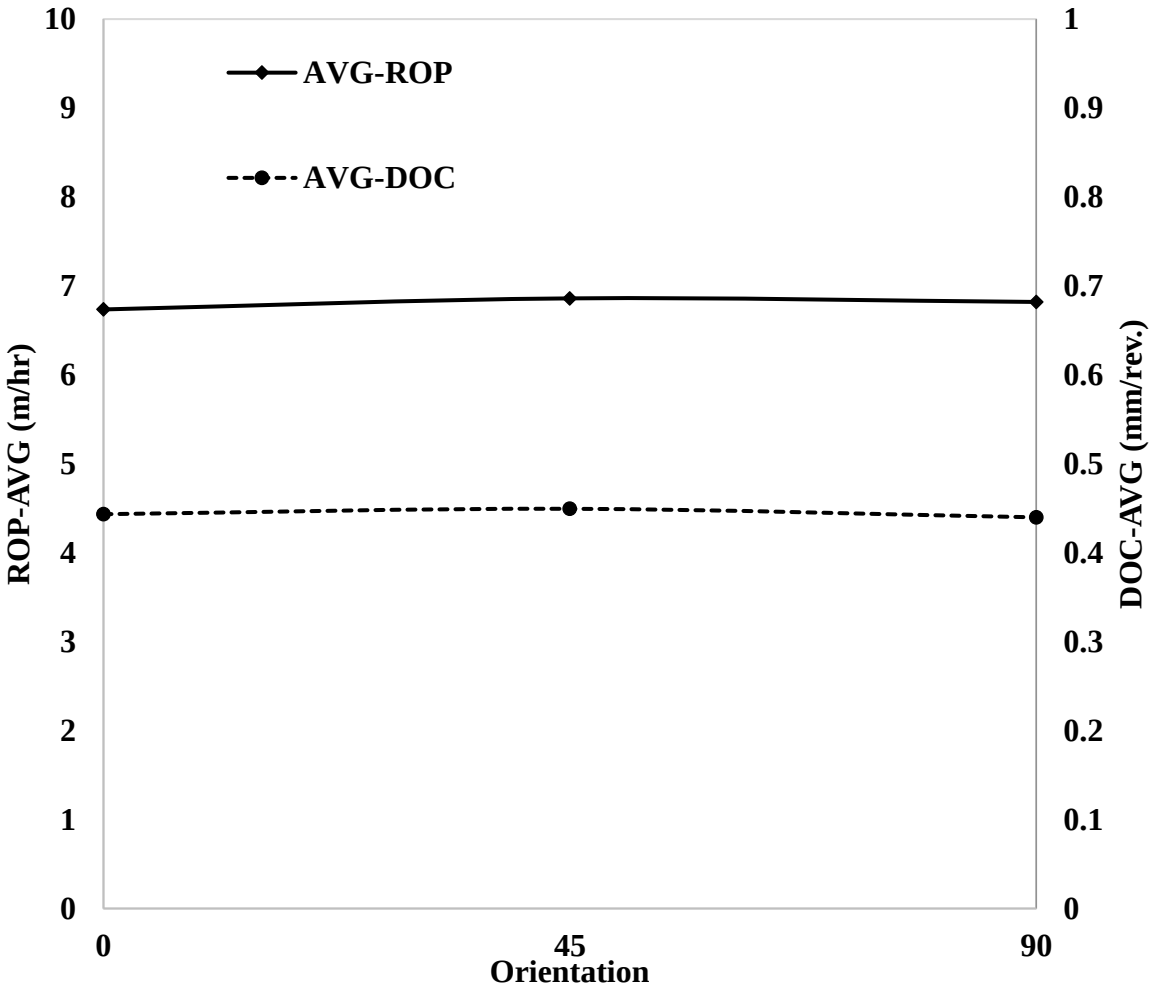

Figure 6-24. Relationship between oriented ROP-AVG and oriented AVG-DOC from RLM drilling

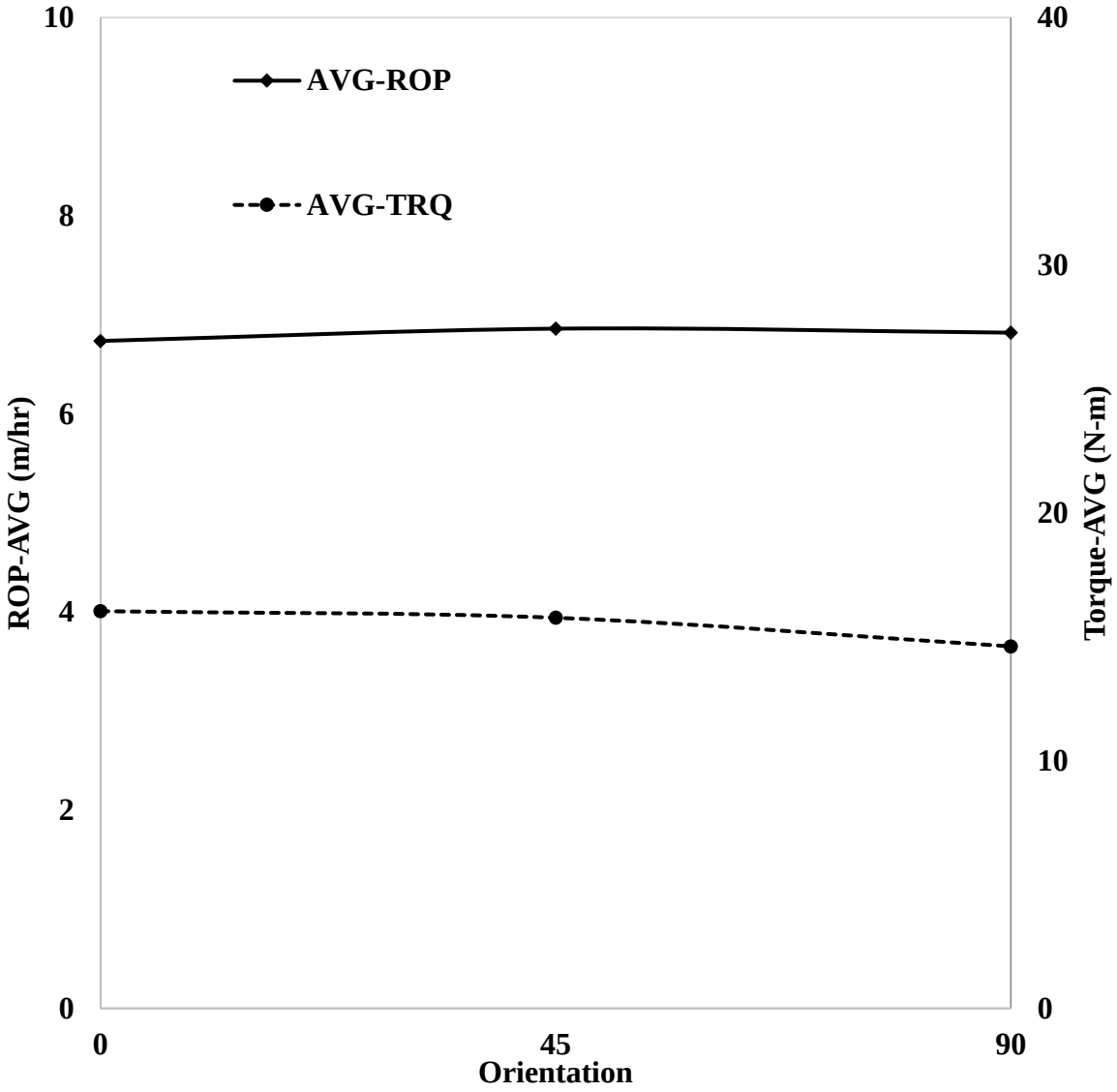

Figure 6-25. Relationship between oriented ROP-AVG and oriented TRQ-AVG from RLM drilling

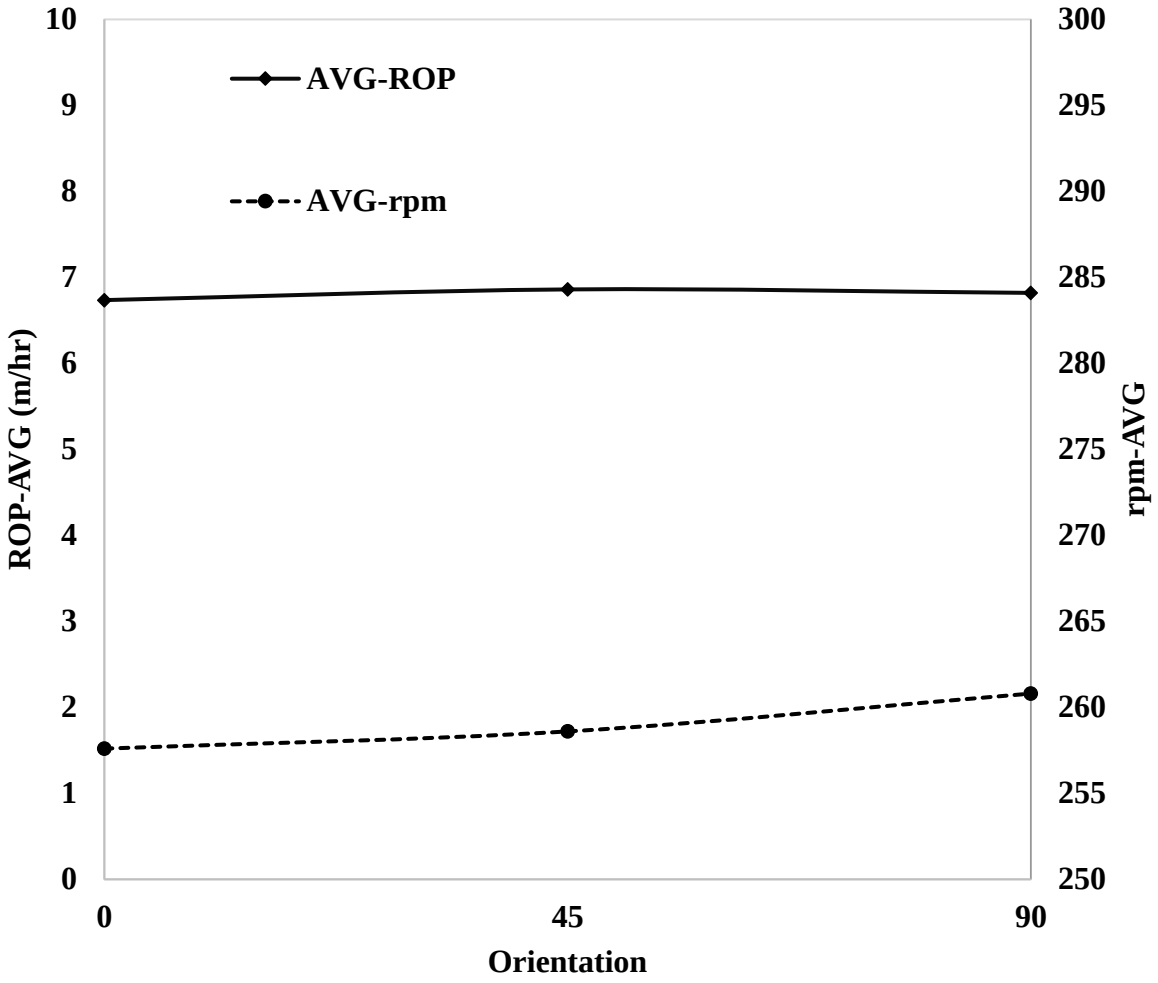

Figure 6-26. Relationship between oriented ROP-AVG and oriented TRQ-AVG from RLM drilling

6.8 Summary

- Circular Vp and Vs measurements were conducted on shale, RLM, and granite and they exhibited shale anisotropy, and granite and RLM isotropy.

- This study involved evaluation of multiple drilling parameters as a function of shale bedding orientations at various WOB.
- Study of the variations of ROP, DOC, RPM, and Torque in shale drilling resulted from drilling in different orientations showed shale anisotropy.
- In shale, the oriented drilling showed higher ROP in oblique drilling than that in vertical and horizontal drilling.
- Averaged oriented DOC and TRQ are directly proportional to ROP and their values are higher in the oblique direction due to the lower strength than that in vertical and horizontal direction where strength is higher.
- Averaged oriented rpm was observed to be inversely proportional to ROP.
- In RLM, averaged oriented ROP was in the same range in the three directions.
- Averaged DOC, TRQ, and rpm in drilling RLM were observed to experience no significant variation, which indicates RLM isotropy.

6.9 Future Work

In-depth study of shale drilling parameters, including smaller increment orientations (i.e. 15°. 30°, 60°, and 75°) and as a function of various conditions of flow rates, confining pressures, and rotary speeds.

- Studying of shale physical and mechanical properties under pressurized conditions.

- Simulating shale shear and tensile fracturing modes during drilling operation and linking such modes to drill bit types used under various conditions of confining pressures, flow rates, and shale rock types.

6.10 Acknowledgement

This work was performed at the Drilling Technology Laboratory (DTL) at Memorial University of Newfoundland, St. John's, Newfoundland and Labrador, Canada and it was funded by:

A. Atlantic Canada Opportunity Agency (AIF contract number: 781-2636-1920044), involving Husky Energy, Suncor Energy and Research and Development Corporation (RDC) of Newfoundland and Labrador.
B. The Ministry of Higher Education and Scientific Research, Libya, through the Canadian Bureau for International Education, Canada (CBIE-Canada).

6.11 References

1. McLamore, R. T. (1971). "The Role of Rock Strength Anisotropy in Natural Hole Deviation", Journal of Petroleum Technology, 23(11), pp. 1315-1321.

2. Brown, E.T., Green, S. J., and Sinha, K. P. (1981). "The Influence of Rock Anisotropy on Hole Deviation in Rotary Drilling- A Review", International Journal of Rock Mechanics, Mining Sciences, and Geomechanics Abstracts, Vol. 18, pp.387- 401.

3. Karfakis, M. G., and Evers, J. F. (1987). “Technical Note- Effects of Rock Lamination Anisotropy on Drilling Penetration and Deviation”, International Journal of Rock Mechanics, Mining Sciences, and Geomechanics Abstracts, 24 (6), pp. 371-374.

4. Boualleg, R., Sellami, H., and Menand, S. (2006). “Effect of Formations Anisotropy on Directional Tendencies of Drilling Systems” IADC/SPE Drilling Conference, Miami, Florida, USA, 21-23 February.

5. Boualleg, R., Sellami, H., Rouabhi, A., and Menand, S. (2007). “Effect of Rock Anisotropy on Deviation Tendencies of Drilling Systems”, 11TH Congress of the International Society for Rock Mechanics, Taylor and Francis Group, London.

6. Maurice B. D. (2013). “Geomechanical Aspects of Shale Gas Development”, Rock Mechanics for Energy and Environment- Taylor and Frances Group, London.

7. Cheatham, J. B., & Daniels, W. H. (1979). “A Study of Factors Influencing the Drillability of Shales: Single-Cutter Experiments With STRATAPAX (T) Drill Blanks,” ASME J. Energy Resour. Technol., 101(3), pp. 189-195.

8. Wang, W., & Taleghani, A. D. (2014). “Simulating multizone fracturing in vertical wells,” ASME J. Energy Resour. Technol., 136(4), p. 042902.

9. Zhou, D., Zheng, P., Peng, J., & He, P. (2015). “Induced stress and interaction of fractures during hydraulic fracturing in shale formation,” ASME J. Energy Resour. Technol., 137(6), p. 062902.

10. Ahn, C. H., Dilmore, R., & Wang, J. Y. (2017). “Modeling of hydraulic fracture propagation in shale gas reservoirs: a three-dimensional, two-phase model ASME J. Energy Resour. Technol., 139(1), p. 012903.

11. Chen, X., Gao, D., Yang, J., Luo, M., Feng, Y., & Li, X. (2018). “A Comprehensive Wellbore Stability Model Considering Poroelastic and Thermal Effects for Inclined Wellbores in Deepwater Drilling,” ASME J. Energy Resour. Technol., 140(9), p. 092903.

12. Fjaer, E., Holt, R. M., Raaen, A. M., Risnes, R., and P. Horsrud. (2008). “Petroleum Related Rock Mechanics”, (53), Elsevier.

13. Chang, C., Zoback, M.D., and Khaksar, A. (2006). “Empirical Relations between Rock Strength and Physical Properties in Sedimentary Rocks”, Journal of Petroleum Science and Engineering, 51(3), pp.223-237.

14. Pan, R., Zhang, G., Li, S., An, F., Xing, Y., Xu, D., and Xie, R. (2016). “Influence of Mineral Compositions of Rocks on Mechanical Properties”, the 50th us rock Mechanics / Geomechanics symposium, American rock mechanics association, Houston, TX, USA, 26-29 June 2016.

15. Friedman, M. (1976). “Porosity, Permeability, and Rock Mechanics - A Review”, the 7th US Symposium on Rock Mechanics. American Rock Mechanics Association.

16. Abugharara, A. N., Alwaar, M. A., Hurich, A. C., and Butt, S.D. (2016). “Laboratory Investigation on Directional Drilling Performance in Isotropic and Anisotropic Rocks.” The 50th US Rock mechanics / Geomechanics Symposium, American Rock Mechanics Association, Houston, TX, USA, 26-29 June.

17. Abugharara, A. N., Alwaar, A. M., Butt, S. D., and Hurich, C. A. (2016). "Baseline Development on Rock Anisotropy Investigation Utilizing Empirical Relationships Between Oriented Physical and Mechanical Measurement and Drilling Performance", The 35th International Conference on Ocean, Offshore and Arctic Engineering, Drilling Symposium, June 19-24, Busan, South Korea.

18. ASTM Standard D2845. (2008). "Standard Test Method for Laboratory Determination of Pulse Velocities and Ultrasonic Elastic Constants of Rock," ASTM International, West Conshohocken, PA, www.astm.org.

19. Ewy, R. T. and Bovberg, C. A. (2010). "Strength Anisotropy of Mudstones and Shales", the 44th US-Canada Rock Mechanics / Geomechanics Symposium, American Rock Mechanics Association, Salt Lake City, UT, June 27-30.

20. Crawford, B.R., Dedontney, N. L., and Ottesen, S. (2012). "Shear Strength Anisotropy in Fine-Grained Rocks", the 46th US Rock Mechanics / Geomechanics Symposium, American Rock Mechanics Association, Chicago, IL, USA, 24-27 June.

21. Holt, R. M., Nes, O.M., Stenebraten, J.F., and Fajaer, E. (2012). "Static Vs. Dynamic Behaviour of Shale", the 46th US Rock Mechanics / Geomechanics Symposium, American Rock Mechanics Association, Chicago, IL, USA, 24-27 June.

22. Fjaer, E. and Nes, O. M. (2013). "Strength Anisotropy of Mancos Shale" the 47th US Rock Mechanics / Geomechanics Symposium, American Rock Mechanics Association, San Francisco, CA, USA, 23-26 June.

23. Simpson, N. D. J., Stroisz, A., Bauer, A., Vervoort, A., and Holt, R.M. (2014). “Failure Mechanics of Anisotropic Shale during Brazilian Tests”, the 48th US Rock Mechanics / Geomechanics Symposium, American Rock Mechanics Association, Minneapolis, MN, USA, 1-4 June.

24. Holt, R.M., Bauer, A., Fjaer, A., Stenebraten, J. F., Szewczyk, D., and Horsrud, P. (2015). “Relating Static and Dynamic Mechanical Anisotropies of Shale”, the 49th US Rock Mechanics / Geomechanics Symposium, Sanfrancisco, CA, USA, 28 June-1 July.

25. Cho, J., Kim, H., Jeon, S., and Min, K. (2012). “Deformation and Strength Anisotropy of Asan, Gneiss, Boryeong Shale, and Yeoncheon Schist”, International Journal of Rock Mechanics and Mining Sciences, (50), pp. 158-169, Elsevier.

26. Park, B., and Min, K. (2013). “Discrete Element Modelling of Transversely Isotropic Rock”, the 47th US Rock Mechanics / Geomechanics Symposium, American Rock Mechanics Association, San Francisco, CA, USA, 23-26 June.

27. Nygaard, R., and Hareland, G. (2007). “Application of Rock Strength in Drilling Evaluation”, SPE Latin American and Caribbean Petroleum Engineering Conference, Buenos Aires, Argentina, April 15-19.

28. Kerkar, P. B., Hareland, G., Fonseca, E. R., and Hackbarth, C. J. (2014). “Estimation of Rock Compressive Strength Using Downhole Weight-on-Bit and Drilling Models” International Petroleum Technology Conference, Doha, Qatar, January 20-22.

29. Horsrud, P. (2001). “Estimating Mechanical Properties of Shale from Empirical Correlations”, Society of Petroleum Engineers, SPE Drilling and Completion.

30. David, N. D., Joel, S., Claudio, D. P., Anthony, F. S., Mark, D. R. (2010). “Prediction of Shale Mechanical Properties from Global and Local Empirical Correlations”, SEG Denver, Annual Meeting.

31. Altindag, R. (2012). “Correlation between P-Wave Velocity and Some Mechanical Properties for Sedimentary Rocks”, the Journal of the Southern African Institute of Mining and Metallurgy, 112(3), pp. 229-237.

32. Mishra, D. A., and Basu, A. (2013). “Estimation of Uniaxial Compressive Strength of Rock Materials by Index Tests Using Regression Analysis and Fuzzy Inference System”, Journal of Engineering Geology, (160), pp. 54-68, Elsevier.

33. Fear, M. J. (1999). “How to improve rate of penetration in field operations,” SPE drilling & completion, 14(01), pp. 42-49.

34. Hamza, F., Chen, C., Gu, M., Quirein, J., Martysevich, V., and Matzar, L. (2015). “Characterization of Anisotopic Elastic Moduli and Stress for Unconventional Reservoirs Using Laboratory Static and Dynamic Geomechanical Data”, SPE/CSUR Unconventional Resources Conference, Calgary, Alberta, Canada, October 20-22.

CHAPTER 7: NUMERICAL STUDY USING PFC-2D OF THE INFLUENCE OF PASSIVE VIBRATION ASSISTED ROTARY DRILLING TOOL (PVARD) ON ENHANCING DRILLING PERFORMANCE

Abdelsalam N. Abugharara [a], PhD candidate

Abourawi Alwaar [a], Graduate Student

John Molgaard [b], Professor

Charles Hurich [c], Associate Professor

Stephen D. Butt [a], Professor

[a] Drilling Technology Laboratory, Memorial University of Newfoundland, St. John's, NL, Canada A1B 3X5

[b] Department of Mechanical Engineering, Memorial University of Newfoundland, St. John's, NL, Canada A1B 3X5

[c] Department of Earth Sciences, Memorial University of Newfoundland, St. John's, NL, Canada A1B 3X5

This chapter is based on the objectives defined in section 1.3.5 and was submitted to the Journal of Energy Resources and Technology (ASME) on March 2, 2019 and are currently under review.

7.1 Co-authorship Statement

The contributions of this collaborative work are described in the following seven parts. 1) Identification of research topic is collaborative between all co-authors. 2) Design of experiments are contributed by Abdelsalam Abugharara, Abourawi Alwaar, and Dr. S. D. Butt. 3) Preparation of cores and construction of ultrasonic and mechanical measurements are solely contributed by Abdelsalam Abugharara. 4) Performance of drilling experiments are cooperated by Abdelsalam Abugharara and Abourawi Alwaar, 5) PFC-2D simulation is contributed by Abdelsalam Abugharara and Abourawi Alwaar, 6) Data analysis and discussion of results is a collaborative work contributed by all co-authors, 7) Manuscript preparation is mainly contributed by Abdelsalam Abugharara, with revision assistance provided by all other coauthors

7.2 Abstract

This work concentrates on implementing the Particle Flow Code – 2Dimension (PFC-2D) in simulating empirical drilling of using the Passive Vibration Assisted Rotary Drilling (pVARD) tool reported in Rana et al. [1]. The laboratory input drilling parameters that were simulated in the PFC-2D included several levels of weight on bit (WOB), one rotary speed of 300 rpm, one constant flow rate, at two sets of bottomhole pressure (BHP). The laboratory drilling was performed on 10.61 * 15.24 cm cylinders of rock like material (RLM) of about 50 MPa strength, using a fully instrumented laboratory-scale rig. Moreover, the experiments were conducted using three different pVARD configurations as well as rigid “conventional” drilling. The three pVARD configurations differed in their compliances controlled by various spring stiffness as low, medium, and high as controlled by the stiffness of the incorporated springs. In the PFC-2D, the experimental drilling was simulated with the equivalent WOB values, constant cutter horizontal velocity, and constant

cutting removal. By including the above parameters and conditions, PFC-2D successfully, simulated drilling with pVARD and a rigid drillstring. The evaluated output parameters included rate of penetration (ROP), depth of cut (DOC), and mechanical specific energy (MSE). The numerical simulation showed good agreement with, and validated, the experimental work, and indicated the positive effect of utilizing the downhole pVARD (in three configurations) on improving ROP.

7.3 Introduction

It is well established that efficient drilling is achieved by operating at a maximum feasible rate of penetration (ROP) i.e. the depth of cut per unit time, which also means a minimum mechanical specific energy (MSE), the energy required to remove a unit volume of rock [2 -5]. These are functions of the weight on bit (WOB), drill mud pressure and flow rate and rotary speed (e.g. in rpm) of the drill bit [6 - 8]. Drill off test (DOT) is the typical practice to determine optimal drilling parameters for efficient drilling performance [5, 9 -11]. Other parameters such as best bit selection and optimal bit hydraulics with enough flow rate that clears rock cuttings, avoids blockages, prevents bit ball, and brings cuttings to the surface, also influence drilling performance [6, 12-18]. In current drilling technology some key parameters, including WOB and rotary speed, are applied and controlled at the bottom hole assembly (BHA) rather than solely at the surface as discussed in the next section. This helps to reduce energy loss along the drill string by avoiding friction, eliminate damage at a rotating drill string in vertical or non-vertical wells, and better transmit of surface load and torque to drill bit. The flow of drill mud may also be used to drive the rotation of the drill bit and the pressure in the drill mud at the drill bit and the bottom hole pressure

(BHP) influence the WOB and the ROP. Vibration of the drill string and/or of the drill bit was conventionally considered undesirable, even dangerous and to be avoided, as it has been linked to damage, including premature failure to drill bits and hence to costly excessive down-time [18 – 27]. However, as outlined in the following section, vibration can be beneficial rather than detrimental.

7.4 Applications of Vibrations to Improve ROP

Considering that the conventional way to improve ROP requires an increase of the parameters (WOB, rpm, torque, etc.) only at the surface and then transmitted through the entire drill string to the drill bit. However, a new frequent way to improve ROP involves installing special tools as part of the BHA that utilize the parameters most influence the ROP (i.e. WOB and rpm) to be increased, stabilized, or efficiently transmitted to the drill bit. Some applications of non-dangerous vibrations have been reported in several studies. de Bruijin et al. [10] reported up to 100% ROP improvement achieved through minimizing fluctuation in rpm by using a Turbodrill. Gaynor [28] reported the improvement of ROP in directional drilling using steerable straight-hole turbodrills, which provided eccentric bit rotation and controlled well deviations. Jansen et al. [29] reported a significant increase in ROP and reduction of downhole equipment failure by using an active damping system that acted as a tuned vibration damper that eliminated stick/slip and torsional drillstring vibration, the main two types of destructive vibrations. Motahhari et al. [30] reported maximizing ROP by using a positive displacement motor (PDM) at the bit, whose performance data is coupled with an ROP model to optimize drilling parameters including WOB and improving ROP. Alali et al. [31] reported ROP improvement by using axial oscillation generator tool (AGT), whose axial oscillation reduced friction and enhanced weight transfer. Clausen et al. [32] reported

maximizing ROP, limiting bit damage, and extending bit life by using an axial excitation tool (AET) at the bit in vertical and directional wells that generated downhole beneficial axial vibrations. Gee et al. [33] reported field and mathematical simulation data that showed significant increase in ROP due to generating downhole benign vibration that enhanced weight transfer and reduced friction by using axial oscillation tool (AOT) verses a lateral vibration tool (LVT). Jones et al. [34] reported increasing drilling performance using a friction reduction tool (FRT) that was effective in transmitting axial oscillation, reducing friction, and eliminating BHA damage. Wu et al. [25] reported a higher ROP at lower overall drilling cost by identifying the root cause of the harmful effect of the stick slip and axial vibrations. By minimizing the harmful effect of the stick slip and axial vibrations, the life of the bit and BHA can be extended and the drilling performance can be enhanced. This was done by Finite Element Analysis (FEA). Wang et al. [35] reported theoretical, laboratory and field results showing reduction of friction and improved ROP using a novel self-resonating oscillator. Wilson and Noynaert [36] reported ROP improvement not only due to reducing friction and enhancing weight transfer, but more importantly due to generating dynamic axial force by using axial excitation tools (AET) in drilling non-vertical wells. Li et al. [37] and Akbari et al. [38] reported improvement in ROP by using downhole vibration assisted rotary drilling (VARD) through experimental and PFD-2D simulation, respectively. They found the excitation of controlled vibration at the bit influences increasing ROP at applied low WOB. Babatunde et al. [39] reported the influence of vibration frequencies at the bit on enhancing ROP using a diamond drag bit. Xiao et al. [11] reported ROP improvement using an active vibration assisted drilling tool installed at the bit during laboratory coring with a diamond impregnated bit. Their experimental results showed that at any given WOB, the ROP was increased with higher

amplitude of bit-rock vibration and with cutting size increased. Moreover, their spectral analysis of the Acoustic Emission (AE) indicated higher ROP with larger cutting size, higher AE energy, and lower AE frequency.

As a continuation of a series of investigations of the influence of downhole controlled and desirable axial vibrations (with various frequencies, amplitudes, compliances, etc.) performed by the drilling technology laboratory at Memorial University of Newfoundland (DTL-MUN) [1, 11, 31, 32, 34, 40, 41, 42, 43], DTL-MUN has been using PFC-2D to simulate drilling performance and investigate improving ROP, involving various conditions of pressure, rock properties, flow rates, vibration and non-vibration systems [32, 40, 41, 44]. This paper focuses on a simulation of a laboratory study in which ROP was enhanced using pVARD. In the simulation, using PFC-2D three pVARD configurations, in addition to matching drilling parameters (i.e. WOB, rpm, etc.), their compliances were modeled, inducing three axial vibration levels, which were not found to be dangerous in the laboratory study. The PFC-2D simulation results agreed with the significant increase in ROP and decrease in MSE, achieved by using pVARD.

7.5 Description of pVARD

Implementing the pVARD tool in drilling has been shown already to enhance drilling performance. It induces useful axial oscillation that generates downhole dynamic weight on bit (DDWOB) and minimizes destructive vibrations to within the controlled and safe vibration window. Details of the pVARD design and laboratory and field implementation is reported by Rana et al., [1] and a Discrete Element Method simulation of pVARD is reported by Zang, et al., [40]. One of the main functions of pVARD is to allow the drilling string to have some axial oscillations with different magnitudes generated by bit-rock interaction. The axial oscillation of pVARD is controlled by

inserted springs. Arrangement of pVARD springs varies the pVARD compliance, and as a sequence, the oscillation amplitude range. In this study, pVARD tool was configured using three different axial compliances and with a rigid (non-compliance) configuration as outlined in Table 7.1.

Table 7.1. Summary of PFC-2D parameters and their magnitudes

Property	Magnitude
Ratio of Maximum to Minimum Ball Size	1.8
Parallel Bond Shear Strength	44e6 Pa
Parallel Bond Normal Strength	44e6 Pa
Minimum Ball Radius	0.35e-3 m
Ball and Bond Elastic Modulus	44e9 Pa
Ratio of Normal to Shear Stiffness	2.5
Ball-Ball and Ball-Wall Friction	0.5
Density	2650 kg/m^3
Porosity	18 %
Normal Damping Ratio	0.2
Shear Damping Ration	0.2
Local Damping Ratio	0.5
Unconfined Compressive Strength (UCS)	55 MPa
Young Modulus	40 GPa

7.6 Studied Parameters

The parameters included in the analysis of this study involve the following:

7.6.1 Input Drilling Parameters (IDP)

- Different Bottomhole Pressure (BHP)
- Different Weights On Bit (WOB).
- Three configurations of pVARD (with three different compliance configurations) versus Rigid (non-compliance configuration).

7.6.2 Output Drilling Parameters (ODP)

- Rate of Penetration (ROP)
- Depth Of Cut (DOC).
- Mechanical Specific Energy (MSE).

Figure 7-1 shows the drilling procedure modeled with PFC-2D. It shows the cutter, weight configurations applied, and the region of study in PFD-2D. The three balls displayed above the cutter in Figure 7-1 represent the static weight, the spring stiffness pf pVARD, and the damping. BHP was another factor involved in the PFC-2D simulation. This was to evaluate the influence of BHP on drilling performance using pVARD against rigid drilling. Figure 7-2 shows an example of the effect of BHP on decreasing ROP. Moreover, the results show higher ROP with pVARD vs. rigid at the same BHP.

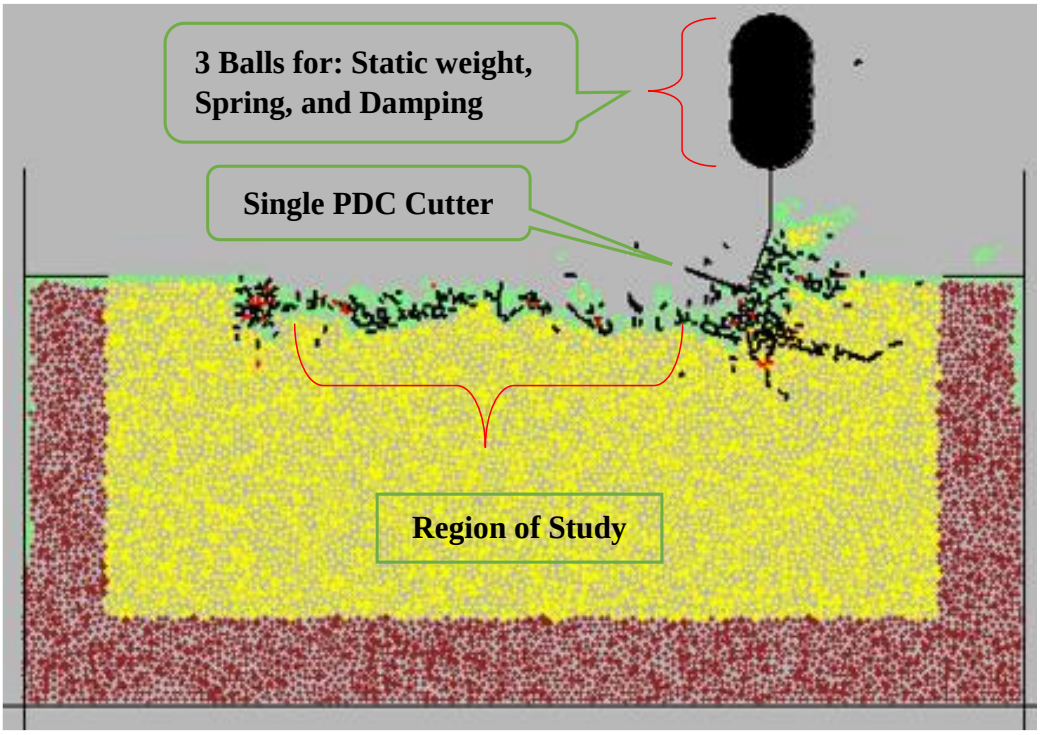

Figure 7-1. Screenshot of the cutting process modeled in PFC-2D

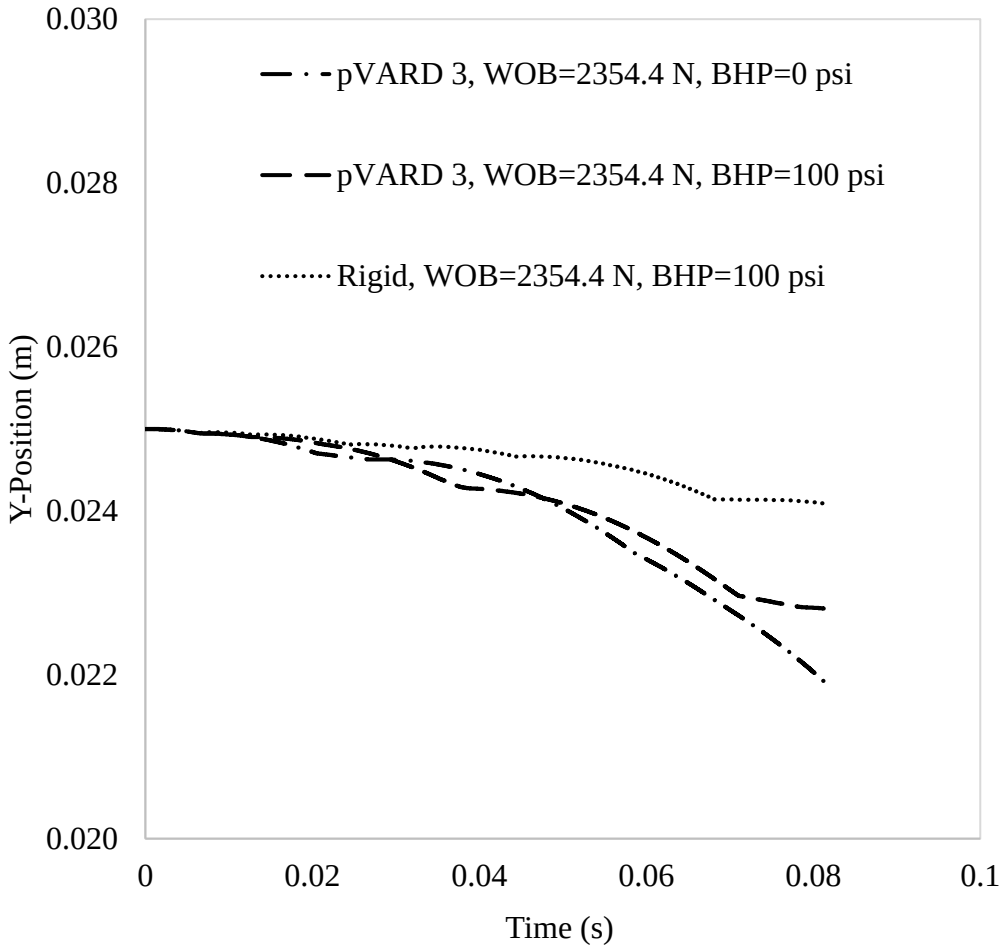

Figure 7-2. One set of PFC-2D output using 3rd pVARD configuration vs. rigid drilling applying different BHP and at the same WOB

7.7 Results

In this section, data is presented based on the drilling performance implementing pVARD vs. rigid with comparative study of PFC-2D results with the experimental results that were reported by Rana et al., [1]. Drilling with DOC equal or less than chamfer depth is considered inefficient drilling performance; therefore, such data was not included in the study with the PDC cutter used in the experimental work. The chamfer depth is 0.15 mm, as reported by Khorshidian, [14]. The

corresponding DOC results of the experimental study are shown in Table 7.2, which included only the DOC data greater than the depth of the chamfer. After categorizing the valid drilling data to be included in the analysis based on the DOC, the study proceeded for ROP and MSE data evaluation. Figure 7-3 shows an example of the comparation of a simulation and experimental results for ROP using the 3rd pVARD configuration. There was a consistent magnitude ratio between the outputs in the simulations and the laboratory experiments. However, it was considered sufficient in the PFC-2D simulation study to achieve outputs in ROP, DOC and MSE that matched the trends in the experimental data obtained with varying WOB.

Table 7.2. Summary of DOC result in PFC-2D and laboratory work

Drilling Mode	Depth of Cut	
	EXPERIMENT	SIMULATION
pVARD 1	0.281	0.333
	0.815	0.557
	0.856	0.698
	1.080	1.320
	1.200	2.320
pVARD 2	0.350	0.357
	0.465	0.601
	0.754	1.064
	1.110	1.490
	1.002	2.348
pVARD 3	0.440	0.403
	0.674	0.674
	0.842	1.090
	1.049	1.380
	1.200	2.400
RIGID	0.262	0.303
	0.414	0.357
	0.445	0.439
	0.786	0.524
	0.766	0.911

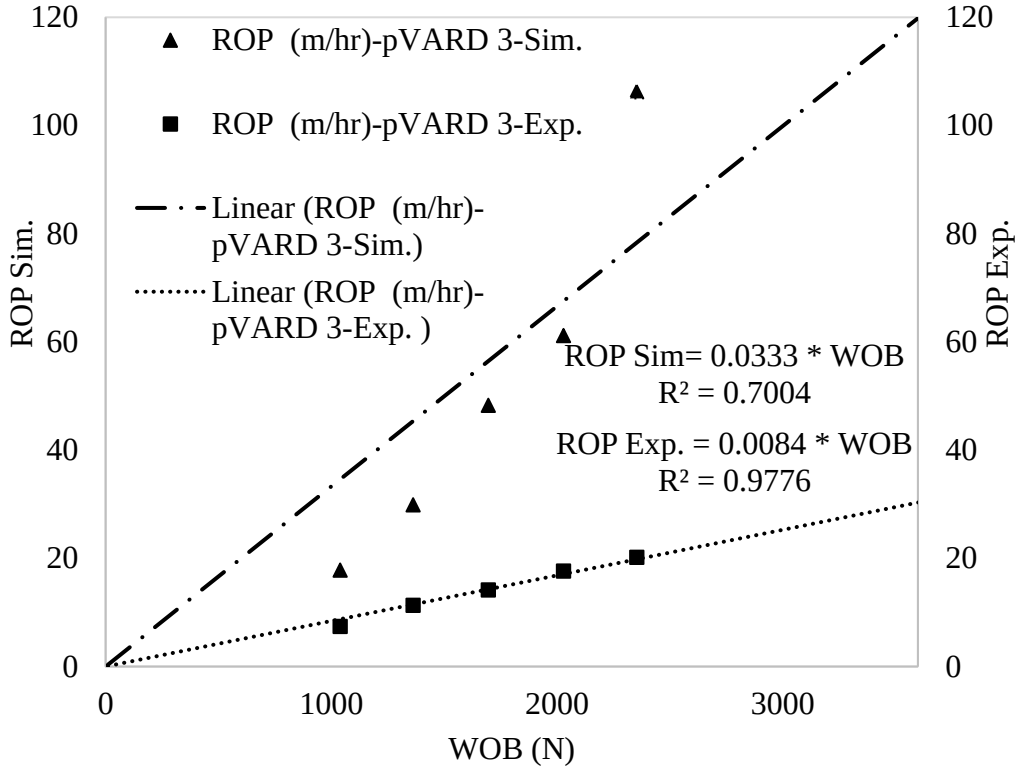

Figure 7-3. One example of data comparison between simulation and experimental work using 3rd configuration of pVARD

7.8 Single Parameter Analysis

This is one category of data analysis adopted in this study. It applies on all figures that includes only one drilling parameter with WOB (see discussion section). In this section, results of each single drilling parameter, including ROP, DOC, and MSE are analyzed based on experimental versus numerical studies with WOB.

7.8.1 Double Parameter Analysis

In this analysis, in each drilling configuration two drilling parameters are analyzed as function of WOB. Figure 7-4 to Figure 7-7 show the analysis of ROP and DOC. These figures show that DOC was directly proportional to ROP. Figure 7-8 to Figure 7-11 show the analysis of the drilling performance based on the study of ROP and MSE at 5 different WOBs using the three pVARD configurations vs. rigid drilling in the numerical study, in which MSE was reversely proportional to ROP. These relationships are generally accepted as indicators of efficient drilling.

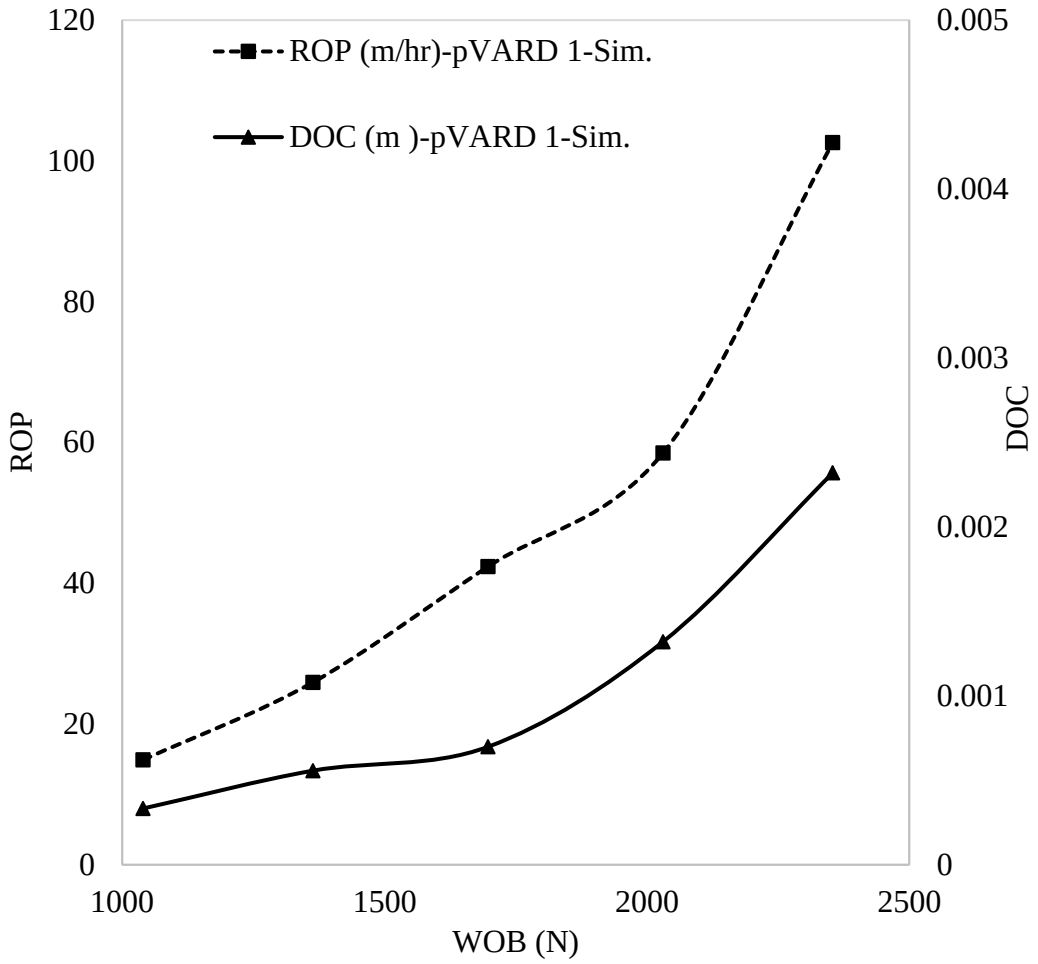

Figure 7-4. ROP and DOC vs. WOB for simulated pVARD 1

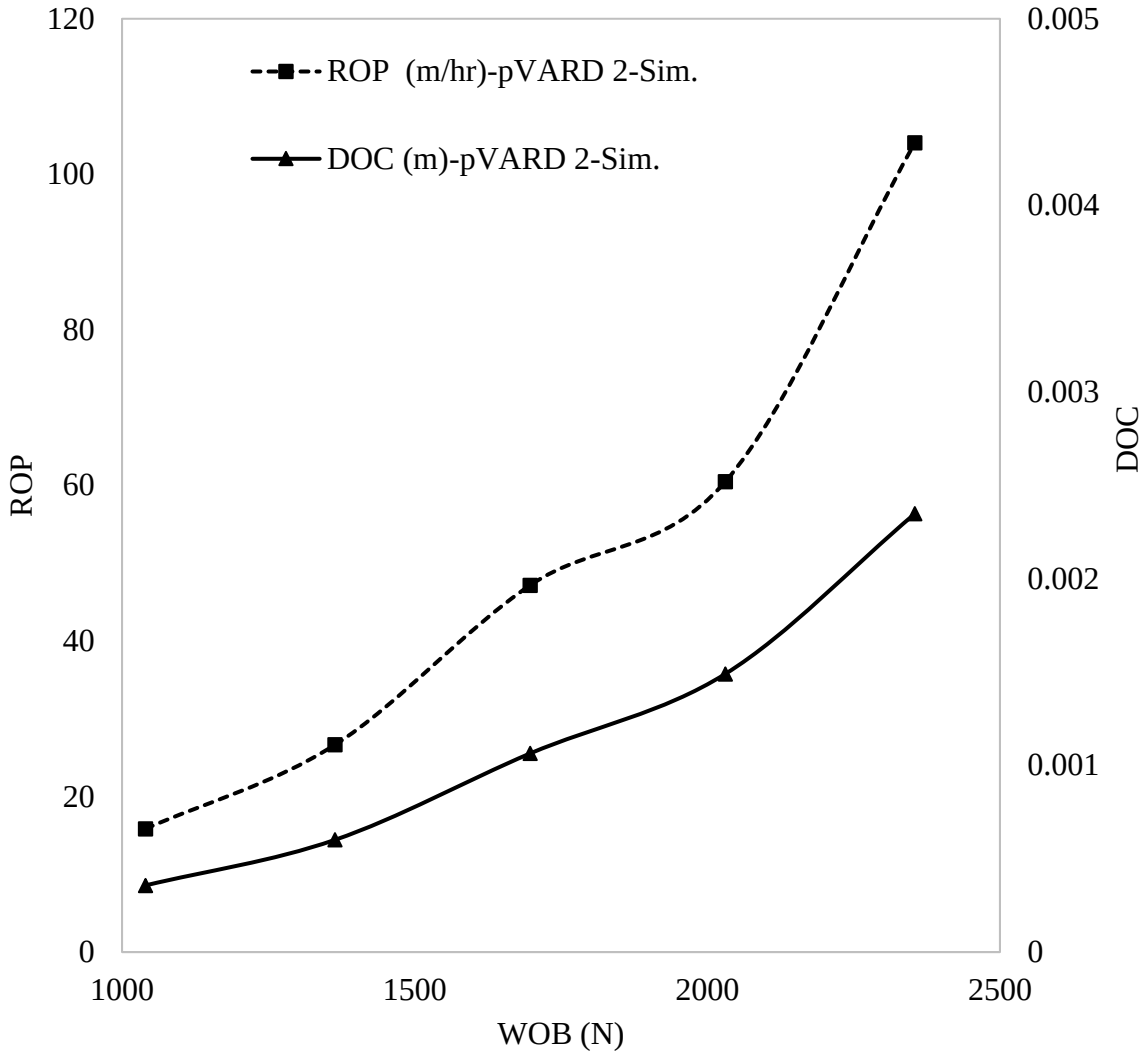

Figure 7-5. ROP and DOC vs. WOB for simulated pVARD 2

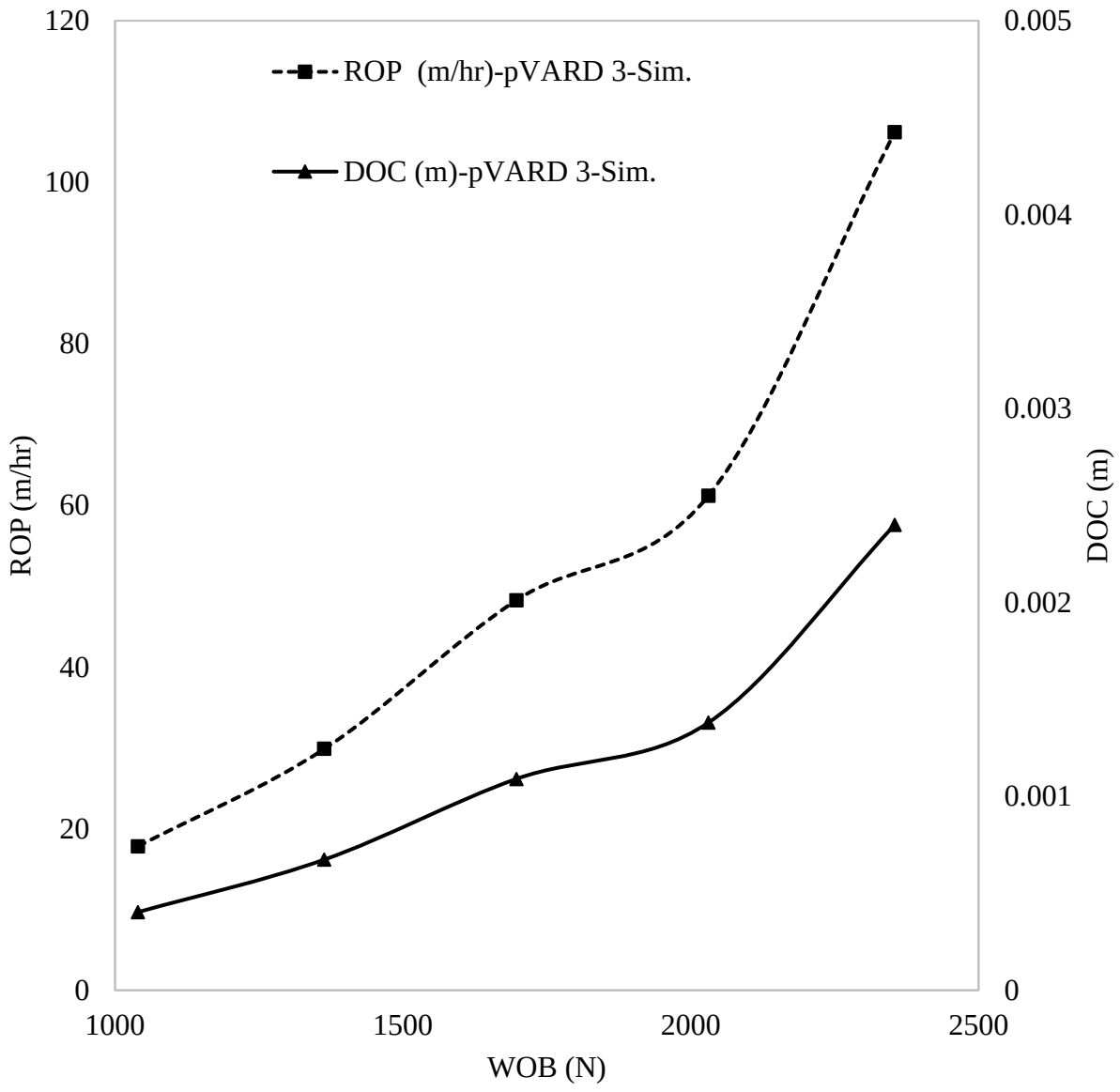

Figure 7-6. ROP and DOC vs. WOB for simulated pVARD 3

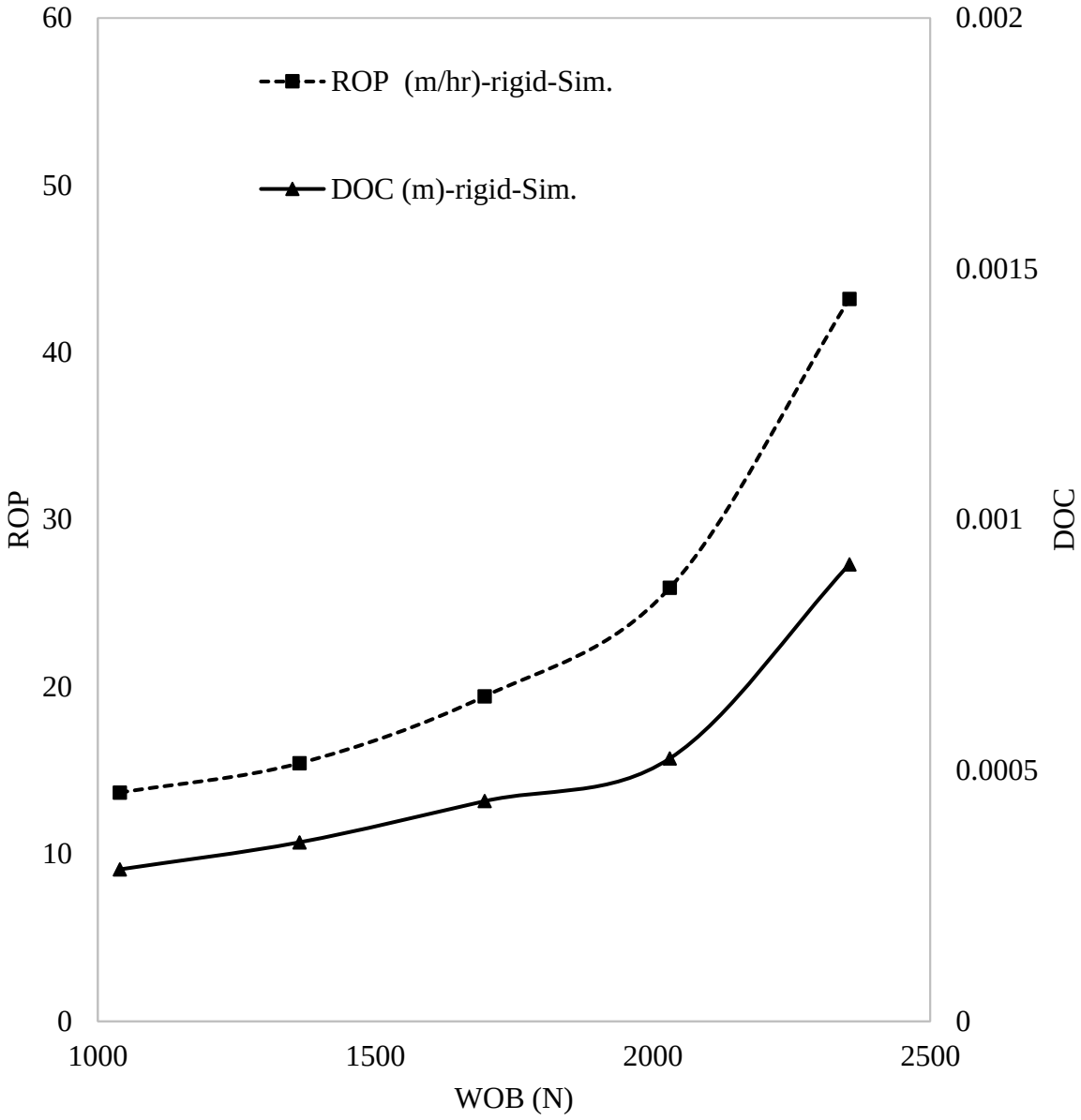

Figure 7-7. ROP and DOC vs. WOB for simulated rigid

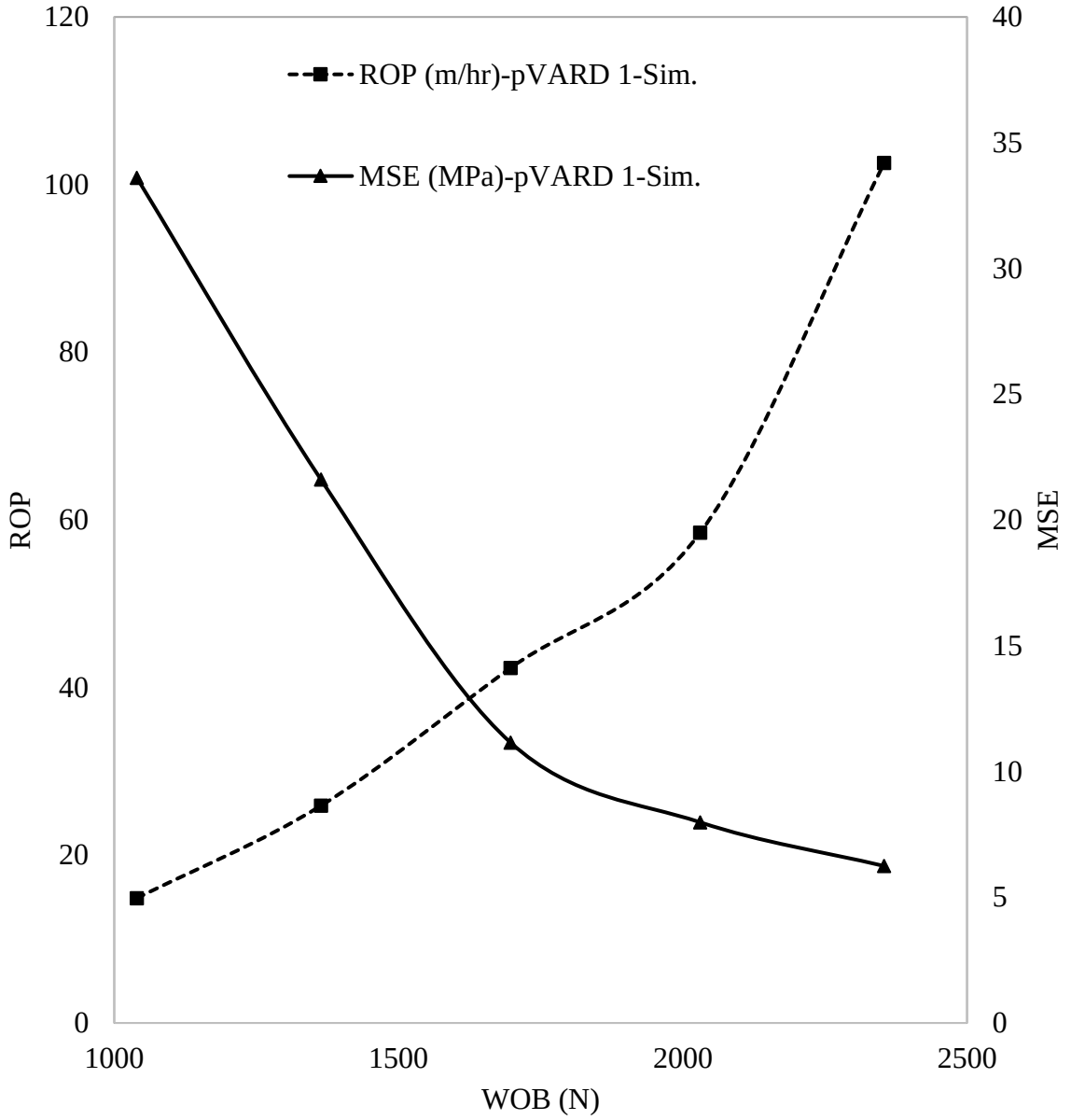

Figure 7-8. ROP and MSE vs. WOB for simulated pVARD1

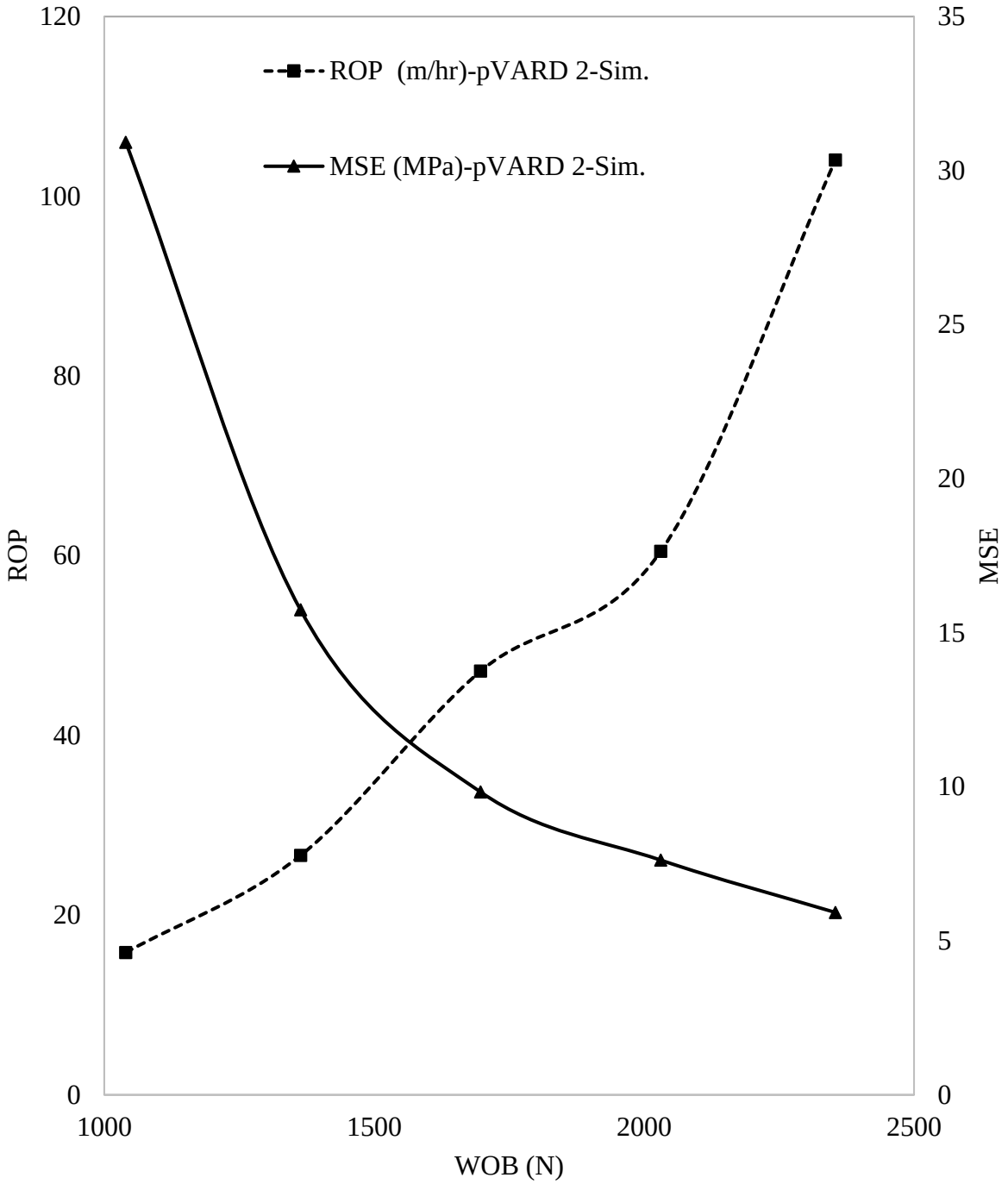

Figure 7-9. ROP and MSE vs. WOB for simulated pVARD 2

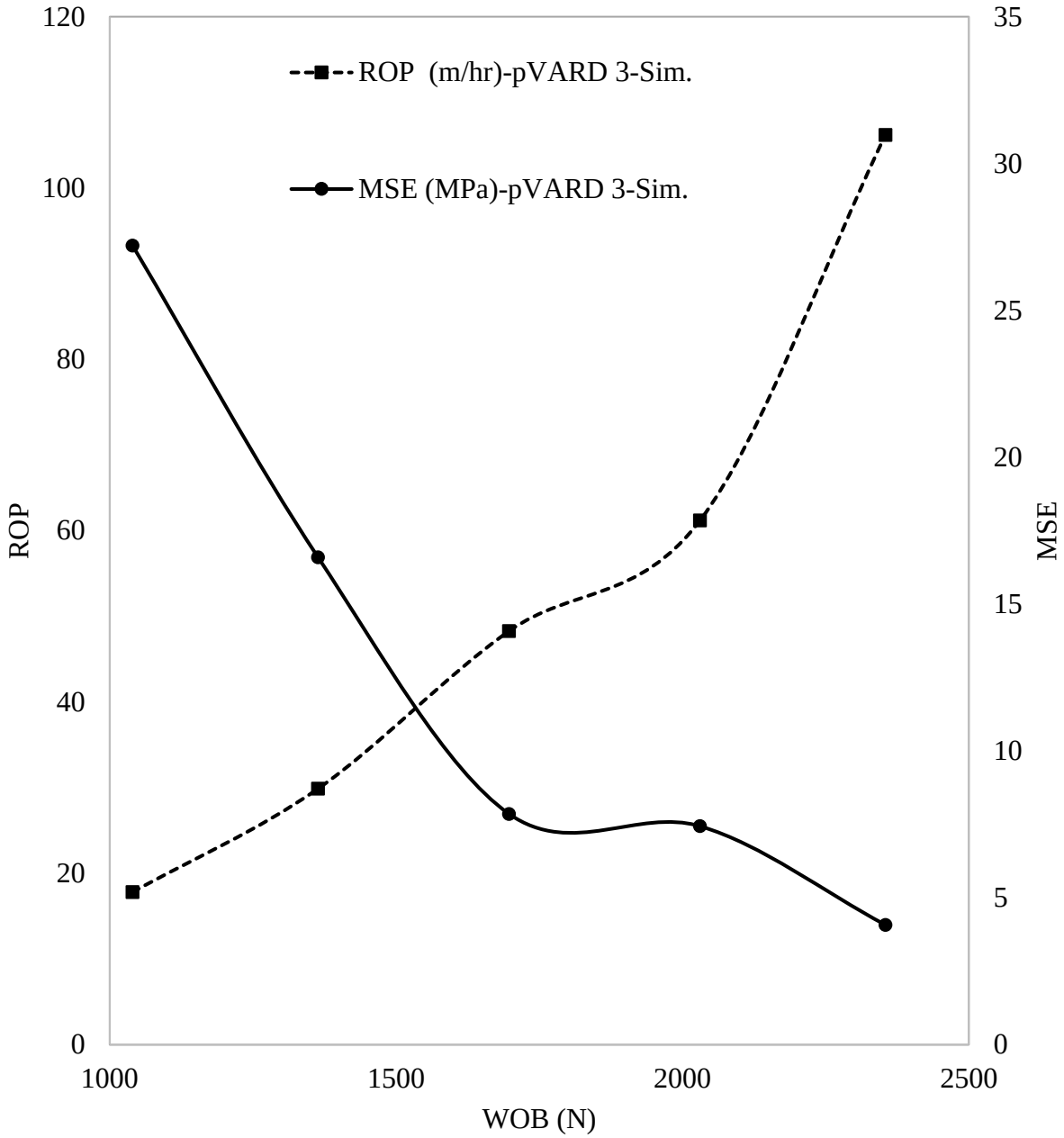

Figure 7-10. ROP and MSE vs. WOB for simulated pVARD 3

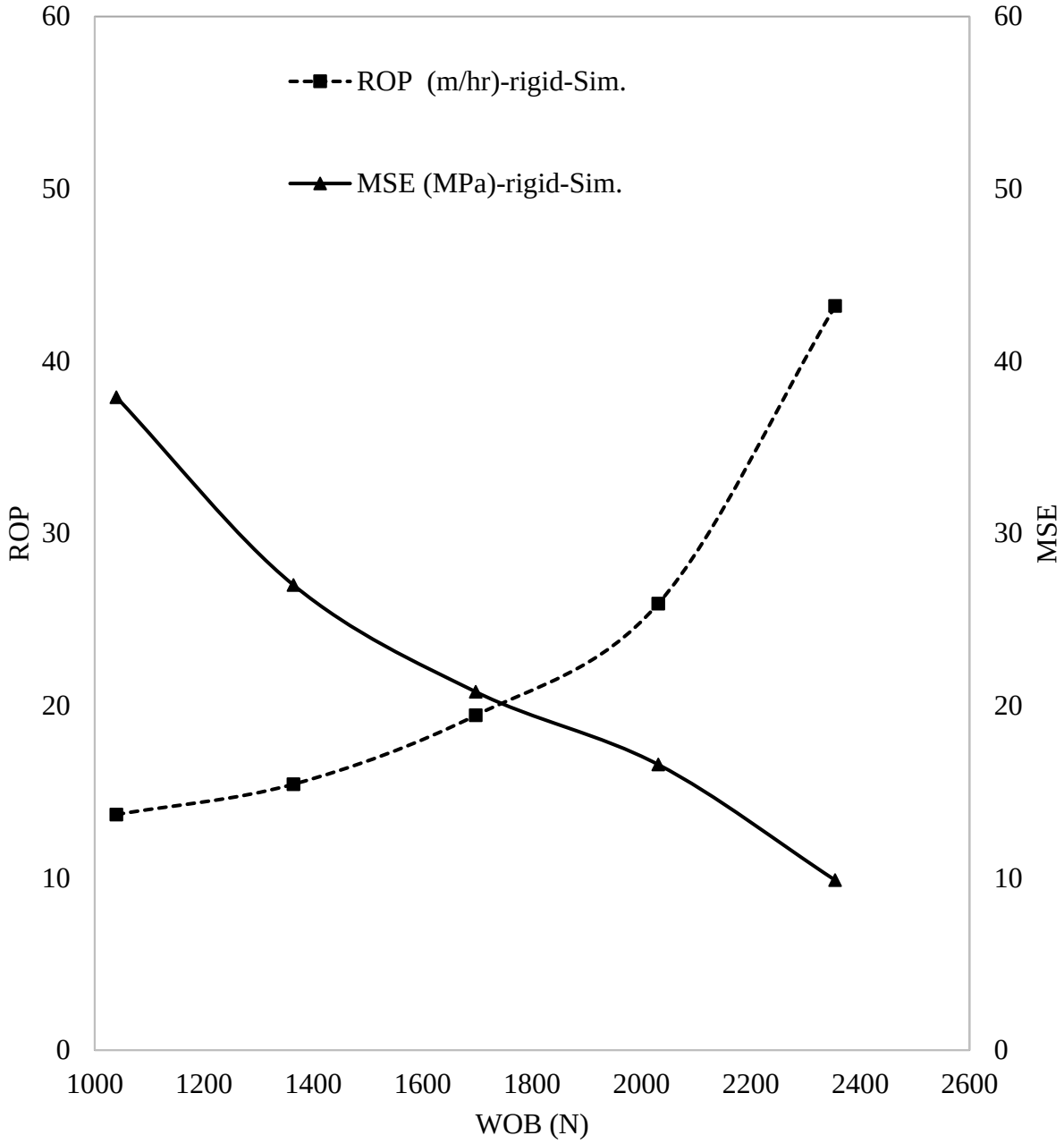

Figure 7-11. ROP and MSE vs. WOB for simulated rigid

7.8.2 Multiple Parameter Analysis

In this analysis, all drilling results of ROP, DOC, and MSE were analyzed together using different drilling modes of pVARD and rigid, based on experiment and simulation. Figure 7-12 and Figure 7-13 show the comparative results of ROP vs. WOB in different drilling modes experimentally and numerically, respectively. Figure 7-14 and Figure 7-15 compares DOC in different drilling modes experimentally and numerically, respectively. Figure 7-16 and Figure 7-17 show MSE is compared in different drilling modes, experimentally and numerically, respectively. Figure 7-18 shows the ROP values obtained experimentally vs. numerically. The results show that ROP is always higher in all pVARD configurations versus rigid drilling. Figure 7-19 shows the combined results of MSE experimentally vs. numerically. The results show that MSE is always lower in all pVARD configurations versus rigid drilling. The results of Figure 7-18 and Figure 7-19 confirm the positive influence of pVARD on enhancing drilling performance. This confirmation was further validated using field, laboratory, and numerical work.

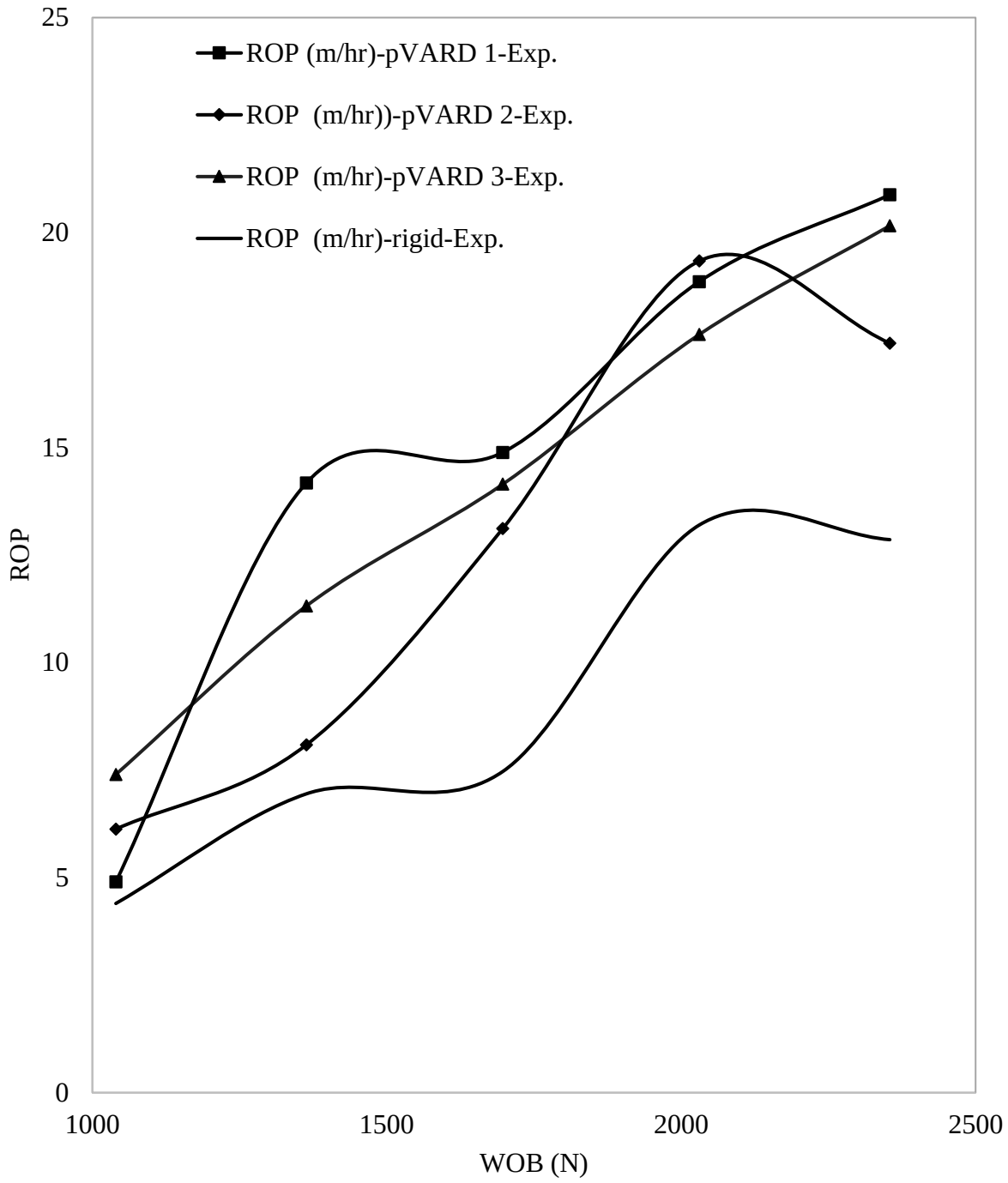

Figure 7-12. Compared experimental ROP vs. WOB in all drilling modes of pVARD and rigid

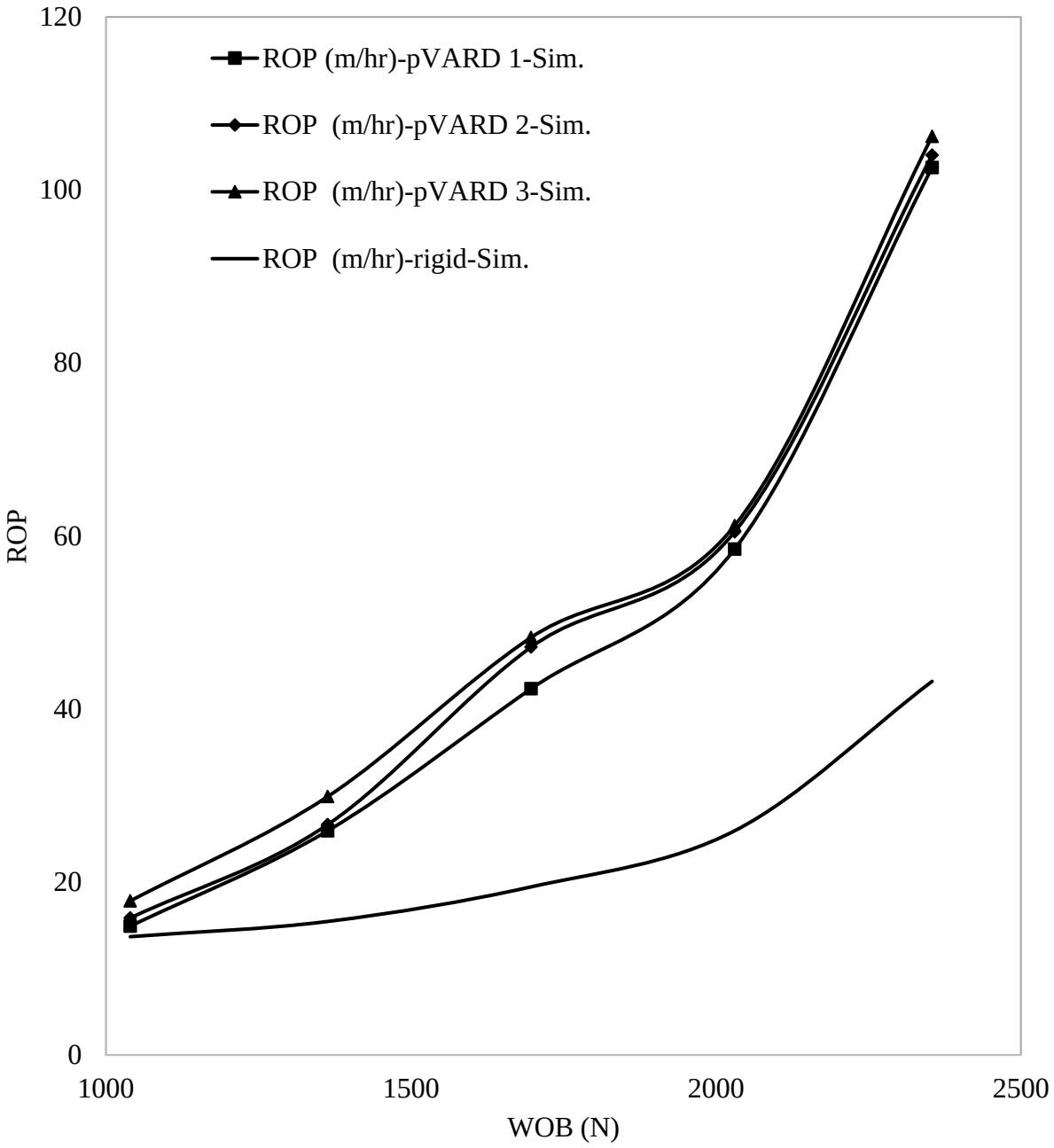

Figure 7-13. Compared simulated ROP vs. WOB in all drilling modes of pVARD and rigid

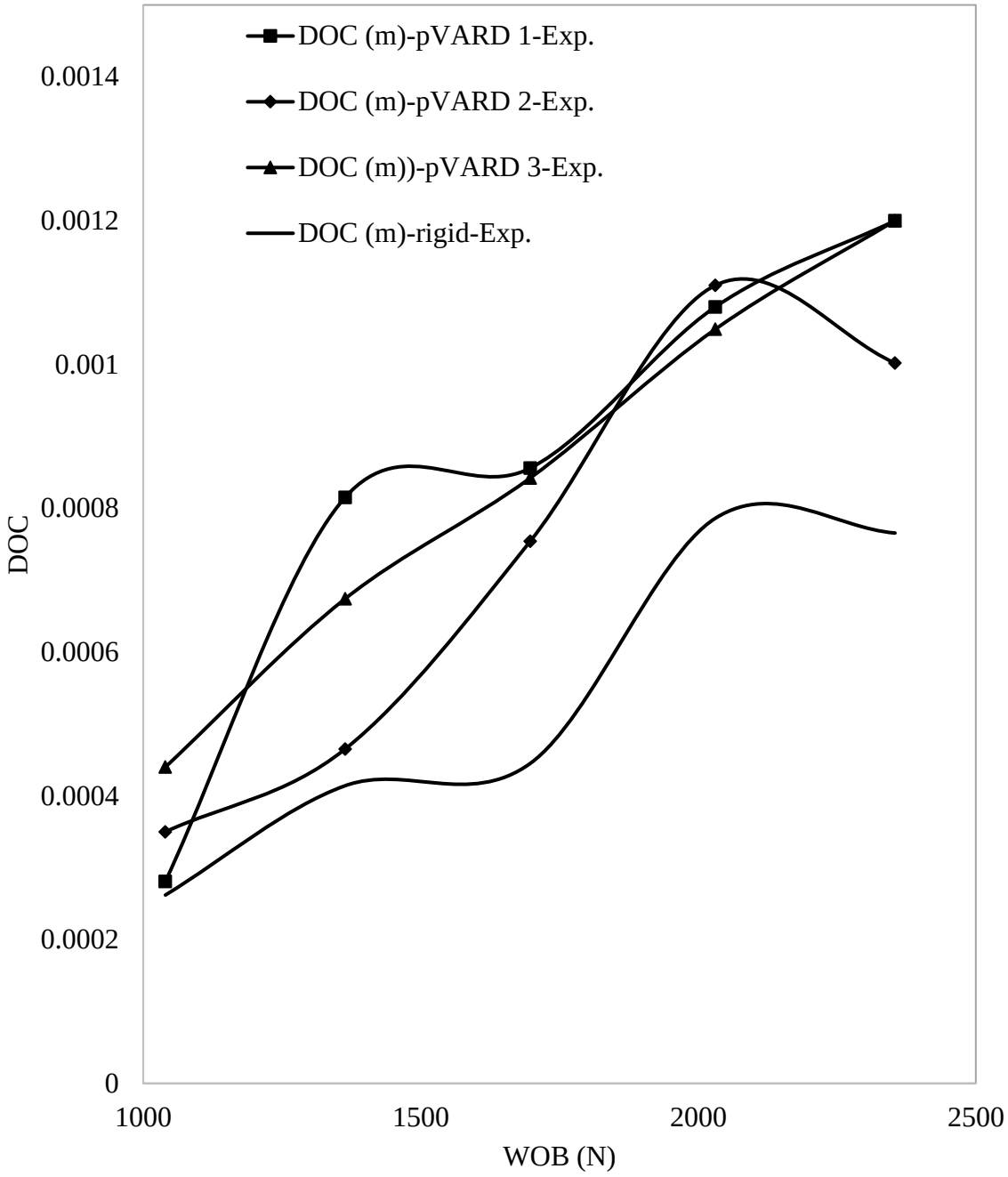

Figure 7-14. Compared experimental DOC vs. WOB in all drilling modes of pVARD and rigid

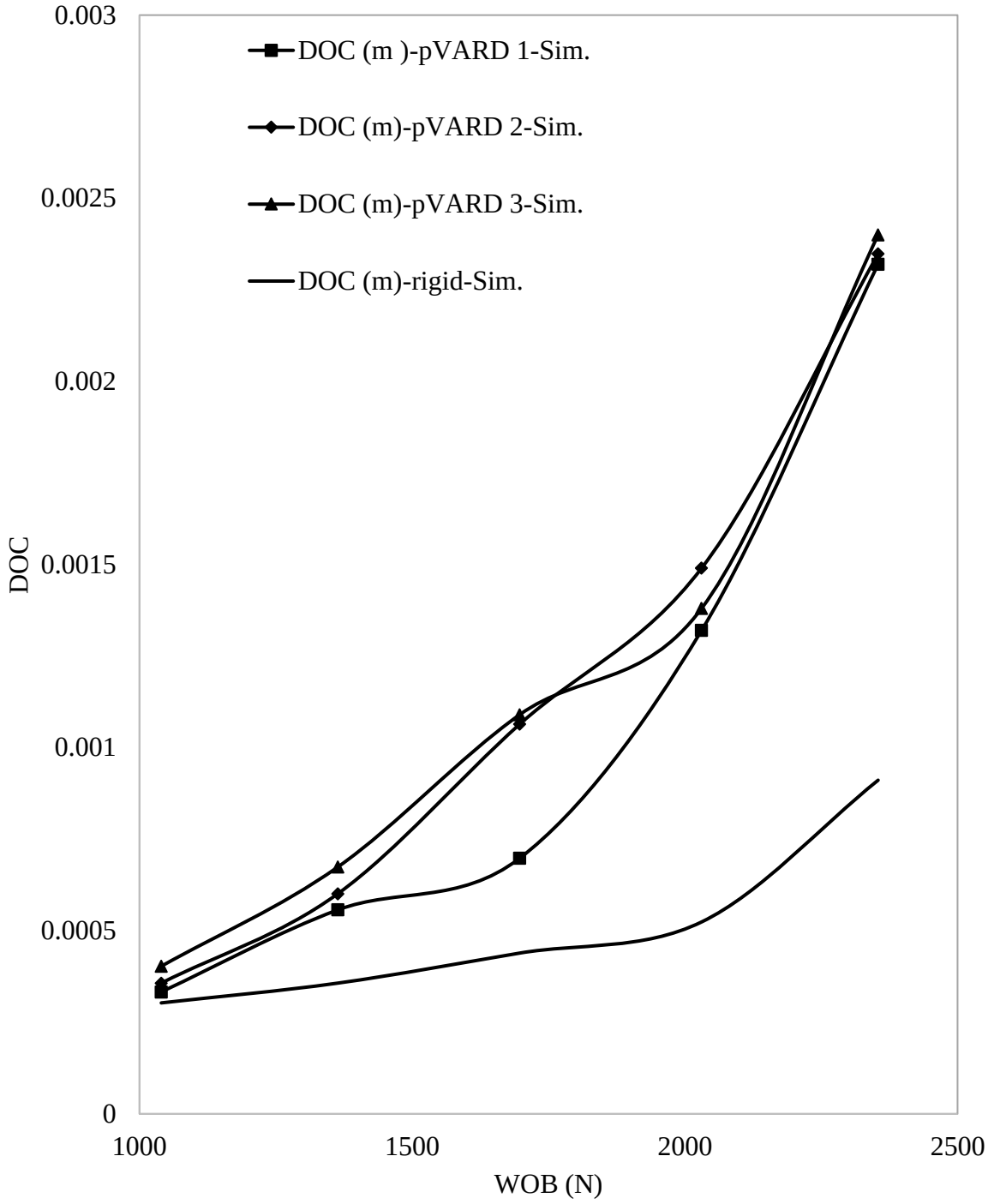

Figure 7-15. Compared simulated DOC vs. WOB in all drilling modes of pVARD and rigid

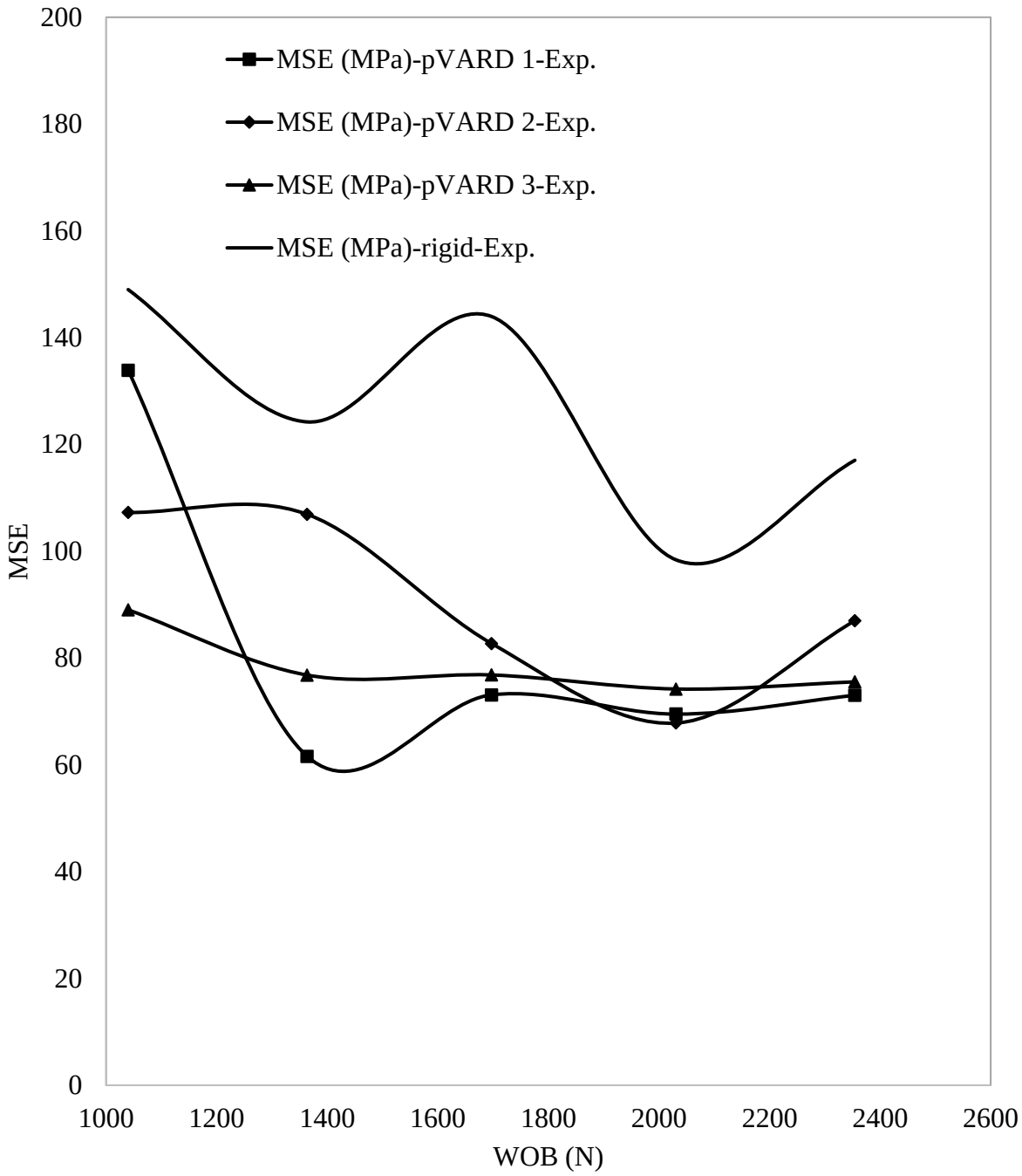

Figure 7-16. Compared experimental MSE vs. WOB in all drilling modes of pVARD and rigid

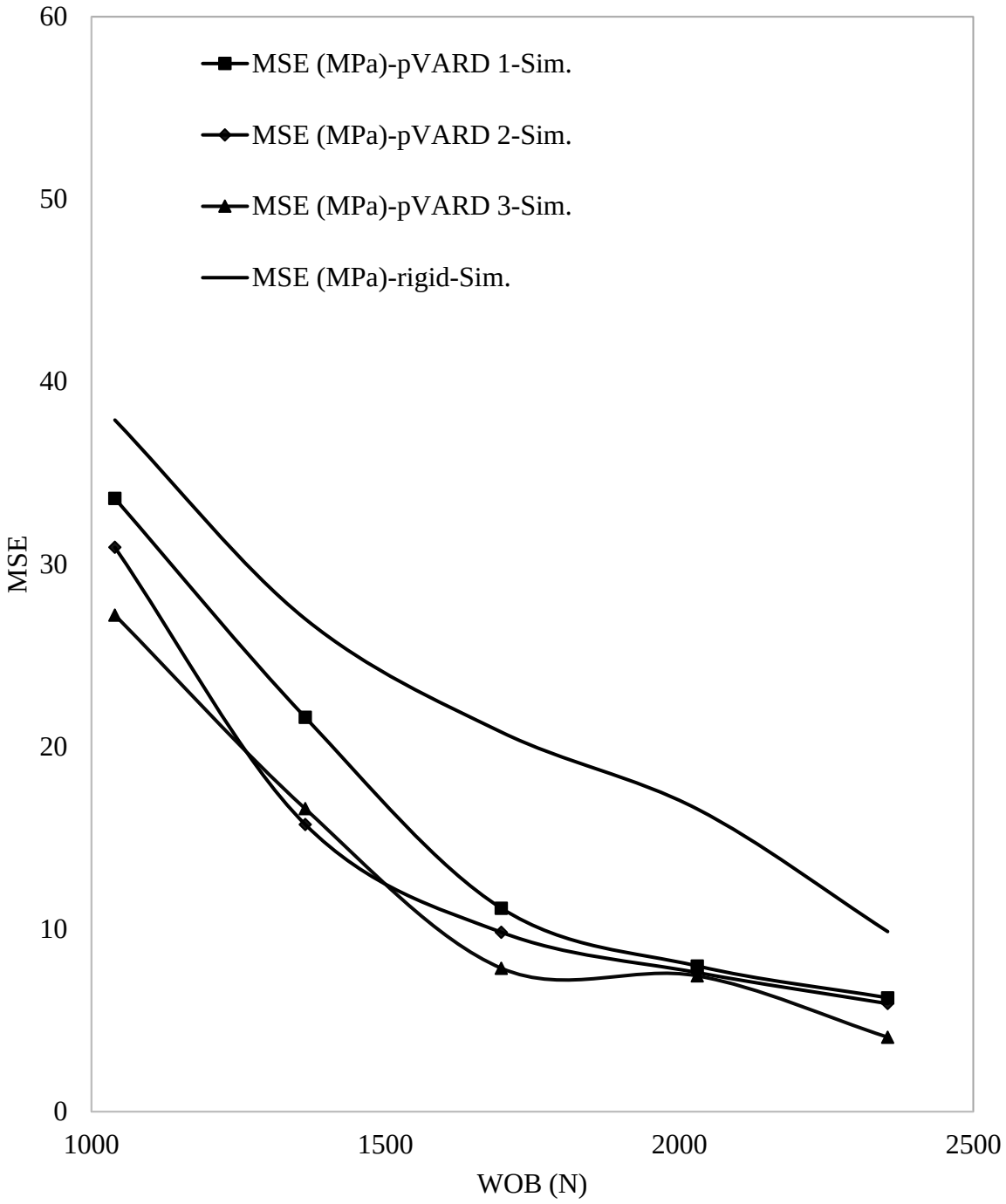

Figure 7-17. Compared simulated ROP vs. WOB in all drilling modes of pVARD and rigid

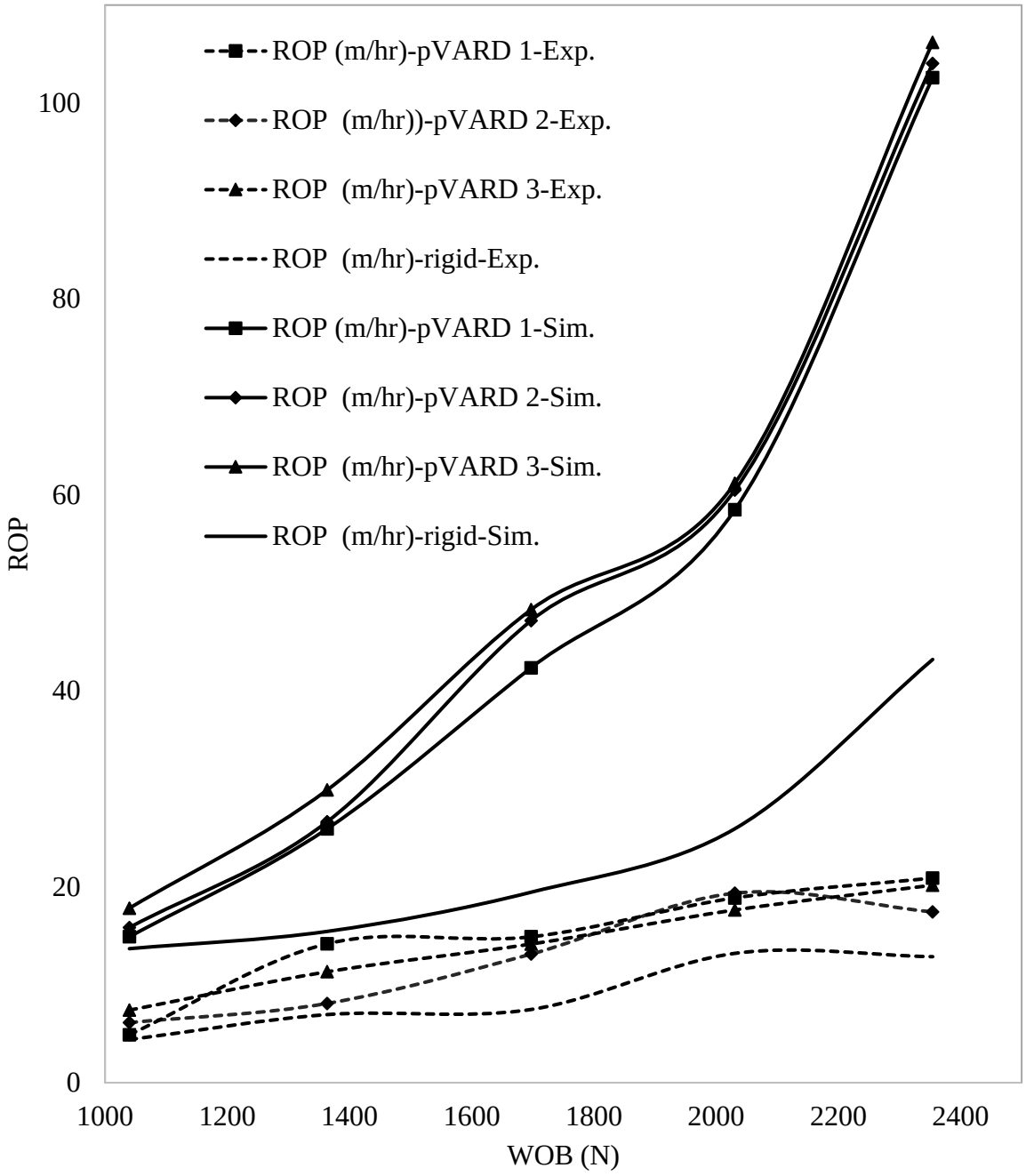

Figure 7-18. Compared result of ROP vs. WOB for all drilling modes of experiments and PFC-2D

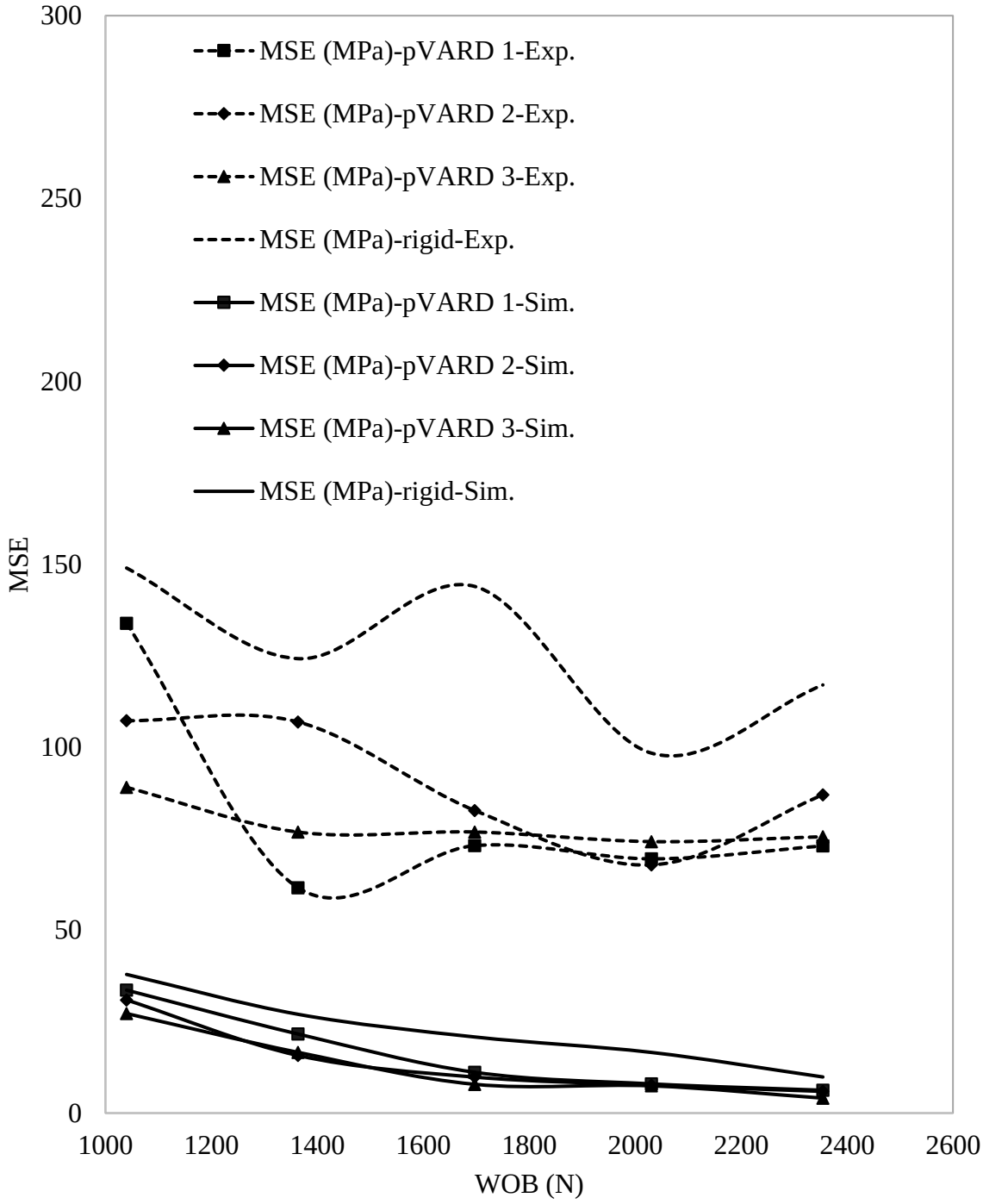

Figure 7-19. Compared result of MSE vs. WOB for all drilling modes of experiments and PFC-2D

7.8.3 Curve fitting and numerical models' analysis

This section provides a comparative analysis of the drilling parameters of ROP, DOC, and MSE based on single parameter analysis. Figure 7-20 to Figure 7-203 show relationships for four different sets of results between experimental and simulation, including ROP of pVARD configuration1, DOC of pVARD configuration 2, MSE of pVARD configuration 3, and MSE of rigid configuration. Table 7.3 summarizes the numerical models of all the experimental and PFD-2D studies performed using the three pVARD configurations compared to the rigid. Figure 7-20 displays the experimental and numerical ROP results applying a linear fitting function. This figure shows the results of pVARD-1 that represents the softest pVARD spring configuration and generates the highest oscillation amplitude. Results of this figure show an increase of ROP with the increase of WOB. Figure 7-21 exhibits the experimental and numerical DOC results applying a linear fitting function. This figure shows the results of pVARD-2 that represents the medium soft pVARD spring configuration and generates the medium oscillation amplitude. The results of this figure show an increase of DOC with the increase of WOB. Figure 7-22 demonstrate the experimental and numerical MSE results applying a linear fitting function. This figure shows the results of pVARD-3 that represents the stiffest pVARD spring configuration and generates the lowest oscillation amplitude. The results of this figure show a decrease of MSE with the increase of WOB. Figure 7-23 exhibits the experimental and numerical MSE results applying a linear fitting function. This figure shows the results of rigid drilling mode that involves no generation of downhole oscillation. The results of this figure show a decrease of MSE with the increase of WOB.

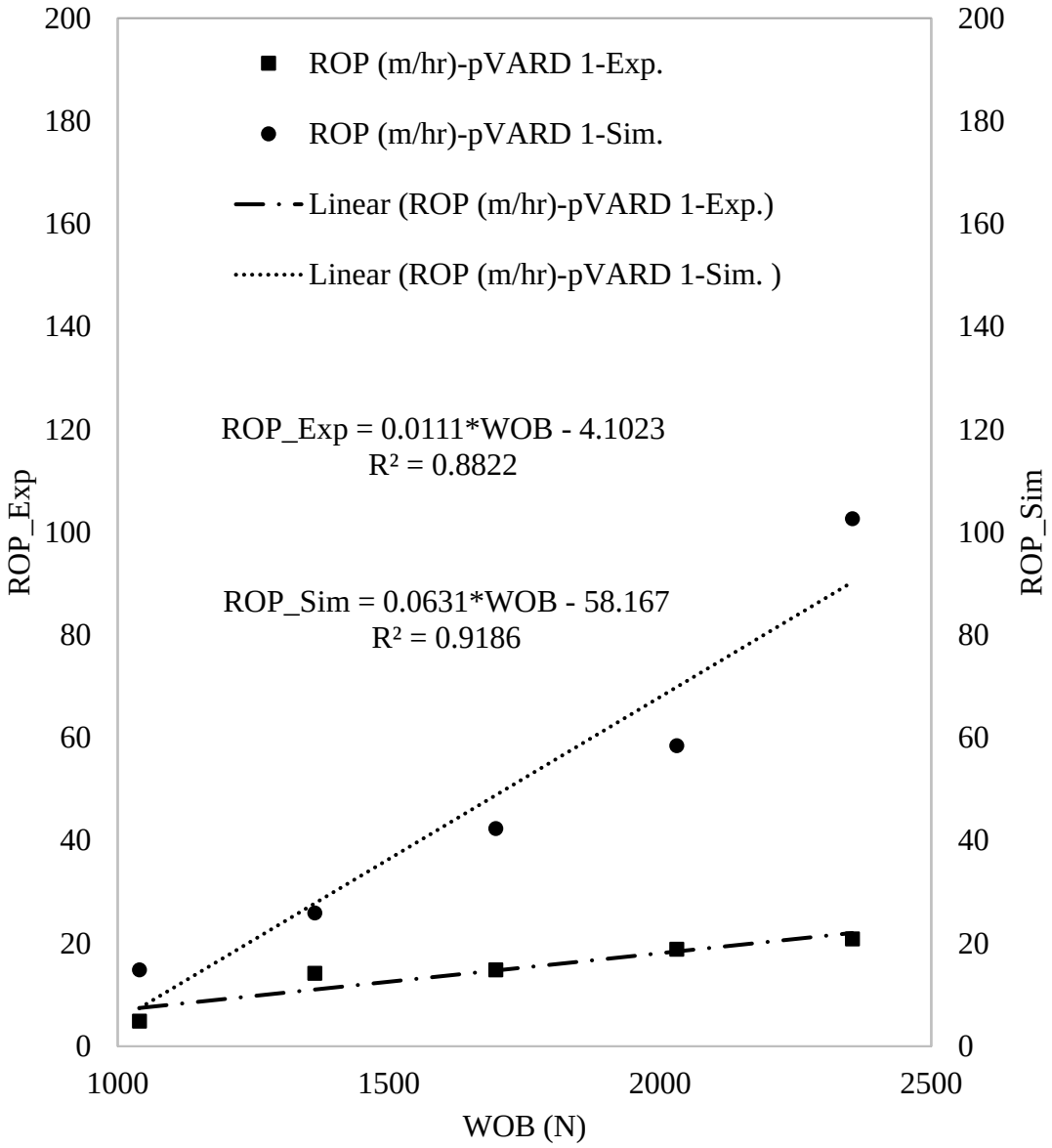

Figure 7-20. ROP_ Exp. and ROP_Sim. Vs. WOB using pVARD 1

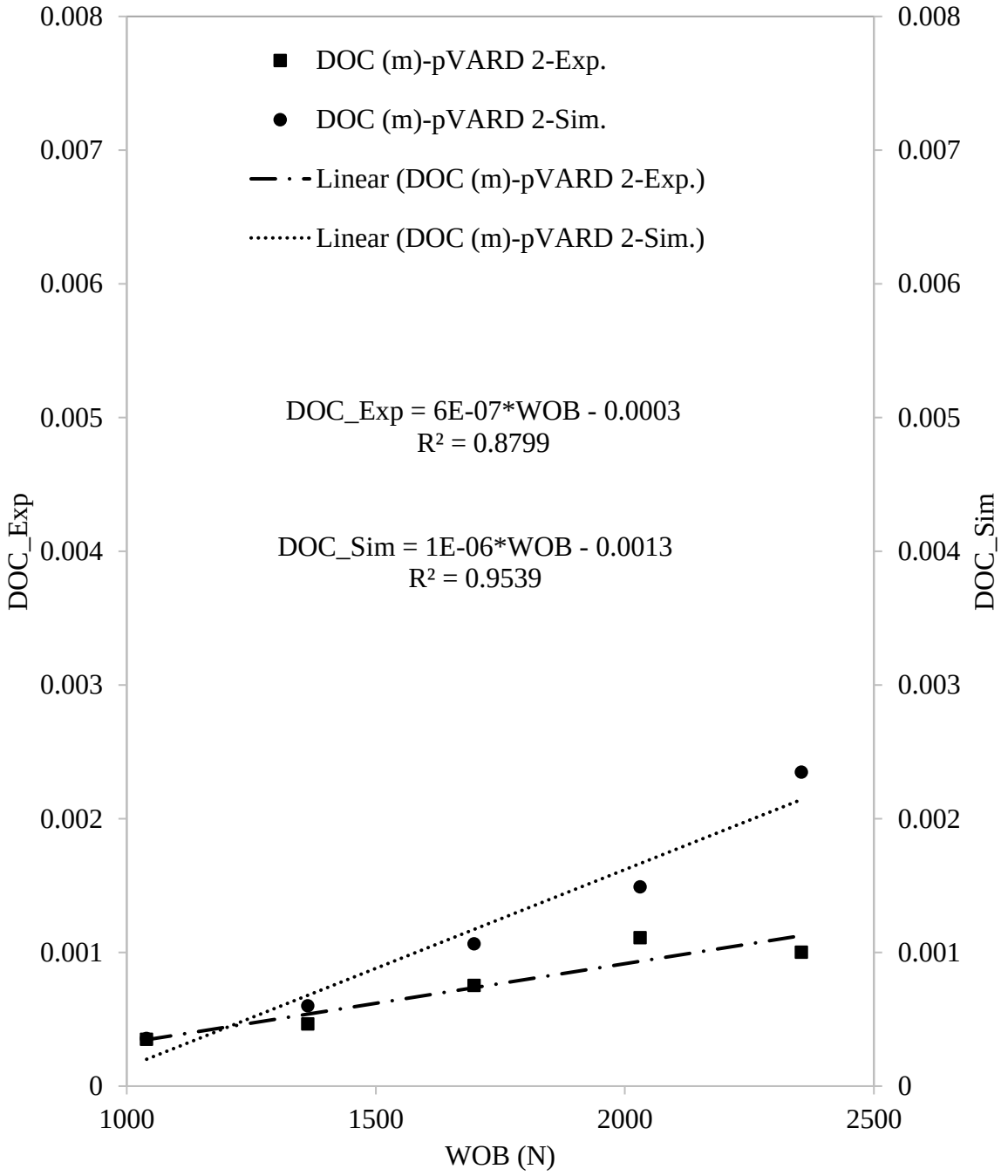

Figure 7-21. DOC_ Exp. and DOC_Sim. vs. WOB using pVARD 2

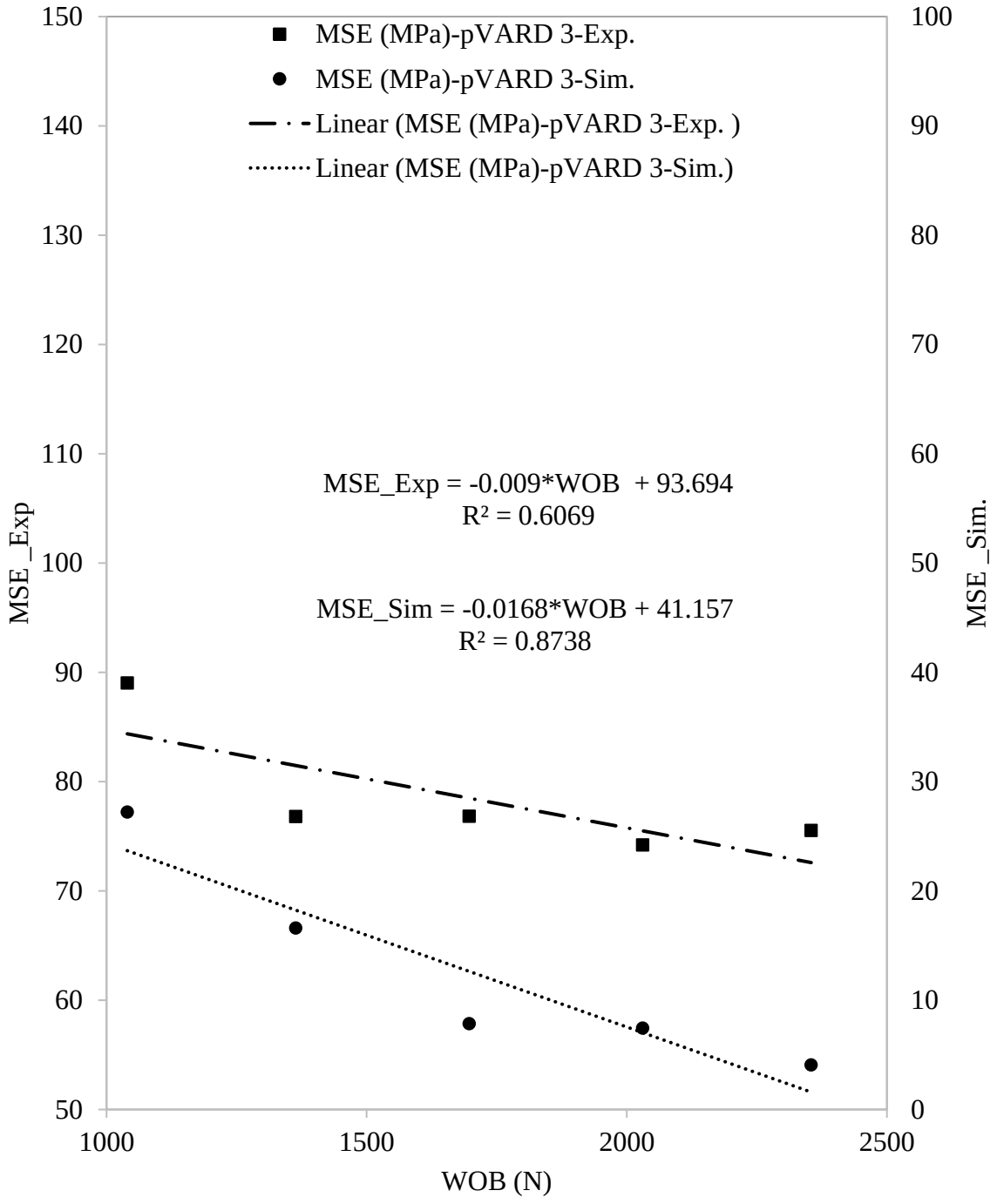

Figure 7-22. MSE_ Exp. and MSE_Sim. vs. WOB using pVARD -3

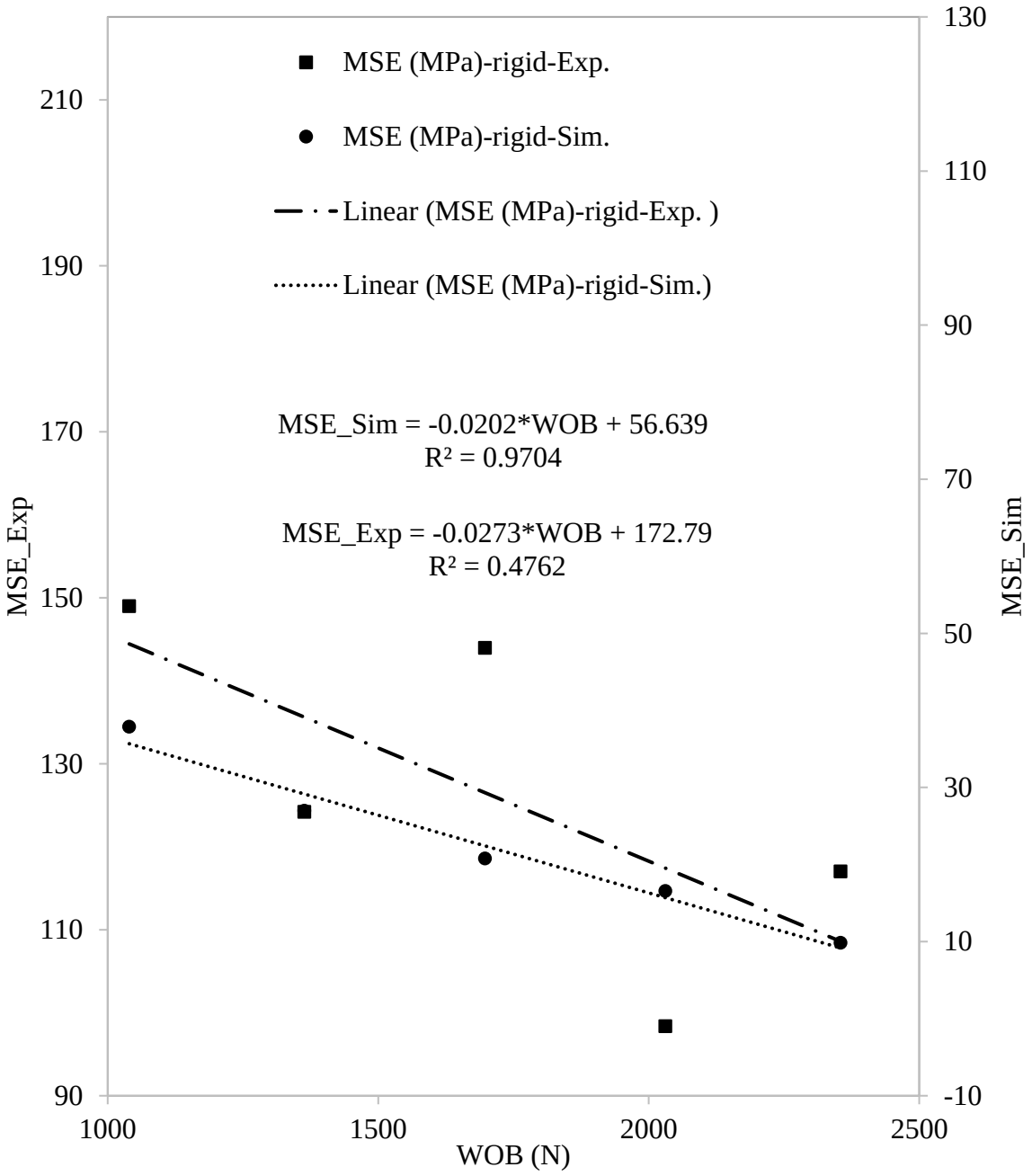

Figure 7-23. MSE_ Exp. and MSE_Sim. vs. WOB using rigid drilling

Table 7.3. Summary of numerical models of experimental versus PFD-2D studies using pVARD and rigid drilling

Drilling Mode	pVARD Set	ROP		DOC		MSE	
		Equations	R^2	Equations	R^2	Equations	R^2
pVARD	1	ROP_Exp = 0.0111*WOB - 4.1023	0.8822	DOC_Exp = 6E-07*WOB - 0.0002	0.8819	MES_Exp = -0.0344*WOB + 140.62	0.3754
pVARD	2	ROP_Exp = 0.0103*WOB - 4.6404	0.8782	DOC_Exp = 6E-07*WOB - 0.0003	0.8799	MSE_ Exp = -0.0243*WOB + 131.51	0.562
pVARD	3	ROP_Exp = 0.0097*WOB - 2.2557	0.9951	DOC_Exp = 6E-07*WOB - 0.0001	0.9951	MSE_Exp = -0.009*WOB + 93.694	0.6069
Rigid		ROP_Exp = 0.007*WOB - 2.9658	0.893	DOC _Exp = 4E-07*WOB - 0.0002	0.8929	MSE_Exp = -0.0273*WOB + 172.79	0.4762
pVARD	1	ROP_Sim = 0.0631*WOB - 58.167	0.9186	DOC_Sim = 1E-06*WOB - 0.0014	0.8732	MSE_Sim = -0.0207*WOB + 51.307	0.8911
pVARD	2	ROP_Sim = 0.0637*WOB - 57.35	0.9299	DOC_Sim = 1E-06*WOB - 0.0013	0.9539	MSE_ Sim = -0.0176*WOB + 43.903	0.817
pVARD	3	ROP_Sim = 0.0631*WOB - 54.39	0.9216	DOC_Sim = 1E-06*WOB - 0.0012	0.9206	MSE_Sim = -0.0168*WOB + 41.157	0.8738
Rigid		ROP_Sim = 0.0211*WOB - 12.231	0.8439	DOC _Sim = 4E-07*WOB - 0.0002	0.8215	MSE_Sim = -0.0202*WOB + 56.639	0.9704

7.9 Discussion

PFC-2D was utilized for simulating the work reported by Rana et al., [1]. The simulation work involved comparative studies between pVARD and rigid drilling systems. The simulation study included modeled drilling parameters including ROP, DOC, and MSE. For further study of the effect of different pVARD compliance levels on the drilling performance in contrast with rigid drilling, three various configurations of pVARD were involved.

In the single parameter analysis, drilling parameters were individually analyzed vs. different levels of WOB. Result showed an increase in ROP and DOC, and a decrease in MSE in all pVARD configurations as well as rigid drilling in the experimental and PFC-2D studies. For ROP and DOC, the result showed higher values in drilling using all pVARD configurations than that of rigid drilling in the experimental and PFC-2D studies. For MSE, the result showed lower values using all pVARD configurations than that of rigid drilling in the experimental and PFC-2D studies.

For dual drilling parameter analysis, result shown in Figure 7-4 through Figure 7-7 of PFC-2D study demonstrate the relationship between ROP and DOC at different WOBs using all pVARD 1, pVARD 2, pVARD 3, and rigid drilling, respectively. Result show an increase in ROP with the increase of DOC in all drilling modes. This was found in all drilling tests of the experimental and the simulation studies. The result also showed that ROP and DOC were higher in all pVARD drilling than that of rigid drilling, experimentally and numerically showing the positive effect of using pVARD enhancing drilling penetration.

The results shown in Figure 7-8 through Figure 7-11 of PFC study demonstrate the relationship between MSE and ROP at different WOBs using pVARD 1, pVARD 2, pVARD 3, and rigid drilling, respectively. Result show a decrease in MSE with an increase of ROP in all drilling modes, experimentally and numerically.

In the multiple parameter analysis, two drilling parameters were analyzed together as function of WOB, experimentally and numerically. Result shown in Figure 7-12 through Figure 7-17 are of combination of result of each drilling parameter of ROP, DOC, and MSE from experimental and numerical study in one set. The comparative result of ROP and MSE were found to have similar trends of increase or decrease in all drilling modes, experimentally and numerically. For further multiple drilling parameter analysis, result of each drilling parameter of ROP and MSE using all drilling modes from experimental and numerical studies were compared in Figure 7-18 and Figure 7-19, respectively. This analysis further demonstrated the influence of using pVARD on enhancing drilling performance. Figure 7-20 through Figure 7-23 are four of twelve samples that represent comparative analysis of the same drilling parameters (ROP, DOC, and MSE) as a result of experimental and numerical studies in two drilling modes, including pVARD and rigid applying linear curve fitting function. Figure 7-20 shows increasing in ROP as a function of WOB in both drilling modes, experimentally and numerically using pVARD 1. Figure 7-21 shows increasing in DOC as a function of WOB that results in increasing ROP in both drilling modes, experimentally and numerically using pVARD 2. Figure 7-22 shows decreasing in MSE as a function of WOB as a sign of enhanced drilling performance in both drilling modes, experimentally and numerically using pVARD 3.

Figure 7-23 shows a decreasing in MSE as a function of WOB as in both drilling modes, experimentally and numerically using rigid drilling. The drilling parameters that were implemented in this evaluation supported the enhancement of the drilling performance using pVARD tool against rigid drilling.

7.10 Conclusion

The numerical study using the PFC-2D simulating the experimental results reported by Rana et al., [1] can be summarized in the following points:

- The numerical study supported the experimental work in demonstrating the positive influence of pVARD implementation on drilling performance enhancement.
- Involving more drilling parameters including DOC, MSE, and BHP supported the comparative study and strengthened the validation of the simulation and the experimental results.
- This work showed good agreements between all drilling parameters in both drilling modes, including three p-VARD configurations and rigid drilling.
- ROP and DOC were directly proportion to the increase of WOB
- MSE was inversely proportion ROP and DOC

7.11 Acknowledgment

This work was funded by Atlantic Canada Opportunity Agency (AIF contract number: 781-2636-1920044), involving Husky Energy, Suncor Energy and Research and Development Corporation

(RDC) of Newfoundland and Labrador. Also, Ministry of Higher Education and Scientific Research, Libya, through Canadian Bureau for International Education, Canada (CBIE-Canada).

7.12 References

1. Rana, P. S., Abugharara, A. N., Butt, S. D., and Molgaard, J. (2015). "Experimental and Field Application of Passive-Vibration Assisted Rotary Drilling (pVARD) Tool to Enhance Drilling Performance, " Proc. 49th US Rock Mechanics/Geomechanics Symposium, San Francisco, CA.

2. Teale, R. (1965). “The concept of specific energy in rock drilling”. In International journal of rock mechanics and mining sciences & geomechanics abstracts (Vol. 2, No. 1, pp. 57-73). Pergamon.

3. Hegde, C., Daigle, H., Millwater, H., & Gray, K. (2017). “Analysis of rate of penetration (ROP) prediction in drilling using physics-based and data-driven models”. Journal of Petroleum Science and Engineering, 159, pp. 295-306.

4. Pessier, R. C., Wallace, S. N., & Oueslati, H. (2012). “Drilling performance is a function of power at the bit and drilling efficiency”. In IADC/SPE Drilling Conference and Exhibition. Society of Petroleum Engineers. San Diego, California, USA. Paper No. SPE-151389-MS

5. Dupriest, F. E., & Koederitz, W. L. (2005). “Maximizing drill rates with real-time surveillance of mechanical specific energy”. In SPE/IADC Drilling Conference. Society of Petroleum Engineers. Amsterdam, Netherlands. Paper No. SPE/ IADC 92194.

6. Fear, M. J. (1999). “How to improve rate of penetration in field operations”. SPE drilling & completion, 14(01), pp. 42-49.

7. Soares, C., Daigle, H., & Gray, K. (2016). “Evaluation of PDC bit ROP models and the effect of rock strength on model coefficients”. Journal of Natural Gas Science and Engineering, 34, pp. 1225-1236.

8. AL-Mahasneh, M. A. (2017). “Optimization Drilling Parameters Performance During Drilling in Gas Wells. International Journal of Oil, Gas and Coal Engineering”, 5(2), pp. 19-26.

9. Bourdon, J. C., Cooper, G. A., Curry, D. A., McCann, D., & Peltler, B. (1989). “Comparison of field and laboratory-simulated drill-off tests. SPE drilling engineering”, 4(04), pp. 329-334.

10. de Bruijn, H. J., Kemp, A. J., & Van Dongen, J. C. M. (1986). “Use of MWD for Turbodrill Performance Optimization as a Means To Improve ROP”. SPE Drilling Engineering, 1(04), PP. 309-314.

11. Xiao, Y., Hurich, C., Molgaard, J., & Butt, S. D. (2018). “Investigation of active vibration drilling using acoustic emission and cutting size analysis”. Journal of Rock Mechanics and Geotechnical Engineering, 10(2), pp. 390-401.

12. Detournay, E., & Defourny, P. (1992). “A phenomenological model for the drilling action of drag bits”. In International journal of rock mechanics and mining sciences & geomechanics abstracts (Vol. 29, No. 1, pp. 13-23). Pergamon.

13. Black, A. D., Walker, B. H., Tibbitts, G. A., & Sandstrom, J. L. (1986). “PDC bit performance for rotary, mud motor, and turbine drilling applications”. SPE Drilling Engineering, 1(06), pp. 409-416.

14. Tibbitts, G. A., Sandstrom, J. L., Black, A. D., & Green, S. J. (1981). “Effects of bit hydraulics on full-scale laboratory drilled shale”. Journal of Petroleum Technology, 33(07), pp. 1-180.

15. Warren, T. M., & Armagost, W. K. (1988). “Laboratory drilling performance of PDC bits”. SPE drilling engineering, 3(02), pp. 125-135.

16. Gerbaud, L., Menand, S., & Sellami, H. (2006). “PDC bits: all comes from the cutter rock interaction”. In IADC/SPE Drilling Conference. Miami, US. Paper No. IADC/SPE 98988.

17. Pessier, R., & Damschen, M. (2011). “Hybrid bits offer distinct advantages in selected roller-cone and PDC-bit applications”. SPE Drilling & Completion, 26(01), pp. 96-103.

18. Wang, Y., & Salehi, S. (2015). “Application of real-time field data to optimize drilling hydraulics using neural network approach”. Journal of Energy Resources Technology, 137(6), p. 062903.

19. Ren, Y., Wang, N., Jiang, J., Zhu, J., Song, G., & Chen, X. (2019). “The Application of Downhole Vibration Factor in Drilling Tool Reliability Big Data Analytics—A Review”. ASCE-ASME Journal of Risk and Uncertainty in Engineering Systems, Part B: Mechanical Engineering, 5(1), p. 010801.

20. Al Dushaishi, M. F., Nygaard, R., & Stutts, D. S. (2018). “An analysis of common drill stem vibration models”. Journal of Energy Resources Technology, 140(1), p. 012905.

21. Yigit, A. S., & Christoforou, A. P. (2006). “Stick-slip and bit-bounce interaction in oil-well drillstrings”. Journal of Energy Resources Technology, 128(4), pp. 268-274.

22. Dareing, D., Tlusty, J., & Zamudio, C. (1990). “Self-excited vibrations induced by drag bits”. Journal of Energy Resources Technology, 112(1), pp. 54-61.

23. Elsayed, M. A. (2007). “A novel approach to dynamic representation of drill strings in test rigs”. Journal of Energy Resources Technology, 129(4), pp. 281-288.

24. Raymond, D. W., Elsayed, M. A., Polsky, Y., & Kuszmaul, S. S. (2008). “Laboratory simulation of drill bit dynamics using a model-based servohydraulic controller”. Journal of Energy Resources Technology, 130(4), p. 043103.

25. Wu, X., Karuppiah, V., Nagaraj, M., Partin, U. T., Machado, M., Franco, M., & Duvvuru, H. K. (2012). “Identifying the root cause of drilling vibration and stick-slip enables fit-for-purpose solutions”. In IADC/SPE Drilling Conference and Exhibition. Society of Petroleum Engineers. San Diego, California, USA. Paper No. SPE-151347-MS

26. Salminen, K., Cheatham, C., Smith, M., & Valiullin, K. (2017). “Stuck-Pipe Prediction by Use of Automated Real-Time Modeling and Data Analysis”. SPE Drilling & Completion, 32(03), pp. 184-193.

27. Dong, G., & Chen, P. (2016). “A review of the evaluation, control, and application technologies for drill string vibrations and shocks in oil and gas well”. Shock and Vibration. Volume 2016, Article ID 7418635

28. Gaynor, T. M. (1988). “Downhole control of deviation with steerable straight-hole turbodrills”. SPE Drilling Engineering, 3(01), pp. 50-56.

29. Jansen, J. D., van den Steen, L., & Zachariasen, E. (1995). “Active damping of torsional drillstring vibrations with a hydraulic top drive”. SPE Drilling & Completion, 10(04), pp. 250-254.

30. Motahhari, H. R., Hareland, G., Nygaard, R., & Bond, B. (2009). “Method of Optimizing Motor and Bit Performance for Maximum ROP”. Journal of Canadian Petroleum Technology, 48(6), pp. 44-49.

31. Alali, A., & Barton, S. P. (2011). “Unique axial oscillation tool enhances performance of directional tools in extended reach applications”. In Brasil Offshore. Society of Petroleum Engineers. Macaé, Brazil. Paper No, SPE-143216-MS.

32. Clausen, J. R., Schen, A. E., Forster, I., Prill, J., & Gee, R. (2014). “Drilling with induced vibrations improves ROP and mitigates stick/slip in vertical and directional wells”. In IADC/SPE Drilling Conference and Exhibition. Society of Petroleum Engineers. Paper No. IADC/SPE 168034.

33. Gee, R., Hanley, C., Hussain, R., Canuel, L., & Martinez, J. (2015). “Axial Oscillation Tools vs. Lateral Vibration Tools for Friction Reduction–What's the Best Way to Shake the Pipe?” In SPE/IADC Drilling Conference and Exhibition. Society of Petroleum Engineers. London, England, UK. Paper No. SPE-173024-MS.

34. Jones, S., Feddema, C., Sugiura, J., & Lightey, J. (2016). “A New Friction Reduction Tool with Axial Oscillation Increases Drilling Performance: Field-Testing with Multiple Vibration Sensors in One Drill String”. In IADC/SPE Drilling Conference and Exhibition. Society of Petroleum Engineers. Fort Worth, Texas, USA. Paper No. SPE-178792-MS.

35. Wang, P., Ni, H., & Wang, R. (2018). “A novel vibration drilling tool used for reducing friction and improve the penetration rate of petroleum drilling”. Journal of Petroleum Science and Engineering, 165, pp. 436-443.

36. Wilson, J. K., & Noynaert, S. F. (2017). “Inducing Axial Vibrations in Unconventional Wells: New Insights through Comprehensive Modeling”. In SPE/IADC Drilling Conference and Exhibition. Society of Petroleum Engineers.

37. Li, H., Butt, S., Munaswamy, K., & Arvani, F. (2010). “Experimental investigation of bit vibration on rotary drilling penetration rate”. In 44th US Rock Mechanics Symposium and 5th US-Canada Rock Mechanics Symposium. American Rock Mechanics Association. Paper No. ARMA 10-426

38. Akbari, B., Butt, S. D., Munaswamy, K., & Arvani, F. (2011). “Dynamic single PDC cutter rock drilling modeling and simulations focusing on rate of penetration using distinct element method”. In 45th US Rock Mechanics/Geomechanics Symposium. American Rock Mechanics Association. San Francisco, California. Paper No. ARMA-11-379.

39. Wilson, J. K., & Noynaert, S. F. (2017). “Inducing Axial Vibrations in Unconventional Wells: New Insights through Comprehensive Modeling”. In SPE/IADC Drilling Conference and Exhibition. Society of Petroleum Engineers.

40. Babatunde, Y., Butt, S., Molgaard, J., & Arvani, F. (2011). “Investigation of the effects of vibration frequency on rotary drilling penetration rate using diamond drag bit”. In 45th US rock mechanics/geomechanics symposium. American Rock Mechanics Association. San Francisco, California. Paper No. ARMA-11-527.

41. Zhang, J., Yang, J., & Butt, S. (2016). “DEM simulation of enhancing drilling penetration using vibration and experimental validation”. In Proceedings of the 49th Annual Simulation Symposium (p. 12). Society for Computer Simulation International.

42. Alwaar, A., Abugharara, A. N., & Butt, S. D. (2018). “PFC-2D Numerical Study of the Influence of Passive Vibration Assisted Rotary Drilling Tool (pVARD) on Drilling Performance Enhancement”. In ASME 2018 37th International Conference on Ocean, Offshore and Arctic Engineering (pp. V008T11A014-V008T11A014). American Society of Mechanical Engineers.

43. Mohamed, B., Abugharara, A. N., Rahman, M. A., & Butt, S. D. (2018). “CFD Numerical Simulation for Downhole Thruster Performance Evaluation”. In ASME 2018 37th International Conference on Ocean, Offshore and Arctic Engineering. American Society of Mechanical Engineers. Paper No. OMAE2018-78101

44. Abugharara, A., Molgaard, J., Hurich, C., and Butt, S. (2019). “Study of the influence of Controlled Axial Oscillations of pVARD on Generating Downhole Dynamic WOB and Improving Coring and Drilling Performance in shale”. Proceedings of the ASME 2019. 38th International Conference on Ocean, Offshore and Arctic Engineering, Glasgow, Scotland, UK. OMAE2019-96189

45. Khorshidian, H., Mozaffari, M., & Butt, S. D. (2012). “The Role of Natural Vibrations in Penetration Mechanism of a single PDC cutter”. In 46th US Rock mechanics/geomechanics symposium, 24-27 June, Chicago, Illinois. American Rock Mechanics Association. Paper No. ARMA-2012-402.

CHAPTER 8: STUDY OF THE INFLUENCE OF CONTROLLED AXIAL OSCILLATIONS OF PVARD ON GENERATING DOWNHOLE DYNAMIC WOB AND IMPROVING CORING AND DRILLING PERFORMANCE IN SHALE

Abdelsalam N. Abugharara [a], PhD candidate

John Molgaard [b], Professor

Charles A. Hurich [c], Associated Professor

Stephen D. Butt [a], Professor

[a] Drilling Technology Laboratory, Memorial University of Newfoundland, St. John's, NL, Canada A1B 3X5

[b] Department of Mechanical Engineering, Memorial University of Newfoundland, St. John's, NL, Canada A1B 3X5

[c] Department of Earth Sciences, Memorial University of Newfoundland, St. John's, NL, Canada A1B 3X5

This chapter is based on the objectives defined in section 1.3.6 and was presented at the 38th International Conference on Ocean, Offshore and Arctic Engineering OMAE2019 held in Glasgow, Scotland, UK, on 9-14 June 2019.

8.1 Co-authorship Statement

The contributions of this collaborative work are described in the following four parts. 1) Identification of research topic and design of experiments are contributed by Abdelsalam Abugharara and Dr. S. D. Butt. 2) Preparation of cores, construction mechanical measurements are solely contributed by Abdelsalam Abugharara. 3) Performance of coring experiments are solely contributed by Abdelsalam Abugharara. 4) Manuscript preparation are contributed by Abdelsalam Abugharara with revision assistance provided by all co-authors.

8.2 Abstract

This work concentrates on investigating enhancing the drilling performance, through increasing drilling rate of penetration (ROP), using passive vibration assisted rotary drilling (pVARD). This work involved analysis of how ROP was significantly increased when drilling using pVARD compared to drilling using conventional system “rigid”. This work was performed using shale rocks. The apparatus used was a fully instrument laboratory scale rig and the bits were dual-cutter polycrystalline diamond compact (PDC) bit for drilling and diamond impregnated coring bit for coring. The flow rate was constant of (7 litter / min) using clean water at atmospheric pressure environment. In addition, for accuracy data recording, a data acquisition system (DAQ-Sys) using a LabVIEW software was utilized to record data at 1000HZ sampling rate. The output drilling parameters involved in the analysis included operational rpm, torque (TRQ), and ROP. All the output-drilling parameters were analyzed with relation to downhole dynamic weight on bit

(DDWOB). The result of this work explained how pVARD can increase the DDWON and improve ROP. The result also demonstrated generating a balanced and concentric increase in DDWOB and minimizing the wide-range fluctuation of DDWOB generated in rigid drilling, specifically at high DDWOB.

8.3 Introduction

Shale drilling has been experiencing significant attention nowadays. This attention is mainly driven by the recent shale oil and gas substantial discoveries, and the improvement of technologies used for well control, horizontal drilling, and horizontal fracturing. The importance of shale coring is also high. The need for evaluating the encountered shale section in the drilling path and in reservoir zone is essential, where shale coring comes into play. However, shale coring and drilling is subjected to numerous challenges. For better shale coring and drilling performance, these challenges are required to be addressed for bit, bottomhole assembly protection, downhole drilling operating condition enhancement, non-productive time (NPT) and consumed energy, and cost reduction, and rate of penetration enhancement. Achieving such requirement cannot be handy with the intensive reporting of harmful and destructive drillstring vibrations.

In the context of the existence of drillstring vibrations, it is reported by many studies to be generated in drilling oil and gas wells in various modes and levels [1, 2, 3, 4, 5]. They are also reported to be classified to dangerous and non-dangerous vibrations [6].

In the context of enhancing drilling performance, numerous studies have been conducted through typical drill-off-tests (DOT) to signify the most influencing drilling parameters on drilling performance by constructing the performance curve and optimizing the founders [7, 8, 9, 10, 11].

These studies showed how to optimize ROP through the founder point, which is mainly affected by downhole wellbore conditions that are related to bit design and selection, surface WOB and rpm transmitting, and bit hydraulics and cutting removal process [12, 13].

In the context of eliminating wellbore vibrations, many reported simulation, laboratory, and field studies demonstrated the relationship between enhancing borehole drilling conditions and minimizing dangerous bit and drillstring vibrations and controlling non-dangerous downhole vibrations at the safely operating window, which benefits significantly enhances drilling performance. This can be achieved through several means, including improving communication and transmitting between surface and downhole drilling parameters by installing near-bit axial-vibrations inducing tools [3, 14, 15, 16, 17, 18, 19, 20,]. This enhances optimizing required and efficient surface load, narrows the gap between surface and downhole rpm and minimizes bit rpm acceleration (the source of bit stick-slip) [1, 3, 21], provides continues drillstring motion through induced non-dangerous axial vibrations, which with the addition to the above benefits reducing consumed energy, protecting bit and BHA, decreasing NPT, cuts down costs, and improving ROP. This work reports, through two laboratory study of coring and drilling experiments in shale rocks, the benefits of implementing pVARD that controls the downhole vibrations and enhances the drilling parameters and improves ROP. These experiments were performed using pVARD versus rigid drilling, where pVARD was locked and acted as a part of the rigid drilling system.

8.4 Sample Preparation

Samples were prepared using a specially developed procedure. Firstly, shale blocks were collected from Conception Bay South (CBS), Newfoundland, Canada, where three wells were drilled in a

field trial as part of a continuous research conducted at drilling technology laboratory at Memorial University of Newfoundland (DTL-MUN). Secondly, using a diamond saw, the shale blocks were cut into cubs of dimensions ranging between 15 cm to 30 cm in all three lengths with some variations in lengths. The reason the dimensions were made equal was to balance the sample on the load cell and accurately record the DDWOB. Thirdly, after determining shale bedding orientations, shale cubs were properly-oriented placed in transparent plastic containers to enable monitoring cement confinement in the next step. Fourthly, low viscosity cement was poured between shale cubes and wall of plastic containers with maintenance of cement top to be risen horizontally for balanced cover and confining of shale cubes. Fifthly, after drying off, the plastic containers were removed, the shale orientations were identified, based on which the edges of the cement confining shale cubes were cut by the diamond saw for perfecting their cubical shape in preparation for drilling experiments. Lastly, cement confining shale cubes were grouped based on their bedding orientations to three sets, including parallel, oblique, and perpendicular to bedding. The work of this paper, with respect to shale drilling reports only the results of drilling parallel to shale bedding. For shale coring, the samples were, firstly, cored using 7.62 cm diamond coring bit to obtain shale cylinders. Then, shale cylinders were cut from both ends to flatten their ends, after which they were placed in 10.16 cm plastic cylinders and filled with cement. When dried, the samples were cored using a 2.54 cm diamond impregnated coring bit.

8.5 Experimental Procedure and Apparatus

The work of this paper reports only the results of laboratory drilling parallel to shale bedding. The apparatus, fully described by Rana et al., [20], used for drilling was a fully instrumented laboratory

scale rig supported with 1000 HZ sampling rate Data Acquisition System (DAC-Sys) utilizing professional LabVIEW Software for data recording. Several sensors were connected to the drilling rig to record data, including a draw wire linear position transducer (LPT) that measures axial displacement between the motor head and the drill pipe used to calculate the ROP, a laser triangulation sensor (LTS) that measures (i) the relative displacement between the motor head and drill pipe, which assisted in analyzing data of various drilling systems (i.e. pVARD, rigid), (ii) the actual rpm, a hall effect sensor that is in line with the electric motor, which used to measure the motor current for torque calculation, and a load cell fixed beneath the shale samples, which used to record the downhole dynamic weight on bit (DDWOB). Two bits were used for shale drilling and coring. A dual-cutter polycrystalline diamond compact (PDC) bit was used for shale drilling parallel to bedding, and a diamond impregnated coring bit was used for shale coring parallel to bedding as well. The fluid used for cutting removal and borehole cleaning was clean water with about 7 liter / minute flow rate. To drill or core, shale samples were fixed in the center of the sample holder to be balanced in the load cell. At each suspended weight, the coring and the drilling process was repeated several times as explained in the results. The purpose of the repetition was to provide more data sets for each weight. The drilling and coring were conducted using two drillstring configurations, including pVARD and rigid “conventional” systems. pVARD was set on medium compliance mode, where it induced medium-range-amplitude of downhole oscillations. In rigid drilling and coring, pVARD was locked and acted as a part of the drill string. Figure 8-1 shows the apparatus for shale coring and drilling as well as the coring and drill bit types used.

Figure 8-1. Apparatus for shale coring and drilling experiments with coring and drill bits

8.6 Results and Discussion

Results presented in this paper are categorized into two main groups, including (i) shale coring results and (ii) shale drilling results, respectively. The results of the first group (shale coring) were obtained by applying one set of suspended weight, which was repeated multiple times. In this

group rpm and torque are also presented and plotted against DDWOB. The results of the second group (shale drilling) were obtained by using three different sets of suspended weight, including low suspended weight (LSW), medium suspended weight (MSW), and high suspended weight (HSW). In this group distribution of DDWB in two sets of suspended weight are presented to demonstrate the DDWO fluctuation in pVARD vs. rigid drilling.

8.6.1 Shale Coring Results

Shale coring performance was improved, but not significantly as the case in shale drilling performance (see shale drilling results). There are two main reasons that can be stated here explaining this. Firstly, the low surface area active for bit-rock inaction and low coring resistance compared to a full-face drilling bit. Secondly, the configuration of pVARD and the precise pVARD operating window. As pVARD can be pre-configure based on rock type and property before coring, and the pVARD configuration used in this test was medium compliance governed by medium strength springs, the performance could have been improved more by if the configuration was with low compliance. Confirmations of this are in progress in a current pVARD project. Results of ROP with DDWOB of shale coring using pVARD vs. rigid with their average values are shown in Figure 8-2.

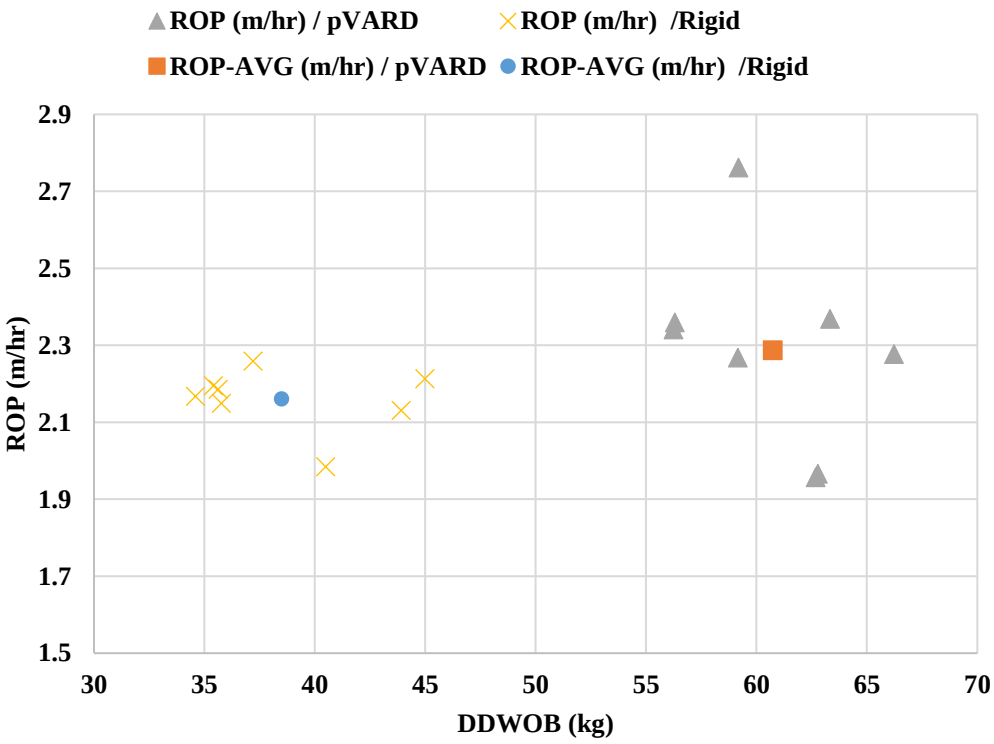

Figure 8-2. Results of ROP with DDWOB of shale coring using pVARD vs. rigid with their average values

Figure 8-3 show the results of rpm with DDWOB of shale coring using pVARD vs. rigid with their average values. The results demonstrate the decrease in rpm (this was first observed by Abugharara et al 2017 [22]) due to ROP increase as a sign of more resistance encountered was exposed for such improvement in ROP. It was noticed that the decrease in rpm did not negatively affect ROP. As stated in the introduction, coring dose not encounter high resistance and big fluctuation in rpm, as the case in drilling, the influence of using pVARD in stabilizing bit rotary speed to eliminate stick-slip is also currently investigate.

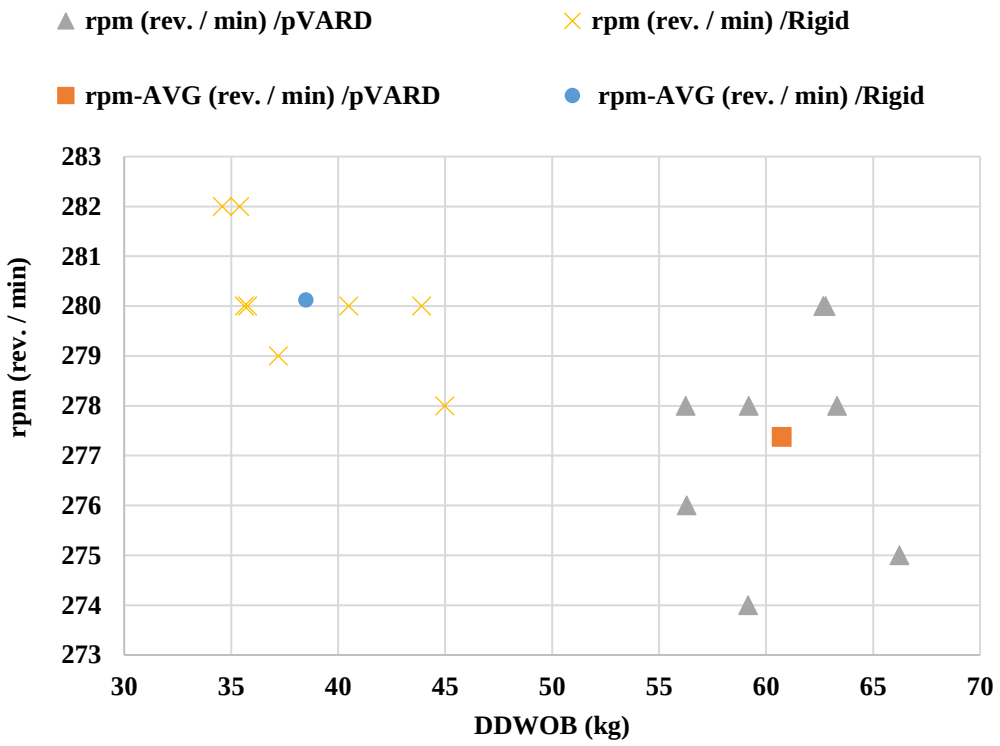

Figure 8-3. Results of rpm with DDWOB of shale coring using pVARD vs. rigid with their average values

Figure 8-4 shows the results of torque with DDWOB of shale coring using pVARD vs. rigid with their average values. The increase of torque with the increase of DDWOB and ROP was also observed by Abugharara et al., 2017 [22] during oriented shale drilling representing direction drilling in shale, where the author explained the change in torque to the shale strength variation with respect to shale bedding orientation. The increase of torque is a sign of increasing the resistance that the bit encounters with the increase of DDWOB to cut more rock at higher depth of cut for higher ROP. The torque magnitude can be small in coring using a diamond impregnated

coring bit and can be large in drilling using a full face PDC bit governed by bit rock interaction contact area.

The potential fluctuation in torque which can be observed while drilling more than in coring due to the same reason of the contact area, can be a sign for bit stick-slip dangerous vibrations. When bit sticks, resistance increases and torque increases. When bit slips, resistance decreases and torque releases, too. However, the increase of the torque reported here is not a sign of stick slip because it is not fluctuated torque, but it increases due to the increase of DDWOB that increases the depth of cut that leads to increasing ROP.

Results shown in Figure 8-4 uncovers another important area of research investigating the influence of implementing pVARD in eliminating torque and rpm fluctuation as a sign for eliminating downhole destructive vibrations and improving generating controlled downhole drilling conditions (i.e. DDWOB) and enhancing drilling penetration.

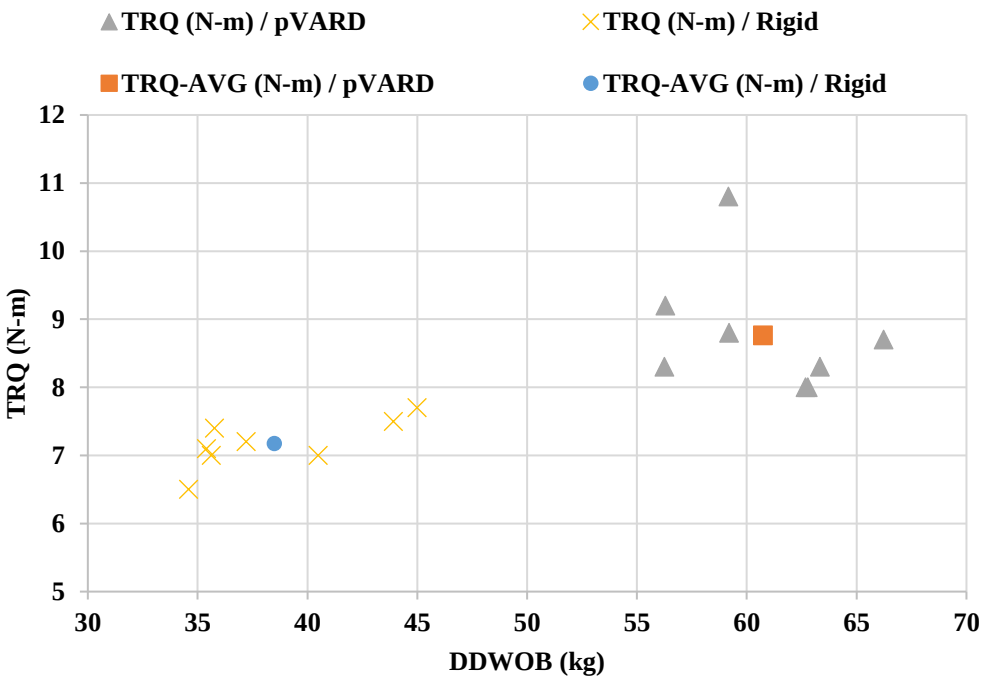

Figure 8-4. Results of torque with DDWOB of shale coring using pVARD vs. rigid with their average values

8.6.2 Shale Drilling Results

Shale drilling has, recently gained more attention influenced by the large shale oil and gas discoveries and the technology advancement for shale horizontal drilling and hydraulic fracturing operations. However, challenges have been continuously reported during shale drilling. One main challenge is drillstring destructive vibrations. As drilling uses full face drill bits, challenges are expected to be greater compared to coring. This section explains pVARD operational mechanism in improving ROP by applying balanced and concentric DDWOB, especially at higher suspended weight with comparison to rigid drilling. Figure 5 shows the results of ROP with DDWOB of shale drilling using pVARD applying three sets of suspended weight with their average values. The three

suspended weight sets are low, medium and high suspended weight, (LSW), (MSW), and (HSW), respectively. ROP was increased with the increase of suspended weight. Load cell data provided DDWOB that showed significant increase in ROP due to applying higher DDWOB when drilling with pVARD in comparison to rigid drilling. Detailed comparison is provided in Figure 8-5 and Figure 8-6.

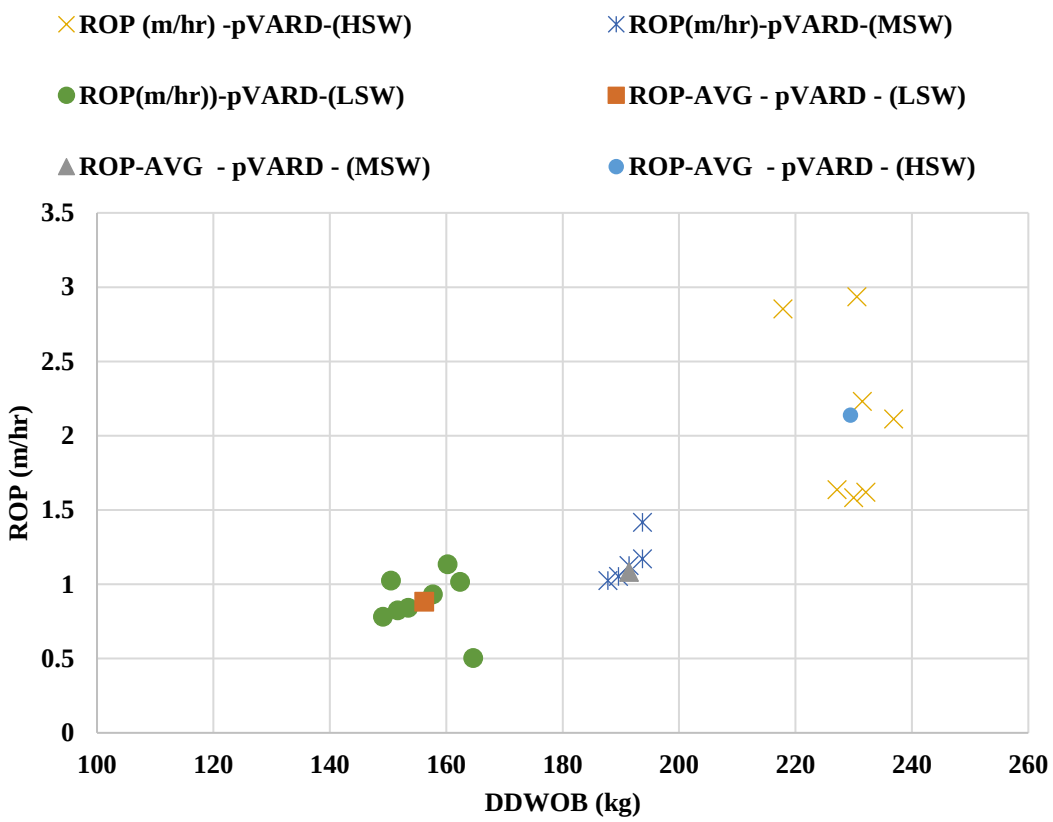

Figure 8-5. Results of ROP with DDWOB of shale drilling using pVARD applying three sets of suspended weight with their average values

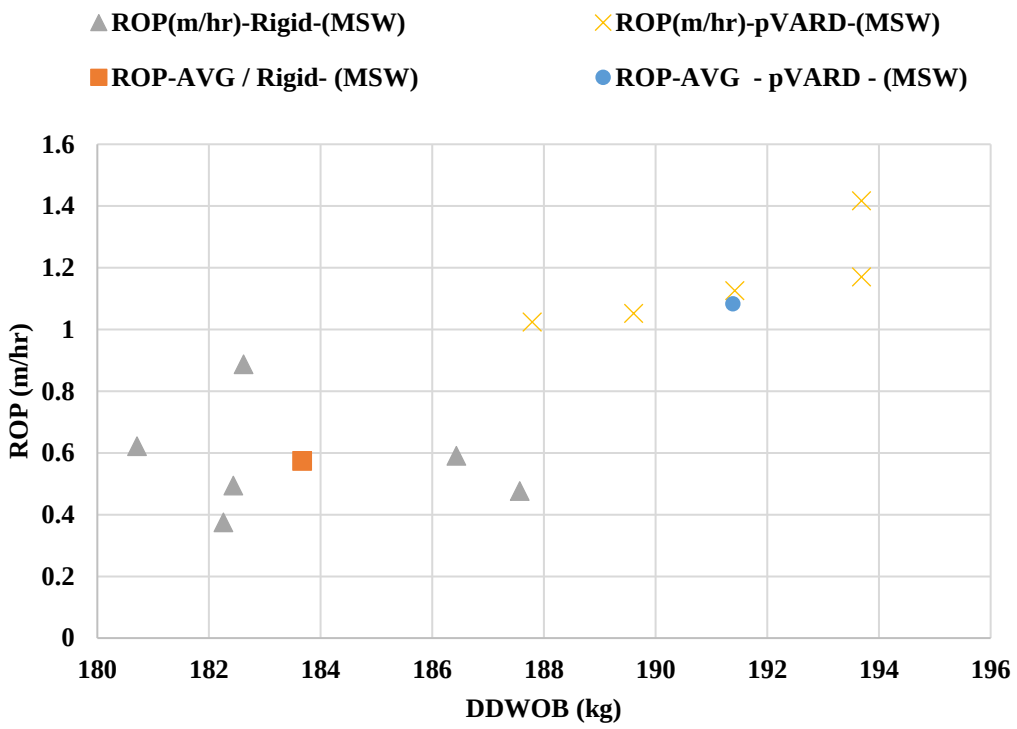

Figure 8-6. Results of ROP with DDWOB of shale drilling using pVARD vs. rigid applying medium suspended weight with their average values

Figure 8-6 shows the results of ROP with DDWOB of shale drilling using pVARD vs. rigid applying medium suspended weight with their average values. The results show significant improvement in ROP-AVG influenced by DDWOB increase using pVARD compared to rigid drilling. DDWOB's increasing range demonstrated more focused, concentric, and balanced of pVARD in improving ROP against rigid drilling, which is demonstrated more in Figure 8-7. Figure 8-7 shows the results of ROP with DDWOB of shale drilling using pVARD vs. rigid applying high suspended weight with their average values. This result shows the significant influence of pVARD in balancing DDWOB resulting in substantial improvement in ROP. The results also show pVARD

function in narrowing-down DDWOB range as a sign for stabilizing downhole operating conditions and eliminating the sources for dangerous vibrations.

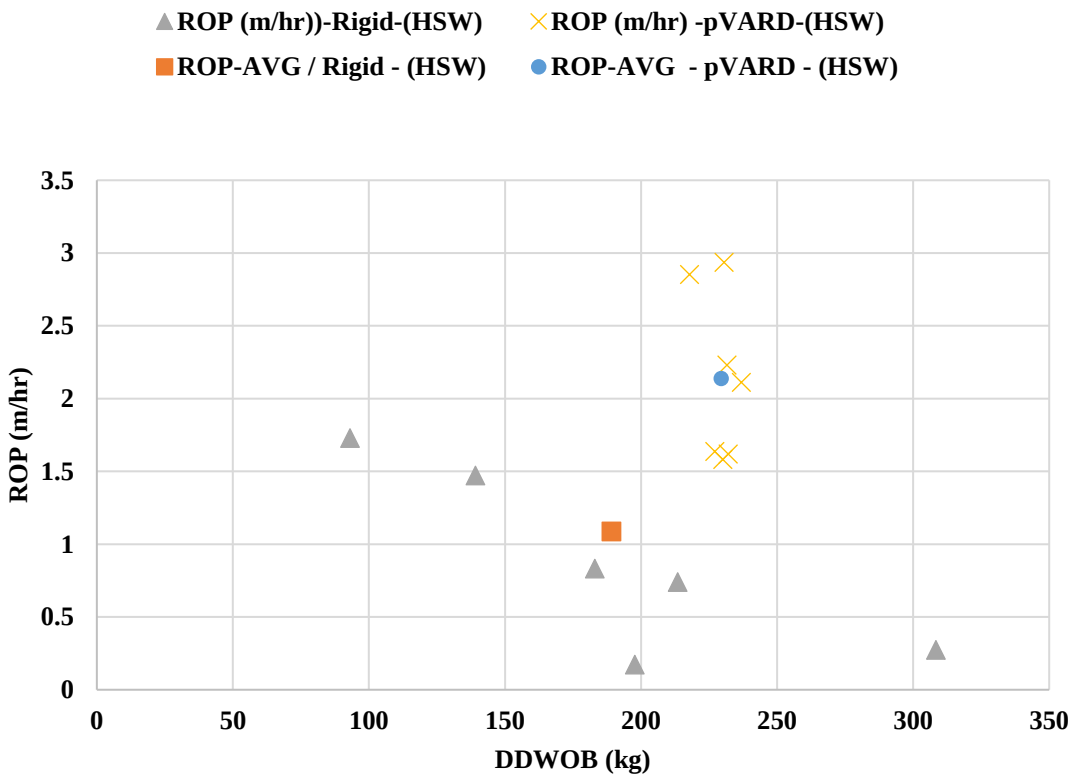

Figure 8-7. Results of ROP with DDWOB of shale drilling using pVARD vs. rigid applying high suspended weight with their average values

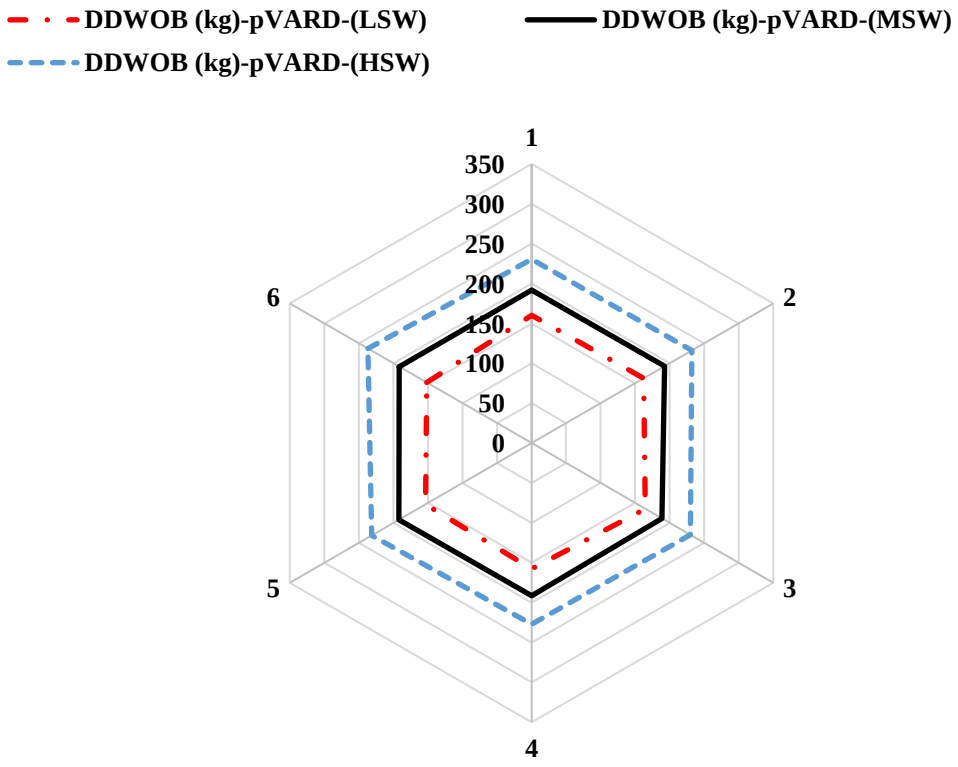

Figure 8-8. Demonstration of pVARD balanced and concentric DDWOB distribution at three sets of suspended weight

Figure 8-8 and Figure 8-9 demonstrate, using radar data plot, pVARD balanced and concentric DDWOB distribution at three sets of suspended weight, and rigid imbalanced DDWOB distribution at HSW, especially at higher DDWOB, respectively. These results show the influence of using pVARD in controlling downhole operating conditions and stabilizing them for enhancing drilling performance.

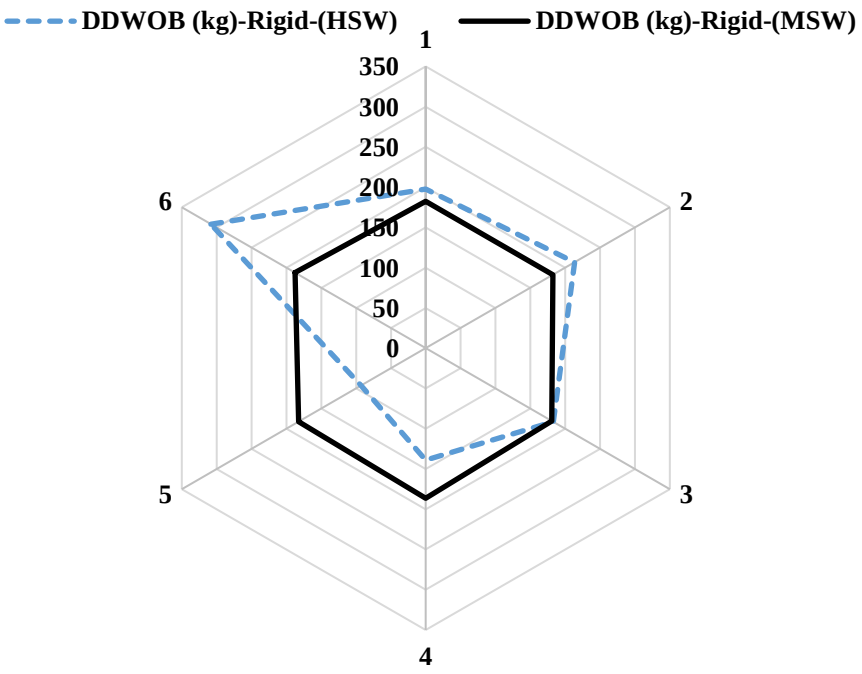

Figure 8-9. Demonstration of rigid imbalanced DDWOB distribution at two sets of suspended weight

8.7 Conclusion

This work involved analysis of shale coring and drilling performance using pVARD vs. rigid drilling. The results of both, shale coring and shale drilling parallel to shale bedding showed performance improvement using pVARD. The results also showed that one main reason for such improvement was the increase of DDWOB. More impotently, the results demonstrated the concentric increased in DDWOB using pVARD against rigid drilling. Some other observations are summarized in the following points:

- In shale coring, due to the small contact area between coring bit and shale, DDWO did not experience large improvement, however, the coring could exhibit more improvement with pVARD configuration adjustment.

- Similar observations in rpm and torque reported in Abugharara et al., 2017 [22] found in this work. Torque increase with the increase of DDWB and resulted increase in ROP. On the other hand, rpm was decreased, which can be related to the increase of depth of cut and torque.
- In shale drilling, due to a larger contact area between the PDC bit cutters and shale comparing to the diamond coring impregnated bit, that was pVARD was including more axial oscillations and generating higher DDWOB that that of rigid drilling, which led to higher ROP.
- The uniqueness of pVARD DDWOB was more concentric and balanced than that in rigid drilling. Generating balanced DDWOB, not only improves drilling performance, but also does not expose bit and bottomhole assembly BHA to destructive vibrations.
- The wide range in DDWOB experienced in HSW rigid drilling was not only associated with low ROP, but also could elevate the chance of damaging bit and BHA, increase NPT, and drive up the drilling cost.

8.8 Acknowledgment

This work was performed at the Drilling Technology Laboratory (DTL) at Memorial University of Newfoundland in St. John's, Canada. This work is funded by the Atlantic Canada Opportunity Agency (AIF contract number: 781-2636-1920044), involving Husky Energy, Suncor Energy and Research and Development Corporation (RDC) of Newfoundland and Labrador. The Financial support is also provided by the Ministry of Higher Education and Scientific Research, Libya through Canadian Bureau for International Education (CBIE).

8.9 References

1. Ren, Y., Wang, N., Jiang, J., Zhu, J., Song, G., & Chen, X. (2019). The Application of Downhole Vibration Factor in Drilling Tool Reliability Big Data Analytics—A Review. ASCE-ASME Journal of Risk and Uncertainty in Engineering Systems, Part B: Mechanical Engineering, 5(1), p. 010801.

2. Al Dushaishi, M. F., Nygaard, R., & Stutts, D. S. (2018). An analysis of common drill stem vibration models. Journal of Energy Resources Technology, 140(1), p. 012905.

3. Yigit, A. S., & Christoforou, A. P. (2006). Stick-slip and bit-bounce interaction in oil-well drillstrings. Journal of Energy Resources Technology, 128(4), pp. 268-274.

4. Dareing, D., Tlusty, J., & Zamudio, C. (1990). Self-excited vibrations induced by drag bits. Journal of Energy Resources Technology, 112(1), pp. 54-61.

5. Dykstra, M. W., Chen, D. K., Warren, T. M., & Azar, J. J. (1996). Drillstring component mass imbalance: a major source of downhole vibrations. SPE drilling & completion, 11(04), pp. 234-241.

6. Dunayevsky, V. A., Abbassian, F., & Judzis, A. (1993). Dynamic stability of drillstrings under fluctuating weight on bit. SPE drilling & completion, 8(02), pp. 84-92.

7. Detournay, E., & Defourny, P. (1992, January). A phenomenological model for the drilling action of drag bits. In International journal of rock mechanics and mining sciences & geomechanics abstracts (Vol. 29, No. 1, pp. 13-23). Pergamon.

8. Bourdon, J. C., Cooper, G. A., Curry, D. A., McCann, D., & Peltler, B. (1989). Comparison of field and laboratory-simulated drill-off tests. SPE drilling engineering, 4(04), pp. 329-334.

9. Fear, M. J. (1999). How to improve rate of penetration in field operations. SPE drilling & completion, 14(01), pp. 42-49.

10. Pessier, R. C., Wallace, S. N., & Oueslati, H. (2012, January). Drilling performance is a function of power at the bit and drilling efficiency. In IADC/SPE Drilling Conference and Exhibition. Society of Petroleum Engineers.

11. AL-Mahasneh, M. A. (2017). Optimization Drilling Parameters Performance During Drilling in Gas Wells. International Journal of Oil, Gas and Coal Engineering, 5(2), pp. 19-26.

12. Bielstein, W. J., & Cannon, G. E. (1950). Factors Affecting the Rate of Penetration of Rock Bits. Drilling and Production Practice, 61(4).

13. Warren, T. M., & Armagost, W. K. (1988). Laboratory drilling performance of PDC bits. SPE drilling engineering, 3(02), pp. 125-135.

14. Li, H., Butt, S., Munaswamy, K., & Arvani, F. (2010, January). Experimental investigation of bit vibration on rotary drilling penetration rate. In 44th US Rock Mechanics Symposium and 5th US-Canada Rock Mechanics Symposium. American Rock Mechanics Association. Paper No. ARMA 10-426

15. Gee, R., Hanley, C., Hussain, R., Canuel, L., & Martinez, J. (2015, March). Axial Oscillation Tools vs. Lateral Vibration Tools for Friction Reduction–What's the Best Way to Shake the Pipe?. In SPE/IADC Drilling Conference and Exhibition. Society of Petroleum Engineers.

16. Wang, P., Ni, H., & Wang, R. (2018). A novel vibration drilling tool used for reducing friction and improve the penetration rate of petroleum drilling. Journal of Petroleum Science and Engineering, 165, pp. 436-443.

17. Alwaar, A., Abugharara, A. N., & Butt, S. D. (2018, June). PFC-2D Numerical Study of the Influence of Passive Vibration Assisted Rotary Drilling Tool (pVARD) on Drilling Performance Enhancement. In ASME 2018 37th International Conference on Ocean, Offshore and Arctic Engineering (pp. V008T11A014-V008T11A014). American Society of Mechanical Engineers.

18. Mohamed, B., Abugharara, A. N., Rahman, M. A., & Butt, S. D. (2018, June). CFD Numerical Simulation for Downhole Thruster Performance Evaluation. In ASME 2018 37th International Conference on Ocean, Offshore and Arctic Engineering (pp. V008T11A016-V008T11A016). American Society of Mechanical Engineers.

19. Wu, X., Karuppiah, V., Nagaraj, M., Partin, U. T., Machado, M., Franco, M., & Duvvuru, H. K. (2012, January). Identifying the root cause of drilling vibration and stick-slip enables fit-for-purpose solutions. In IADC/SPE Drilling Conference and Exhibition. Society of Petroleum Engineers.

20. Rana, P. S., Abugharara, A. N., Butt, S. D., and Molgaard, J., 2015, "Experimental and Field Application of Passive-Vibration Assisted Rotary Drilling (pVARD) Tool to Enhance Drilling Performance, " Proc. 49th US Rock Mechanics/Geomechanics Symposium, San Francisco, CA.

21. Patil, P. A., & Teodoriu, C. (2013). Model development of torsional drillstring and investigating parametrically the stick-slips influencing factors. Journal of Energy Resources Technology, 135(1), p. 013103.

22. Abugharara, A. N., Hurich, C. A., Molgaard, J., & Butt, S. D. (2017, June). Study of the Influence of Shale Anisotropy Orientation on Directional Drilling Performance in Shale. In ASME 2017 36th International Conference on Ocean, Offshore and Arctic Engineering (pp. V008T11A011-V008T11A011). American Society of Mechanical Engineers.

CHAPTER 9: A COMPREHENSIVE LABORATORY INVESTIGATION OF ROCK ANISOTROPY EVALUATION USING FINE-GRAINED SANDSTONE FORMATION

Abdelsalam N. Abugharara [a], PhD candidate

John Molgaard [b], Professor

Charles A. Hurich [c], Associate Professor

Stephen D. Butt [a], Professor

[a] Drilling Technology Laboratory, Memorial University of Newfoundland, St. John's, NL, Canada A1B 3X5

[b] Department of Mechanical Engineering, Memorial University of Newfoundland, St. John's, NL, Canada A1B 3X5

[c] Department of Earth Sciences, Memorial University of Newfoundland, St. John's, NL, Canada A1B 3X5

This chapter is based on the objectives defined in section 1.3.7 and was submitted to Canadian Geotechnical Journal on July 2, 2019.

9.1 Co-authorship Statement

The contributions of this collaborative work are described in the following four parts. 1) Identification of research topic and design of experiments are contributed by Abdelsalam Abugharara and Dr. S. D. Butt. 2) Preparation of cores, construction mechanical measurements are solely contributed by Abdelsalam Abugharara. 3) Performance of coring experiments are solely contributed by Abdelsalam Abugharara. 4) Manuscript preparation are contributed by Abdelsalam Abugharara with revision assistance provided by all co-authors

9.2 Abstract

Rock anisotropy is an important topic for numerous areas including optimizing performance of oil and gas drilling and mining excavations, minimizing wellbore instability, and improving the safety of civil engineering structures. An experimental procedure for investigating rock anisotropy characterization using fine-grained sandstone evaluation is reported. The procedure involved several tests. Each test was conducted in three main orientations: vertical, diagonal, and horizontal with respect to one quarter of the Cartesian coordinate system. Tests were performed on samples obtained from the same sandstone block. Tests included (i) circular ultrasonic compressional and shear wave velocity measurements (VP, VS), (ii) oriented unconfined compressive strength (OUCS), (iii) multidirectional oriented indirect tensile strength (OITS), (iv) oriented axial point load strength (OPLS), and (v) directional compliant and non-compliant drilling. First, the oriented ultrasonic wave velocity was measured to classify the anisotropy of the tested sandstone. Second, the oriented strength tests were conducted, and their data was correlated. Third, the oriented compliant and non-compliant drilling was performed, and the oriented drilling performance was

analyzed as a function of downhole dynamic weight on bit (DDWOB). Results of oriented ultrasonic wave velocity measurements, oriented strength, oriented strength correlations, and oriented compliant and non-compliant drilling showed isotropy of the tested fine-grained sandstone. By using published oriented ultrasonic wave velocity and strength indices, sandstone was also determined to be isotropy. The reported testing procedure is a comprehensive practical methodology of rock anisotropy evaluation.

9.3 Introduction

Rocks are classified to be either isotropic, if their properties (i.e. mechanical, physical, etc.) are directional independent, or anisotropic, if their properties are directional dependent [1,2]. Anisotropy can vary between the most basic vertically transversely isotropic / horizontally transversely isotropic, or VTI and HTI, respectively, and the very high anisotropy [3].

Rock anisotropy can highly affect various applications, including oil and gas drilling process, well-logging measurements, reservoir evaluation, oil sand formations' permeability enhancement, mining operations, and civil structures [4,5,6]. The influence of anisotropy of shale, an example of VTI rocks, on oriented drilling, as reported in [7, 8] highlighted the importance of studying the anisotropy of interbedded rocks.

The evaluation and determination of rock anisotropy assists in controlling well trajectory, enhancing drilling performance, optimizing hydrocarbon production, strengthening civil structures, and minimizing errors in produced data and results [5].

Rock anisotropy has an important effect on ultrasonic wave propagation. Another important property of rock that can vary with direction due to inherent rock anisotropy is strength. Rock

strength has been studied using numerous methods both destructive and non-destructive. Some of the destructive methods include confined and unconfined compressive strength, CCS and UCS, respectively [6]. UCS can be estimated from several other testing types, such as indirect tensile test (IT) or Brazilian tensile test (BTS) [9-12] and point load index (PLI) [13-15], which have been proven to have reliable correlations with UCS.

Rock tensile strength is determined through both direct and indirect tensile tests in both laboratories and through simulation under various conditions. However, the indirect tensile strength determined multidirectionally has not been applied for rock anisotropy / isotropy classification. Several reasons for choosing such a test method are its ease of sample preparation, its low cost, and its simple apparatus and experimental procedure [10, 18, 19].

An experimental procedure was developed [22] to establish a baseline for rock anisotropy evaluation utilizing two types of rocks, rock-like-material and granite (a synthetic rock and a natural rock, respectively), but it did not include an indirect tensile strength (ITS) test as is reported here.

The purpose of developing the baseline procedure that evaluates rock anisotropy, even though, its results showed the isotropy of the tested rocks, was to establish a practice that connects some main tests that represent verity of measurements (physical, mechanical, and drilling) to one another, and to structure a chain of relationships between tests and responses, which can eventually be used for evaluation of both isotropic and anisotropic rocks [7,20, 21, 22]. The indices used for such procedure are initially based on the published ones, but along the maturity of the procedure, are indices that can be proposed.

Although the proposed procedure has been initially developed [22], then was broadened, as presented in this work, and was mainly practiced on rocks that turned to be isotropic, this procedure was also involving some data analysis and evaluations that were performed on rocks of obvious anisotropic properties (shale), which requires more investigation on determined anisotropic rocks (i.e. shale) as research continuation as indicated in the future work section [7, 21].

The aim of this paper is to report a comprehensive laboratory procedure for rock anisotropy evaluation using a fine-grained sandstone formation through oriented ultrasonic wave propagation, oriented and multidirectionally oriented strength estimation, and directional compliant and non-compliant drilling application.

9.4 Sample preparation

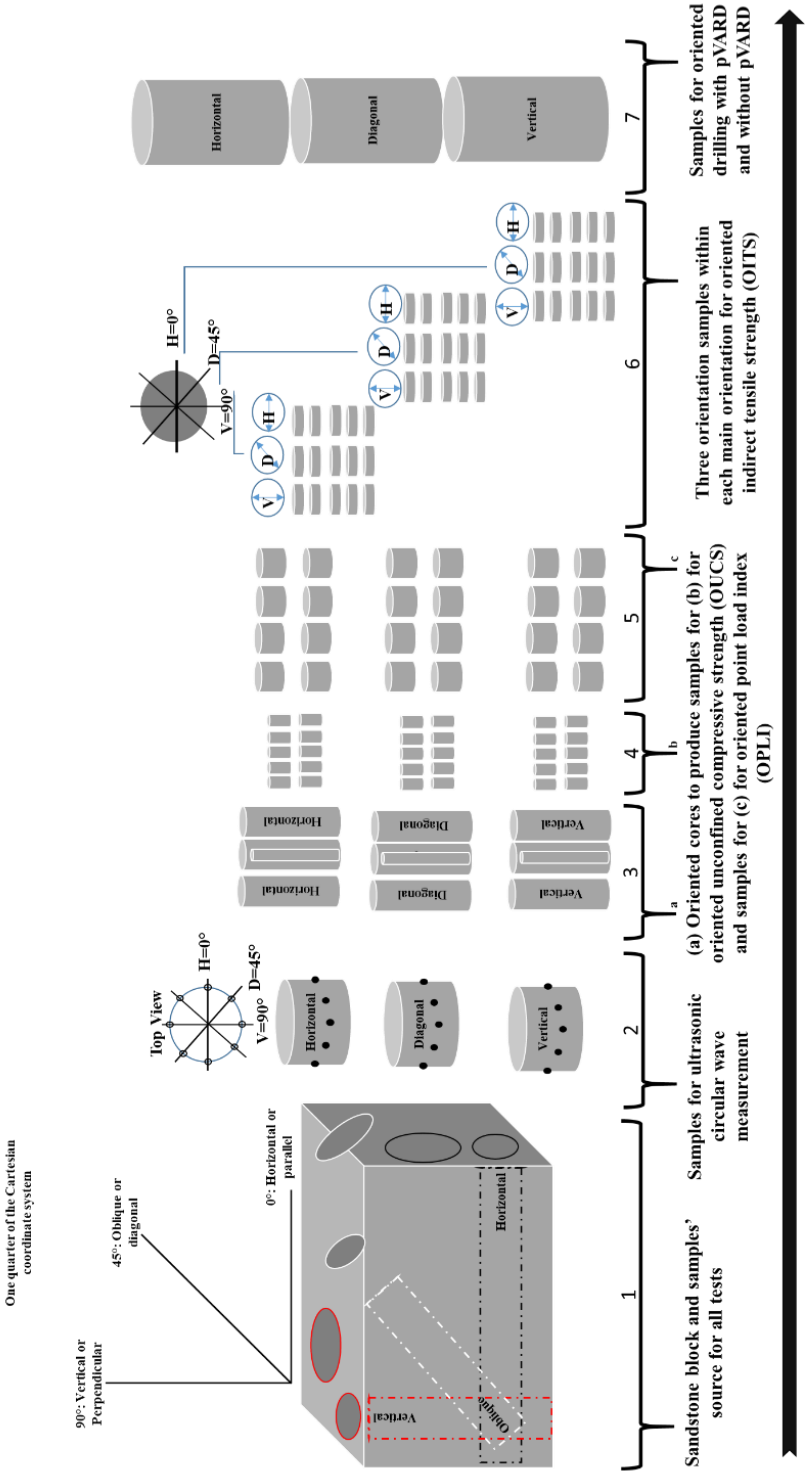

Figure 9-1. Fine-grained sandstone block as a source for oriented samples for all tests

Samples were produced from one block of a fine-grained sandstone and used for all tests as shown in Figure 9-1. Samples were obtained in various dimensions in accordance with American Society for Testing and Materials (ASTM) standards and the International Society of Rock Mechanics (ISRM) suggested methods. The dimensions of the main block were 70 cm long, 40 cm wide, and 50 cm high. Different diameter coring bits were used to core sandstone in three orientations: vertical, diagonal, and horizontal.

For oriented ultrasonic wave velocity measurements, samples were cores of 10.16 cm diameter and about 10 cm long as shown in Figure 9-1 (2), with indications of directions of circular wave velocity measurements. For oriented strength measurements, samples were cores of 4.76 cm diameter and about 30 cm long or more depending on the coring directions. Samples in each orientation were then categorized to three groups. Each group was denoted for a particular oriented strength testing type including oriented unconfined compressive strength (OUCS), oriented point load Index (OPLI), and oriented indirect tensile (OIT), Figure 9-1 (4, 5 and 6) respectively. For the oriented unconfined compressive strength test, samples were cored axially from the 4.76 cm samples using a 2.54 cm coring bit. The samples were then cut into a 2:1 ratio of length to diameter. For the OPLI test, samples were cut from the 2.54 cm cores in accordance with [23]. Figure 9-2 shows the requirements for sample dimension for the oriented axial point load test.

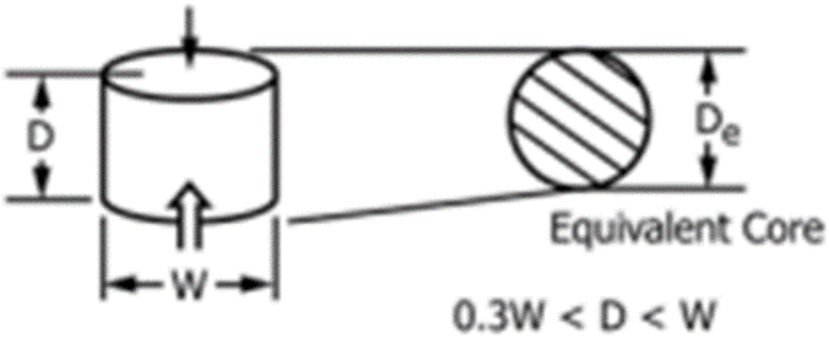

Figure 9-2. Sample dimensions for oriented point load test [23]

For the oriented indirect tensile test, disk samples were cut after color-coding the original cores as shown in Figure 9-1 (6) and *Figure 9-3* (right) to denote multidirectional orientations within each primary orientation.

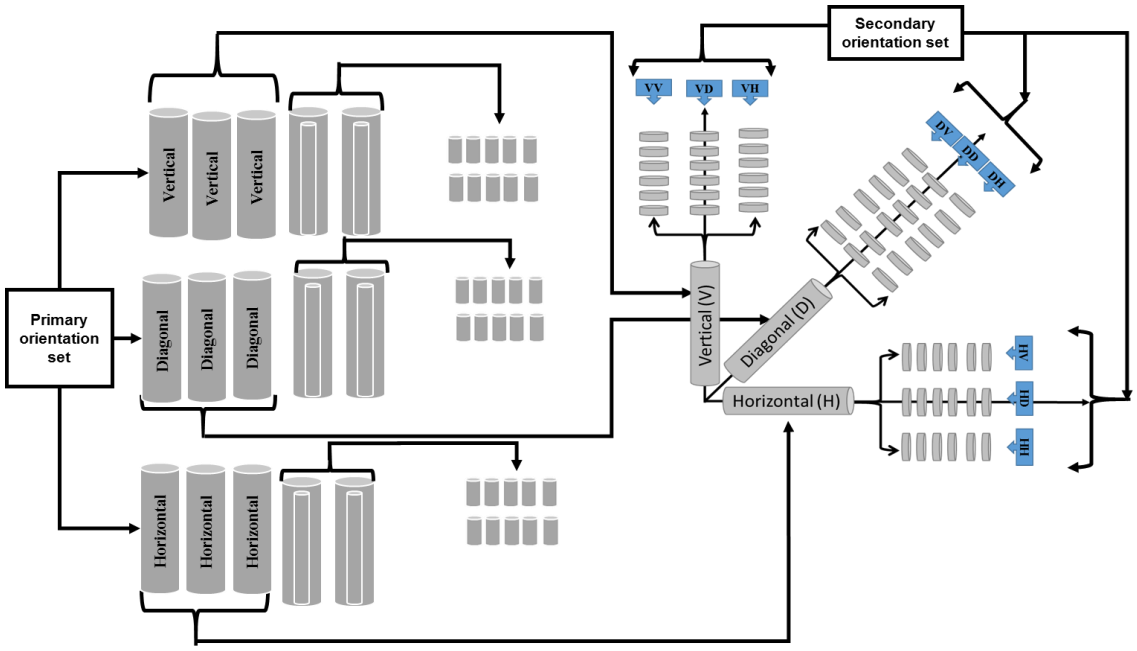

Figure 9-3. Diagram of sample preparation for UCS and multidirectional oriented IT

For both compliant and non-compliant drilling, samples were cored using a 10.16 cm coring bit. Each sample represents a different orientation. Samples are shown in Figure 9-1 (7).

9.5 Experimental Procedure

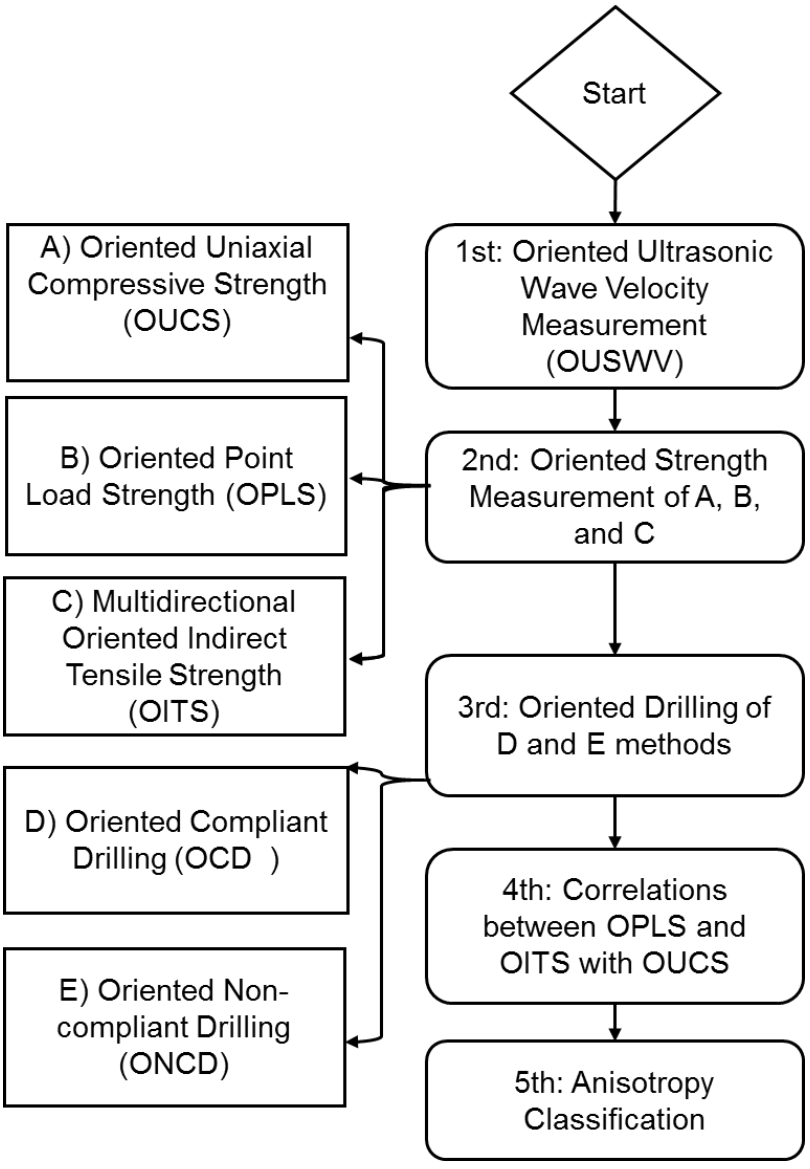

Figure 9-4. Experimental procedure flowchart.

Experiments were performed in the order described in Figure 9-4. First, for oriented ultrasonic wave velocity (OUSWV) including both compressional and shear wave velocity. The purpose of performing the OUSWV first was to test the sandstone for anisotropy with the non-destructive tests and to use some existing OUSWV anisotropy indices.

Second, oriented strength was determined through the destructive strength tests of OUCS, OPLS, and OITS. For the OUCS, tests were performed on samples prepared according to the primary set of vertical, diagonal, and horizontal. The purpose of these tests was to confirm the sandstone anisotropy classification obtained by OUSWV with the oriented strength tests. The OITS tests were conducted on disk samples prepared in the multidirectional orientations as shown in Figure 9-3 (right).

Third, a compliant drilling using a passive vibration assisted rotary drilling (pVARD) tool, and a non-compliant drilling were performed on samples produced from three orientations. Both drilling types were performed on the same samples, but each drilling was performed from opposite ends.

Fourth, correlations between OPLS and OITS with OUCS were constructed for further sandstone anisotropy evaluation and characterization. Lastly, a comparative analysis between the results of this work and work reported elsewhere was performed.

9.6 Performed Tests and Apparatus

This section shows all the tests that were conducted for the investigation of sandstone anisotropy by oriented ultrasonic wave velocity measurements, oriented strength measurements, and oriented drillings.

9.6.1 Oriented Ultrasonic Wave Velocity

The purpose of this measurement was mainly to investigate anisotropy through a non-destructive method.

Compared to other sound wave velocity measurements (i.e. low frequency sonic wave method and the frequency resonant method), the high frequency ultrasonic method was adopted for this work because it is more reliable and practical. Also, because it is a non-destructive, low cost, and high precision measurement. In this test, the compressional and shear wave velocities (VP and VS, respectively) were measured across eight spots around a circumference of each sample with an increment of 45 degrees as shown in Figure 9-1. The ultrasonic wave velocity apparatus used for this measurement was fully described by Abugharara et al., 2016 [22].

9.6.2 Oriented Strength

This section shows the three types of strength tests used: OUCS, OPLS, and OITS.

Figure 9-5 shows the apparatus used for all strength tests. A Point load apparatus was modified for OUCS and OITS tests.

Figure 9-5. PLI Apparatus with modifications with flat-end pistons for OITS and OUCS

9.6.3 Oriented Unconfined Compressive Strength

About 30 samples were tested for the OUCS. Samples were classified into three groups to represent three orientations. Figure 9-6 shows the samples before (top) and after (bottom) conducting the OUCS test.

Figure 9-6. Samples before (top) and after (bottom) performing OUCS test showing a consistent shear fracture pattern

9.6.4 Oriented Point Load Strength

44 samples were tested following the axial point load index. Figure 9-7 shows samples before (top) and after (bottom) performing the OPLS test.

Figure 9-7. Samples before (top) and after (bottom) performing the OPLS test and showing consistent valid fracturing modes

9.6.5 Oriented Indirect Tensile Strength

For this test, 90 sandstone disk samples were prepared and classified into three groups as described in Figure 9-1. Following a color code, three smaller groups each of about 10 samples represented the three orientations. Each group consists of about 30 samples representing three secondary orientations within each larger core: (VV, VD, VH), (DV, DD, DH), and (HV, HD, and HH) within each primary orientation of vertical (V), diagonal (D), and horizontal (H). The purpose of the classification of the disk samples into primary and secondary orientations was to investigate the sandstone anisotropy. Figure 9-3 shows the procedure of testing the disk samples following the color code for the secondary orientations.

Many studies reported the influence of rock anisotropy on the fracture direction deviation from the two load points when the splitting (fracturing) of the sandstone disk samples were monitored while testing. The straight and direct fracture between the two load points in all OITS testing was determined as shown in Figure 9-10 and was considered as another sign of sandstone isotropy. Figure 9-9 and Figure 9-10 show the oriented disk samples before and after the OITS tests, respectively.

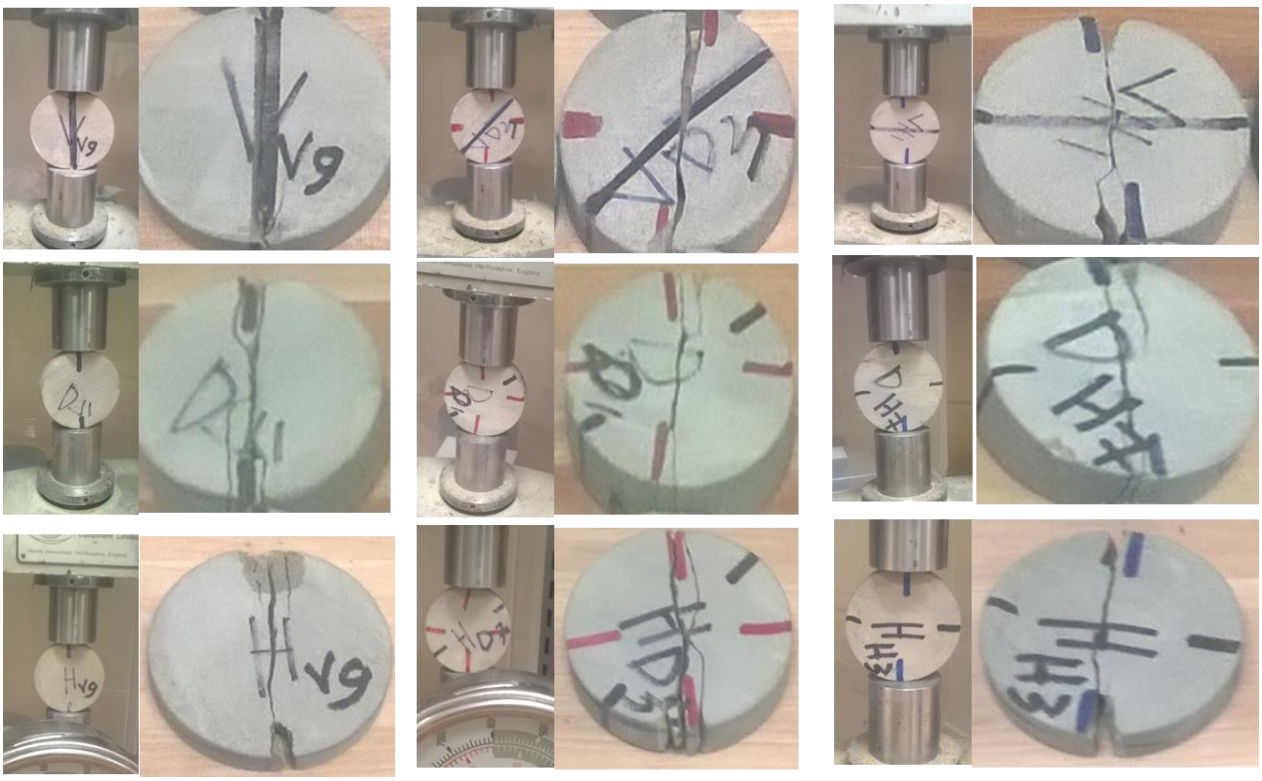

Figure 9-8. Procedure of the OITS test on sandstone disk samples (left) and fractured samples after OITS (right) showing consistently straight splitting fractures

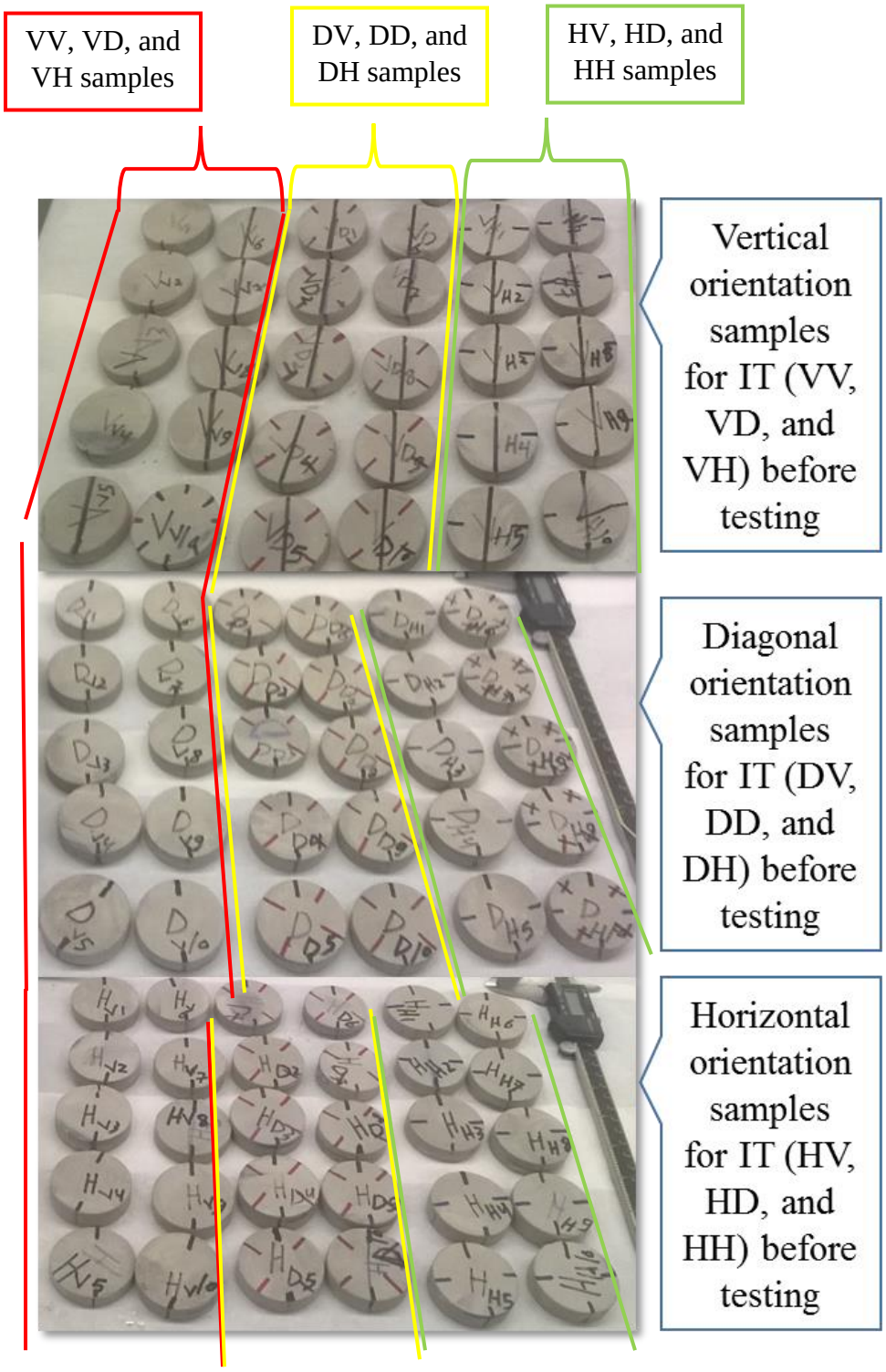

Figure 9-9. Sandstone disk samples before OITS testing

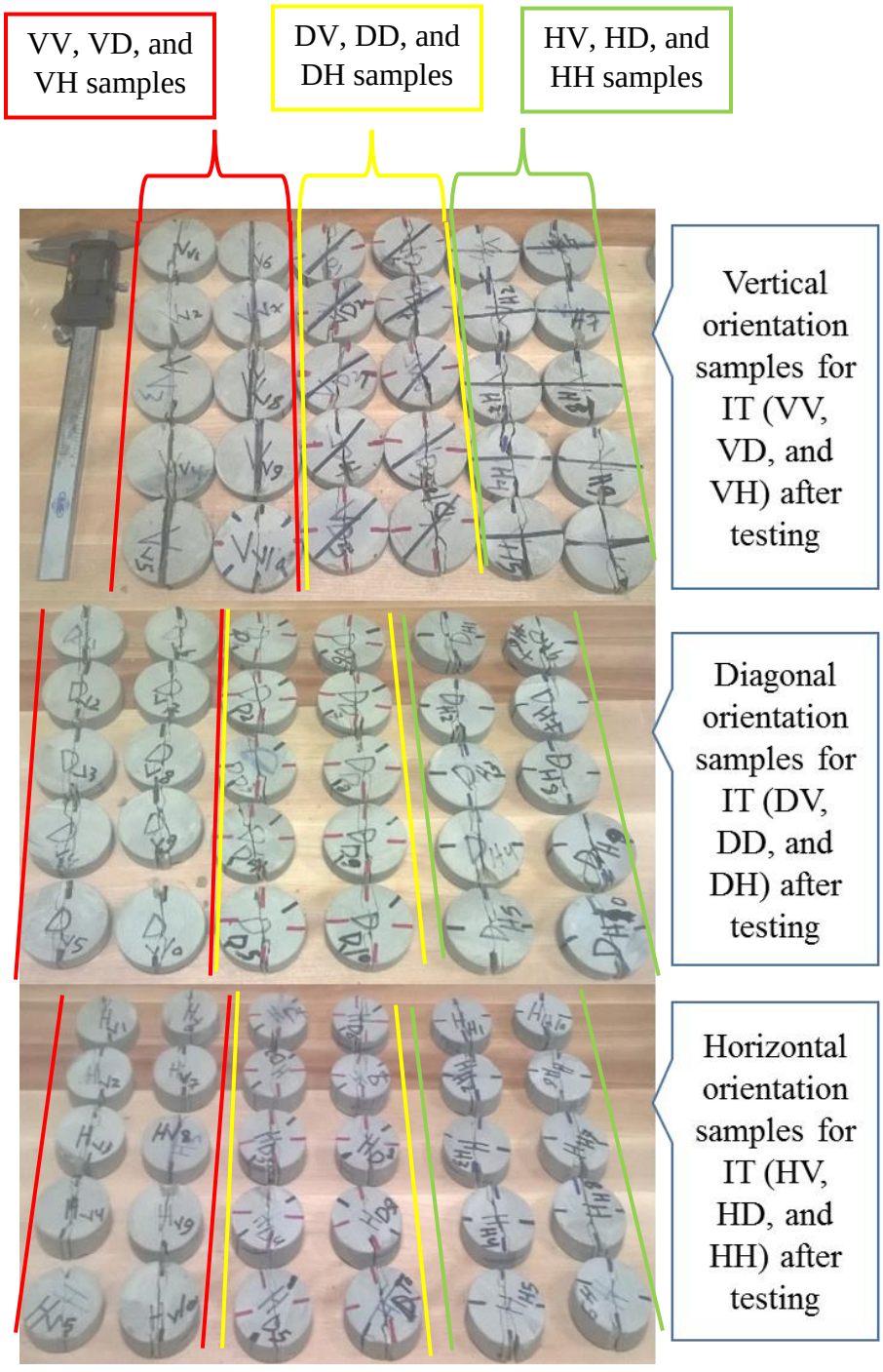

Figure 9-10. Sandstone disk samples after OITS testing

9.6.6 Oriented Compliant and Non-compliant Drilling

Compliant drilling using pVARD and non-compliant drilling were the last tests. Figure 9-11 shows the compliant and non-compliant drilling apparatus with a dual cutter Polycrystalline Diamond Compact (PDC) bit.

Figure 9-12 shows drilled samples by compliant and non-compliant drilling using a fully instrumented laboratory scale rotary drilling rig (Figure 9-11). The pVARD tool was used to drill with induced vibrations, which makes it different from non-compliant drilling, where pVARD was locked. The purpose of using two different drilling modes of compliant and non-compliant drilling was to further evaluate sandstone anisotropy.

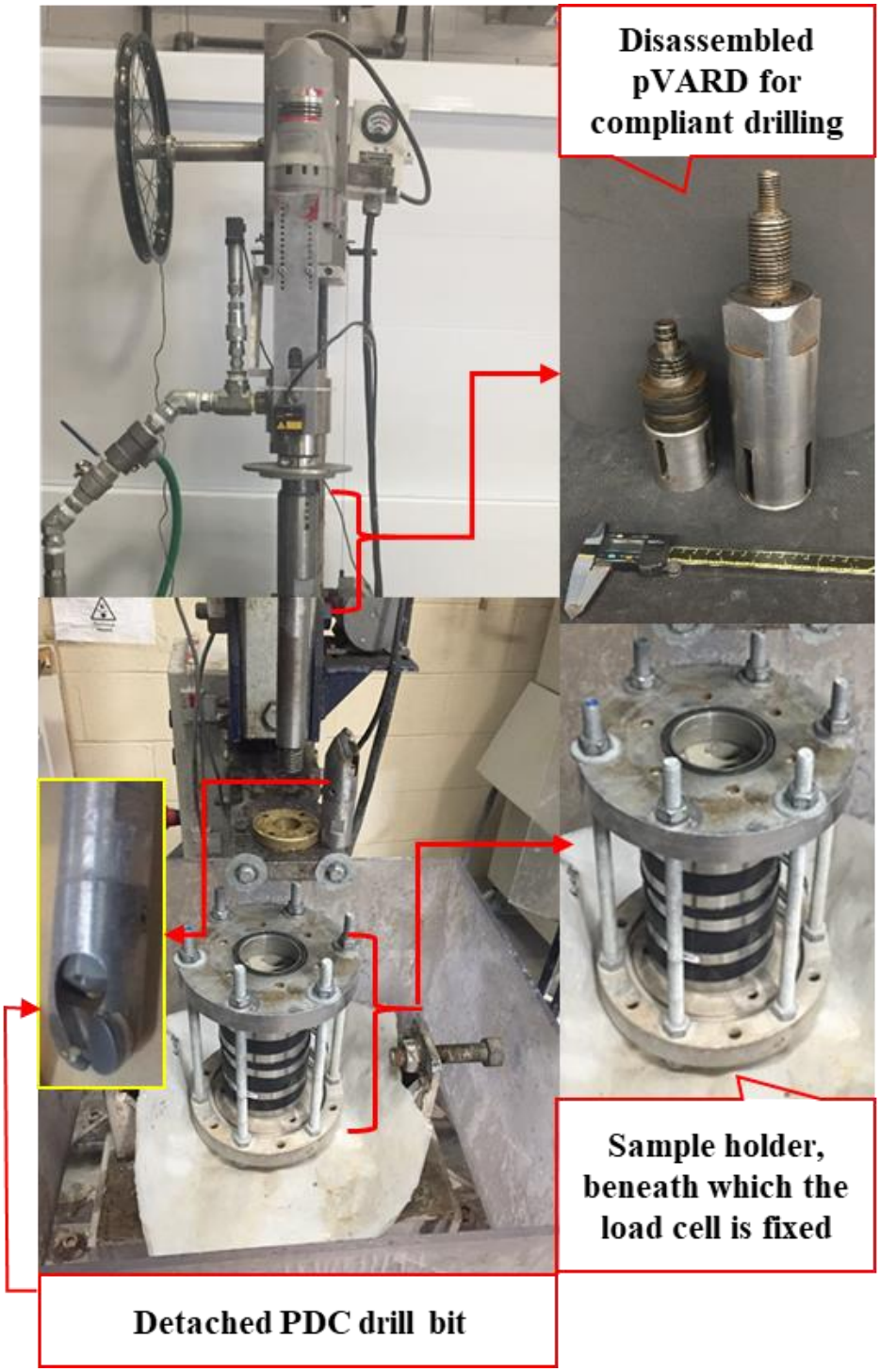

Figure 9-11. Fully instrumented laboratory scale drilling rig

Figure 9-12. Strength samples' source (top) drilled samples using compliant and non-compliant drilling (bottom)

9.7 Results

This section contains the results of the measured oriented ultrasonic wave velocities, by which the isotropy of sandstone was firstly determined. It also contains the results of the oriented UCS, PLS, IT, and their correlations.

9.7.1 Results of Oriented Ultrasonic Wave Measurement

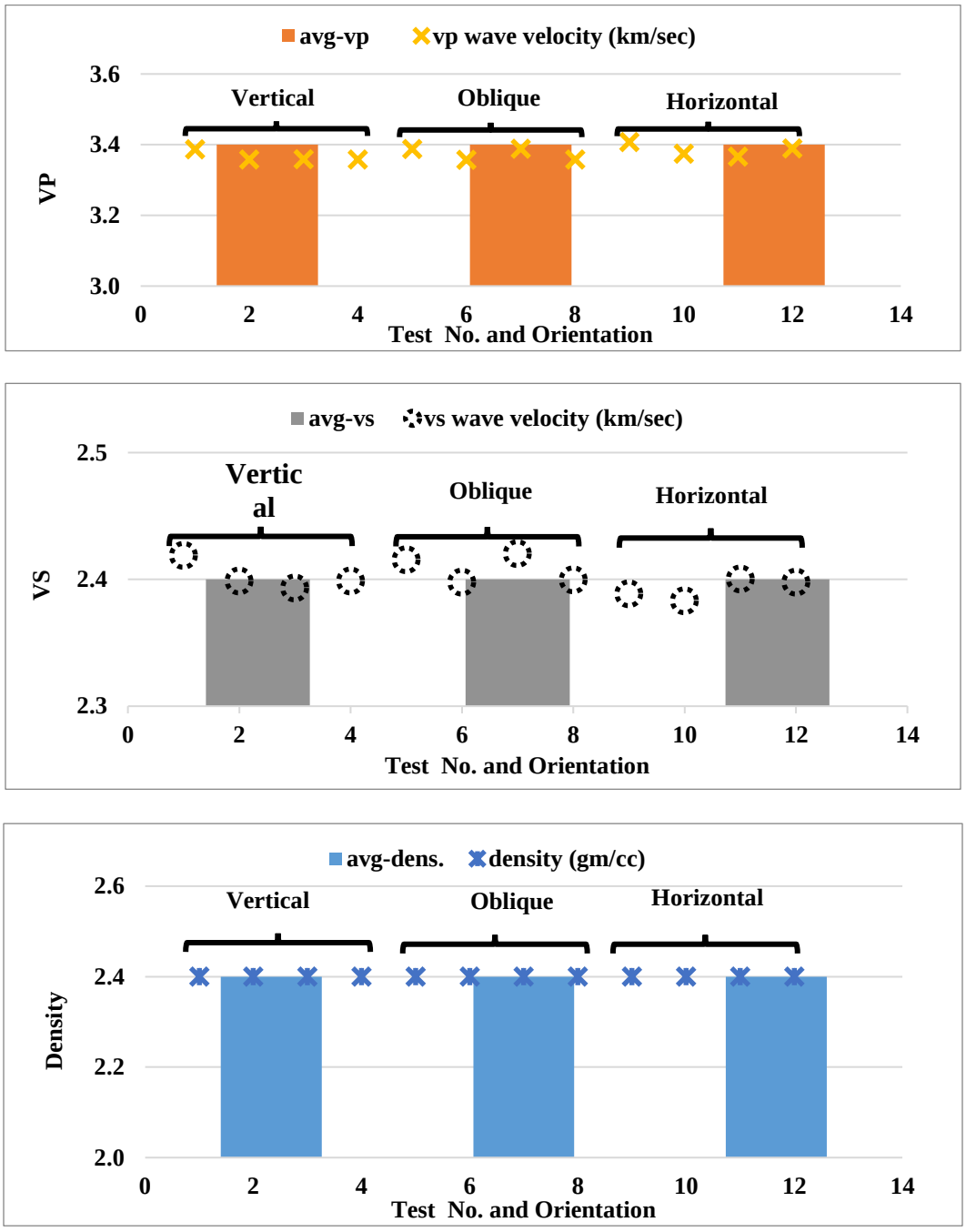

Figure 9-13. Oriented ultrasonic compressional (top) and shear (middle) wave velocity measurements as well as density with their average values

Figure 9-13 shows results of the circular ultrasonic compressional (top) and shear (middle) wave velocity measurements from three oriented sandstone cores with their average values. Figure 9-13 also shows density measurements of these oriented samples and the other cores in the three orientations with their average values.

Results of the anisotropy classification of tested sandstone was according to some of the published anisotropy indices reported by Tsidzi, 1997 and Saroglou, 2007 [24, 25], and they are summarized in Table 9.1. Table 9.1 also contains the anisotropy strength indices and the results of the current work. The work reported by Tsidzi and Saroglou was conducted on various types of rocks that varied in their anisotropy and their classification included all isotropy and anisotropy classification ranges. This work used only one type of rock but conducted all tests on samples obtained from the same block of the rock. This considered as unique, as such a high number of tests were involved for the same purpose of rock anisotropy investigation. There was neither indication of this work's unique sample preparation reported in previously published work addressing rock anisotropy investigation, nor was an involvement of several testing types performed for the same purpose and the same study.

Table 9.1 summarizes published indices of wave velocity and strength anisotropy with their conditions for anisotropy classification, along with the results of the current study.

Table 9.1. Published wave velocity and strength anisotropy indices with their conditions for anisotropy classification with results of current study

Author	Test type	Anisotropy Index	Equation	Criterion	Result of current study	Descriptive term
Tsidizi (1997) [24]	Wave velocity	Velocity Anisotropy (VA) Index	VA= [(Vmax-Vmin)/Vmean] (%)	< 2.0 : Isotropy	0.55 (%)	Isotropy
Saroglou (2007) [25]			IVP =VP (0°)/VP (90°)			
ISRM (1981) [26]	PLI	Point load strength anisotropy index	Ia(50) = Is (50) (90°) / Is (50) (0°)	1.0 : Isotropy	0.05	Isotropy
ISRM (1985) [27]						
Tsidzi (1990) [15]						
Ramamurthy (1993) [28]	UCS	Uniaxial compressive strength anisotropy index	Iσc = σc (90°) / σc (min)	1.0 - 1.1: Isotropy	0.99	Isotropy

9.7.2 Results of Oriented Strength

9.7.2.1 Oriented Unconfined Compressive Strength

This section shows the results of sandstone oriented strength measured by OUCS. Figure 9-14 shows the results of all OUCS tests with their average values.

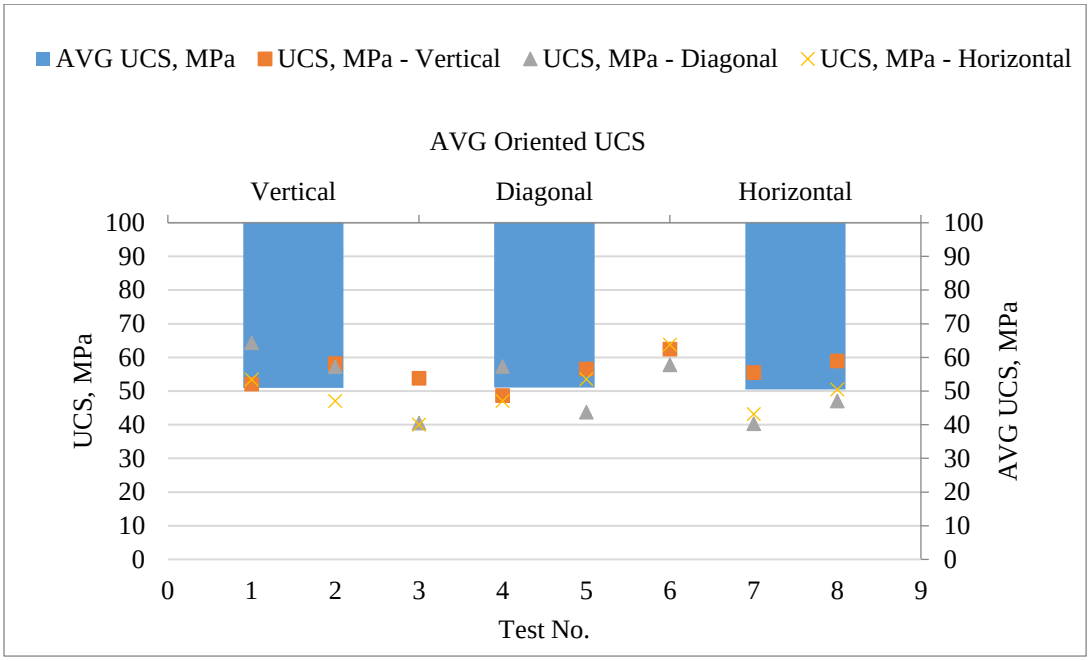

Figure 9-14. Oriented unconfined compressive strength and their average values

9.7.2.2 Oriented Point Load Strength

The results of the OPLS and their average values are shown in Figure 9-15. Correlation between all data of OUCS and OPLS is shown in Figure 9-16. Values of average strength by OUCS and OPLS are shown in Figure 9-17.

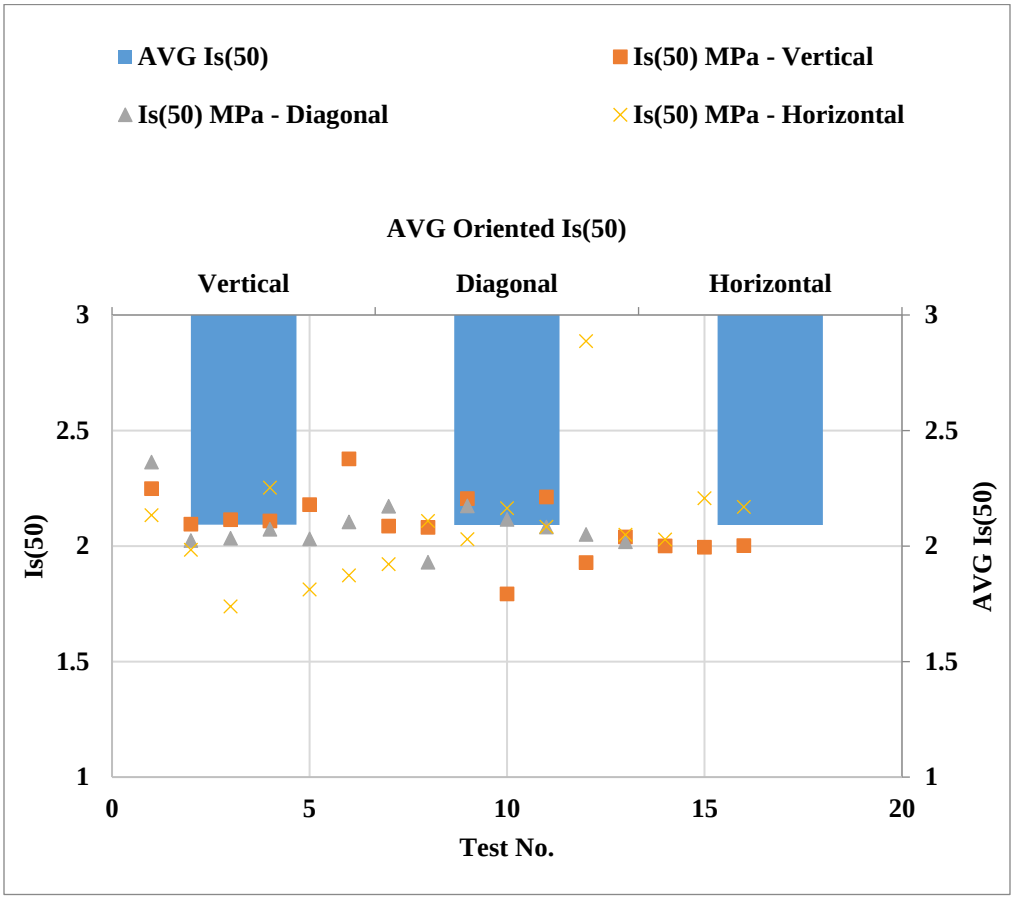

Figure 9-15. Oriented point load strength and their average values

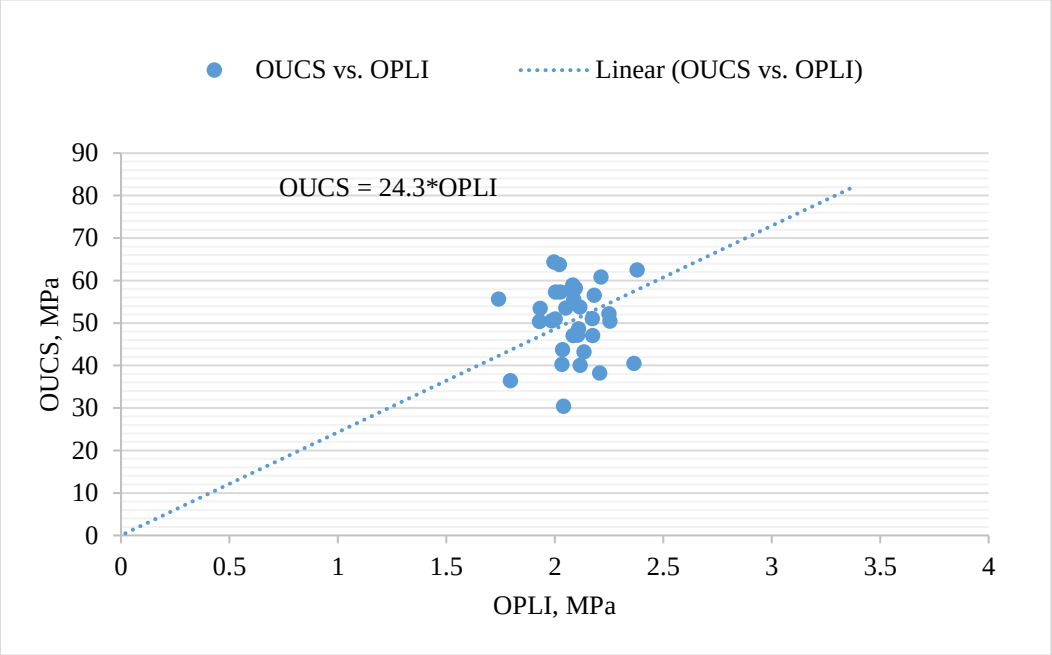

Figure 9-16. All data of oriented UCS vs. PLS

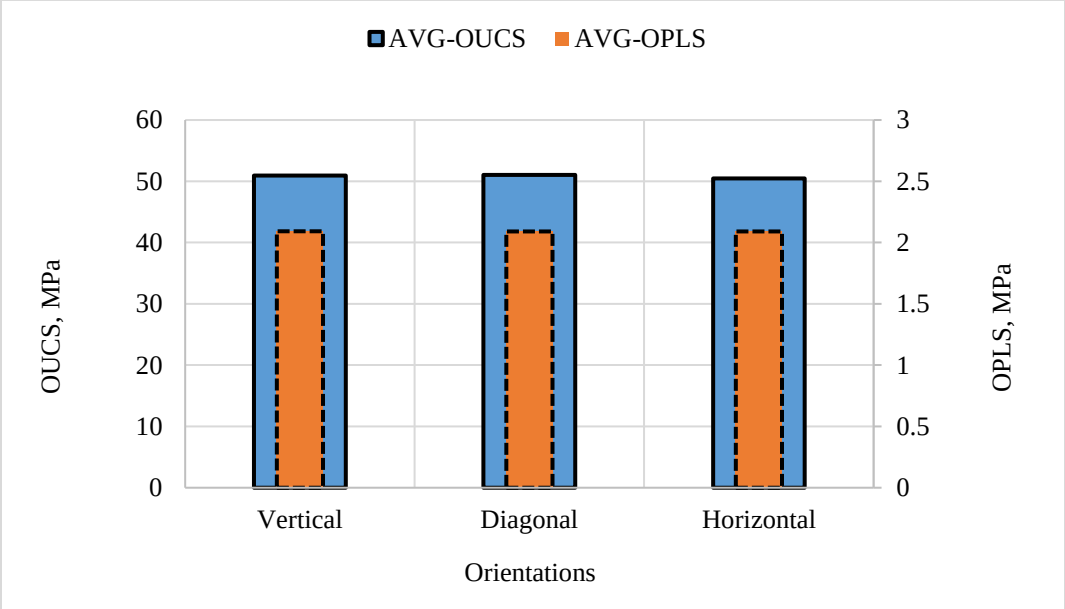

Figure 9-17. Averaged values of oriented UCS vs. PLS

9.7.2.3 Oriented Indirect Tensile Strength

This section shows the results of oriented strength determined by multidirectional indirect tensile strength. It also includes the correlation between OUCS and OITS. Figure 9-18 shows the data of oriented strength obtained by multidirectional indirect tensile strength and their average values.

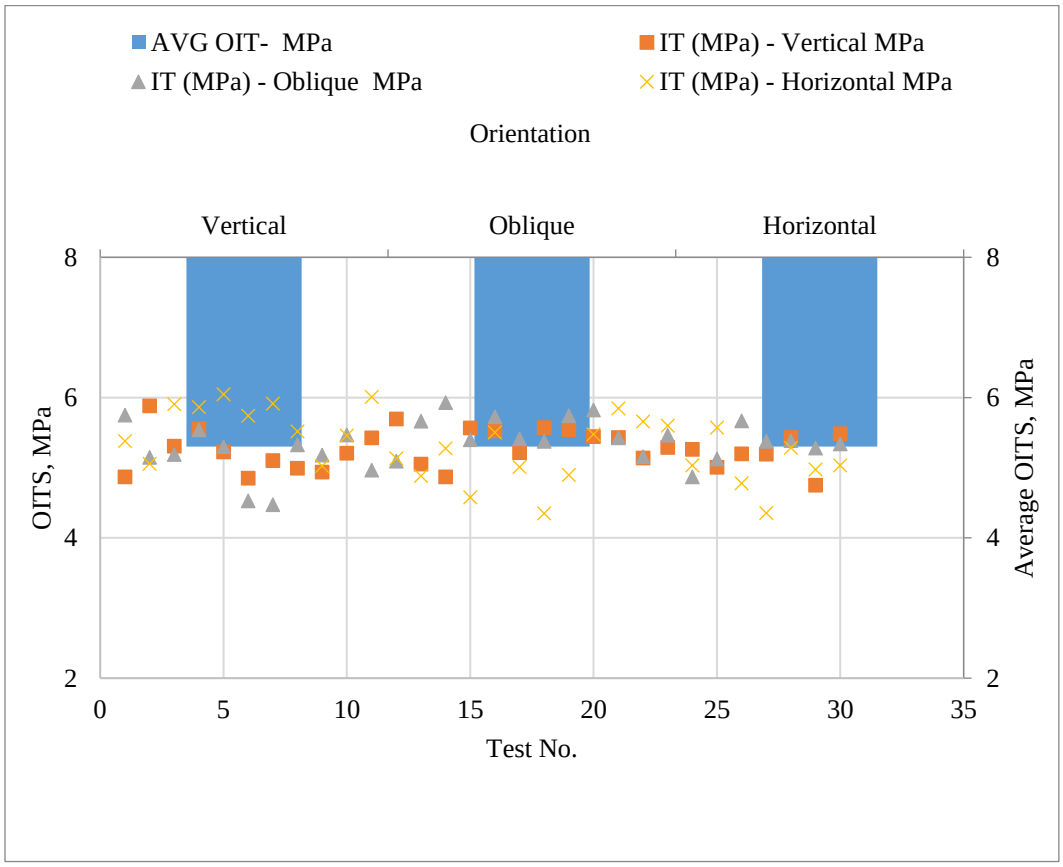

Figure 9-18. Oriented strength obtained by multidirectional indirect tensile test

Figure 9-19 shows the correlation of all data of OUCS and OITS. Figure 9-20 shows the results of oriented average strength obtained by OUCS and OITS.

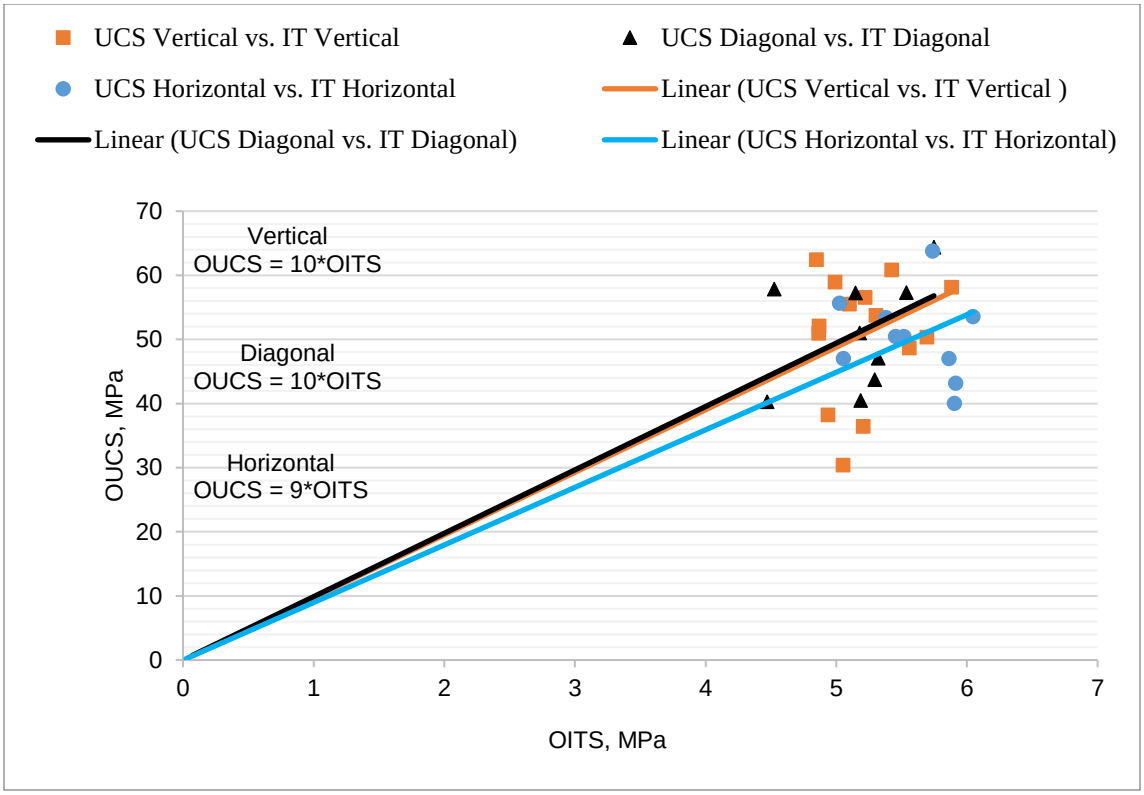

Figure 9-19. All data of oriented UCS vs. IT

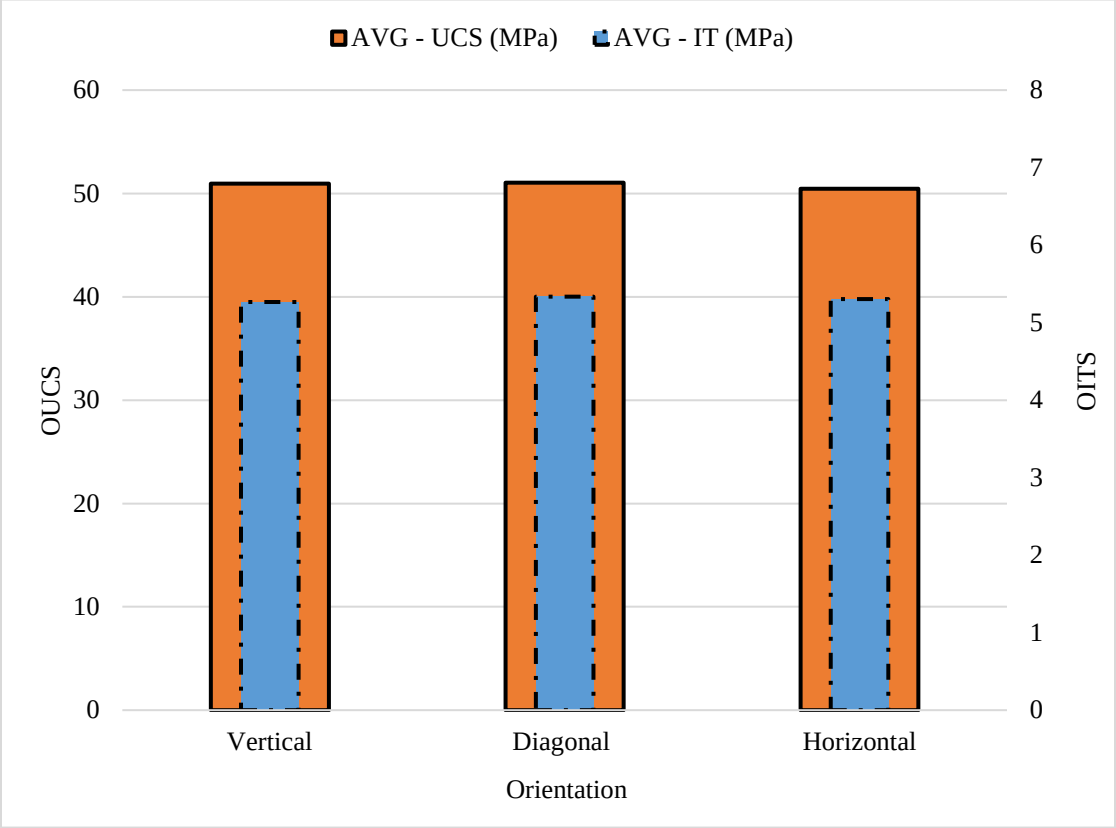

Figure 9-20. Averaged values of oriented strength obtained by UCS and IT

Table 9.2 contains correlations for PLI and UCS from both published and the current Study.

Table 9.2. Summary of published correlations for PLI and UCS with correlations of the current study

Reported correlations			
Author	Source of rock	Rock type	Correlation
Broch and Franklin (1972) [13]	UK	Various rocks	UCS = 23.7*PLI
Bieniawski (1975) [29]	South Africa	Sandstones	UCS = 23.9*PLI
Hawkins and Olver (1986) [30]	UK	Sandstones	UCS = 24.8*PLI
Vallejo et al. (1989) [31]	USA	Sandstones	UCS = 17.4*PLI
Das (1985) [32]	Canada	Sandstones	UCS = 18*PLI
Smith (1997) [33]	Various locations	Sandstones	UCS = 24*PLI
Current study correlations: Abugharara (2019)			
Vertical UCS vs. Vertical PLI	Canada	Sandstones	UCS=24*PLI
Diagonal UCS vs. Diagonal PLI	Canada	Sandstones	UCS=24*PLI
Horizontal UCS vs. Horizontal PLI	Canada	Sandstones	UCS=25*PLI
Vertical UCS vs. Diagonal PLI	Canada	Sandstones	UCS = 24*PLI
Vertical UCS vs. Horizontal PLI	Canada	Sandstones	UCS = 24*PLI
Diagonal UCS vs. Vertical PLI	Canada	Sandstones	UCS = 24*PLI
Diagonal UCS vs. Horizontal PLI	Canada	Sandstones	UCS = 26*PLI
Horizontal UCS vs. Diagonal PLI	Canada	Sandstones	UCS = 24*PLI
Horizontal UCS vs. Vertical PLI	Canada	Sandstones	UCS = 24*PLI
OUCS vs. OPLS (all data in all orientations)	Canada	Sandstones	UCS=24*PLI

Table 9.3 summarizes correlations between multidirectional OITS and OUCS.

Table 9.3. Summary of correlations between OITS and OUCS in all scenarios of multiple and singular orientation

Correlations between IT and UCS of Previous studies				
Ref.	Author	Equation	Rock Type	Orientation
1	Kahraman et al, 2012 [11]	UCS=10.61*BTS	Different rock types including sandstone	/
2	Altindag and Guney, 2010 [34]	UCS=12.308*TS^1.0725	Different rock types including sandstone	/
3	Altindag and Guney, 2010 [34]	UCS=12.38*TS^1.025	Different rock types including sandstone	/
Correlations between IT and UCS of this study				
Ref.	Author	Equation	Rock Type	Orientation
4		UCS = 10*IT	Fine-grain Sandstone	UCS Vertical vs. IT Vertical
5		UCS = 10*IT	Fine-grain Sandstone	UCS Diagonal vs. IT Vertical
6		UCS = 10*IT	Fine-grain Sandstone	UCS Horizontal vs. IT Vertical
7		UCS = 10*IT	Fine-grain Sandstone	UCS Vertical vs. IT Diagonal
8	Abugharara et al, 2019,	UCS = 10*IT	Fine-grain Sandstone	UCS Diagonal vs. IT Diagonal
9	Current study	UCS = 10*IT	Fine-grain Sandstone	UCS Horizontal vs. IT Diagonal
10		UCS = 9*IT	Fine-grain Sandstone	UCS Vertical vs. IT Horizontal
11		UCS = 9*IT	Fine-grain Sandstone	UCS Diagonal vs. IT Horizontal
12		UCS = 9*IT	Fine-grain Sandstone	UCS Horizontal vs. IT Horizontal
13		UCS = 10*IT	Fine-grain Sandstone	Multidirectional orientation of UCS vs. IT
14		UCS = 10*IT	Fine-grain Sandstone	AVG of AVG OUCS vs. OITS

9.7.2.4 Oriented Compliant and Non-Compliant Drilling

This section contains the results of oriented drilling in the three orientations using the compliant and non-compliant drilling system. The results involved comparison between the downhole dynamic weight on bit (DDWOB) measured by the load cell attached beneath the sample holder. The DDWOB is a result of an input of three levels of static weight, low static weight (LSW), medium static weight (MSW), and high static weight (HSW). Drilling using compliant and non-compliant induces different levels of vibrations that influence the DDWOB, and as a result influence ROP. The purpose here is to conduct a comparative analysis of DDWOB in compliant and non-compliant drilling as a function of sandstone orientation and static weight, then, evaluate their changes with orientation.

Figure 9-21 and Figure 9-22 show consistency in results as a function of static weight levels and orientation indicating sandstone isotropy. The similarity appears in DDWOB as well as in rate of penetration (ROP) in both compliant and noncompliant drilling as a function of orientation.

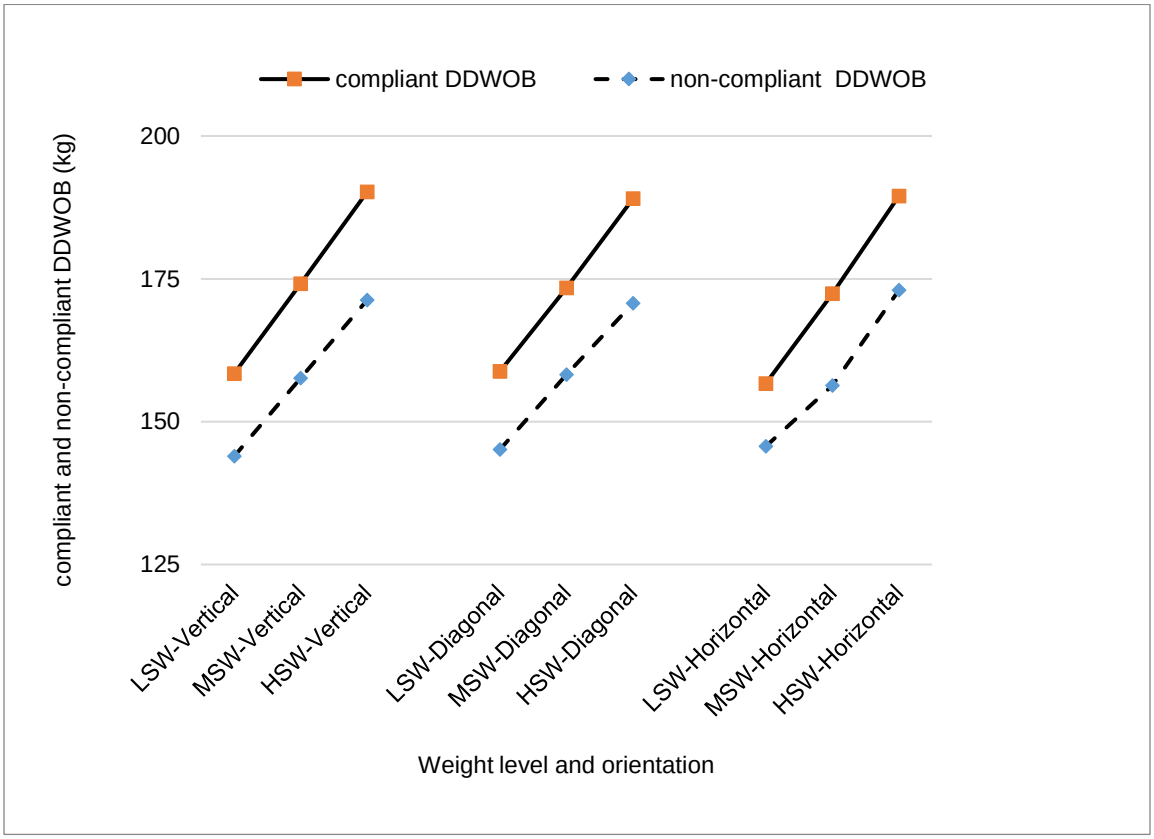

Figure 9-21. Averaged values of DDWOB of compliant and non-compliant drilling as a function of three sets of static weight and orientations

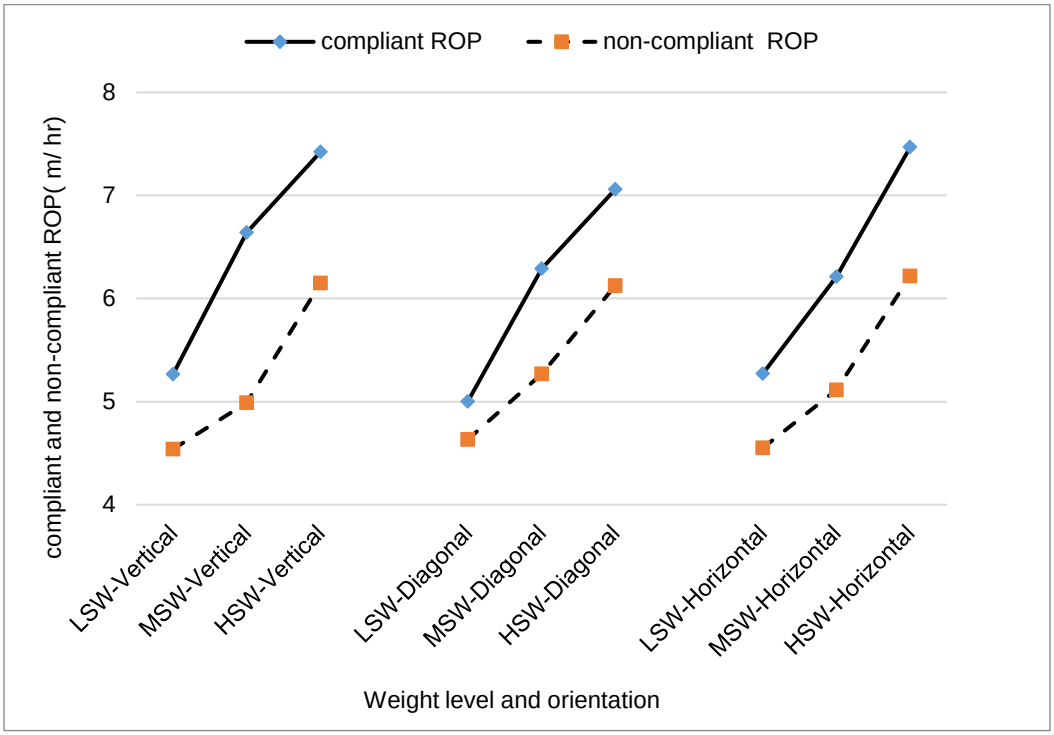

Figure 9-22. Averaged values of ROP of compliant and non-compliant drilling as a function of three sets of static weight and orientations

9.8 Discussion

Sandstone anisotropy was evaluated based on averaged values of the results of all tests. For each set of testing in each orientation, there was repetition of tests as the same inputs and results were averaged.

This work investigated the anisotropy of sandstone by using several types of tests and through performing some new techniques of sample preparation and testing procedures. First, OUSWV measurements were performed. The results of OUSWV were analyzed with comparison to published wave velocity indices and are shown in Figure 9-13. Sandstone isotropy classification through OUSWV is indicated in Table 9.1 (top). Second, sandstone anisotropy was investigated

through applying three main strength tests (OUCS, OPLIS, and OITS). The results of the oriented strength tests of OUCS and OPLIS were analyzed with comparison to published OUCS and OPLS indices. The sandstone isotropy classification through OUCS and OPLIS is reported in Table 9.1 (bottom and middle, respectively). As a new contribution of oriented indirect tensile strength, a multidirectional indirect tensile strength test was performed to evaluate the anisotropy of the tested sandstone, in particular, and to support the developed procedure for rock anisotropy evaluation, in general. Third, oriented correlations, as a new rock anisotropy investigation technique between OUCS and OPLIS as well as between OUCS and OITS were performed and their summary is reported in Table 9.2 and Table 9.3, respectively. It can be noted that some of the published correlations were non-linear relationships. The reason for such non-linear relationships could be due to plotting various rock types together, where, in this work, only one rock types was tested. Lastly, as a novel technique for investigating rock anisotropy, oriented compliant and non-compliant drilling was performed involving various levels of axially induced oscillations. The purpose behind including these experiments and involving them in the rock anisotropy investigation was to evaluate the influence of the inner structure of rocks that lead to property variation with direction on inducing axial oscillation, which can impact drilling parameters and drilling performance. Moreover, if rock properties are consistent with orientation, then results can be consistent. The results of the new involvement of the oriented (directional) compliant and non-compliant drilling techniques were analyzed as a function of rock orientations as well as DDWOB.

Figure 9-13 shows results of the oriented compressional wave velocity (top) and the oriented shear wave velocity (middle) with their averaged values plotted on the same figures as a function of the sample orientations. Several circular wave measurements were taken from each sample cored in a

different orientation. Then measurements of wave velocity performed on the same core are averaged and plotted as a function of orientation (vertical, oblique, and horizontal). Figure 9-13 (bottom) shows oriented densities of the tested sandstone. The samples used for the density measurements were the oriented samples used for OUSWV. The samples prepared for strength and drilling tests of different shapes and dimensions were also used for measuring the oriented density as a function of orientation.

Figure 9-14, Figure 9-15, and Figure 9-18 show oriented strength obtained by UCS, PLI, and IT with their average values, respectively. The results of strength anisotropy were used for the tested sandstone anisotropy using published indices that are reported in Table 9.1. The sandstone anisotropy investigation using published strength indices showed sandstone isotropy and are summarized in Table 9.1 (middle and bottom).

Figure 9-17 and Figure 9-20 show the average values of the oriented UCS with OPLS and OITS as a function of orientation, respectively.

Although strength correlations between UCS with PLI and IT were widely used by numerous researchers, the main purpose for such correlations was to provide alternatives to estimate rock strengths by different methods. This study, however, uses correlation as a new technique to evaluate rock anisotropy.

Correlations were constructed collectively and individually as functions of orientations. Figure 9-16 and Figure 9-19 show the collective correlations between OUCS with OPLS and OITS, respectively. The results of the strength correlations between OUCS, OPLS and OITS are summarized in Table 9.2 and Table 9.3, respectively.

Oriented drilling using different induced oscillations was included in this study as a novel technique that was not applied before to investigate rock anisotropy. The purpose of involving compliant and non-compliant drilling was to further analyze the tested sandstone anisotropy using a dual cutter PDC bit, which can drill in a balanced mode, and to expand the rock anisotropy evaluation procedure. Another reason for including the drilling of compliant and non-compliant was to investigate the relationship between DDWOB and rock anisotropy / isotropy as a function of orientation and the magnitude of axial oscillations.

The positive influence of compliant drilling on drilling performance against non-compliant drilling was previously investigate, using static WOB as well as DDWOB [34, 35, 36], and both compliant and non-compliant oriented drilling were implemented in this work. Their results were analyzed for the purpose of rock anisotropy evaluation.

Figure 9-21 and Figure 9-22 show results of oriented DDWOB and oriented ROP using both drilling modes as a function of three sets (low, medium, and high) of static weight and rock orientation. The averaged results of DDWOB and ROP as a function of the three static weight sets and orientation showed result consistency and similar trend variations, which indicates sandstone isotropy, as was determined by OUSWV, OUCS, OPLS, and OITS.

Constructing the comprehensive laboratory procedure that involved physical, mechanical, and drilling performance measurements to evaluate rock anisotropy utilizing fine-grained sandstone is a new technique. All the tests support and validate one another in evaluating rock anisotropy.

9.9 Conclusion

This work reports results of an ongoing project that uses various techniques, among which are compliant and non–compliant drilling as well as strength tests, for rock anisotropy characterization.

Using fine-grained sandstone, tests were supporting one another in showing the isotropy in wave velocity and strength tests where comparison with published studies was performed. As a new testing contribution for rock anisotropy investigation, the drilling tests using various axial compliant magnitudes also showed data consistency, indicating sandstone isotropy and supporting sandstone isotropy, which was first determined by the oriented wave and strength tests.

9.10 Future Work

- Considering smaller orientation increments in all parts of the study of similar sandstone structure to detailed procedure.
- Involving various types of rocks, in particular rocks of obvious anisotropy such as shale or other interbedded rocks for the purpose of anisotropy evaluation.
- Conducting further study for rock anisotropy evaluation under various conditions such as pressurized conditions.
- Producing pressurized indices of the published ones as well as indices for compliant and non-compliant drilling for the purpose of rock anisotropy evaluation.

9.11 Acknowledgement

This work was performed in the Drilling Technology Laboratory (DTL) at Memorial University of Newfoundland, St. John's, Newfoundland and Labrador, Canada.

9.12 Funding Data

- Atlantic Canada Opportunity Agency (AIF contract number: 781-2636-1920044), involving Husky Energy, Suncor Energy and Research and Development Corporation (RDC) of Newfoundland and Labrador.
- The Ministry of Higher Education and Scientific Research, Libya, through the Canadian Bureau for International Education, Canada (CBIE-Canada).

9.13 References

1. Brown, E. T., & Hudson, J. A. (Eds.). (1993). "Comprehensive rock engineering: principles, practice & projects". 1. Fundamentals. Pergamon Press.

2. Goodman, R. E. (1980). "*Introduction to Rock Mechanics*". John Wiley:12.

3. Brady, B. H. G., and E. T. Brown. (2006). "*Rock Mechanics for underground mining",* Kluwer Academic Publishing: 36.

4. Mokhtari, M., Honarpour, M. M., Tutuncu, A. N., & Boitnott, G. N. (2016). "Characterization of elastic anisotropy in Eagle Ford Shale: Impact of heterogeneity and measurement scale", SPE Reservoir Evaluation & Engineering, 19(03), 429-439.

5. Gu, M. (2018). “Impact of anisotropy induced by shale lamination and natural fractures on reservoir development and operational designs”. SPE Reservoir Evaluation & Engineering, 21(04), 850-862.

6. Ashour, H. A. (1988). “A Compressive Strength Criterion for Anisotropic Rock Materials”, Canadian Geotechnical Journal, 25(2), 233-237.

7. Abugharara, A. N., Mohamed, B., Hurich, C., Molgaard, J., & Butt, S. D. (2019). “Experimental investigation of the effect of shale anisotropy orientation on the main drilling parameters influencing oriented drilling performance in shale”. Journal of Energy Resources Technology, 141(10), 102904. DOI: 10.1115/1.4043435.

8. Brown, E.T., Green, S.J. and Sinha, K.P. (1981). “The influence of rock anisotropy on hole deviation in rotary drilling—A review”. In International Journal of Rock Mechanics and Mining Sciences & Geomechanics Abstracts, 18(5), 387-401. Pergamon.

9. Sheorey, P.R. (1997). “Empirical rock failure criteria,” A. A. Balkema", p: 176.

10. Komurlu, E., Kesimal, A., & Demir, S. (2015). “Experimental and Numerical Study on Determination of Indirect (Splitting) Tensile Strength of Rocks under Various Load Apparatus”. Canadian Geotechnical Journal, 53(2), 360-372.

11. Kahraman, S., Fener, M., and Kozman, E. (2012). Predicting the compressive and tensile strength of rocks from indentation hardness index. Journal of the Southern African Institute of Mining and Metallurgy, 112 (5), 331-339.

12. Diederichs, M.S. (2007). “The 2003 Canadian geotechnical colloquium: Mechanistic interpretation and practical application of damage and spalling prediction criteria for deep tunneling”. Canadian Geotechnical Journal. 44(9), 1082-1116.

13. Broch, E. and Franklin, J. A. (1972). “The point load strength test”, International Journal Rock Mechanics and Mining Sciences & Geomechanics Abstracts, 9 (6), 669-697. Pergamon Press.

14. Mendieta, H. J. (2012). “Determination of a correlation between intact rock unconfined compressive strength and index parameters”. Harmonising Rock Engineering and the Environment - Proceedings of the 12th ISRM International Congress on Rock Mechanics. P.735-739.

15. Tsidzi, K. (1990). “The influence of foliation on point load strength anisotropy of foliated rocks”. Bull. Int. Association of Eng. Geology, 29: 49-58.

16. ISRM. (1978). “Suggested methods for determining tensile strength of rock materials”. International Journal Rock Mechanics and Mining Sciences & Geomechanics Abstracts, 15(3), 99–103. DOI:10.1016/0148-9062(78)90003-7.

17. Chen, C.S., Pan, E. and Amadei, B. (1998). “Determination of deformability and tensile strength of anisotropic rock using Brazilian tests”. International Journal of Rock Mechanics and Mining Sciences, 35(1), 43-61.

18. Li, D. and Wong, L.N.Y. (2013). “The Brazilian Disc Test for rock Mechanics Applications: Review and New Insights”. Rock mechanics and rock engineering, 46(2): 269-287.

19. Perras, M.A. and Diederichs, M.S. (2014). “A Review of the Tensile Strength of Rock: Concepts and Testing”, Geotechnical and geological engineering, 32(2): 525-546.

20. Abugharara, A. N., Hurich, C. A., Molgaard, J., and Butt, S. D. (2017). “Implementation of Circular Wave Measurements and Multiple Drilling Parameter Analysis in Rock Isotropy Evaluation”, the 36th International Conference on Ocean, Offshore and Arctic Engineering, held in Trondheim, Norway. Paper No.: OMAE2017-62088.

21. Abugharara, A. N., Alwaar, M. A., Hurich, A. C., and Butt, S.D., (2016), "Laboratory Investigation on Directional Drilling Performance in Isotropic and Anisotropic Rocks," the 50th US Rock mechanics / Geomechanics Symposium, American Rock Mechanics Association, held in Houston, TX, USA. Paper No.: ARMA-2016-868.

22. Abugharara, A. N., Alwaar, A. M., Butt, S. D., and Hurich, C. A. (2016). "Baseline Development on Rock Anisotropy Investigation Utilizing Empirical Relationships Between Oriented Physical and Mechanical Measurement and Drilling Performance," The 35th International Conference on Ocean, Offshore and Arctic Engineering, Drilling Symposium, Busan, South Korea. Paper No. OMAE2016-5514.

23. ASTM International. ASTM D5731. (2016). "Standard Test Method for Determination of the Point Load Strength Index of Rock and Application to Rock Strength Classifications". West Conshohocken, PA; ASTM International, 2016.

24. Tsidzi, K. E. N. (1997). "Propagation characteristics of ultrasonic waves in foliated rocks. *Bulletin of the International Association of Engineering Geology*, (56), 103-114..

25. Saroglou, H. and Tsiambaos, G. (2007). "Classification of Anisotropic Rocks," In 11th Congress of the International Society for Rock Mechanics, In: Ribeiro e Sousa, Otalla, Grossmann, editors. Taylor & Francis Group, London, 1: 191-196.

26. ISRM. (1981). "Rock characterization testing and monitoring," ISRM Suggested methods, Brown E.T. (ed.), Pergamon Press, Oxford.

27. ISRM (1985). "Suggested method for determining point load strength". International Journal of Rock Mechanics and Mining Sciences and Geomechanical Abstract, 22(2), 51-60. 21)

28. Ramamurthy, T. (1993). “Strength and Modulus Responses of Anisotropic Rocks,” Comprehensive Rock Engineering, Pergamon Press, Oxford, 1: 313-329.

29. Bieniawski Z. T. (1975). “Point load test in geotechnical practice,” Engineering Geology, 9(1), 1-11.

30. Hawkins, A. B., Olver, J. A. G. (1986). “Point Load Tests: Correlation Factor and Contractual Use, An Example from the Corallian at Weymouth. In: Hawkins, A.B. (Ed.), Site Investigation Practice: Assessing BS 5930,” Geological Society, London, 269-271.

31. Vallejo, L. E., Welsh, R. A., Robinson, M. K. (1989). “Correlation between Unconfined Compressive and Point Load Strength for Appalachian Rocks,” Proceeding of 30th US Symposium on Rock Mechanics, Morgantown, 461-468.

32. Das, B. M. (1985). “Evaluation of the point load strength for soft rock classification, Proceedings of the fourth international conference ground control in mining,” Morgantown, WV, 220-226.

33. Smith, H. J. (1997). “The Point Load Test for Weak Rock in Dredging Applications,” International Journal of Rock Mechanics and Mining Sciences, 34, 295, 3-4.

34. Altindag, R. and Guney, A. (2010). “Predicting the Relationships between Brittleness and Mechanical Properties (UCS, TS and SH) of Rocks,” Scientific Research and Essays", 5(16): pp.2107-2118.

35. Abugharara, A. N, Alwaar, A., C Hurich, J Molgaard, SD Butt. (2019). “PFC-2D” Numerical Study of the Influence of Passive Vibration Assisted Rotary Drilling (pVARD) Tool On Drilling Performance Enhancement,” Submitted to Journal of Energy Resources Technology, under review.

36. Abugharara, A. N., Molgaard, J., Hurich, C. A., and Butt, S. D. (2019) “Study of the Relationship between Oriented Downhole Dynamic Weight on Bit and Drilling parameters in Coring Isotropic Natural and Synthetic Rocks,” accepted for proceedings of the ASME 38th International Conference on Ocean, Offshore and Arctic Engineering, will be held in Glasgow, Scotland, UK. Paper No.: OMAE2019-96176.

37. Abugharara, A. N., Molgaard, J., Hurich, C. A., and Butt, S. D. (2019). “Study of The Influence of Controlled Axial Oscillations of pVARD on Generating Downhole Dynamic WOB and Improving Coring and Drilling Performance in Shale,” accepted for proceedings of the ASME 38th International Conference on Ocean, Offshore and Arctic Engineering, will be held in Glasgow, Scotland, UK. Paper No.: OMAE2019-96189.

CHAPTER 10: CONCLUSIONS

10.1 Summary

The work of this dissertation involved a comprehensive research of study of rock isotropy /anisotropy evaluation, (ii) study of the influence of rock anisotropy of shale on drilling performance, and (iii) study of the influence of the induced axial oscillations by the newly developed pVARD on drilling performance. This three-unit research focused on investigating how rocks, classified as isotropy / anisotropy, and the induced axial oscillations can influence directional drilling performance? In terms of rock isotropy / anisotropy evaluation, a comprehensive procedure was developed and tested that involved several newly developed and proposed interlinked techniques to measure the oriented physical and mechanical properties of rocks as well as different drilling systems of compliant and non-compliant.

The influence of shale anisotropy on directional drilling performance was intensively studies in this thesis through a comprehensive research that involved synthetic and natural isotropic rocks (RLM, fine-grained granite and fine-grained sandstone) and vertically transverse isotropic rocks (shale).

The study of the influence of the induced axial oscillations on drilling and coring performance was conducted through involving (i) the newly developed pVARD, as a compliant drilling system and (ii) the DDWOB.

Results showed (i) a reliable developed procedure for rock isotropy / anisotropy evaluation, through which good agreements of tests and measurements were found, (ii) directionally dependent rock properties (i.e. strength anisotropy) were found to be highly influencing the directional drilling performance as well as the main drilling parameters: DOC, rpm, and TRQ when compared to directional drilling in isotropic rocks, and (iii) axially induced oscillations by pVARD with the consideration of DDWOB found to be improving drilling and coring performance through increasing ROP.

The details of the seven research areas in this dissertation are provided in chapters 3, 4, 5, 6, 7, 8, and 9. These research areas are commented on as follows:

10.2 Concluding Remarks

Chapter 3 reports on developing a baseline procedure for rock isotropy / anisotropy evaluation that can be used as a base for the next projects research. The work of this chapter involved oriented physical measurements: VP and VS, mechanical measurements: strength obtained from various tests, and oriented drilling performance experiments: mainly ROP. The tests used mainly synthetic specimens of RLM produced at the Drilling Technology Laboratory and adopted some of the published anisotropy indices for the physical and some of the strength tests. The work of this chapter showed the practical potential for developing a baseline procedure that can be broadened to include more tests and can be tested on other rock types.

Chapter 4 reports on supporting the baseline procedure developed in Ch. 3. by (i) involving more rocks (granite and shale), (2) expanding the range of VP and VS to be circular measurements on RLM and newly involved rocks, and (iii) calculating the RLM and granite oriented stiffness matrices, after determining their isotropy. The reason for including more rocks was to validate, calibrate, and test the developed procedure by conducting more measurements on more rocks of various types, as well as to prepare for the next research through initial and basic involvement of shale in this chapter. The work of this chapter provided confirmations on the isotropy of fine-grained granite and RLM. It also provided initial data for the vertically transvers isotropy of shale, which required more tests and focus in the next chapters.

Chapter 5 reports an investigation for more confirmation of isotropy of RLM and vertically transverse isotropy of shale by involving more of physical, mechanical, and drilling tests. For the physical measurements, calculations of the oriented dynamic elastic moduli were involved that included: compressional wave modulus, shear wave modulus, rigidity modulus, Poisson's ratio, bulk modulus, young's modulus, and Lame's constant. Also, the VTI of shale was confirmed more in this chapter through multi-measurements of VP and VS parallel to shale beddings. For the mechanical measurements, indirect tensile test was involved for mode data provision for RLM isotropy, and mono-direction (perpendicular to shale bedding) point load index test was performed for shale strength estimation. For the drilling measurements, oriented drilling performance (ROP) was measured for drilling in RLM and shale, however, this drilling was to investigate the differences between shale and RLM through directional drilling performance as well as through

the oriented cutting size analysis. This chapter provided more data on isotropy of RLM and VTI of shale through newly involved physical, mechanical, and drilling measurements.

Chapter 6 reports an investigation of the influence of shale anisotropy on directional drilling performance. After determining shale as VTI through circular wave velocities and its anisotropy through different responses in drilling performance and cutting size analysis than that of RLM, a set of research was carried to focus on the influence of shale anisotropy on drilling performance with the inclusion of main drilling parameters with representation of field direction drilling scenarios. Relationships were drawn between the inclination of the shale anisotropy and the main drilling parameters that were involved that included ROP, DOC, rpm, and TRQ and shale anisotropy as a function of the applied WOB. Prior to conducting the non-compliant drilling experiments, a three-point strength anisotropy curve was developed using published data in the literature, based on which the relationships between shale anisotropy orientations and main drilling parameters were investigated. The research of this work showed that there was high influence of shale anisotropy on drilling performance and the main drilling parameters as a function of the static WOB and the anisotropy orientation. ROP was found to be the highest in the direction of incline drilling, where the angle between the drilling direction and the shale bedding plane was 45 degrees and was low in the vertical (perpendicular to shale bedding) and the horizontal (parallel to shale bedding) directions. DOC was found to be directly proportion, rpm reversely proportion, and TRQ directly proportion with ROP as a function of static WOB and shale anisotropy orientation.

Chapter 7 reports a study of the influence pVARD on improving mono-direction drilling performance. pVARD, as a newly developed tool that induces controllable axial oscillations, was tested in the laboratory in drilling RLM samples, in field trials in drilling three wells of various types of shale formations, as well as was numerically simulated using PFC-2D simulation. pVARD was firstly tested in the laboratory have three different configuration with different compliant levels: low compliant with low, medium, and high compliances, which all were tested against the rigid drilling system (with no induced axial oscillations) under various conditions of various water flow rates and bottomhole pressures as a function of static WOB. In the three testing environments (laboratory, field, and simulation) pVARD was found to have ROP higher than that of rigid drilling in in all pVARD configurations and under all conditions. However, the performance of pVARD was found to vary between its three configurations. Moreover, PFC-2D was successfully used to simulate the laboratory and field drilling using pVARD vs. rigid drilling. The work of this chapter showed the influence of pVARD on enhancing ROP, which opened a window of research of the next chapters to investigate the mechanism behind such influence (Ch. 8.) and the potential inclusion of pVARD in the rock isotropy / anisotropy evaluation procedure (Ch. 9.)

Chapter 8 reports a study of the influence of the induced axial oscillations of by pVARD on DDWOB and that improves coring and drilling performance in shale. This research involved the dynamic WOB that was recorded by the load cell fixed beneath the sample holder in drilling parallel to shale bedding using both systems: pVARD and rigid. Shale was also tested through coring using impregnated diamond coring bit perpendicular to shale bedding. Both of shale drilling and coring experiments were repeated several times at the same input parameters of flow rates,

applied static weight, and rpm. Results showed higher DDWOB recorded during coring and drilling in shale using pVARD than that of rigid coring and drilling, which resulted in increasing ROP. Another outcome of this research was that the DDWOB was found to be more stable and balanced when using pVARD than that when using rigid, which could have led to the DDWOB to be more effective in pVARD than that of rigid.

Chapter 9 reports a study of a comprehensive laboratory procedure for isotropy / anisotropy evaluation using fine-grained sandstone. The work of this chapter was an advanced research of the initial baseline procedure developed in (Ch. 3.) The work of this chapter involved more tests that were conducted on samples that were cored and prepared in a newly developed methodology. Samples of all tests were produced, uniquely from the same block, which made them more representative of the source rock (the block). For the first time, the multidirectional orientation was included in the indirect tensile test for the oriented strength determination. Oriented strength correlations were also studied to support the isotropy / anisotropy evaluation procedure. For the oriented drilling performance, pVARD drilling was included in the study with comparison to rigid drilling as a function of the DDWOB. The research of this chapter provided a procedure of a chain of tests and measurements that collectively supported the proposed isotropy / anisotropy evaluation procedure.

10.3 Dissertation Highlights and Contributions

10.3.1 Rock isotropy / anisotropy classification procedure

1) All physical, mechanical, and drilling tests were found to have good agreements in supporting rock isotropy / anisotropy evaluation.

2) From the stage of the baseline to the stage of the comprehensive procedure, it was found that the more tests included in the procedure, the stronger the evaluation can be.

3) This proposed procedure shows the connectivity between the involved tests in supporting one another and enriching the evaluation procedure.

10.3.2 Influence of rock anisotropy on drilling performance

1) Strength anisotropy curve was developed as a single-factor relationship, based on which trends of drilling ROP, DOC, rpm, and TRQ were constructed.

2) With the advancement of well control equipment and tools, shale anisotropy orientation was found to have a positive influence on directional drilling performance.

3) As a single-factor relationship, shale strength anisotropy was found to be one of the main influencing reasons to have a higher ROP in the oblique drilling and lower ROP in the vertical and horizontal drilling in shale under the atmospheric pressure.

10.3.3 Influence of induced axial oscillations on enhancing drilling performance

1) pVARD has a significant role in increasing the effectiveness of the DDWOB and, therefore improving drilling performance.

2) pVARD found to increase both, the drilling and the coring performance comparing to the non-compliant system.

3) When including devices of well-trajectory-control and well-deviation prevention, the induced controllable and non-destructive axial oscillations play an important role in improving the downhole drilling conditions and enhancing the drilling and coring ROP.

10.4 Recommendations for Future Work

1) As properties of synthetic rock changes with time (i.e. strength increases), pre-determination of properties prior to each experimental set is recommended to conduct.

2) Due to the fragileness of shale, it is recommended to confine shale samples with cement before drilling. The smaller the shale samples are the more needed to have the samples confined with cement.

3) Due to that every machine has its own operating conditions and mechanical specifications, it is recommended to have a full set of research and experiments to be conducted on the same machine.

4) It is recommended to include more rock types to enrich the research and validate the proposed procedures.

5) It is recommended to conduct the tests of the proposed procedure under various conditions of pressure, loading rates, etc.

6) For all oriented tests involved in the proposed isotropy / anisotropy procedure, samples should be produced from one block for the real formation representation, when using mono-rock-type.

10.5 Research limitations

1) When conducting strength tests in research of this thesis, the point load index was the main used apparatus. The loading rate was hand-controlled, and it is expected that data be more precise when using a constant loading rate apparatus.

2) In the comprehensive laboratory procedure for the isotropy / anisotropy evaluation, although some tests were performed on various types of rocks at different times and stages in various chapters, but only a fine-grained sandstone block was used at the final stage that turned out to be isotropic. It can be more useful when the same set of the procedure applied on other blocks of a well-determined VTI shale block that contained oblivious bedding structure.

APPENDICES

APPENDIX 1: STUDY OF THE INFLUENCE OF SHALE ANISOTROPY ORIENTATION ON DIRECTIONAL DRILLING PERFORMANCE IN SHALE

Proceedings of the ASME 2017 36th International Conference on Ocean, Offshore and Arctic Engineering
OMAE2017
June 25-30, 2017, Trondheim, Norway

OMAE2017-62071

STUDY OF THE INFLUENCE OF SHALE ANISOTROPY ORIENTATION ON DIRECTIONAL DRILLING PERFORMANCE IN SHALE

Abdelsalam N. Abugharara[1], Charles A. Hurich[2], John Molgaard[3], and Stephen D. Butt[1]

[1] Faculty of Engineering and Applied Science
Department of Process Engineering
Memorial University of Newfoundland
St. John's, Newfoundland and Labrador,
Canada

[2] Faculty of Science – Earth Sciences
Memorial University of Newfoundland
St. John's, Newfoundland and Labrador,
Canada

[3] Faculty of Engineering and Applied Science
Department of Mechanical Engineering
Memorial University of Newfoundland
St. John's, Newfoundland and Labrador,
Canada

ABSTRACT

The influence of shale anisotropy orientation on shale drilling performance has been studied using a new laboratory procedure. This procedure includes drilling and testing three sets of shale samples in different orientations from a single rock sample. Shale samples of different types were collected from outcrops located at Conception Bay South (CBS) in Newfoundland, Canada. For predrilling tests, oriented physical and mechanical measurements on each type of shale were conducted on the same rocks that will be drilled later. For drilling tests, three sets of tests were conducted. Each set was in a different orientation, corresponding to those in the physical and mechanical measurements. Each set was conducted under the same drilling parameters of pressure, flow rate (FR), and weight on bit (WOB) using a fully instrumented laboratory scale drilling rig. Two different types of drill bits were used, including a 35 mm dual cutter PDC bit and a 25.4 mm diamond coring bit. The drilling data was analyzed by constructing relationships between drilling rate of penetration (ROP) versus orientation (i.e. 0˚, 45˚, or 90˚). The analysis also included relationships between WOB and bit cutter Depth of Cut (DOC), Revolution Per Minute (RPM), and Torque (TRQ). All the above relations were evaluated as a function of shale bedding orientation. This evaluation can assist in understanding the influence of shale anisotropy on oriented drilling. Details of the conducted tests and results are reported.

INTRODUCTION

Challenges faced when drilling shale (i.e. well deviations influenced by shale anisotropy and well control solutions) [1-5], the importance of increasing shale gas and oil production through shale Hydraulic Fracturing (HF), and shale horizontal drilling positive impacts [6] all raise the demand for laboratory research on shale.

The oriented measurements of the physical and mechanical properties of shale are some of the main laboratory research areas and topics of interest being investigated by many research institutes, including but not limited to, Chevron Energy Technology Co., ExxonMobil Upstream Research and Development companies, NTNU and SINTEF Petroleum Research, Statoil, and the Department of Physics at the University of Alberta.

In addition to the oriented measurements of the shale physical and mechanical properties, the Drilling Technology Laboratory at Memorial University of Newfoundland and Labrador (DTL-MUN) - Canada performed experimental studies evaluating the oriented drilling performance in isotropic and anisotropic rocks. This evaluation was supported by studies of oriented physical and mechanical measurements of same rocks [17, 22, 29].

There are many influences on the strength of rocks in general and on shale more specifically. Some of these influences include the content of mineral types and inner structures (i.e. fractures, bedding, porosity, permeability, grain sizes and distributions, etc.) and the contained mineral properties, and mineral compositions [7-10].

The properties of shale are influenced mainly by the special inner bedding structure, clay content, and compaction magnitude of the shale layers.

The shale physical properties can be determined by measuring the velocities of compressional and shear waves (VP and VS, respectively) and the shale mechanical properties can be

determined by measuring the strength of shale. More specifically, the oriented shale physical and mechanical properties can be determined by measuring the velocities of VP, VS, and the strength, respectively in the corresponding direction relative to the selected drilling orientation.

The mechanical characteristics of shale have two main strength patterns. The first pattern is the shear fracture pattern, which occurs as a result of the uniaxial and triaxle compressive strength tests (referred to as UCS and CCS, respectively). The second pattern is the shale tensile strength pattern, which occurs as a result of the tensile tests [11–19].

Shale drilling applications is another research topic of interest. This involves an implementation of laboratory physical and mechanical properties under simulated conditions for drilling evaluation. It also links the laboratory-determined shale fracturing patterns (i.e. tensile fracturing) to shale HF applications [6, 20, 21].

DTL-MUN has been conducting research that evaluates shale drilling techniques, using different drill bit types under different conditions of flow rates as a function of shale bedding inclinations [17, 22]. This research, which this paper is part of investigates the oriented shale drilling performance in relation to other important drilling parameters including RPM, DOC, and Torque.

SAMPLE PREPARATION

Samples of two types of shales (red shale and green shale) were prepared for tests including mainly physical and drilling tests. The mechanical data representing the shale strength variations with shale bedding inclinations were collected from the literature review for comparison purposes and for evaluation of the experimental data included in this paper. The shale samples were cored parallel to the shale layers to determine the VP and VS. Cores of 50.8 mm, 88.9 mm and 101.6 mm were obtained using diamond coring bits. As challenges were encountered in shale coring due to the weakness of shale, a procedure was developed to assist in shale coring. Shale rocks were cut into cubes by a diamond saw. They were then cast in cement after determining and marking the shale bedding orientations. Lastly, a diamond coring bit of the desirable diameter was used to core shale samples. It was determined that coring parallel to shale bedding was more successful for retrieving good and intact cores. This was because of a wider surface contact between the layers, which provided more resistance in splitting the layers. Figure 1 shows some of the obtained cores of red shale in different diameters. All cores were cored parallel to the shale bedding. For drilling experiments, leaving the cubed shale samples cast in cement to be drilled later is sufficient for drilling tests under atmospheric pressure. Figure 2 shows samples of green shale after drilling one-hole parallel to bedding using PDC bit (top-right) and one red shale sample after drilling multiple holes. Each hole was in a different orientation using a 25.4 mm coring bit (bottom). Applying drilling tests using a coring bit did not require shale samples to be cast with cement due to that the coring bit transmits less lateral force to the layers that may cause damage and sample splitting, as it is the case in drilling using a PDC bit.

FIGURE 1.RED SHALE CORES IN DIFFERENT DIAMETERS. ALL SAMPLES ARE CORED PARALLEL TO THE SHALE BEDDING.

FIGURE 2. GREEN SHALE SAMPLE CAST AND DRILLED PARALLEL TO BEDDING USING 35 MM PDC BIT (TOP RIGHT). RED SHALE SAMPLE READY TO BE DRILLED (BOTTOM LEFT) AND RED SHALE SAMPLE DRILLED IN DIFFERENT ORIENTATIONS USING 25.4 MM DIAMOND CORING BIT (BOTTOM RIGHT)

CONDUCTED TESTS

Ultrasonic measurements

The Ultrasonic velocity measurements were performed to measure VP and VS. The equipment included TDS 1002B two channel digital storage Oscilloscope, square wave Pulser/Receiver Model 5077PR, and two Panametrics shear-

wave sensors. Shear wave coupling was used to ensure complete contact between sensors and the surface of the tested rock samples. Figure 3 shows the apparatus for this test.

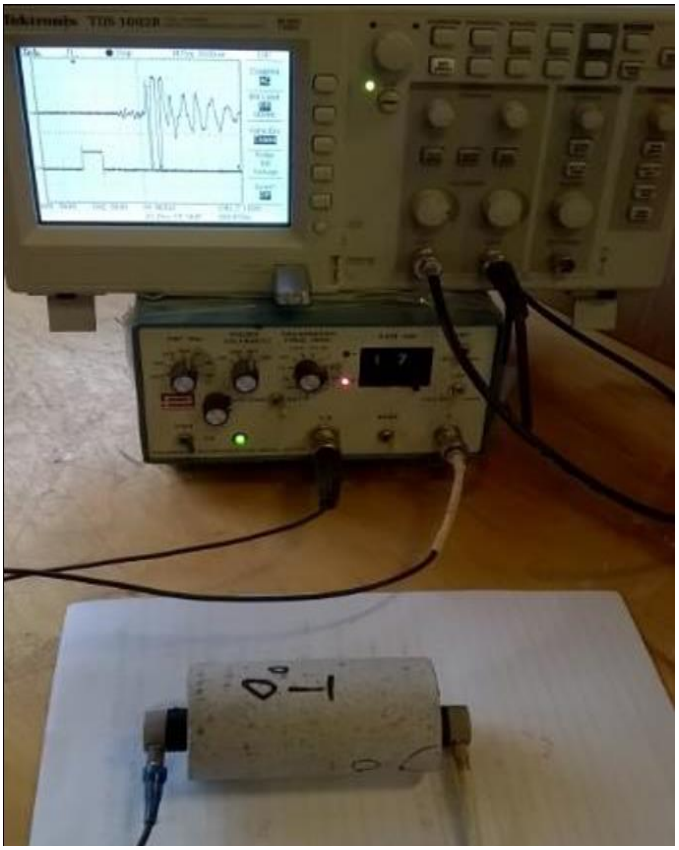

FIGURE 3. ULTRASONIC APPARATUS. AFTER (ABUGHARARA ET AL., 2016) [22].

The target of this study is a deeper characterization of shale (as VTI rocks) in a circular pattern, to obtain relationships between oriented physical and mechanical properties and shale drilling performance in the corresponding orientations, and to include more drilling parameters in the study.

The effect of shale bedding inclinations on the oriented shale physical measurement can be evaluated by VP and VS measured in different orientations. The effect of shale bedding inclinations on the shale oriented mechanical properties can be evaluated by strength tests conducted in different orientations. In this paper, the effect of shale bedding orientations on drilling performance is evaluated. This evaluation included a study of the variation of the oriented ROP, DOC, and Torque (see section on drilling tests).

VP and VS in all rock types tested in this paper were measured through 360° as circular VP and VS measurements, with increments of 45°. Samples of RLM, on which VP and VS measurements were conducted are shown in Fig 4.

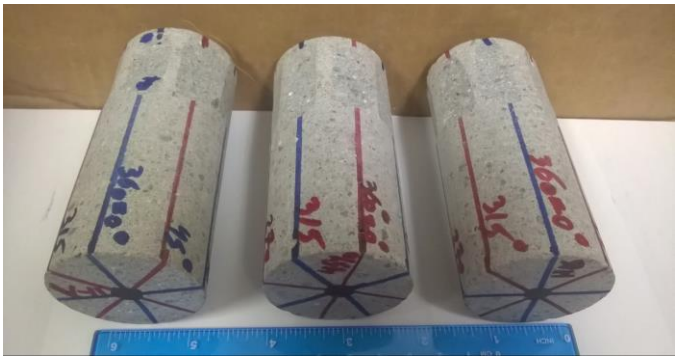

FIGURE 4. THREE RLM SAMPLES CORED IN THREE DIFFERENT ORIENTATIONS. EACH SAMPLE HAS PREPARED POSITIONS AT THE TOP ENDS FOR FULL CIRCULAR VP AND VS MEASUREMENTS

Figure 5 shows the circular VP and VS obtained from RLM, confirming in a full circle what was confirmed in one quarter of a circle of RLM by Abugharara et al., 2016 [17]. Figure 5, also shows measurements conducted on one RLM sample that are shown in Fig. 4.

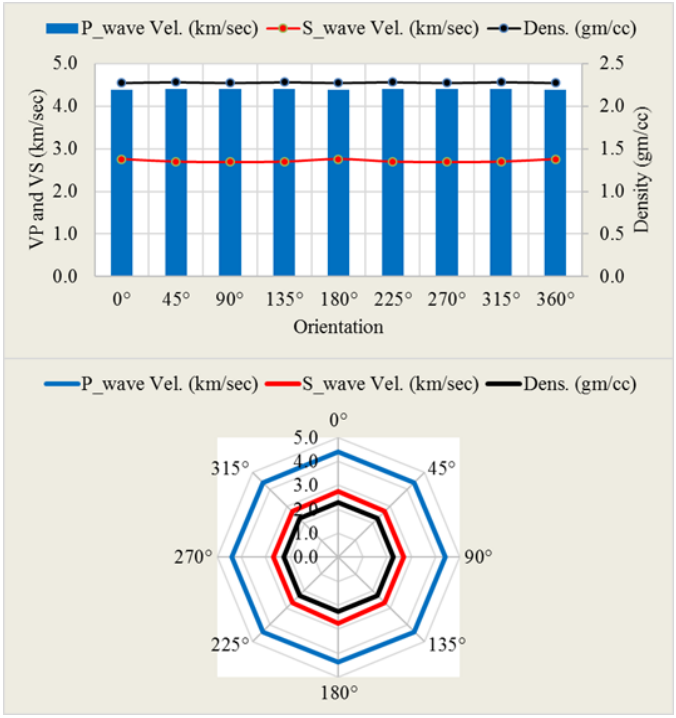

FIGURE 5. CIRCULAR VP AND VS MEASUREMENTSCONDUCTED ON ONE RLM SAMPLE SHOWN IN FIGURE 4.

Orthogonally oriented samples of granite with no visible preferred petro fabric were tested as a second example of an isotropic rock on the horizontal core and the vertical core as shown in Fig. 6, 7 and 8 respectively.

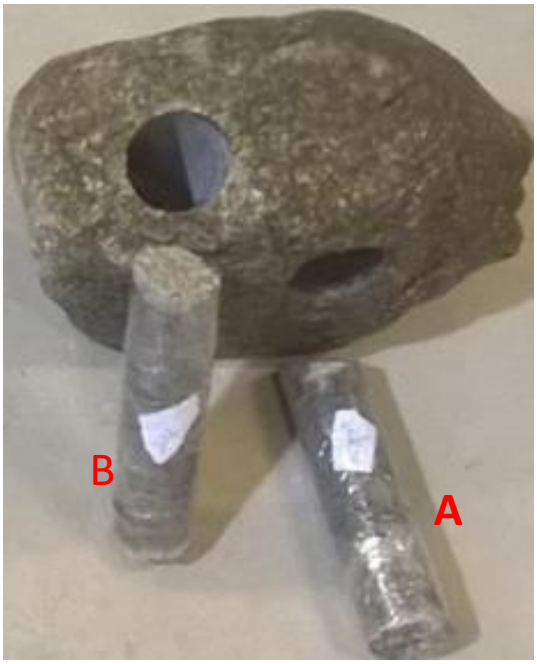

FIGURE 6. GRANITE ROCK WITH VERTICAL AND HORIZONTAL CORES.

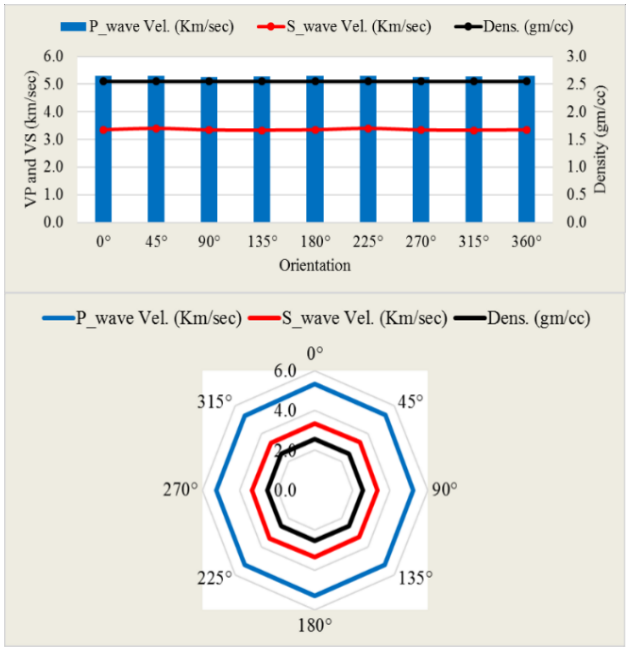

Figure 7. Circular VP and VS measurement conducted on cored granite sample # A as shown in Fig. 5.

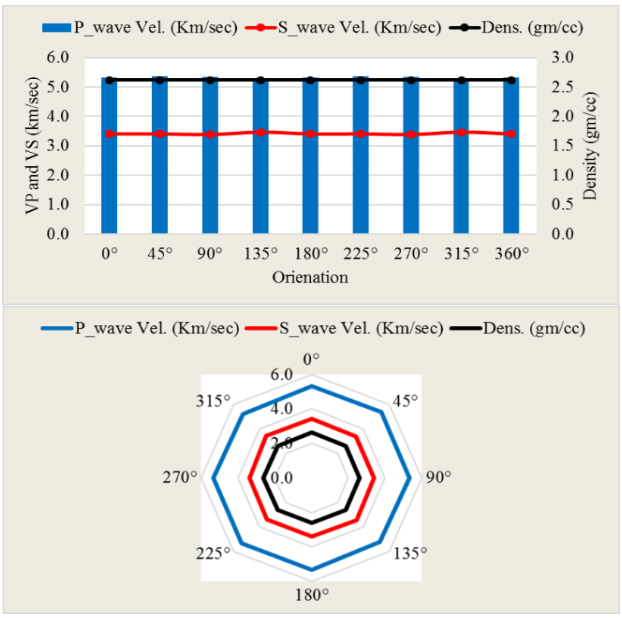

FIGURE 8. CIRCULAR VP AND VS MEASUREMENT CONDUCTED ON CORED GRANITE SAMPLE # B SHOWN IN FIG. 5.

Due to the bedding structure of red shale, a procedure for measuring the circular VP and VS as shown in Fig. 9 was adopted. Variations of the measured VP and VS as function of the shale bedding orientations was observed. The variations are induced by the rock inner structure. For shale, the layers act as different medias that affects the wave velocities propagating through. The higher the number of the layers the wave propagates through, the slower the velocity. For the same shale rock, the maximum number of layers is encountered when waves propagate perpendicular to layers, resulting in the minimum wave velocity. When waves propagate parallel to the layers, the wave velocity is the maximum. The wave velocity is medium when propagating at 45°.

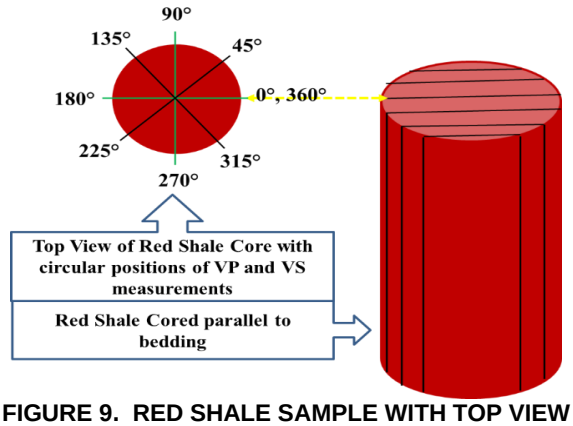

FIGURE 9. RED SHALE SAMPLE WITH TOP VIEW SHOWING VP AND VS MEASURING PROCEDURE.

Figure 10 shows the result of circular VP and VS measurement in red shale, which was cored horizontally following the measurement procedure shown in Fig. 9. The result shows the VTI of the tested red shale.

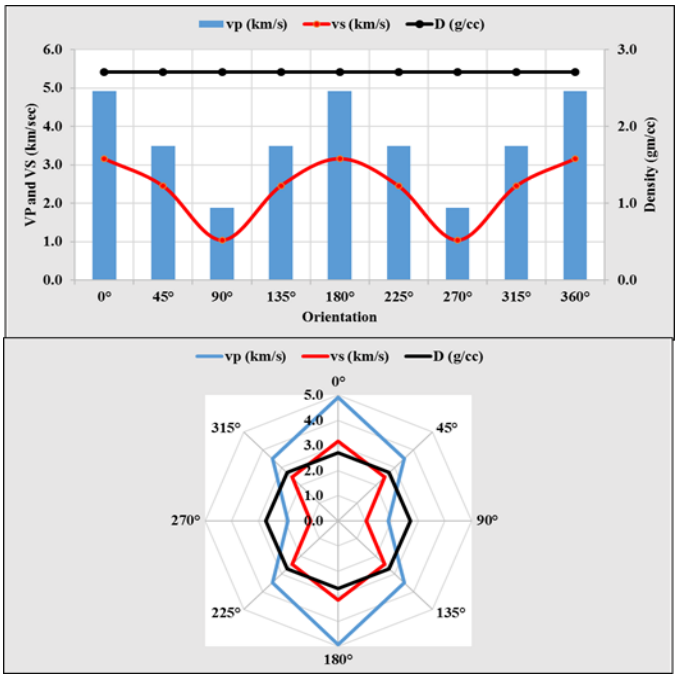

FIGURE 10. CIRCULAR VP AND VS MEASUREMENTS OBTAINED FROM ONE CORE OF RED SHALE.

Mechanical tests

The mechanical tests in this paper depended on shale strength estimation data that was collected from the literature review. A number of studies of laboratory research on shale strength investigation determination, and modelling have been conducted in many institutes and research centers as well as educational and research laboratories. Several papers report research investigating shale strength under confined compressive and unconfined compressive strengths (CCS and UCS, respectively) as well as shale tensile strength through the Indirect Tensile (IT) test and the Point Load Index (PLIT) test [11-19].

Shale strength was also estimated through empirical correlations supporting the shale strength pattern theory of the U-Strength curve [23-26].

Modelling of the shale strength using various models, including Plane of Weakness model, Patchy Weakness model, Bonded Particle model, and Smooth Joint model was also in agreement with the other shale strength methods [18, 19, 27, 28].

The significance of the collective work performed in the area of shale strength estimation through laboratory, field and modelling is that they all agreed with the pattern of shale strength depending on the performed test type, applied conditions, chosen loading rates, and selected tested rock orientations.

The pattern of shale strength in the CCS and the UCS tests leading to shear fracture mode is that the highest strength is at the orientations of 0° and 90° (perpendicular and parallel to shale bedding, respectively) and the lowest strength is in orientations between 30° and 60°. However, the pattern of shale strength in the IT test leading to tensile fracture mode has two reported modes. Generally, the strength is the lowest at 0° orientation (parallel to the bedding) and the highest at 90° orientation (perpendicular to the bedding) and the strength increases in between. [14, 18]. It was also reported that the IT has the lowest strength at about 15° orientation, where the other strengths at the other orientations follow the same pattern as the above. [15].

The implementation of both types of strength testing, mentioned above and the resulting patterns of rock failure modes (i.e. shear, tensile) in the area of drilling performance is analyzed as described in the following section.

Drilling tests

The drilling experiments were conducted on VTI red shale samples as they were conducted on Isotropic rock samples, including RLM and granite. The purpose of conducting drilling tests on RLM and granite was for comparison and validation of the oriented shale "σ - ROP" theory presented in this paper.

A fully instrumented laboratory scale rotary drilling rig was used for the drilling tests. Water flow rate of 5.6 l/min was used for removing the cutting, cleaning the hole, ensuring continues contact between rock and the drill bit and preventing non-productive time (NPT) spent on fracturing the cuttings into smaller pieces. Two different drill bits were used, including 25.4 mm diamond coring bit. It was used in the oriented drilling of RLM, granite, and red shale. The other drill bit was a 35 mm PDC bit for oriented drilling of green shale. Two different rotary speed settings were used, 300 and 600 rpm. However, the actual RPM, which was recorded varies somewhat depending on the torque involved. The drilling parameters measured by sensors connected to a DAQ System utilizing professional LabVIEW software included bit travel for drilling depth measurement, operational RPM, consumed current, and dynamic WOB. Drilling performance was then evaluated by constructing relationships between WOB vs. ROP, DOC, RPM, and Torque. This evaluation was performed on data recorded from drilling in different orientations in all three rock types, focusing primarily on drilling in shale.

The results of the oriented drilling tests conducted on green shale using the 35 mm PDC bit and flow rate of 18 l/min are shown in Fig. 11 to 15. Figure 11 shows WOB vs. ROP as a function of green shale bedding orientations. This figure confirms that ROP is significantly affected by the shale strength anisotropy due to shale bedding orientation. Figures 12 to 15

show the results of drilling parameters and their variations with respect to green shale bedding orientations in various WOB.

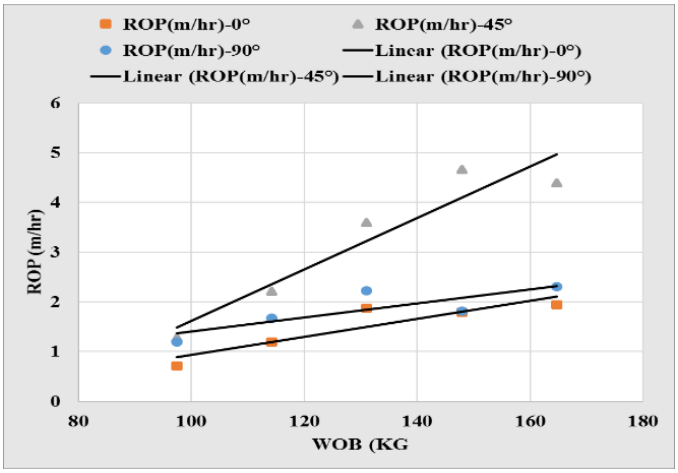

FIGURE 11. WOB VS. ROP IN GREEN SHALE AS FUNCTION OF BEDDING PLAN INCLINATION.

The drilling parameters included in this evaluation are DOC, RPM and Torque, respectively. The results of drilling in green shale show trends of ROP, DOC, RPM, and Torque that can be linked to the shale strength trend reported by authors mentioned in the section on mechanical tests. Figure 12, shows the relationship between WOB and ROP in three orientations of green shale. This relationship indicates higher ROP at 45°, where shale shear strength is low and lower ROP at 0° and 90°, where shale shear strength is high. In these drilling experiments in shale, the PDC bit advances in depth by cutting the rock in shear fracture. Figure 12 also shows the variations of ROP in drilling green shale as a function of the bedding inclinations. The variations were analyzed at the same WOB. Figure 13 shows the variations of the DOC in drilling green shale in three different orientations with different WOB. The variations of DOC have a trend that is directly proportional to the trend of ROP. This trend indicates that the ROP increases in parallel with increasing DOC. For drilling in any particular orientation, DOC increases with WOB in the orientation that has the same strength. Figure 14 shows the variations of RPM in drilling green shale in different orientations corresponding to different levels of WOB. In this figure, the RPM is having an opposite relationship to the ROP and DOC. Such opposite relationship can be explained as that increasing the DOC that leads to increasing the ROP provides an increasing resistance that leads to RPM reduction. However, the reduction of the RPM does not affect negatively the ROP, but it only indicates the involvement of higher resistance when the bit cutters get deeper into the formation as a result of increasing the DOC.

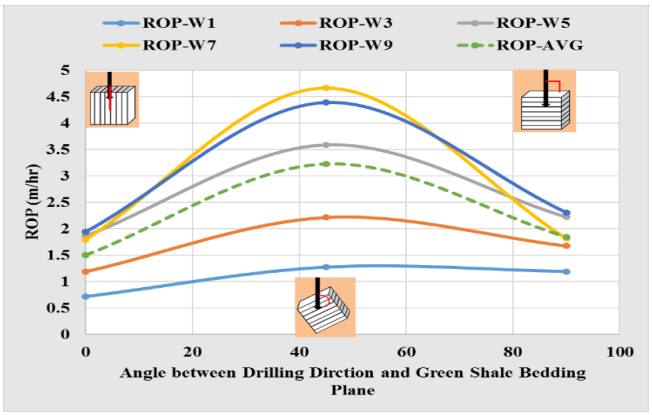

FIGURE 12. ROP VARIATION RESULTED FROM GREEN SHALE DRILLING IN DIFFERENT ORIENTATIONS.

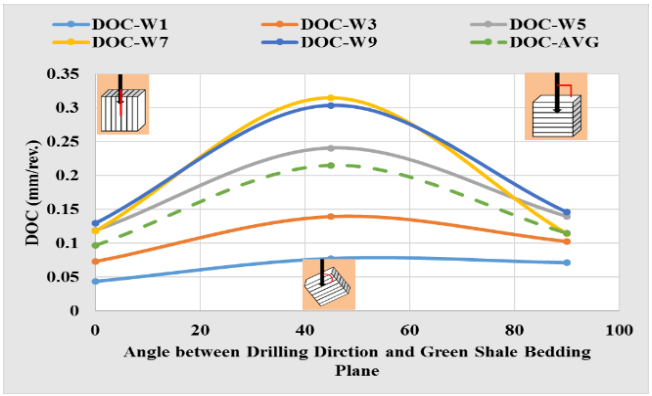

FIGURE 13. VARIATION OF DOC IN GREEN SHALE DRILLING IN DIFFERENT ORIENTATIONS.

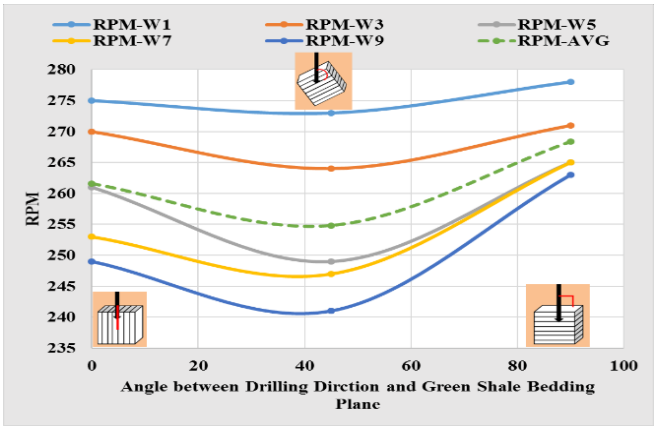

FIGURE 14. VARIATION OF RPM AS FUNCTION OF GREEN SHALE BEDDING PLAN INCLINATION.

Figure 15 shows variations of the torque resulted in drilling green shale in different orientations. The torque variations are analyzed in each level of WOB as WOB increases. The increasing of torque has a direct proportional relationship with

ROP and DOC, indicating that the higher DOC requires higher torque to increase ROP.

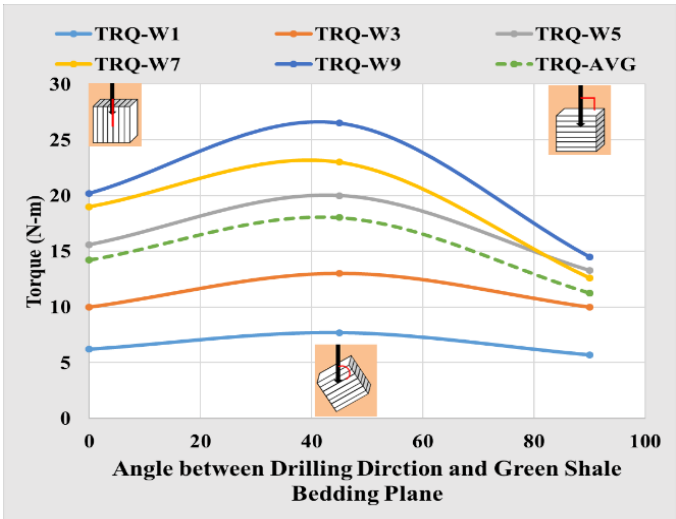

FIGURE 15. CALCULATED TORQUE IN DRILLING GREEN SHALE IN DIFFERENT ORIENTATIONS.

Figures 16 to 18 show the results of the oriented drilling tests in red shale utilizing flow rate of 5.6 l/min and using 25.4 mm diamond coring bit. These figures show smaller variations in ROP, DOC, and RPM than in figures 12 to 15 for green shale drilling using the 35 mm PDC bit. Although the variations are smaller, they follow the same trend as in Fig. 12 to 15. The variations that are shown in Fig. 12 to 18 indicate anisotropy of shale related to shale bedding.

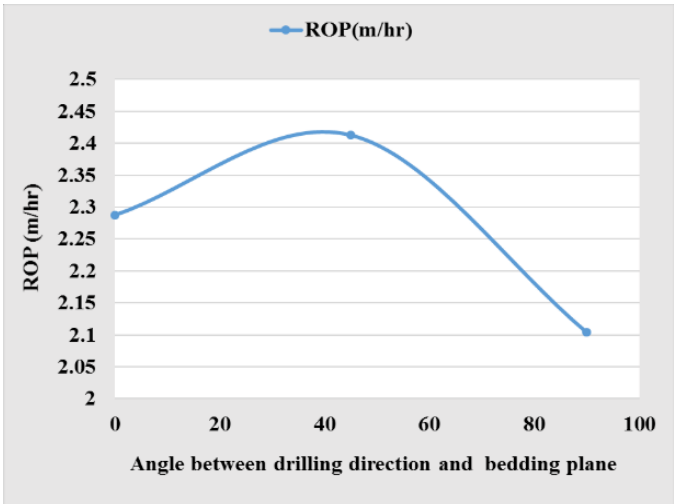

FIGURE 16. ROP VARIATION WITH RESPECT TO RED SHALE ORIENTATION AT DYN-WOB OF ~ 55 KG.

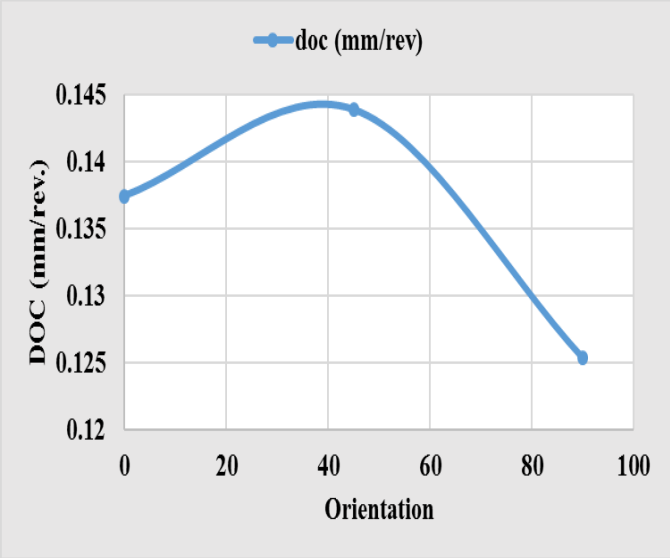

FIGURE 17. DOC VARIATION SHOWING HIGHER DOC AT 45°.

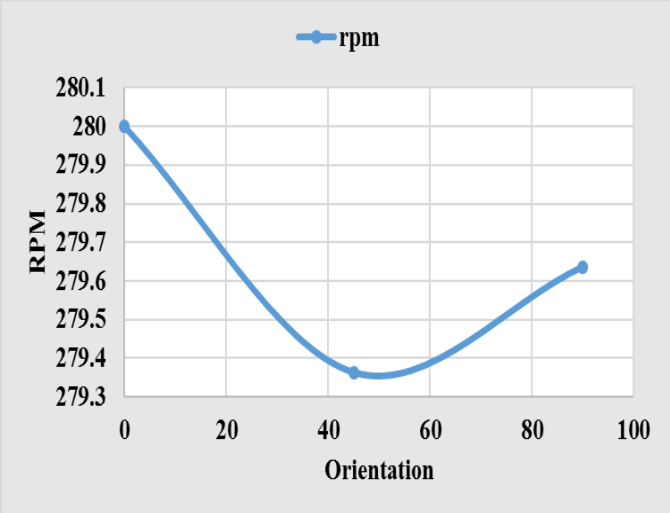

FIGURE 18. RPM VARIATION IN DRILLING RED SHALE IN DIFFERENT ORIENTATIONS.

For comparison purposes between isotropic and anisotropic rocks, Fig. 19 shows the results of DOC-AVG obtained from drilling an isotropic rock of RLM in different orientations corresponding to different levels of WOB. The results of this drilling parameter are in good agreement with the isotropy results obtained from the physical and mechanical tests illustrating the differences in drilling isotropic and anisotropic rocks (Abugharara, et al., 2017) [29].

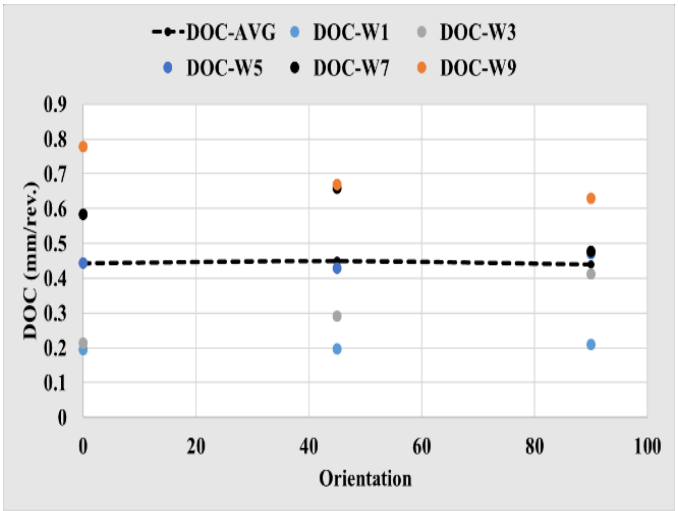

FIGURE 19. DOC AND AVERAGED DOC OBTAINED FROM DRILLING RLM IN DIFFERENT ORIENTATIONS.

SUMMARY

- A study of the effect of orientation with respect the bedding plane's inclination in red and green shale rocks was conducted.
- Circular VP and VS measurements in RLM and granite showed tested rock isotropy.
- Circular VP and VS measurements showed anisotropy of both shale types.
- Study of variations of ROP, DOC, RPM, and Torque in RLM and granite in drilling in different orientations showed isotropy in these tested rocks.
- Study of variations of ROP, DOC, RPM, and Torque in red and green shale resulted from drilling in different showed shale anisotropy.

FUTURE WORK

- Greater in-depth study of the shale drilling parameters in more other orientations under various conditions of flow rates, confining pressures and rotary speeds will be conducted and will be reported in future publications.
- Relationships between shale physical and mechanical properties under pressurized conditions will be constructed.
- Relationships between shale strength, shale drilling parameters as a function of shale bedding plane inclinations, and drilling performance, will be analyzed in more depth also under pressurized conditions.
- Analysis of the relationships above that will simulate shale shear and tensile fracturing during drilling operation and linking such relations to drill bit types and rock failure mode under various conditions of confining pressure, flow rates, and shale rock types will also be analyzed.

NOMENCLATURE

CBS	Conception Bay South
CCS	Confined Compressive Strength, MPa
DOC	Depth Of Cut, mm/rev.
FR	Flow Rate, l/min
IT	Indirect Tensile, MPa
MDP	Multiple Drilling Parameter
PDC	Polycrystalline Diamond Compact
PLIT	Point Load Index Test, MPa
RLM	Rock Like Material
ROP	Rate of Penetration, m/hr
RPM	Revolution Per Minute
TRQ	Torque, N-m
UCS	Unconfined Compressive Strength, MPa
VP	Primary or Compressional Wave Velocity, km/sec
VS	Secondary or Shear Wave Velocity, km/sec
VTI	Vertically Transverse Isotropy
WOB	Weight On Bit

ACKNOWLEDGEMENT

This work was done at the Drilling Laboratory Technology (DTL) at Memorial University of Newfoundland in St. John's, Canada. The project is funded by Atlantic Canada Opportunity Agency (AIF contract number: 781-2636-1920044), involving Husky Energy, Suncor Energy and Research and Development Corporation (RDC) of Newfoundland and Labrador. Financial support is also provided by the Ministry of Higher Education and Scientific Research, Libya. Special thanks to DTL members for their help in laboratory work, in particular Abdlsalam Ihmoudah and Bashir Alrujbani. Thanks are also sent to Peter Samaan.

REFERENCES

[1] McLamore, R. T., 1971, "The Role of Rock Strength Anisotropy in Natural Hole Deviation", Journal of Petroleum Technology, SPE-3229.

[2] Brown, E.T., Green, S. J., and Sinha, K. P., 1981, "The Influence of Rock Anisotropy on Hole Deviation in Rotary Drilling- A Review", International Journal of Rock Mechanics, Mining Sciences, and Geomechanics Abstracts, Vol. 18, pp.387- 401.

[3] Karfakis, M. G., and Evers, J. F., 1987, "Technical Note-Effects of Rock Lamination Anisotropy on Drilling Penetration and Deviation", International Journal of Rock Mechanics, Mining Sciences, and Geomechanics Abstracts, Vol. 24, No. 6, pp. 371-374.

[4] Boualleg, R., Sellami, H., and Menand, S., 2006, "Effect of Formations Anisotropy on Directional Tendencies of Drilling Systems" IADC/SPE Drilling Conference, Miami, Florida, USA, 21-23 February.

[5] Boualleg, R., Sellami, H., Rouabhi, A., and Menand, S., 2007, "Effect of Rock Anisotropy on Deviation Tendencies of Drilling Systems", 11TH Congress of the International Society for Rock Mechanics, Taylor and Francis Group, London.

[6] Maurice B. D., 2013, "Geomechanical Aspects of Shale Gas Development", Rock Mechanics for Energy and Environment-Tylor and Frances Group, London.

[7] Fjaer, E., Holt, R. M., Raaen, A. M., Risnes, R., and P. Horsrud, 2008, "Petroleum Related Rock Mechanics", (53), Elsevier.

[8] Chang, C., Zoback, M.D., and Khaksar, A., 2006, "Empirical Relations between Rock Strength and Physical Properties in Sedimentary Rocks", Journal of Petroleum Science and Engineering, 51(3), pp.223-237.

[9] Pan, R., Zhang, G., Li, S., An, F., Xing, Y., Xu, D., and Xie, R., 2016, "Influence of Mineral Compositions of Rocks on Mechanical Properties", the 50th us rock Mechanics / Geomechanics symposium, American rock mechanics association, Houston, TX, USA, 26-29 June 2016.

[10] Friedman, M., 1976, "Porosity, Permeability, and Rock Mechanics - A Review", the 7th US Symposium on Rock Mechanics. American Rock Mechanics Association.

[11] Ewy, R. T. and Bovberg, C. A., 2010, "Strength Anisotropy of Mudstones and Shales", the 44th US-Canada Rock Mechanics / Geomechanics Symposium, American Rock Mechanics Association, Salt Lake City, UT, June 27-30.

[12] Crawford, B.R., Dedontney, N. L., and Ottesen, S., 2012, "Shear Strength Anisotropy in Fine-Grained Rocks", the 46th US Rock Mechanics / Geomechanics Symposium, American Rock Mechanics Association, Chicago, IL, USA, 24-27 June.

[13] Holt, R. M., Nes, O.M., Stenebraten, J.F., and Fajaer, E., 2012, "Static Vs. Dynamic Behaviour of Shale", the 46th US Rock Mechanics / Geomechanics Symposium, American Rock Mechanics Association, Chicago, IL, USA, 24-27 June.

[14] Fjaer, E. and Nes, O. M., 2013, "Strength Anisotropy of Mancos Shale" the 47th US Rock Mechanics / Geomechanics Symposium, American Rock Mechanics Association, San Francisco, CA, USA, 23-26 June.

[15] Simpson, N. D. J., Stroisz, A., Bauer, A., Vervoort, A., and Holt, R.M., 2014, "Failure Mechanics of Anisotropic Shale during Brazilian Tests", the 48th US Rock Mechanics / Geomechanics Symposium, American Rock Mechanics Association, Minneapolis, MN, USA, 1-4 June.

[16] Holt, R.M., Bauer, A., Fjaer, A., Stenebraten, J. F., Szewczyk, D., and Horsrud, P., 2015, "Relating Static and Dynamic Mechanical Anisotropies of Shale", the 49th US Rock Mechanics / Geomechanics Symposium, Sanfrancisco, CA, USA, 28 June-1 July.

[17] Abugharara, A. N., Alwaar, M. A., Hurich, A. C., and Butt, S.D., 2016, "Laboratory Investigation on Directional Drilling Performance in Isotropic and Anisotropic Rocks." The 50th US Rock mechanics / Geomechanics Symposium, American Rock Mechanics Association, Houston, TX, USA, 26-29 June.

[18] Cho, J., Kim, H., Jeon, S., and Min, K., 2012, "Deformation and Strength Anisotropy of Asan, Gneiss, Boryeong Shale, and Yeoncheon Schist", International Journal of Rock Mechanics and Mining Sciences, (50), pp. 158-169, Elsevier.

[19] Park, B., and Min, K., 2013, "Discrete Element Modelling of Transversely Isotropic Rock", the 47th US Rock Mechanics / Geomechanics Symposium, American Rock Mechanics Association, San Francisco, CA, USA, 23-26 June.

[20] Nygaard, R., and Hareland, G., 2007, "Application of Rock Strength in Drilling Evaluation", SPE Latin American and Caribbean Petroleum Engineering Conference, Buenos Aires, Argentina, April, 15-19.

[21] Kerkar, P. B., Hareland, G., Fonseca, E. R., and Hackbarth, C. J., 2014, "Estimation of Rock Compressive Strength Using Downhole Weight-on-Bit and Drilling Models" International Petroleum Technology Conference, Doha, Qatar, January, 20-22.

[22] Abugharara, A. N., Alwaar, A. M., Butt, S. D., and Hurich, C. A., 2016, "Baseline Development on Rock Anisotropy Investigation Utilizing Empirical Relationships Between Oriented Physical and Mechanical Measurement and Drilling Performance", The 35th International Conference on Ocean, Offshore and Arctic Engineering, Drilling Symposium, June 19-24, Busan, South Korea.

[23] Horsrud, P., 2001, "Estimating Mechanical Properties of Shale from Empirical Correlations", Society of Petroleum Engineers, SPE Drilling and Completion.

[24] David, N. D., Joel, S., Claudio, D. P., Anthony, F. S., Mark, D. R., 2010, "Prediction of Shale Mechanical Properties from Global and Local Empirical Correlations", SEG Denver, Annual Meeting.

[25] Altindag, R., 2012, "Correlation between P-Wave Velocity and Some Mechanical Properties for Sedimentary Rocks", the Journal of the Southern African Institute of Mining and Metallurgy, 112(3), pp. 229-237.

[26] Mishra, D. A., and Basu, A., 2013, "Estimation of Uniaxial Compressive Strength of Rock Materials by Index Tests Using Regression Analysis and Fuzzy Inference System", Journal of Engineering Geology, (160), pp. 54-68, Elsevier.

[27] Fjaer, E., Stenebraten, J. F., Holt, R. M., Bauer, A., Horsrud, P., and Nes, O., 2014, "Modelling Strength Anisotropy", Rock Mechanics for Natural Resources and

Infrastructure, ISRM-Specialized Conference 9-13 September, Goiania, Brazil.

[28] Hamza, F., Chen, C., Gu, M., Quirein, J., Martysevich, V., and Matzar, L., 2015, "Characterization of Anisotopic Elastic Moduli and Stress for Unconventional Reservoirs Using Laboratory Static and Dynamic Geomechanical Data", SPE/CSUR Unconventional Resources Conference, Calgary, Alberta, Canada, October, 20-22.

[29] Abugharara, A. N., Hurich, C. A., Molgaard, J., and Butt, S. D., 2017, "Implementation of Circular Wave Measurements and Multi-Drilling Parameters' Analysis in Rock Isotropy Evaluation", Proceeding of the 36th International Conference on Ocean, Offshore and Arctic Engineering, drilling symposium, June 25-30, Trondheim, Norway.

APPENDIX 2: EXPERIMENTAL EVALUATION OF PASSIVE-VIBRATION ASSISTED ROTARY DRILLING (PVARD) TOOL TO ENHANCE DRILLING PERFORMANCE

ARMA 15-492

Experimental Evaluation of passive-Vibration Assisted Rotary Drilling (p-VARD) tool to Enhance Drilling Performance

Rana, P.S., Abugharara, A.N., Molgaard, J. and Butt, S.D.

Advance Drilling Laboratories (ADL), Memorial University of Newfoundland, St. John's, NL, Canada

This paper was prepared for presentation at the 49th US Rock Mechanics / Geomechanics Symposium held in San Francisco, CA, USA, 28 June-1 July 2015.

ABSTRACT: The passive-Vibration Assisted Rotary Drilling (p-VARD) technology was developed to enhance the drilling Rate of Penetration (ROP) for using Poly-crystalline Diamond Compact (PDC) drill bits by modulating the rock-bit interactions. A lab-scale p-VARD prototype was tested by drilling rock analogue fine-grained concrete samples with an Unconfined Compressive Strength (UCS) ~50 MPa. Results showed that within the operational range of the tool, defined by the range of WOB applied during drilling, ROP was consistently 50% or more greater as compared to conventional drilling without the p-VARD tool, as other drilling conditions being the same. A field-scale p-VARD prototype was developed and tested during field trials in September 2014. Evaluation of data from the field trials is ongoing; however, representative drilling results for drilling a red shale formation (with mechanical properties similar to the laboratory concrete material) showed similar results with ROP increased 50% to 100% when WOB was in the operational range of the tool.

1. INTRODUCTION

By studying Vibration Assisted Rotary Drilling (VARD), the Advance Drilling Laboratories (ADL) of Memorial University of Newfoundland aims to introduce technologies that provide higher penetration rates and greater economic values in the process of drilling. Vibrations are mostly considered undesirable in the field of drilling and efforts are done to mitigate them. Vibrations are linked to whirl, stick-slip and non-uniform dynamic loading, which cause damage to bits and down-hole equipment. The Institute of Technical Mechanics, Ukraine tested devices that work on the principle of cavitation. A two to three times increase in ROP was reported [1]. Another study was done on an Axial Oscillation Generator tool (AGT) and it was found that the AGT improves weight transfer to the bit and reduces torque on bit. Also it was found that it significantly reduces stick-slip [2]. National Oil-well Varco Down-hole Ltd. (NOV) developed a small scale vibration test-rig, to simulate stick-slip and study stick-slip mitigation methods. Axial friction reduction and axial load transfer can be achieved by introducing axial excitations in the oil-well, which results in an improvement in ROP and better Mechanical Specific Energy (MSE) [3]. Heng Li et al reported that the combined effect of vibrations and rotation increases the rate of penetration for a coring bit [4]; also ROP improvement was reported as a function of amplitude of vibrations. Babatunde et al studied the effect of vibration frequency on penetration rates using natural diamond drag bits. Here again VARD improved the penetration rates [5]. Both Heng Li et al and Babatunde et al used a shaker table under the sample as a source of vibrations. To further study the effect of vibrations on drilling performance, a prototype in-line tool (lab scale p-VARD tool) was designed and tested. Initial results were promising and significant increase in ROP using concrete specimens of medium strength was observed.

2. EXPERIMENTAL EQUIPMENT AND PROCEDURE

For lab scale testing of a p-VARD tool, an electrical powered, drilling setup was used. This drilling setup was used before and is described in detail by Khorshidian et al [6]. Figure1 shows the lab scale drilling setup displaying main parts and equipment including a laser triangulation sensor and p-VARD tool. The drilling system comprises of three units, a rotary system, fluid circulation system and suspended weight loading system. The rotary system consists of a Milwawkee motor with a maximum thrust and torque of 3500 N and 80 Nm, respectively, at 300 RPM and 40 Nm of torque at 600 RPM. For the circulation system a triplex pump with maximum flow rate of 150 L/min and maximum pressure of 6900 KPa was used. Weight on bit (WOB)

was applied using suspended weight and a rack and pinion arrangement.

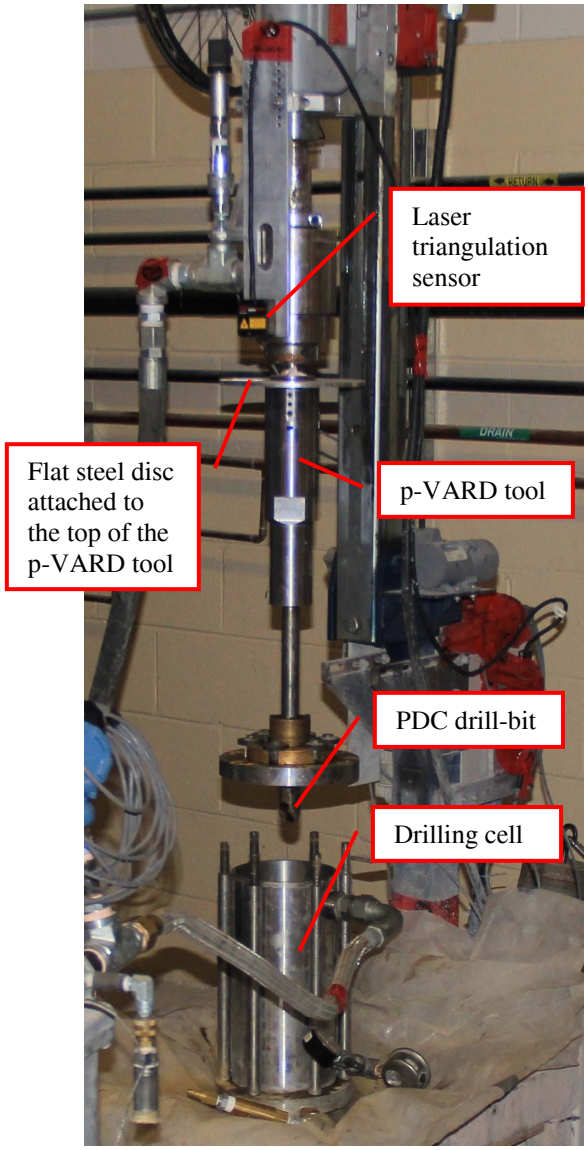

Figure: 1. Lab-scale drilling setup

To measure the axial displacement generated by the tool, a Micro-Epsilon laser triangulation sensor was used. A polished flat disc of steel was attached to the tool (shown in figure 1). Three groves were machined. The Sensor was able to detect and precisely record relative motion of tool and drill-string. Also on each revolution three peaks of signal were recorded, corresponding to three machined groves. This way the Revolutions per Minute (RPM) were recorded. Figure 2 shows the laser sensor recordings of axial displacement and RPM. Tests were performed at a rated RPM of 300. An average value of 280 RPM was recorded by the sensor. Figure 3 represents a comparison of average RPM recorded in conventional and with p-VARD drilling. A load cell was attached at the bottom of the drilling cell, to measure the dynamic Weight on Bit (WOB).

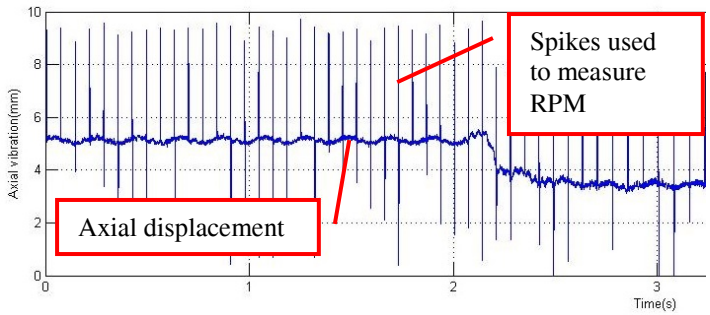

Figure: 2. Output of laser-triangulation sensor

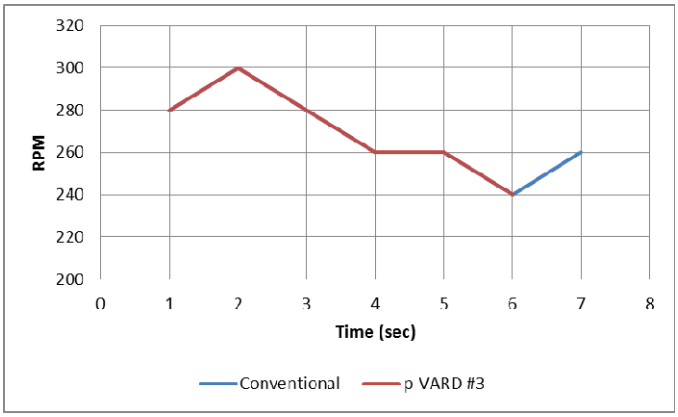

Figure: 3. Comparison of RPM over a course of drilling (both with and without p-VARD) at 173 Kg WOB and a flow-rate of 72 L/min

2.1 *Drill off Tests*

Drills off Tests (DOT) were performed at various flow rates. A founder point was not reached due to limitations of the drilling system used. A linear relationship was observed between ROP and WOB. Three p-VARD tool settings were tested against conventional drilling. The tested p-VARD settings were (a) high compliance setting (p-VARD #1), (b) medium compliance setting (p-VARD #2) and (c) low compliance setting (p-VARD #3). Figure 4 displays the disassembled lab-scale prototype of p-VARD.

A 35 mm two-cutter PDC drill-bit was used for the experiments. Details about nozzle configuration are provided by Khorshidian et al [6].

Previous tests indicated that an enhanced ROP is observed with the use of compliance. Based on these findings, a tool was developed that utilizes rock-bit interactions and generates axial vibrations, providing full rotary speed and torque to the drill-bit. The tool was designed to be installed directly above the drill bit. It has three sections; a compliant section (converts natural axial vibrations of drill-bit to axial displacements), a dampening section (absorbs the vibrations that can damage the Bottom Hole Assembly) and a torque transmitting unit.

The tool comprises of an inner hollow shaft and outer shell that provides relative motion between opposite ends of the tool; for transmitting torque key-ways are used. The compliance of the tool can be adjusted to different values.

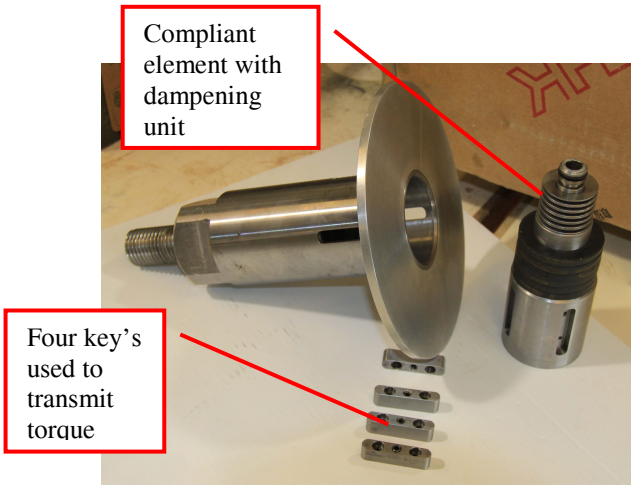

Figure: 4. Lab-scale prototype of p-VARD

2.2 Rock properties

For lab-scale testing, rock analogue concrete specimens were cast using water, Portland cement and fine grained rock aggregate. The ASTM D2938-95 standard was followed. To measure the rock strength Unconfined Compressive Strength (UCS) tests were conducted on 14 NQ (46mm) sized cored samples. ASTM Standards detailed in D5731-08, regarding the Point Load Index Test (PLIT) were followed for testing samples of natural rock collected from the site of the field trials. The type of rocks tested varied between sandstones, granite, red and grey shale. To test the abrasiveness of rock CERCHAR tests were performed; as per ASTM D7625-10. Acoustic Emission (AE) tests were performed to measure P and S wave velocities for the samples. Main obtained results of various elastic moduli and mechanical tests are shown in table 1.

Table: 1. Rock characterization

Rock type	Concrete	Red-shale
P-wave velocity (m/s)	4423	5154
S-wave velocity (m/s)	2448	3767
P-wave modulus (M) Gpa	44	72
S-wave modulus (G) Gpa	13	38
Elastic Modulus (E)Gpa	34	71
Bulk Modulus (K) Gpa	5	27
UCS (Mpa)	51	56
CAI	1.98	1.06

3. LAB EXPERIMENT RESULTS

Four main groups of tests with different drilling system compliance (i.e. conventional drilling, p-VARD #1, p-VARD #2 and p-VARD #3) were performed. Also, within each main group of system compliance, four different flow rates were used. Finally for each flow rate (i.e.16, 44, 72 and 100 L/min), five different WOB (i.e. 106, 139, 173, 207 and 240 kg) were applied.

Table: 2. Test matrix for lab tests with recorded ROP

Test Matrix (80 test runs in total)					
Tool configuration	WOB (Kg)	Flow Rate (litres/min) (ROP-m/hr)			
Conventional	106	16 (4.40)	44 (7.08)	72 (4.39)	100 (8.21)
	139	16 (6.95)	44 (7.28)	72 (7.31)	100 (11.68)
	173	16 (7.47)	44 (11.90)	72 (8.21)	100 (9.77)
	207	16 (13.20)	44 (14.89)	72 (12.30)	100 (11.87)
	240	16 (12.86)	44 (16.06)	72 (15.48)	100 (18.52)
p-VARD #1	106	16 (4.90)	44 (5.72)	72 (4.46)	100 (3.50)
	139	16 (14.18)	44 (9.93)	72 (8.84)	100 (8.69)
	173	16 (14.89)	44 (10.50)	72 (13.45)	100 (13.95)
	207	16 (18.86)	44 (18.53)	72 (12.50)	100 (12.84)
	240	16 (20.88)	44 (20.89)	72 (21.41)	100 (17.36)
p-VARD #2	106	16 (6.13)	44 (6.72)	72 (6.24)	100 (5.45)
	139	16 (8.09)	44 (10.35)	72 (11.49)	100 (7.50)
	173	16 (13.21)	44 (11.26)	72 (13.58)	100 (15.32)
	207	16 (19.34)	44 (16.75)	72 (19.72)	100 (16.14)
	240	16 (17.43)	44 (11.87)	72 (20.40)	100 (17.25)
p-VARD #3	106	16 (7.40)	44 (4.55)	72 (8.71)	100 (4.01)
	139	16 (11.32)	44 (8.61)	72 (8.79)	100 (10.41)
	173	16 (14.15)	44 (15.30)	72 (12.66)	100 (10.36)
	207	16 (17.63)	44 (12.24)	72 (16.48)	100 (11.96)
	240	16 (20.16)	44 (16.27)	72 (19.94)	100 (15.70)

A total of 80 runs were drilled using a 4" diameter concrete specimen. Data was recorded using a Data Acquisition System (DAQ). Table 2 shows detailed lab experimental plan with implemented values of WOB and Flow Rate against the resultant ROP.

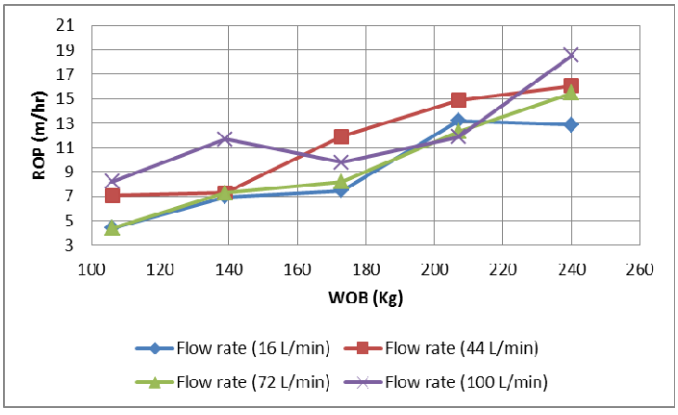

Figure: 5. ROP versus WOB at various flow rates for conventional drilling (no p-VARD used)

For conventional drilling (without using p-VARD) ROP was proportional to applied WOB. Although no clear founder point was observed, a rise in WOB translates to a rise in ROP as can be observed in figure 5. At a flow rate of 44 L/min, the DOT conducted provided the highest ROP. For the p-VARD #1 configuration or high compliance setting, as represented in figure 6, even at a flow rate of 16 L/min cuttings were removed properly, yielding better ROP for low WOB. As WOB is increased curves started to converge. At higher flow rates the 72 L/min and 100 L/min ROP versus WOB curves are almost identical. The p-VARD #1 (high compliance) setting has the highest amplitude of vibrations. The high amplitude of vibrations seems to be helping the removal of cuttings, even at very low flow rates.

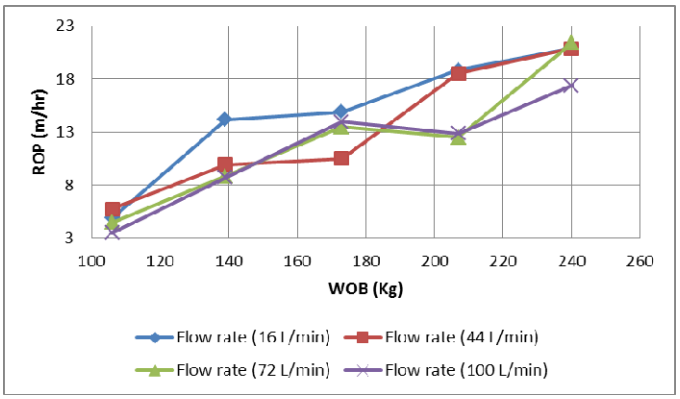

Figure: 6. ROP versus WOB at various flow rates for p-VARD #1 (high compliance)

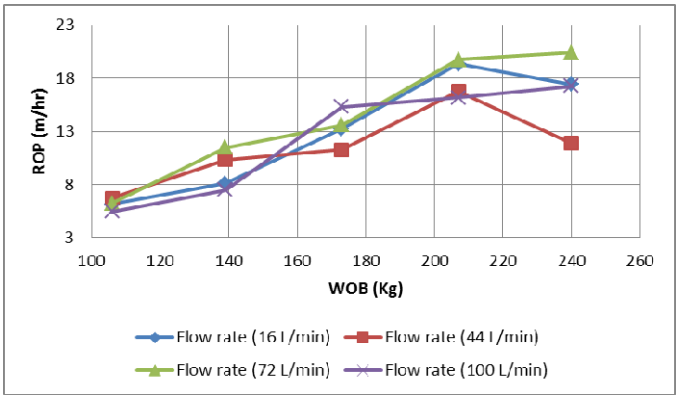

Figure: 7. ROP versus WOB at various flow rates for p-VARD #2 (medium compliance)

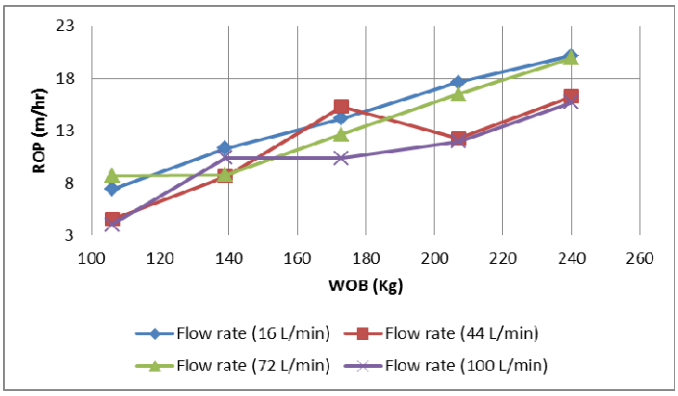

Figure: 8. ROP versus WOB at various flow rates for p-VARD #3 (low compliance)

In case of medium and high compliance setting of p-VARD tool, very little effect of flow rate is observed.

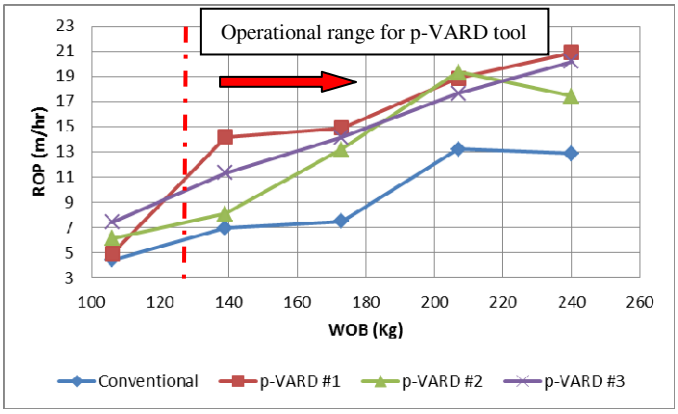

Figure: 9. ROP versus WOB for various compliance settings of the tool (flow rate 16 L/min)

On comparing conventional drilling against various p-VARD configurations, at a low flow rate (16 L/min) a clear range of operation for p-VARD can be observed. All p-VARD configurations were better than conventional drilling. Roughly 50 % or more, increase in ROP was recorded, as being displayed in figure 9.

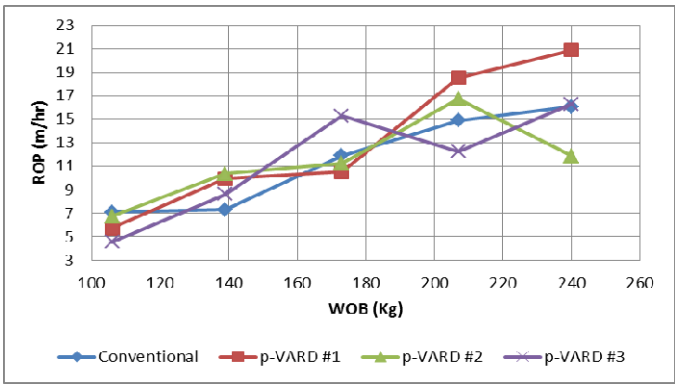

Figure: 10. ROP versus WOB for various compliance settings of the tool (flow rate 44 L/min)

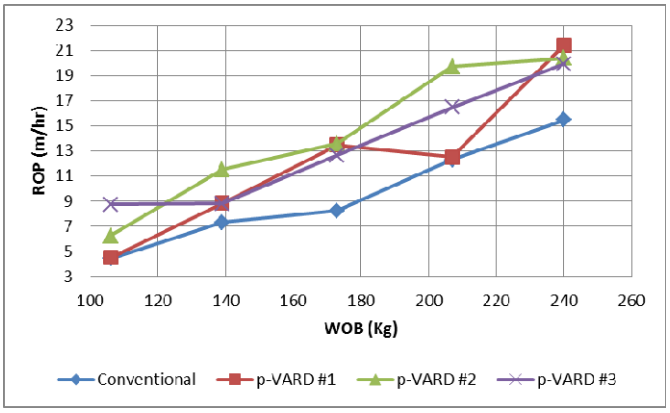

Figure: 11. ROP versus WOB for various compliance settings of the tool (flow rate 72 L/min)

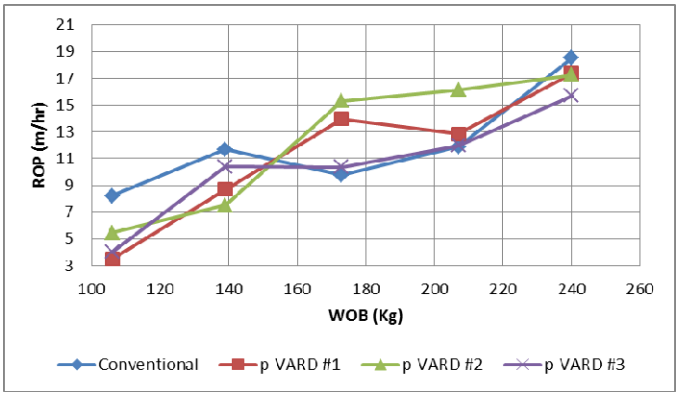

Figure: 12. ROP versus WOB for various compliance settings of the tool (flow rate 100 L/min)

As we have observed before, for conventional drilling 44 L/min was the best flow rate. On plotting all tool configurations for 44 L/min (figure 10), no significant improvement was recorded. In fact conventional drilling (no-VARD) was better under some circumstances. However, as shown in figures11 and 12, higher flow rates of (72 L/min and 100 L/min) respectively medium compliance setting (p-VARD #2), out performs all other.

4. FIELD TRIALS

A field-scale version of the p-VARD tool was developed with the same basic configuration as the lab-scale tool. This tool was evaluated during field drilling trials in September 2014, where multiple wells were drilled through several shale formations to approximate depths of 122 m. As with the laboratory experiments, multiple successive DOT were conducted using a 152 mm diameter PDC bit without the p-VARD tool and then repeated with the p-VARD tool in three different compliance configurations. A down-hole Sensor-Sub recorded axial, lateral and torsional accelerations and magnetometer data to determine near-bit motions to aid with p-VARD evaluation. The Bottom hole Assembly (BHA) including the PDC bit, Sensor-Sub and p-VARD tools is shown in Figure 13. The field drilling trials also involved drilling with other bit types; cuttings collection and evaluation, seismic while drilling data collection and evaluation, dynamic drill string motion recording, and detailed bit and tool wear and damage evaluation. Evaluation of these broader field trial data is ongoing and will be detailed in future publications, however, a representative example of p-VARD performance evaluation is given in this paper. An Ingersoll Rand T3W rig was contracted for the field trials. The rig configurations were: Total pull-back: 70,000 lbs. Deck engine: Cat C15 575 HP, Derrick length: 15 Ft and 600 Ft of onboard rod rack.

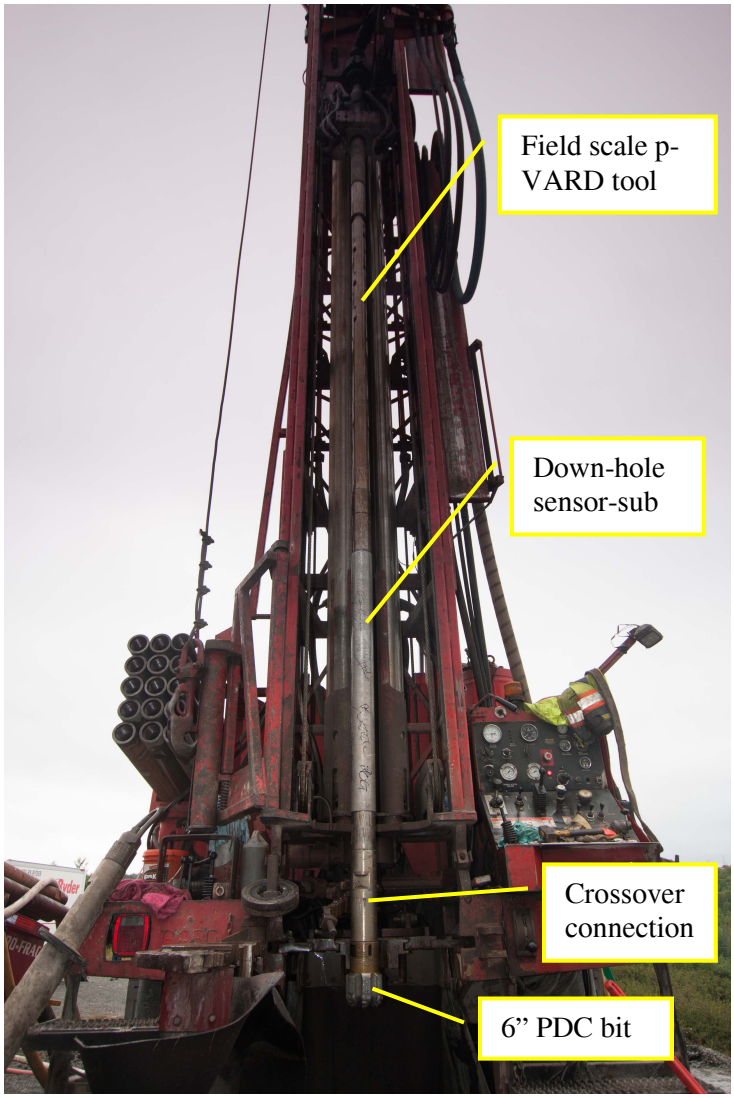

Figure: 13. Bottom Hole Assembly (BHA) for field trials

4.1 Field trial results

One of the formations penetrated during the field trials was red shale, which has mechanical properties similar to the concrete material used for the laboratory trials as shown in Table 1. DOT data comparing conventional drilling with two different compliance configuration of

the p-VARD tool are given in Figure 14. As can be seen, the p-VARD tool with configuration #1 has essentially the same drilling ROP as for conventional drilling (no p-VARD tool). However, the p-VARD tool with configuration #2 (which is better matched for the range of WOB used for the DOT) has ROP ranging on average 50% to 100% higher in the WOB range from 6000 to 8500 kg, with decreasing improvement at higher WOB. This is in general agreement with the laboratory p-VARD evaluation.

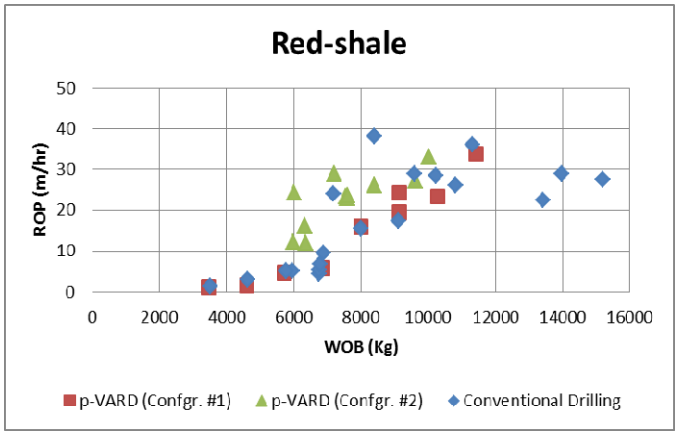

Figure: 14. DOTs for conventional drilling and p-VARD configurations on Red shale

5. CONCLUSIONS

- From experiments done in lab and in field it is clear that a p-VARD tool can enhance ROP.
- Enhancement in ROP is noticed only after a certain amount of WOB is applied. An operational range for the observed effective use of the p-VARD tool based on WOB is reported.
- From the lab results it is clear that flow rate has a significant effect on p-VARD tool performance. In general a much lower flow rate was required using the p-VARD tool to get cuttings removed. Axial vibrations generated by the tool played an important role in the removal of cuttings.

6. FUTUREWORK

As it is clear from the results, that p-VARD can outperform conventional drilling. But further studies are required to optimize the performance of the p-VARD tool. The effect of amplitude of vibration on drilling performance should be studied further. Experiments involving bottom-hole pressure are suggested for future work.

7. ACKNOWLEDGEMENT

Special thanks to Brady Mining for providing 32 mm PDC bits used in lab scale testing of p-VARD tool. Also thanks to Suncor Energy for providing the 6 inch PDC and 6 inch Roller Cone bits, both used in field tests of the tool. The project is funded by Atlantic Canada Opportunity Agency (AIF contract number: 781-2636-1920044), involving Husky Energy, Suncor Energy and Research and Development Corporation (RDC) of Newfoundland and Labrador. Thanks to all ADL members for their help in field trials and lab data processing, in particular Yingjian Xiao.

REFERENCES

1. Pilipenko V. V, I. K. Man'ko, S. I. Dolgopoloy and O. D. Nikolayey, 2005, Characteristics of a high frequency cavitation hydrovibrator for setting up dynamic loads on the rock cutting tool of a drilling assembly, Naukoyy Vistnyk NDU, No 1, Dniepropetrovsk, National Mining University Publishers, pp 66-70.
2. A. Al Ali, S. Barton and A. Mohanna, 2011, Unique Axial Oscillation tool enhances performance of directional tools in extended reach applications, SPE 143216, SPE Annual Technical and Exhibition, Macae, Brasil, June 14-17.
3. Ian Forster, 2011, Axial excitation as a means of stick-slip mitigation - small scale rig testing and full scale field testing, SPE/IADC 139830, SPE/IADC Drilling Conference and Exhibition, Amsterdam, Netherlands, March 1-3.
4. Li. H, S. Butt, K. Munaswamy and Farid Arvani, 2010, Experimental investigation of bit vibrations on rotary drilling penetration rate. 44th US Rock Mechanics Symposium and 5th US-Canada Rock Mechanics Symposium, Salt Lake city, UT, June 27-30.
5. Babatunde, Y., Butt, S., Molgaard, J., & Arvani, F, 2011, Investigation of the Effects of Vibration Frequency on Rotary Drilling Penetration Rate Using Diamond Drag Bit, 45th US Rock Mechanics/Geo Mechanics symposium, San Francisco, CA, June 26-29.
6. Khorshidian H, S. D. Butt and Farid Arvani, 2014, Influence of high velocity jet on drilling performance of PDC bit under pressurized condition, 48th US Rock Mechanics/Geo Mechanics Symposium, Minneapolis, MN, 1-4 June.

APPENDIX 3: PFC-2D NUMERICAL STUDY OF THE INFLUENCE OF PASSIVE VIBRATION ASSISTED ROTARY DRILLING TOOL (PVARD) ON DRILLING PERFORMANCE ENHANCEMENT

Proceedings of the ASME 2018 37th International Conference on Ocean, Offshore and Arctic Engineering
OMAE2018
June 17-22, 2018, Madrid, Spain

OMAE2018-78057

PFC-2D NUMERICAL STUDY OF THE INFLUENCE OF PASSIVE VIBRATION ASSISTED ROTARY DRILLING TOOL (pVARD) ON DRILLING PERFORMANCE ENHANCEMENT

Abourawi Alwaar, Abdelsalam N. Abugharara, and Stephen D. Butt

Process Engineering Department
Faculty of Engineering and Applied Sciences
Memorial University of Newfoundland
St. John's, Newfoundland and Labrador, Canada

ABSTRACT

The objective of this work is to evaluate the influence of the implementing the downhole Passive Vibration Assisting Rotary Drilling (pVARD) Tool on enhancing drilling performance using a numerical study utilizing a Particle Flow Code (PFC-2D). The work is comprised of a numerical study of a simulation using the PFC-2D on an experimental work described in ARMA 15-492 (Rana et al, 2015). The numerical study was performed to validate the experimental work following the steps, procedure, and conditions performed in the laboratory work.

The numerical study of the laboratory work involves not only the evaluation of drilling rate of penetration (ROP), but it also includes the Depth of Cut (DOC) of the bit cutters and the Mechanical Specific Energy (MSE). This numerical work also includes comparison study of drilling performance under various configurations of the pVARD tool, which represents a controlled downhole vibration against the rigid drilling configuration that represents the conventional rotary drilling. The pVARD configurations involves pVARD low spring compliance, medium spring compliance, and high spring compliance. The drilling output parameters of DOC, MSE, and ROP are then studied and analyzed in all pVARD and non-pVARD configurations.

Likewise of the experimental work, the result of the numerical simulation approves the experimental work and it indicates the positive effect of utilizing the downhole pVARD on improving ROP. The drilling performance enhancement is also supported by the DOC and the MSE result.

Keyword: PFC-2D, pVARD, ROP, MSE, DOC.

INTRODUCTION AND BACKGROUND

Field and laboratory drilling experiments approved the positive effect of the employment of pVARD on enhancing ROP [1, 3, 4, 5, 6, 9, 10, and 12].

Research describes the efficient drilling of oil and gas wells in various ways. One way includes reduction of the non-productive time (NPT) by extending the downhole tools' lives, preventing damaging drill bit as a result of encountered downhole lateral and stick/slip vibrations, improving the downhole drillstring mechanical behavior, reducing downhole frictions in non-vertical wells, and ultimately enhancing ROP by inducing downhole axial vibrations [1, 2, 7, 9, 10, and 12].

PFC-2D has been used as an applicable method to simulate drilling performance [2, 3, 4, 8, and 13]. Various conditions of pressure, rock properties, flow rates vibration and non-vibration modes were applied during implementing PFC-2D studies for numerical drilling investigations [2, 4, and 11].

The enhancement of the drilling ROP can be achieved through numerous ways. The conventional way of improving the ROP can be reached by manipulating with the inputs of the drilling parameters including drill mud flow rates, rotary speeds, rotary torque, and weights on bit (WOB). However, the increase of the above drilling parameters can negatively impact the drilling performance if not applied optimally. For example, an intensive increase of the WOB could cause bucking of the drill string. Also, the intensive increase of the rotary rpm and torque could damage the teeth of the drill bit associated with a high DOC when using a polycrystalline diamond compact (PDC) bit that follows rock shear fracture mode. Considering the fact that the increase of each of the above parameters can

only be entered at the top of the drill string and would be transmitted through the entire drill string to reach the drill bit.

The unconventional method to improve the drilling ROP can be achieved by utilizing the available, moderate, and practical inputs of the drilling parameters at the drill bit by tools installed as part of the Bottomhole assembly (BHA). One approach of increasing the ROP by this method is by implementing the downhole pVARD tool [1].

pVARD tool was designed at the Drilling Technology Laboratory (DTL) in Memorial University of Newfoundland, St. John's, Canada. The pVARD tool was also tested to study its influence on drilling performance applying numerous drilling conditions. The drilling conditions included pressure, flow rates, rotary speeds, formation strengths, formation orientations in laboratory and field scales. Under the above drilling conditions, the pVARD tool was approved to play an important role in improving the drilling performance. This paper validates the results of improving ROP of the field and laboratory work published in ARMA 15-492 (Rana et al, 2015) [1] by employing a comparison study between the experimental study with the simulation study using PFC-2D.

DESCRIPTION OF PVARD

Implementing pVARD tool in drilling has numerous advantages. One of its main functions is to allow the drilling string to have some axial movement with different magnitudes based on the equation of bit-rock-interaction. The axial movements that the pVARD tool has is controlled by the strength of the contained springs of the tool components that produce the pVARD compliance magnitude. The range of the spring compliance has a relationship with the strength of the rock being drilled and therefore it governs the operation range of the tool.

The three main configurations of the pVARD tool that are analyzed in this paper includes sets of low compliance, medium compliance, and high compliance, which represent a high magnitude of low spring strength, a medium magnitude of medium spring strength, and a low magnitude of high spring strength; respectively.

With the additions of the various drilling conditions that the pVARD tool was tested for that were mentioned in the introduction section, the field and laboratory pVARD tool was also experimentally tested under different applications and configurations included the above three sets mentioned above.

Table 1 summarizes the parameters and their magnitudes that were implemented in the PFC-2D simulation study of the pVARD.

STUDIED PARAMETERS

The parameters included in the analysis are the same in the experimental work as well as in the numerical work. They involve the followings:

1. **Input Drilling Parameters (IDP):**
   - Different Bottomhole Pressure (BHP).
   - Different Weights On Bit (WOB).
   - Three configurations of PVARD versus Rigid.
2. **Output Drilling Parameters (ODP):**
   - Drilling Rate of Penetration (ROP)
   - Depth Of Cut (DOC).
   - Mechanical Specific Energy (MSE).

Table 1. Summary of PFC-2D parameters and their magnitudes.

Property	Magnitude
Ratio of Maximum to Minimum Ball Size	1.8
Parallel Bond Shear Strength	44e6 Pa
Parallel Bond Normal Strength	44e6 Pa
Minimum Ball Radius	0.35e-3 m
Ball and Bond Elastic Modulus	44e9 Pa
Ratio of Normal to Shear Stiffness	2.5
Ball-Ball and Ball-Wall Friction	0.5
Density	2650 kg/m^3
Porosity	18 %
Normal Damping Ratio	0.2
Shear Damping Ration	0.2
Local Damping Ratio	0.5
Unconfined Compressive Strength (UCS)	55 MPa
Young Modulus	40 GPa

Figure 1 shows the drilling procedure of PFC-2D. It also shows the cutter, weight configurations applied, and region of study in the PFD-2D study. The three balls displayed in Fig. 2 represent the static weight on bit, the spring stiffness for each pVARD configuration, and the damping.

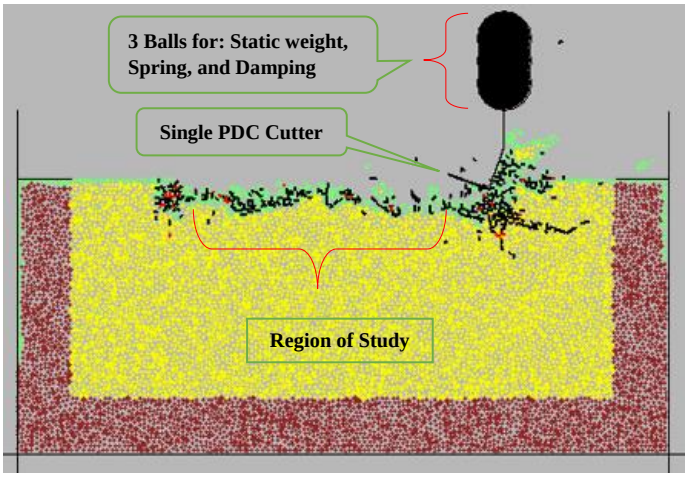

Figure 1. Description of the numerical study of the drilling process using PFC-2D, including weight on bit in case of pVARD.

BHP was another factor implemented in the PFC-2D simulation. The purpose of considering this is to evaluate the

influence of BHP on drilling performance using pVARD VS. rigid drilling. The result of one set of the study of the effect of BHP on the drilling performance is shown in Fig. 2

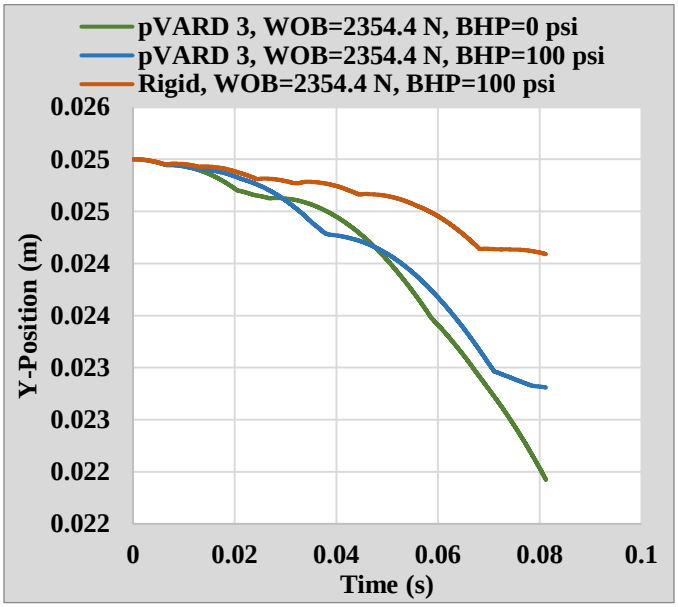

Figure 2. One set of PFC-2D output using rigid drilling for different BHP and at the same WOB=2354.4 N.

RESULTS

The following method of data analysis adopts the graphical display of the results, in which there is comparison analysis between pVARD PFC-2D numerical study and the experimental result obtained from ARMA 15-492 (Rana et al, 2015). The comparison study is based on a double-parameter-analysis with respect to their drilling ROP, which means that the analysis is referenced to the drilling performance as well as a multiple parameter analysis. However, the drilling performance is represented by a pre-analyzed ROP. The pre-analysis is based on the associated DOC; if the DOC is greater than the depth of the chamfer of the bit cutter, then the drilling results are in the accepted range and they are considered to be used for the study. The depth of the chamfer in the PDC cutter used for the experimental work is 0.15 mm. Since we use the same PDC bit used by Hossein Khorshidian, 2012 [14]. He reported the related specifications for this PDC bit. Drilling data of the PFC-2D is considered all valid and all included in the analysis with reference to DOC due to that no chamfer is considered in the design of PDC-2D cutter. Table 2 contains the DOC data, based on which the drilling performance is analyzed and classified.

After determining the valid drilling data to be included in the analysis based on the DOC, the study proceeded for more data evaluation including the ROP and MSE. Figure 3 shows one example of the comparison study of the simulation and the experimental results of ROP using the 3rd pVARD configuration. The result of this study shows good agreement between the two ROP results obtained experimentally and numerically.

Table 2. Summary of DOC result in PFC-2D and laboratory work.

Drilling Mode	Depth Of Cut	
	EXPERIMENT	SIMULATION
pVARD 1	0.281	0.333
	0.815	0.557
	0.856	0.698
	1.080	1.320
	1.200	2.320
pVARD 2	0.350	0.357
	0.465	0.601
	0.754	1.064
	1.110	1.490
	1.002	2.348
pVARD 3	0.440	0.403
	0.674	0.674
	0.842	1.090
	1.049	1.380
	1.200	2.400
RIGID	0.262	0.303
	0.414	0.357
	0.445	0.439
	0.786	0.524
	0.766	0.911

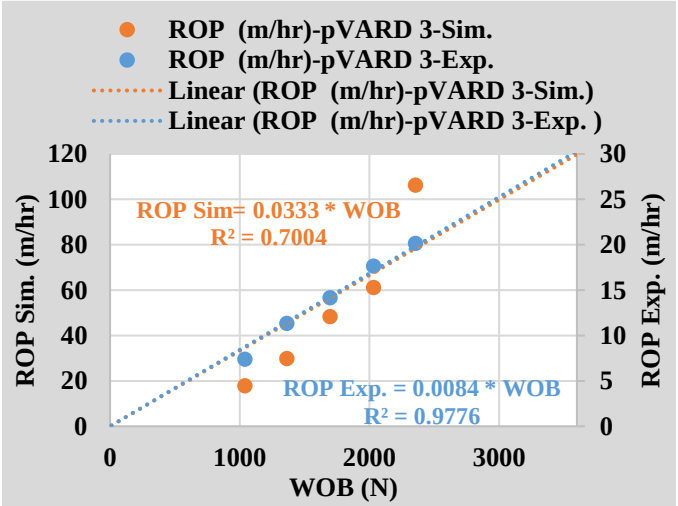

Figure 3. One example of data comparison between simulation and experimental work using the 3rd pVARD configuration.

Double parameter analysis

In this analysis, in each individual drilling configurations, two drilling parameters were analyzed with the drilling ROP, including DOC and MSE. Figures 4, 5, 6, and 7 show the analysis of the drilling performance based on the study of ROP and DOC. The figures show that DOC was directly proportional to ROP. Figures 8, 9, 10, and 11 show the analysis of the drilling performance based on the study of ROP and MSE in 5 different WOBs using the three pVARD configurations vs. rigid drilling in the numerical study, in which MSE was reversely proportional to ROP.

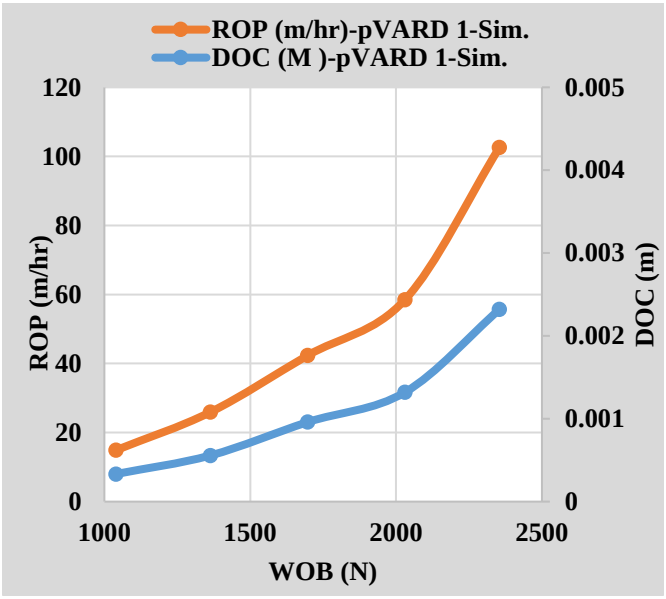

Figure 4. ROP vs. DOC for simulated pVARD 1.

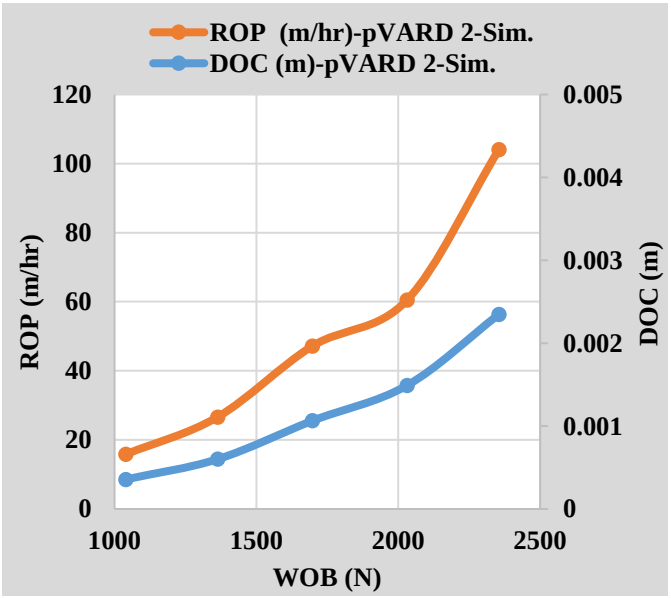

Figure 5. ROP vs. DOC for simulated pVARD 2.

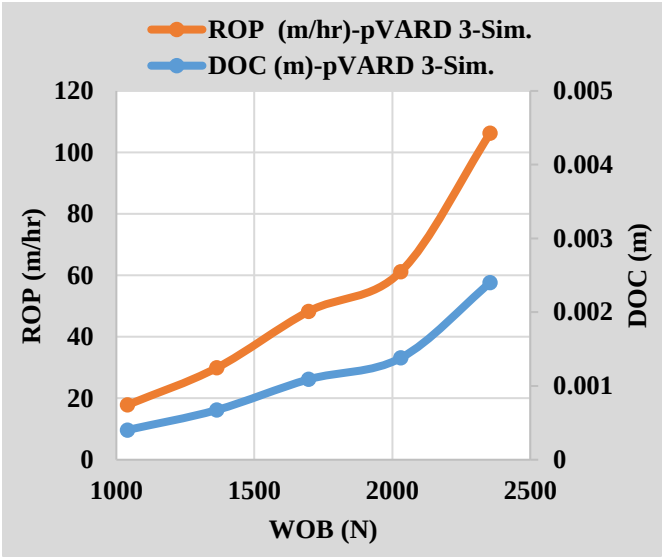

Figure 6. ROP vs. DOC for simulated pVARD 3.

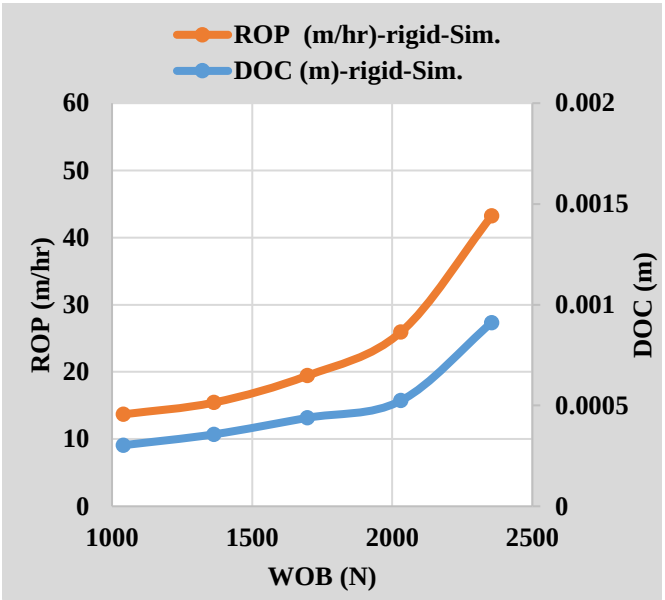

Figure 7. ROP vs. DOC for simulated rigid.

Results of Fig. 4 to Fig. 11 show good agreement between ROP, DOC, and MSE in all drilling tests of pVARD vs. rigid and experimental work vs. simulation.

Figures 4 to 7 show the relationship between ROP and DOC in the simulation work by PDC-2D. These figures show that ROP is directly proportional to DOC showing the positive influence of the increase of DOC on ROP.

Figures 8 to 11 show the relationship between ROP and MSE in the simulation using the PFC-2D. These figures show that ROP is reversely proportional to MSE, confirming the positive influence of the reduction of MSE on the efficient

drilling performance through ROP. The result of these figures agrees with the general trend and relationship between ROP and MSE which is reversal as a sign of an efficient drilling.

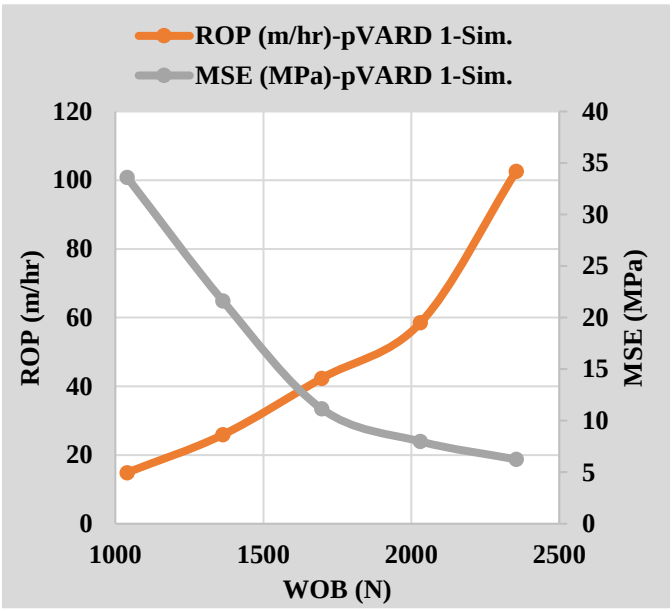

Figure 8. ROP vs. MSE for simulated pVARD1.

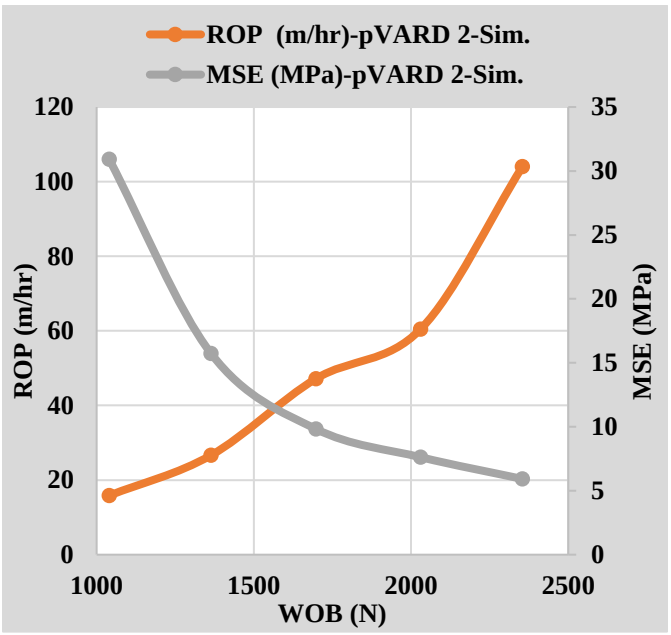

Figure 9. ROP vs. MSE for simulated pVARD 2.

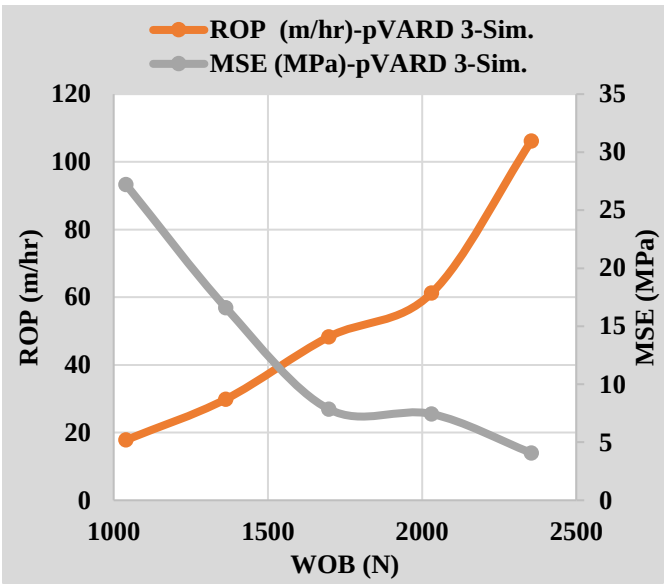

Figure 10. ROP vs. MSE for simulated pVARD3.

Figure 11. ROP vs. MSE for simulated rigid.

Multiple parameter analysis

In this analysis, all drilling results of ROP, DOC, and MSE were analyzed together using different drilling modes of pVARD and rigid based on experimental and simulation. Figures 12 and 13 show the comparative results of ROP in different drilling modes experimentally and numerically, respectively.

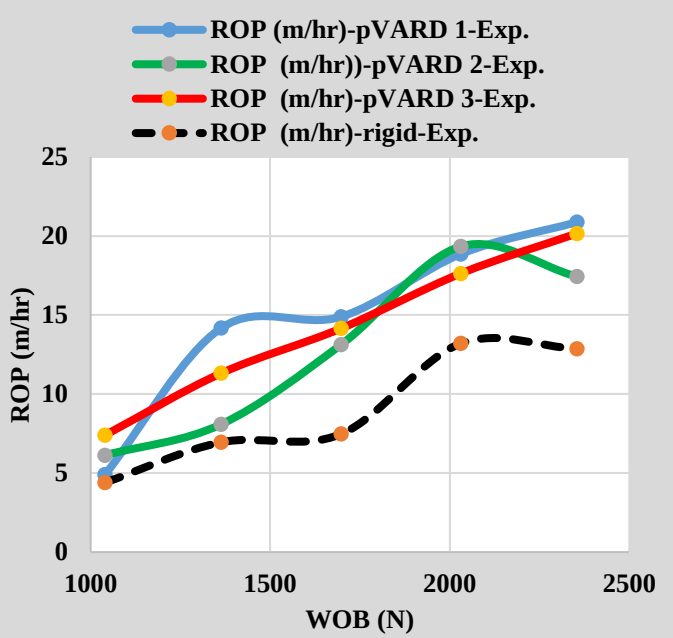

Figure 12. Compared experimental ROP in all drilling modes of pVARD and rigid.

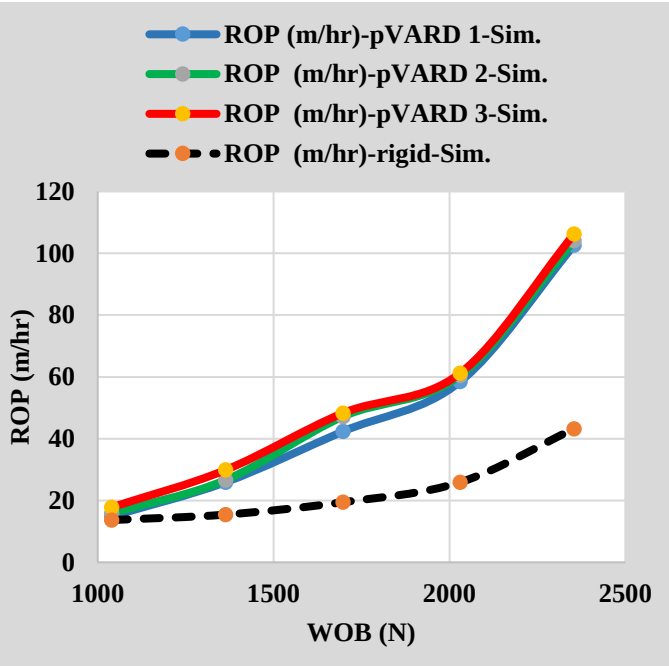

Figure 13. Compared simulated ROP in all drilling modes of pVARD and rigid.

Figures 14 and 15 show the comparison results of DOC in different drilling modes experimentally and numerically, respectively.

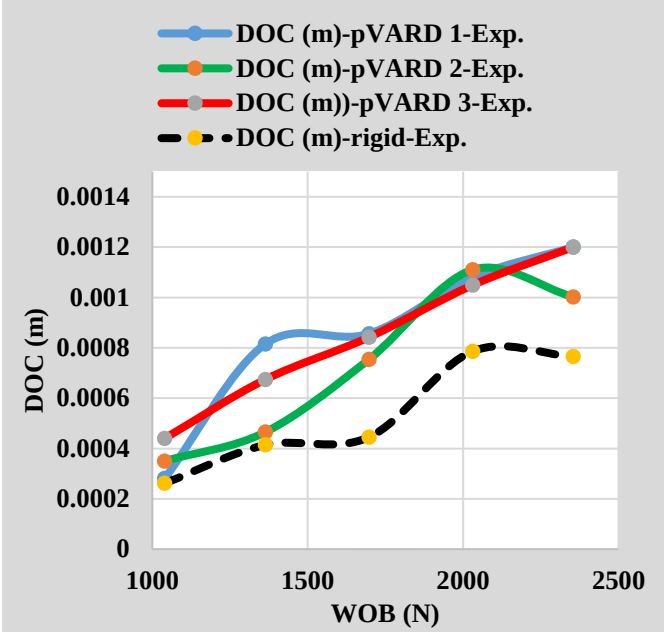

Figure 14. Compared experimental DOC in all drilling modes of pVARD and rigid

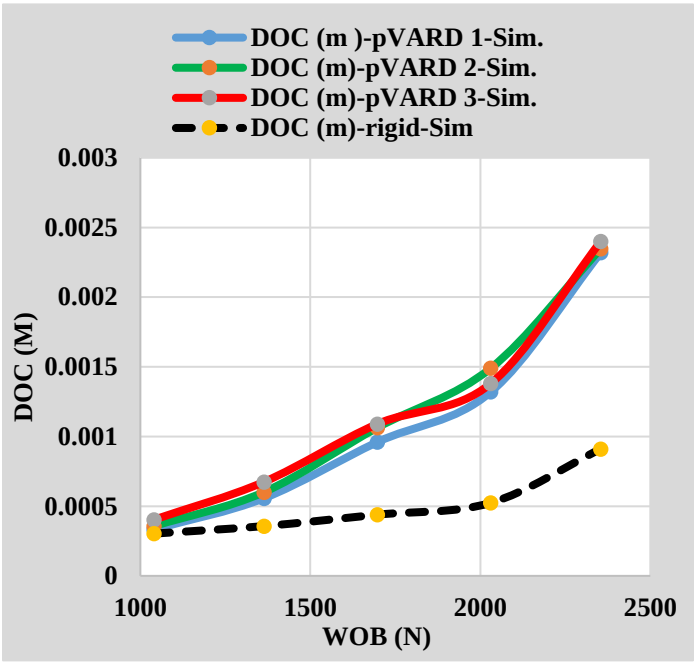

Figure 15. Compared simulated DOC in all drilling modes of pVARD and rigid.

Figures 16 and 17 show the comparison results of MSE in different drilling modes experimentally and numerically, respectively.

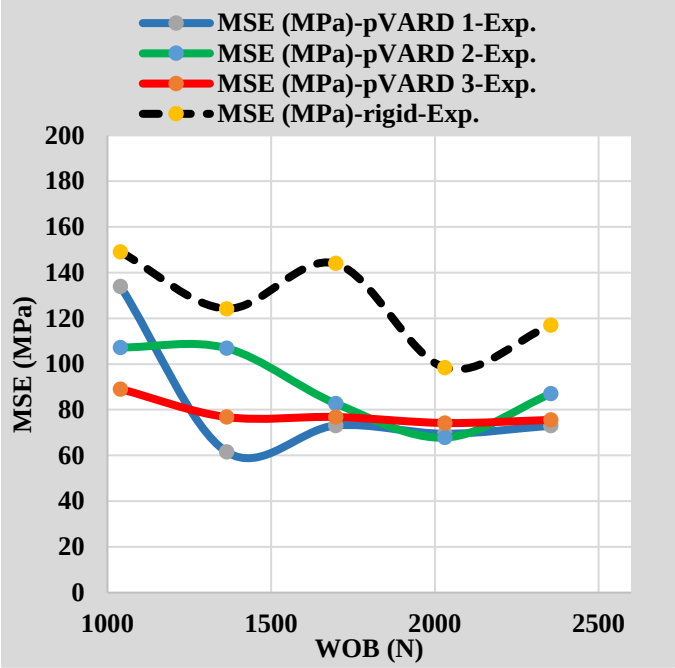

Figure 16. Compared experimental MSE in all drilling modes of pVARD and rigid.

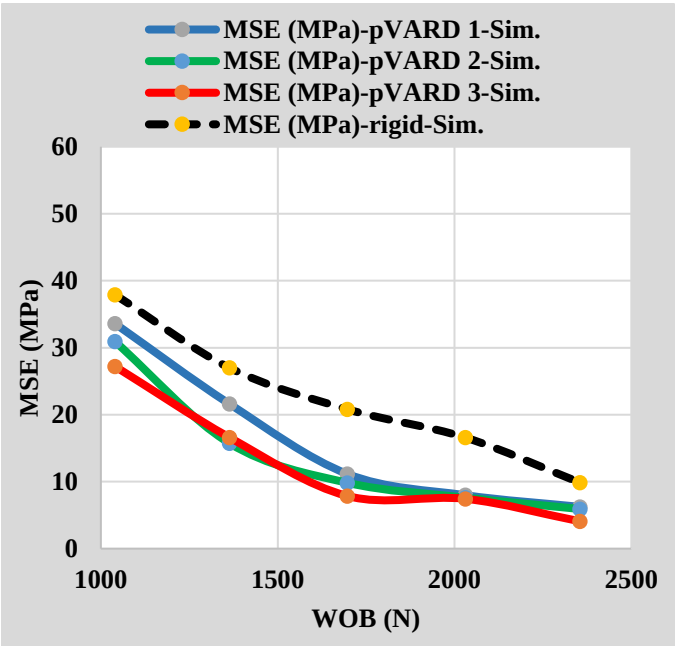

Figure 17. Compared simulated ROP in all drilling modes of pVARD and rigid.

Figure 18 shows the combined result of ROP experimentally vs. numerically. The result shows that ROP is always higher in all pVARD configurations versus rigid drilling in both experimental and numerical work. Figure 19 shows the combined result of MSE experimentally vs. numerically. The result shows that MSE is always lower in all pVARD configurations versus rigid drilling in both experimental and numerical work. The result of Fig. 18 and Fig. 19 confirms the positive influence of pVARD on enhancing drilling performance. This confirmation was further a proved by field laboratory, and numerical work.

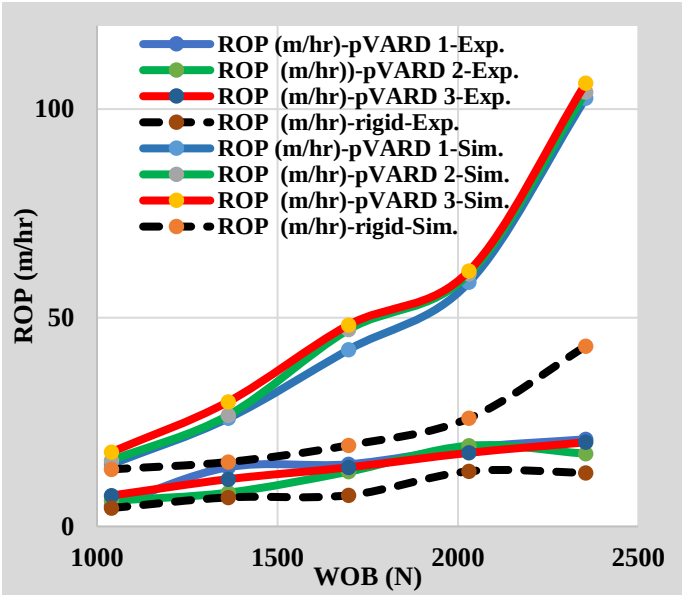

Figure 18. Compared result of ROP for all drilling modes of experimental work vs. PFC-2D numerical work.

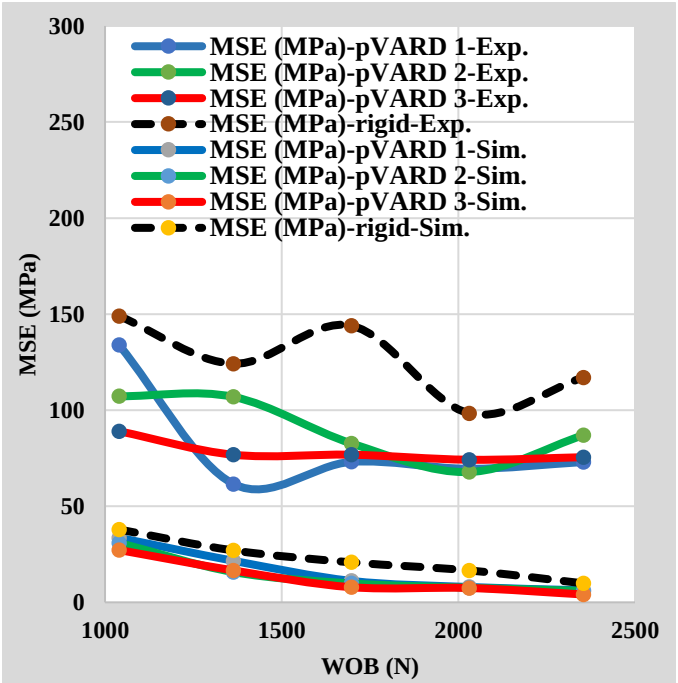

Figure 19. Compared result of MSE for all drilling modes of experimental work vs. PFC-2D numerical work.

DISCUSSION

PFC-2D was utilized for simulating and validating the work published in ARMA 15-492 (Rana et al, 2015) [1]. The simulation work involved comparative studies between pVARD and rigid drilling systems. The simulation study, also, included multiple drilling parameters such as ROP, DOC, MSE and BHP. For further analysis of the effect of pVARD on the drilling performance in contrast with rigid, three various configurations of pVARD were involved.

As shown in all figures of the double parameter section, the drilling ROP increases with the increase of DOC. This was found in all drilling tests of the experimental and the simulation. Also, the drilling ROP was found to be increasing with the decrease of the MSE. This is found in all drilling tests of the experimental and the simulation as well.

As shown in figures (Fig. 12 to Fig. 17) in the multiple parameter section, the combined relationships between ROP, DOC, and MSE were found to have good agreements in all drilling modes , including the experimental and the simulation when applying all drilling modes, involving the three sets of pVARD as well as the rigid.

As the drilling ROP increases with the increase of WOB, all ROP results from the numerical and experimental work were found to have a good agreement and they showed an increase of ROP with the increase of WOB. In Fig. 13, the result of the simulated ROP was found to be the lowest in the rigid drilling compared to all pVARD configurations, which was good validation to the experimental work of the ROP that is shown in Fig. 12. This confirms the positive influence of implementing pVARD on enhancing drilling performance through the analysis of WOB vs. ROP.

Based on that the increase of DOC causes an increase in the drilling ROP, all DOC relationships were found to have good agreement and their increase found to result an increase of ROP. Such positive agreement of WOB vs. DOC was found in both numerical and experimental work. In Fig. 15, the simulated DOC was found to be the lowest in the rigid drilling compared to all pVARD sets that had good agreement and validated the experimental results of the DOC displayed in Fig. 14.

As MSE has a reveres relationship with the drilling ROP and that its decrease while increasing the drilling ROP is a sign of an efficient drilling performance, all MSE results were found to be decreasing with the increase of ROP. In Fig. 17, the simulated MSE result was found to be the highest in the rigid drilling compared to all pVARD configurations, which was confirming the positive influence of implementing pVARD on drilling efficiently and enhancing the drilling performance.

The drilling parameters that were implemented in this experimental and numerical evaluation through various drilling settings, supported the enhancement of the drilling performance when using pVARD tool.

SUMMARY

The numerical study using the PFC-2D of this work can be summarized in the following points:

- The numerical study supported the experimental work in approving the positive influence of pVARD implementation on drilling performance enhancement.
- Involving more drilling parameters including DOC, MSE, and BHP supported the comparative study and strengthened the validation work of the simulation and the experimental results.
- As the PFC-2D was the software used for data validation, it showed good agreements between all studied drilling parameters and drilling mods.

ACKNOWLEDGMENT

This work was performed at the Drilling Technology Laboratory (DTL) at Memorial University of Newfoundland in St. John's, Canada. This project is financially funded by the Atlantic Canada Opportunity Agency (AIF contract number: 781-2636-1920044), involving Husky Energy, Suncor Energy and Research and Development Corporation (RDC) of Newfoundland and Labrador. The Financial support is also provided by the Ministry of Higher Education and Scientific Research, Libya through Canadian Bureau International Education (CBIE).

NOMENCLATURE

BHP: Bottom Hole Pressure
CBIE: Canadian Bureau International Education
DOC: Depth Of Cut
DTL: Drilling Technology Laboratory
Exp.: Experimental
IDP: Input Drilling Parameters
MSE: Mechanical Specific Energy
NPT: Non-Productive Time
ODP: Output Drilling Parameters
PDC: Polycrystalline Diamond Compact
PFC-2D: Particle Flow Code-2 Dimension
pVARD: passive Vibration Assisted Rotary Drilling
RDC: Research Development Cooperation
ROP: Rate Of Penetration
Sim: Simulation
WOB: Weight On Bit

REFERENCES

[1] Rana, P.S, A.N. Abugharara, S.D. Butt and J. Molgaard. Experimental and Field Application of Passive-Vibration Assisted Rotary Drilling (pVARD) Tool to Enhance Drilling Performance. The 49th US Rock Mechanics / Geomechanics Symposium held in San Francisco, CA, USA, 28 June- 1 July 2015.

[2] Khorshidian, H., Mozaffari, M., & Butt, S. D. (2012, January 1). The Role of Natural Vibrations In Penetration Mechanism of a Single PDC Cutter. The 46th US Rock Mechanics / Geomechanics Symposium held in Chicag, IL, USA, 24-27 June 2012.

[3] Zhong, J., Yang, J., and Butt, S.D. (2016). DEM Simulation OF Enhancing Drilling Penetration Using Vibration and Experimental Validation. Society for Modelling and Simulation International, 2016 Summer Simulation Multi-Conference, Montreal Convention Center, Quebec, Canada, Feb 1 - 3, 2016.

[4] Akbari, B., Butt, S. D., Munaswamy, K., & Arvani, F. (2011, January 1). Dynamic Single PDC Cutter Rock Drilling Modeling and Simulations Focusing On Rate of Penetration Using Distinct Element Method. American Rock Mechanics Association. The 45th US Rock Mechanics / Geomechanics Symposium held in San Francisco, CA, June 26–29, 2011.

[5] Li, H., Butt, S., Munaswamy, K., & Arvani, F. (2010, January 1). Experimental Investigation of Bit Vibration On Rotary Drilling Penetration Rate. American Rock Mechanics Association. The 44th US Rock Mechanics / Geomechanics Symposium and 5th U.S.- Canada Rock Mechanics Symposium held in Salt Lake City, UT June 27-30, 2010.

[6] Babatunde, Y., Butt, S., Molgaard, J., & Arvani, F. (2011, January 1). Investigation of the Effects of Vibration Frequency on Rotary Drilling Penetration Rate Using Diamond Drag Bit. American Rock Mechanics Association. The 45th US Rock Mechanics / Geomechanics Symposium held in San Francisco, CA, June 26–29, 2011.

[7] Abtahi, A., Butt, S., Molgaard, J., & Arvani, F. (2011, January 1). Wear Analysis and Optimization on Impregnated Diamond Bits in Vibration Assisted Rotary Drilling (VARD). American Rock Mechanics Association. The 45th US Rock Mechanics / Geomechanics Symposium held in San Francisco, CA, June 26–29, 2011.

[8] Wilson, J. K., & Noynaert, S. F. (2017, March 14). Inducing Axial Vibrations in Unconventional Wells: New Insights through Comprehensive Modeling. Society of Petroleum Engineers. The SPE/IADC Drilling Conference and Exhibition held in The Hague, The Netherlands, 14-16 March 2017. doi:10.2118/184635-MS

[9] Clausen, J. R., Schen, A. E., Forster, I., Prill, J., & Gee, R. (2014, March 4). Drilling with Induced Vibrations Improves ROP and Mitigates Stick/Slip in Vertical and Directional Wells.

Society of Petroleum Engineers. The IADC/SPE Drilling Conference and Exhibition held in Fort Worth, Texas, USA, 4-6 March 2014. doi:10.2118/168034-MS

[10] Jones, S., Feddema, C., Sugiura, J., & Lightey, J. (2016, March 1). A New Friction Reduction Tool with Axial Oscillation Increases Drilling Performance: Field-Testing with Multiple Vibration Sensors in One Drill String. Society of Petroleum Engineers. The SPE/IADC Drilling Conference and Exhibition held in in Fort Worth, Texas, USA, 1-3 March 2016. doi:10.2118/178792-MS

[11] Akbari, B., Miska, S. Z., Yu, M., & Rahmani, R. (2014, August 18). The Effects of Size, Chamfer Geometry, and Back Rake Angle on Frictional Response of PDC Cutters. American Rock Mechanics Association. The 48th US Rock Mechanics / Geomechanics Symposium held in Ninneapolis, MN, USA, 1-4 June 2014

[12] Gee, R., Hanley, C., Hussain, R., Canuel, L., & Martinez, J. (2015, March 17). Axial Oscillation Tools vs. Lateral Vibration Tools for Friction Reduction- What's the Best Way to Shake the Pipe? Society of Petroleum Engineers.The SPE/IADC Drilling Conference and Exhibition held in London, United Kingdom, 17-19 March 2015. doi:10.2118/173024-MS

[13] Carrapatoso, C., da Fontoura, S. A. B., Martinez, I. M. R., Inoue, N., Lourenço, A., & Curry, D. (2013, January 1). Simulation of Single Cutter Experiments in Evaporite using the Discrete Element Method. International Society for Rock Mechanics and Rock Engineering. Rok Mechanics for Resources, Energy and Environment-Taylor and Francis Group, London, ISBN 978-1-138-00080-3

[14] Khorshidian, Hossein (2012) Phenomena affecting penetration mechanisms of polycrystalline diamond compact bits. Masters thesis, Memorial University of Newfoundland

APPENDIX 4: STUDY OF THE RELATIONSHIP BETWEEN ORIENTED DOWNHOLE DYNAMIC WEIGHT ON BIT AND DRILLING PARAMETERS IN CORING ISOTROPIC NATURAL AND SYNTHETIC ROCKS

Proceedings of the ASME 2019 38th International Conference on Ocean, Offshore and Arctic Engineering
OMAE2019
June 9-14, 2019, Glasgow, Scotland

OMAE2019-96176

STUDY OF THE RELATIONSHIP BETWEEN ORIENTED DOWNHOLE DYNAMIC WEIGHT ON BIT AND DRILLING PARAMETERS IN CORING ISOTROPIC NATURAL AND SYNTHETIC ROCKS

Abdelsalam N. Abugharara
Memorial University of Newfoundland
St. John's, Newfoundland, Canada

John Molgaard
Memorial University of Newfoundland
St. John's, Newfoundland, Canada

Charles A. Hurich
Memorial University of Newfoundland
St. John's, Newfoundland, Canada

Stephen D. Butt
Memorial University of Newfoundland
St. John's, Newfoundland, Canada

ABSTRACT

Coring natural rocks (granite) and synthetic rocks (rock like material, RLM) using diamond impregnated coring bit was performed by A rigid coring system. RLM and granite were previously tested to be isotropic rocks by the author [1, 2, 3, 4] A baseline procedure was developed for isotropic rock characterization [2] and this work is to contribute to the developed baseline procedure by considering downhole dynamic weight on bit (DDWOB). The drilling parameters involved in the analysis included rate of penetration (ROP) depth of cut (DOC), rpm, and torque. All parameters were studied as a function of DDWOB at 300 and 600 input rpm. A fully instrumented laboratory scale rotary drilling rig was used with 5 liter/minute water flow rate. Samples were first cored in 47.6 mm diameter in the desired orientations. Samples of granite were cored in two perpendicular directions (vertical and horizontal) and samples of RLM were cored in three directions including vertical, oblique, and horizontal. The coring experiments were performed using 25.4 mm diamond impregnated coring bit. At each input rpm and at each applied static weight, multiple coring runs were repeated and then averaged; therefore, each point of the displayed data was averaged of at least three repeated experiments at the same inputs. DDWOB was recorded by a load cell fixed beneath the sample holder and connected to a Data Acquisition System that records at 1000 HZ sampling rate. Several sensors were used to record the required data, including operational rotary speed, advancement of drill bit for ROP calculation, and motor current for torque measurement. Results showed similar trends in different orientations at the same inputs demonstrating RLM and granite isotropy. The results also showed the influence of DDWOB on ROP, DOC, rpm, and torque (TRQ) expanding the baseline procedure through considering DDWOB for isotropic rock characterization.

INTRODUCTION

Drilling and coring efficiently require optimum application and transfer of drilling parameters from the surface to the drill and coring bit. For coring, there are two main systems: induced non-dangerous vibration coring or drilling system and rigid (non-compliance and conventional) coring or drilling system. Abugharara et al.,

[5] reported A comprehensive comparative study between the two systems while coring and drilling in various rocks (i.e. shale). As challenges are continuously encountered during drilling and coring, achieving efficient coring or drilling may not be possible, especially in directional and horizontal operations. Some of the challenges that may be faced while coring and drilling in non-vertical wells include coring bit jamming, buckling of drill pipes, pre-mature wear and failure of bit and bottomhole assembly due to excessive application of surface load and generating destructive vibrations. Surface WOB and rpm are difficult to control, particularly in non-vertical wells, which could lead to in-efficient coring process. Therefore, laboratory experiments are needed more than ever to understand the relationship between all drilling parameters, in particular WOB, to increase confidence in coring applications. One of the challenges faced in non-vertical drilling is applying optimum WOB, exceeding which could lead to drill pipe buckling, wellbore enlargement and washout, generating destructive vibrations, etcetera. Vibrations have always existed in the drill string and have effects on tool life and drilling performance, but some drilling systems have more vibrations than others. However, numerous studies show that some vibrations are controllable, low level, and non-dangerous, and they can be desirably implemented to improve downhole drilling conditions and eventually, enhance drilling rate of penetration (ROP) [5, 6, 7, 8].

For accurate downhole data recording, downhole sensors are required. Jones, et al., [9, 10] reported the importance of implementing downhole measurements to record data while drilling for drilling performance improvement, core retrieving enhancement, and coring cost reduction. Raymond, et al., [11] and Myers, et al., [12] reported a laboratory simulation of a coring and drilling bit dynamics using a model-based servohydraulic controller and a data acquisition system to record bit dynamics while coring and drilling.

Similar relationships were found between the dependent variables (ROP, DOC, rpm, and TRQ) and orientation and DDWOB, as were found previously with static WOB, with both granite and RLM [1, 2, 3, 4].

SAMPLE PREPARATION

The first step with RLM was to cast cylinders 152.4 mm diameter, 304.8 mm long. 47.6 mm cores were drilled from these, some aligned with the vertical axis of the cylinders; some perpendicular to the vertical axis; also some at 45º to the vertical axis, as shown in Fig. 1.

The 47.6 mm RLM cores were then cored using a 25.4 mm diameter impregnated diamond coring bit as shown in Fig. 2. The left hand side of Fig. 4 shows 19 such cores the smaller cores are shown within the larger core samples. The six at the very far left are 47.6 mm diameter cores drilled vertically from cylinders. The top four of these were drilled axially (inline with both their axes and the axis of the cylinders). However, the lower two 47.6 mm diameter cores were drilled with a 25.4 mm bit perpendicular to the to the axis of each 47.6 mm diameter core, but in different directions in that plane - 0º, 45º, 90º to each other.

The same pattern was true for the middle set of seven 47.6 mm diameter cores but, as noted, these cores were produced at 45º to the axis of 152.4 mm diameter cylinders.

Likewise, the six 47.6 mm cores to the right of the 19 RLM samples, were produced perpendicularly to the axis of 152.4 mm diameter cylinders.

Figure 4 also shows four 47.6 mm diameter cores from granite. The two on the left were drilled perpendicularly to the two on the right. As in Fig. 2, the direction chosen for reference was arbitrary.

Figure 1. Three 152.4 mm diameter and 304.8 mm long, out of which 47.6 mm diameter RLM samples were cored

Figure 2. Granite (natural rock) after coring 47.6 mm diameter vertical and horizontal samples

Figure 3. Sample holder while coring a 47.6 mm RLM sample using 25.4 mm impregnated diamond coring bit

Figure 4. 47.6 mm RLM and granite samples after coring by 25.4 mm diamond impregnated coring bit in different orientations

EXPERIMENTAL PROCEDURE AND APPARATUSE

During each drilling with the 25.4 mm coring bit, the sample holder shown in Fig 3 was used, beneath which a load cell was fixed as a part of the laboratory drilling rig.

The complete apparatus is reported by Rana et al., [8], with changes, which include locking pVARD, for rigid coring and replacing the pressure cell with the sample holder shown in Fig. 3. The sample holder is one small part of a fully instrumented laboratory scale rig with several sensors that record data for determining the actual (operational) rpm, bit advancement for ROP calculation and motor current for torque measurement as reported by Rana et al., 2015 [8]. Two input rotational speeds were used for coring, including 300 rpm and 600 rpm. A flow rate of 5 liter / minute of a clean water was used for hole cleaning and cutting removing. Three static weights were applied, including low, medium, and high static weight, (LSW), (MSW), and (HSW), respectively.

RESULTS

The main purpose of this analysis and discussion is to enrich the baseline procedure developed by the author in Abugharara, et al., [2] in anisotropic rock classifications by involving downhole dynamic weight on bit (DDWOB), using diamond impregnated coring bit in rigid system. As RLM has been previously tested [1, 2, 3, 4, 5], granite results have more in-depth analysis here than RLM.

Results of Granite Coring

The parameters involved in the analysis include (i) corresponding DDWOB to three different sets of static weight of low, medium and high (LSW), (MSW), and (HSW), respectively, (ii) rate of penetration (ROP), (iii) Depth of cut (DOC), (iv) Operational rotary speed corresponding to nominal rpm of 300 and 600, and (v) Torque. In term of orientation, granite was cored in two perpendicular directions, vertical and horizontal.

Coring with 300 rpm:

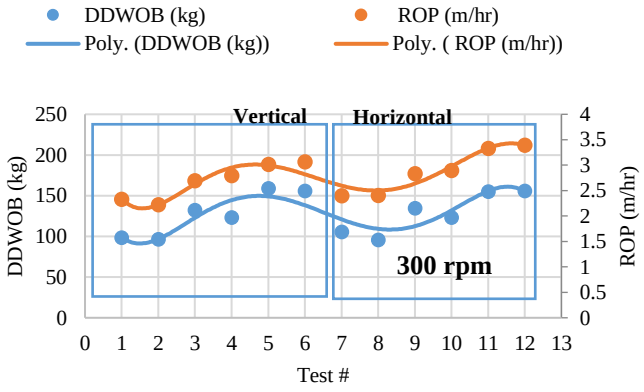

Figure 5. Relationship between ROP and DDWOB in vertical and horizontal granite coring at 300 input rpm using three sets of static weight in each orientation

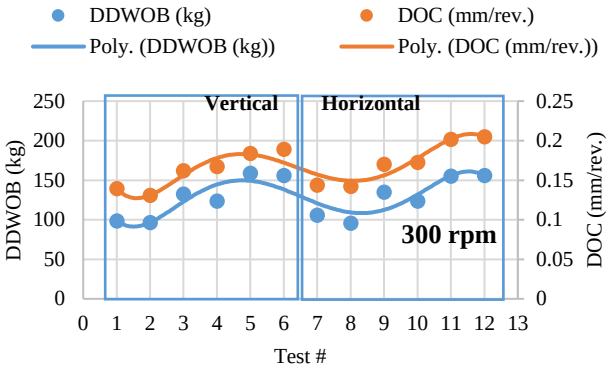

Figure 6. Relationship between DOC and DDWOB in vertical and horizontal granite coring at 300 input rpm using three sets of static weight in each orientation

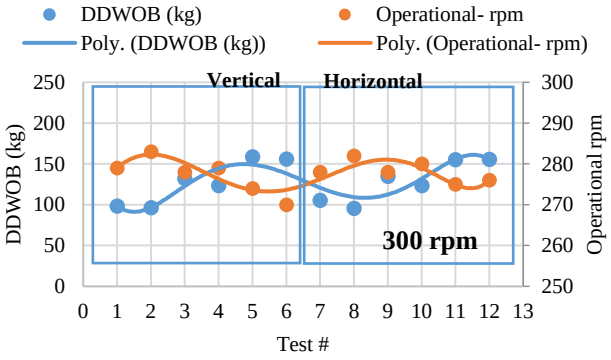

Figure 7. Relationship between operational rpm and DDWOB in vertical and horizontal granite coring at 300 input rpm using three sets of static weight in each orientation

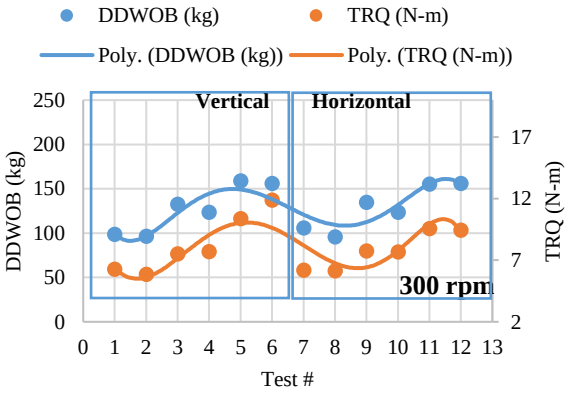

Figure 8. Relationship between TRQ and DDWOB in vertical and horizontal granite coring at 300 input rpm using three sets of static weight in each orientation

Coring with 600 rpm:

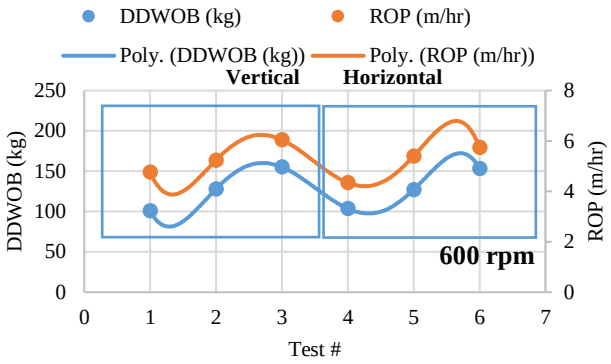

Figure 9. Relationship between ROP and DDWOB in vertical and horizontal granite coring at 600 input rpm using three sets of static weight in each orientation

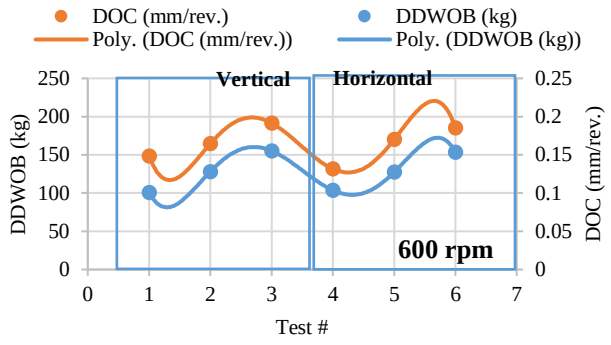

Figure 10. Relationship between DOC and DDWOB in vertical and horizontal granite coring at 600 input rpm using three sets of static weight in each orientation

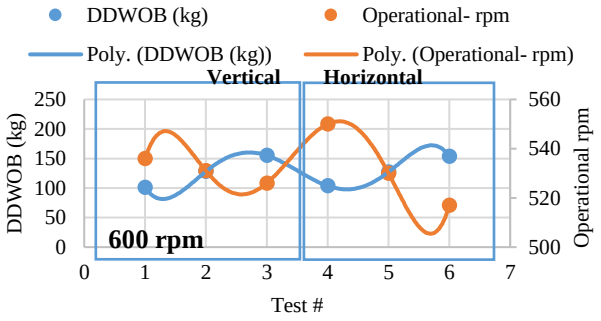

Figure 11. Relationship between operational rpm and DDWOB in vertical and horizontal granite coring at 600 input rpm using three sets of static weight in each orientation

Results of RLM Coring

Same drilling parameters of the granite coring were applied in RLM coring. Results of RLM shown in this

section are of RLM coring in three different orientations, including vertical (V), diagonal (45º), and horizontal (H). Three sets of static weight were applied, including low, medium, and high (LSW), (MSW), and (HSW), respectively. RLM coring results are only for 600 nominal rpm.

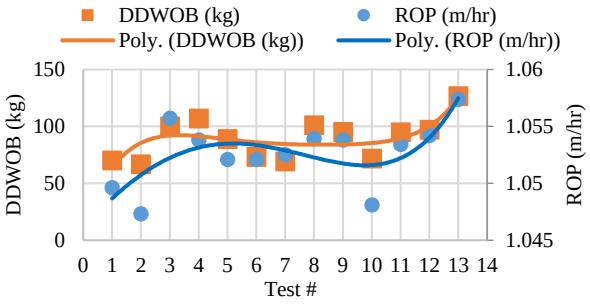

Figure 12. A number of RLM coring runs showing the relationship between DDWOB and ROP

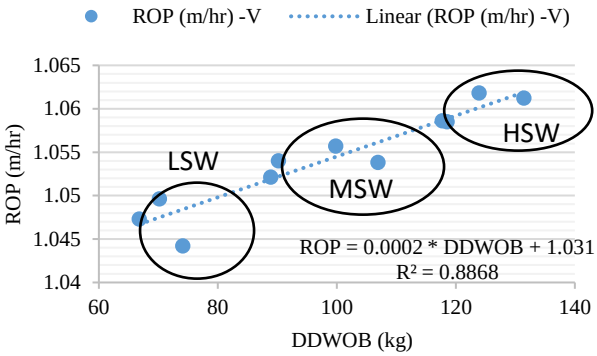

Figure 13. DDWOB vs. ROP in coring vertical RLM samples in three sets of static weight

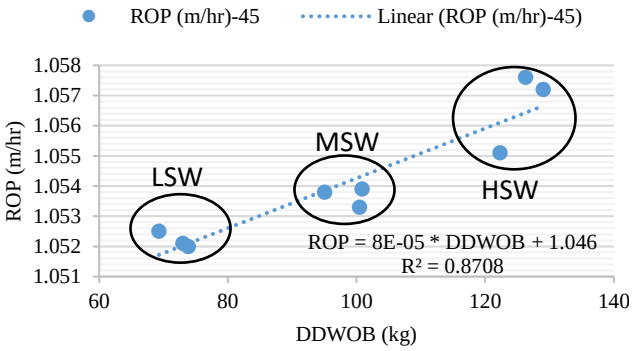

Figure 14. DDWOB vs. ROP in coring oblique RLM samples in three sets of static weight

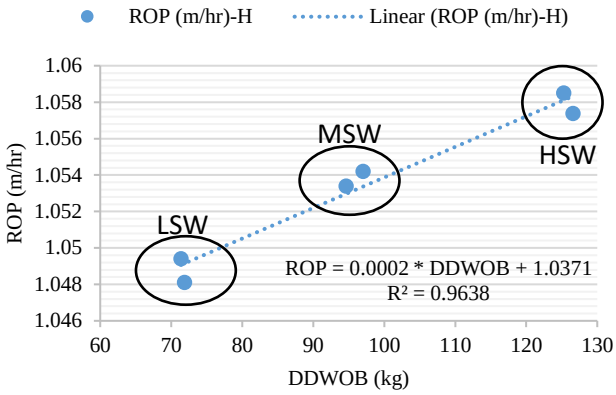

Figure 15. DDWOB vs. ROP in coring horizontal RLM samples in three sets of static weight

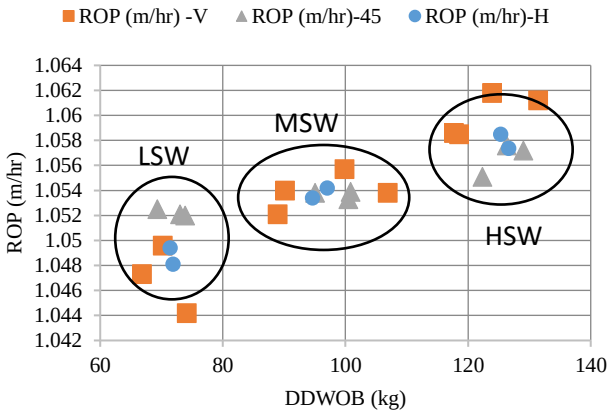

Figure 16. DDWOB vs. ROP in coring RLM samples in three orientations using three sets of static weight

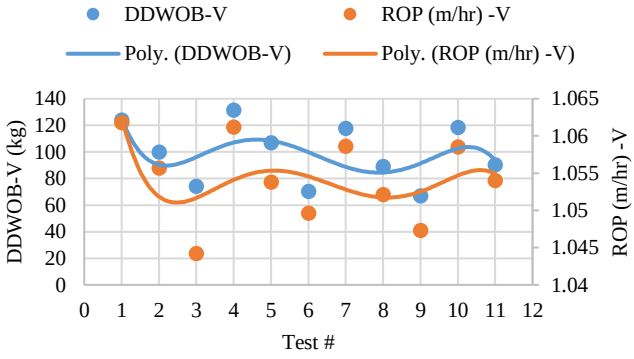

Figure 17. DDWOB versus ROP in vertical RLM coring

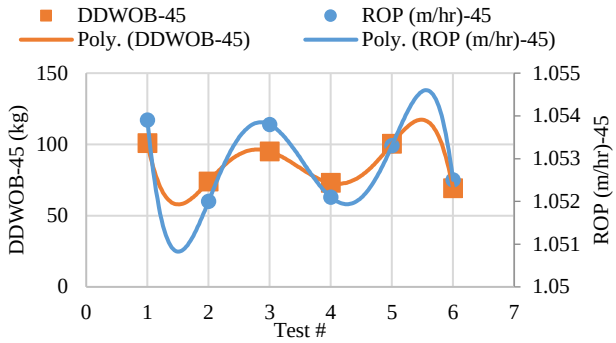

Figure 18. DDWOB versus ROP in oblique RLM coring

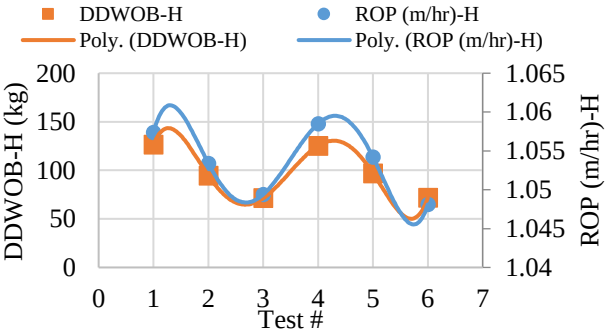

Figure 19. DDWOB versus ROP in horizontal RLM coring

DISCUSSION

Results of coring RLM and granite samples were analyzed with the DDWOB recorded by the load cell connected to the DAQ system that has a 1000hz sampling rate. Results of coring RLM and granite in three orientations and two perpendicular orientations, respectively are shown in Fig. 5 through Fig.

Figure 5 to 8 show the relationship between DDWOB and ROP, DOC, actual (operational) rpm, and torque in coring vertical and horizontal granite samples using 300 input rpm applying three different sets of static weight. The ROP, DOC, and torque increased with the increase of DDWOB, where rpm decreased with the increase of DDWOB.

Figure 9 to 11 show relationships between DDWOB and ROP, DOC, and actual rpm for coring vertical and horizontal granite samples using 600 input rpm applying three sets of static weight. ROP, DOC, and torque increased with the increase of DDWOB, where the actual rpm decreased with the increase of DDWOB. Figure 5 through 11 showed granite isotropy, similarly to what was reported by Abugharara, et al., [1, 2, 3, 4] but with the application of DDWOB.

Figure 12 through 19 show results of RLM coring in three orientations using only 600 input rpm. These results show relationships between DDWOB and ROP at three levels of static weight.

Figure 12 shows the consistent trend of the relationship between DDWOB and ROP at three sets of static weight of a randomly selected number of coring tests, which demonstrate the influence of DDWOB on ROP, and that ROP increases and decreases with the increase and the decrease of DDWOB, respectively.

Figure 13 through 15 exhibit the increase of ROP with the increase of DDWOB in coring RLM vertically, diagonally, and horizontally; respectively, at three sets of static weight and at 600 input rpm. Figure 16 combines in one figure the results of Fig. 13 to Fig. 15 showing the consistent relationship between ROP and DDWOB in the three orientations.

Figure 17 through 19 show the influence of increasing DDWOB on ROP in coring RLM in three orientations using 600 input rpm. Data of Fig. 17 through Fig. 19 was not averaged as was the case in granite coring; however, the results exhibited the importance of considering DDWOB when coring using rigid coring systems.

CONCLUSION

Downhole dynamic weight on bit (DDWOB) fluctuated as did the dependent parameters, ROP, DOC, rpm, and torque. However, the relationships follow the same trend as with the static WOB.

Actual rpm of 300 and 600 were found to be decreasing with the increase of DDWOB, increase of torque, and increase of ROP.

Relationships between DDOWB and drilling parameters showed granite isotropy and that ROP, DOC, and torque increases with the increase of DDWOB, where the actual rpm decreases with the increase of DDWOB. Coring granite samples using 300 and 600 rpm showed similar trends in relationships between DDWOB and drilling parameters, but in different magnitudes.

RLM coring results, showed increase in ROP with the increase of DDWOB regardless of the three drilling orientations.

NOMENCLATURE

DDWOB	Downhole dynamic weight on bit (kg)
DOC	Depth of cut (mm/rev.)
HSW	High static weight (kg)
LSW	Low static weight (kg)
MSW	Medium static weight (kg)
RLM	Rock like material
ROP	Rate of penetration (m/hr)
rpm	Revolution per minuet
WOB	Weight on bit (kg)

ACKNOWLEDGMENT

This work was performed at the Drilling Technology Laboratory (DTL) at Memorial University of Newfoundland in St. John's, Canada. This project is financially funded by the Atlantic Canada Opportunity Agency (AIF contract number: 781-2636-1920044), involving Husky Energy, Suncor Energy and Research and Development Corporation (RDC) of Newfoundland and Labrador. The Financial support is also provided by the Ministry of Higher Education and Scientific Research, Libya through Canadian Bureau for International Education (CBIE-Libya).

REFERENCES

[1] Abugharara, A. N., Alwaar, M. A., Hurich, A. C., & Butt, S. D. (2016, June). Laboratory investigation on directional drilling performance in isotropic and anisotropic rocks. In 50th US Rock Mechanics/Geomechanics Symposium. American Rock Mechanics Association. Houston, Texas. Paper No. ARMA-2016-868.

[2] Abugharara, A. N., Alwaar, A. M., Butt, S. D., & Hurich, C. A. (2016, June). Baseline Development of Rock Anisotropy Investigation Utilizing Empirical Relationships Between Oriented Physical and Mechanical Measurements and Drilling Performance. In ASME 2016 35th International Conference on Ocean, Offshore and Arctic Engineering (pp. V008T11A016-V008T11A016). American Society of Mechanical Engineers. Busan, South Korea. Paper No. OMAE2016-55141.

[3] Abugharara, A. N., Hurich, C. A., Molgaard, J., & Butt, S. D. (2017, June). Study of the Influence of Shale Anisotropy Orientation on Directional Drilling Performance in Shale. In ASME 2017 36th International Conference on Ocean, Offshore and Arctic Engineering (pp. V008T11A011-V008T11A011). American Society of Mechanical Engineers. Trondheim, Norway. Paper No. OMAE2017-62071.

[4] Abugharara, A. N., Hurich, C. A., Molgaard, J., & Butt, S. D. (2017, June). Implementation of Circular Wave Measurements and Multiple Drilling Parameter Analysis in Rock Anisotropy Evaluation. In ASME 2017 36th International Conference on Ocean, Offshore and Arctic Engineering (pp. V008T11A012-V008T11A012). American Society of Mechanical Engineers. Trondheim, Norway. Paper No. OMAE2017-62088.

[5] Abugharara, A., Molgaard, J., Hurich, C., and Butt, S., 2019, Study of the influence of Controlled Axial Oscillations of pVARD on Generating Downhole Dynamic WOB and Improving Coring and Drilling Performance in shale. Proceedings of the ASME 2019 38th International Conference on Ocean, Offshore and Arctic Engineering, Glasgow, Scotland, UK. OMAE2019-96189.

[6] Mohamed, B., Abugharara, A. N., Rahman, M. A., & Butt, S. D. (2018, June). CFD Numerical Simulation for Downhole Thruster Performance Evaluation. In ASME 2018 37th International Conference on Ocean, Offshore and Arctic Engineering. American Society of Mechanical Engineers. Madrid, Spain. Paper No. OMAE2018-78101

[7] Alwaar, A., Abugharara, A. N., & Butt, S. D. (2018, June). PFC-2D Numerical Study of the Influence of Passive Vibration Assisted Rotary Drilling Tool (pVARD) on Drilling Performance Enhancement. In ASME 2018 37th International Conference on Ocean, Offshore and Arctic Engineering (pp. V008T11A014-V008T11A014). American Society of Mechanical Engineers. Madrid, Spain. Paper No. OMAE2018-78057.

[8] Rana, P. S., Abugharara, A. N., Butt, S. D., & Molgaard, J. (2015). Experimental and Field Application of Passive-Vibration Assisted Rotary Drilling (pVARD) Tool to Enhance Drilling Performance. In Proceedings of 49th US Rock Mechanics/Geomechanics Symposium. San Francisco, CA, USA. Paper No. ARMA 15-492

[9] Jones, S., Sugiura, J., Rose, K., & Schnuriger, M. (2017, March). Drilling Dynamics Data Recorders Now Cost-Effective for Every Operator-Compact Embedded Sensors in Bit and BHA Capture Small Data to Make the Right Decisions Fast. In SPE/IADC Drilling Conference and Exhibition. Society of Petroleum Engineers. Hague, The Netherlands. Paper No. SPE-184738-MS.

[10] Jones, S., Sugiura, J., & Wood, H. (2017, March). Recorded Dynamics Measurements While Coring Enhances Performance and Recovery. In SPE/IADC Drilling Conference and Exhibition. Society of Petroleum Engineers. The Hague, The Netherlands. Paper No. SPE/IADC-184740-MS.

[11] Raymond, D. W., Elsayed, M. A., Polsky, Y., & Kuszmaul, S. S. (2008). Laboratory simulation of drill bit dynamics using a model-based servohydraulic controller. Journal of Energy Resources Technology, 130(4), p. 043103.

[12] Myers, G., Schroeder, D., Keogh, W., Grigar, K., & Masterson, W. (2006, January). Coring Dynamics: Data Acquisition While Coring. In Offshore Technology Conference. Offshore Technology Conference. Houston, Texas, USA. Paper No. OTC-17920-MS.

APPENDIX 5: EMPIRICAL PROCEDURE INVESTIGATION FOR SANDSTONE ANISOTROPY EVALUATION: PART I

Title - Empirical Procedure Investigation for Sandstone Anisotropy Evaluation: Part I

Abdelsalam Abugharara and Stephen Butt
Department of Process Engineering, Memorial University of Newfoundland, St. John's, Newfoundland and Labrador, Canada
John Molgaard
Department of Mechanical Engineering, Memorial University of Newfoundland, St. John's, Newfoundland and Labrador, Canada
Charles Hurich
Department of Earth Sciences, Memorial University of Newfoundland, St. John's, Newfoundland and Labrador, Canada

ABSTRACT
An experimental procedure to examine fine-grain sandstone rock anisotropy is reported. The procedure involved several tests. Each test was conducted in three main orientations: vertical, diagonal, and horizontal. Tests included ultrasonic wave velocity and strength. The oriented ultrasonic compressional and shear wave velocity measurements were performed to characterize the anisotropy of the tested sandstone using reported anisotropy indices. The oriented unconfined compressive strength was followed by a multidirectionally oriented indirect tensile strength. Correlations between the unconfined and the indirect tensile strength tests were constructed and compared to published correlations. Results showed isotropy of the tested sandstone, throughout the conducted tests.

RÉSUMÉ
Cette communication traite d'une expérimentation pour examiner l'anisotropie des roches de grès à grains fins. La procédure a impliqué plusieurs tests. Chaque test a été mené selon trois orientations principales : verticale, diagonale et horizontale. Les tests ont inclus la mesure de la vitesse et la résistance de l'onde ultrasonique. On a procédé à des mesures axées sur la vitesse des ondes de compression et de cisaillement pour caractériser l'anisotropie du grès testé, en utilisant les indices d'anisotropie rapportés. Le test de résistance à la compression uniaxiale orientée a été suivi par un test multidirectionnel de résistance à la compression diamétrale. Les corrélations entre les tests de compressions simples et ceux des compressions diamétrales ont été élaborées et comparées à des résultats ont été publiés. Les résultats ont indiqué une isotropie du grès analysé tout au long des tests réalisés.

1 INTRODUCTION

Rock strength was studied using numerous methods both destructive and nondestructive. Some of the destructive methods include confined and unconfined compressive strength, CCS and UCS, respectively, (Syed et al., 2018). UCS can be estimated from several other testing types such as indirect tensile test (IT) or Brazilian tensile test (BTS) (Sheory 1997, Asadi 2015, Kharaman et al. 2012, Diederichs, 2007) and point load index (PLI) (Broch and Franklin 1972, Mendieta 2012, Tsidzi 1990), which have been proved to have reliable correlations with UCS.

Many factors including time consuming sample preparation and test procedure complications, data variability, as well as the high cost of the destructive tests, which can vary from one method to another are behind the demand for alternative methods to estimate rock strength.

Ultrasonic wave propagation is one main nondestructive method for rock strength estimation. It gained its high recognition and attention with the increase of studies correlating measured rock strength from destructive methods with the estimated rock strength from the nondestructive methods.

Rock anisotropy classification is another main topic of research, where the destructive and nondestructive rock strength methods have been used. Several indices have been produced to evaluate rock anisotropy through the variation of the ultrasonic wave velocity (Tsidzi 1997, Saroglou 2007). Other indices were produced to classify rock anisotropy based on their strength variation in different directions using UCS (Ramamurthy 1993). Such methods vary in the cost, time consumed, and complexity.

Rock strength determination has been intensively studied in both laboratories and through simulation under various conditions providing a massive amount of data and methodologies within various range of inclinations (degree increments). However, the indirect tensile strength determined multidirectionally, has not been applied for rock

anisotropy / isotropy classification. One reason for choosing such application is the ease of sample preparation, low cost, simple apparatus and experimental procedure.

Rock tensile strength is determined through both direct and indirect tensile tests (ASTM 2008a, ASTM 2008b, ISRM 1987, Chen et al. 1998, Li and Wong 2013, Perras and Diederichs 2014).

An experimental procedure was previously developed by the authors, Abugharara et al. (2015), which was implemented to evaluate anisotropy of rock like material and granite. However, the indirect tensile strength (ITS) was not included. This study can support the procedure as a handy method for rock anisotropy evaluation.

The work of this paper concentrates on using indirect tensile strength (IT), conducted in multiple orientations to classify the anisotropy of the tested fine-grain sandstone.

2 SAMPLE PREPARATION

One sandstone block was the source for samples used for all tests. Samples were obtained in various dimensions in accordance with the American Society for Testing and Materials (ASTM) and International Society of Rock Mechanics (ISRM) suggested methods. The dimensions of the main block were about 70 cm * 40 cm * 50 cm (length * width * height). Samples of various diameters were cored in the three main orientations of vertical, diagonal, and horizontal.

Samples for oriented ultrasonic measurements were cores of 10.16 cm diameter and about 10 cm long. Figure 1 shows the sandstone block, core samples for OUSWV, and the top view of each sample indicating the degree increments for the circular wave measurement from left to right, respectively.

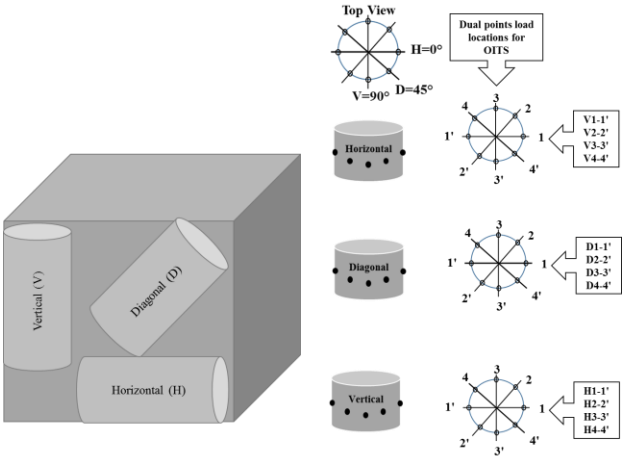

Figure 1. Sandstone block, core samples for OUSWV, and top view of each sample indicating the degree increments for the circular wave measurement from left to right, respectively

Samples for oriented strength measurements were cored using a natural diamond coring bit to obtain cores of 4.76 cm diameter samples and about 30 cm long or more depending on the coring directions. Several cores were obtained in each orientation to produce sufficient number of samples for each test. Samples in each orientation were then categorized into three groups. Each group was denoted for particular oriented strength testing type.

For the unconfined compressive strength test, samples where cored axially from the 4.76 cm samples using a 2.54 cm coring bit. These samples are shown in Figure 2, (middle). The samples were then cut to 2:1 ratio of length to diameter with accordance to standards.

For the indirect tensile test, disk samples were cut to after colour-coding the original cores as shown in Fig. 2 (left), to denote three secondary orientations within each primary orientation.

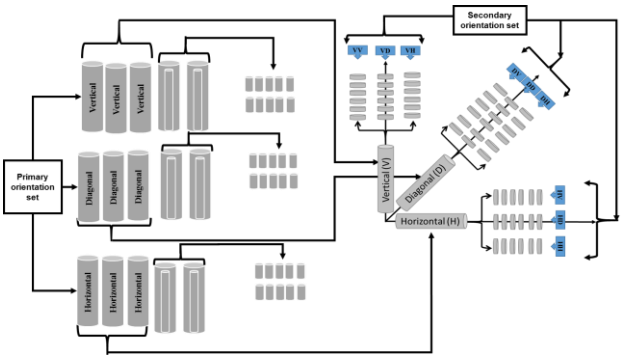

Figure 2. Oriented cores of sandstones (left), OUCS samples (middle), and OITS disks (right)

3 EXPERIMENTAL PROCEDURE

Experiments were performed in the following order. First: for oriented ultrasonic wave velocity (OUSWV) including compressional and shear wave velocity, vp and vs, respectively. The purpose of performing the OUSWV first was to determine the anisotropy of the sandstone through the non-destructive tests using some existing anisotropy indices.

Second, the multidirectional oriented indirect tensile strength test (OITS) as well as the oriented unconfined (uniaxial) compressive strength test (OUCS) were performed. The OITS was conduced on disk samples prepared according to two orientation sets: primary and secondary as shown in Fig. 3. The OUCS was performed on samples prepared according to the primary set of vertical, diagonal, and horizontal. The purpose of these tests was to confirm the sandstone anisotropy classification obtained by OUSWV with the oriented strength tests.

Third, a comparative analysis between the results of this work and work reported elsewhere was performed.

4 PERFORMED TESTS AND APPARATUS

This section shows the tests that were conducted for sandstone anisotropy investigation including ultrasonic wave and strength measurements.

4.1 Oriented Ultrasonic Wave Velocity

The purpose of this measurement was mainly to classify the sandstone anisotropy through a nondestructive method.

Compared to other sound wave velocity measurements (e.g. low frequency sonic wave method and the frequency resonant method), the high frequency ultrasonic method is more reliable and practical. A reason for using this method that it is the associated non-destructive, low cost, and the high precision measurement. In this test the compressional and shear wave velocities (vp and vs, respectively) were measured across eight spots around a circumference of each sample with an increment of 45 degrees as shown in Fig 1.

The ultrasonic wave velocity apparatus used for this measurement was fully described by “Abugharara et al., “2016)”.

4.2 Oriented Strength

This section shows the two main types of strength tests used: the oriented indirect tensile strength (OITS) and the oriented uniaxial compressive strength (OUCS). Figure 3 shows the apparatus used for all strength tests including the oriented indirect tensile (OIT) test and the oriented unconfined compressive strength (OUCS) test. The apparatus was modified to suit the OIT and OUCS tests by replacing the conical pistons to flat-end pistons.

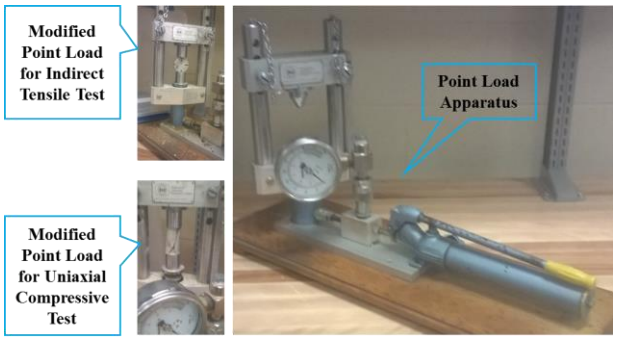

Figure 3. PLI tester Apparatus modified for OITS and OUCS strength measurement with flat-end pistons

4.2.1 Oriented Indirect Tensile Strength

For this test, 90 sandstone disk samples were prepared and classified into three groups as described in Fig. 2. Following a colour code, three smaller groups of about 10 samples were representing three orientations. Each group consists of about 30 samples representing three secondary orientations (VV, VD, VH), (DV, DD, DH), and (HV, HD, and HH) within each primary orientation of vertical (V), diagonal (D), and horizontal (H). The purpose of this classification of the disk samples into primary and secondary was for investigation of the sandstone anisotropy. Figure 4 shows the procedure of testing the disk samples following the colour code for the secondary orientations.

Figure 4. Procedure of OITS test on sandstone disk sample

As many studies reported the influence of rock anisotropy on the fracture direction deviation from the two load points, splitting (fracturing) of sandstone disk samples was monitored while testing. The straight and direct fracture between the two load points in all OITS testing was another was determined as shown in Fig. 6. and was considered as another sign of sandstone isotropy. Figure 5 and 6 show the oriented disk samples before and after OITS, respectively.

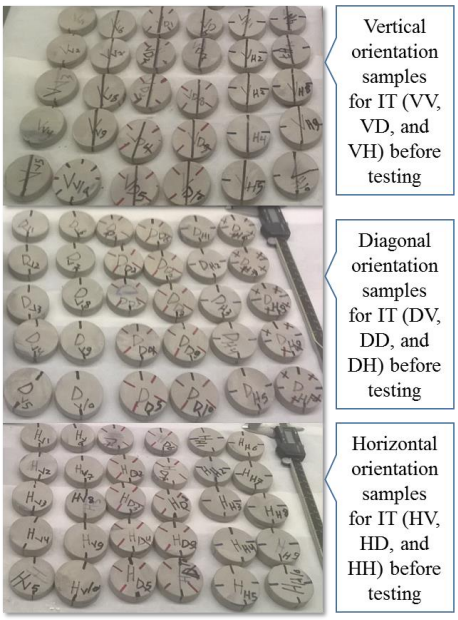

Figure 5. Sandstone disk samples before OITS testing

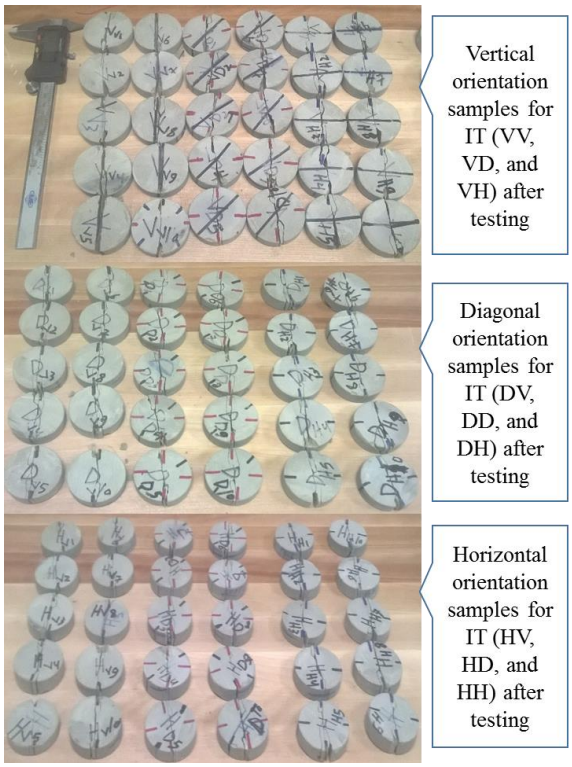

Figure 6. Sandstone disk samples after OITS testing

4.2.2 Oriented Unconfined Compressive Strength

About 30 samples were tested for the OUCS. Samples were classified into three groups to represent three orientations. Figure 7 shows the samples before (top) and after (bottom) conducting the UCS test.

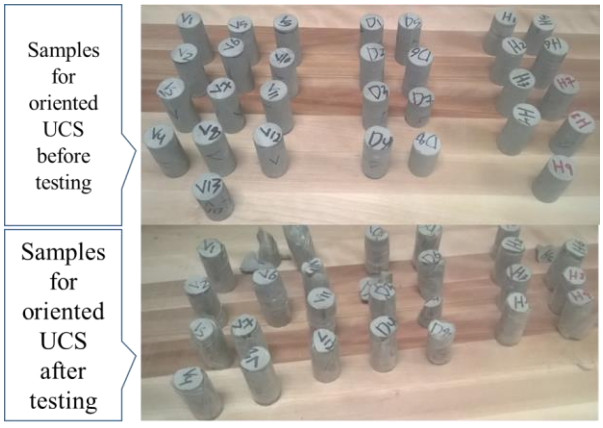

Figure 7. Sandstone core samples before (top) and after (bottom) OUCS testing

5 RESULTS

This section contains the results of the measurement of the oriented ultrasonic, by which the isotropy of sandstone was firstly confirmed. It also contains the results of the oriented IT, UCS, and their correlations.

5.1 Oriented Ultrasonic Wave Measurement and Anisotropy Classification

Using the ultrasonic apparatus reported by Abugharara et al. (2016), oriented compressional and shear wave velocities were measured from the three sandstone cores (vertical, diagonal, and horizontal) as described in Fig. 1.

Compressional and shear wave velocities were measured around the complete circumference of three cylinders. The measuring locations were 45 degrees apart. The purpose of this measurement was to evaluate the sandstone isotropy and calculate its strength using existing numerical models. Such calculated strength would be compared with the measured sandstone strength of this paper. Figure 8 shows results of OUSWV measurements as well as the density of the samples used.

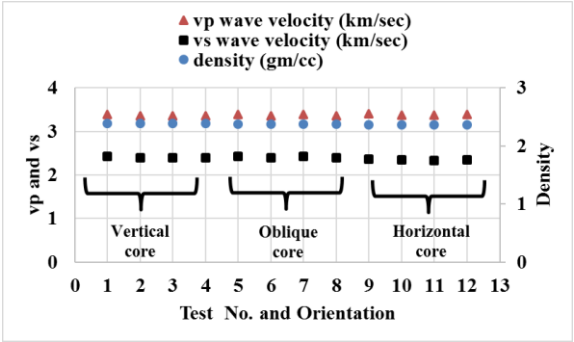

Figure 8. Oriented compressional and shear wave velocities using ultrasonic method with density

Ultrasonic wave velocity anisotropy (VA) was classified by Tsidzi (1997) and Saroglou (2007). This classification was also used by Birch (1961) for description of seismic waves.

(Tsidzi 1997) reported the velocity anisotropy index (VA) based on Eq. 1. Table 1 shows the anisotropy classification according to Tsidzi (1997).

$$VA = \frac{\text{Vmax}-\text{Vmin}}{Vmean}\ (\%) \qquad (1)$$

Where Vmax: the maximum ultrasonic velocity, Vmin: the minimum ultrasonic velocity, and Vmean: the mean velocity.

Table 1. Degree of velocity anisotropy VA (%) according to Tsidzi (1997).

Degree of velocity anisotropy VA (%)	Descriptive term
< 2	Isotropy
2 to 6	Fairly Anisotropy
6 to 20	Moderately Anisotropy
20 to 40	Highly Anisotropy
> 40	Very highly Anisotropy

(Saroglou, 2007) proposed Eq. 2 for rock anisotropy classification.

$$\mathrm{Ivp} = \frac{\mathrm{Vp}(0°)}{\mathrm{Vp}(90°)} \quad (2)$$

Results of this study using Eq. 1 and 2 including the criterion of each author's index are shown in Table 2.

Table 2. Results of sandstone isotropy using OUSWV measurement

According to	Criterion	Description	Result of this study
Tsidzi, 1997	Less than 2(%)	Isotropy	0.55 (%)
Saroglou, 2007	Equal or less than 1	Isotropy	1.006

5.2 Sandstone Oriented Strength and Strength Anisotropy Classification

This section contains results of (i) strength anisotropy classification and (ii) the calculated sandstone strength using OITS and OUCS.

According to Ramamurthy (1993) a strength anisotropy index was proposed as presented in Eq. 3.

$$\mathrm{I}\sigma c = \frac{\mathrm{I}\sigma ci\ (90°)}{\mathrm{I}\sigma ci\ (min)} \quad (3)$$

Where Iσc is the uniaxial compressive strength (UCS) anisotropy, Iσci (90º) is the maximum UCS, and Iσci (0º) is the minimum UCS. The tested sandstone was determine as an isotropy rock according to the criterion described in Table 3.

Table 3. Uniaxial compressive strength anisotropy according to Ramamurthy (1993)

According to	Criterion	Description	Result of this study
Ramamurthy, 1993	1.0 to 1.1	Isotropy	1.01

Through the OUCS test, the strength was measured at three primary orientations. However, the OITS test was measured in the three secondary orientations within the three primary orientations.

After performing each of the OITS and OUCS tests, their results were correlated. The purpose this correlation was for a comparative study analysis with some reported results elsewhere for further evaluation of sandstone isotropy.

5.2.1 Collective Results of OITS vs. OUCS

Strength results of all OITS tests verses OUCS tests were plotted collectively with respect to each primary orientation and are shown in Fig. 9. The average values of these tests are shown in Fig. 10.

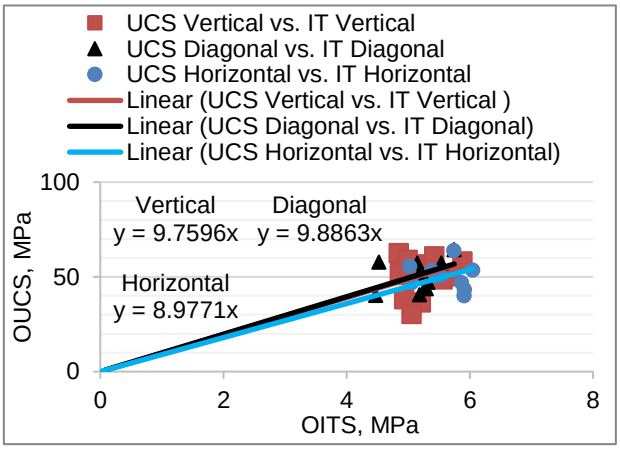

Figure 9. Strength values of OUCS vs. OITS

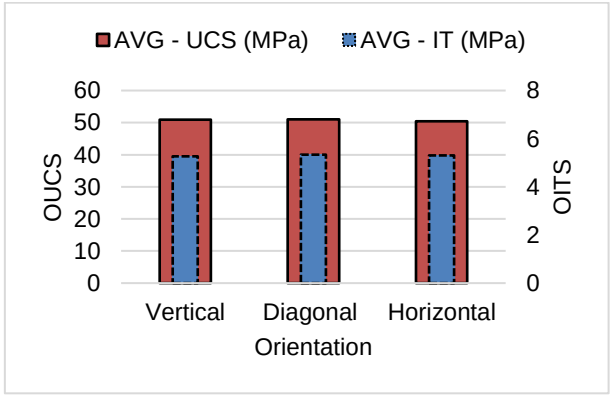

Figure 10. Average strength values of OITS and OUCS

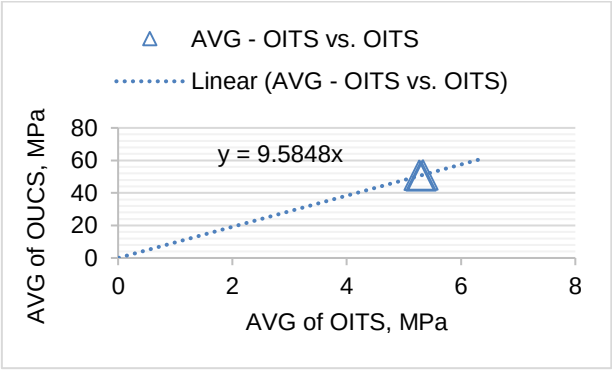

Figure 11. Correlation between the average values of OITS and OUCS

Figure 11 shows the correlation between the average values of OITS versus average values of OUCS demonstrating sandstone isotropy. The three average

values of OITS and OUCS represent the three primary orientations of vertical, diagonal, and horizontal.

5.2.2 Individual Results of OITS vs. OUCS

Data of each orientation was considered in separate graphs of OUCS vs. OITS for each orientation, as shown for one orientation in Fig. 12. Results of all correlations between OUCS and OITS are summarized in Table 2 (bottom) with some published models (top).

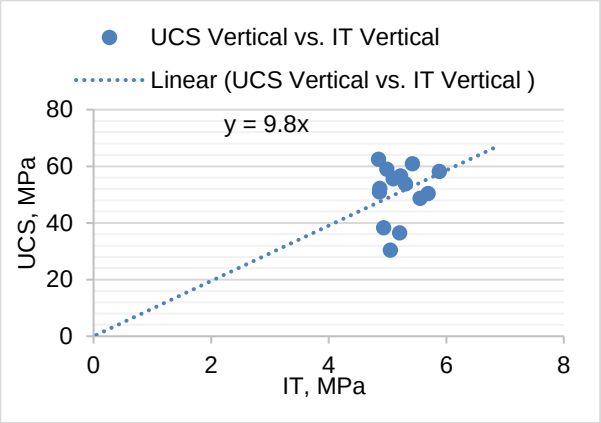

Figure 12. Correlations between vertically oriented strength of IT vs. UCS

6 DISCUSSION

Sandstone anisotropy was classified firstly by OUSWV according to reported wave velocity indices. Then, by OUCS. Finally by OITS.

After anisotropy classification, which was determined by OUSWV as indicated in Table 1, OUCS tests were conducted to provide more data for correlation with OITS. Figure 9 contains all data of OITS performed on disk samples vs. OUCS performed on standard samples that are shown in Fig. 7.

Correlating equations shown in Fig. 9 demonstrate sandstone isotropy. Sandstone isotropy is also shown when correlating AVG-OITS with AVG-OUCS producing a similar equation as shown in Fig. 10 and 11.

7 CONCLUSION

This is a report of an ongoing study of methodology for evaluating rock anisotropy.

8 FUTURE WORK

- Considering smaller orientation increments in all parts of the study.
- Involving various types of rocks to enrich the current procedure for broader anisotropy evaluation.
- Further study for rock anisotropy evaluation under various conditions such as pressurized condition is recommended.

Table 4. Summary of correlations between OITS and OUCS in all scenarios of multiple and singular orientation

Correlations between IT and UCS of Previous studies				
Ref.	Author	Equation	Rock Type	Orientation
1	Kahraman et al, 2012	UCS=10.61*BTS	Different rock types including sandstone	/
2	Altidag and Guney, 2010	UCS=12.308*TS^1.0725	Different rock types including sandstone	/
3	Altidag and Guney, 2010	UCS=12.38*TS^1.025	Different rock types including sandstone	/
Correlations between IT and UCS of this study				
Ref.	Author	Equation	Rock Type	Orientation
4	Abugharara et al, 2019, Current study	UCS = 9.7596*IT	Fine-grain Sandstone	UCS Vertical vs. IT Vertical
5		UCS = 9.7955*IT	Fine-grain Sandstone	UCS Diagonal vs. IT Vertical
6		UCS = 9.6437*IT	Fine-grain Sandstone	UCS Horizontal vs. IT Vertical
7		UCS = 9.8863*IT	Fine-grain Sandstone	UCS Vertical vs. IT Diagonal
8		UCS = 9.5817*IT	Fine-grain Sandstone	UCS Diagonal vs. IT Diagonal
9		UCS = 9.6625*IT	Fine-grain Sandstone	UCS Horizontal vs. IT Diagonal
10		UCS = 8.9771*IT	Fine-grain Sandstone	UCS Vertical vs. IT Horizontal
11		UCS = 9.0219*IT	Fine-grain Sandstone	UCS Diagonal vs. IT Horizontal
12		UCS = 9.2662*IT	Fine-grain Sandstone	UCS Horizontal vs. IT Horizontal
13		UCS = 9.6165*IT	Fine-grain Sandstone	Multi-orientation of UCS vs. IT
14		UCS = 9.5848*IT	Fine-grain Sandstone	AVG of AVG OUCS vs. OITS

9 ACKNOWLEDGEMENT

This work was performed at the drilling technology laboratory (DTL) at Memorial university of Newfoundland, St. John's, Newfoundland and Labrador, Canada.

10 FUNDING DATA

- Atlantic Canada Opportunity Agency (AIF contract number: 781-2636-1920044), involving Husky Energy, Suncor Energy and Research and Development Corporation (RDC) of Newfoundland and Labrador.
- The Ministry of Higher Education and Scientific Research, Libya, through the Canadian Bureau for International Education, Canada (CBIE-Canada).

11 NOMENCLATURE

BTS	Brazilian Tensile Strength
CBIE	Canadian Bureau for International Education, Canada
VP	Compressional (Primary) Wave Velocity
IVP	Compressional Wave Velocity Index
DTL	Drilling Technology Laboratory
IT	Indirect Tensile Strength
OITS	Oriented Indirect Tensile Strength
OUSWV	Oriented Ultrasonic Wave Velocity
OUCS	Oriented Unconfined "Uniaxial" Compressive Strength
RDC	Research and Development Corporation
VS	Shear (Secondary) Wave Velocity
ST	Splitting Strength
VA	Velocity Anisotropy

12 REFERENCES

Abugharara, A. N., Alwaar, A. M., Butt, S. D., and Hurich, C. A. 2016. Baseline Development on Rock Anisotropy Investigation Utilizing Empirical Relationships Between Oriented Physical and Mechanical Measurement and Drilling Performance, The 35th International Conference on Ocean, Offshore and Arctic Engineering, Drilling Symposium, Busan, South Korea. Paper No. OMAE2016-5514.

Altindag, R. and Guney, A. 2010. Predicting the relationships between brittleness and mechanical properties (UCS, TS and SH) of rocks, *Scientific research and Essays*, *5*(16): pp.2107-2118.

Asadi, A. 2015. Application of artificial neural networks in estimation of uniaxial compressive strength using indirect tensile strength data of limestone rocks, In ISRM Regional Symposium-EUROCK 2015, International Society for Rock Mechanics and Rock Engineering. Salzburg, Austria Paper No. ISRM-EUROCK-2015-081.

ASTM. 2008a. 2936-08: Standard Test Method for Direct Tensile Strength of Intact Rock Core Specimens, ASTM International, West Conshohocken.

ASTM. 2008b. 3967-08: Standard Test Method for Splitting Tensile Strength of Intact Rock Core Specimens, ASTM International, West Conshohocken

Broch, E. and Franklin, J. A. 1972. The point load strength test, *International Journal Rock Mechanics and Mining Sciences & Geomechanics Abstracts*, 9 (6): 669-697. Pergamon Press.

Chen, C.S., Pan, E. and Amadei, B. 1998. Determination of Deformability and Tensile Strength of Anisotropic Rock Using Brazilian Tests, *International Journal of Rock Mechanics and Mining Sciences*, *35*(1): 43-61.

Diederichs, M.S. 2007. The 2003 Canadian Geotechnical Colloquium: Mechanistic interpretation and practical application of damage and spalling prediction criteria for deep tunnelling, *Canadian Geotechnical Journal*, *44*(9):1082-1116.

ISRM. 1978. Suggested methods for determining tensile strength of rock materials, Int J Rock Mech Min Sci Geomech Abstr 15(3):99–103. DOI:10.1016/0148-9062(78)90003-7

Kahraman, S., Fener, M., Kozman, E. 2012. Predicting the compressive and tensile strength of rocks from indentation hardness index, *Journal of the Southern African Institute of Mining and Metallurgy*, 112 (5): 331-339.

Li, D. and Wong, L.N.Y. 2013. The Brazilian Disc Test for rock Mechanics Applications: Review and New Insights. *Rock mechanics and rock engineering*, 46(2): 269-287.

Mendieta, H. J. 2012. Determination of a correlation between intact rock unconfined compressive strength and index parameters, *Harmonising Rock Engineering and the Environment - Proceedings of the 12th ISRM International Congress on Rock Mechanics*, P.735-739.

Perras, M.A. and Diederichs, M.S. 2014. A Review of the Tensile Strength of Rock: Concepts and Testing, *Geotechnical and geological engineering*, *32*(2): 525-546.

Ramamurthy, T. 1993. Strength and Modulus Responses of Anisotropic Rocks, *Comprehensive Rock Engineering*, Pergamon Press, Oxford, 1: 313-329.

Saroglou, H. and Tsiambaos, G. 2007. Classification of anisotropic rocks, *In 11th Congress of the International Society for Rock Mechanics,* In: Ribeiro e Sousa, Otalla, Grossmann, editors. Taylor & Francis Group, London, 1: 191-196.

Sheorey, P.R. 1997. *Empirical rock failure criteria*, A. A. Balkema, p:176.

Syed, S. A., Jin, G., Al Dhamen, A. A., and Saad, B. 2018. Enhancing rock mechanical characterization – new approach to quantatively determine the imminent failure state during multi-stage triaxial testing, *Presented at the SPWLA 59th Annual Logging Symposium* held in London, UK. Paper ID: SPWLA-2018-FFF.

Tsidzi, K. 1990. The Influence of Foliation on Point Load Strength Anisotropy of Foliated Rocks, *Bull. Int. Association of Eng. Geology,* 29: 49-58.

Tsidzi, K. 1997. Propagation characteristics of ultrasonic waves in foliated rocks, *Bull. Int. Association of Eng. Geology,* 56: 103-113.

APPENDIX 6 EMPIRICAL PROCEDURE INVESTIGATION FOR SANDSTONE ANISOTROPY EVALUATION: PART II

Title - Empirical Procedure Investigation for Sandstone Anisotropy Evaluation: Part II

Abdelsalam Abugharara and Stephen Butt
Department of Process Engineering, Memorial University of Newfoundland, St. John's, Newfoundland and Labrador, Canada
John Molgaard
Department of Mechanical Engineering, Memorial University of Newfoundland, St. John's, Newfoundland and Labrador, Canada
Charles Hurich
Department of Earth Sciences, Memorial University of Newfoundland, St. John's, Newfoundland and Labrador, Canada

ABSTRACT
A laboratory methodology of an anisotropy evaluation for fine grain sandstone is reported. The methodology involved four types of tests: (i) point load strength (OPLS) and (ii) compliant and non-compliant drilling as two primary tests, and (iii) ultrasonic wave velocity (OUSWV) measurement and (iv) unconfined (uniaxial) compressive strength (UCS) as supporting tests. Each test was conducted on samples produced from the same natural sandstone block in three orientations: vertical, diagonal, and horizontal. The primary tests were conducted for sandstone characterization determined by OUSWV using published anisotropy indices, and correlated with UCS. The tests showed sandstone isotropy, and are part of an ongoing study to develop a rock anisotropy characterization procedure.

RÉSUMÉ
Cette communication examine une méthode de laboratoire utilisée pour l'évaluation anisotropique du grès à grains fins. La méthodologie a impliqué quatre types de tests: (i) l'intensité des charges ponctuelles (OPLS), (ii) forages conformes et non-conformes étant les deux premiers tests effectués et (iii) la mesure de la vitesse des ondes ultrasoniques (OUSWV), (iv) celle de la résistance à la compression uniaxiale (UCS) en tant que tests complémentaires. Chaque test a été mené sur des échantillons provenant de la même roche naturelle de grès selon trois orientations principals: verticale, diagonale et horizontale. Les tests principaux ont été conduits pour caractériser le grès tel que déterminé par le procédé de la mesure de la vitesse des ondes ultrasoniques (OUSWV) en utilisant les indices d'anisotropie publiés et corrélés avec ceux de la résistance à la compression (UCS). Les tests ont démontré l'isotropie du grès et font partie d'une étude en cours dans le but de développer un procédé de caractérisation de l'anisotropie de la roche.

1 INTRODUCTION

Rocks are classified to be either isotropic, whose properties (i.e. mechanical, physical, etc.) are directional independent or anisotropic, whose properties are directional dependent (Brown el al. 1993, Goodman 1980). Anisotropy can vary between the most basic vertically transversely isotropic / horizontally transversely isotropic, VTI and HTI, respectively and the very highly anisotropy (Brady and Brown 2006)

Rock anisotropy can highly affect various applications, including oil and gas drilling process, well-logging measurements, reservoir evaluation, and mining operations as well as civil structures (Mokhtari et al. 2016, Gu 2018, Abugharara 2019).

Evaluating and determining rock anisotropy assist in controlling well trajectory, enhancing drilling performance, optimizing hydrocarbon production, strengthening civil structures, and minimizing errors in produced data and results.

The influence of anisotropy of shale, as an example of VTI rocks on oriented drilling by Abugharara et al. (2019) highlighted the importance of studying the anisotropy.

Published studies reported rock anisotropy evaluation methods through several tests of destructive and non-destructive tests.

The aim of this paper is to study the tested fine grain sandstone through oriented strength tests (OPLS, OUCS and their correlations) and directional compliant and non-compliant drilling as a part of ongoing research, whose ultimate goal is to develop a comprehensive procedure for rock anisotropy characterization.

2 SAMPLE PREPARATION

Samples were produced from one fine-grain sandstone block and used for all tests as shown in Fig. 1. Samples were obtained in various dimensions in accordance with American Society for Testing and Materials (ASTM) standards and International Society of Rock Mechanics (ISRM) suggested methods. The dimensions of the main

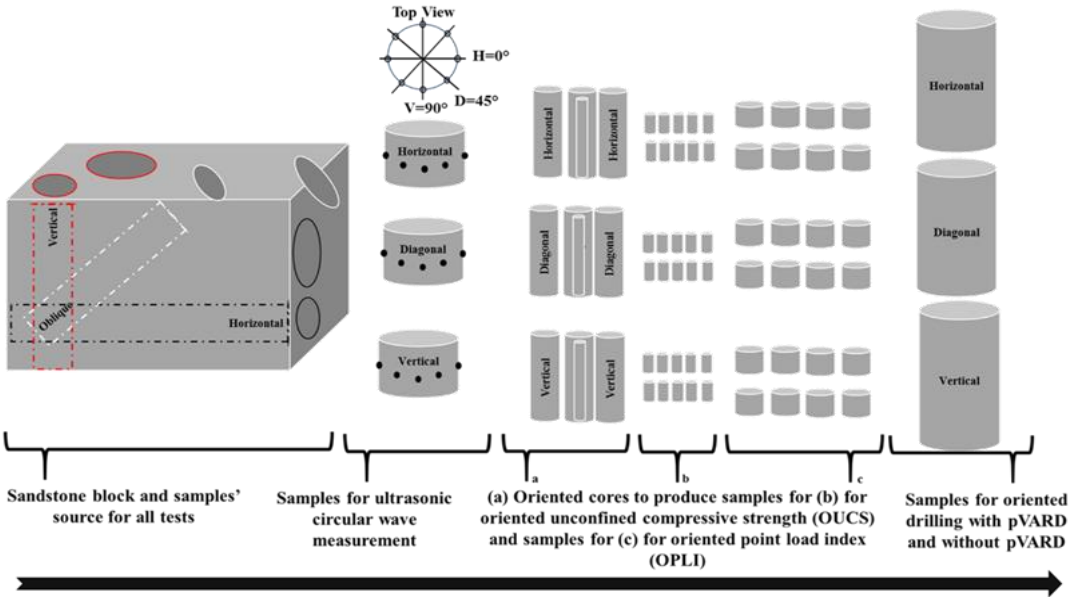

Figure 1. Sandstone coring source and samples sets for all tests of ultrasonic, strength and drilling

block were about 70 cm long, 40 cm wide, and 50 cm high. Different diameter coring bits were used to core sandstone in three orientations: vertical, diagonal, and horizontal.

For OUSWV measurements, samples were cores of 10.16 cm diameter and about 10 cm long as shown in Fig.1 second left, with indications of circular wave velocity measurements as well as samples' top view. For oriented strength measurements, samples were cores of 4.76 cm diameter and about 30 cm long or more depending on the coring directions. Samples in each orientation were then categorized to three groups. Each group was denoted for particular oriented strength testing type.

For the unconfined compressive strength test, samples where cored axially from the 4.76 cm samples using a 2.54 cm coring bit. These samples are shown in Figure 2-a AND b. The samples were then cut to a 2:1 ratio of length to diameter with accordance to standards. For the PLI test, samples were prepared for the point load axial test. Samples were cut from the 2.54 cm cores in accordance with "ASTM D5731 – 2016" as shown in Fig. 1-c. Figure 2 shows sample dimension requirements for the point load axial test.

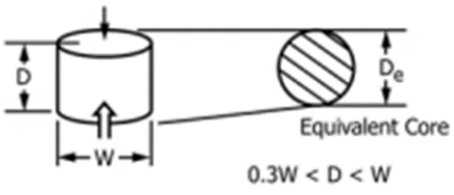

Figure 2. sample dimension requirement for point load test "according to ASTM D5731 – 2016".

For both compliant and non-compliant drilling, samples were cored using a 10.16 cm coring bit. Samples are shown in Fig. 1- Right.

3 EXPERIMENTAL PROCEDURE

Experiments were conducted in the following order. First: for oriented ultrasonic wave velocity (OUSWV) including compressional and shear wave velocity (vp and vs respectively). The purpose of this test was to characterize the tested sandstone anisotropy in accordance with some published ultrasonic wave velocity anisotropy indices.

Second, sandstone oriented strength was determined through the destructive strength tests of both OPLS and OUCS.

Third, a compliance drilling using a passive vibration assisted rotary drilling (pVARD) tool, followed by a non-compliant drilling were performed in three orientations. Both drilling types were performed on the same samples, but each drilling from a different side as detailed in.

Fourth, constructing correlations between OPLIS and OUCS for further sandstone anisotropy evaluation and characterization, followed by the fifth step of determination of sandstone anisotropy.

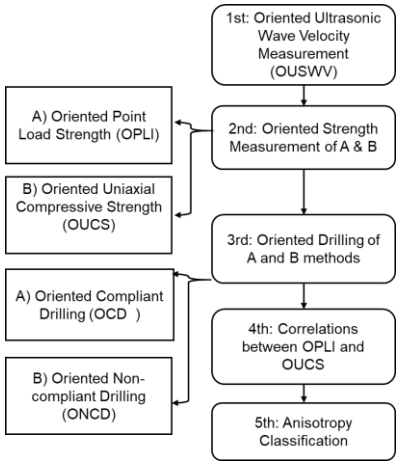

Figure 3. Experimental procedure flowchart.

4 PERFORMED TESTS AND APPARATUS

Several tests were performed to characterize the fine-grain sandstone's anisotropy. These tests included a non-destructive test of oriented ultrasonic compressional and shear wave velocity (OUSWV), and destructive tests of oriented point load Index (OPLI) and oriented uniaxial compressive strength (OUCS).

The purpose of conducting OUSWV, whose apparatus was fully described by Abugharara et al. (2016), was to characterize the anisotropy of the tested fine-grain sandstone using published indices, and then using this anisotropy characterization as a base for the strength and drilling tests. The purpose of applying destructive strength tests of OPLS and OUCS, whose apparatus is shown in Fig. 4, was (i) to confirm the tested rock anisotropy classifications, determined through OUSWV, by using reported strength anisotropy classification indices, (ii) to evaluate the sandstone strength anisotropy based on OPLI results, and (iii) to correlate results of OPLI and OUCS and compare their correlation models to published models.

Figure 4. Point load apparatus and its modified version for OUCS.

Compliant drilling using pVARD and non-compliant drilling were the last tests. Figure 5 shows compliant and non-compliant drilling apparatus with a dual cutter Polycrystalline Diamond Compact (PDC) bit. Figure 6 shows samples PLI and UCS before testing as well as samples after compliant and non-compliant drilling tests using a fully instrumented laboratory scale rotary drilling rig. pVARD tool was used to drill with induced vibrations that makes it different from non-compliant drilling, where pVARD was locked. The purpose of using two different drilling modes of compliant and non-compliant was to further evaluate sandstone anisotropy.

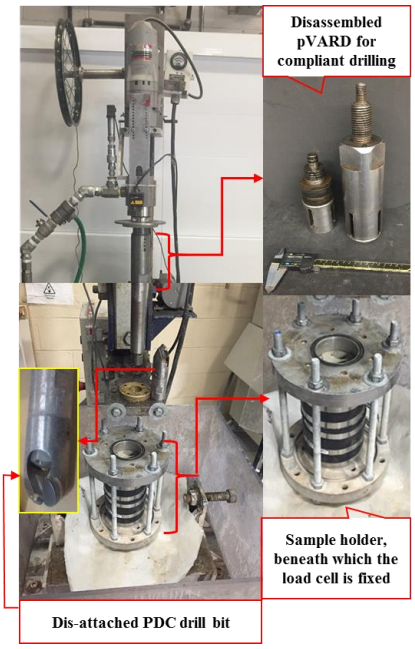

Figure 5. Fully instrumented laboratory scale drilling rig

Figure 6. Samples for PLI and UCS before testing as well as drilled samples.

5 RESULTS

This section contains results of OUSWV, OPLS, OUCS, compliant and non-compliant drilling, as well as correlations between OPLS and OUCS.

5.1 Results of Oriented Ultrasonic Wave Measurement and Sandstone Anisotropy classification

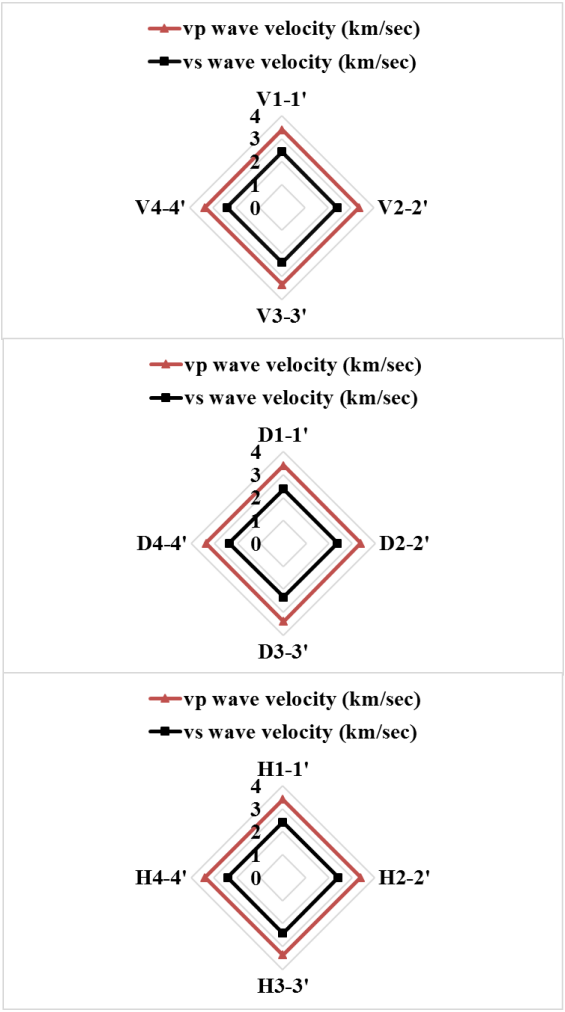

Figure 7. Circular ultrasonic compressional and shear wave velocity measurement

Figure 7 shows results of the circular ultrasonic compressional and shear wave velocity measurements from three oriented sandstone cores.

Results of the anisotropy classification of this sandstone according to some of the published anisotropy indices by Tsidzi (1997) and Saroglou (2007) are summarized in Table 1. Table 1 also contains the anisotropy strength indices and the results of their current work.

5.2 Results of Oriented Sandstone Strength

5.2.1 Oriented Unconfined Compressive Strength

This section shows results of sandstone oriented strength measured by OUCS and OPLS as shown in Fig. 8 and 9, respectively. The average values of strength results measured from both tests show consistency indicating sandstone isotropy.

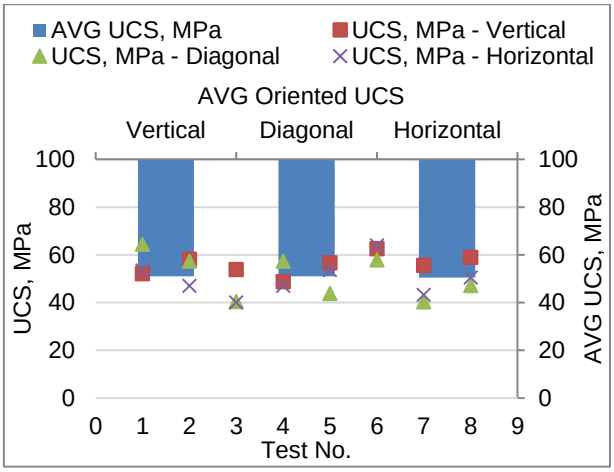

Figure 8. Oriented unconfined compressive strength and their average values.

5.3 Oriented Point Load Strength

Results of OPLS and their values are shown in Fig. 9. The average strength values of OPLS and OUCS are shown in Fig. 10.

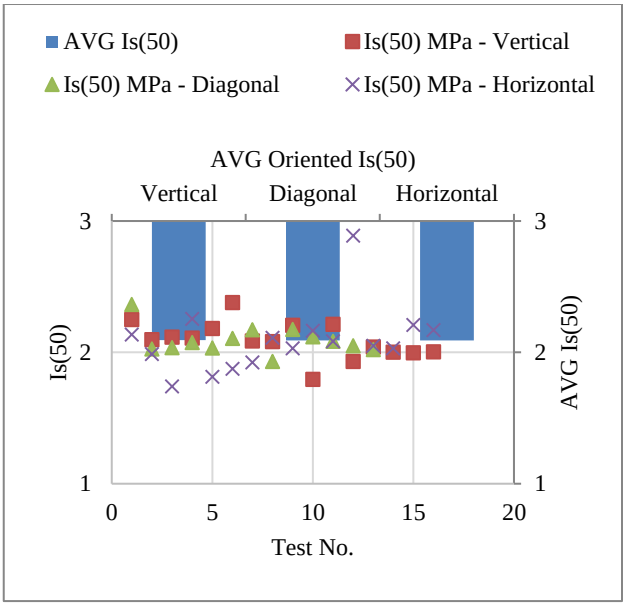

Figure 9. Oriented point load strength and their average values

to be isotropy is that the value equals 1. For this study

Table 1. Published wave velocity and strength anisotropy indices with their conditions for isotropy classification and results of current study

Author	Test type	Anisotropy Index	Equation	Criterion	Result of current study	Descriptive term
Tsidizi (1997)	Wave velocity	Velocity Anisotropy (VA) Index	VA= [(Vmax-Vmin)/Vmean] (%)	< 2.0 : Isotropy	0.55 (%)	Isotropy
Saroglou (2007)			Ivp=Vp(0°)/Vp(90°)			
ISRM (1981)	PLI	Point load strength anisotropy index	Ia(50) = Is (50) (90°) / Is (50) (0°)	1.0 : Isotropy	0.05	Isotropy
ISRM (1985)						
Tsidzi (1990)						
Ramamurthy (1993)	UCS	Uniaxial compressive strength anisotropy index	Iσc = σc (90°) / σc (min)	1.0 - 1.1: Isotropy	0.99	Isotropy

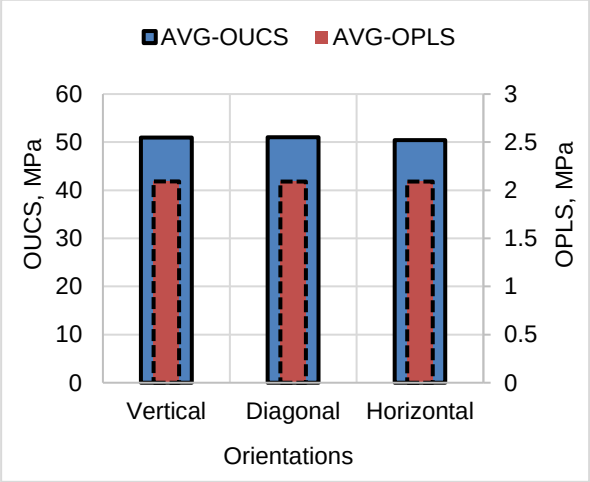

Figure 10. Average values of OUSC and OPLS

According to ISRM (1981), ISRM (1985), and Tsidzi (1990), rock strength anisotropy can be classified using PLI using Eq. 1.

$$Ia(50) = \frac{Is\,(50)(90°)}{Is\,(50)(0°)} \quad (1)$$

Where, $Ia(50)$ is a point load strength anisotropy index, $Is\,(50)(90°)$ and $Is\,(50)(0°)$ is point load strength anisotropy index applied vertically and horizontally, respectively. The associated conditions for Eq.1 for a rock $Ia(50)$ = 0.05, classifying the tested sandstone as isotropic.

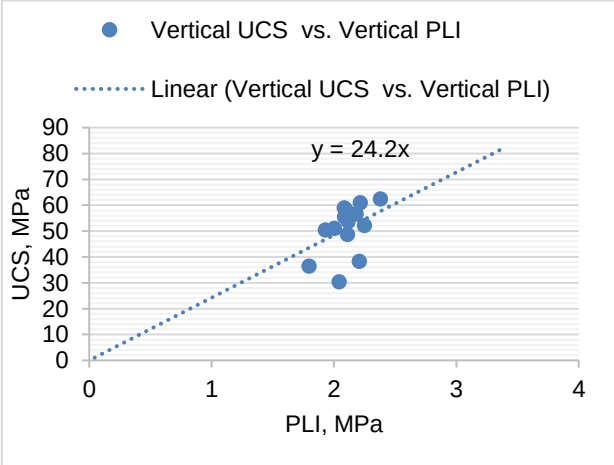

Figure 11. Correlation between vertical PLI and vertical UCS

Figures 11 to 14 are 4 figures of 10, which show correlations between UCS and PLI in all scenarios of orientations. Figure 11 shows correlations between vertical UCS and vertical PLI. Figure 12 shows correlations between diagonal UCS and diagonal PLI. Figure 13 shows correlations between horizontal UCS and horizontal PLI. Figure 14 shows correlations between OUCS and OPLI.

Table 2. Summary of published correlations for PLI and UCS with correlations with the current study

Reported correlations			
Author	Source of rock	Rock type	Correlation
Broch and Franklin (1972)	UK	Various rocks	UCS = 23.7*PLI
Bieniawski (1975)	South Africa	Sandstones	UCS = 23.9*PLI
Hawkins and Olver (1986)	UK	Sandstones	UCS = 24.8*PLI
Vallejo et al. (1989)	USA	Sandstones	UCS = 17.4*PLI
Das (1985)	Canada	Sandstones	UCS = 18*PLI
Smith (1997)	Various locations	Sandstones	UCS = 24*PLI
Current study correlations: Abugharara (2019)			
Vertical UCS vs. Vertical PLI	Canada	Sandstones	UCS=24.3*PLI
Diagonal UCS vs. Diagonal PLI	Canada	Sandstones	UCS=24.3*PLI
Horizontal UCS vs. Horizontal PLI	Canada	Sandstones	UCS=24.1*PLI
Vertical UCS vs. Diagonal PLI	Canada	Sandstones	UCS = 24.3*PLI
Vertical UCS vs. Horizontal PLI	Canada	Sandstones	UCS = 24*PLI
Diagonal UCS vs. Vertical PLI	Canada	Sandstones	UCS = 23.6*PLI
Diagonal UCS vs. Horizontal PLI	Canada	Sandstones	UCS = 25.8*PLI
Horizontal UCS vs. Diagonal PLI	Canada	Sandstones	UCS = 24*PLI
Horizontal UCS vs. Vertical PLI	Canada	Sandstones	UCS = 23.7*PLI
OUCS vs. OPLS (all data in all orientations)	Canada	Sandstones	UCS=24.3*PLI

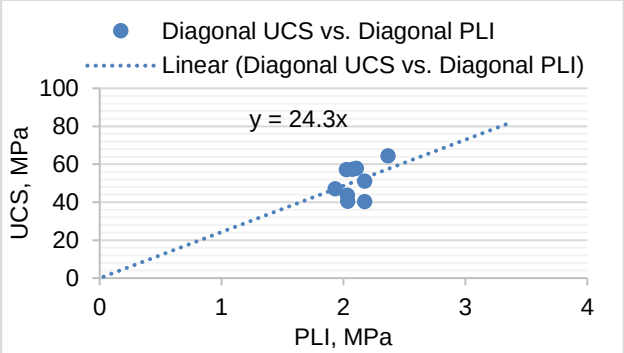

Figure 12. Correlation between diagonal PLI and diagonal UCS

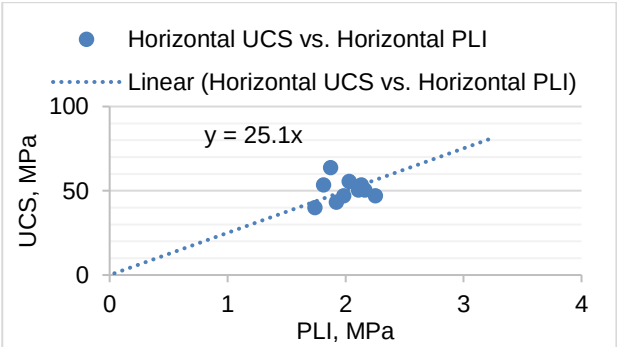

Figure 13. Correlation between horizontal PLI and horizontal UCS

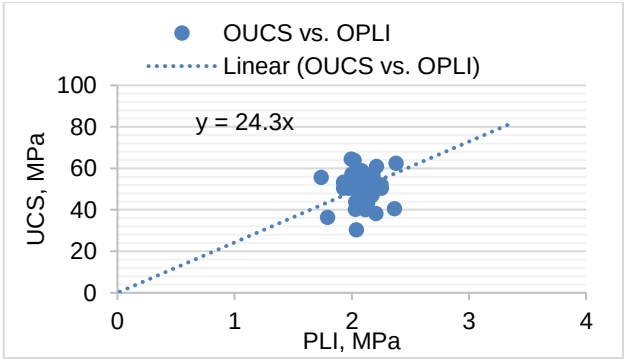

Figure 14. Correlation between OPLI and OUCS involving their data in the three orientations

5.4 Oriented Compliant and Non-Complaint Drilling

This section contains the results of oriented drilling sandstone in three orientations using compliant and non-compliant. The results involved comparison between the downhole dynamic weight on bit (DDWOB) measured by the load cell attached beneath the sample holder. Drilling using compliant and non-compliant induces different levels of vibrations that influences the DDWOB. The purpose here is to conduct a comparative analysis DDWOB in compliant and non-compliant drilling as a function of sandstone orientation and static weight and evaluate their changes with orientation. Differences in results with orientation indicates sandstone anisotropy and similar results indicates sandstone isotropy.

Fig. 15 and 16 show consistency indicating sandstone isotropy. This similarity appears in DDWOB as well as rate of penetration (ROP) compliant and noncompliant drilling as a function of orientation.

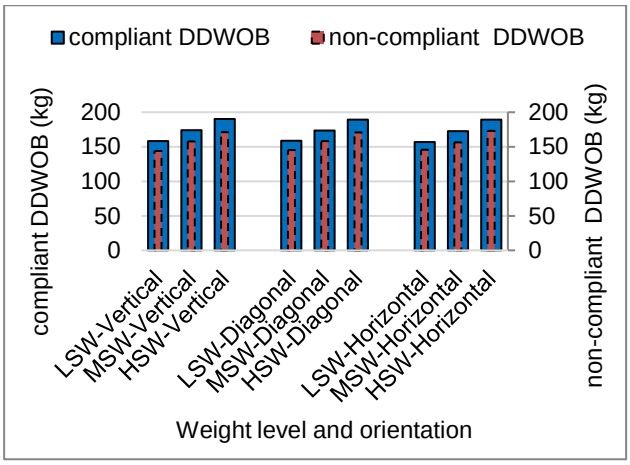

Figure 15. Compliant and non-compliant DDWOB as a function of sandstone orientation and weight levels of low, medium, and high static weight

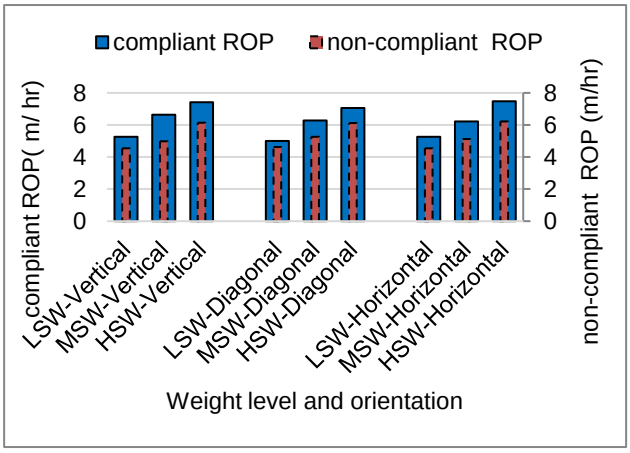

Figure 16. Compliant and non-compliant ROP as a function of sandstone orientation and weight levels of low, medium, and high static weight

6 Discussion

The anisotropy of the fine grain sandstone was studies using the oriented ultrasonic, strength and drilling tests. Ultrasonic method was conducted first on three samples. The results of ultrasonic wave velocity measurement are shown in Fig. 7.

Figure 8 and 9 show oriented strength results and their average values, which were obtained by OUCS and OPLS, respectively. Strength anisotropy indices were determined based on the averaged values of all tests. Although Abugharara (2019) reported the UCS anisotropy for sandstone, the purpose of presenting OUCS in this paper is to have correlation between OUCS and OPLS.

Figure 10 shows the average values of the oriented strengths. These average values were used for the sandstone strength anisotropy classification. For PLI anisotropy index, Eq. 1 was used. Results showed sandstone isotropy as summarized in Table 1.

Figures 11 to 14 show correlations between PLI and UCS in similar orientations: individually as shown in Fig. 11 to 13 and collectively as shown in Fig. 14). Correlations of possible scenarios of all orientations are summarized in Table 1.

Drilling was performed for evaluating sandstone's anisotropy. The two drilling parameters involved were DDWOB and ROP (Fig 15 and 16; respectively). Both parameters were studied as a function of orientation in two drilling modes of compliant and non-compliant. First, the compliant drilling was better in performance and had higher ROP against non-compliant. Second, DDWOB was recorded higher in compliant drilling than that of non-compliant. They various weight levels of low, medium, and high static weight levels were applied to study DDOWB and ROP. The results of DDWOB and ROP show consistency, which could be considered as a sigh of sandstone isotropy as was determined by the ultrasonic wave velocity and the strength methods.

7 CONCLUSION

The work of this paper reports results of an ongoing project that uses various techniques, among which are compliant and non–complaint drilling as well as strength tests, for rock anisotropy characterization.

Tests were supporting one another in showing sandstone isotropy, in particular wave velocity and strength tests. The drilling tests showed data consistency, indicating sandstone isotropy.

8 FUTURE WORK

Involving different rock types and performing tests under pressurized conditions will be considered.

9 ACKNOWLEDGEMENT

This work was performed at the Drilling Technology Laboratory (DTL) at Memorial University of Newfoundland, St. John's, Newfoundland and Labrador, Canada.

10 FUNDING DATA

- Atlantic Canada Opportunity Agency (AIF contract number: 781-2636-1920044), involving Husky Energy, Suncor Energy and Research and Development Corporation (RDC) of Newfoundland and Labrador.
- The Ministry of Higher Education and Scientific Research, Libya, through the Canadian Bureau for International Education, Canada (CBIE-Canada).

11 NOMENCLATURE

CBIE	Canadian Bureau for International Education, Canada

VP	Compressional (Primary) Wave Velocity
IVP	Compressional Wave Velocity Index
DDWOB	Downhole Dynamic Weight on Bit
DTL	Drilling Technology Laboratory
HSW	High Static weight
LSW	Low Static weight
Vmax	Maximum velocity
Vmean	Mean velocity
MSW	Medium Static weight
Vmin	Minimum velocity
OPLS	Oriented Point Load Strength
OUSWV	Oriented Ultrasonic Wave Velocity
OUCS	Oriented Unconfined "Uniaxial" Compressive Strength
pVARD	passive Vibration Assisted Rotary Drilling
PLI	Point Load Index
Ia(50)	Point load strength anisotropy index
Is	Point load strength index
PDC	Polycrystalline Diamond Compacts
ROP	Rate of Penetration
RDC	Research and Development Corporation
VS	Shear (Secondary) Wave Velocity
Iσc	Uniaxial compressive strength anisotropy index
VA	Velocity Anisotropy

12 REFERENCES

Abugharara, A. N., Alwaar, A. M., Butt, S. D., and Hurich, C. A. 2016. Baseline Development on Rock Anisotropy Investigation Utilizing Empirical Relationships Between Oriented Physical and Mechanical Measurement and Drilling Performance, The 35th International Conference on Ocean, Offshore and Arctic Engineering, Drilling Symposium, Busan, South Korea. Paper No. OMAE2016-5514.

Abugharara, A. N., Mohamed, B., Hurich, C., Molgaard, J., & Butt, S. D. 2019. Experimental Investigation of the Effect of Shale Anisotropy Orientation on the Main Drilling Parameters Influencing Oriented Drilling Performance in Shale, *Journal of Energy Resources Technology*, *141*(10):102904. DOI: 10.1115/1.4043435

ASTM International. ASTM D5731-16 Standard Test Method for Determination of the Point Load Strength Index of Rock and Application to Rock Strength Classifications. West Conshohocken, PA; ASTM International, 2016.

Bieniawski Z. T. 1975: Point load test in geotechnical practice. Engineering Geology, 9(1), 1-11.

Brady, B. H. G., and E. T. Brown. 2006. *Rock Mechanics for underground mining,* Kluwer Academic Publishing: 36.

Broch, E. and Franklin, J. A. (1972). The point load strength test, *International Journal Rock Mechanics and Mining Sciences & Geomechanics Abstracts*, 9 (6): 669-697. Pergamon Press.

Brown, Edwin T., and John A. Hudson, eds. 1993. *Comprehensive rock engineering: principles, practice & projects. 1. Fundamentals*, Pergamon Press, p.285, DOI: 10.1016/0148-9062(94)90473-1

Chau, K.T., Wong, R. H. C. 1996: Uniaxial compressive strength and point load strength of rocks, International Journal of Rock Mechanics and Mining Sciences, Geomechanical Abstract, 33, 183-188.

Das, B. M. 1985. Evaluation of the point load strength for soft rock classification, Proceedings of the fourth international conference ground control in mining, Morgantown, WV, 220-226.

Goodman, Richard E. 1980. *Introduction to Rock Mechanics*. No. BOOK. John Wiley:12.

Gu, M. 2018. Impact of Anisotropy Induced by Shale Lamination and Natural Fractures on Reservoir Development and Operational Designs. *SPE Reservoir Evaluation & Engineering*, *21*(04): 850-862.

Hawkins, A. B., Olver, J. A. G. 1986. Point load tests: correlation factor and contractual use, An example from the Corallian at Weymouth. In: Hawkins, A.B. (Ed.), Site Investigation Practice: Assessing BS 5930, Geological Society, London, 269-271.

INTERNATIONAL SOCIETY OF ROCK MECHANICS (ISRM). 1981. Rock characterization testing and monitoring, *ISRM Suggested methods*, Brown E.T. (ed.), Pergamon Press, Oxford.

ISRM 1985: Suggested method for determining point load strength. *International Journal of Rock Mechanics and Mining Sciences and Geomechanical Abstract*, 22(2), 51-60. 21)

Mokhtari, M., Honarpour, M. M., Tutuncu, A. N., & Boitnott, G. N. 2016. Characterization of elastic anisotropy in Eagle Ford Shale: Impact of heterogeneity and measurement scale, *SPE Reservoir Evaluation & Engineering,* 19(03): 429-439.

Ramamurthy, T. 1993. Strength and Modulus Responses of Anisotropic Rocks, *Comprehensive Rock Engineering*, Pergamon Press, Oxford, 1: 313-329.

Saroglou, H., and G. Tsiambaos. 2007. Classification of anisotropic rocks, *In 11th Congress of the International Society for Rock Mechanics*. In: Ribeiro e Sousa, Otalla, Grossmann, editors. Taylor & Francis Group, London, p. 191.

Smith, H. J. 1997: The point load test for weak rock in dredging applications, International Journal of Rock Mechanics and Mining Sciences, 34, 295, 3-4.

Tsidzi, K. 1990. The Influence of Foliation on Point Load Strength Anisotropy of Foliated Rocks, *Bull. Int. Association of Eng. Geology,* 29: 49-58.

Tsidzi, K. 1997. Propagation characteristics of ultrasonic waves in foliated rocks, *Bull. Int. Association of Eng. Geology,* 56: 103-113.

Vallejo, L. E., Welsh, R. A., Robinson, M. K. 1989: Correlation between unconfined compressive and point load strength for Appalachian rocks, *Proceeding of 30th US Symposium on Rock Mechanics*, Morgantown, 461-468.